

DEVELOPMENT OF A SYNTHETIC STRATEGY TOWARD
TRANS-CYCLOBUTANE-CONTAINING NATURAL PRODUCTS:
ENANTIOSELECTIVE TOTAL SYNTHESIS OF (+)-PSIGUADIAL B

Thesis by

Lauren Marie Chapman

In Partial Fulfillment of the Requirements

for the Degree of

Doctor of Philosophy

The logo for the California Institute of Technology (Caltech), featuring the word "Caltech" in a bold, orange, sans-serif font.

CALIFORNIA INSTITUTE OF TECHNOLOGY

Pasadena, California

2017

(Defended May 31, 2017)

© 2017

Lauren Marie Chapman

All Rights Reserved

To Dad

I hope heaven needs you more than I do.

ACKNOWLEDGEMENTS

First and foremost, I wish to thank my research advisor, Professor Sarah Reisman, for her unwavering support while conducting my doctoral studies in her laboratory. She has given me just the right amount of guidance when I needed it most, but also the freedom to develop into an independent, critically thinking scientist. Sarah ascribes to the motto, “if you work hard for me, I’ll work hard for you,” a contract that has been extraordinarily motivating for me, and I thank her for being my strongest advocate in turn. Without question, Sarah cares deeply for all of her students and I am truly grateful to have had the privilege of working for an exceptional mentor who I’ve always felt has my best interests at heart.

I would also like to thank my committee chairman, Professor Brian Stoltz, whose presence on the third floor of Schlinger makes many of us in the Reisman lab feel as though we have a second advisor. Throughout my graduate degree, he has provided thoughtful feedback on my work and his support in my search for employment has been instrumental to my success at Caltech. I have also greatly appreciated the insightful questions and guidance provided by the rest of my committee members, Professor Jonas Peters, Professor David Tirrell, and Dr. Scott Virgil.

Not only has Scott served on my committee, but has also spent many, *many* hours with me discussing every possible topic, including reaction optimization, the electrical circuitry of the polarimeter, and raising seahorses. Scott’s wealth of knowledge and enthusiasm for chemistry is contagious; I am deeply indebted to him for his dedication in helping me to solve numerous problems in synthesis, while teaching me patience through arduous HPLC purifications. Likewise, I am grateful to Dr. David VanderVelde whose

extensive expertise in NMR has greatly benefited my pursuits in total synthesis. The time he has spent with me pouring over 2D data is singlehandedly responsible for my proficiency in structure elucidation and stereochemical assignment.

The entire division of Chemistry and Chemical Engineering at Caltech is an exceptional place to do science; the highly collaborative and supportive environment here has been essential to my development as a chemist. I have had the privilege and pleasure to work alongside many extraordinary colleagues over the years. As a first year student, I felt welcomed by the senior students in the lab, and am especially obliged to Sarah's first class, Dr. Julian Codelli, Dr. Roger Nani, Dr. Raul Navarro, Dr. Lindsay Repka, and Dr. John Yeoman, for developing a foundational lab culture that has made the Reisman group such a fun place to work.

I could not have asked for a better project partner and confidant than Jordan Beck, who is an exceptionally talented chemist and an all-around joy to spend time with. It has been an honor to mentor him as a first year graduate student and a true joy to witness him now independently drive his own total synthesis project. I've also greatly enjoyed training one of our newest group members, Caitlin Lacker, who undoubtedly has a very bright scientific future ahead of her. To the rest of my collaborators that I've worked with throughout the years: ShuMing Huang, Leon Moskatel, and Dr. Linglin Wu, I thank you for your contributions and for helping me grow as a mentor.

I could not have made it through this journey without the friendship and support of many former lab members: Professor Anton Dubrovskiy, Dr. Christopher Haley, Dr. Matthew Hesse, Dr. Nathaniel Kadunce, Katerina Korch, Dr. Raul Navarro, Dr. Jane Ni, Matthieu Richter, Dr. Haoxuan Wang, and Dr. John Yeoman. I really don't know where

I'd be without all the time you've generously spent with me. I am tremendously grateful to all the current Reisman lab members: Nick Cowper, Dr. Elliot Farney, Nick Fastuca, Sean Feng, Denise Grünenfelder, Arthur Han, Dr. Luke Hanna, Julie Hofstra, Victor Mak, Skyler Mendoza, Dr. Yasu Nakayama, Tatsuya Okita, Kelsey Poremba, Dr. Susan Stevenson, Dr. Justin Su, and Alice Wong. Thank you for making every day a joy to come into work. Wishing you all the very best in your careers, I will truly miss you!

I have arguably spent more time alongside my baymate and dear friend, Dr. Chen Xu, than anyone else throughout my PhD. I will never forget the many cultural and linguistic adventures we have had throughout our four years of late-night chemistry together. I would especially like to thank Shoshana Bachman for her personal support during difficult times; her courage and honesty is unmatched by anyone else I have met at Caltech and continues to inspire me. I also am indebted to my friends outside of Caltech who have been vital to my personal growth and a consistent source of support and perspective each week: to Albie, Andy, Julie, and Monique—the insights and lessons I have learned from our time together are among the greatest gifts I will take with me.

My decision to pursue a graduate degree in chemistry was heavily influenced by my time working as an associate chemist at Cubist Pharmaceuticals. In particular, my former supervisor, Qingyi Li, led the charge in encouraging me to take my career to the next level. She has set my standard for what it means to be an extraordinary mentor, and I thank her for always believing in me. A heartfelt thank you goes out to *all* of my former Cubist colleagues who showed me how rewarding a scientific career is when you get to work alongside brilliant people who really care about the impact we make in patients' lives. I am proud to say that I'll be continuing the fight to combat infectious disease at

Novartis, Emeryville and am very grateful to the medicinal chemists there for giving me the opportunity to join their team.

It should be noted that, as Brian's substitute during the 2012 Prospective Student Visit Weekend, Dr. Jeffrey Holder is partially responsible for recruiting me to Caltech in the first place. The friendship that we quickly cultivated that summer has evolved into a bond that continues to grow each day. His strength, love, and commitment to building a life together are unlike I've ever known. I am forever thankful for his patience with me as I've worked many long hours to complete my graduate degree, and I am so looking forward to our exciting new chapter in San Francisco.

Finally, words cannot express how grateful I am for the unconditional love and support of my "adopted" family, Linda and Casey Silverberg, who have always kept me grounded, celebrated my successes, and never let me give up on pursuing the things I want most in life. My perseverance in the face of adversity would simply not be possible without them. I also want to thank my Mother and the rest of my family for providing a sense of love and belonging (and an endless amount entertainment) throughout my life. More than anything else, I am eternally grateful to have had the best father in the entire world, whose personal integrity constantly inspires me to become a better version of myself. He taught me that your greatest legacy is left in the impact you make on others; his has certainly been a guiding beacon in my life, and I strive to follow his example.

ABSTRACT

Trans-cyclobutane-containing meroterpenoids are a structurally intriguing class of natural products with a diverse array of pharmacologically interesting properties. Herein, the development of a synthetic strategy for *de novo* construction of the *trans*-cyclobutane motif is described, which has enabled the first enantioselective total synthesis of the cytotoxic natural product, (+)-psiguadial B. Specifically, we have developed a photochemical Wolff rearrangement with tandem catalytic, asymmetric addition to a ketene generated *in situ*. To our knowledge, this work represents the first example of this methodology used to prepare enantioenriched amides. A palladium-catalyzed, directed C(sp³)-H alkenylation reaction is used to quickly build molecular complexity, and two distinct epimerization strategies permit access to either enantiomer of the natural product from a single enantiomer of organocatalyst.

In the course of this work, three different synthetic routes toward (+)-psiguadial B were investigated and each is discussed. These studies have led to the execution of several challenging key transformations, including an *ortho*-quinone methide hetero-Diels-Alder cycloaddition with a cyclohexanone-derived enol ether, a vinyl sulfide-mediated Prins cyclization, and a modified Norrish-Yang cyclization. Ultimately, the successful synthetic strategy was realized by employing a ring-closing metathesis to form the strained, 7-membered terpene framework, and a late-stage benzylic oxidation/arylation strategy to complete the core of the natural product.

Finally, in an effort to apply these key strategy concepts in the context of other bioactive *trans*-cyclobutane-containing natural products, initial results toward a concise total synthesis of (+)-rumphellaone A are presented.

PUBLISHED CONTENT AND CONTRIBUTIONS

Portions of the work described herein were disclosed in the following communication:

Chapman, L. M.; Beck, J. C.; Wu, L.; Reisman, S. E. *J. Am. Chem. Soc.* **2016**, *138*, 9803.

DOI: 10.1021/jacs.6b07229

This article is available online at: <http://pubs.acs.org/doi/abs/10.1021/jacs.6b07229>

Copyright © 2016 American Chemical Society

L.M.C. contributed to conception of the synthetic strategy, conducted the experiments described herein, prepared the supporting data, and participated in writing the manuscript.

TABLE OF CONTENTS

CHAPTER 1	1
(+)–Psiguadial B and Structurally-Related Natural Products	
1.1 INTRODUCTION	1
1.2 DIFORMYL PHLOROGLUCINOL MEROTERPENOID	
NATURAL PRODUCTS	2
1.2.1 Biological Activity and Medicinal Properties.....	3
1.2.2 Synthetic Aspects: Hetero-Diels–Alder Strategies	4
1.3 TRANS-CYCLOBUTANE-CONTAINING NATURAL PRODUCTS	5
1.3.1 Natural Products Derived from β -Caryophyllene	5
1.3.2 Seminal Synthetic Approaches Toward Natural Products	
Containing <i>Trans</i> -Fused Cyclobutanes	6
1.3.3 Biomimetic Strategies for Semi-Synthesis	9
1.4 THE PSIGUADIAL FAMILY OF NATURAL PRODUCTS	11
1.4.1 Isolation of Psiguadials A–D	11
1.4.2 Proposed Biosynthesis of the Psiguadial Family	12
1.4.3 Total Synthesis Efforts Toward Psiguadial B	16
1.5 NOTES AND REFERENCES	18

CHAPTER 2 **24**

First Generation Synthetic Strategy Toward (+)-Psiguadial B
and Development of a Catalytic, Asymmetric Wolff Rearrangement

2.1 INTRODUCTION	24
2.1.1 C(sp ³)-H Activation: A Guiding Strategic Bond Disconnection.....	25
2.1.2 Retrosynthetic Analysis: Precedent and Anticipated Challenges	27
2.2 FORWARD SYNTHETIC EFFORTS: RACEMIC STUDIES	32
2.3 DEVELOPMENT OF A TANDEM PHOTOCHEMICAL WOLFF REARRANGEMENT/ASYMMETRIC KETENE ADDITION	37
2.3.1 Reaction Design and Relevant Precedent	37
2.3.2 Optimization of an Enantioselective Wolff Rearrangement	39
2.3.3 Efforts Toward Flow Photochemistry	46
2.3.4 Mechanistic Considerations	49
2.3.5 Efforts Toward Expansion of Substrate Scope	53
2.4 FORWARD SYNTHETIC EFFORTS: ASYMMETRIC ROUTE	54
2.4.1 Quaternary Center Formation via Conjugate Addition.....	55
2.4.2 Evaluation of the Key <i>o</i> -QMHDA Cycloaddition Reaction	59
2.4.3 Model Studies Toward a Vinyl Sulfide Prins Cyclization	64
2.5 CONCLUDING REMARKS	65
2.6 EXPERIMENTAL SECTION	67
2.6.1 Materials and Methods	67
2.6.2 Preparative Procedures and Spectroscopic Data	68
2.7 NOTES AND REFERENCES	103

APPENDIX 1	111
Spectra Relevant to Chapter 2	
APPENDIX 2	171
X-Ray Crystallography Reports Relevant to Chapter 2	
CHAPTER 3	192
Revised Strategies for the Enantioselective Total Synthesis of (+)-Psiguadial B	
3.1 INTRODUCTION	192
3.1.1 Revised Retrosynthetic Analysis	193
3.2 FORWARD SYNTHETIC EFFORTS	198
3.2.1 Development of an Alternative Epimerization Strategy	198
3.2.2 Optimization of a Catalytic Conjugate Addition Reaction	200
3.2.3 Evaluation of the Key Norrish–Yang Cyclization	203
3.3 REVISED SYNTHETIC ROUTE AND NEW ENDGAME STRATEGY	206
3.3.1 Completion of the Central Psiguadial Framework.....	206
3.3.2 Appendage of C1' Phenyl and Final Functionalization	211
3.4 CONCLUDING REMARKS	215
3.5 EXPERIMENTAL SECTION	217
3.5.1 Materials and Methods.....	217
3.5.2 Preparative Procedures and Spectroscopic Data	218
3.6 NOTES AND REFERENCES	260

APPENDIX 3 **266**

Spectra Relevant to Chapter 3

APPENDIX 4 **324**

Progress Toward a Concise Total Synthesis of (+)-Rumphellaone A

4.1 INTRODUCTION	324
4.1.1 Isolation and Biosynthetic Origins.....	324
4.2 PREVIOUS TOTAL SYNTHESSES OF (+)-RUMPHELLAONE A	326
4.2.1 Kuwahara's Enantioselective Synthesis	326
4.2.2 Echavarren's Asymmetric Synthesis	327
4.3 RETROSYNTHETIC ANALYSIS	328
4.4 FORWARD SYNTHETIC EFFORTS	328
4.5 CONCLUDING REMARKS AND FUTURE DIRECTIONS	333
4.6 EXPERIMENTAL SECTION	334
4.6.1 Materials and Methods.....	334
4.6.2 Preparative Procedures and Spectroscopic Data	335
4.7 NOTES AND REFERENCES	346

APPENDIX 5 **349**

Spectra Relevant to Appendix 4

ABOUT THE AUTHOR **363**

LIST OF ABBREVIATIONS

$[\alpha]_D$	angle of optical rotation of plane-polarized light
Å	angstrom(s)
<i>p</i> -ABSA	<i>para</i> -acetamidobenzenesulfonyl azide
Ac	acetyl
acac	acetylacetonate
AIBN	azobisisobutyronitrile
aq	aqueous
AQN	anthraquinone-1,4-diyl diether
Ar	aryl group
atm	atmosphere(s)
BINOL	1,1'-bi-2,2'-naphthol
bipy	2,2'-bipyridine
Bn	benzyl
Boc	<i>tert</i> -butoxycarbonyl
bp	boiling point
br	broad
Bu	butyl
<i>i</i> -Bu	<i>iso</i> -butyl
<i>n</i> -Bu	butyl or <i>norm</i> -butyl
<i>t</i> -Bu	<i>tert</i> -butyl
BQ	1,4-benzoquinone
Bz	benzoyl

c	concentration of sample for measurement of optical rotation
^{13}C	carbon-13 isotope
/C	supported on activated carbon charcoal
$^{\circ}\text{C}$	degrees Celcius
calc'd	calculated
CAN	ceric ammonium nitrate
cat.	catalyst
Cbz	benzyloxycarbonyl
CD	Cinchonidine
cf.	consult or compare to (Latin: <i>confer</i>)
<i>cis</i>	on the same side
cm^{-1}	wavenumber(s)
CN	Cinchonine
CoA	Coenzyme A
conc.	concentrated
conv.	conversion
Cp	cyclopentadienyl
CSA	camphor sulfonic acid
Cy	cyclohexyl
Δ	heat or difference
δ	chemical shift in ppm
d	doublet
d	deutero or dextrorotatory

D	deuterium
dba	dibenzylideneacetone
DBU	1,8-diazabicyclo[5.4.0]undec-7-ene
DCE	1,2-dichloroethane
DDQ	2,3-dichloro-5,6-dicyano-1,4-benzoquinone
<i>de novo</i>	starting from the beginning; anew
DIPEA	<i>N,N</i> -diisopropylethylamine
DHQ	dihydroquinine
DHQD	dihydroquinidine
DIBAL	diisobutylaluminum hydride
DMAP	4-(dimethylamino)pyridine
DME	1,2-dimethoxyethane
DMEDA	<i>N,N'</i> -dimethylethylenediamine
DMF	<i>N,N</i> -dimethylformamide
DMPU	1,3-dimethyl-3,4,5,6-tetrahydro-2(1H)-pyrimidinone
DMSO	dimethylsulfoxide
dppe	1,2-bis(diphenylphosphino)ethane
dppf	1,1'-bis(diphenylphosphino)ferrocene
dr	diastereomeric ratio
<i>ee</i>	enantiomeric excess
E	methyl carboxylate (CO_2CH_3)
E^+	electrophile
<i>E</i>	<i>trans</i> (entgegen) olefin geometry

EDCI	<i>N</i> -(3-dimethylaminopropyl)- <i>N'</i> -ethylcarbodiimide hydrochloride
e.g.	for example (Latin: <i>exempli gratia</i>)
EI	electron impact
<i>ent</i>	enantiomer of
<i>epi</i>	epimeric
equiv	equivalent(s)
ESI	electrospray ionization
Et	ethyl
<i>et al.</i>	and others (Latin: <i>et alii</i>)
FAB	fast atom bombardment
FTIR	fourier transform infrared spectroscopy
g	gram(s)
Grubbs-II	Grubbs' catalyst™ 2nd generation
h	hour(s)
¹ H	proton
[H]	reduction
HDA	hetero-Diels–Alder
HFIP	hexafluoroisopropanol
HG-II	Hoveyda–Grubbs' catalyst™ 2nd generation
HIV	human immunodeficiency virus
HMBC	heteronuclear multiple-bond correlation spectroscopy
HMDS	hexamethyldisilazide
HMPA	hexamethylphosphoramide

$h\nu$	irradiation with light
HPLC	high performance liquid chromatography
HRMS	high resolution mass spectrometry
Hz	hertz
IC ₅₀	half maximal inhibitory concentration (50%)
i.e.	that is (Latin: <i>id est</i>)
<i>iso</i>	isomeric
<i>in situ</i>	in the reaction mixture
J	coupling constant in Hz
k	rate constant
kcal	kilocalorie(s)
kg	kilogram(s)
L	liter or neutral ligand
l	levorotatory
LA	Lewis acid
LC/MS	liquid chromatography–mass spectrometry
LDA	lithium diisopropylamide
m	multiplet or meter(s)
M	molar or molecular ion
m	<i>meta</i>
μ	micro
<i>m</i> -CPBA	<i>meta</i> -chloroperbenzoic acid
Me	methyl

mg	milligram(s)
MHz	megahertz
MIC	minimum inhibitory concentration
min	minute(s)
mL	milliliter(s)
MM	mixed method
mol	mole(s)
MOM	methoxymethyl
Ms	methanesulfonyl (mesyl)
MS	molecular sieves
MTT	3-(4,5-dimethylthiazol-2-yl)-2,5-diphenyltetrazolium bromide
m/z	mass-to-charge ratio
NBS	<i>N</i> -bromosuccinimide
ND	not determined
NHC	<i>N</i> -heterocyclic carbene
nm	nanometer(s)
nM	nanomolar
NMO	<i>N</i> -methylmorpholine <i>N</i> -oxide
NMR	nuclear magnetic resonance
NOE	nuclear Overhauser effect
NOESY	nuclear Overhauser enhancement spectroscopy
NPh	naphthyl
Nu [−]	nucleophile

<i>o</i>	<i>ortho</i>
<i>o</i> -QM	<i>ortho</i> -quinone methide
[O]	oxidation
P	peak
<i>p</i>	<i>para</i>
PCC	pyridinium chlorochromate
PDC	pyridinium dichromate
Ph	phenyl
pH	hydrogen ion concentration in aqueous solution
PHAL	1,4-phthalazinediyl diether
PIFA	[bis(trifluoroacetoxy)iodo]benzene
Pin	pinacol
PivOH	pivalic acid
pK_a	acid dissociation constant
pm	picometer(s)
PMB	<i>para</i> -methoxybenzyl
ppm	parts per million
PPTS	pyridinium <i>para</i> -toluenesulfonate
Pr	propyl
<i>i</i> -Pr	isopropyl
<i>n</i> -Pr	propyl or <i>norm</i> -propyl
psi	pounds per square inch
py	pyridine

PYR	2,5-diphenyl-4,6-pyrimidinediyl diether
q	quartet
QD	Quinidine
QN	Quinine
quant.	quantitative
R	generic (alkyl) group
R _L	large group
R	rectus
RCM	ring-closing metathesis
recry.	recrystallization
ref	reference
R _f	retention factor
rgt.	reagent
rt	room temperature
s	singlet or seconds
S	sinister
sat.	saturated
t	triplet
TBAF	tetra- <i>n</i> -butylammonium fluoride
TBME	<i>tert</i> -butyl methyl ether
TBS	<i>tert</i> -butyldimethylsilyl
TC	thiophene-2-carboxylate
temp	temperature

Tf	trifluoromethanesulfonyl
TFA	trifluoroacetic acid
THF	tetrahydrofuran
TLC	thin layer chromatography
TMS	trimethylsilyl
TOF	time-of-flight
tol	tolyl
TPAP	tetrapropylammonium perruthenate
<i>trans</i>	on the opposite side
Ts	<i>para</i> -toluenesulfonyl (tosyl)
UV	ultraviolet
<i>vide infra</i>	see below
w/v	weight per volume
X	anionic ligand or halide
xs	excess
Z	<i>cis</i> (zusammen) olefin geometry

Chapter 1

(+)-Psiguadial B and Structurally-Related Natural Products

1.1 INTRODUCTION

Natural products are a large and diverse class of bioactive molecules that hold tremendous potential as medicinal agents. To date, natural products and their derivatives rank among the most successful lead compounds that have been developed into drug candidates and evaluated in clinical trials.¹ Although 33% of approved drugs are derived from natural products,² the pharmaceutical industry has shifted away from natural-product based discovery programs over the last two decades,³ due in part to prohibitively difficult synthetic challenges associated with accessing architecturally complex molecules. Moreover, chemical derivatization of natural product-based scaffolds is often non-trivial, hindering the systematic study of structure activity relationships (SAR).

To the synthetic chemist, it is precisely these challenges that drive the pursuit of natural product total synthesis. The intriguing structural frameworks of these molecules provide a platform to inspire the invention of new chemical methods that facilitate rapid

construction of particularly formidable synthetic targets. In this regard, we strive for creativity as well as efficiency when designing new synthetic strategies, unencumbered by the notion that we may only utilize the tools that are already at our disposal. From this ideal perspective, only the limits of imagination preclude us from advancing the frontiers of chemical science. To the extent that we are successful in developing novel transformations with the goal of improving synthetic efficiency, there is no better venue to showcase the versatility of a new method than in the context of total synthesis.

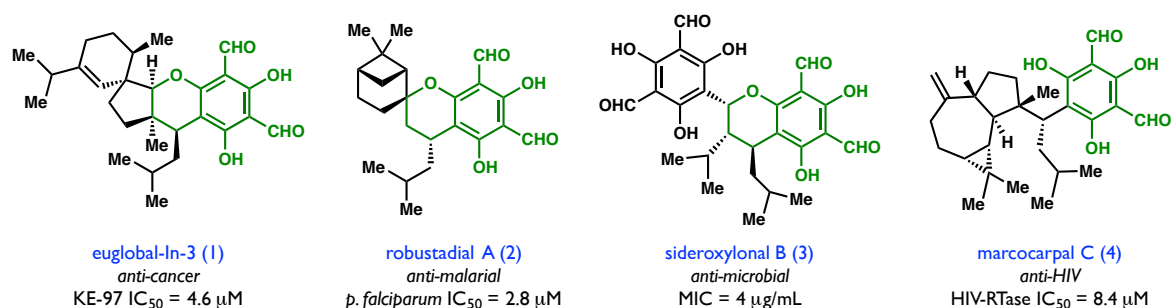
1.2 DIFORMYL PHLOROGLUCINOL MEROTERPENOID NATURAL PRODUCTS

As their name suggests, meroterpenoids are classified as hybrid natural products that are partially derived from terpene biosynthesis pathways. The term “phloroglucinol” refers to a 1,3,5-trihydroxybenzene unit, which arises in nature from malonyl-CoA by a series of condensation and cyclization events facilitated by polyketide synthases.⁴ Specifically, diformyl phloroglucinol constitutes a highly oxidized arene containing two aldehydes and three phenols in an alternating arrangement (see Figure 1.1). Diformyl phloroglucinol meroterpenoids therefore possess two distinct sets of physiochemical properties: the terpene portion is often stereochemically-rich, largely hydrophobic, and chemically inert, while the diformyl phloroglucinol motif is flat, aromatic, reactive, and has great capacity for multiple hydrogen-bonding interactions. The fusion of these disparate features in one molecule makes this class of natural products particularly fascinating and has captivated the interest of chemists and biologists alike for decades.

1.2.1 Biological Activity and Medicinal Properties

Phloroglucinol-containing natural products are a large class of bioactive molecules, comprising over 700 compounds known to date.⁵ Diformyl phloroglucinol meroterpenoids are a subset of this family whose diverse medicinal properties^{5,6} are exemplified by molecules such as euglobal-In-3 (**1**),⁷ robustadial A (**2**),⁸ sideroxylonal B (**3**),⁹ and marcocarpal C (**4**, Figure 1.1),¹⁰ which exhibit anti-cancer, anti-malarial, anti-bacterial, and anti-viral bioactivity, respectively. Owing to their therapeutic potential, there is growing interest in preparing various derivatives of these natural products, which have recently appeared in patents describing their utility as neurotransmitter-reuptake inhibitors for the treatment of a variety of neurological disorders such as depression, obesity, addiction, and Alzheimer's disease.¹¹ Given the intriguing bioactivity of diformyl phloroglucinol meroterpenoids, many research groups continue to pursue the isolation and characterization of new molecules in this family that are derived from natural sources.¹² In particular, the extracts of plants used in traditional folk medicine have long served as rich sources of bioactive natural meroterpenoids with novel structures.

Figure 1.1. Bioactive diformyl phloroglucinol terpenes

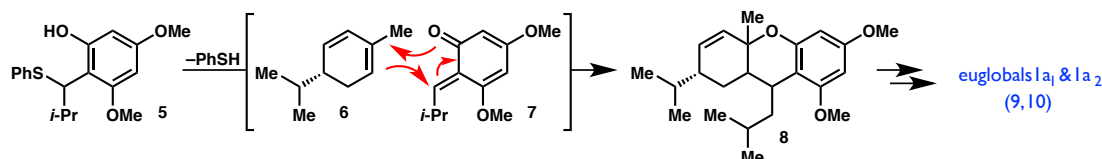


1.2.2 Synthetic Aspects: Hetero-Diels–Alder Strategies

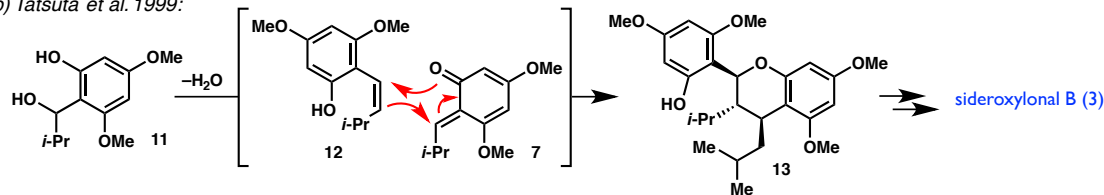
Decades of synthetic studies have led to a variety of chemical tools for the construction of diformyl phloroglucinol meroterpenoids.⁵ In particular, those containing central pyran rings prompt a hetero-Diels–Alder (HDA) cycloaddition as an obvious retrosynthetic disconnection. Such transformations commonly proceed with hetero-dienes known as *ortho*-quinone methides (*o*-QM, i.e. **7** and **17**, Scheme 1.1). These highly reactive species can be generated *in situ* using a variety of methods,¹³ often involving loss of a stable molecule, such as thiophenol or water. Notable examples of concise, biomimetic syntheses using this strategy to rapidly assemble the frameworks of several prototypical diformyl phloroglucinol meroterpenoid natural products include early work by Chiba,¹⁴ Tatsuta,¹⁵ and Singh.¹⁶

Scheme 1.1. Synthesis of diformyl phloroglucinol meroterpenoids via *o*-QM/HDA

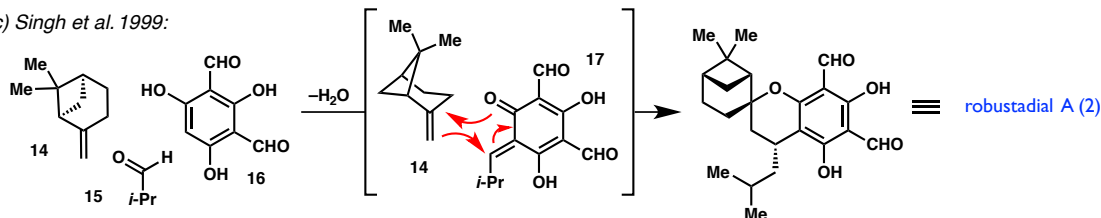
a) Chiba et al. 1995:



b) Tatsuta et al. 1999:



c) Singh et al. 1999:

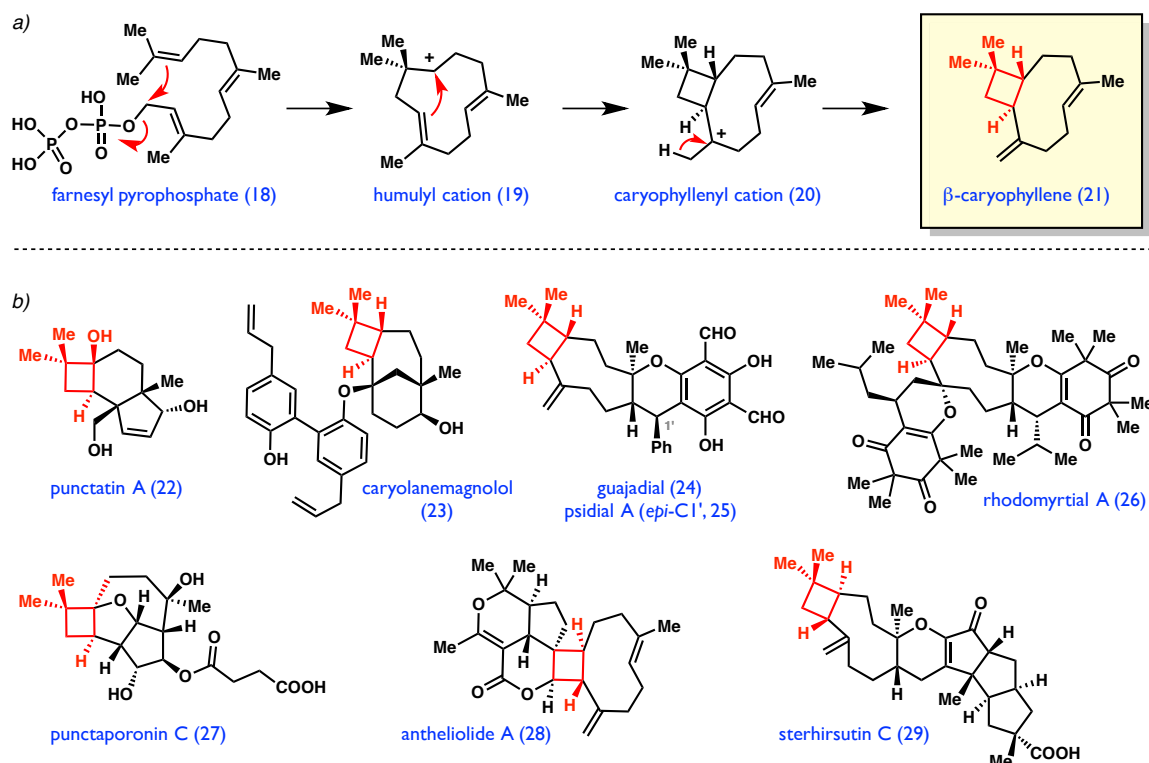


1.3 TRANS-CYCLOBUTANE-CONTAINING NATURAL PRODUCTS

1.3.1 Natural Products Derived from β -Caryophyllene

Cyclobutane-containing natural products are a structurally intriguing class of metabolites produced by a variety of organisms, with over 210 compounds in this family displaying a wide range of interesting bioactive properties.¹⁷ While 4-membered rings are relatively common among natural products, *trans*-fused cyclobutanes are rare due to the strain associated with this stereochemical arrangement, and almost exclusively found in molecules derived from β -caryophyllene (**21**). First isolated in 1834, **21** is an optically active, naturally abundant sesquiterpenoid from which a multitude of polycyclic natural products originate.¹⁸ Biosynthetically, **21** is proposed to arise by caryophyllene synthase-mediated intramolecular cyclization of farnesyl pyrophosphate (**18**, Figure 1.2a) to

Figure 1.2. *Trans*-cyclobutane natural products derived from β -caryophyllene



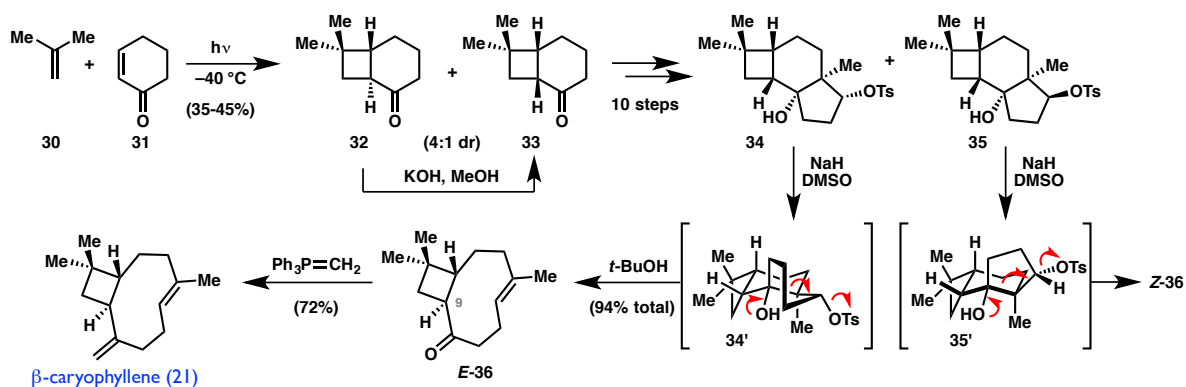
generate humulyl cation **19**,¹⁹ which undergoes subsequent ring closure to produce the 4-membered ring. This enzymatic process is proposed to guide the stereoselective formation of the unusual *trans*-fused cyclobutane in **21**. Further cationic, enzyme-mediated rearrangement of **21** leads to divergent biosyntheses of many complex terpenoid scaffolds.^{18,20} Indeed, the structural hallmarks of caryophyllene are clearly evident in a diverse array of natural products, especially those displaying the *trans*-cyclobutane motif (**22–29**, Figure 1.2b).²¹ Unsurprisingly, the unique structural features of β -caryophyllene and related natural products have generated much interest from the synthetic community in the last 50 years.

1.3.2 Seminal Synthetic Approaches Toward Natural Products Containing *Trans*-Fused Cyclobutanes

In 1963, Corey and coworkers reported the first landmark total synthesis of β -caryophyllene (**21**, Scheme 1.2).²² Construction of the cyclobutane ring was accomplished at the outset via a regioselective, photochemical [2+2] cycloaddition

Scheme 1.2. Corey's total synthesis of β -caryophyllene via [2+2] and fragmentation

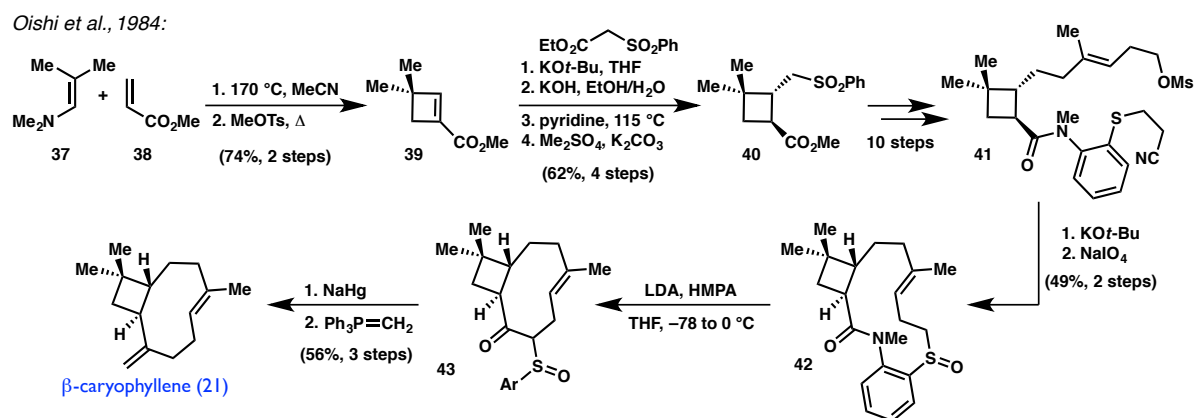
Corey et al., 1963:



between isobutylene (**30**) and 2-cyclohexenone (**31**). Interestingly, the reaction produced unstable *trans*-fused cyclobutane **32** as the major diastereomer,²³ which was subsequently epimerized to the more stable *cis* cyclobutane **33** upon treatment with KOH in methanol. Elaboration to a diastereomeric mixture of tosylates **34** and **35** then enabled formation of the 9-membered ring by a Grob fragmentation, forming either the *E* or *Z* olefin through the antiperiplanar transition states **34'** and **35'**, respectively. Addition of *tert*-butanol then facilitated base-mediated epimerization at C9 over the course of 15 hours to produce penultimate ketone **36**. A final Wittig methylenation reaction proceeded smoothly to furnish the natural product in 13 steps.

Twenty years after Corey's initial disclosure, Oishi and coworkers reported a markedly different strategy toward **21** (Scheme 1.3).²⁴ Cyclobutene **39** was accessed using Brannock's method for enamine-promoted formal [2+2] cycloaddition between **37** and **38** under thermal conditions.²⁵ Base-mediated conjugate addition of ethyl 2-(phenylsulfonyl)acetate established the thermodynamically preferred *trans*-stereochemistry across the cyclobutane ring, and following selective decarboxylation and

Scheme 1.3. Oishi's total synthesis of β -caryophyllene via intramolecular alkylation

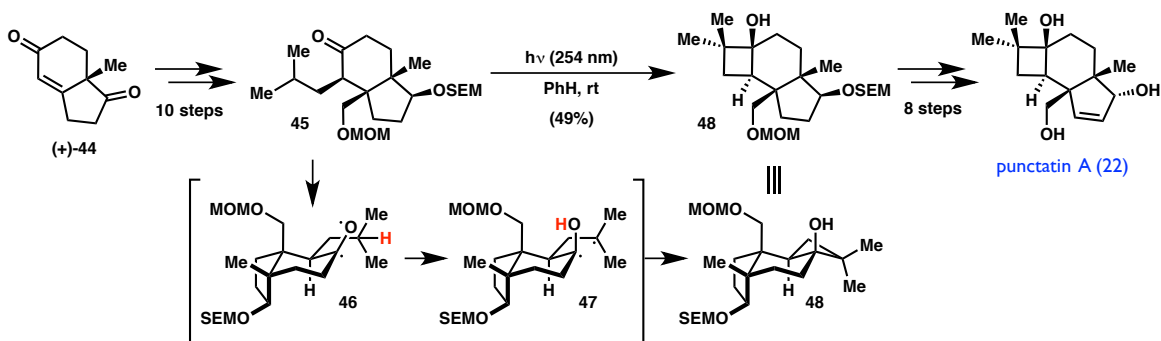


re-esterification, provided phenylsulfone **40** in 62% over the 4-step sequence. Exposure of nitrile **41** to KO*t*-Bu triggered formation of a thiolate anion (not shown), which underwent intramolecular alkylation to give 13-membered macrocycle **42** after oxidation to the corresponding sulfoxide. In a key step, ring contraction was achieved via acyl transfer reaction upon treatment of **42** with LDA in the presence of HMPA. With the 9-membered ring secured, reductive cleavage of the aryl sulfoxide and Wittig methylenation then delivered β -caryophyllene in a total of 22 steps.

Shortly after Oishi's report, Paquette and Sugimura described the first asymmetric synthesis of a related β -caryophyllene-derived natural product, (–)-punctatin A (**22**, Scheme 1.4).²⁶ Enantioenriched Hajos–Parrish ketone (**44**)²⁷ was advanced to bicyclic ketone **45**, which was conformationally poised to undergo stereoselective Norrish–Yang cyclization²⁸ upon irradiation with 254 nm light. This elegantly employed transformation is known to proceed by excitation of the carbonyl π system to the photoexcited triplet state, which exhibits diradical character²⁹ (i.e. **46**). The oxygen-centered radical then abstracted a proximal hydrogen atom (highlighted in red), which resulted in two carbon-centered radicals (i.e. **47**) that recombined to furnish cyclobutanol **48**. This intermediate

Scheme 1.4. Paquette's total synthesis of punctatin A via Norrish–Yang cyclization

Paquette & Sugimura, 1986:



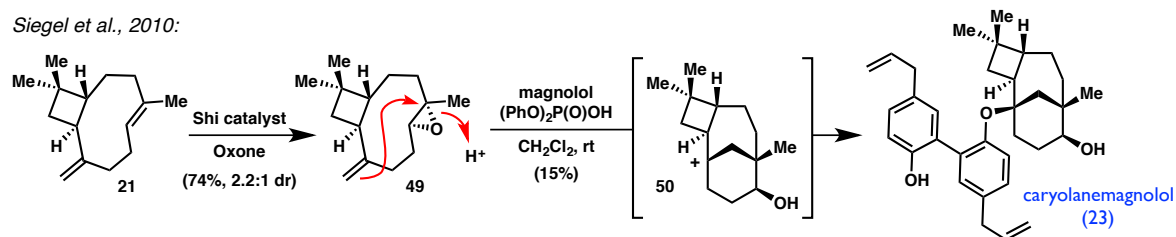
was then converted to the natural product in a further 8 steps.

These early reports exemplify some common synthetic strategies to construct cyclobutanes in natural product total synthesis. Moreover, the challenges associated with building this motif with the requisite *trans*-fused arrangement, in high yield and stereoselectivity, are apparent. Although many lessons have been learned through the synthetic efforts aimed at accessing terpenes such as β -caryophyllene (**21**) through total synthesis, others have exploited the natural abundance of **21** by utilizing it as a starting material in the semi-synthesis of other biosynthetically related natural products.

1.3.3 Biomimetic Strategies for Semi-Synthesis

Caryolanemagnolol (**23**) is a sesquiterpene-neolignan isolated from the bark of *Magnolina obovata* that exhibits striking neurological activity,³⁰ as well as demonstrated *in vivo* efficacy for improving motor function in patients with Huntington's disease.³¹ In 2010, Siegel and coworkers reported a concise semi-synthesis of **23**, proceeding in just 2 steps from **21**, according to the biosynthetic proposal for its origin (Scheme 1.5).³² Selective epoxidation of the more electron-rich, trisubstituted olefin in **21** was accomplished to afford **49** with moderate diastereoselectivity. Notably, Shi's catalyst was used to override the substrate's inherent preference to produce the undesired α -epoxide.

Scheme 1.5. Siegel's semi-synthesis of caryolanemagnolol

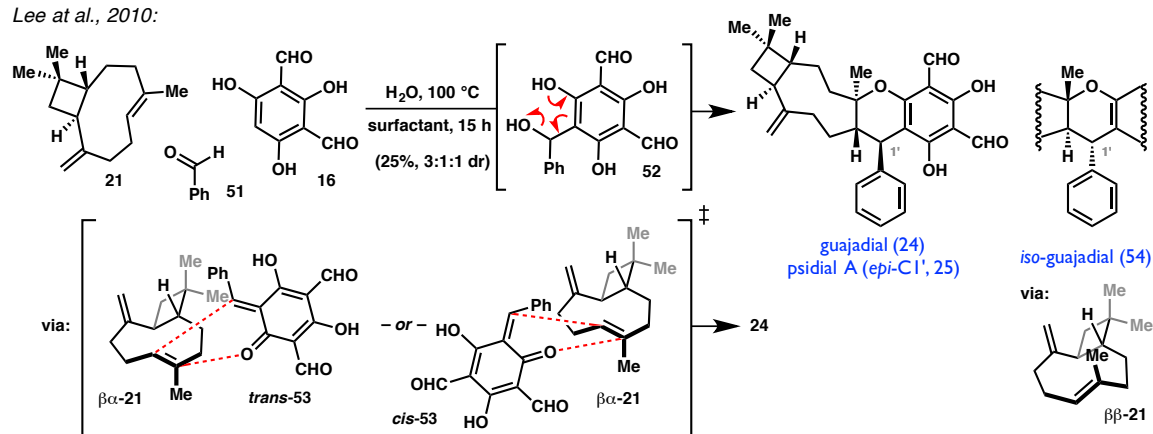


Transannular epoxide opening was effected with diphenyl phosphate, thus generating bridgehead carbocation **50**, which was trapped by magnolol to provide direct access to the natural product, albeit in a modest 15% yield.³³

Concurrent with these studies, Lee and coworkers explored a three-component, one-pot assembly of the diformyl phloroglucinol meroterpenoids, guajadial (**24**) and psidial A (**25**).³⁴ Knoevenagel condensation between benzaldehyde (**51**) and diformyl phloroglucinol **16** produced 2-hydroxybenzyl alcohol **52**, which can extrude water to generate *ortho*-quinone methide (*o*-QM) **53** *in situ* (Scheme 1.6). This reactive heterodiene then underwent [4+2] cycloaddition with the most stable $\beta\alpha$ -configuration of **21**³⁵ through either of the two transition states depicted below to yield **24** as the major diastereomer isolated from the reaction. Alternative approach of either *cis* or *trans*-**53** accounts for the complementary stereochemical outcome observed in **25**, while the formation of **54** may arise via cycloaddition with the diastereomeric $\beta\beta$ -conformation of **21**. As in Siegel's case, although this biomimetic cycloaddition (*vide infra*) proceeds in low overall yield, semi-synthesis from **21** benefits from exceptionally expedient access to caryophyllene-derived *trans*-cyclobutane-containing natural products.

Scheme 1.6. Lee's semi-syntheses of guajadial and psidial A

Lee *et al.*, 2010:

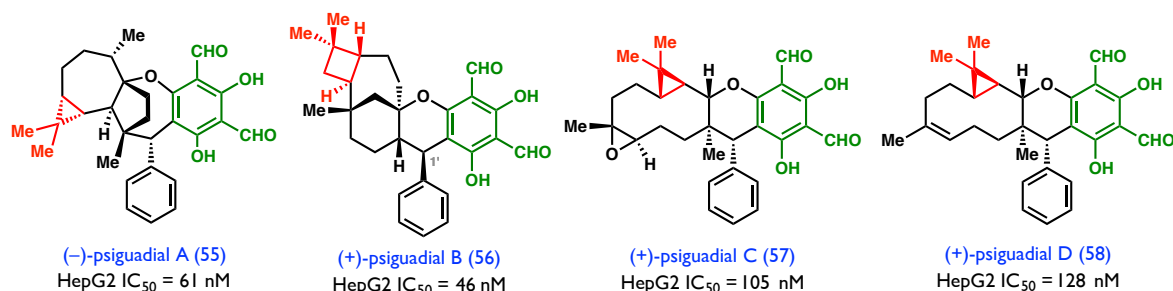


1.4 THE PSIGUADIAL FAMILY OF NATURAL PRODUCTS

1.4.1 Isolation of Psiguadials A–D

In 2010, Shao and coworkers reported the discovery of psiguadials A (**55**) and B (**56**), two new phloroglucinol meroterpenoids (Figure 1.3)³⁶ isolated from the leaves of *Psidium guajava*, a plant that has been used in traditional Chinese medicine for centuries to treat a variety of ailments, including diabetes and hypertension.³⁷ Two years later, the same group disclosed additional members of this family, psiguadials C (**57**) and D (**58**).³⁸ From a structural standpoint, the psiguadials are characterized by a polycyclic terpene unit featuring a 3- or 4- membered ring, which is fused to a diformyl phloroglucinol arene through a cyclic ether bearing a phenyl substituent at C1'.

Figure 1.3. Structures and biological activity of psiguadials A–D

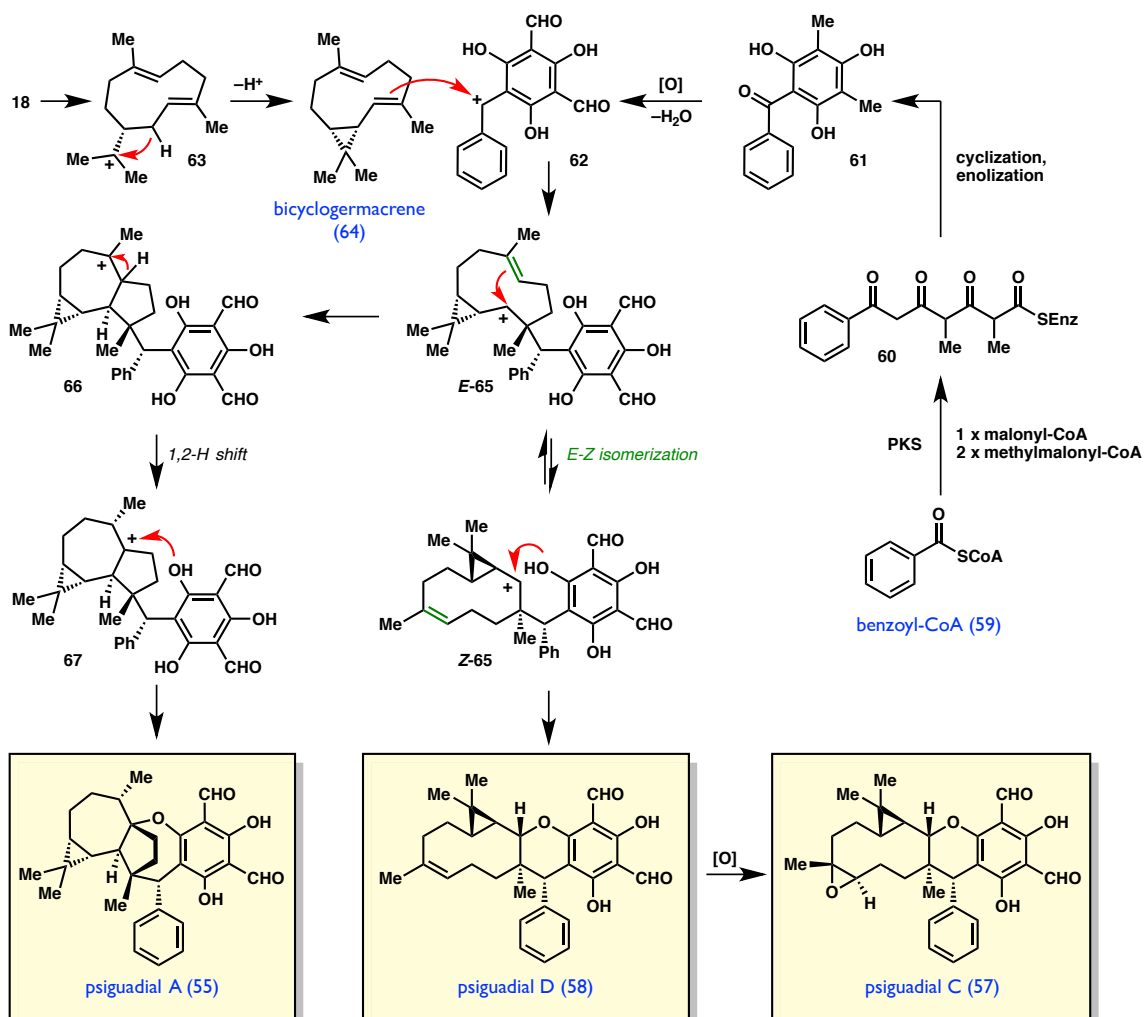


Biological investigations using an *in vitro* colorimetric MTT assay revealed that **55–58** exhibit strong anti-proliferative activity against a human hepatoma cancer cell line (HepG2), with (+)-psiguadial B (**56**) being the most potent anti-tumor agent in its class (IC₅₀ = 46 nM). While its biological target remains unknown at this time, **56** holds promise as a tool compound that could be useful for elucidating a potentially novel mechanism-of-action, which may benefit the development of new therapeutic agents in the ongoing fight against cancer.

In addition to its biological significance, **56** is also notable as the only member of the psiguadial family to possess a *trans*-cyclobutane ring, which is fused to a bridging 7-6 strained polycyclic terpene that includes an all-carbon quaternary center at C1. Coupled with the presence of six stereogenic centers throughout the molecule, we became interested in pursuing a total synthesis of **56** to address the synthetic challenges presented by these unique structural features. While we ultimately sought to develop a novel synthetic strategy toward *trans*-cyclobutane containing natural products, it is instructive to consider nature's unified approach toward construction of the psiguadial family.

1.4.2 Proposed Biosynthesis of the *Psiguadial* Family

In their isolation report of psiguadials C and D, Shao et al. provided an extensive and detailed proposal for the biosynthetic origins of the broader natural product family.³⁸ Beginning with benzoyl-CoA (**59**), a plausible series of condensation, cyclization, and enolization events result in the formation of **61**,^{4,39} a compound that has also been extracted from *Psidium guajava* previously (Scheme 1.7). Oxidation and loss of water from a protonated species results in benzylic cation **62**. This highly electrophilic species can engage one of the two olefins in the bicyclogermacrene (**64**), a terpene that like β -caryophyllene, is also derived from farnesyl pyrophosphate (**18**). Reaction between **64** and **62** produces cyclopropylcarbinyl cation *E*-**65**, which triggers either of two cationic cyclization pathways; C-C bond formation forges the 7-5 ring system that leads to **55**, while **58** arises by isomerization of the olefin, followed by trapping of carbocation in *Z*-**65** with the pendant phenol. Finally, **57** may be produced by oxidation of the trisubstituted olefin in **58**.

Scheme 1.7. Proposed biosynthesis of psguadials A, C, and D

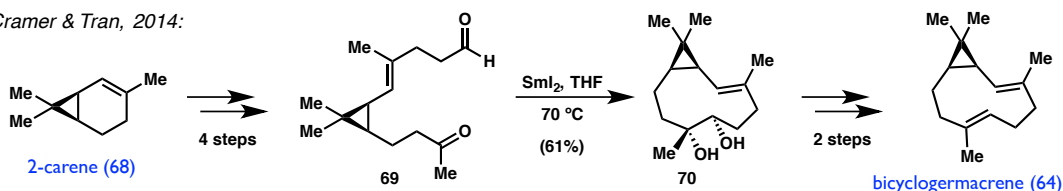
Support for the proposed biosynthetic origins of psguadials A, C, and D is evident in Cramer and Tran's recently reported synthesis of bicyclogermacrene (64), which proceeds in 7 steps from the readily available terpene, 2-carene (68, Scheme 1.8a).⁴⁰ Oxidative cleavage of the olefin in 68 and homologation to dialdehyde 69 allowed for a key SmI_2 -mediated reductive cyclization to form the 10-membered ring in 70 with complete diastereoselectivity. This diol was then advanced to 64 in 2 steps,

employing a modified Corey–Winter protocol⁴¹ for installation of the trisubstituted olefin with the requisite *E*-configuration.

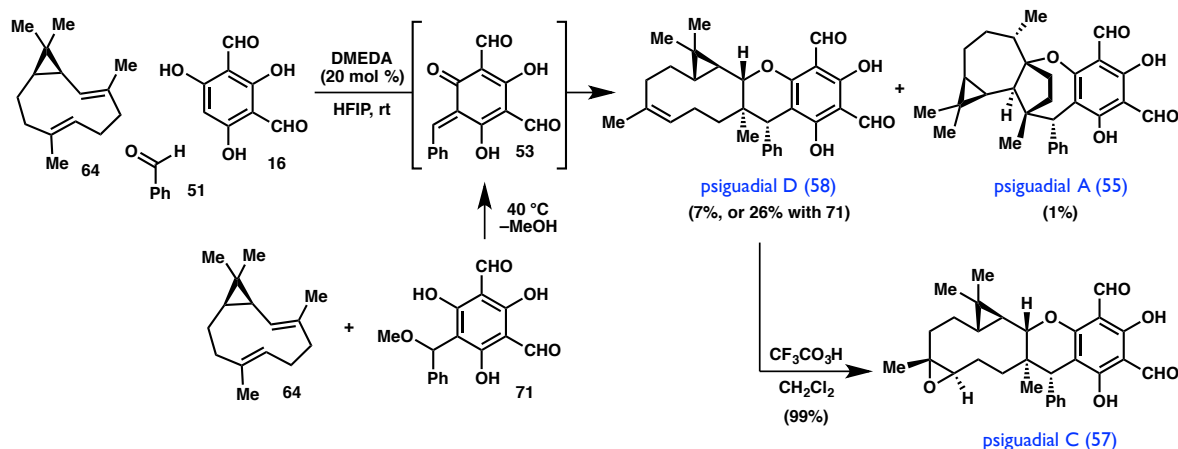
With **64** in hand, the authors validate the notion that this terpene is indeed a plausible biosynthetic precursor to **55**, **57**, and **58** by applying Lee’s strategy to access **53** *in situ*, which engages with **64** according to Shao’s proposal (Scheme 1.8b).³⁸ However, **64** proved quite sensitive under Lee’s previously established thermal reaction conditions, leading to the development of a milder protocol to effect the biomimetic cationic cascade cyclization, which provided **58** and **55** in a modest 7% and 1% yield, respectively. Alternatively, it was found that reaction with a more reactive *o*-QM precursor (**71**) allowed psguadial D (**58**) to be isolated in an improved 26% yield. Psguadial C (**57**) was then obtained by epoxidation of **58** using trifluoroacetic acid in near quantitative yield.

Scheme 1.8. Cramer’s biomimetic synthesis of psguadials A, C, and D

a) Cramer & Tran, 2014:



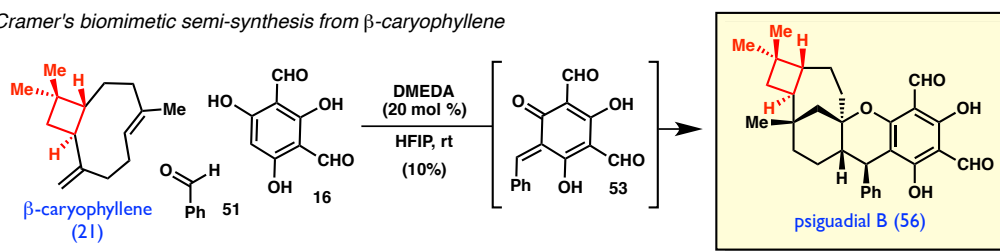
b) Biomimetic synthesis of psguadials A, C, and D



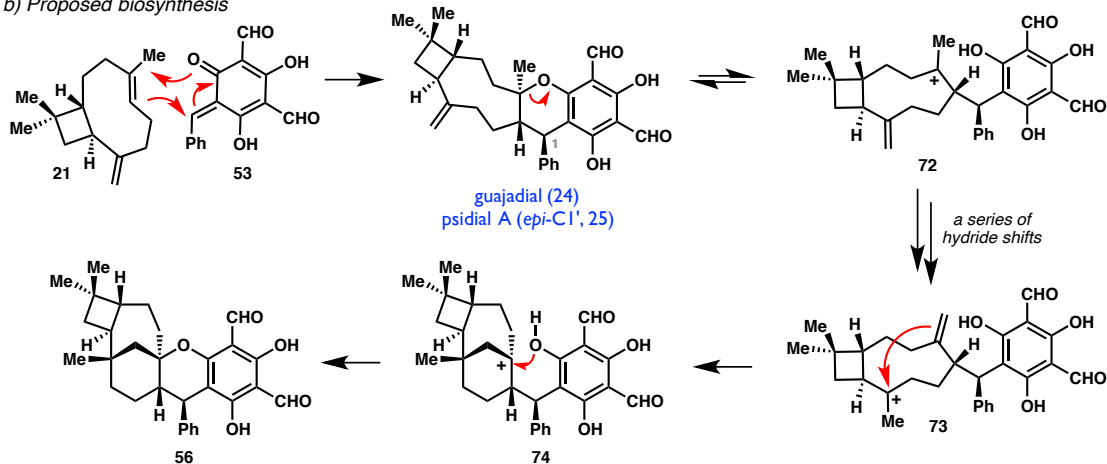
In the same year, an analogous semi-synthesis of psiguadial B (**56**) appeared in the author's thesis,⁴² utilizing the same reaction conditions with β -caryophyllene (**21**) in place of **64** to furnish the natural product in 10% yield (Scheme 1.9a). As with their published biomimetic syntheses of the other members of the psiguadial family, this study lends support for Shao's biosynthetic proposal (Scheme 1.9b),³⁸ which is initiated by ring-opening of the related natural products, guajadial (**24**)^{37a} and psidial A⁴³ (**25**). The resulting carbocation **72** can isomerize to **73** through a series of hydride shifts, and suffer transannular attack by the *exo*-olefin to generate bridgehead cation **74**. As demonstrated by Seigel (see Scheme 1.5), this species can then be trapped by the pendant phenol to form the central pyran ring and furnish **56**.

Scheme 1.9. Cramer's biomimetic semi-synthesis of psiguadial B

a) Cramer's biomimetic semi-synthesis from β -caryophyllene

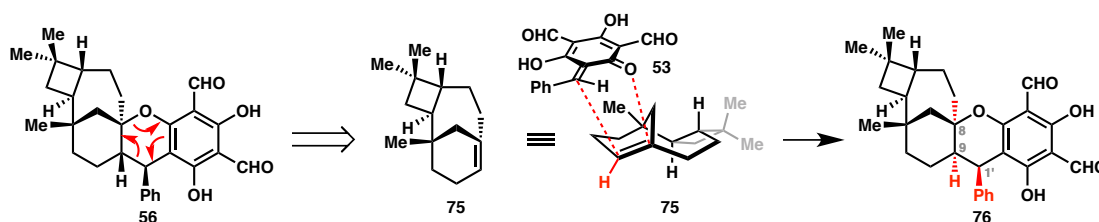


b) Proposed biosynthesis



It is interesting to note that this cationic cascade cyclization stands in contrast to a hypothetical, concerted hetero-Diels–Alder cycloaddition with **53** from the convex face of anti-Bredt olefin **75**⁴⁴ (Figure 1.4). If such a reaction were possible, it would be expected to provide the corresponding product **76** with the *incorrect* relative stereochemistry between C8, C9, and C1'. Thus, the three-dimensional profile of the natural product also provides some evidence for the cationic pathway outlined above.

Figure 1.4. Hypothetical “biomimetic” concerted hetero-Diels–Alder cycloaddition



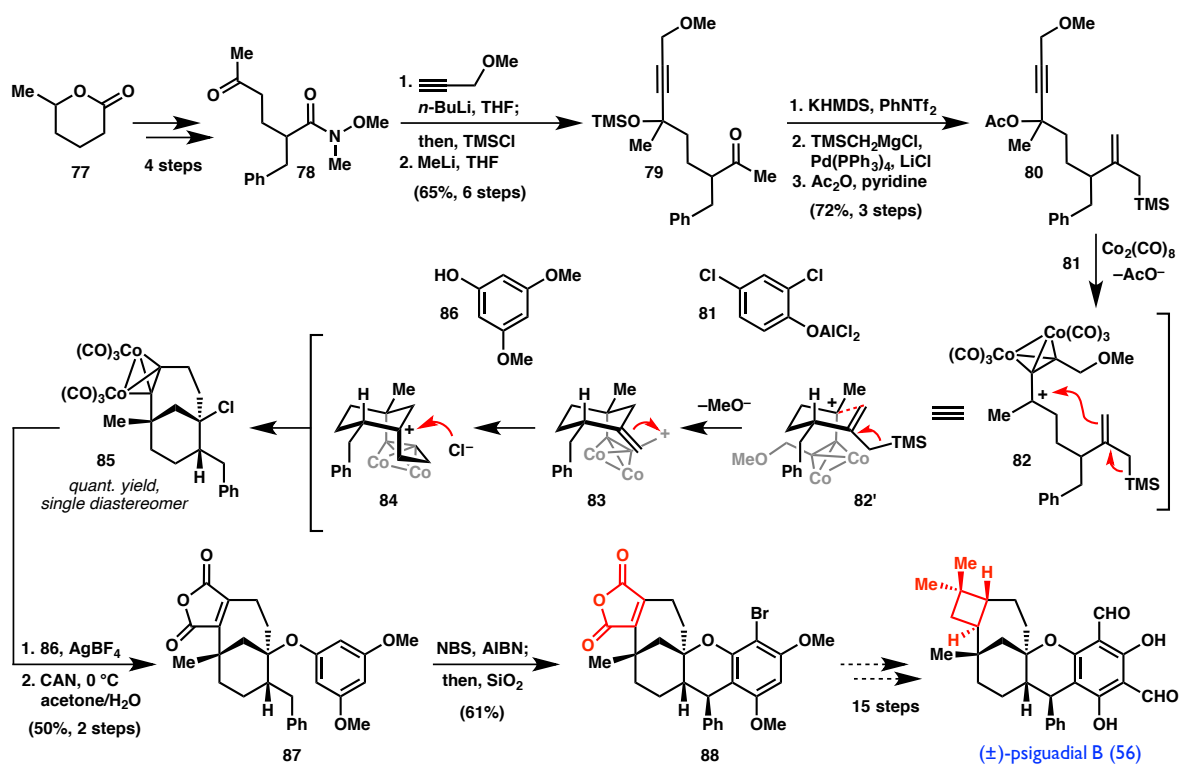
1.4.3 Total Synthesis Efforts Toward *Psiguadial B*

In February of 2017, Tanino and coworkers disclosed their progress toward a total synthesis of (±)-**56** (Scheme 1.10).⁴⁵ Beginning with commercially available lactone **77**, a 4-step protocol provided ketone **78**, which allowed facile installation of a key methoxymethyl alkyne via 1,2-addition. Treatment of the resulting Weinreb amide with MeLi afforded methyl ketone **79**, which provided a handle at C1' for conversion to allyl silane **80** through formation of the corresponding vinyl triflate and Pd-catalyzed coupling with (trimethylsilyl)methylmagnesium chloride.

In a key cyclization event, the bridging 7-6 bicycle was constructed in a single step using the formal [5+2] cycloaddition method the authors had developed previously.⁴⁶ Complexation of the alkyne in **80** with Co₂(CO)₈ induces the neighboring acetate to

leave, thus generating tertiary carbocation **82**. This species underwent intramolecular cyclization with the pendant allyl silane through a chair-like transition state (i.e. **82'**). Cation **83** was then formed in the presence of Lewis acid **86** and attacked by the *exo*-olefin, thus establishing the 7-membered ring. The reaction cascade was terminated by trapping of bridgehead cation **84** with an equivalent of chloride released from **86** to furnish bicycle **85** in quantitative yield, as a single diastereomer.

Scheme 1.10. Tanino's progress toward a total synthesis of (\pm)-psiguadial B



Silver-promoted abstraction of the chloride in **85** allowed trapping with phenol **86**, and following oxidative decomplexation using CAN, furnished aryl ether **87**. Treatment of **87** with NBS in the presence of AIBN effected benzylic bromination at C1' and subsequent Friedel–Crafts cyclization with the electron-rich arene occurred spontaneously upon exposure to silica gel, affording **88** in 61% yield. With the entire core of the natural product secured, the authors conclude their report by stating that efforts to

convert the maleic anhydride in **88** into the *trans*-fused cyclobutane ring of **56** are currently ongoing.⁴⁷ To the best of our knowledge, the work reviewed herein constitutes the only synthetic studies toward psiguadial B.

1.5 NOTES AND REFERENCES

- (1) (a) David, B.; Wolfender, J. L.; Dias, D. A. *Phytochemistry Reviews* **2015**, *14*, 299. (b) Dias, D. A.; Urban, S.; Roessner, U. *Metabolites* **2012**, *2*, 303.
- (2) Newman, D. J.; Cragg, G. M. *J. Nat. Prod.* **2016**, *79*, 629.
- (3) Beutler, J. A. *Curr. Protoc. Pharmacol.* **2009**, *46*, 9.11.1.
- (4) For the biosynthesis of phloroglucinol, see: (a) Achkar, J.; Xian, M.; Zhao, H.; Frost, J. W. *J. Am. Chem. Soc.* **2005**, *127*, 5332. For examples of polyketide synthases in phloroglucinol biosynthesis, see: (b) Yu, D.; Xu, F.; Zeng, J.; Zhan, J. *IUBMB Life* **2012**, *64*, 285.
- (5) Singh, I. P.; Sidana, J.; Bharate, S. B.; Foley, W. J. *Nat. Prod. Rep.* **2010**, *27*, 393.
- (6) (a) Ghisalberti, E. L. *Phytochemistry* **1996**, *41*, 7. (b) Wang, J.; Zhai, W.-Z.; Zou, Y.; Zhu, J.-J.; Xiong, J.; Zhao, Y.; Yang, G.-X.; Fan, H.; Hamann, M. T.; Xia, G.; Hu, J.-F. *Tetrahedron Lett.* **2012**, *53*, 2654. (c) Yang, X.-W.; Guo, Q.-M.; Wang, Y.; Xu, W.; Tian, L.; Tian, X.-J. *Bioorg. Med. Chem. Lett.* **2007**, *17*, 1107.
- (7) Wang, J.; Zhai, W.-Z.; Zou, Y.; Zhu, J.-J.; Xiong, J.; Zhao, Y.; Yang, G.-X.; Fan, H.; Hamann, M. T.; Xia, G.; Hu, J.-F. *Tetrahedron Lett.* **2012**, *53*, 2654.
- (8) Bharate, S. B.; Khan, S. I.; Tekwani, B. L.; Jacob, M.; Khan, I. A.; Singh, I. P. *Bioorg. Med. Chem.* **2008**, *16*, 1328.

- (9) Satoh, H.; Etoh, H.; Watanabe, N.; Kawagishi, H.; Arai, K.; Ina, K. *Chem. Lett.* **1992**, 21, 1917.
- (10) Nishizawa, M.; Emura, M.; Kan, Y.; Yamada, H.; Ogawa, K. *Tetrahedron Lett.* **1992**, 33, 2983.
- (11) (a) Roemer, E.; Grothe, T. *Plant extracts for use in brain modulation*. WO2008074420, 2008. (b) Zhu, J. J. L. *Analogues of phloroglucinols from eucalyptus plant varieties and related compounds and use for neurodegenerative disorders*. GB2465228, 2010. (c) Fiorini-Puybaret, C.; Joulia, P. 5-[1'-(decahydro-7-hydroxy-1,1,3A,7-tetramethyl-1H-cyclopropa[A]naphthalen-4-yl)-3'-methylbutyl]-2,4,6-trihydroxy-1,3-benzenedicarboxaldehyde used as drugs. WO2009106769, 2009.
- (12) (a) Tang, G.-H.; Dong, Z.; Guo, Y.-Q.; Cheng, Z.-B.; Zhou, C.-J.; Yin, S. *Sci. Rep.* **2017**, 7, 1952. Qin, X.-J.; Yan, H.; Ni, W.; Yu, M.-Y.; Khan, A.; Liu, H.; Zhang, H.-X.; He, L.; Hao, X.-J.; Di, Y.-T.; Liu, H.-Y. *Sci. Rep.* **2016**, 6, 1726. (b) Shang, Z.-C.; Yang, M.-H.; Liu, R.-H.; Wang, X.-B.; Kong, L.-Y. *Sci. Rep.* **2016**, 6, 2983.
- (13) For a review, see: Willis, N. J.; Bray, C. D. *Chem. Eur. J.* **2012**, 18, 9160. For a more extensive discussion of *o*-QM-hetero-Diels–Alder reactivity, see Chapter 2.
- (14) (a) Chiba, K.; Sonoyama, J.; Tada M. *J. Chem. Soc., Perkin Trans. 1*, **1996**, 1435. (b) Chiba, K.; Arakawa, T.; Tada, M. *Chem. Commun.* **1996**, 1763.
- (15) Tatsuta, K.; Tamura, T.; Mase, T. *Tetrahedron Lett.* **1999**, 40, 1925.
- (16) (a) Bharate, S. B; Singh, I. P. *Tetrahedron Lett.* **2006**, 47, 7021. (b) Bharate, S.

- B.; Bhutani, K. K.; Khan, S. I.; Tekwani, B. L.; Jacob, M. R.; Khan, I. A.; Singh, I. P. *Bioorg. Med. Chem.* **2006**, *14*, 1750. (c) Bharate, S. B.; Khan, S. I.; Tekwani, B. L.; Jacob, M.; Khan, I. A.; Singh, I. P. *Bioorg. Med. Chem.* **2008**, *16*, 1328.
- (17) (a) Dembitsky, V. M. *J. Nat. Med.* **2007**, *62*, 1. (b) Dembitsky, V. M. *Phytomedicine* **2014**, *21*, 1559. (c) Sergeiko, A.; Poroikov, V. V.; Hanus, L. O.; Dembitsky, V. M. *Open Med. Chem. J.* **2008**, *2*, 26.
- (18) Fitjer, L.; Malich, A.; Paschke, C.; Kluge, S.; Gerke, R.; Rissom, B.; Weiser, J.; Noltemeyer, M. *J. Am. Chem. Soc.* **1995**, *117*, 9180, and references cited therein.
- (19) (a) Dehal, S. S.; Croteau, R. *Arch. Biochem. Biophys.* **1988**, *261*, 346. (b) Cai, Y.; Jia, J.-W.; Crock, J.; Lin, Z.-X.; Chen, X.-Y.; Croteau, R. *Phytochemistry* **2002**, *61*, 523.
- (20) For a representative example, see: Hong, A. Y.; Stoltz, B. M. *Angew. Chem. Int. Ed.* **2014**, *53*, 5248.
- (21) For **22–25**, *vide infra*. For isolation of **26–29**, see: (a) Zhang, Y.-L.; Chen, C.; Wang, X.-B.; Wu, L.; Yang, M.-H.; Luo, J.; Zhang, C.; Sun, H.-B.; Luo, J.-G.; Kong, L.-Y. *Org. Lett.* **2016**, *18*, 4068. (b) Anderson, J. R.; Edwards, R. L.; Poyser, J. P.; Whalley, A. J. S. *J. Chem. Soc., Perkin Trans. 1* **1988**, *4*, 823. (c) Green, D.; Carmely, S.; Benayahu, Y.; Kashman, Y. *Tetrahedron Lett.* **1988**, *29*, 1605. (d) Qi, Q.-Y.; Ren, J.-W.; Sun, L.-W.; He, L.-W.; Bao, L.; Yue, W.; Sun, Q.-M.; Yao, Y.-J.; Yin, W.-B.; Liu, H.-W. *Org. Lett.* **2015**, *17*, 3098.
- (22) (a) Corey, E. J.; Mitra, R. B.; Uda, H. *J. Am. Chem. Soc.* **1963**, *85*, 362. (b) Corey, E. J.; Mitra, R. B.; Uda, H. *J. Am. Chem. Soc.* **1964**, *86*, 485. (c) For the first

- enantioselective total synthesis of **21**, see: Larionov, O. V.; Corey, E. J. *J. Am. Chem. Soc.* **2008**, *130*, 2954.
- (23) Subsequent mechanistic studies suggest that this [2+2] cycloaddition occurs stepwise via the intermediacy of diradical species produced by photoexcitation of 2-cyclohexenone: Corey, E. J.; Bass, J. D.; LeMahieu, R.; Mitra, R. B. *J. Am. Chem. Soc.* **1964**, *86*, 5570.
- (24) Ohtsuka, Y.; Niitsuma, S.; Tadokoro, H.; Hayashi, T.; Oishi, T. *J. Org. Chem.* **1984**, *49*, 2326.
- (25) Brannock, K. C.; Burpitt, R. D.; Goodlett, V. W. *J. Org. Chem.* **1964**, *29*, 801.
- (26) (a) Paquette, L. A.; Sugimura, T. *J. Am. Chem. Soc.* **1986**, *108*, 3841. (b) Sugimura, T.; Paquette, L. A. *J. Am. Chem. Soc.* **1987**, *109*, 3017.
- (27) Hajos, Z. G.; Parrish, D. R. *Org. Synth.* **1984**, *63*, 26.
- (28) (a) N. C. Yang, D.-D. H. Yang, *J. Am. Chem. Soc.* **1958**, *80*, 2913. (b) For a recent review, see: Chen, C. *Org. Biomol. Chem.* **2016**, *14*, 8641.
- (29) Fleming, I.; Kemp-Jones, A. V.; Long, W. E.; Thomas, E. J. *J. Chem. Soc., Perkin Trans. 2* **1976**, *1*, 7.
- (30) Fukuyama, Y.; Otsu, Y.; Miyoshi, K.; Nakamura, K.; Kodama, M.; Nagasawa, M.; Hasegawa, T.; Okazaki, H.; Sugawara, M. *Tetrahedron* **1992**, *48*, 377.
- (31) Du, R. *Trop. J. Pharm. Res.* **2015**, *14*, 1713.
- (32) Cheng, X.; Harzdorf, N. L.; Shaw, T.; Siegel, D. *Org. Lett.* **2010**, *12*, 1304.
- (33) The authors in reference 32 also describe an alternative 6-step protocol from **49** that proceeds in slightly higher overall yield (19%).
- (34) Lawrence, A. L.; Adlington, R. M.; Baldwin, J. E.; Lee, V.; Kershaw, J. A.;

- Thompson, A. L. *Org. Lett.* **2010**, *12*, 1676.
- (35) Collado, I. G.; Hanson, J. R.; Maicas-Sánchez, A. J. *Nat. Prod. Rep.* **1998**, *15*, 187, and references cited therein.
- (36) Shao, M.; Wang, Y.; Liu, Z.; Zhang, D.-M.; Cao, H.-H.; Jiang, R.-W.; Fan, C.-L.; Zhang, X.-Q.; Chen, H.-R.; Yao, X.-S.; Ye, W.-C. *Org. Lett.* **2010**, *12*, 5040.
- (37) (a) Yang, X.-L.; Hsieh, K.-L.; Liu, J.-K. *Org. Lett.* **2007**, *9*, 5135, and references cited therein. (b) Díaz-de-Cerio, E.; Verardo, V.; Gómez-Caravaca, A.; Fernández-Gutiérrez, A.; Segura-Carretero, A. *Int. J. Mol. Sci.* **2017**, *18* (4), 897. (c) Lin, J.; Puckree, T.; Mvelase, T. P. *J. Ethnopharmacol.* **2002**, *79*, 53.
- (38) Shao, M.; Wang, Y.; Jian, Y.-Q.; Huang, X.-J.; Zhang, D.-M.; Tang, Q.-F.; Jiang, R.-W.; Sun, X.-G.; Lv, Z.-P.; Zhang, X.-Q.; Ye, W.-C. *Org. Lett.* **2012**, *14*, 5262.
- (39) Moussa, G. E. *Acta Chem. Scand.* **1968**, *22*, 3319.
- (40) Tran, D. N.; Cramer, N. *Chem. Eur. J.* **2014**, *20*, 10654.
- (41) (a) Corey, E. J.; Winter, R. A. E. *J. Am. Chem. Soc.* **1963**, *85*, 2677. (b) Corey, E. J.; Hopkins, B. *Tetrahedron Lett.* **1982**, *23*, 1979.
- (42) Tran, D. N. *Rhodium-Catalyzed Imine-Directed C-H Bond Activation and Biomimetic Synthesis of Sesquiterpenoids*. PhD Thesis, ETH Zürich **2014**.
- (43) Fu, H.-Z.; Luo, Y.-M.; Li, C.-J.; Yang, J.-Z.; Zhang, D.-M. *Org. Lett.* **2010**, *12*, 656.
- (44) Bridgehead olefin **75** is reportedly accessible from **21**: (a) Khomenko, T. M.; Korchagina, D. V.; Gatilov, Y. V.; Bagryanskaya, I. Y.; Tkachev, A. V.; Vyalkov, A. I.; Kun, O. B.; Salenko, V. L.; Dubovenko, Z. V.; Barkash, V. A. *Zh. Org. Khim.* **1990**, *26*, 2129.; Khomenko, T. M.; Korchagina, D. V.; Gatilov, Y. V.;

- Bagryanskaya, I. Y.; Tkachev, A. V.; Vyalkov, A. I.; Kun, O. B.; Salenko, V. L.; Dubovenko, Z. V.; Barkash, V. A. *Russ. J. Org. Chem. (English Translation)* **1990**, *26*, 1839. (b) See also: Khomenko, T. M.; Bagryanskaya, I. Y.; Gatilov, Y. V.; Korchagina, D. V.; Gatilova, V. P.; Dubovenko, Z. V.; Barkhash, V. A. *Zh. Org. Khim.* **1985**, *21*, 677.; Khomenko, T. M.; Bagryanskaya, I. Y.; Gatilov, Y. V.; Korchagina, D. V.; Gatilova, V. P.; Dubovenko, Z. V.; Barkhash, V. A. *Russ. J. Org. Chem. (English Translation)* **1985**, *21*, 614.
- (45) Kinebuchi, M.; Uematsu, R.; Tanino, K. *Tetrahedron Lett.* **2017**, *58*, 1382.
- (46) Kudo, M.; Kondo, F.; Maekawa, H.; Shimizu, T.; Miyashita, M.; Tanino, K. *Tetrahedron Lett.* **2014**, *55*, 1192. For a closely related, seminal example of cobalt-mediated cyclization in total synthesis, see: Jamison, T. F.; Shambayati, S.; Crowe, W. E.; Schreiber, S. L. *J. Am. Chem. Soc.* **1994**, *116*, 5505.
- (47) A document detailing the synthetic strategy in reference 45 was released in association with a symposium that suggests an undisclosed 15-step sequence to reach **56** from **88**. See: Tanino, K. et al. *Symposium Papers of 56th Symposium on the Chemistry of Natural Products*, Kochi, Japan, October 15-17, 2014, 133-137. Available from: http://www.pharm.tohoku.ac.jp/~gousei/synthetic/mondai/zemi-toi/zemitoi_2014-15/zemi_toi_M2-D_2014-15/toi%2020141115.pdf (accessed March 27th, 2017).

Chapter 2

First Generation Synthetic Strategy Toward (+)-Psiguadial B and Development of a Catalytic, Asymmetric Wolff Rearrangement[†]

2.1 INTRODUCTION

Owing to the diverse and intriguing bioactive properties of diformyl phloroglucinol natural products, we became interested in pursuing (+)-psiguadial B (**56**) as a target for total synthesis. As discussed in Chapter 1, biomimetic approaches to phloroglucinol meroterpenoids are well precedented, and often provide direct access to β -caryophyllene-derived natural products.¹ However, we recognized that an abiotic synthesis of **56** would allow us to develop new chemistry and strategy concepts that we hoped would be useful in broader synthetic contexts. We began by focusing on the design of a *de novo* approach to construct the *trans*-fused cyclobutane in **56**—a task for which a

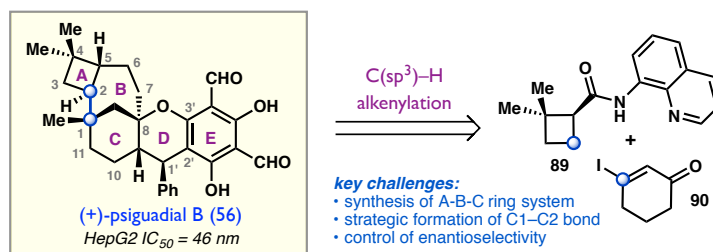
[†] Portions of this chapter were adapted from the following communication: Chapman, L. M.; Beck, J. C.; Wu, L.; Reisman, S. E. *J. Am. Chem. Soc.* **2016**, *138*, 9803, DOI: 10.1021/jacs.6b07229, copyright 2016 American Chemical Society. The research discussed in this chapter was completed in collaboration with Jordan C. Beck, a graduate student in the Reisman Lab.

practical solution was not readily apparent, particularly in the context of asymmetric catalysis.

2.1.1 C(sp³)–H Activation: A Guiding Strategic Bond Disconnection

From a synthetic standpoint, we reasoned that the primary challenge posed by **56** is construction of the central bicyclo[4.3.1]decane, which is *trans*-fused to a cyclobutane. Specifically, we identified the C1–C2 bond, which links the A and C rings through vicinal stereogenic centers, as a strategic disconnection (Figure 2.1). On the basis of this analysis, we became interested in forming this bond by a Pd-catalyzed C(sp³)–H alkenylation reaction between cyclobutane **89** and vinyl iodide **90**. Although the direct product of this reaction would be a *cis*-cyclobutane, we envisioned accessing the thermodynamically more stable *trans*-cyclobutane through an epimerization process.

Figure 2.1. Identification of a guiding strategic bond disconnection

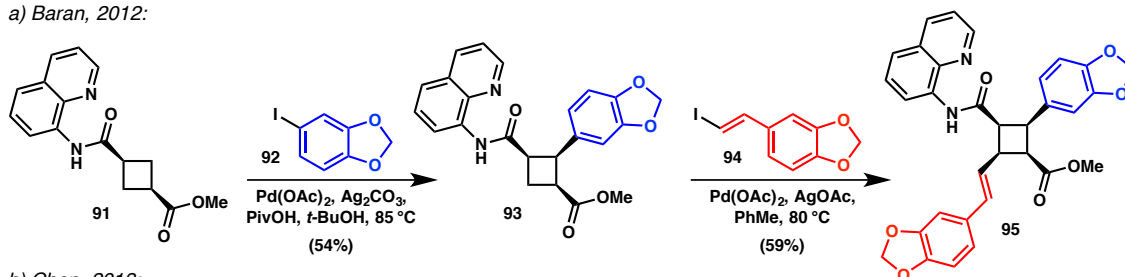


At the outset of our studies, C(sp³)–H functionalization using 8-aminoquinoline as an auxiliary was well established² and elegantly demonstrated as a powerful strategy in the context of total synthesis.³ In particular, we were encouraged by two key reports^{3a,b} that showcased cyclobutanes as suitable substrates for this chemistry. In 2012, Baran subjected cyclobutamide **91** to sequential C(sp³)–H arylation and alkenylation reactions to obtain fully *cis*-substituted cyclobutane **95** *en route* to pipericyclobutanamide A

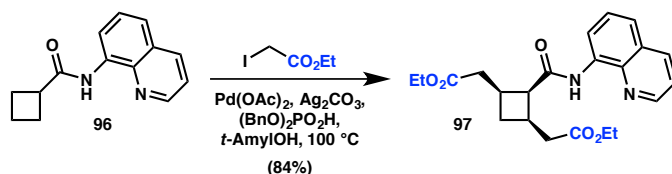
(Scheme 2.1a). While this example lent credence to our proposed C(sp³)-H alkenylation reaction, there was some uncertainty about whether the proximal methyl C-H bonds in **89** would intervene unproductively. Concurrent with our own efforts, Chen and coworkers described a general C(sp³)-H alkylation reaction,⁴ including an example of a simple cyclobutane substrate (**96**, Scheme 2.1b). More recently, Yu has applied a distinct amide-based directing group in combination with chiral ligand **100** to access enantioenriched arylated cyclobutanes (Scheme 2.1c).⁵ These studies highlight the general utility of this substrate class in C(sp³)-H activation chemistry.

Scheme 2.1. Relevant C(sp³)-H functionalizations of cyclobutane substrates

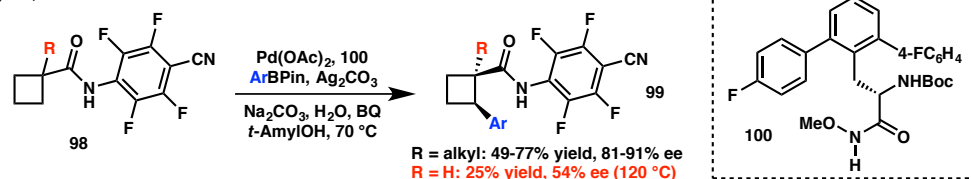
a) Baran, 2012:



b) Chen, 2013:



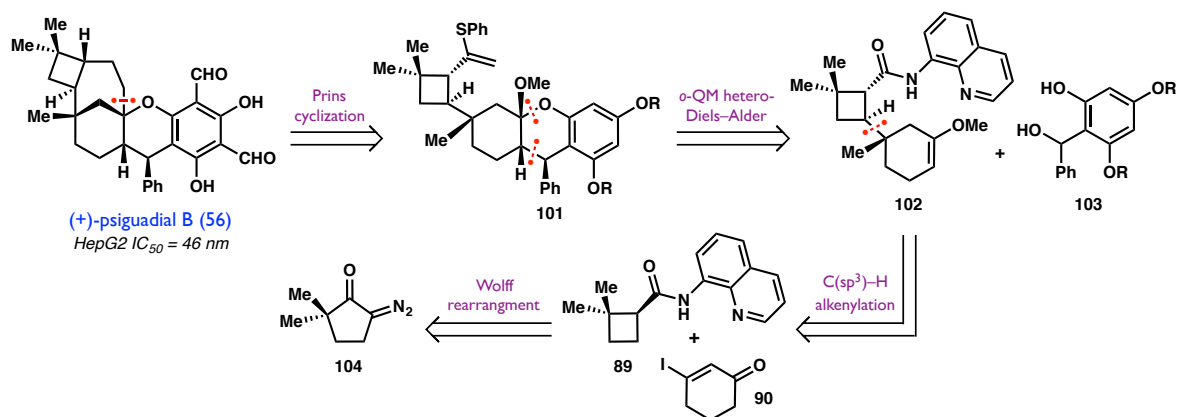
c) Yu, 2014:



2.1.2 Retrosynthetic Analysis: Precedent and Anticipated Challenges

Mapping this strategic bond construction onto a more complete retrosynthesis of (+)-psiguadial B (**56**), we planned to construct the 7-membered ring at a late stage in the synthesis via intramolecular Prins cyclization of a pendant vinyl sulfide onto an oxocarbenium ion derived from cyclic ketal **101** (Figure 2.2). Although ring closure to form this strained system was expected to be challenging, the Prins reaction has been successfully used for the preparation of complex, polycyclic ring systems.

Figure 2.2. Retrosynthetic analysis

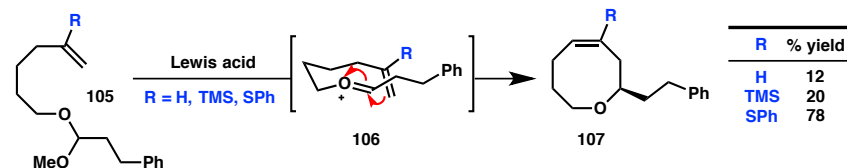


In 1990, Overman showed that medium-size cyclic ethers could be readily prepared via Lewis acid-promoted intramolecular cyclization of mixed acetals with tethered olefins (Scheme 2.2a).⁶ Later reports by Maier⁷ and Mascareñas⁸ were particularly encouraging, as they demonstrated that cyclic oxocarbenium ions⁹ could undergo intramolecular attack by activated olefins (e.g. **108** and **110**, Scheme 2.2b, c) to form bridging, 7-membered bicycles, similar to the system we hoped to build.

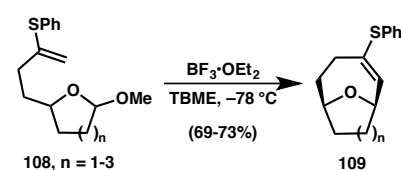
This first disconnection allowed simplification to a tricyclic core scaffold (**101**) that we imagined could be assembled in a convergent manner by employing an *ortho*-quinone methide hetero-Diels-Alder (*o*-QMhDA) reaction. Thermolysis of a suitably

Scheme 2.2. Examples of Prins cyclizations to form medium-sized rings

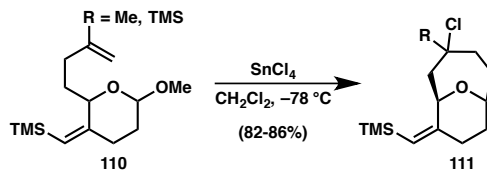
a) Overman et al., 1990:



b) Sasmal and Maier, 2002:



c) Mascareñas et al., 2005:

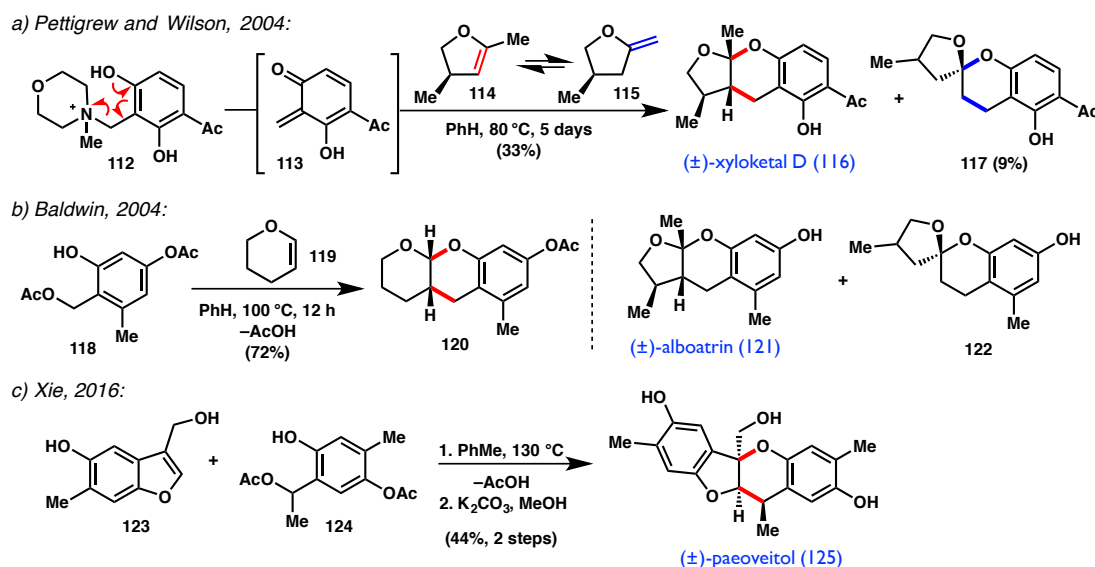


functionalized 2-hydroxybenzyl alcohol derivative (e.g. **103**) was expected to provide an *E*-configured *ortho*-quinone methide (*o*-QM) *in situ*,¹⁰ which was envisioned to undergo intermolecular [4 + 2] cycloaddition with a cyclic enol ether such as **102** to furnish the tricyclic chroman core of the natural product. While *o*-QMHTA reactions are widely used to construct similar bicyclic chroman frameworks,¹¹ the dieneophiles employed are typically limited to simple acyclic enol ethers or styrenes that are used in large excess to avoid side products resulting from *o*-QM dimerization. In contrast, our proposed strategy necessitated reaction with a more elaborate, cyclohexanone-derived enol ether that would be used as the limiting reagent.

Surprisingly few reports of endocyclic enol ethers participating in *o*-QMHTA reactions exist in the literature. In 2004, Wilson and coworkers described the first example of these substrates as competent hetero-dienophiles in their synthesis of (±)-xyloketal D (**116**, Scheme 2.3a).¹² Thermolytic extrusion of *N*-methyl morpholine from **112** provided *o*-QM **113**, which underwent cycloaddition with dihydrofuran **114** to provide **116** directly, albeit in low yield. Similar work by Baldwin showed that this transformation could also be accomplished using dihydropyran **119** in a single example

published alongside their synthesis of (\pm)-alboatrin (**121**), which utilized an analogous *o*-QMHDA strategy (Scheme 2.3b).¹³ Notably, both reactions required a three- to tenfold excess of the enol ether, and suffered from formation of unwanted spiroketal side products, **117** and **122**, which resulted from isomerization to exocyclic enol ether **115** under the reaction conditions. Recently, Xie and coworkers leveraged this same disconnection to prepare (\pm)-Paeoveitol (**125**) as a single diastereomer in just 2 steps from benzofuran **123**.¹⁴

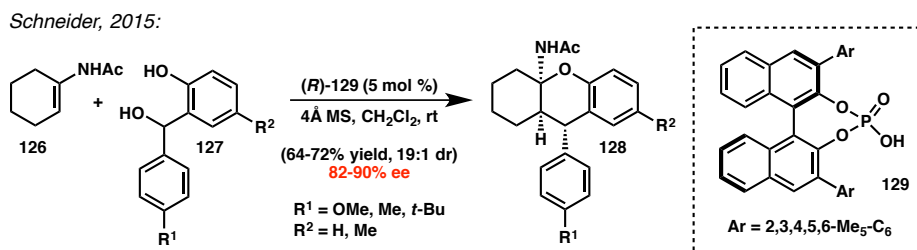
Scheme 2.3. *o*-QMHDA reactions with cyclic enol ethers in total synthesis



At the outset of our studies, we were unaware of any reported examples of *cyclohexanone-derived* enol ethers used as dienophiles in *o*-QMHDA cycloadditions. However, at the time of this writing, several examples have appeared in the literature that address the challenge of controlling facial selectivity in *o*-QMHDA reactions using simple, cyclic enamides such as **126** (Scheme 2.4).¹⁵ Schneider and coworkers leveraged the ability of BINOL-based phosphoric acid **129** to simultaneously form hydrogen bonds with **126** and the *o*-QM generated from **127**, which presumably leads to an organized

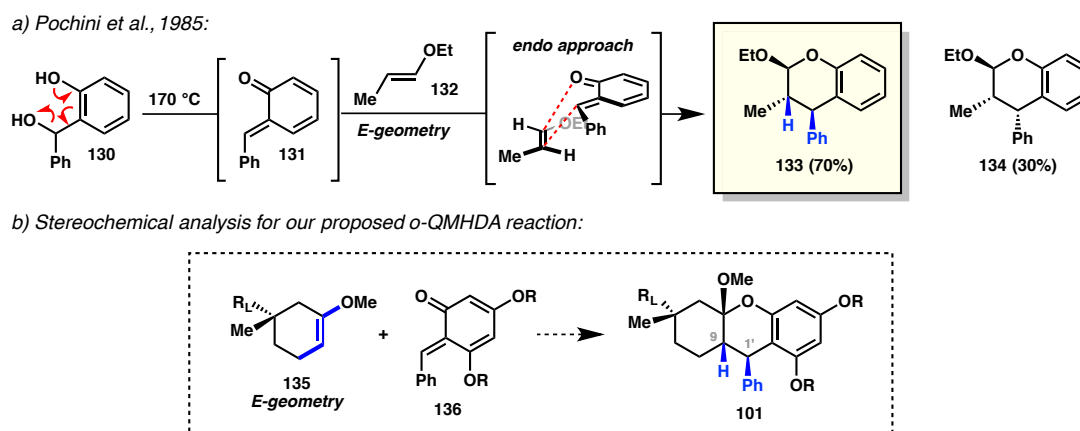
transition state that exerts high levels of enantiocontrol in formation of the corresponding cyclic *N,O*-acetal products **128**.

Scheme 2.4. Enantioselective *o*-QM enamide cycloaddition reaction



Although the feasibility of this reaction was uncertain at the time, we were hopeful that successful implementation of this strategy would serve to 1) quickly build complexity in a convergent sense, 2) provide a means to install a highly oxidized arene, and, 3) set two vicinal stereocenters in a single step. With respect to the relative stereochemistry between C9 and C1', Pochini has observed the diastereoselectivity we desired for elaboration to **101** with acyclic vinyl ethers, such as **132**, which were found to react with *E*-configured *o*-QM **131** through an *endo* transition state (Scheme 2.5a).¹⁰ Accordingly, it was expected that phenyl substitution of the proposed *o*-QM **136** would sterically enforce *E*-geometry, which upon reaction with *E*-enol ether **135** should deliver

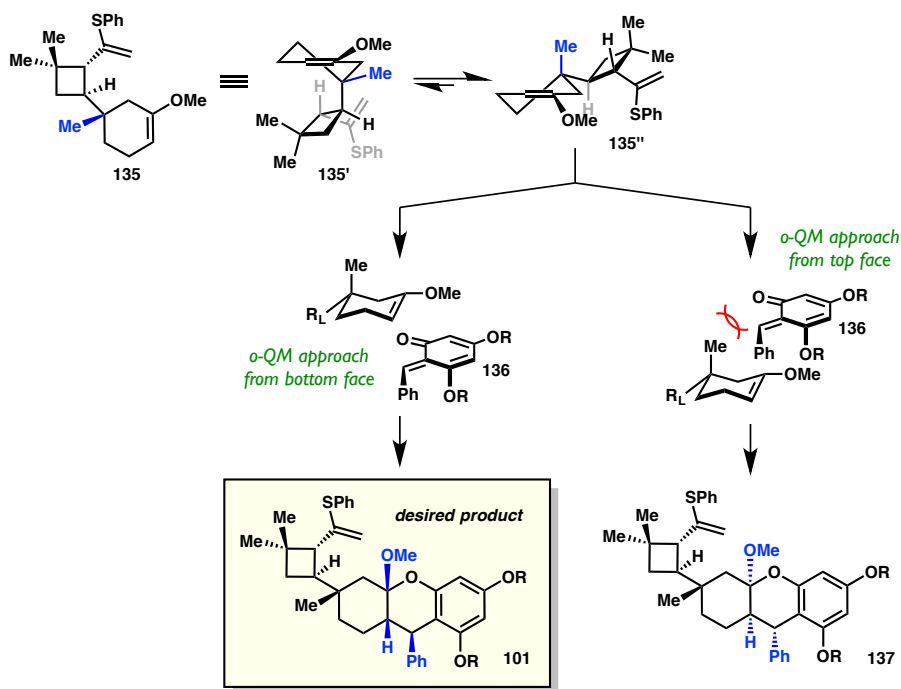
Scheme 2.5. Diastereoselectivity of *o*-QM HDA reactions with *E*-enol ethers



101 with the desired *anti* relationship of the adjacent protons (Scheme 2.5b).

With respect to the stereochemistry about C9 and C1' in an *absolute* sense, the proposed *o*-QMHA reaction could give rise to two possible *endo* diastereomers: **101** and **137** (Figure 2.3). Pettus has shown that chiral enol ethers may be used to achieve facial selectivity in substrate-controlled cycloadditions with *o*-QMs.¹⁶ Conformational analysis of the proposed substrate reveals that the large cyclobutane substituent should most likely occupy an equatorial position, resulting in twist-chair conformation **135''** in which the axial methyl could potentially block the top face. This suggested that the *o*-QM might prefer to approach from the bottom instead, leading to **101** with the stereochemical arrangement found in (+)-psiguadial B (**56**). However, we were cognizant of the fact that this “blocking” methyl group is relatively small and might not impose the steric influence that could be required for high levels of diastereoselectivity. Moreover, the methyl group

Figure 2.3. Analysis of facial selectivity of proposed *o*-QMHA cycloaddition



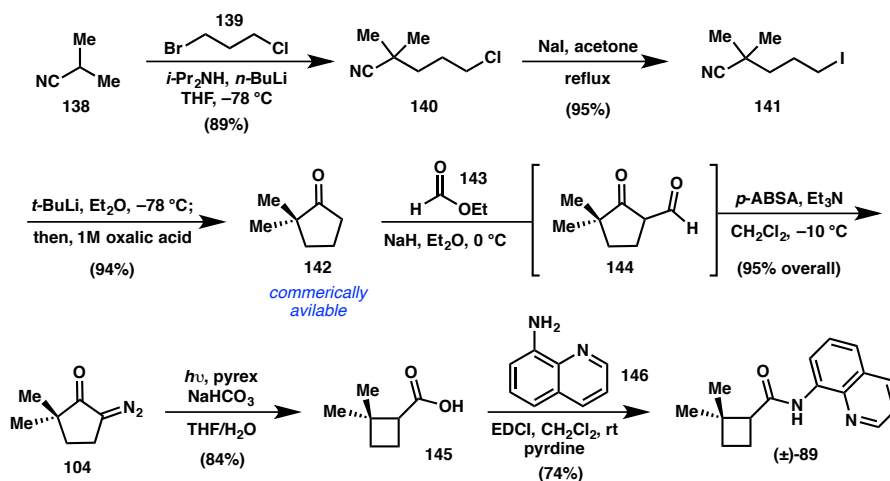
is situated further from the reaction center than in example substrates that exhibit good substrate diastereocontrol. Thus, it remained unclear whether the chiral information built into enol ether **135** would impart facial selectivity to give the desired *endo* diastereomer **101**. Nonetheless, we elected to pursue the development of this key reaction.

Continuing on with our retrosynthetic analysis, **102** was envisioned to be accessible in short order from the product of the directed C(sp³)-H alkenylation reaction, joining fragments **89** and **90**. In turn, we expected that cyclobutamide **89** could be easily prepared from known diazoketone **30** via photochemical Wolff rearrangement.¹⁷

2.2 FORWARD SYNTHETIC EFFORTS: RACEMIC STUDIES

Since our immediate objective was to evaluate the practicality of the C(sp³)-H alkenylation reaction, a straightforward synthesis of cyclobutamide **89** was first pursued as a racemate (Scheme 2.6). In the forward direction, the synthesis begins with an adaptation of a known route to access the expensive, yet commercially available 2,2-dimethylcyclopentanone (**142**).¹⁸ Alkylation of isobutyronitrile (**138**) with 1-bromo-3-

Scheme 2.6. Scalable, racemic route to access key cyclobutamide



chloropropane (**139**) and subsequent Finkelstein reaction proceeded smoothly to give alkyl iodide **141** in near quantitative yield. Next, lithium–halogen exchange, followed by cyclization and hydrolysis provided access to large quantities of **142**. Formylation then allowed for a Regitz-diazo transfer reaction, furnishing diazoketone **104** in excellent yield.¹⁷ Finally, photolytic ring contraction of **104** in the presence of aqueous base afforded cyclobutane carboxylic acid **145**, which was easily coupled with 8-aminoquinoline (**146**) under standard conditions to deliver (±)-**89** in good overall yield.

Upon subjection of **89** to reported Pd-catalyzed C(sp³)–H functionalization reaction conditions, we were pleased to detect a combined 42% yield of the desired coupling products **147** and **148** (Table 2.1, entry 1). A brief survey of reaction parameters revealed that increased concentration of pivalic acid shut down the desired reaction, whereas omission of this additive gave a single diastereomer (entries 2 and 3). While alternative bases led to lower overall conversions (entries 4 and 5), solvent choice proved critical, with the highest yields observed in TBME (entry 8). Although most reactions

Table 2.1. Optimization of the racemic C(sp³)–H alkenylation reaction

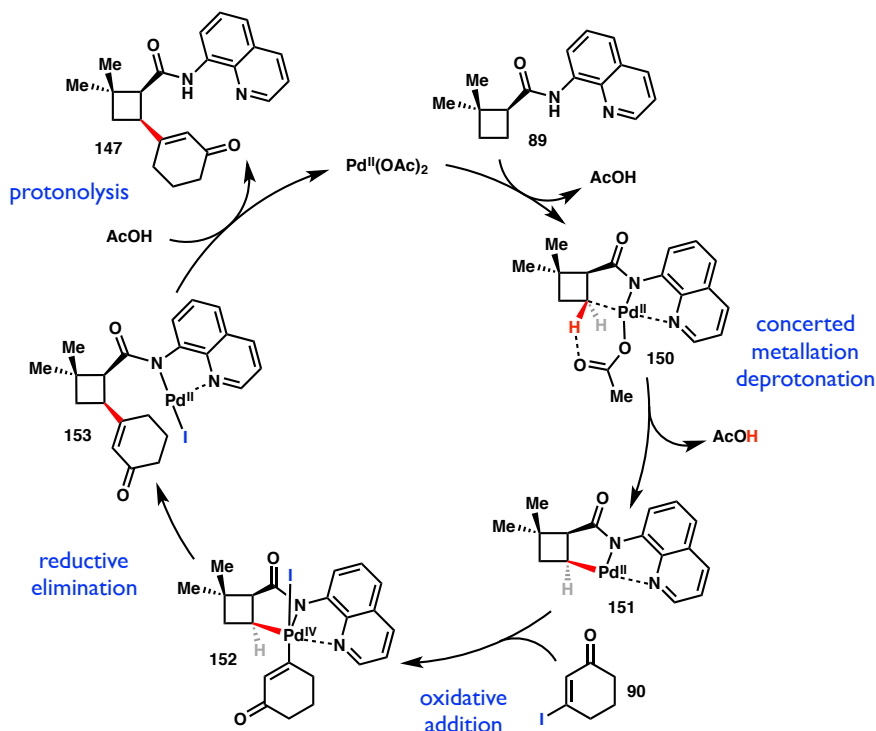
entry	solvent	base	equiv pivOH	% conv. ^a	% 147 (cis) ^a	% 148 (trans) ^a	% 149 (lactam) ^a	% bis ^a
1	<i>t</i> -BuOH	Ag ₂ CO ₃	1	100	32	10	44	12
2	<i>t</i> -BuOH	Ag ₂ CO ₃	3	100	7	0	19	18
3	<i>t</i> -BuOH	Ag ₂ CO ₃	–	92	22	0	57	2
4	<i>t</i> -BuOH	AgOAc	1	81	7	30	34	0
5	<i>t</i> -BuOH	Cs ₂ CO ₃	1	52	0	4	0	10
6	PhMe	Ag ₂ CO ₃	–	100	51	0	26	14
7	dioxane	Ag ₂ CO ₃	–	63	47	5	6	4
8	TBME	Ag ₂ CO ₃	–	91	71	11	4	0
9	DMF	Ag ₂ CO ₃	–	53	0	40	10	0

^a Conversion and relative product distribution determined by LC/MS.

favorable formation of the *cis* diastereomer **147**, interestingly *trans* **148** predominated under certain conditions (entries 4 and 9). Analysis by mass spectrometry also suggested the formation of a bis-olefinated side product¹⁹ and appreciable amounts of spirocyclic lactam **149**, which presumably arises via intramolecular aza-Michael addition of the corresponding imide (not shown) into the proximal enone.²⁰

Since the proposed mechanism of this transformation^{2a,4} proceeds through oxidative addition of **90** to a 5-membered palladacycle (**151**, Figure 2.4), it is expected that, following reductive elimination and protonolysis, the enone should be delivered from the same face as the aminoquinoline directing group. Thus, we reasoned that **148** must arise by epimerization of the initially formed *cis*-product (**147**), presumably facilitated by the presence of base and protic solvent. Since the *trans* relationship across the cyclobutane ring was ultimately required, reaction conditions were sought to effect

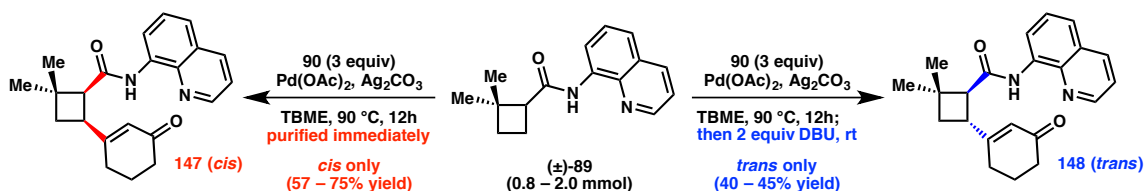
Figure 2.4. Proposed mechanism for the $C(sp^3)$ -H alkenylation reaction



complete *in situ* epimerization and allow the direct isolation of **148**.

Additional screening revealed that reactions run under identical conditions gave highly variable ratios of **147** to **148**, and upon scale-up, we were surprised to find that the product ratio switched almost entirely to favor **147**. This result led us to suspect that adventitious water could be playing a role in the epimerization; however, control experiments did not support this hypothesis.²¹ Next, DBU was added to the crude reaction mixture after the C(sp³)-H alkenylation had finished in an attempt to drive the epimerization to completion (Scheme 2.7). Over the course of our efforts to bring material through on larger scale, a general observation was made: if **147** were purified immediately, the yields were consistently higher than if **148** were isolated after treatment with DBU. In these cases, the yields were comparatively poor, but with much lower variance, only ranging from 40 to 45%.

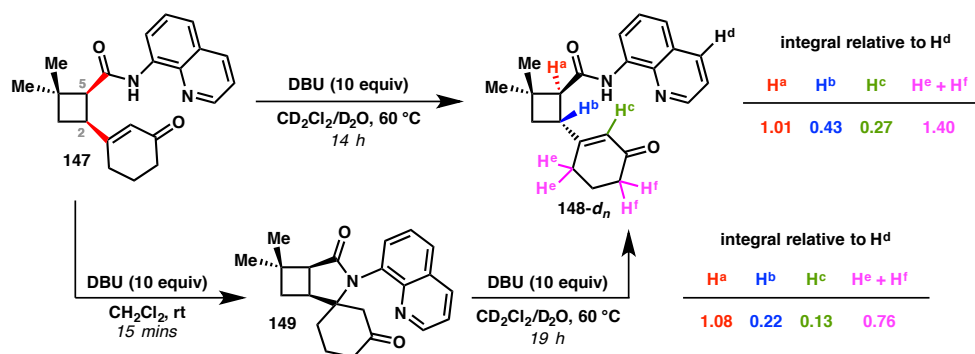
Scheme 2.7. Toward a one-pot C(sp³)-H alkenylation/epimerization process



Ultimately, it was discovered that treatment of pure **147** with DBU resulted in immediate and complete conversion to spirocyclic lactam **149** (Scheme 2.8). Resubjection of **149** to the same epimerization conditions confirmed that this intermediate slowly converts to the thermodynamically preferred *trans* diastereomer **148**, but never does so completely at room temperature. This accounts for the lower yields of **148** obtained when additional base was added *after* the coupling reaction. With these lessons learned, the workup and purification protocol was improved to afford **147** in

consistently high yields; further optimization efforts established that the epimerization was best accomplished by treating purified **147** with an excess of DBU in dichloromethane at 60 °C, which accelerated conversion to **148**.

Scheme 2.8. Determining the site of epimerization via deuteration experiments

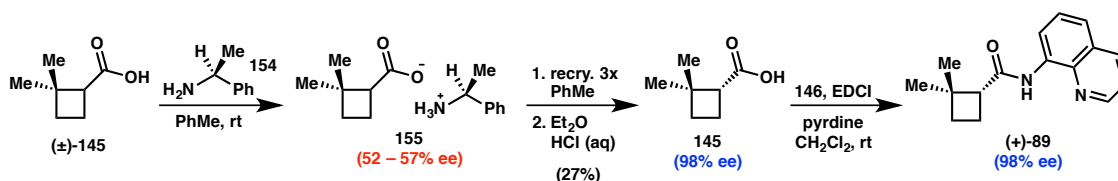


At this stage, it was unclear whether the formation of **148** was mediated by a true epimerization event at only one stereocenter, or in fact a complete racemization of both C2 and C5. To answer this critical question, deuterium-labeling studies were conducted in which **147** was subjected to the standard epimerization reaction conditions in CD₂Cl₂, doped with a small amount of D₂O. Analysis by ¹H NMR revealed diminished integrals for signals corresponding to protons expected to be exchangeable (H^c, H^e, and H^f), including the allylic proton H^b at C2. To our delight, no deuterium incorporation was detected at C5, indicating that a selective epimerization process had been achieved. A similar outcome was obtained when isolated lactam **149** was subjected to the deuterium-containing epimerization reaction conditions. With these exciting results in-hand, attention turned to the preparation of **89** as a single enantiomer.

Chiral resolution of carboxylic acids is often accomplished by separation of diastereomeric salts, prepared from the racemic mixture.²² This technique was utilized in an initial approach to access **89** as a single enantiomer; treatment of racemic acid **145**

with (*S*)-1-phenethylamine (**154**, Scheme 2.9)²³ provided salt **155**, which was formed in 52–57% ee. We found that at least three recrystallizations were required to achieve high levels of enantiopurity. As is often the case with classical resolutions, this process reliably provided **145** in 98% ee, albeit in only 27% overall yield. As before, amide coupling under standard conditions furnished (+)-**89** with no racemization.

Scheme 2.9. Classical resolution of cyclobutane carboxylic acid **145**



2.3 DEVELOPMENT OF A TANDEM PHOTOCHEMICAL WOLFF REARRANGEMENT/ ASYMMETRIC KETENE ADDITION

2.3.1 Reaction Design and Relevant Precedent

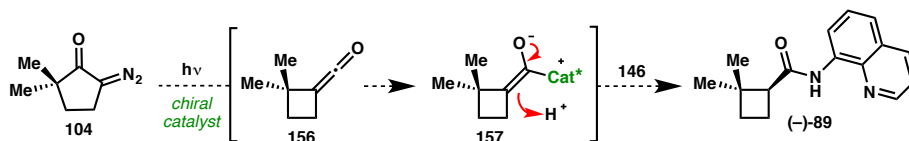
Although classical resolution provided access to (+)-**89**, the synthetically intractable yields led us to consider the development of an asymmetric method that would ideally deliver the desired amide in a single operation from **104** (Scheme 2.10a). Recognizing that photolysis of diazoketone **104** produces ketene **156** via Wolff rearrangement,²⁴ we hypothesized that this reactive intermediate might engage with a chiral catalyst, and in the presence of **146**, afford enantioenriched **89**.

Indeed, Fu has demonstrated that amides can be prepared with excellent enantioselectivity from aryl ketenes and 2-cyanopyrrole (**159**) in the presence of chiral DMAP catalyst (–)-**161** (Scheme 2.10b).²⁵ Notably, this protocol requires slow addition

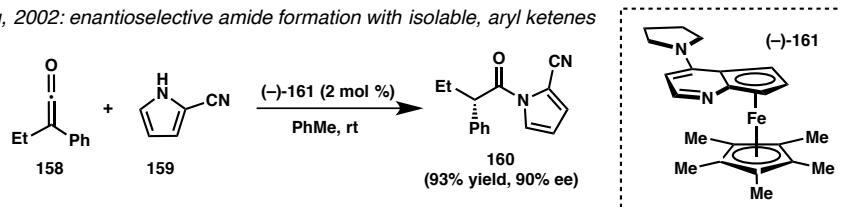
of stable, isolable ketenes; thus, it was not clear that Fu's methodology would be directly applicable using a ketene such as **156**, generated *in situ* under photochemical conditions. In this regard, Lectka's single example of asymmetric interception of a ketene generated by Wolff rearrangement to form α -chloroester **165** was encouraging (Scheme 2.10c).²⁶ With respect to nitrogen nucleophiles engaging with ketenes generated *in situ*, Wang and Hou have prepared lactam **169** by intramolecular attack of a tethered tosyl amine onto the ketene in **168**, which arises by Ag-mediated dediazotization of α -diazoketone **167** (Scheme 2.10d).²⁷ With these key reports in mind, we set out to first establish conditions under which the desired reactivity could be achieved in a racemic sense.

Scheme 2.10. Enantioselective Wolff rearrangement reaction design & precedent

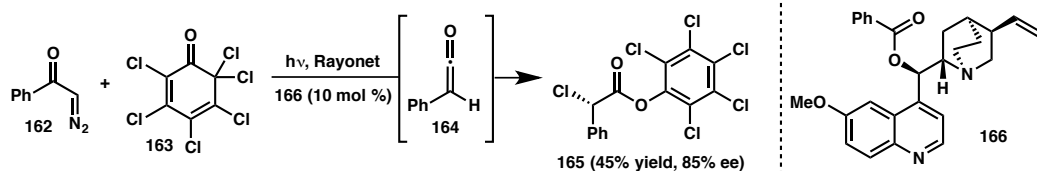
a) Reaction design: enantioselective amide formation with an alkyl diazoketone



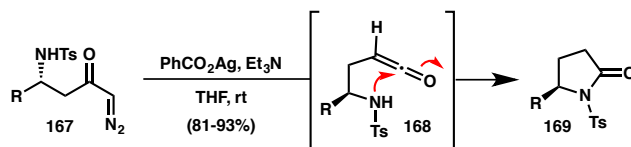
b) Fu, 2002: enantioselective amide formation with isolable, aryl ketenes



c) Lectka, 2004: enantioselective ester formation with an aryl diazoketone

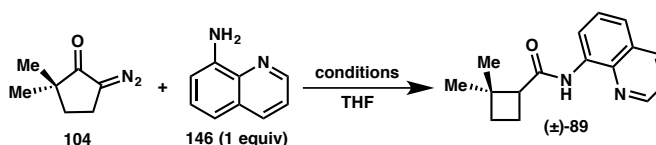


d) Wang and Hou, 1998: Addition of a nitrogen nucleophile to a ketene generated by Wolff rearrangement



Gratifyingly, it was found that irradiation of a mixture of **104** and **146** produced (±)-**89** in 46% yield (Table 2.2, entry 1). Interestingly, addition of 10 mol % DMAP *diminished* reactivity under otherwise identical conditions, although longer reaction time and heating rescued the yield somewhat (entries 2 and 3). Silver salts, such as Ag₂O and AgOBz, failed to promote dediazotization leaving **104** intact at room temperature or 50 °C (entries 4–8). Having established that this reaction was feasible under photolytic conditions, the ability of a chiral catalyst to exert enantiocontrol was explored next.

Table 2.2. Establishing desired reactivity in tandem with Wolff rearrangement



entry	de-diazo method	additive (equiv)	temp (°C)	time (h)	% yield (isolated)
1	<i>hν</i> , pyrex ^a	–	rt	4	46
2	<i>hν</i> , pyrex ^a	DMAP (0.1)	rt	4	16
3	<i>hν</i> , pyrex ^a	DMAP (0.1)	~60 ^b	18	28
4	Ag ₂ O	–	rt	18	0
5	Ag ₂ O	Et ₃ N (1.0)	rt	18	0
6	Ag ₂ O	Et ₃ N (1.0)	50	18	0
7	AgOBz	Et ₃ N (1.0)	rt	18	0
8	AgOBz	Et ₃ N (1.0)	50	18	0

^a Irradiated with a 450W medium-pressure Hanovia Hg lamp.

^b Increase in reaction temperature results from heat produced by the lamp, generated upon prolonged irradiation.

2.3.2 Optimization of a Tandem Asymmetric Ketene Addition[‡]

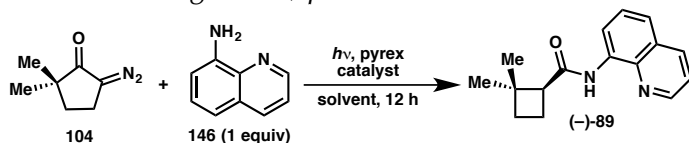
Due to the significant background reaction discovered in the absence of a chiral reagent, initial evaluations began using high catalyst loadings. In the event, we were pleased to find that in the presence of Fu's catalyst, (+)-**161**, the Wolff rearrangement furnished (–)-**89** in good yields, with promising levels of enantioinduction (34–42% ee,

[‡] Optimization studies in this section were conducted in collaboration with Dr. Linglin Wu, a postdoctoral researcher in the Fu Lab.

Table 2.3, entries 1–4). Based on the observation that high loadings of (+)-**161** produce a very dark, deep purple solution, the significant drop in yield at 50 mol % (entry 5) is attributed to poor light penetration through the reaction mixture. Attempts to improve selectivity by lowering the reaction temperature, or adding **104** slowly counterintuitively led to lower ee's (entries 6 and 7). A survey of different solvents also proved unsuccessful in providing high levels of enantioselectivity (entries 8–12). Hoping to identify a more efficacious structural analog to **161**, **170** and **171** were examined, but unfortunately both catalysts returned racemic product (entries 13 and 14).

At this juncture it was determined that use of the high wattage, heat-producing Hanovia lamp could be avoided by switching to irradiation with a household 254 nm lamp manufactured by Honeywell.²⁸ Reactions using this lamp were performed in quartz

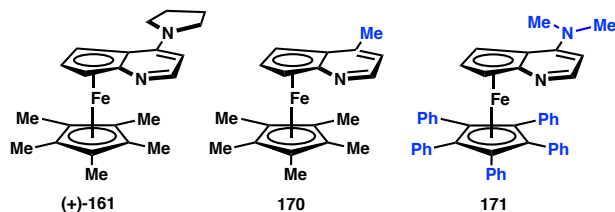
Table 2.3. Initial evaluation using chiral, planar Fe-DMAP derivatives



entry ^a	solvent	catalyst (mol %)	% yield	% ee
1	THF	161 (10)	75	34
2	THF	161 (15)	64	42
3	THF	161 (20)	64	41
4	THF	161 (30)	67	42
5	THF	161 (50)	39	46
6 ^b	THF	161 (15)	30	12
7 ^c	THF	161 (15)	60	36
8	TBME	161 (10)	–	28
9	dioxane	161 (10)	49	37
10	MeCN	161 (10)	44	22
11	DCE	161 (15)	50	24
12	PhMe	161 (10)	25	26
13	THF	170 (10)	58	0
14	THF	171 (10)	74	0

^a Irradiated with a 450W medium-pressure Hanovia Hg lamp.

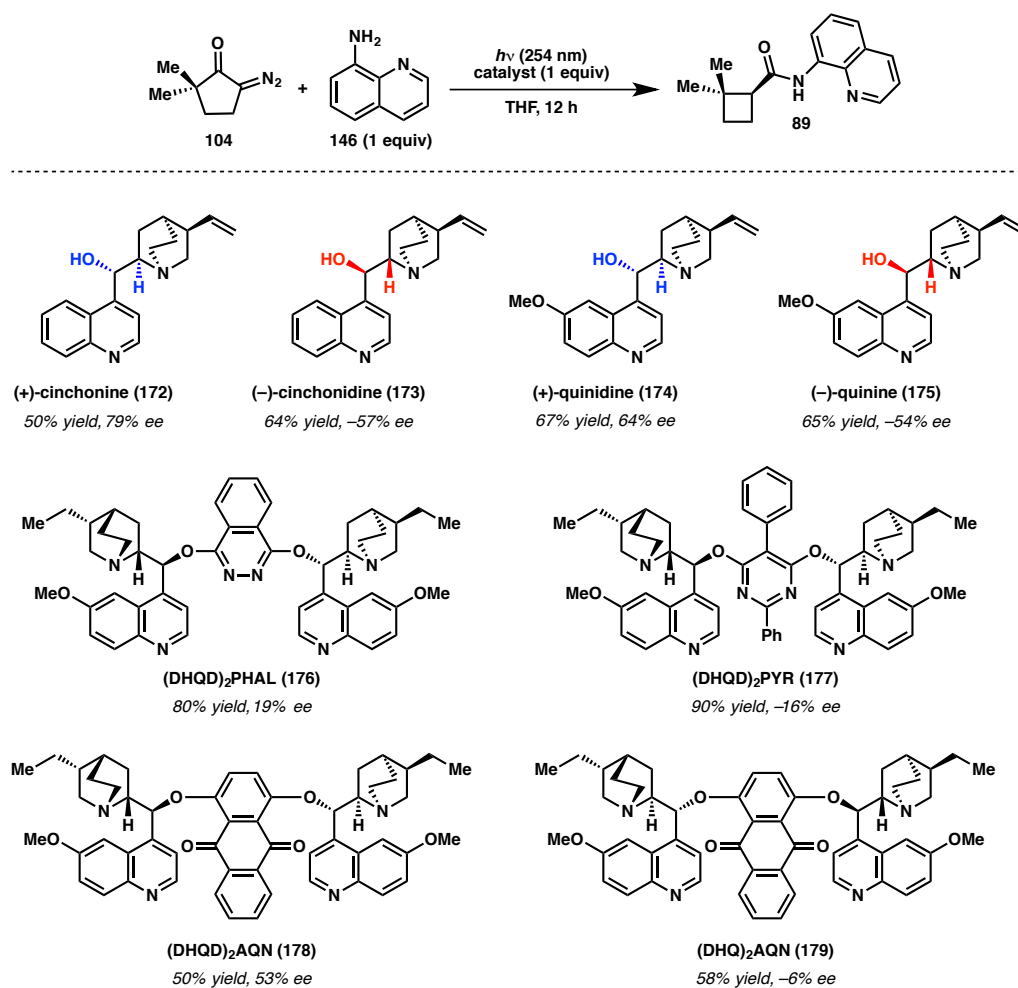
^b Reaction conducted at 0 °C. ^c Slow addition of 104.



tubes to maximize 254 nm light transmittance, and although this did not improve selectivity with **161**, this convenient setup was used moving forward.

With no leads toward an improvement in enantioselectivity using Fu's Fe-DMAP catalysts, we next decided to explore the cinchona alkaloids—another class of catalysts known to engage in catalytic, asymmetric reactions with ketenes.²⁹ Beginning with stoichiometric quantities of **172–179**, we were delighted to obtain ee's exceeding 50% for the first time (Table 2.4). (+)-Cinchonine (**172**) provided (–)-**89** with the highest selectivity (79% ee) in 50% yield. Interestingly, (+)-quinidine (**174**), which only differs

Table 2.4. Evaluation of chiral cinchona alkaloids



from **172** by the presence of a methoxy group on the quinoline ring, gave (–)-**89** in 64% ee—a marked difference for such a small structural variation. The corresponding pseudo-enantiomers, (–)-cinchonidine (**173**) and (–)-quinine (**175**), each gave lower selectivities in the opposite enantiomeric series. This observation was significant since the absolute configuration of **89** could not be determined at the time. While dimeric cinchona (DHQD)₂PHAL (**176**) and (DHQD)₂PYR (**177**) gave high yields of 80% and 90%, respectively, both provided very low levels of enantioselectivity.

Encouraged by these results, a few more known cinchona derivatives were evaluated. Unfortunately, epimerization of the secondary alcohol (**181–184**, Table 2.5)³⁰

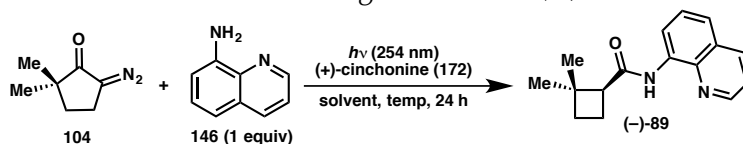
Table 2.5. Cinchona-derivatives and other classes of nucleophilic catalysts

<hr/>		
 Benzoyl-DHQ (180): 10 mol % 53% yield, 0% ee	 R = H: <i>epi</i> -CN (181): 50 mol % 50% yield, 24% ee R = OMe: <i>epi</i> -QD (182): 50 mol % 58% yield, 48% ee	 R = H: <i>epi</i> -CD (183): 50 mol % 51% yield, 4% ee R = OMe: <i>epi</i> -QN (184): 50 mol % 58% yield, –9% ee
 Indanyl-NHC (185): 50 mol % 32% yield, –66% ee	 OTBS-NHC (186): 20 mol % 68% yield, 39% ee	 Imidazolium-NHC (187): 50 mol % 0% yield
 188: 20 mol % 25% yield, 0% ee	 R = NEt ₂ (189): 20 mol % 30% yield, 0% ee R = Ph (190), <i>t</i> -Bu (191): 20 mol % 0% yield	 192: 20 mol % 0% yield

significantly diminished ee, while acylation (**180**)^{29f,31} abolished selectivity entirely. NHC precursors **185** and **186**³² were moderately successful, though these results proved very irreproducible and therefore this catalyst class was not pursued further. Finally, nucleophilic chiral phosphine catalysts **188** and **189** were found to only provide small amounts of racemic product.

With (+)-cinchonine (**172**) identified as the best catalyst, the reaction conditions were optimized for this particular alkaloid. Since **172** is only sparingly soluble in THF, the lower yield using 1 equivalent was again attributed to poor light penetration through the heterogeneous mixture (Table 2.6, entry 1). Reducing the loading of **172** led to improved yields of (–)-**89** without eroding enantioselectivity (entries 2 and 3). As before, lowering the reaction temperature to 0 °C did not improve selectivity (entry 4). Irradiation through either pyrex or vycor glass gave lower yields with significant amounts of starting material remaining (entries 5 and 6); this confirmed that conducting the reactions in quartz tubes was optimal for high conversion. Screening alternative solvents did not prove fruitful (8–11), although dioxane gave comparable results to THF (entry 7).

Table 2.6. Optimization of Wolff rearrangement with (+)-cinchonine



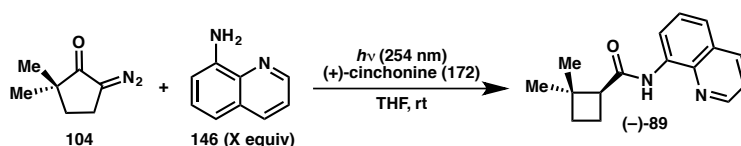
entry	solvent	172 (mol %)	temp (°C)	vessel	% yield	% ee
1	THF	100	rt	quartz	50	79
2	THF	50	rt	quartz	72	77
3	THF	20	rt	quartz	66	81
4	THF	20	0	quartz	28	79
5	THF	20	rt	vycor	29	79
6	THF	20	rt	pyrex	20	75
7	dioxane	20	rt	quartz	69	79
8	MeCN	20	rt	quartz	43	74
9	DMF	20	rt	quartz	76	50
10	CH ₂ Cl ₂	20	rt	quartz	62	47
11	PhMe	20	rt	quartz	65	59

^a Determined by ¹H NMR via integration relative to an added internal standard.

^b Determined by SFC using a chiral stationary phase.

The conditions in entry 3 were chosen as optimal reaction parameters, and attention turned toward reproducing these results on large scale. To our dismay, we found that an increase in scale from 0.10 mmol to 11.0 mmol led to a drastic drop in yield from 66% to 37%, although the enantioselectivity observed previously was maintained (Table 2.7 entries 1 and 2). After confirming this result several times, we considered that the discrepancy in yield could be due to a difference in the large-scale reaction setup. On small scale (~1.0 mL solvent) the reactions were performed in sealed quartz tubes; however, given that the photolysis of **104** produces N₂ gas, the large-scale reactions were conducted in a quartz flask with an outlet needle to prevent excessive pressure buildup. To discern whether the low yields were the result of an inherent scalability problem, or due to the alternative reaction setup, a small-scale reaction left open to air was conducted; interestingly, this experiment gave **89** in only 18% yield³³ (entry 3) with no remaining **104**, indicating that a sealed reaction vessel was indeed important.

Table 2.7. Translating the Wolff rearrangement to large scale



entry	mmol	172 (mol %)	atm	equiv 146	% yield ^a	% ee ^b
1 ^c	0.10	20	N ₂	1	66	81
2	11.0	20	N ₂	1	37	79
3	0.10	20	air	1	18	75
4	0.10	20	CO	1	33	69
5	15.0	20	N ₂	3	62	80
6	15.0	10	N ₂	3	65	79
7	30.0	10	N ₂	3	62	79

^a Determined by ¹H NMR: relative to an added internal standard.

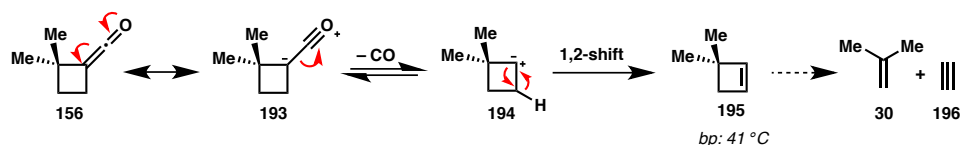
^b Determined by SFC using a chiral stationary phase.

^c Conducted in a sealed tube.

Considering these data together with the fact that we were unable to detect any side products that would account for the mass balance lost, it was hypothesized that

ketene **153** might decompose via photodecarbonylation (Scheme 2.11)³⁴ to produce volatile side products (i.e. **195**, and/or **30** and **196**). This idea was corroborated upon detection of CO when the atmosphere of a sealed reaction was vented into a hand-held CO detector. Having elucidated this deleterious pathway, the reaction was run under an atmosphere of CO in an attempt to take advantage of the equilibrium between **193** and **194** and funnel back toward the ketene; however, this only resulted in lower yield and ee (Table 2.7, entry 4).

Scheme 2.11. Elucidation of a deleterious photodecarbonylation pathway

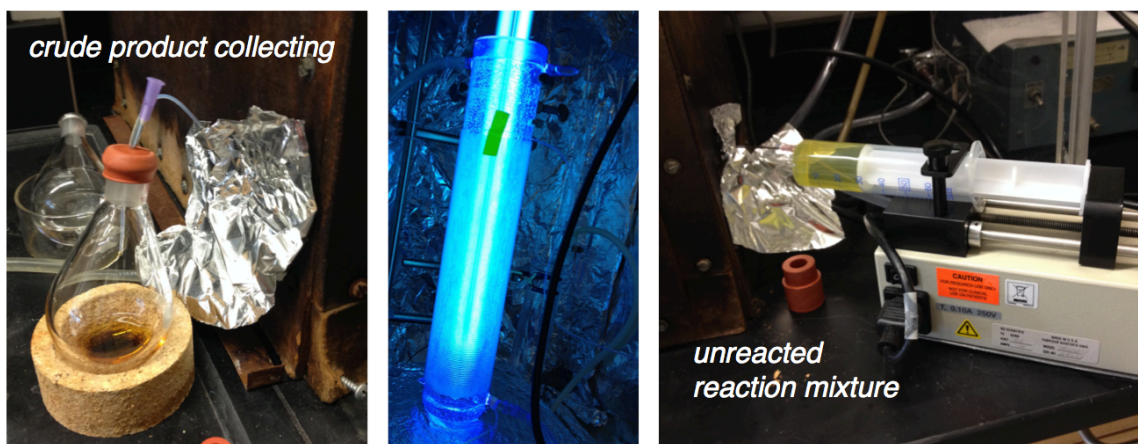


In order to drive the product distribution toward nucleophilic trapping, the concentration of **146** was increased, which gratifyingly restored the desired reactivity and afforded (–)-**89** in 62% yield with 80% ee on a 15 mmol scale (entry 5). Moreover, the catalyst loading could be reduced further to 10 mol % using this protocol, which reliably produced (–)-**89** in 62% yield with 79% ee on a 30 mmol scale (entry 7). Although (–)-**89** is obtained with modest ee directly from the reaction, a single recrystallization by layer diffusion provided this key intermediate in enantiomerically pure form. To the best of our knowledge, this is the first example of a tandem photolytic Wolff rearrangement/catalytic asymmetric ketene addition to afford enantioenriched amides.

2.3.3 Efforts Toward Flow Photochemistry

In recent years, flow chemistry has emerged as an efficient technique for enabling large-scale execution of photochemical reactions.³⁵ In order to maximize material throughput for this first step of our total synthesis, we became interested in developing a flow reactor from readily available laboratory materials. To this end, 100 ft of PFTE Teflon cannula tubing was wrapped around a jacketed quartz immersion well²⁸ and secured on each end with tape (Figure 2.5). A 16-gauge needle was fit inside the cannula at the top end of the photoreactor, allowing a large syringe to be connected to the inlet. A prepared reaction mixture could then be taken up into the syringe and driven through the photoreactor at a consistent flow rate, controlled by a syringe pump. Based on the inner diameter of the cannula (1.07 mm) and its volume capacity (29 mL), appropriate flow rates were calculated to allow the travelling reaction mixture to be irradiated for a total of approximately 2-4 hours.

Figure 2.5. Syringe-pump driven flow reactor setup



It is important for reaction mixtures to remain homogenous when flowing through a photoreactor. As discussed previously, (+)-cinchonine (**172**) is only sparingly soluble in

THF, which necessitates dilute (0.05 M) reaction concentrations to achieve a homogenous solution. Therefore, in order to maximize material throughput using the flow reactor setup, a suitable co-solvent that would help maintain homogenous mixtures at higher concentrations was required. Unfortunately, **172** was found to be insoluble in a variety of solvents, including EtOAc, CH₂Cl₂, THF/CH₂Cl₂, MeCN, DME, and even DMF. However, we found that both DMPU and 2-MeTHF helped to solubilize **172**. Test reactions in quartz tubes revealed that use of these solvents alone were detrimental to the reaction (Table 2.8, entries 3 and 4); however the addition of a small amount of DMPU in THF was well tolerated and allowed a two-fold increase in concentration (entry 2).

Table 2.8. Flow photochemistry test reactions and results

104 + 146 $\xrightarrow[\text{solvent, rt}]{h\nu (254 \text{ nm}), (+)\text{-cinchonine (20 mol \%)}}$ (-)-89

Co-solvent test reactions:

entry ^a	[M]	solvent	% yield	% ee
1	0.05	THF	66	81
2	0.10	14% DMPU/THF	57	78
3	0.10	DMPU	14	70
4	0.10	2-MeTHF	28	56

^a Reactions conducted in sealed quartz tubes on 0.10 mmol scale, with 1 equiv 146.

Flow results:

entry	scale (mmol)	flow rate (ml/h)	solvent, [M]	146 (equiv)	% yield	% ee
6 ^b	5.0	20	14% DMPU/THF (0.10 M)	1	38	78
7 ^b	2.4	10	THF (0.05 M)	1	40	82
8 ^b	2.5	15	THF (0.05 M)	3	54	79
9 ^c	51	15	THF (0.05 M)	3	10	80

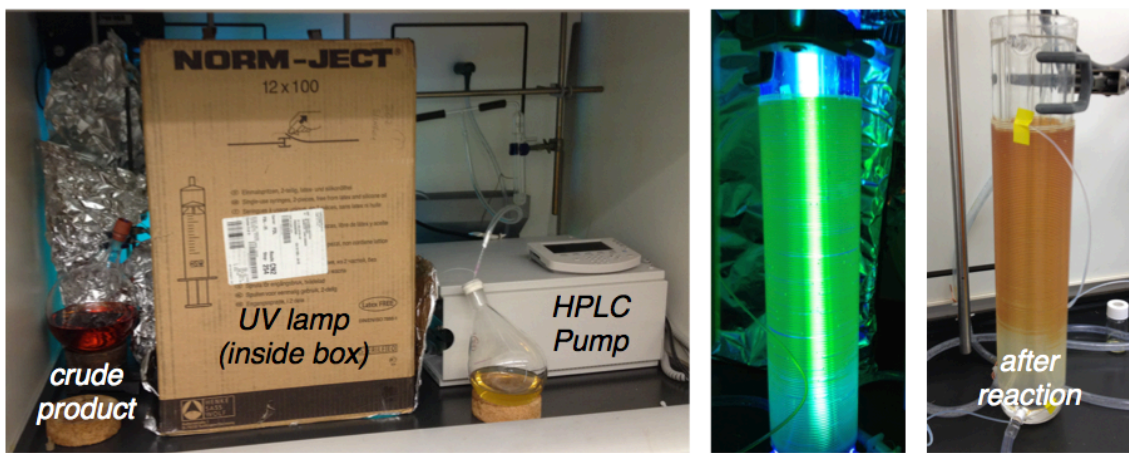
^b Conducted using flow chemistry setup with syringe pump.
^c Conducted using flow chemistry setup with HPLC pump.

Applying this solvent system in the context of syringe-pump driven flow photochemistry led to a disappointing 38% yield (entry 6), compared with 57% in the corresponding test reaction. Likewise, a flow reaction using standard conditions suffered the same outcome, even at a slower flow rate (entry 7). After the discovery of the ketene photodecarbonylation problem, the flow setup was evaluated again using 3 equivalents of **146** and resulted in an increased 54% yield (entry 8). Although this yield was slightly lower than anticipated (cf: entry 1), the ability to process many grams of material through

a continuous flow reactor was deemed preferable to running sequential batches, and thus worth the tradeoff in yield.

To achieve a continuous flow system, we required a device capable of sending more volume through the flow reactor than a simple 50 mL syringe would allow. To accomplish this, the cannula was attached to a threaded HPLC fitting and a remote-controlled HPLC pump was used to send the reaction mixture through the flow reactor (Figure 2.6). The crude product collected in the receiving flask was monitored periodically by TLC. Curiously, starting material was detected after ~12 hours, indicating that the reaction had stalled. Once the lamp was turned off, we discovered that the side of the cannula facing the UV lamp had become severely discolored upon prolonged irradiation, which precluded light from passing through to the reaction mixture. As a result, the attempt at a 51 mmol scale using flow photochemistry afforded **89** in only 10% yield (entry 9), with the unreacted starting material recovered almost entirely. While the cannula discoloration is unfortunate, we note that further evaluation of alternative materials, including other grades of Teflon, or ideally quartz tubing, may prove fruitful in

Figure 2.6. HPLC-pump driven flow reactor setup and discolored cannula

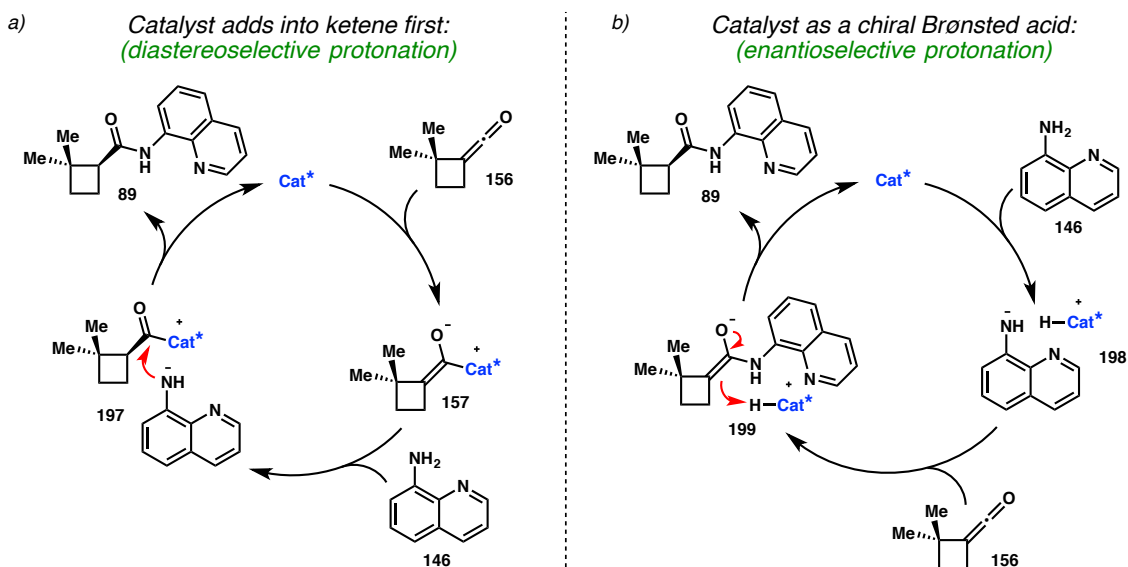


mitigating this problem. Moreover, these experiments provide an important proof-of-concept that the newly developed asymmetric Wolff rearrangement chemistry is inherently compatible with flow photochemistry systems.

2.3.4 Mechanistic Considerations

Experiments designed to probe the mechanism of this transformation were guided by two principle possibilities: First, many cinchona alkaloid-mediated asymmetric transformations involving ketene intermediates are proposed to proceed by addition of the catalyst to the ketene, forming a chiral, zwitterionic enolate complex^{26,29} such as **157** (Figure 2.7a). In the context of the tandem Wolff rearrangement/asymmetric ketene addition, it is envisioned that **157** may undergo a diastereoselective protonation with **146**, which serves as an achiral proton source to produce ion pair **197**. Transacylation of this species then generates **89** and expels the catalyst, allowing it to reenter the cycle.

Figure 2.7. Two mechanistic possibilities for the asymmetric ketene addition

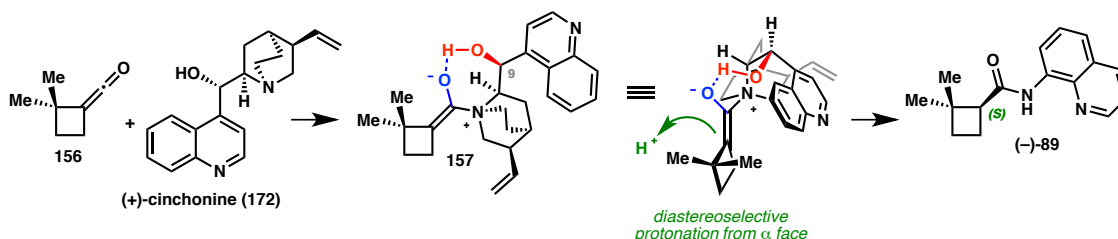


Another possibility put forth by Fu²⁵ in the context of the ferrocenyl DMAP catalysts (e.g. **161**) invokes an asymmetric protonation as the enantiodetermining step (Figure 2.7b). In this mechanism, the free catalyst first acts as a base to deprotonate an achiral proton source, such as **146**, to generate chiral ion pair **198**; in the context of their system, Fu and coworkers have observed an analogous ion pair by NMR spectroscopy as the resting state of the catalyst. The aminoquinoline anion in **198** can then add into ketene **156**, and the resulting achiral enolate undergoes protonation with a chiral Brønsted acid in **199** to furnish the product and regenerate the free-base form of the catalyst.

Lectka has used computational support to show that the alkoxide of zwitterionic enolates like **157** are capable of forming various hydrogen bonds with the quinuclidine nucleus of cinchona catalysts.^{29e, 36} These interactions serve to rigidify the three-dimensional conformation of **157**, thus leading to predictable levels of enantioselectivity. Based on this, and the fact that significant drops in asymmetric induction are observed using cinchona alkaloids without free hydroxyl groups (e.g. **176–180**), a possible scenario can be envisioned in which the enolate alkoxide in **157** forms a stabilizing hydrogen bond with the free C9 hydroxyl on the catalyst (Figure 2.8). Notably, examination of molecular models reveals that, with this key interaction in place, the quinolone ring in **172** folds down alongside the *re* face of the enolate in **157**, leaving the other side of the complex exposed for preferential protonation from the *si* face. Although somewhat crude, this analysis correctly predicts the absolute stereochemistry of the major enantiomer that is obtained experimentally. Moreover, models built of the pseudoenantiomeric enolate complex derived from **173** shows that the *si* face is blocked with lower efficiency, which

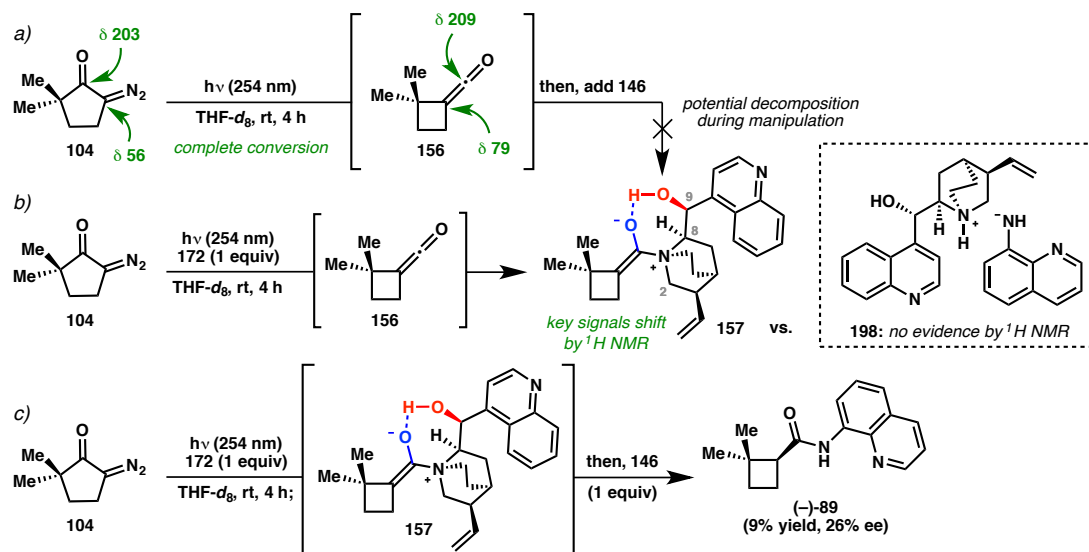
could explain the diminished levels of enantioinduction that are observed with the diastereomeric series of cinchona catalysts.

Figure 2.8. A possible model for diastereoselective protonation



A series of experiments that might lend support for the formation of zwitterionic complex **157** was conducted. To begin, it was important to determine whether ketene **153** could be formed discretely. To answer this question, diazoketone **104** was irradiated for 4 hours in THF- d_8 and transferred directly to a dry NMR tube. Spectroscopic analysis by NMR revealed complete and relatively clean conversion of **104** to **153**, exhibiting signature ^1H and ^{13}C NMR shifts consistent with a ketene (Scheme 2.12a). Subsequent addition of a 1 equiv **146** to this solution did not result in any evidence of **89**, most likely due to decomposition of the sensitive ketene during subsequent manipulation.

On the other hand, irradiation of **104** in the presence of 1 equiv **172** in THF- d_8 for the same amount of time provided a different ^1H NMR: key signals corresponding to protons at C2, C8, and C9 on the quinuclidine nucleus were shifted substantially, and these integrated well with respect to two new methyl signals with the hallmark characteristics of the cyclobutyl-geminal dimethyl pattern (Figure 2.12b). On the other hand, no change in the ^1H NMR spectrum of **172** was observed in the presence of **146** in THF- d_8 , indicating that ion pair **198** likely does not constitute the resting state of the active catalyst, as in the enantioselective protonation mechanism.²⁵

Scheme 2.12. Attempts to identify critical intermediates/reactive species.

Lastly, to confirm that the proposed zwitterionic complex **157** is capable of forming ion pair **197** and undergoing subsequent transacylation, 1 equiv **146** was added to the reaction mixture following irradiation of **104** and **172** for 4 hours. The expected product **89** was obtained from this experiment, albeit in only 9% yield and 26% ee.³⁷ While it is unclear why the yield is so low in this case, we attribute the low levels of enantioselectivity to a higher rate of background reaction in the presence of excess ketene **153**, which was observed by $^1\text{H NMR}$ analysis of the crude reaction mixture. Taken together with recent computational studies,³⁸ we believe these preliminary results lend some support for the diastereoselective protonation mechanism outlined in Figure 2.7a. However, more experiments are required to fully elucidate the operative mechanism.

2.3.5 Efforts Toward Expansion of Substrate Scope[§]

In tandem with ongoing work to learn more about the mechanism of the asymmetric Wolff rearrangement, efforts to explore the generality of the substrate scope for this transformation have been initiated.³⁹ A preliminary summary of our findings is summarized in Table 2.9. In moving away from **104**, simple, systematic changes were made to new substrates tested (**200–203**); therefore, it was surprising to find that both yield and enantioselectivity dropped dramatically for α -diazoindanone **200**. On the other hand, α -diazotetralone **202** performed very well in the presence of (DHQD)₂PYR (**177**), providing the corresponding product in 61% yield and 75% ee. Notably, this substrate was the first identified to give high levels of selectivity using a dimeric cinchona catalyst; interestingly, the optimal catalyst for **104** afforded only 48% yield and 34% ee in this system. Whereas the epimeric cinchona alkaloids **182** and **181** performed poorly with

Table 2.9. Summary of optimal catalysts for alternative substrates

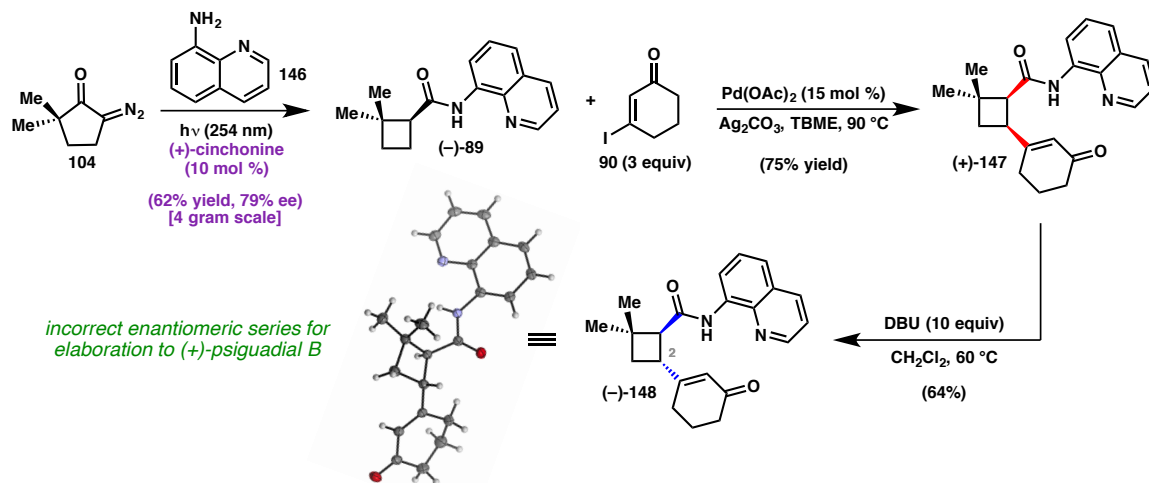
 104	 200	 201	 202	 203
optimal catalyst: (+)-cinchonine (172) 66% yield, 81% ee	(DHQD) ₂ AQN (178) 40% yield, 34% ee	epi-quinidine (182) 66% yield, 70% ee	(DHQD) ₂ PYR (177) 61% yield, –75% ee	(+)-quinidine (174) 65% yield, 68% ee
second best catalyst: (+)-quinidine (174) 67% yield, 64% ee	(–)-quinine (175) 48% yield, –26% ee	epi-cinchonine (181) 52% yield, 64% ee	epi-cinchonine (181) 65% yield, 42% ee	(+)-cinchonine (172) 49% yield, 64% ee

[§] Exploration of the substrate scope for the tandem Wolff rearrangement/asymmetric ketene addition reaction is currently underway in collaboration with Caitlin Lacker, a graduate student in the Reisman Lab.

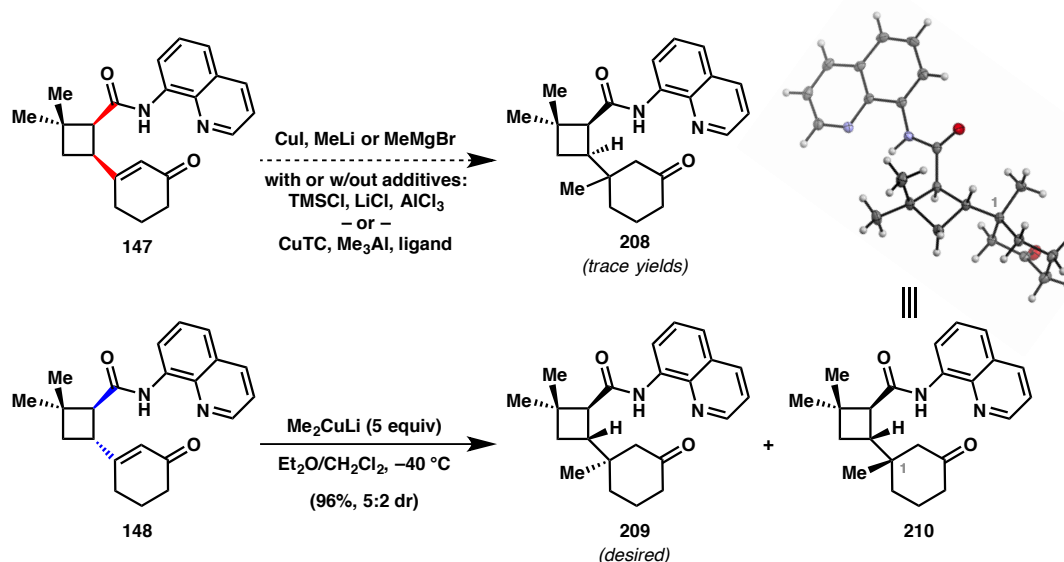
104, these catalysts afforded the *best* results for **201**, a strikingly close 6-membered analog of **104**. Although the dimeric and epimeric cinchona catalysts gave the highest ee for substrates **200–202**, this trend did *not* hold for 7-membered diazoketone **203**. In this case, (+)-quinidine (**174**) was determined as the optimal catalyst, furnishing the corresponding Wolff product in 65% yield and 69% ee. At present, a generally optimal catalyst has not been identified for the preparation of enantioenriched amides using this method, though mechanistic investigations may inform efforts to improve the substrate scope of this transformation. Future work will also be directed at exploring a variety of different nucleophiles as alternatives to **146**.

2.4 FORWARD SYNTHETIC EFFORTS: ASYMMETRIC ROUTE

With rapid access to multigram quantities of **89** in enantiopure form, the C(sp³)-H alkenylation reaction was conducted on gram scale to give (+)-**147** in 75% yield (Scheme 2.13). The requisite *trans*-cyclobutane was obtained with no erosion of ee by selective epimerization at C2, as determined by earlier deuterium-labeling studies. It was at this stage that we were able to obtain single crystals of *trans*-cyclobutane **148** suitable for X-ray diffraction. Unfortunately, **148** was found to be in the incorrect enantiomeric series for elaboration to natural **56**. To our dismay, this problem could not be circumvented by simply employing (–)-cinchonidine (**173**) in the tandem Wolff rearrangement/asymmetric ketene addition, as this *diastereomeric* catalyst afforded (+)-**89** in lower yield with only 57% ee (see Table 2.4). Nevertheless, (–)-**148** was advanced in the interest of validating the key reactions in our retrosynthetic analysis as soon as possible.

Scheme 2.13. Alkenylation/epimerization using enantiopure cyclobutamide**2.4.1 Quaternary Center Formation via Conjugate Addition**

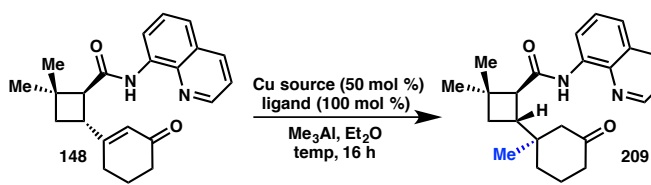
The next task focused on installing the methyl group to form the C1 quaternary center. Subjection of *cis*-cyclobutane **147** to a number of standard conjugate addition conditions provided only trace yields of the desired product **208**, presumably due to steric crowding by the proximal large aminoquinoline group (Scheme 2.14). On the other hand, treatment of *trans*-cyclobutane **148** with excess Gilman's reagent smoothly furnished **209** and **210** in near quantitative yield as a 5:2 mixture of diastereomers, respectively. Separation of the diastereomers by HPLC purification allowed single crystals of **210** to be obtained for X-ray diffraction analysis, which unambiguously confirmed that the *minor* diastereomer possessed the *undesired* configuration of the methyl group at the C1 quaternary center.

Scheme 2.14. Initial foray into conjugate addition to set the C1 quaternary center

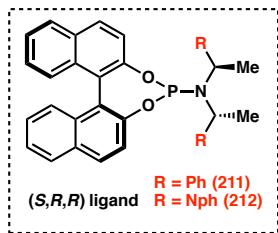
Although reaction with **148** inherently favored formation of the desired diastereomer, asymmetric conjugate addition conditions were evaluated in order to improve the selectivity of this transformation. Fortunately, application of the asymmetric copper-catalyzed conditions developed by Alexakis and coworkers⁴⁰ accomplished this goal, albeit with 50 mol % copper and a stoichiometric equivalent of phosphoramidite ligand (**211**, Table 2.10). Such a high catalyst loading is likely necessary due to the presence of the highly coordinating aminoquinoline auxiliary. Identification of optimal reaction conditions required some experimentation to provide an acceptable balance of reasonable yield. Application of Alexakis' canonical conditions gave only trace yield (Table 2.10, entry 1); however, we found that using $\text{Cu}(\text{OAc})_2$ in place of CuTC boosted the yield significantly and provided high levels of diastereoselectivity (entry 2). Switching to a bulkier, naphthyl-substituted ligand (**212**) counterintuitively lowered selectivity; likewise, raising the reaction temperature led to depressed yields (entries 3–5). Fortunately, it was found that $[\text{Cu}(\text{OTf})_2 \cdot \text{PhMe}]$ boosted the yield to a serviceable 44%, and since other

copper sources did not prove fruitful (entry 7), this set of reaction conditions was chosen to move forward with.

Table 2.10. Copper-catalyzed conjugate addition



entry ^a	Cu source	R	temp (°C)	% yield (brsm) ^b	dr
1	CuTC	Ph	-30	trace	–
2	Cu(OAc) ₂	Ph	-30	28 (44)	97:1
3	Cu(OAc) ₂	Nph	-30	24 (35)	19:1
4	Cu(OAc) ₂	Ph	0	18 (20)	1:0
5	Cu(OAc) ₂	Ph	rt	4 (6)	22:1
6	[Cu(OTf)] ₂ ·PhMe	Ph	-30	44 (62)	81:1
7	Cu(MeCN) ₄ BF ₄	Ph	-30	trace	–

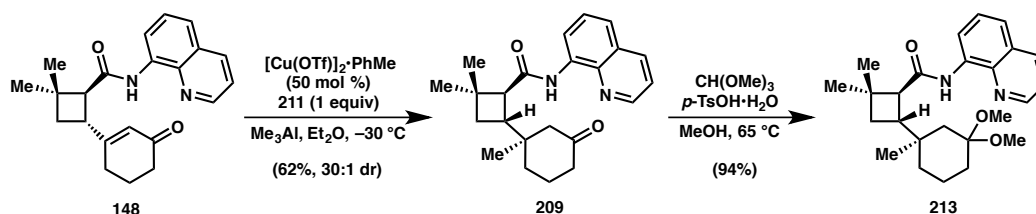


(S,R,R) ligand
R = Ph (211)
R = Nph (212)

^a Reactions conducted on 0.09 mmol scale. ^b Determined by ¹H NMR relative to added internal standard.

Upon scale-up, an exotherm was observed when Me₃Al was added to the reaction mixture, which was mitigated by adding the reagent more slowly. Using this protocol, **209** was obtained in an improved 62% yield and 30:1 dr on a 0.6 mmol scale (Scheme 2.15). With the correct configuration at the quaternary center secured, this ketone was converted to the corresponding ketal **213**, which could be used directly in the planned *o*-QMHA reaction (*vide infra*, see Scheme 2.17).

Scheme 2.15. Optimal conjugate addition conditions and ketal protection

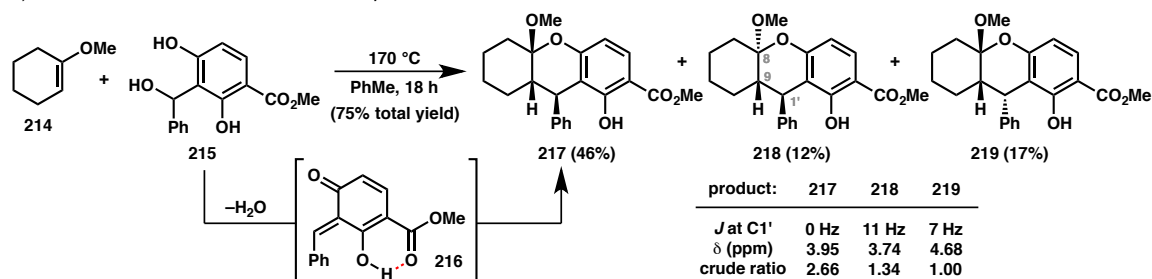


In parallel with these efforts, a variety of *o*-QM precursors were evaluated with different arene oxidation patterns and phenol protecting groups using a simple model

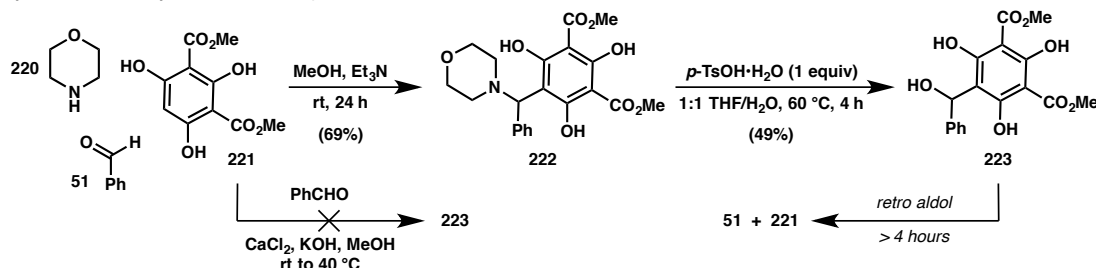
system to study the reactivity of each. Interestingly, phloroglucinol derivatives lacking carbonyl functionality (see **103**, Figure 2.2) were generally unreactive with 1-methoxycyclohex-1-ene (**214**, Scheme 2.16a). Conversely, we were gratified to find that use of aryl ester **215** afforded the desired cycloaddition products as a mixture of three diastereomers, in a combined 75% yield. Stereochemical analysis of **217–219** was aided by the signature ^1H NMR coupling patterns of the vicinal protons at C1' and C9; the signal of the doubly benzylic proton at δ 3.95 ppm in **217** corresponds to a singlet that is characteristic of a 90° dihedral angle ($J = 0$ Hz) with the adjacent proton at C9. On the other hand, thermal equilibration of the ketal leads to a *trans* fusion across C8–C9 in **218**, thus placing these protons at a 180° dihedral angle, which is consistent with the observed $J = 11$ Hz coupling also present in (+)-psiguadial B (**56**). Integration of these key signals in the crude reaction mixture revealed that products with the desired relative stereochemistry, **217** and **219**, predominated in an overall *endo/exo* ratio of 4:1.

Scheme 2.16. Model [4+2] and synthesis of fully oxidized *o*-QM precursor

a) Model studies used to evaluate *o*-QM precursors



b) Synthesis of a fully oxidized *o*-QM precursor



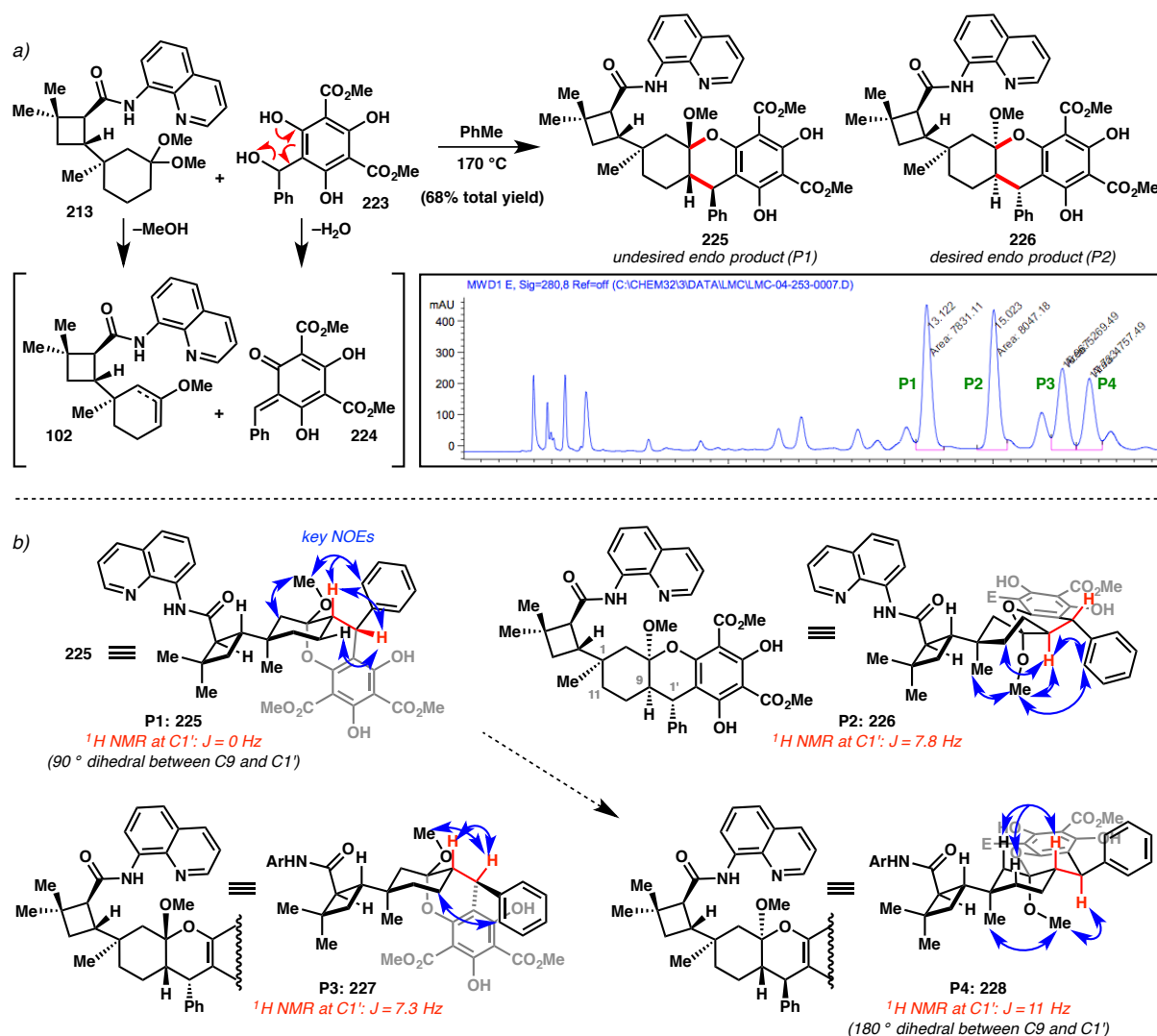
The aryl ester in **215** is proposed to form a key hydrogen bond to the neighboring phenol, thus orienting the proton away from the co-planar phenyl group in *o*-QM **216**. This interaction accounts for the successful thermolysis of **215** vs. other *o*-QM precursors, as well as the observed regioselectivity of the cycloaddition. Given the apparent necessity of this H-bonding assistance, a fully functionalized *o*-QM precursor was sought, which would obviate the need for arene oxidation at a later stage. Unfortunately, subjection of **221**⁴¹ to the same phenolic aldol conditions used to synthesize **215**⁴² did not result in any productive reaction (Scheme 2.16b). On the other hand, generation of a more electrophilic imine, derived from benzaldehyde (**51**) and morpholine (**220**) engaged readily with **221** to provide **222** in 69% yield. Access to 2-hydroxy benzyl alcohol **223** was then realized by leveraging Wilson's tactic to access *o*-QMs from morpholine derivatives;⁴³ **222** was activated with *p*-TsOH, and in the presence of water, gave **223** in 49% yield after 4 hours. Notably, **223** proved sensitive under the acidic reaction conditions and would slowly revert back to **221** and **51**, presumably via protonation and retro aldol processes.

2.4.2 Evaluation of the Key *o*-QMHDA Cycloaddition Reaction

With both cycloaddition partners finally in hand, the proposed *o*-QMHDA reaction was investigated. After some experimentation, it was found that **213** could be used directly to afford a 1:1 equilibrating mixture of enol ethers (**102**) upon thermal extrusion of methanol at 170 °C (Scheme 2.17a).⁴⁴ Concurrently, 2-hydroxy benzyl alcohol **223** underwent thermolysis to generate the corresponding *o*-QM **224**. We were pleased to observe a remarkably efficient cycloaddition between these two *in situ*-

generated species furnishing a 68% total yield of the fused tricycle products, albeit as a complex mixture of diastereomers that proved inseparable by standard silica gel column chromatography. Fortunately, analytically pure samples of each of the four diastereomers formed in highest abundance (Peaks 1–4) were obtained by subsequent HPLC purification to assess the stereochemical outcome of the reaction.

Scheme 2.17. Realization of the *o*-QMHA reaction



Spectroscopic analysis by 2D NMR led to the assignment of *endo* products, **225** and **226**, as the two major diastereomers, isolated in a ~1:1 ratio. For **225**, key NOE

signals between the newly formed methine at C9, the methoxy ketal, and an *ortho*-proton on the phenyl ring—all of which correlate to each other—establish that these three substituents reside on the same face of the molecule (Scheme 2.17b). Furthermore, the ^1H NMR signal at C1' corresponds to a characteristic singlet that is indicative of a 90° dihedral angle ($J = 0$ Hz) with the adjacent proton at C9. Whereas the methyl group at the C1 quaternary center does not exhibit any discerning signals in the 2D NOESY spectrum of **225**, the C1 methyl in **226** *does* show a key correlation with the methoxy ketal. In turn, **226**'s methoxy ketal also shares an NOE with the C9 methine and a small, but discernable signal is observed with an *ortho*-phenyl proton, indicating that these groups are all oriented in the same direction. Notably, **226** appears to adopt a boat conformation, as evidenced by the NOE correlation between the C9 methine and axial proton on C11.

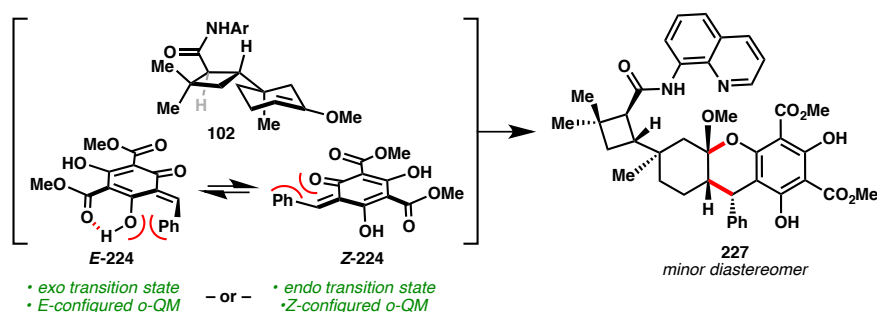
Spectroscopic characterization of the minor products revealed that peak 3 corresponds to **227**, which displays some analogous features to **225**, except that the methoxy ketal now correlates to the C1' methine, and the coupling constant ($J = 7.3$ Hz) between vicinal protons at C1' and C9 suggests a *cis*-orientation, as drawn. Interestingly, this same coupling constant in **228** (corresponding to peak 4) is 11 Hz, which is most consistent with a 180° dihedral angle between C9 and C1', and thus a *trans*-fusion across the newly formed ring. This assignment is further supported by characteristically prominent NOEs shared between all the axial protons indicated, as well as correlations from the methoxy ketal to both the C1 methyl group and the benzylic proton at C1'.

Analysis of the diastereomeric mixture by mass spectrometry confirms that many of the minor constituents apparent in the chromatogram shown in Scheme 2.17a possess the same molecular weight as **225–228**. These minor components likely represent the

remainder of the expected diastereomers, namely, the *exo* product complementary to **226**, as well as *trans*-fused isomers resulting from thermal equilibration of the ketal, as observed in **228**.

With these stereochemical assignments in-hand, we were pleased to observe that *endo* products, **225** and **226**, were in fact produced in the highest abundance as predicted. However, given the near 1:1 ratio of these intermediates, it was clear that the C1 methyl group did *not* serve to block *o*-QM approach from the bottom face of enol ether **102**.⁴⁵ Rather, isolation of minor products, **227** and **228**, suggest that cycloaddition from the bottom face of **102** is actually preferred. With regard to *endo/exo* selectivity, **227** may arise by one of two possibilities: either *E*- or *Z*-**224** can react with **102** through an *exo* or *endo* transition state, respectively, to yield the same stereochemical outcome (Figure 2.9). Although formation of *E*-configured *o*-QMs is typically favored in order to avoid steric clashing with the lone pairs on oxygen,¹¹ this interaction is unavoidable in the case of fully oxidized *o*-QM **224**. Thus, without a clear steric bias to favor one configuration over the other, the precise nature of how **227** arises remains unclear at this time.

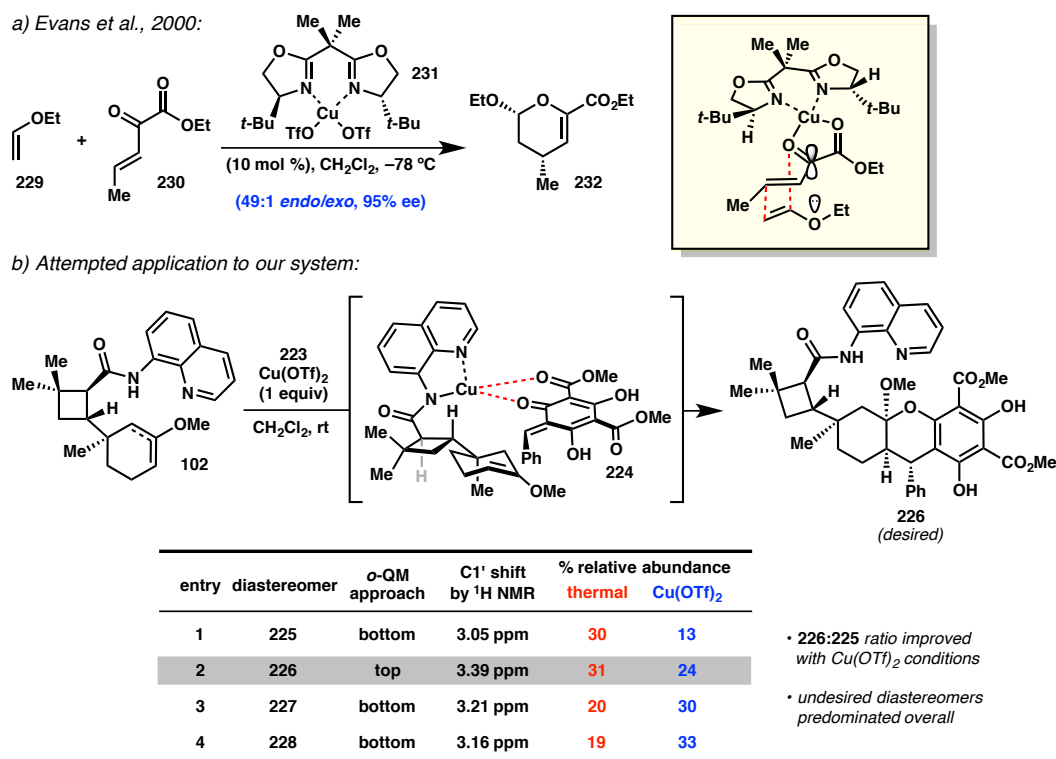
Figure 2.9. Possibilities for *o*-QM configuration and approach to form **227**



Disappointed by the overall low yield of **226**, a potential solution was conceived to improve the facial selectivity of this transformation by leveraging the auxiliary in **102**

to *direct* the approach of the *o*-QM. Drawing inspiration from Evans' highly selective Cu-catalyzed inverse-demand hetero-Diels–Alder chemistry (Scheme 2.18a),⁴⁶ it was envisioned that the Cu-chelating aminoquinoline could engage **224** in a similar two-point binding mode, which would deliver the *o*-QM from the top face of enol ether **102** and set the desired stereochemistry at C9 and C1' (Scheme 2.18b). Formation of **224** would be triggered at room temperature by the equivalent of triflic acid generated via complexation of Cu(OTf)₂ with aminoquinoline.^{15,47}

Scheme 2.18. Toward an aminoquinoline-directed *o*-QMHDHA reaction



To test this hypothesis, enol ether **102** was prepared by thermal heating in PhMe, and after replacing the solvent with CH₂Cl₂, **113** was added in the presence of Cu(OTf)₂. Analysis of the crude mixture by ¹H NMR revealed that although the ratio of **226:225** had improved relative to the thermal reaction, formation of undesired products, **227** and **228**,

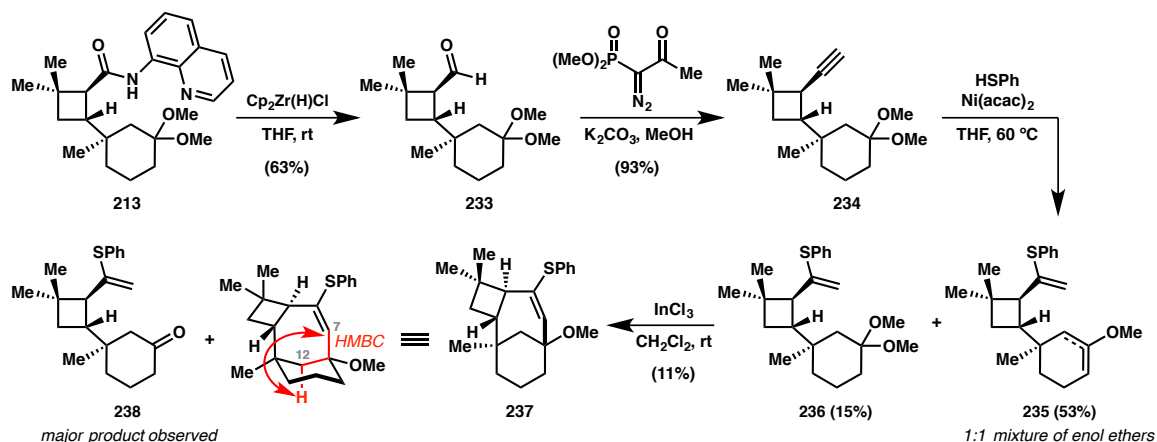
now predominated overall. Moreover, this reaction suffered from rapid hydrolysis of **102** to ketone **209** and formation of retro aldol product **221**—an unsurprising consequence of triflic acid generation. At this stage, it was clear that implementation of this strategy would require a significant investment in reaction optimization and we felt that such an effort would only be warranted if the proposed late-stage Prins reaction were proved feasible. Thus, attention turned to assessing this key reaction in a model system.

2.4.3 Model Studies Toward a Vinyl Sulfide Prins Cyclization

Reductive cleavage of the aminoquinoline auxiliary in **213** was accomplished with Schwartz's reagent to furnish aldehyde **233**, which was smoothly homologated to alkyne **234** using an Ohira–Bestmann reaction (Scheme 2.19). Nickel-catalyzed hydrothiolation⁴⁸ proceeded with complete regioselectivity to give vinyl sulfide **236** in low yield, mainly due to the facile conversion of this intermediate to a mixture of enol ethers **235** during the course of the reaction. Nonetheless, having arrived at a substrate capable of validating the desired Prins reactivity, ketal **236** was subjected to a variety of Lewis acids, and in nearly all cases simple deprotection to the corresponding ketone **238** was observed. Gratifyingly however, the use of InCl_3 ^{9b} delivered the desired Prins product **237**, representing successful assembly of the bridging bicyclic terpene framework for the first time. Formation of the 7-membered ring was confirmed by a key HMBC correlation between the C12 axial proton and the distinct sp^2 C7 signal at δ 140 ppm. Although the realization of a successful Prins cyclization was promising, our excitement was tempered by the fact that **237** was obtained in poor yield and unfortunately, this initial result proved irreproducible. Taken together with the significant

diastereoselectivity issues plaguing the *o*-QMHA reaction, these setbacks ultimately motivated the decision to revise our retrosynthetic analysis.

Scheme 2.19. Evaluating the feasibility of Prins cyclization in a model system



2.5 CONCLUDING REMARKS

In conclusion, a first-generation route to (+)-psiguadial B (**56**) was investigated, which led to several key discoveries. First, the synthetic challenge posed by *de novo* construction of the *trans*-fused cyclobutane ring in **56** inspired the development of a photochemical Wolff rearrangement with tandem asymmetric ketene addition to provide direct access to enantioenriched amides in good yield and selectivity. This novel transformation provided the foundation for the ability to access optically active advanced intermediates, which were rapidly assembled using a key Pd-catalyzed C(sp³)-H alkenylation reaction.

In addition, a remarkably efficient *o*-QMhDA cycloaddition was successfully achieved between a highly functionalized cyclohexanone-derived enol ether *used as the limiting reagent* and a fully oxidized *o*-QM under thermal conditions. Elucidation of the

stereochemical outcome of the reaction led to the conclusion that the presence of the C1 methyl group was insufficient to enforce the desired facial selectivity in *o*-QM approach. Lastly, exploratory efforts aimed at realizing the proposed Prins cyclization in a model system were met with limited success. Having completed the evaluation of our key retrosynthetic disconnections, attention ultimately turned to the development of a second-generation synthetic strategy, as described in Chapter 3.

2.6 EXPERIMENTAL SECTION

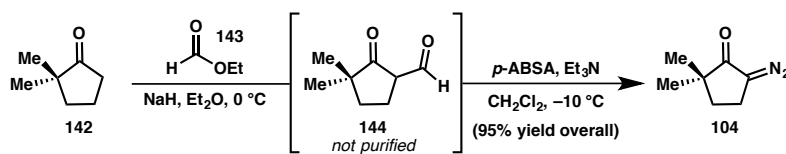
2.6.1 Materials and Methods

General Procedures. Unless otherwise stated, reactions were performed under a nitrogen atmosphere using freshly dried solvents. Tetrahydrofuran (THF), methylene chloride (CH_2Cl_2), acetonitrile (MeCN), *tert*-butyl methyl ether (TBME), benzene (PhH), and toluene (PhMe) were dried by passing through activated alumina columns. Triethylamine (Et_3N), *N,N*-diisopropylethylamine (DIPEA), and methanol (MeOH) were distilled over calcium hydride prior to use. Unless otherwise stated, chemicals and reagents were used as received. All reactions were monitored by thin-layer chromatography using EMD/Merck silica gel 60 F254 pre-coated plates (0.25 mm) and were visualized by UV, *p*-anisaldehyde, or 2,4-dinitrophenylhydrazine staining. Flash column chromatography was performed either as described by Still et al.⁴⁹ using silica gel (particle size 0.032-0.063) purchased from Silicycle or using pre-packaged RediSep[®]Rf columns on a CombiFlash Rf system (Teledyne ISCO Inc.). Optical rotations were measured on a Jasco P-2000 polarimeter using a 100 mm path-length cell at 589 nm. ^1H and ^{13}C NMR spectra were recorded on a Bruker Avance III HD with Prodigy cryoprobe (at 400 MHz and 101 MHz respectively), a Varian 400 MR (at 400 MHz and 101 MHz, respectively), a Varian Inova 500 (at 500 MHz and 126 MHz, respectively), or a Varian Inova 600 (at 600 MHz and 150 MHz, respectively), and are reported relative to internal CHCl_3 (^1H , $\delta = 7.26$) and CDCl_3 (^{13}C , $\delta = 77.1$), THF (^1H , $\delta = 3.58$) and THF- d_8 (^{13}C , $\delta = 67.6$), or C_6H_5 (^1H , $\delta = 7.16$), and C_6D_6 (^{13}C , $\delta = 128$). Data for ^1H NMR spectra are reported as follows: chemical shift (δ ppm) (multiplicity, coupling constant (Hz), integration). Multiplicity and qualifier abbreviations are as follows: s = singlet, d =

doublet, t = triplet, q = quartet, m = multiplet, br = broad, app = apparent. IR spectra were recorded on a Perkin Elmer Paragon 1000 spectrometer and are reported in frequency of absorption (cm^{-1}). HRMS were acquired using an Agilent 6200 Series TOF with an Agilent G1978A Multimode source in electrospray ionization (ESI), or mixed (MM) ionization mode, or obtained from the Caltech Mass Spectral Facility in fast-atom bombardment mode (FAB). Analytical SFC was performed with a Mettler SFC supercritical CO_2 analytical chromatography system with a Chiralcel AD-H column (4.6 mm x 25 cm).

2.6.2 Preparative Procedures and Spectroscopic Data

Preparation of diazoketone **104**.¹⁷



To each of two flame-dried 1 L round-bottom flasks was added NaH (60% dispersion in mineral oil, 3.17 g, 79.2 mmol, 1.20 equiv) and the atmosphere was exchanged for N_2 one time. Dry Et_2O (30.0 mL) was then added via syringe and the suspension cooled to $0\text{ }^\circ\text{C}$. Ethyl formate (12.4 mL, 152 mmol, 2.30 equiv) was then added, followed by 2,2-dimethylcyclopentanone **142**¹⁸ (7.40 g, 66.0 mmol) either neat, or as a 3.0 M solution in Et_2O . A catalytic amount of wet methanol ($\sim 100\text{ }\mu\text{L}$) was then added and the reaction left to stir at $0\text{ }^\circ\text{C}$.⁵⁰ Upon completion, the reaction solidifies to a chunky, white solid that dissolved readily upon the addition of DI H_2O . At this point, both reaction mixtures were combined for workup: after dilution with Et_2O , the layers

were separated and the aqueous layer was washed with Et₂O 3x to remove organic impurities and a small amount of unreacted starting material. The aqueous layer was then cooled to 0 °C and acidified to pH = 3 using 5 M HCl. Et₂O was then added and the acidified aqueous layer was extracted 6x. The combined organics were then dried over Mg₂SO₄, filtered, and concentrated *in vacuo* into a 500 mL round-bottom flask.

The crude formyl ketone **144** was taken up in CH₂Cl₂ (132 mL) and the solution cooled to –10 °C. Triethylamine (55.2 mL, 396 mmol, 5.00 equiv) was added, followed by solid *p*-ABSA⁵¹ (31.8 g, 132 mmol, 1.00 equiv) in three portions. The reaction was stirred for 3 hours and allowed to gradually reach 10 °C, at which point an aqueous solution of KOH (55.0 mL, 4 M) was added. Additional CH₂Cl₂ and H₂O were added, the layers were separated and the aqueous layer extracted with CH₂Cl₂ until no product remains by TLC. The combined organics were dried over Mg₂SO₄, filtered, and concentrated *in vacuo*. The crude residue was purified by silica gel flash chromatography (20–30% Et₂O/pentane) to afford **104** (17.4 g, 95% yield) as a bright yellow oil.

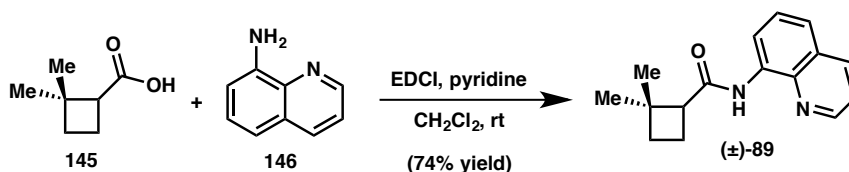
¹H NMR (400 MHz, CDCl₃) δ 2.88 (t, *J* = 7.0 Hz, 2H), 1.77 (t, *J* = 7.2 Hz, 2H), 1.04 (d, *J* = 1.0 Hz, 6H).; **¹H NMR** (400 MHz, THF-*d*₈) δ 2.94 (t, *J* = 7.0 Hz, 2H), 1.79 (t, *J* = 7.2 Hz, 2H), 1.04 (s, 6H).

¹³C NMR (101 MHz, CDCl₃) δ 204.8, 56.6, 46.3, 35.7, 24.1, 21.2.; **¹³C NMR** (101 MHz, THF-*d*₈) δ 203.6, 56.1, 46.9, 36.6, 24.5, 21.9.

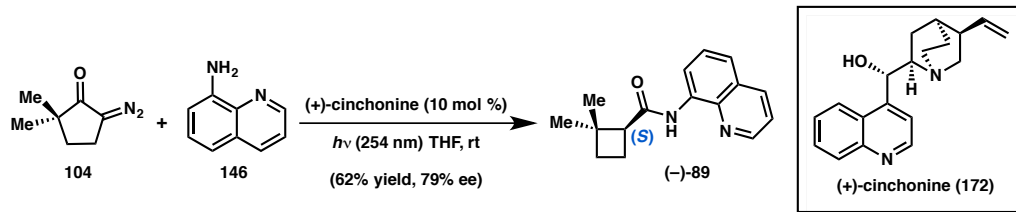
FTIR (NaCl, thin film) 3754, 3414, 3332, 2962, 2934, 2892, 2869, 2672, 2642, 2578, 2510, 2080, 1981, 1673, 1581, 1471, 1460, 1382, 1362, 1339, 1309, 1267, 1245, 1204, 1133, 1110, 1058, 1030, 994, 977, 948, 919, 893, 780, 726, 697 cm.⁻¹

HRMS (MM) calc'd for $C_7H_{11}N_2O$ $[M+H]^+$ 139.0866, found 139.0860.

Preparation of racemic cyclobutamide (\pm)-89**.**



To a flame-dried 200 mL flask were added carboxylic acid **145**¹⁷ (806 mg, 6.29 mmol), 8-aminoquinoline **146** (952 mg, 6.60 mmol, 1.05 equiv), and *N*-(3-dimethylaminopropyl)-*N'*-ethylcarbodiimide hydrochloride (1.45 g, 7.56 mmol, 1.20 equiv). The dry reagents were dissolved in CH_2Cl_2 (60 mL) and pyridine (610 μ L, 7.56 mmol, 1.20 equiv) was then added quickly via syringe. The reaction was stirred at room temperature for 18 hours, then diluted with H_2O and extracted with CH_2Cl_2 (2 x 50 mL). The combined organics were dried over $MgSO_4$, filtered, and concentrated *in vacuo*. The crude residue was purified by silica gel flash chromatography (isocratic: 5% EtOAc/Hexane) to give (\pm)-**89** (1.19 g, 74% yield) as a thick, pale yellow oil that solidified to a solid upon standing at $-20^\circ C$. For spectroscopic characterization data, see large-scale preparation detailed below.

Large-scale preparation of enantioenriched cyclobutamide (–)-**89**.

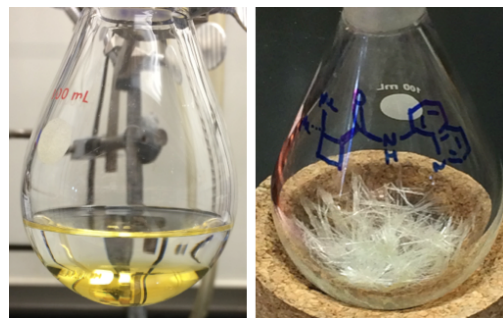
To a flame-dried, 1 L quartz flask were added 8-aminoquinoline (**146**) (12.9 g, 89.5 mmol, 3.00 equiv) and (+)-cinchonine (**172**) (879 mg, 2.99 mmol, 0.100 equiv). The flask was evacuated and backfilled with N₂ three times and dry THF (600 mL) was then added via cannula. Diazoketone **104** (4.12 g, 29.8 mmol, 1.00 equiv) was added last via syringe and the reaction was irradiated with stirring using a Honeywell 254 nm lamp at room temperature. Reaction progress was monitored by TLC (72-168 hours are typically required for complete conversion on this scale, and rotation of the flask every day provided faster conversion).⁵² Upon completion, the reaction mixture was concentrated *in vacuo*, the solids (**172**) were taken up in CH₂Cl₂, and the suspension filtered. The filter cake was washed with CH₂Cl₂ three times and the filtrate was concentrated *in vacuo* to give a crude residue that



was purified by silica gel flash chromatography (isocratic: 6% EtOAc/hexane) to provide **89** (4.69 g, 62% yield) as a pale-yellow solid. The enantiomeric excess was determined to be 79% by chiral SFC analysis (AD-H, 2.5 mL/min, 20% IPA in CO₂, $\lambda = 254$ nm): t_R (major) = 4.23 min, t_R (minor) = 5.64 min. $[\alpha]_D^{25.0} = -66.0^\circ$ ($c = 0.560$, CHCl₃).

Recrystallization procedure:

Enantioenriched cyclobutane **89** was dissolved in a minimal amount of CH₂Cl₂ in a 100 mL round-bottom flask. An equal amount of hexanes was carefully layered on top of the CH₂Cl₂ to form a biphasic mixture. The layers



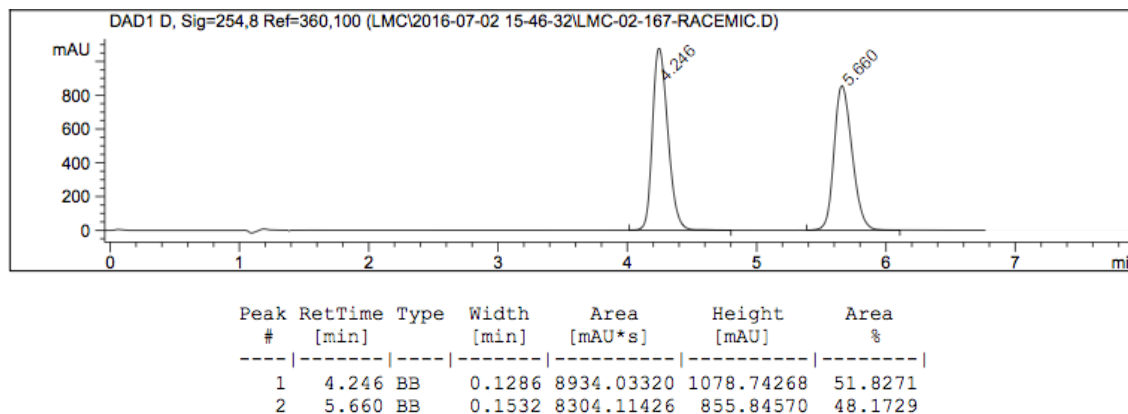
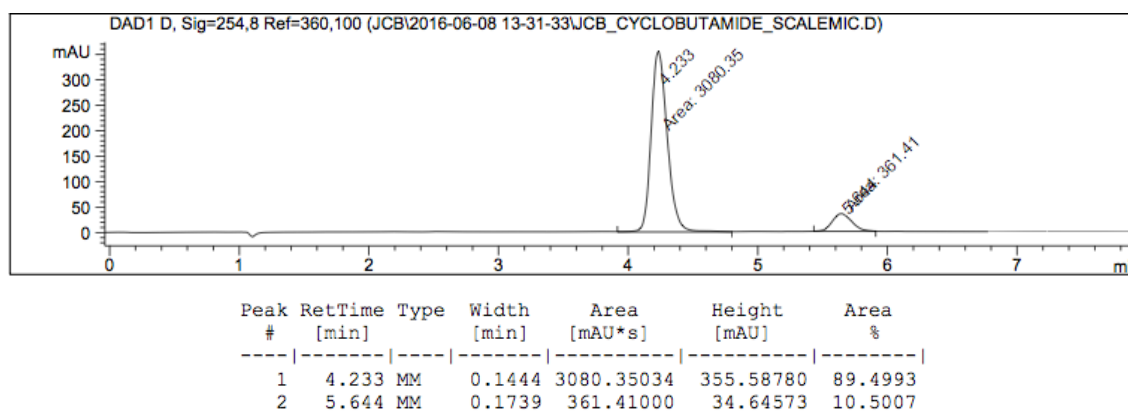
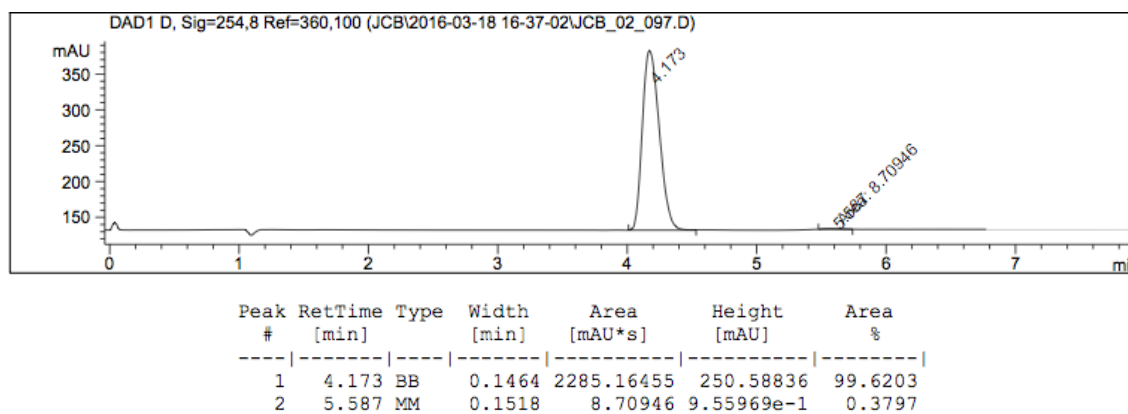
were allowed to diffuse overnight to provide (–)-**89** as white needles. The supernatant was concentrated under reduced pressure and this process was repeated again to provide additional (–)-**89** (3.50 g total, 83% recovery of theoretical total of the desired enantiomer, 46% overall yield from **104**): $[\alpha]_D^{25.0} = -109^\circ$ ($c = 0.720$, CHCl₃).

¹H NMR (400 MHz, CDCl₃) δ 9.68 (s, 1H), 8.80 (t, $J = 1.8$ Hz, 1H), 8.79 (dd, $J = 13.6$, 1.6 Hz, 1H), 8.15 (dd, $J = 8.3$, 1.7 Hz, 1H), 7.52 (q, $J = 8.2$, 7.5 Hz, 1H), 7.48 (dd, $J = 8.3$, 1.6 Hz, 1H), 7.45 (dd, $J = 8.3$, 4.2 Hz, 1H), 3.07 (ddd, $J = 9.1$, 8.2, 0.9 Hz, 1H), 2.48 (dq, $J = 11.4$, 9.4 Hz, 1H), 2.06 (dtd, $J = 11.6$, 8.6, 3.3 Hz, 1H), 1.85 (dt, $J = 10.8$, 9.1 Hz, 1H), 1.74 (dddd, $J = 10.7$, 9.5, 3.3, 0.9 Hz, 1H), 1.39 (s, 3H), 1.14 (s, 3H).

¹³C NMR δ 171.8, 148.3, 138.6, 136.4, 134.7, 128.1, 127.6, 121.7, 121.3, 116.4, 51.0, 40.4, 32.3, 30.9, 23.4, 17.4.

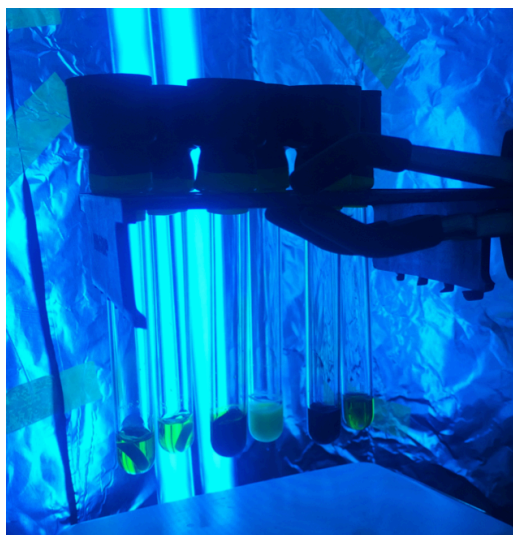
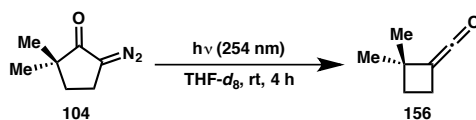
FTIR (NaCl, thin film) 3353, 3047, 2952, 2861, 1685, 1595, 1577, 1526, 1485, 1460, 1424, 1385, 1324, 1261, 1239, 1187, 1169, 1153, 825, 791, 756 cm.⁻¹

HRMS (MM) calc'd for C₁₆H₁₉N₂O [M+H]⁺ 255.1492, found 255.1501.

SFC data for racemic 89:**Enantioenriched 89 isolated directly from reaction:****Enantiopure (–)-89 after a single recrystallization:**

General small-scale protocol for the asymmetric Wolff rearrangement.

Inside a N₂-filled glovebox, six oven-dried 13 x 100 quartz test tubes were each charged with aminoquinoline **146** (14.4 mg, 0.100 mmol, 1.00 equiv) and the specified catalyst (typically, 20–50 mol %). Diazoketone **104** (13.8 mg, 0.100 mmol) was then added to each as a solution in 1.00 mL THF and the reactions fitted with a 19/38 rubber septum around the outside of each tube and sealed with electrical tape. The reactions were brought out of the glovebox and placed in a bottomless test tube rack in front of a Honeywell 254 nm lamp. The reactions were irradiated with stirring at room temperature for the indicated length of time (typically 18–24 hours). The reactions were then concentrated *in vacuo* and the crude reactions mixtures either analyzed by ¹H NMR with an added internal standard, or purified by silica gel flash chromatography (isocratic: 6% EtOAc/hexane) to provide **89** in varying yields and enantiopurities.

***In situ* generation of ketene **156**.**

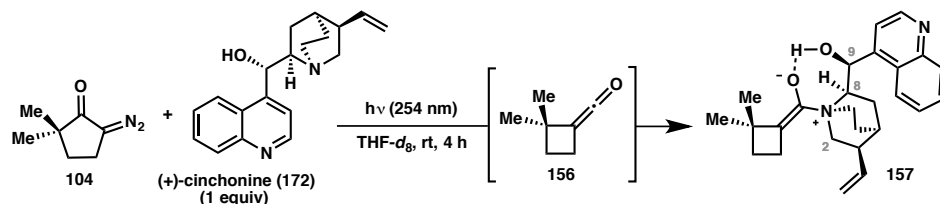
Inside a N₂-filled glovebox, an oven-dried quartz tube was charged with diazoketone **104** (13.8 mg, 0.100 mmol) and dissolved in THF-*d*₈ (750 μL). The reaction was fitted with a 19/38 rubber septum around the outside of the tube and sealed with

electrical tape. The reaction was brought out of the glovebox and irradiated for 4 hours in front of a Honeywell 254 nm lamp, as described above. The reaction mixture was then opened to air and pipetted directly into a dry NMR tube for immediate spectroscopic analysis.⁵³

¹H NMR (400 MHz, THF-*d*₈) δ 2.20 (t, *J* = 7.9 Hz, 2H), 1.66 (t, *J* = 8.1 Hz, 2H), 1.19 (s, 6H).

¹³C NMR (101 MHz, THF-*d*₈) δ 209.1, 78.8, 45.9, 30.9, 25.9, 22.0.

Spectroscopic observation of zwitterion **157**.



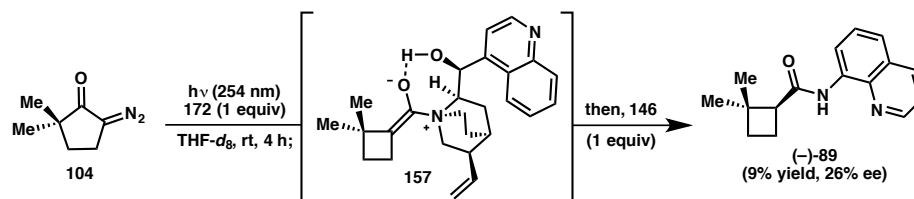
Inside a N₂-filled glovebox, an oven-dried quartz tube was charged with (+)-cinchonine (**172**) (29.4 mg, 0.100 mmol, 1.00 equiv) and suspended in THF-*d*₈ (750 μ L). Diazoketone **104** (13.8 mg, 0.100 mmol) was then added, and the reaction was fitted with a 19/38 rubber septum around the outside of the tube and sealed with electrical tape. The reaction was brought out of the glovebox and irradiated for 4 hours in front of a Honeywell 254 nm lamp, as described above. The reaction mixture was then opened to air and excess **172** was removed by rapid filtration through a 0.45 μ m Whatman syringe filter. The filtrate was added directly to a dry NMR tube for immediate spectroscopic analysis and compared against the ¹H for spectrum for **172**:

Key signals in (+)-cinchonine (**172**) are bolded below:

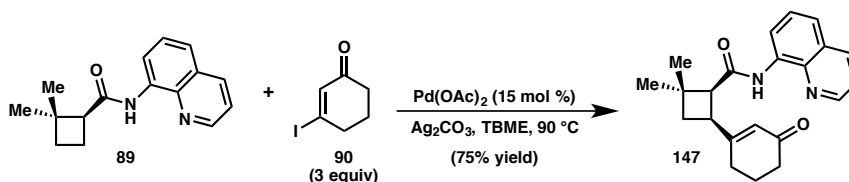
¹H NMR (400 MHz, THF-*d*₈) δ 8.78 (d, *J* = 4.4 Hz, 1H), 8.17 (dd, *J* = 8.5, 1.3 Hz, 1H), 8.02 (dd, *J* = 8.5, 1.4 Hz, 1H), 7.62 (ddd, *J* = 8.4, 6.8, 1.5 Hz, 1H), 7.54 (d, *J* = 4.5 Hz, 1H), 7.50 (ddd, *J* = 8.3, 6.8, 1.5 Hz, 1H), 6.15 (ddd, *J* = 17.2, 10.3, 7.9 Hz, 1H), **5.49 (C9: d, *J* = 4.3 Hz, 1H)**, 5.10 – 4.96 (m, 2H), 4.90 (d, *J* = 3.9 Hz, 1H), **3.25 (C2: ddd, *J* = 13.7, 7.7, 2.4 Hz, 1H)**, **3.02 (C8: td, *J* = 9.0, 5.1 Hz, 1H)**, 2.82 – 2.70 (m, 2H), 2.67 – 2.61 (m, 1H), 2.19 (q, *J* = 8.4 Hz, 1H), 2.10 (ddd, *J* = 13.0, 8.7, 2.0 Hz, 1H), 1.68 (t, *J* = 2.4 Hz, 1H), 1.50 – 1.43 (m, 2H), 1.27 (dddd, *J* = 13.8, 9.4, 4.7, 1.7 Hz, 1H).

Key signals in **157** that have shifted or appeared are bolded below:

¹H NMR (400 MHz, THF-*d*₈) δ 8.78 (d, *J* = 4.5 Hz, 1H), 8.18 (dd, *J* = 8.5, 1.3 Hz, 1H), 8.07 – 7.98 (m, 1H), 7.63 (ddd, *J* = 8.4, 6.8, 1.4 Hz, 1H), 7.55 (dd, *J* = 4.5, 0.7 Hz, 1H), 7.50 (ddd, *J* = 8.3, 6.8, 1.4 Hz, 1H), 6.15 (ddd, *J* = 17.2, 10.3, 7.9 Hz, 1H), **5.55 (C9: d, *J* = 5.1 Hz, 1H)**, 5.09 – 4.96 (m, 2H), **3.31 (C2: ddd, *J* = 13.7, 7.7, 2.4 Hz, 1H)**, **3.05 (C8: td, *J* = 8.7, 4.3 Hz, 1H)**, **2.96 (dddd, *J* = 9.2, 8.2, 5.6, 1.0 Hz, 1H)**, 2.85 – 2.71 (m, 3H), 2.66 (dt, *J* = 13.2, 8.7 Hz, 1H), 2.17 – 2.04 (m, 2H), **1.96 – 1.77 (m, 3H)**, 1.48 (dddd, *J* = 8.9, 4.7, 3.6, 1.8 Hz, 3H), **1.23 (s, 3H)**, **1.14 (s, 3H)**.

Stepwise preparation of **89 by discrete formation of zwitterion **157**.**

Inside a N₂-filled glovebox, an oven-dried quartz tube was charged with (+)-cinchonine (**172**) (29.4 mg, 0.100 mmol, 1.00 equiv) and suspended in THF-*d*₈ (750 μL). Diazoketone **104** (13.8 mg, 0.100 mmol) was then added, and the reaction was fitted with a 19/38 rubber septum around the outside of the tube and sealed with electrical tape. The reaction was brought out of the glovebox and irradiated for 4 hours in front of a Honeywell 254 nm lamp, as described above. The reaction mixture was then opened to air and solid aminoquinoline **146** (14.4 mg, 0.100 mmol, 1.00 equiv) was added in one portion. The reaction was stirred at room temperature (without irradiation) overnight. The reaction mixture was concentrated *in vacuo* and the crude residue purified by preparative thin-layer chromatography (20% EtOAc/Hexane) to afford **89** (2.20 mg, 8.7% yield). The enantiomeric excess was determined to be 26% by chiral SFC analysis (AD-H, 2.5 mL/min, 20% IPA in CO₂, λ = 254 nm): *t*_R(major) = 4.23 min, *t*_R(minor) = 5.64 min.

Preparation of *cis*-cyclobutane 147.

To a flame-dried 150 mL pressure vessel were added cyclobutane **89** (2.87 g, 11.3 mmol), vinyl iodide **90**⁵⁴ (7.50 g, 33.8 mmol, 3.00 equiv), Pd(OAc)₂ (379 mg, 1.69 mmol, 0.150 equiv), and Ag₂CO₃ (3.11 g, 11.3 mmol, 1.00 equiv). The reagents were suspended in TBME (56.0 mL) and the vessel sealed under ambient conditions. The reaction was heated to 90 °C for 16 hours, then cooled to room temperature and filtered over a pad of celite. The filtrate was concentrated directly onto celite and purified by silica gel flash chromatography (20–40% EtOAc/hexane) to afford *cis*-cyclobutane **147** (2.95 g, 75% yield) as a pale yellow foam: $[\alpha]_D^{25.0} = +84.4^\circ$ ($c = 0.350$, CHCl₃).

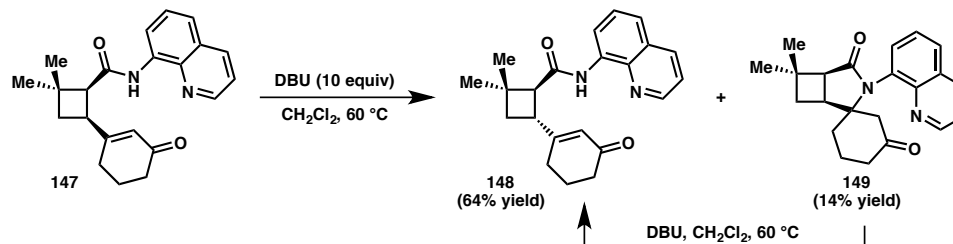
¹H NMR (500 MHz, CDCl₃) δ 9.73 (s, 1H), 8.78 (dd, $J = 12.4, 2.1$ Hz, 1H), 8.78 (t, $J = 1.8$ Hz, 1H), 8.16 (dd, $J = 8.3, 1.7$ Hz, 1H), 7.51 (dd, $J = 8.3, 5.0$ Hz, 1H), 7.50 (d, $J = 0.9$ Hz, 1H), 7.45 (dd, $J = 8.3, 4.2$ Hz, 1H), 6.00 (q, $J = 1.6$ Hz, 1H), 3.45 (dddd, $J = 10.8, 8.5, 7.6, 2.1, 1.0$ Hz, 1H), 3.27 (ddd, $J = 8.8, 2.8, 0.8$ Hz, 1H), 2.48 (t, $J = 10.8$ Hz, 1H), 2.31 (ddd, $J = 7.5, 5.7, 3.5$ Hz, 2H), 2.20 (qd, $J = 6.0, 5.5, 1.1$ Hz, 2H), 2.01 (ddd, $J = 11.0, 8.3, 2.8$ Hz, 1H), 1.95 – 1.84 (m, 2H), 1.46 (s, 3H), 1.13 (s, 3H).

¹³C NMR (126 MHz, CDCl₃) δ 199.5, 170.2, 166.5, 148.3, 138.4, 136.3, 134.4, 127.9, 127.4, 124.9, 121.6, 121.5, 116.5, 56.9, 37.5, 37.5, 36.8, 35.7, 29.9, 27.8, 24.9, 22.6.

FTIR (NaCl, thin film) 3348, 2929, 2865, 1662, 1623, 1595, 1576, 1522, 1485, 1424, 1386, 1347, 1322, 1258, 1191, 1165, 1132, 827, 793 cm.⁻¹

HRMS (MM) calc'd for $C_{22}H_{25}N_2O_2$ $[M+H]^+$ 349.1911, found 349.1910.

Preparation of *trans*-cyclobutane **148 and spirolactam **149**.**



To a 150 mL pressure vessel were added *cis*-cyclobutane **148** (2.74 g, 7.86 mmol) and wet CH_2Cl_2 (27.5 mL). The colorless solution was treated with DBU (11.7 mL, 78.6 mmol, 10.0 equiv) and a bright yellow color was observed immediately. The vessel was sealed under ambient conditions and heated to 60 °C for 20 hours. The reaction mixture was diluted with 100 mL of water and 100 mL of CH_2Cl_2 . The layers were separated, and the aqueous layer was extracted with CH_2Cl_2 (3 x 50 mL). The combined organic layers were dried over Na_2SO_4 , filtered, and concentrated *in vacuo*. The crude residue was purified by silica gel flash chromatography (isocratic: 40% EtOAc/hexane until **148** eluted completely, then 10% MeOH/ CH_2Cl_2) to afford **148** (1.74 g, 64% yield) and **149** (367 mg, 14% yield), each as a pale yellow solid.

Data for *trans*-cyclobutane **148**: $[\alpha]_D^{25.0} = -129.0^\circ$ ($c = 1.43$, $CHCl_3$).

1H NMR (500 MHz, $CDCl_3$) δ 9.68 (s, 1H), 8.79 (dd, $J = 4.2, 1.7$ Hz, 1H), 8.73 (dd, $J = 7.2, 1.8$ Hz, 1H), 8.15 (dd, $J = 8.3, 1.7$ Hz, 1H), 7.52 (dd, $J = 8.3, 7.2$ Hz, 1H), 7.49 (dd, $J = 8.3, 1.8$ Hz, 1H), 7.44 (dd, $J = 8.3, 4.2$ Hz, 1H), 5.92 (q, $J = 1.5$ Hz, 1H), 3.58 (ddq, $J = 18.5, 8.7, 1.6, 0.8, 0.8$ Hz, 1H), 2.97 (dd, $J = 9.8, 0.7$ Hz, 1H), 2.41 – 2.29 (m, 4H), 2.05 – 1.92 (m, 3H), 1.85 (t, $J = 10.4$ Hz, 1H), 1.40 (s, 3H), 1.19 (s, 3H).

¹³C NMR (126 MHz, CDCl₃) δ 199.8, 169.6, 167.5, 148.3, 138.3, 136.3, 134.2, 127.9, 127.3, 123.9, 121.7, 121.5, 116.3, 55.5, 37.5, 36.8, 36.4, 36.3, 30.7, 27.6, 23.1, 22.6.

FTIR (NaCl, thin film) 3344, 3046, 2952, 2865, 2246, 1669, 1623, 1595, 1577, 1526, 1485, 1461, 1424, 1323, 1346, 1326, 1292, 1253, 1191, 1161, 1133, 915, 884, 827, 792, 757, 731 cm.⁻¹

HRMS (MM) calc'd for C₂₂H₂₅N₂O₂ [M+H]⁺ 349.1911, found 349.1919.

For X-Ray crystallographic analysis of **148**, see Appendix 2.

Data for spirolactam **149**, 2.5:1 mixture of diastereomers: $[\alpha]_D^{25.0} = -56.5^\circ$ (c = 1.085, CHCl₃).

¹H NMR (asterisk denotes minor diast., 400 MHz, CDCl₃) δ 8.92 (dd, *J* = 4.1, 1.8 Hz, 1H), 8.85* (dd, *J* = 4.1, 1.8 Hz, 1H), 8.17 (dd, *J* = 8.3, 1.8 Hz, 1H), 8.13* (dd, *J* = 8.3, 1.8 Hz, 1H), 7.87 (dd, *J* = 8.3, 1.5 Hz, 1H), 7.63 – 7.53 (m, 2H), 7.49 (dd, *J* = 7.2, 1.5 Hz, 1H), 7.42 (dd, *J* = 8.3, 4.1 Hz, 1H), 7.37* (dd, *J* = 8.3, 4.1 Hz, 1H), 3.07* (ddd, *J* = 7.3, 3.2, 0.9 Hz, 1H), 2.93 (dd, *J* = 6.0, 3.3 Hz, 1H), 2.86 (d, *J* = 13.2 Hz, 1H), 2.83 – 2.73 (m, 1H), 2.53 (dt, *J* = 13.1, 2.4 Hz, 1H), 2.41 – 2.33 (m, 1H), 2.27 (ddq, *J* = 15.1, 11.3, 2.1 Hz, 1H), 2.15 – 1.94 (m, 2H), 1.94 – 1.83 (m, 1H), 1.71 (dtd, *J* = 13.2, 8.6, 7.6, 3.0 Hz, 1H), 1.52 – 1.38* (m, 1H), 1.35 (s, 3H), 1.34* (s, 3H), 1.31 (s, 3H), 1.14* (s, 3H), 1.03 (td, *J* = 13.7, 4.0 Hz, 1H).

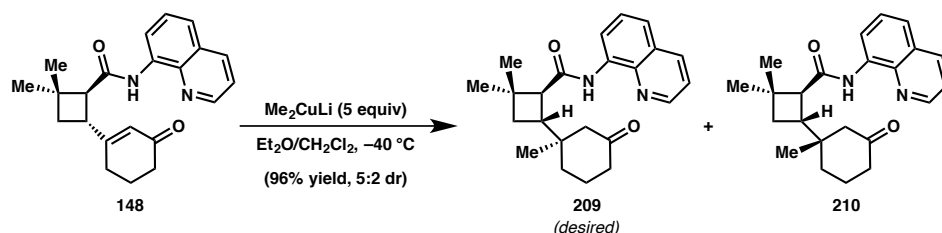
^{13}C NMR (major diastereomer, 101 MHz, CDCl_3) δ 209.2, 175.5, 150.7, 146.3, 136.1, 134.2, 130.7, 129.6, 129.1, 126.2, 121.9, 69.2, 53.2, 49.9, 40.7, 35.8, 34.8, 34.1, 30.2, 29.0, 25.6, 20.1.

^{13}C NMR (minor diastereomer, 101 MHz, CDCl_3) δ 210.0, 175.5, 150.7, 145.6, 136.0, 134.2, 131.5, 129.6, 129.2, 126.0, 121.7, 68.9, 52.9, 49.8, 40.4, 35.0, 34.8, 34.6, 31.3, 30.0, 26.1, 20.1.

FTIR (NaCl, thin film) 3356, 3039, 2953, 2933, 2866, 1705, 1687, 1616, 1596, 1574, 1525, 1496, 1472, 1426, 1391, 1341, 1312, 1279, 1250, 1223, 1134, 1124, 1038, 1027, 905, 831, 795, 753, 664, 643 cm^{-1} .

HRMS (MM) calc'd for $\text{C}_{22}\text{H}_{25}\text{N}_2\text{O}_2$ $[\text{M}+\text{H}]^+$ 349.1911, found 349.1916.

Preparation of ketones 209 and 210 using Gilman's reagent.



To a flame-dried 100 mL flask was added copper (I) iodide (1.48 g, 7.75 mmol, 5.00 equiv) and Et_2O (15.5 mL). The resulting suspension was cooled to $-40\text{ }^\circ\text{C}$ and methyllithium (1.6 M in Et_2O ; 9.68 mL, 15.5 mmol, 10 equiv) was added dropwise. The reaction mixture was stirred at $-40\text{ }^\circ\text{C}$ for 2 hours before **148** (540 mg, 1.55 mmol) was added dropwise as a solution in 5:2 $\text{CH}_2\text{Cl}_2/\text{Et}_2\text{O}$. The reaction mixture was gradually

warmed to 0 °C over 4 hours, then quenched with saturated aqueous NH_4Cl (10 mL) and diluted with EtOAc. NH_4OH was added until all of the solid copper salts were sequestered and two homogenous layers remained. The aqueous layer was extracted with EtOAc (3 x 20 mL) and the combined organics dried over MgSO_4 , filtered, and concentrated *in vacuo*. The crude residue was purified by silica gel flash chromatography (isocratic: 20% EtOAc/Hexane) to afford a 5:2 mixture of **209** and **210** (543 mg, 96% yield), respectively as a white amorphous solid. Subsequent purification by reverse-phase HPLC using two Agilent Eclipse XDB-C8 5 μm 9.4 x 250 mm columns connected in series (gradient: 77–85% MeCN/ H_2O) afforded analytically pure samples of each diastereomer, from which **210** was crystallized (for X-Ray analysis, see Appendix 2).

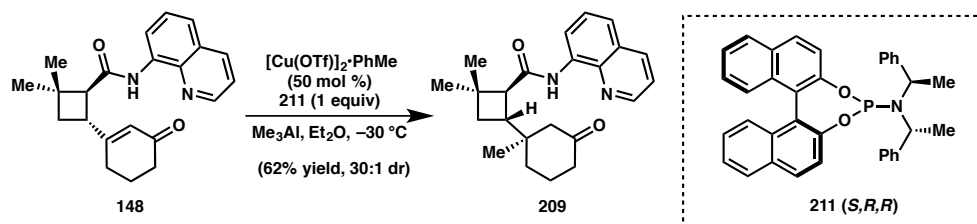
Data for minor diastereomer **210**: $[\alpha]_D^{25.0} = -25.5^\circ$ ($c = 1.50$, CHCl_3).

^1H NMR (500 MHz, CDCl_3) δ 9.64 (s, 1H), 8.82 (dd, $J = 4.2, 1.7$ Hz, 1H), 8.75 (dd, $J = 7.4, 1.6$ Hz, 1H), 8.17 (dd, $J = 8.3, 1.7$ Hz, 1H), 7.56 – 7.48 (m, 2H), 7.46 (dd, $J = 8.2, 4.2$ Hz, 1H), 2.89 – 2.77 (m, 2H), 2.35 – 2.26 (m, 2H), 2.24 (d, $J = 13.3$ Hz, 1H), 2.09 (d, $J = 13.4$ Hz, 1H), 2.07 – 1.99 (m, 1H), 1.88 – 1.77 (m, 1H), 1.72 – 1.61 (m, 3H), 1.55 – 1.48 (m, 1H), 1.35 (s, 3H), 1.13 (s, 3H), 0.92 (s, 3H).

^{13}C NMR (126 MHz, CDCl_3) δ 212.4, 170.6, 148.4, 138.5, 136.5, 134.6, 128.1, 127.6, 121.7, 121.4, 116.4, 51.5, 50.8, 41.2, 39.8, 39.6, 35.2, 34.1, 33.0, 30.8, 23.7, 22.2, 21.3.

FTIR (NaCl, thin film) 3349, 3044, 2952, 2863, 1706, 1687, 1595, 1577, 1523, 1484, 1460, 1424, 1383, 1325, 1238, 1228, 1163, 827, 792 cm^{-1} .

HRMS (MM) calc'd for $\text{C}_{23}\text{H}_{29}\text{N}_2\text{O}_2$ $[\text{M}+\text{H}]^+$ 365.2224, found 365.2261.

Selective preparation of ketone **209 using copper-catalyzed conjugate addition.**

Inside a N_2 -filled glovebox, $[\text{Cu}(\text{OTf})_2] \cdot \text{PhMe}$ (72.4 mg, 0.140 mmol, 0.25 equiv) and (*S,R,R*) ligand **211**⁵⁵ (302 mg, 0.560 mmol, 1.00 equiv) were added to a 25 mL flask. The reagents were suspended in Et_2O (5.60 mL) and stirred at room temperature for 30 mins before *trans*-enone **148** (195 mg, 0.560 mmol) was added as a solid, in one portion. The reaction was sealed under N_2 , removed from the glovebox and cooled to $-30\text{ }^\circ\text{C}$ under argon using a cryocool unit to control the temperature. Me_3Al (2.0 M in heptane; 560 μL , 1.12 mmol, 2.00 equiv) was then added dropwise, taking care to avoid an exotherm and the reaction mixture stirred vigorously at $-30\text{ }^\circ\text{C}$ for 16 hours. MeOH (1.00 mL) was then added to quench excess Me_3Al and then the reaction was warmed to room temperature. The mixture was diluted with EtOAc and H_2O , then the organic layer was separated. The aqueous layer was extracted with EtOAc (3 x 5 mL) and the combined organics dried over MgSO_4 , filtered, and concentrated *in vacuo*. The crude residue was purified by silica gel flash chromatography (2% $\text{Et}_2\text{O}/\text{CH}_2\text{Cl}_2$ until ligand/impurities elute, then 4% $\text{Et}_2\text{O}/\text{CH}_2\text{Cl}_2$) to afford a 30:1 mixture of **209** and **210** (126 mg, 62% yield), respectively as a white solid: $[\alpha]_D^{25.0} = -84.7^\circ$ ($c = 0.600$, CHCl_3).

^1H NMR (400 MHz, CDCl_3) δ 9.64 (s, 1H), 8.81 (dd, $J = 4.2, 1.7$ Hz, 1H), 8.75 (dd, $J = 7.2, 1.8$ Hz, 1H), 8.16 (dd, $J = 8.3, 1.7$ Hz, 1H), 7.56 – 7.47 (m, 2H), 7.45 (dd, $J = 8.3, 4.2$ Hz, 1H), 2.89 – 2.76 (m, 2H), 2.36 – 2.28 (m, 2H), 2.25 (ddd, $J = 12.5, 6.6, 1.1$ Hz,

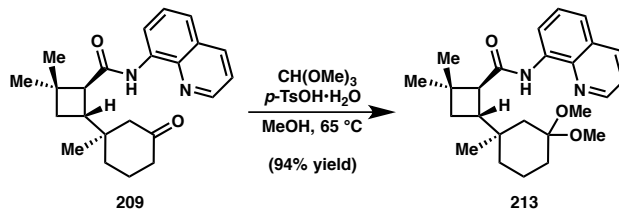
1H), 2.04 (dt, $J = 13.4, 2.0$ Hz, 1H), 1.96 (ddq, $J = 13.7, 7.0, 3.6$ Hz, 1H), 1.81 (dtt, $J = 13.7, 12.0, 5.0$ Hz, 1H), 1.68 – 1.62 (m, 2H), 1.62 – 1.51 (m, 2H), 1.35 (s, 3H), 1.13 (s, 3H), 0.89 (s, 3H).

^{13}C NMR (101 MHz, CDCl_3) δ 212.4, 170.6, 148.3, 138.5, 136.5, 134.6, 128.1, 127.5, 121.7, 121.4, 116.4, 51.5, 50.4, 41.3, 40.9, 39.5, 35.2, 33.8, 32.6, 30.8, 23.7, 22.1, 20.8.

FTIR (NaCl, thin film) 3351, 3047, 2954, 2870, 1708, 1688, 1524, 1485, 1460, 1424, 1384, 1325, 1281, 1259, 1240, 1228, 1163, 919, 827, 792, 757, 732 cm^{-1} .

HRMS (MM) calc'd for $\text{C}_{23}\text{H}_{29}\text{N}_2\text{O}_2$ $[\text{M}+\text{H}]^+$ 365.2224, found 365.2228

Preparation of dimethyl ketal 213.



To a flame-dried 15 mL flask was added ketone **209** (100 mg, 0.274 mmol) and dissolved in freshly distilled MeOH (2.7 mL). Trimethylorthoformate (150 μL , 1.37 mmol, 5.00 equiv) was then added, followed by *p*-toluenesulfonic acid monohydrate (2.60 mg, 0.014 mmol, 0.05 equiv). The reaction was topped with a reflux condenser and heated to 65 °C for 1 hour, then quenched with saturated aqueous NaHCO_3 . The aqueous layer was extracted with EtOAc (3 x 5 mL), and the combined organics were dried over MgSO_4 , filtered, and concentrated *in vacuo*. The crude residue was purified by Florisil[®]

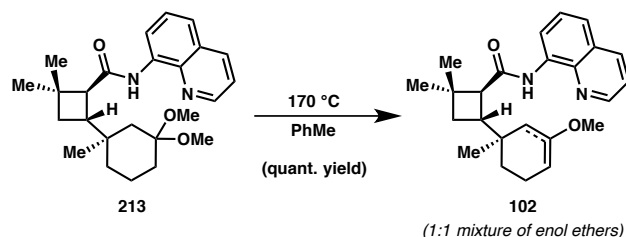
flash chromatography (isocratic: 10% EtOAc/Hexane) to afford **213** (106 mg, 94% yield) as a white, foamy solid: $[\alpha]_D^{25.0} = -83.3^\circ$ ($c = 1.60$, CHCl_3).

^1H NMR (400 MHz, CDCl_3) δ 9.66 (s, 1H), 8.81 (dd, $J = 4.3, 1.7$ Hz, 1H), 8.78 (dd, $J = 7.4, 1.6$ Hz, 1H), 8.14 (dd, $J = 8.3, 1.7$ Hz, 1H), 7.56 – 7.46 (m, 2H), 7.44 (dd, $J = 8.3, 4.2$ Hz, 1H), 3.16 (s, 3H), 3.13 (s, 3H), 2.80 (d, $J = 10.0$ Hz, 1H), 2.69 (q, $J = 9.7$ Hz, 1H), 2.01 (ddd, $J = 13.2, 3.5, 1.6$ Hz, 1H), 1.74 (dt, $J = 14.0, 2.4$ Hz, 1H), 1.70 – 1.50 (m, 4H), 1.31 (s, 3H), 1.28 – 1.13 (m, 4H), 1.11 (s, 3H), 1.01 (s, 3H).

^{13}C NMR (101 MHz, CDCl_3) δ 171.0, 148.3, 138.5, 136.4, 134.7, 128.0, 127.6, 121.6, 121.2, 116.4, 100.8, 51.3, 47.9, 47.3, 42.3, 38.6, 34.8, 34.7, 34.0, 33.3, 32.5, 30.7, 23.9, 21.4, 18.8.

FTIR (NaCl, thin film) 3356, 3048, 2950, 2867, 2828, 1690, 1525, 1485, 1460, 1424, 1384, 1368, 1325, 1288, 1276, 1261, 1242, 1155, 1108, 1096, 1048, 946, 927, 826, 792, 756, 690, 666 cm^{-1} .

HRMS (MM) calc'd for $\text{C}_{24}\text{H}_{31}\text{N}_2\text{O}_2$ $[\text{M}-\text{OCH}_3]^+$ 379.2380, found 379.2376.

Preparation of methyl enol ether 102.

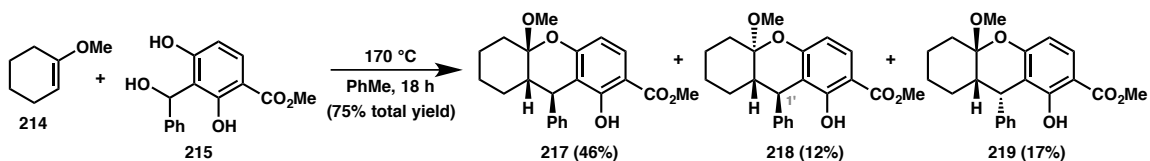
To a 15 mL thick-walled, screw top pressure vessel were added dimethyl ketal **213** (59.8 mg, 0.146 mmol) and PhMe (5.0 mL). The tube sealed under a stream of N₂. The reaction was heated to 170 °C in a preheated oil bath for 3.5 hours. The reaction was then cooled to room temperature and concentrated *in vacuo* to afford **102** (55.1 mg, quantitative yield), an inseparable ~1:1 mixture of enol ether isomers, as a foamy colorless gum: $[\alpha]_D^{25.0} = -78.8^{\circ}$ (c = 1.25, CHCl₃).

¹H NMR (400 MHz, CDCl₃) δ 9.70 (s, 1H), 8.90 – 8.72 (m, 2H), 8.15 (dd, *J* = 8.2, 1.5 Hz, 1H), 7.57 – 7.40 (m, 3H), 4.48 (s, 1H), 3.48 (s, 3H), 2.87 – 2.74 (m, 2H), 2.12 – 1.93 (m, 2H), 1.74 – 1.57 (m, 4H), 1.48 – 1.36 (m, 1H), 1.33 (s, 3H), 1.31 – 1.27 (m, 1H), 1.12 (s, 3H), 0.97 (s, 3H).

¹³C NMR (101 MHz, CDCl₃) δ 171.6, 171.0, 156.3, 154.3, 148.3, 148.3, 138.6, 138.5, 136.4, 136.4, 134.8, 134.7, 128.5, 128.1, 128.1, 127.6, 126.9, 126.8, 121.7, 121.6, 121.2, 121.2, 116.4, 116.3, 99.4, 92.1, 54.1, 53.9, 52.6, 51.5, 40.9, 40.1, 36.4, 35.4, 35.2, 34.0, 33.5, 33.0, 32.6, 30.9, 30.8, 30.7, 29.9, 28.2, 26.1, 25.1, 24.1, 23.9, 21.2, 20.7, 19.5.

FTIR (NaCl, thin film) 3354, 3051, 2949, 2930, 2862, 1690, 1668, 1524, 1484, 1461, 1424, 1384, 1368, 1326, 1238, 1215, 1162, 1147, 1026, 826, 791, 756, 694 cm.⁻¹

HRMS (MM) calc'd for C₂₄H₃₁N₂O₂ [M+H]⁺ 379.2380, found 379.2395.

Preparation of model methoxy ketals 217–219.

To a flame-dried 50 mL thick-walled, screw top pressure vessel were added *o*-QM precursor **215**⁴² (308 mg, 1.12 mmol), enol ether **214**⁵⁶ (756 mg, 6.74 mmol, 6.00 equiv) and PhMe (19.0 mL). The vessel was sealed under a stream of N₂ and heated to 170 °C for 18 hours. The reaction mixture was concentrated *in vacuo* and the crude residue was purified by silica gel flash chromatography (2 – 10% Et₂O/Hexane) to afford a 4:1 inseparable mixture of **217** and **218** (238 mg total, 46% and 12% yield, respectively), and **219** (69.8 mg, 17% yield), each as white solids.

Data for **217** and **218**:

¹H NMR (4:1 dr, asterisk denotes minor diastereomer, 400 MHz, CDCl₃) δ 11.15 (s, 1H), δ 10.91* (s, 1H), 7.77 (dd, *J* = 8.9, 0.6 Hz, 1H), 7.68* (dd, *J* = 8.8, 0.7 Hz, 1H), 7.26 – 7.20 (m, 2H), 7.14 (t, *J* = 7.3 Hz, 1H), 7.08 (d, *J* = 6.9 Hz, 2H), 6.57 (d, *J* = 8.8 Hz, 1H), 6.49* (d, *J* = 8.8 Hz, 1H), 3.95 (s, 1H), 3.90 (s, 3H), 3.83* (s, 3H), 3.74* (d, *J* = 10.9 Hz, 1H), 3.17* (s, 3H), 3.04 (s, 3H), 2.42 – 2.35* (m, 1H), 2.35 – 2.22 (m, 2H), 1.90 – 1.82 (m, 1H), 1.80* (ddd, *J* = 12.1, 10.9, 3.9 Hz, 1H), 1.77 – 1.68 (m, 2H), 1.72 – 1.64* (m, 2H), 1.64 – 1.58* (m, 1H), 1.52 – 1.43 (m, 1H), 1.45* (ddt, *J* = 11.2, 7.3, 3.0 Hz, 2H), 1.42 – 1.32* (m, 1H), 1.36 (ddd, *J* = 9.9, 8.2, 2.5 Hz, 3H), 1.11* (tdd, *J* = 13.3, 8.3, 4.0 Hz, 1H).

^{13}C NMR (**217**, major diastereomer, 101 MHz, CDCl_3) δ 170.8, 162.1, 158.2, 145.6, 129.3, 127.7, 127.5, 125.6, 110.7, 109.1, 105.5, 101.0, 52.1, 47.5, 45.4, 42.1, 32.8, 31.5, 25.3, 22.9.

^{13}C NMR (**218**, minor diastereomer 101 MHz, CDCl_3) δ 170.7, 161.5, 158.3, 145.5, 129.2, 128.0, 127.7, 125.8, 115.5, 109.1, 106.0, 100.2, 52.0, 48.8, 48.4, 41.7, 30.9, 26.9, 25.4, 22.6.

FTIR (NaCl, thin film) 3138 (br), 3085, 3061, 3025, 3002, 2937, 2858, 2832, 1666, 1621, 1590, 1492, 1438, 1368, 1340, 1295, 1251, 1217, 1198, 1140, 1100, 1082, 1058, 1014, 979, 936, 924, 885, 827, 816, 787, 753, 699 cm^{-1} .

HRMS (ESI) calc'd for $\text{C}_{22}\text{H}_{25}\text{O}_5$ $[\text{M}+\text{H}]^+$ 369.1697, found 369.1704.

Data for **219**:

^1H NMR (400 MHz, CDCl_3) δ 11.14 (s, 1H), 7.72 (dd, $J = 8.8, 0.9$ Hz, 1H), 7.43 – 7.24 (br m, 2H), 7.20 (t, $J = 7.1$ Hz, 2H), 7.12 – 6.76 (br m, 1H), 6.51 (d, $J = 8.8$ Hz, 1H), 4.68 (d, $J = 6.9$ Hz, 1H), 3.87 (s, 3H), 3.24 (s, 3H), 2.51 – 2.39 (m, 1H), 1.99 (ddd, $J = 12.5, 6.9, 4.3$ Hz, 1H), 1.77 – 1.65 (m, 1H), 1.60 (dd, $J = 6.7, 4.3$ Hz, 1H), 1.52 (tt, $J = 12.9, 3.8$ Hz, 1H), 1.37 (td, $J = 13.2, 4.5$ Hz, 1H), 1.07 – 0.97 (m, 2H), 0.92 – 0.84 (m, 1H).

^{13}C NMR (101 MHz, CDCl_3) δ 170.9, 162.1, 158.9, 141.8, 129.2, 128.3, 125.8, 111.9, 109.3, 105.9, 100.9, 52.1, 48.6, 43.6, 39.2, 32.6, 25.7, 25.3, 22.7.

FTIR (NaCl, thin film) 3134 (br), 3061, 3085, 3024, 3006, 2952, 2938, 1667, 1618, 1588, 1490, 1438, 1422, 1341, 1292, 1256, 1242, 1219, 1200, 1174, 1142, 1120, 1098, 1054, 1033, 1014, 976, 923, 886, 869, 806, 782, 761, 702, 632 cm^{-1} .

HRMS (ESI) calc'd for $\text{C}_{21}\text{H}_{21}\text{O}_4$ $[\text{M}-\text{OCH}_3]^+$ 337.1434, found 337.1443.

Preparation of benzhydryl morpholine **222**.



To a flame-dried 100 mL round-bottom flask were added phloroglucinol **221** (1.00g, 4.13 mmol), followed by freshly distilled MeOH (41.0 mL). Benzaldehyde (421 μL , 4.13 mmol, 1.00 equiv), morpholine (361 μL , 4.13 mmol, 1.00 equiv), and triethylamine (576 μL , 4.13 mmol, 1.00 equiv) were then added successively via syringe and the reaction stirred at room temperature for 24 hours. The precipitate thus formed was collected by vacuum filtration and washed with MeOH (20 mL) and dried under high vacuum to afford analytically pure **222** (1.19 g, 69% yield) as a white powder.

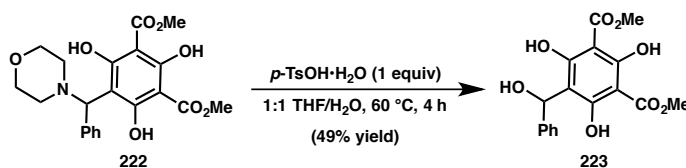
¹H NMR (400 MHz, CDCl_3) δ 15.34 (s, 1H), 13.16 (s, 1H), 12.53 (s, 1H), 7.45 (d, J = 7.2 Hz, 2H), 7.34 – 7.20 (m, 3H), 4.88 (s, 1H), 3.99 (s, 3H), 3.91 (s, 3H), 3.90 – 3.40 (br m, 4H), 3.08 (br s, 1H), 2.46 (ddd, J = 11.9, 6.2, 3.1 Hz, 2H), 2.18 (br s, 1H).

¹³C NMR (101 MHz, CDCl_3) δ 171.7, 166.2, 165.6, 165.1, 138.2, 128.9, 128.4, 103.8, 96.5, 94.2, 69.0, 66.6, 52.7, 52.6.

FTIR (NaCl, thin film) 3404 (br), 3062, 3030, 2955, 2894, 2854, 2716, 2562 (br), 2252, 1953 (br), 1731, 1654, 1603, 1494, 1454, 1431, 1403, 1326, 1290, 1250, 1205, 1169, 1121, 1080, 1029, 1006, 986, 942, 915, 878, 843, 825, 808, 761, 732, 700, 648 cm^{-1}

HRMS (MM) calc'd for $\text{C}_{21}\text{H}_{24}\text{NO}_8$ $[\text{M}+\text{H}]^+$ 418.1496, found 418.1515.

Preparation of fully oxidized *o*-QM precursor **223.**



To a 50 mL round-bottom flask was added benzhydryl morpholine **222** (200 mg, 0.479 mmol), followed by a 1:1 mixture of THF/H₂O (9.6 mL). *p*-toluenesulfonic acid monohydrate (91.1 mg, 0.479 mmol, 1.00 equiv) was then added in one portion and the reaction was heated to 60 °C for 4 hours. Note: it is best to monitor this reaction closely by TLC to mitigate degradation of the product via acid-mediated retro aldol. Upon completion, the reaction was cooled to room temperature and quenched with saturated aqueous NaHCO₃. The reaction was diluted with EtOAc and the organic layer separated. The aqueous layer was extracted with EtOAc (2 x 5 mL) and the combined organic layers were dried over MgSO₄, filtered, and concentrated *in vacuo*. The crude residue was purified by silica gel flash chromatography (isocratic: 5% EtOAc/CH₂Cl₂ + 0.5% AcOH, necessary to avoid streaking on the column). Fractions containing pure product were combined, washed with saturated aqueous NaHCO₃, dried over MgSO₄, filtered, and concentrated *in vacuo* to afford **223** (82.0 mg, 49% yield) as a white solid.

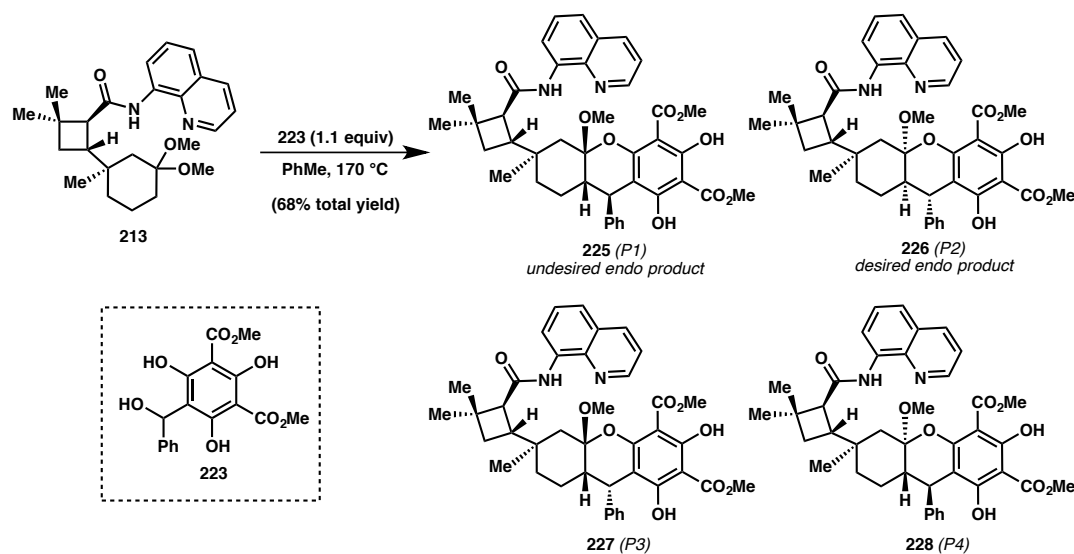
^1H NMR (400 MHz, CDCl_3) δ 11.89 (s, 2H), 11.70 (s, 1H), 7.46 – 7.39 (m, 2H), 7.31 (t, $J = 7.4$ Hz, 2H), 7.26 – 7.19 (m, 1H), 6.38 – 6.23 (m, 1H), 4.09 (d, $J = 11.6$ Hz, 1H), 4.02 (s, 6H).

^{13}C NMR (101 MHz, CDCl_3) δ 170.9, 165.0, 164.7, 143.9, 128.2, 127.0, 125.6, 110.2, 94.5, 68.1, 53.2.

FTIR (NaCl, thin film) 3563 (br), 3357 (br), 3085, 3058, 3028, 3006, 2956, 2851, 2749 (br), 1727, 1655, 1623, 1599, 1492, 1434, 1333, 1318, 1245, 1201, 1170, 1129, 1039, 1026, 972, 909, 836, 816, 733, 698, 622 cm^{-1} .

HRMS (MM) calc'd for $\text{C}_{17}\text{H}_{15}\text{O}_7$ $[\text{M}-\text{OH}]^+$ 331.0812, found 331.0825.

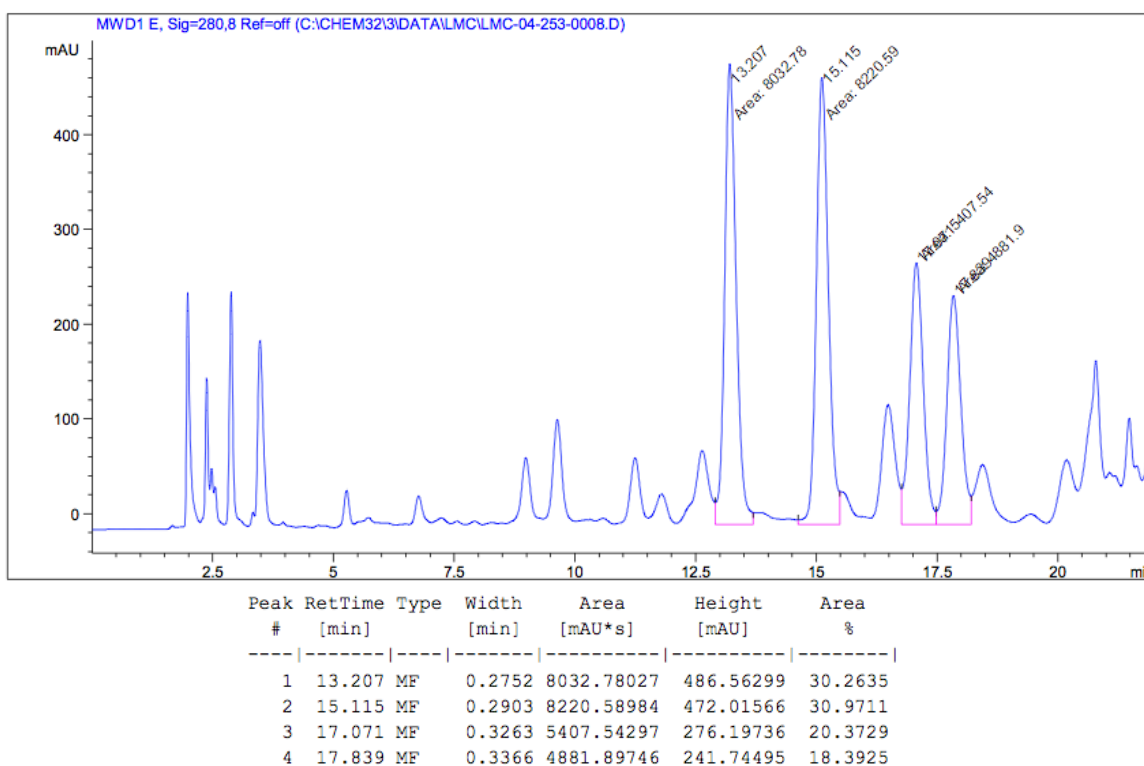
Preparation of tricyclic ketals **225**–**228** by thermal cycloaddition.



To a 15 mL thick-walled, screw top pressure vessel were added dimethyl ketal **213** (105 mg, 0.256 mmol) and *o*-QM precursor **223** (98.0 mg, 0.281 mmol, 1.10 equiv). PhMe (4.3 mL) was then added and the tube sealed under a stream of argon. The reaction

was heated to 170 °C in a preheated oil bath for 21 hours. The reaction was then cooled to room temperature and concentrated *in vacuo*. The crude residue was first purified by silica gel flash chromatography to remove separable impurities (4% EtOAc/CH₂Cl₂ + 0.5% AcOH) to afford a complex mixture of diastereomers, including **225–228** (109 mg, 68% yield). Analytically pure samples of the four diastereomers produced in greatest abundance (i.e. **225–228**) were obtained by subsequent reverse-phase HPLC purification using an Agilent XDB-C18 5 µm 30 x 250 mm column (gradient: 83–100% MeCN/H₂O).

Chromatogram from HPLC separation:



Data for **225** (peak 1): $[\alpha]_D^{25.0} = -13.8^\circ$ (c = 0.420, CHCl₃).

¹H NMR (400 MHz, CDCl₃) δ 12.22 (s, 1H), 11.68 (s, 1H), 9.65 (s, 1H), 8.81 (dd, *J* = 4.2, 1.7 Hz, 1H), 8.77 (dd, *J* = 7.3, 1.7 Hz, 1H), 8.16 (dd, *J* = 8.3, 1.7 Hz, 1H), 7.56 – 7.48 (m, 2H), 7.46 (dd, *J* = 8.3, 4.2 Hz, 1H), 7.24 – 7.16 (m, 2H), 7.16 – 7.09 (m, 1H), 7.09 – 7.02 (m, 2H), 3.96 (s, 3H), 3.93 (s, 3H), 3.91 (s, 1H), 3.05 (s, 3H), 2.82 – 2.67 (m, 2H), 2.16 (dd, *J* = 12.4, 3.5 Hz, 1H), 1.98 (d, *J* = 13.8 Hz, 1H), 1.76 (dd, *J* = 13.3, 4.1 Hz, 1H), 1.70 – 1.39 (m, 6H), 1.32 (s, 3H), 1.12 (s, 3H), 0.96 (s, 3H).

¹³C NMR (101 MHz, CDCl₃) δ 171.0, 170.8, 169.9, 165.0, 163.1, 157.2, 148.3, 145.6, 138.5, 136.5, 134.7, 128.1, 127.8, 127.6, 127.3, 125.6, 121.7, 121.3, 116.4, 102.4, 102.1, 99.0, 95.3, 52.8, 52.5, 51.3, 47.8, 45.3, 41.9, 41.4, 40.1, 34.7, 34.6, 32.7, 32.6, 30.8, 27.4, 23.8, 22.3.

FTIR (NaCl, thin film) 3410 (br), 3355 (br), 3055, 3021, 3000, 2950, 2864, 1734, 1686, 1654, 1643, 1599, 1524, 1484, 1460, 1426, 1384, 1336, 1326, 1279, 1247, 1225, 1163, 1142, 1093, 1063, 988, 973, 949, 841, 826, 791, 754, 698, 667 cm.⁻¹

HRMS (MM) calc'd for C₄₁H₄₅N₂O₉ [M+H]⁺ 709.3120, found 709.3119.

Data for **226** (peak 2): $[\alpha]_D^{25.0} = -32.2^\circ$ (c = 0.360, CHCl₃).

¹H NMR (400 MHz, CDCl₃) δ 12.81 (s, 1H), 12.08 (s, 1H), 9.65 (s, 1H), 8.78 – 8.74 (m, 2H), 8.15 (dd, *J* = 8.3, 1.6 Hz, 1H), 7.53 – 7.46 (m, 2H), 7.43 (dd, *J* = 8.3, 4.2 Hz, 1H), 7.22 (d, *J* = 7.5 Hz, 2H), 7.14 – 7.07 (m, 3H), 3.93 (d, *J* = 0.4 Hz, 3H), 3.93 (d, *J* = 0.3 Hz, 3H), 3.91 (d, *J* = 7.8 Hz, 1H), 3.39 (s, 3H), 2.82 – 2.76 (m, 2H), 2.12 (s, 1H), 1.86 –

1.73 (m, 2H), 1.69 – 1.49 (m, 5H), 1.33 (s, 3H), 1.25 (d, $J = 9.6$ Hz, 1H), 1.10 (s, 3H), 1.05 (s, 3H).

^{13}C NMR (101 MHz, CDCl_3) δ 171.4, 170.8, 169.9, 166.0, 164.7, 158.9, 148.3, 145.9, 138.5, 136.5, 134.7, 128.1, 128.1, 127.8, 127.6, 126.0, 121.7, 121.3, 116.3, 104.2, 104.1, 97.1, 95.7, 52.7, 52.7, 52.2, 49.0, 44.2, 41.7, 39.9, 37.7, 35.1, 35.1, 33.9, 30.8, 28.9, 24.0, 23.5, 22.8.

FTIR (NaCl, thin film) 3412 (br), 3354 (br), 3059, 3022, 3006, 2951, 2928, 2864, 1731, 1686, 1654, 1648, 1643, 1594, 1524, 1484, 1459, 1426, 1384, 1338, 1325, 1249, 1222, 1201, 1157, 1122, 1081, 1092, 1028, 976, 945, 936, 847, 826, 792, 755, 700, 667 cm^{-1} .

HRMS (MM) calc'd for $\text{C}_{41}\text{H}_{45}\text{N}_2\text{O}_9$ $[\text{M}+\text{H}]^+$ 709.3120, found 709.3141.

Data for **227** (peak 3): $[\alpha]_D^{25.0} = -98.4^\circ$ ($c = 0.206$, CHCl_3).

^1H NMR (400 MHz, CDCl_3) δ 12.11 (s, 1H), 11.61 (s, 1H), 9.64 (s, 1H), 8.82 (dd, $J = 4.3, 1.7$ Hz, 1H), 8.76 (dd, $J = 7.3, 1.7$ Hz, 1H), 8.16 (dd, $J = 8.2, 1.7$ Hz, 1H), 7.57 – 7.43 (m, 3H), 7.30 (dd, $J = 8.6, 5.1$ Hz, 2H), 7.17 (s, 2H), 6.81 (s, 1H), 4.54 (d, $J = 7.3$ Hz, 1H), 3.94 (s, 3H), 3.92 (s, 3H), 3.21 (s, 3H), 2.74 (q, $J = 9.8$ Hz, 2H), 2.10 (d, $J = 13.7$ Hz, 1H), 1.97 – 1.83 (m, 1H), 1.62 (d, $J = 8.9$ Hz, 2H), 1.45 (d, $J = 13.8$ Hz, 1H), 1.32 (s, 3H), 1.29 – 1.24 (m, 1H), 1.18 (d, $J = 13.2$ Hz, 1H), 1.11 (s, 3H), 1.10 – 1.06 (m, 1H), 1.04 (s, 3H), 0.76 (dd, $J = 13.1, 3.9$ Hz, 1H).

^{13}C NMR (101 MHz, CDCl_3) δ 171.0, 170.9, 169.7, 164.9, 162.7, 158.0, 148.3, 142.2, 138.5, 136.5, 134.7, 128.5, 128.1, 127.7, 127.6, 125.9, 121.7, 121.3, 116.4, 104.2, 102.2,

99.3, 95.5, 52.8, 52.5, 51.3, 49.0, 43.7, 42.2, 40.3, 38.5, 34.8, 34.4, 33.0, 32.6, 30.8, 23.8, 22.1, 21.7.

FTIR (NaCl, thin film) 3408 (br), 3354 (br), 3059, 3022, 3009, 2952, 2868, 1738, 1732, 1682, 1658, 1652, 1645, 1599, 1525, 1485, 1462, 1455, 1426, 1385, 1327, 1281, 1251, 1225, 1165, 1133, 1090, 1077, 1031, 991, 946, 872, 826, 792, 755, 703 cm^{-1} .

HRMS (MM) calc'd for $\text{C}_{41}\text{H}_{45}\text{N}_2\text{O}_9$ $[\text{M}+\text{H}]^+$ 709.3120, found 709.3133.

Data for **228** (peak 4): $[\alpha]_D^{25.0} = -13.4^\circ$ ($c = 0.226$, CHCl_3).

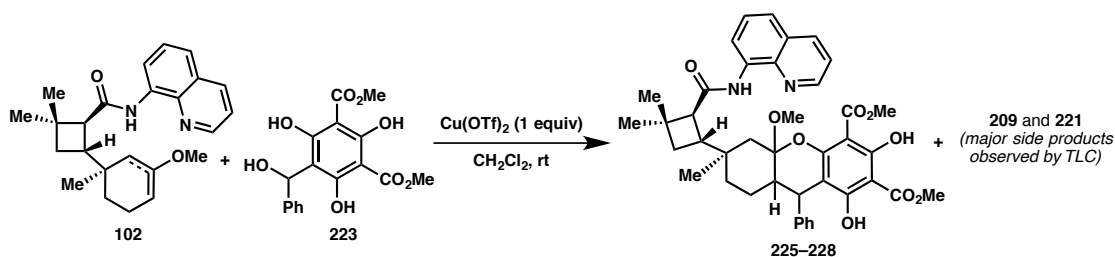
^1H NMR (400 MHz, CDCl_3) δ 11.95 (s, 1H), 11.23 (s, 1H), 9.66 (s, 1H), 8.81 (dd, $J = 4.2, 1.7$ Hz, 1H), 8.76 (dd, $J = 7.3, 1.7$ Hz, 1H), 8.16 (dd, $J = 8.3, 1.7$ Hz, 1H), 7.55 – 7.42 (m, 3H), 7.22 (dd, $J = 7.9, 6.5$ Hz, 2H), 7.18 – 7.13 (m, 1H), 7.10 (d, $J = 7.4$ Hz, 2H), 3.90 (s, 3H), 3.87 (s, 3H), 3.67 (d, $J = 11.0$ Hz, 1H), 3.16 (s, 3H), 2.81 – 2.66 (m, 2H), 2.10 (dd, $J = 14.2, 1.6$ Hz, 1H), 1.71 (td, $J = 10.8, 5.3$ Hz, 1H), 1.64 (dd, $J = 9.2, 2.6$ Hz, 2H), 1.56 – 1.48 (m, 2H), 1.45 (d, $J = 14.3$ Hz, 1H), 1.38 – 1.32 (m, 1H), 1.31 (s, 3H), 1.21 – 1.14 (m, 1H), 1.12 (s, 3H), 1.08 (s, 3H).

^{13}C NMR (101 MHz, CDCl_3) δ 170.8, 170.8, 169.5, 164.0, 162.4, 157.4, 148.3, 145.4, 138.5, 136.5, 134.7, 128.1, 128.1, 127.6, 125.9, 121.7, 121.3, 116.4, 108.0, 101.7, 99.6, 95.5, 52.7, 52.5, 51.2, 49.4, 49.0, 42.0, 41.1, 36.2, 35.3, 34.8, 33.3, 32.6, 30.8, 23.8, 22.5, 21.1.

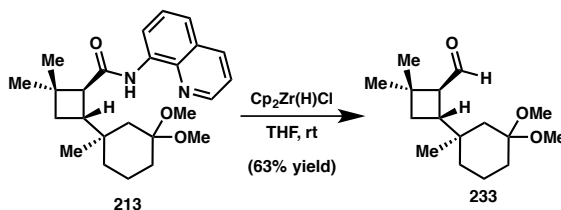
FTIR (NaCl, thin film) 3412 (br), 3354 (br), 3055, 3023, 3003, 2950, 2866, 1732, 1688, 1656, 1598, 1524, 1484, 1453, 1426, 1384, 1327, 1277, 1248, 1225, 1165, 1062, 993, 954, 925, 826, 792, 755, 702 cm^{-1}

HRMS (MM) calc'd for $\text{C}_{41}\text{H}_{45}\text{N}_2\text{O}_9$ $[\text{M}+\text{H}]^+$ 709.3120, found 709.3139.

Preparation of tricyclic ketals 225–228 by $\text{Cu}(\text{OTf})_2$ -mediated cycloaddition.



Inside a N_2 -filled glovebox, methyl enol ether **102** (17.0 mg, 0.045 mmol) and o-quinone methide precursor **223** (16.4 mg, 0.047 mmol, 1.05 equiv) were added to a 1 dram vial and dissolved in CH_2Cl_2 (400 μL). $\text{Cu}(\text{OTf})_2$ was then added as a solid in one portion and the reaction immediately turns a light green color, then yellow-brown within the first 5 minutes. The reaction was stirred at room temperature for 1 hour, then quenched with saturated aqueous NaHCO_3 and diluted with CHCl_3 . The reaction mixture was extracted with CHCl_3 (3 x 1 mL) and the organics filtered through a plug of Na_2SO_4 and concentrated in vacuo. The crude residue was analyzed by ^1H NMR and determined to contain **225**, **226**, **227**, and **228** in a 1.0 : 1.8 : 2.3 : 2.5 ratio, respectively. For spectroscopic characterization data, see above.

Preparation of aldehyde 233.

Inside a N₂-filled glovebox, Schwartz's reagent (119 mg, 0.462 mmol, 2.00 equiv) was added to a 10 mL flask and sealed under N₂. The flask was removed from the glovebox and THF (1.2 mL) was added via syringe. To the milky-white suspension was added ketal **213** (94.8 mg, 0.231 mmol) as a solution in THF (1.2 mL) in a quick drip. The reaction immediately begins to turn yellow, eventually becoming a darker orange color over 1 hour, at which time the reaction was quenched by the addition of saturated aqueous NaHCO₃. The reaction was diluted with EtOAc and the organic layer separated. The aqueous layer was extracted with EtOAc (2 x 5 mL) and the combined organic layers were dried over MgSO₄, filtered, and concentrated *in vacuo*. The crude residue was purified by silica gel flash chromatography (isocratic: 5% EtOAc/hexane + 1% Et₃N) to afford **233** (36.9 mg, 62% yield) as a pale yellow oil: $[\alpha]_D^{25.0} = -33.1^\circ$ (c = 0.500, CHCl₃).

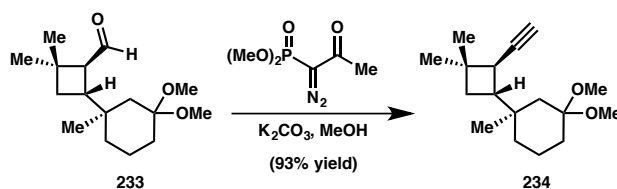
¹H NMR (400 MHz, CDCl₃) δ 9.70 (d, *J* = 3.0 Hz, 1H), 3.14 (s, 3H), 3.09 (s, 3H), 2.64 (td, *J* = 9.7, 8.5 Hz, 1H), 2.58 (dd, *J* = 9.9, 3.0 Hz, 1H), 1.86 (ddt, *J* = 13.6, 4.2, 2.6 Hz, 1H), 1.61 (t, *J* = 10.3 Hz, 1H), 1.57 – 1.44 (m, 4H), 1.34 – 1.18 (m, 2H), 1.16 (s, 3H), 1.14 (s, 3H), 1.13 – 1.05 (m, 2H), 0.89 (s, 3H).

¹³C NMR (101 MHz, CDCl₃) δ 204.7, 100.5, 55.2, 47.6, 47.1, 39.8, 39.3, 35.7, 34.4, 33.9, 33.0, 32.7, 31.1, 24.3, 21.7, 18.6.

FTIR (NaCl, thin film) 2952, 2868, 2828, 2705, 1713, 1461, 1383, 1368, 1341, 1288, 1262, 1246, 1180, 1166, 1110, 1098, 1048, 1009, 945, 924, 823, 828 cm^{-1}

HRMS (MM) calc'd for $\text{C}_{15}\text{H}_{25}\text{O}_2$ $[\text{M}-\text{OCH}_3]^+$ 237.1849, found 237.4454.

Preparation of alkyne **234**.



To a 10 mL round bottom flask were added aldehyde **233** (36.0 mg, 0.134 mmol) and K_2CO_3 (37.0 mg, 0.268 mmol, 2.00 equiv). The flask was fitted with a septum and the atmosphere exchanged 2x for N_2 . Freshly distilled MeOH (1.5 mL) was then added via syringe and the solution cooled to 0 °C. Dimethyl-1-diazo-2-oxopropylphosphonate⁵⁷ (38.6 mg, 0.201 mmol, 1.50 equiv) was weighed into a tared syringe and added dropwise to the reaction, neat. The reaction was allowed to gradually warm to room temperature and stirred for 12 hours. The reaction was then diluted with Et_2O , saturated aqueous NaHCO_3 was added, and the organic layer separated. The aqueous layer was extracted with Et_2O (3 x 5 mL) and the combined organic layers were dried over MgSO_4 , filtered, and concentrated *in vacuo*. The crude residue was purified by Florisil[®] flash chromatography (isocratic: 5% Et_2O /pentane) to afford **234** (32.9 mg, 93% yield) as a pale yellow oil: $[\alpha]_D^{25.0} = -43.6^\circ$ ($c = 0.355$, CHCl_3).

^1H NMR (400 MHz, CDCl_3) δ 3.17 (s, 3H), 3.13 (s, 3H), 2.43 (dd, $J = 10.1, 2.4$ Hz, 1H), 2.16 – 2.05 (m, 2H), 2.04 – 1.93 (m, 1H), 1.69 (ddd, $J = 13.9, 2.8, 1.8$ Hz, 1H), 1.59 –

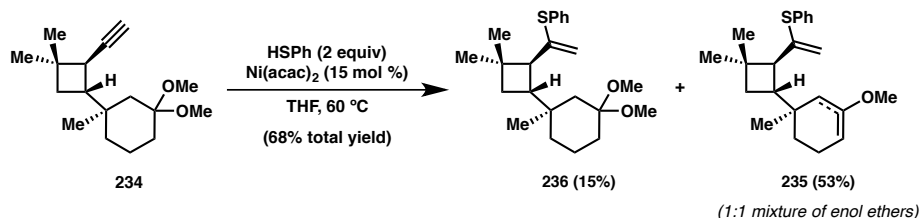
1.50 (m, 2H), 1.48 (d, $J = 9.6$ Hz, 2H), 1.29 – 1.17 (m, 5H), 1.16 (d, $J = 2.7$ Hz, 4H), 1.03 (s, 3H), 0.97 (s, 3H).

^{13}C NMR (101 MHz, CDCl_3) δ 100.7, 85.8, 70.5, 49.1, 47.9, 47.3, 39.1, 35.2, 35.1, 34.0, 33.5, 33.2, 33.2, 29.9, 24.8, 21.1, 18.8.

FTIR (NaCl, thin film) 3310, 3263, 2953, 2866, 2828, 1459, 1383, 1364, 1342, 1323, 1288, 1266, 1243, 1180, 1157, 1106, 1094, 1048, 945, 926, 858, 830, 655, 621 cm^{-1} .

HRMS (MM) calc'd for $\text{C}_{16}\text{H}_{25}\text{O}_2$ $[\text{M}-\text{OCH}_3]^+$ 233.1900, found 233.1887.

Preparation of vinyl sulfides **236** and **235**.



Inside a N_2 -filled glovebox, THF (400 μL) was added to a 1 dram vial containing alkyne **234** (12.4 mg, 0.047 mmol), followed by $\text{Ni}(\text{acac})_2$ as a stock solution in THF (0.10 M, 70 μL , 0.007 mmol, 0.15 equiv). The reaction was stirred for 10 minutes at room temperature before thiophenol (10 μL , 0.094 mmol, 2.00 equiv) was added neat. The reaction was sealed with a Teflon cap and heated to 60 °C in a preheated aluminum block inside the glovebox. After 3 hours, the reaction was cooled to room temperature and diluted with CH_2Cl_2 . The reaction mixture was filtered over a small pad of celite, washed with CH_2Cl_2 until the filtrate runs colorless, and concentrated in vacuo. The crude residue was taken up in EtOAc and shaken with 5M NaOH (to remove excess

thiophenol). The organic layer was then filtered through a plug of Na₂SO₄, concentrated, and purified by preparative thin-layer chromatography (5% EtOAc/hexane + 1% Et₃N) to afford **235** (8.50 mg, 53% yield) and **236** (2.7 mg, 15% yield) each as colorless oils.

Data for ketal **236**: $[\alpha]_D^{25.0} = +12.3^\circ$ (c = 0.115, CHCl₃).

¹H NMR (400 MHz, CDCl₃) δ 7.42 (dd, *J* = 8.1, 1.6 Hz, 2H), 7.36 – 7.28 (m, 3H), 5.17 (d, *J* = 1.3 Hz, 1H), 4.96 (s, 1H), 3.17 (s, 3H), 3.13 (s, 3H), 2.51 (d, *J* = 10.2 Hz, 1H), 2.26 (q, *J* = 9.7 Hz, 1H), 2.04 – 1.92 (m, 1H), 1.65 (ddd, *J* = 13.8, 2.8, 1.6 Hz, 1H), 1.50 (ddd, *J* = 9.6, 7.0, 3.7 Hz, 2H), 1.45 – 1.39 (m, 2H), 1.21 – 1.12 (m, 4H), 1.11 (s, 3H), 0.98 (s, 3H), 0.91 (s, 3H).

¹³C NMR (101 MHz, CDCl₃) δ 145.9, 133.8, 133.4, 129.2, 127.9, 111.6, 100.8, 49.4, 47.9, 47.3, 45.1, 39.7, 35.6, 34.8, 34.6, 33.2, 32.4, 30.6, 23.2, 21.7, 18.9.

FTIR (NaCl, thin film) 2950, 2863, 2827, 1610, 1583, 1476, 1459, 1439, 1379, 1364, 1322, 1274, 1260, 1247, 1178, 1145, 1130, 1100, 1083, 1049, 1024, 946, 926, 856, 831, 822, 747, 691 cm.⁻¹

HRMS (MM) calc'd for C₂₂H₃₁OS [M–OCH₃]⁺ 343.2090, found 343.2073.

Data for enol ether **235**: $[\alpha]_D^{25.0} = -11.0^\circ$ (c = 0.982, CHCl₃).

¹H NMR (400 MHz, CDCl₃) δ 7.46 – 7.36 (m, 2H), 7.36 – 7.27 (m, 3H), 5.23 – 4.84 (m, 2H), 4.63 – 4.29 (m, 1H), 3.40 (s, 3H), 2.58 – 2.50 (m, 1H), 2.40 (dq, *J* = 34.9, 9.5 Hz, 1H), 2.11 – 1.91 (m, 3H), 1.64 (ddd, *J* = 15.0, 5.9, 2.4 Hz, 2H), 1.48 – 1.40 (m, 2H), 1.39

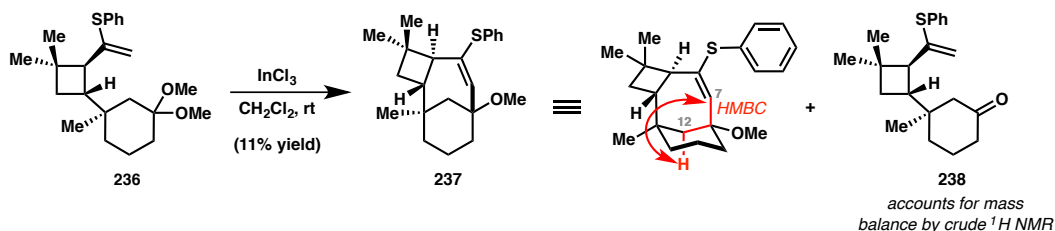
– 1.30 (m, 1H), 1.11 (d, $J = 9.9$ Hz, 3H), 1.00 (d, $J = 2.4$ Hz, 3H), 0.83 (d, $J = 21.0$ Hz, 4H).

^{13}C NMR (101 MHz, CDCl_3) δ 155.3, 154.4, 146.0, 145.9, 133.8, 133.5, 133.4, 133.3, 129.2, 129.1, 127.9, 127.7, 112.3, 111.1, 100.6, 92.0, 54.1, 53.9, 50.2, 49.5, 43.5, 40.9, 37.7, 36.1, 35.1, 35.1, 34.5, 34.1, 32.9, 32.6, 31.6, 30.6, 30.5, 28.2, 25.8, 23.3, 23.2, 22.0, 20.8, 19.4.

FTIR (NaCl, thin film) 3061, 2991, 2950, 2930, 2862, 2843, 1667, 1609, 1583, 1476, 1460, 1453, 1440, 1380, 1366, 1251, 1215, 1148, 1066, 1024, 940, 817, 747, 691 cm^{-1}

HRMS (MM) calc'd for $\text{C}_{22}\text{H}_{31}\text{OS}$ $[\text{M}+\text{H}]^+$ 343.2090, found 343.2087.

Preparation of bridged bicycle 237.



Inside a N_2 -filled glovebox, CH_2Cl_2 was added to a 1 dram vial containing **236** (9.30 mg, 0.025 mmol), followed by InCl_3 (5.49 mg, 0.025 mmol, 1.00 equiv). The reaction was stirred at room temperature for 2 hours, then quenched with saturated aqueous NaHCO_3 and diluted with CH_2Cl_2 . The reaction was extracted with CH_2Cl_2 (3 x 500 μL), the combined organics filtered a plug of Na_2SO_4 , and concentrated *in vacuo*. The crude residue was purified by silica gel flash chromatography (40–60%

CH₂Cl₂/hexane) to afford **237** (0.900 mg, 11% yield) as a colorless oil, with the remaining mass balance accounted for by ketone **238**, as determined by crude ¹H NMR.

Data for bridged bicycle **237**: $[\alpha]_D^{25.0} = +58.2^\circ$ (c = 0.053, CHCl₃).

¹H NMR (400 MHz, CDCl₃) δ 7.40 – 7.36 (m, 2H), 7.30 (ddd, *J* = 8.3, 7.1, 0.8 Hz, 2H), 7.24 – 7.18 (m, 1H), 5.52 (dd, *J* = 2.8, 1.7 Hz, 1H), 3.18 (s, 3H), 2.91 – 2.81 (m, 1H), 2.00 – 1.72 (m, 5H), 1.66 (ddd, *J* = 11.6, 6.8, 3.5 Hz, 1H), 1.44 – 1.37 (m, 2H), 1.35 (dd, *J* = 12.3, 1.7 Hz, 1H), 1.29 (m, 1H), 1.28 (s, 3H), 1.19 (dd, *J* = 14.1, 7.0 Hz, 1H), 1.00 (s, 3H), 0.80 (s, 3H).

¹³C NMR (101 MHz, CDCl₃) δ 139.7, 139.6, 135.0, 131.7, 129.2, 127.2, 80.6, 52.4, 50.2, 49.2, 48.6, 40.1, 38.3, 36.2, 33.7, 31.3, 31.2, 28.9, 22.4, 21.2.

FTIR (NaCl, thin film) 3062, 2945, 2927, 2860, 2820, 1734, 1718, 1701, 1654, 1583, 1560, 1476, 1458, 1438, 1370, 1294, 1254, 1232, 1151, 1086, 1066, 1024, 950, 870, 840, 800, 743, 690 cm.⁻¹

HRMS (MM) calc'd for C₂₂H₃₁OS [M+H]⁺ 343.2090, found 343.2077.

Data for ketone **238**: $[\alpha]_D^{25.0} = +31.6^\circ$ (c = 0.100, CHCl₃).

¹H NMR (400 MHz, CDCl₃) δ 7.46 (dd, *J* = 8.1, 1.6 Hz, 2H), 7.40 – 7.32 (m, 3H), 5.13 (d, *J* = 1.3 Hz, 1H), 4.98 (s, 1H), 2.53 (d, *J* = 10.1 Hz, 1H), 2.38 (td, *J* = 10.0, 8.9 Hz, 1H), 2.32 – 2.23 (m, 2H), 2.17 (d, *J* = 13.6 Hz, 1H), 2.02 (dt, *J* = 13.4, 1.9 Hz, 1H), 1.93

– 1.90 (m, 1H), 1.82 (dddd, $J = 9.7, 8.1, 3.9, 2.3$ Hz, 1H), 1.57 (q, $J = 4.4$ Hz, 1H), 1.49 – 1.44 (m, 1H), 1.44 – 1.33 (m, 2H), 1.16 (s, 3H), 1.03 (s, 3H), 0.82 (s, 3H).

^{13}C NMR (101 MHz, CDCl_3) δ 212.6, 145.5, 134.1, 133.0, 129.3, 128.2, 111.4, 51.1, 49.8, 43.1, 41.3, 40.3, 35.1, 34.2, 32.5, 30.6, 23.1, 22.1, 21.8.

FTIR (NaCl, thin film) 3059, 2953, 2927, 2860, 1711, 1680, 1611, 1583, 1476, 1461, 1440, 1381, 1364, 1347, 1311, 1283, 1253, 1228, 1151, 1087, 1067, 1024, 890, 855, 749, 692 cm^{-1} .

HRMS (MM) calc'd for $\text{C}_{21}\text{H}_{29}\text{OS}$ $[\text{M}+\text{H}]^+$ 329.1934, found 329.1943.

2.7 NOTES AND REFERENCES

- (1) For biomimetic syntheses of phloroglucinol meroterpenoids and β -caryophyllene-derived natural products, see Chapter 1.
- (2) For seminal studies, see: (a) Shabashov, D.; Daugulis, O. *J. Am. Chem. Soc.* **2010**, *132*, 3965. (b) Zaitsev, V. G.; Shabashov, D.; Daugulis, O. *J. Am. Chem. Soc.* **2005**, *127*, 13154. (c) Reddy, B. V. S.; Reddy, L. R.; Corey, E. J. *Org. Lett.* **2006**, *8*, 3391. For reviews, see: (d) Corbet, M.; De Campo, F. *Angew. Chem. Int. Ed.* **2013**, *52*, 9896. (e) Yamaguchi, J.; Itami, K.; Yamaguchi, A. D. *Angew. Chem., Int. Ed.* **2012**, *51*, 8960.
- (3) (a) Gutekunst, W. R.; Baran, P. S. *J. Am. Chem. Soc.* **2011**, *133*, 19076.

- (b) Gutekunst, W. R.; Gianatassio, R.; Baran, P. S. *Angew. Chem., Int. Ed.* **2012**, *51*, 7507. (c) Feng, Y.; Chen, G. *Angew. Chem., Int. Ed.* **2010**, *49*, 958. For reports disclosed after our studies commenced, see: (d) Gutekunst, W. R.; Baran, P. S. *J. Org. Chem.* **2014**, *79*, 2430. (e) Panish, R. A.; Chintala, S. R.; Fox, J. M. *Angew. Chem., Int. Ed.* **2016**, *55*, 4983. (f) Ting, C. P.; Maimone, T. J. *Angew. Chem., Int. Ed.* **2014**, *53*, 3115.
- (4) (a) Zhang, S.-Y.; Li, Q.; He, G.; Nack, W. A.; Chen, G. *J. Am. Chem. Soc.* **2013**, 12135. (b) Wang, B.; Lu, C.; Zhang, S.-Y.; He, G.; Nack, W. A.; Chen, G. *Org. Lett.* **2014**, *16*, 6260.
- (5) Xiao, K.-J.; Lin, D. W.; Miura, M.; Zhu, R.-Y.; Gong, W.; Wasa, M.; Yu, J.-Q. *J. Am. Chem. Soc.* **2014**, *136*, 8138.
- (6) (a) Blumenkopf, T. A.; Bratz, M.; Castaneda, A.; Look, G. C.; Overman, L. E.; Rodriguez, D.; Thompson, A. S. *J. Am. Chem. Soc.* **1990**, *112*, 4386. (b) Blumenkopf, T. A.; Look, G. C.; Overman, L. E. *J. Am. Chem. Soc.* **1990**, *112*, 4399. (c) Overman, L. E.; Blumenkopf, T. A.; Castaneda, A.; Thompson, A. S. *J. Am. Chem. Soc.* **1986**, *108*, 3516. (d) Overman, L. E.; Blumenkopf, T. A.; Castaneda, A.; Thompson, A. S. *J. Am. Chem. Soc.* **1986**, *108*, 3516. (e) Bratz, M.; Bullock, W. H.; Overman, L. E.; Takemoto, T. *J. Am. Chem. Soc.* **1995**, *117*, 5958.
- (7) Sasmal, P. K.; Maier, M. E. *Org. Lett.* **2002**, *4*, 1271.
- (8) López, F.; Castedo, L.; Mascareñas, J. L. *Org. Lett.* **2005**, *7*, 287.
- (9) For other relevant examples, see: (a) Fearnley, S. P.; Lory, P. *Org. Lett.* **2007**, *9*, 3507. (b) Cho, Y. S.; Kim, H. Y.; Cha, J. H.; Pae, A. N.; Koh, H. Y.; Choi, J. H.;

- Chang, M. H. *Org. Lett.* **2002**, *4*, 2025.
- (10) Arduini, A.; Bosi, A.; Pochini, A.; Ungaro, R. *Tetrahedron* **1985**, *41*, 3095.
- (11) For reviews, see: (a) Willis, N. J.; Bray, C. D. *Chem. Eur. J.* **2012**, *18*, 9160. (b) Van De Water, R. W.; Pettus, T. R. *Tetrahedron* **2002**, *58*, 5367. (c) Ferreira, S. B.; da Silva, F. de C.; Pinto, A. C.; Gonzaga, D. T. G.; Ferreira, V. F. *J. Heterocyclic Chem.* **2009**, *46*, 1080.
- (12) (a) Wilson, P. D.; Pettigrew, J. D.; Bexrud, J. A.; Freeman, R. P. *Heterocycles*. **2004**, *62*, 445. (b) Pettigrew, J. D.; Freeman, R. P.; Wilson, P. D. *Can. J. Chem.* **2004**, *82*, 1640.
- (13) (a) Rodriguez, R.; Adlington, R. M.; Moses, J. E.; Cowley, A.; Baldwin, J. E. *Org. Lett.* **2004**, *6*, 3617. (b) Kumbaraci, V.; Ergunes, D.; Midilli, M.; Begen, S.; Talinli, N. *J. Heterocyclic Chem.* **2009**, *46*, 226.
- (14) Zhang, Y.; Guo, Y.; Li, Z.; Xie, Z. *Org. Lett.* **2016**, *18*, 4578.
- (15) (a) Saha, S.; Schneider, C. *Chem. Eur. J.* **2015**, *21*, 2348. (b) El-Sepelgy, O.; Haseloff, S.; Alamsetti, S. K.; Schneider, C. *Angew. Chem., Int. Ed.* **2014**, *53*, 7923. (c) Saha, S.; Schneider, C. *Org. Lett.* **2015**, *17*, 648. (d) Zhao, J.-J.; Zhang, Y.-C.; Xu, M.-M.; Tang, M.; Shi, F. *J. Org. Chem.* **2015**, *80*, 10016.
- (16) (a) Selenski, C.; Mejorado, L. H.; Pettus, T. R. *Synlett* **2004**, *2004*, 1101. (b) Selenski, C.; Pettus, T. R. *J. Org. Chem.* **2004**, *69*, 9196. (c) Wenderski, T. A.; Marsini, M. A.; Pettus, T. R. *Org. Lett.* **2011**, *13*, 118. (d) Marsini, M. A.; Huang, Y.; Lindsey, C. C.; Wu, K.-L.; Pettus, T. R. *Org. Lett.* **2008**, *10*, 1477.
- (17) (a) Ghosh, A.; Banerjee, U. K.; Venkateswaran, R. V. *Tetrahedron* **1990**, *46*, 3077. (b) Banerjes, U. K.; Venkateswaran, R. V. *Tetrahedron Lett.* **1983**, *24*, 423.

- (18) With the exception of substituting hexyllithium with *t*-BuLi, **142** was prepared according to: Caille, S.; Crockett, R.; Ranganathan, K.; Wang, X.; Woo, J. C. S.; Walker, S. D. *J. Org. Chem.* **2011**, 76, 5198.
- (19) We were unable to isolate this side product, and thus could not confirm its structure.
- (20) (a) Wasa, M.; Engle, K. M.; Yu, J.-Q. *J. Am. Chem. Soc.* **2010**, 132, 3680. (b) Stowers, K. J.; Fortner, K. C.; Sanford, M. S. *J. Am. Chem. Soc.* **2011**, 133, 6541. (c) Mehta, S.; Yao, T.; Larock, R. C. *J. Org. Chem.* **2012**, 77, 10938.
- (21) Experiments conducted in DMF on 0.200 mmol scale: rigorous exclusion of water resulted in 72% *trans*-**148** (relative to *cis*-**147**), whereas use of wet solvent gave only 65% **148**. Moreover, the intentional addition of water provided **148** in only 43% yield. These results suggest that adventitious water alone is not responsible for the degree of *in situ* epimerization observed.
- (22) Fogassy, E.; Nógrádi, M.; Kozma, D.; Egri, G.; Pálovics, E.; Kiss, V. *Org. Biomol. Chem.* **2006**, 4, 3011.
- (23) Fehr, C.; Galindo, J. *Helv. Chim. Acta.* **1995**, 78, 539.
- (24) (a) L. Wolff, *Justus Liebigs Ann. Chem.* **1902**, 325, 129. For reviews, see: (b) Meier, H.; Zeller, K. P. *Angew. Chem. Int. Ed.* **1975**, 14, 32. (c) Kirmse, W. *Eur. J. Org. Chem.* **2002**, 2193.
- (25) (a) Hodous, B. L.; Fu, G. C. *J. Am. Chem. Soc.* **2002**, 124, 10006. For preparation of enantioenriched esters in a related report, see: (b) Wiskur, S. L.; Fu, G. C. *J. Am. Chem. Soc.* **2005**, 127, 6176.
- (26) See equation 10: France, S.; Wack, H.; Taggi, A. E.; Hafez, A. M.; Wagerle, T.

- R.; Shah, M. H.; Dusich, C. L.; Lectka, T. *J. Am. Chem. Soc.* **2004**, *126*, 4245.
- (27) Wang, J.; Hou, Y. *J. Chem. Soc., Perkin Trans. I* **1998**, *12*, 1919.
- (28) Setup inspired by and adapted from that pictured in the supporting information (page S-18) of: Do, H.-Q.; Bachman, S.; Bissember, A. C.; Peters, J. C.; Fu, G. C. *J. Am. Chem. Soc.* **2014**, *136*, 2162. See also: Ziegler, D. T.; Choi, J.; Muñoz-Molina, J. M.; Bissember, A. C.; Peters, J. C.; Fu, G. C. *J. Am. Chem. Soc.* **2013**, *135*, 13107.
- (29) (a) Pracejus, H. *Justus Liebigs Ann. Chem.* **1960**, 634, 9. (b) Wynberg, H.; Staring, E. *J. Am. Chem. Soc.* **1982**, *104*, 66. (c) Wynberg, H.; Staring, E. G. J. *J. Org. Chem.* **1985**, *50*, 1977. (d) Calter, M. A. *J. Org. Chem.* **1996**, *61*, 8006. (e) Dogo-Isonagie, C.; Bekele, T.; France, S.; Wolfer, J.; Weatherwax, A.; Taggi, A. E.; Paull, D. H.; Dudding, T.; Lectka, T. *Eur. J. Org. Chem.* **2007**, *2007*, 1091, and references cited therein. (f) For a review of catalytic asymmetric additions to ketenes, see: Paull, D. H.; Weatherwax, A.; Lectka, T. *Tetrahedron* **2009**, *65*, 6771.
- (30) Epimeric cinchona alkaloids (**181–184**) were prepared according to: Hiratake, J.; Inagaki, M.; Yamamoto, Y.; Oda, J. *J. Chem. Soc., Perkin Trans. I* **1987**, 1053.
- (31) Prepared according to: Khripach, V. A.; Zhabinskii, V. A.; Ol'khovik, V. K.; Ivanova, G. I.; Zhernosek, E. V.; Kotyatkina, A. I. *Zh. Org. Khim.* **1994**, *30*, 1650.; Khripach, V. A.; Zhabinskii, V. A.; Ol'khovik, V. K.; Ivanova, G. I.; Zhernosek, E. V.; Kotyatkina, A. I. *Russ. J. Org. Chem. (English Translation)* **1994**, *30*, 1735.
- (32) Prepared according to: Zhang, Y.-R.; He, L.; Wu, X.; Shao, P.-L.; Ye, S. *Org.*

Lett. **2008**, *10*, 277.

- (33) We considered that the low yield of **89** could be due to ambient water trapping the sensitive intermediate ketene, however formation of **145** was not detected.
- (34) Tidwell, T. T. *Ketenes*, 2nd ed.; John Wiley & Sons: Hoboken, NJ, 2006; pp 443–447.
- (35) (a) Knowles, J. P.; Elliott, L. D.; Booker-Milburn, K. I. *Beilstein J. Org. Chem.* **2012**, *8*, 2025. (b) Cambié, D.; Bottecchia, C.; Straathof, N. J. W.; Hessel, V.; Noël, T. *Chem. Rev.* **2016**, *116*, 10276.
- (36) Taggi, A. E.; Hafez, A. M.; Dudding, T.; Lectka, T. *Tetrahedron* **2002**, *58*, 8351.
- (37) We note that this result could also be achieved by the enantioselective protonation mechanism, and therefore does not provide direct evidence for either possibility outlined in Figure 2.7.
- (38) Pattawong, O.; Mustard, T. J. L.; Johnston, R. C.; Cheong, P. H.-Y. *Angew. Chem. Int. Ed.* **2012**, *52*, 1420.
- (39) Substrates **200–203** were prepared using the same procedure employed for **104**. Spectroscopic data for **200** and **202** are consistent with that previously reported: (a) Vuluga, D.; Legros, J.; Crousse, B.; Bonnet-Delpon, D. *Green Chem.* **2009**, *11*, 156. For preparation of the ketones used to access **201** and **203**, see: (b) Cernijenko, A.; Risgaard, R.; Baran, P. S. *J. Am. Chem. Soc.* **2016**, *138*, 9425. (c) Liu, H.; Drizin, I.; Koenig, J. R.; Cowart, M. D.; Wakefield, B. D.; Altenbach, R. J.; Black, L. A.; Zhao, C. *Macrocyclic pyrimidine derivatives*. WO2009123967, 2009.
- (40) (a) d’Augustin, M.; Palais, L. T.; Alexakis, A. *Angew. Chem., Int. Ed.* **2005**, *44*,

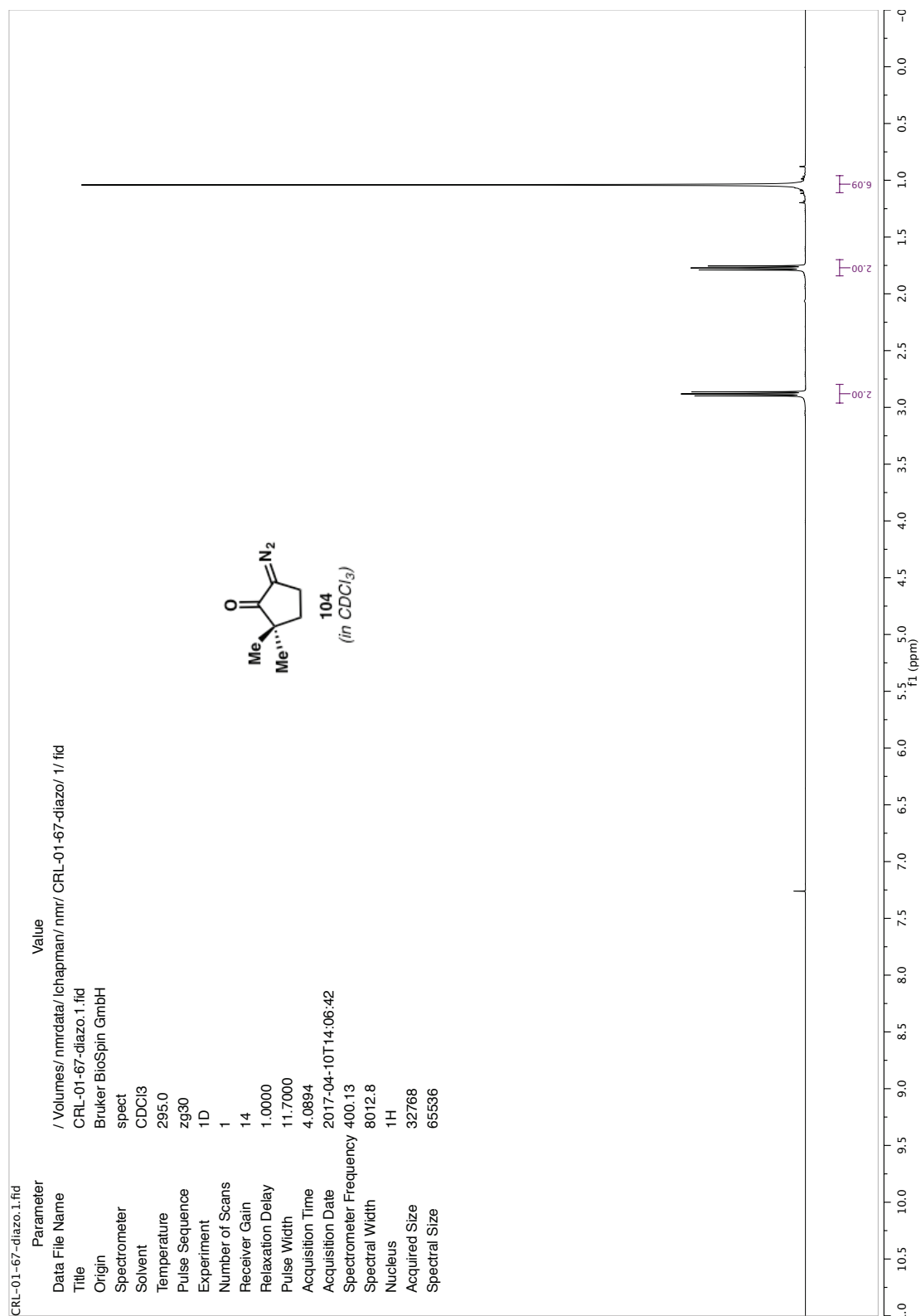
1376. (b) Vuagnoux-d'Augustin, M.; Alexakis, A. *Chem. Eur. J.* **2007**, *13*, 9647.
- (41) (a) Prepared directly in <10% yield according to: Leuchs, H.; Theodorescu, G. *Chem. Ber.* **1910**, *43*, 1243. (b) The corresponding ethyl ester can also be prepared in higher yield (~20%) according to: Zhang, Q.; Botting, N. P.; Kay, C. *Chem. Commun.* **2011**, *47*, 10596.
- (42) Saimoto, H.; Yoshida, K.; Murakami, T.; Morimoto, M.; Sashiwa, H.; Shigemasa, Y. *J. Org. Chem.* **1996**, *61*, 6768.
- (43) See reference 12. It is worth noting that attempts to employ **222** directly as an *o*-QM precursor in the [4+2] complicated the reaction profile, since the equivalent of morpholine (**220**) liberated from **222** adds into the initially formed cycloaddition products via thermal oxonium ion formation. Efforts to mitigate *this* problem by activating **222** via *N*-methylation were unsuccessful.
- (44) Only one enol ether isomer reacts, presumably due to steric hindrance.
- (45) For clarity, recall that these intermediates are in the *opposite* enantiomeric series with respect to the structures presented in the introductory stereochemical analysis discussion (Figure 2.3).
- (46) Evans, D. A.; Johnson, J. S.; Olhava, E. J. *J. Am. Chem. Soc.* **2000**, *122*, 1635.
- (47) For select examples of *o*-QMs generated using Brønsted acids, see: (a) Hsiao, C.-C.; Raja, S.; Liao, H.-H.; Atodiresci, I.; Rueping, M. *Angew. Chem. Int. Ed.* **2015**, *54*, 5762, and references cited therein. (b) Gharpure, S. J.; Sathiyarayanan, A. M.; Vuram, P. K. *RSC Adv.* **2013**, *3*, 18279.
- (48) Ananikov, V. P.; Orlov, N. V.; Beletskaya, I. P. *Organometallics* **2006**, *25*, 1970.
- (49) Still, W. C., Kahn, M. & Mitra, A. *J. Org. Chem.* **1978**, *43*, 2923.

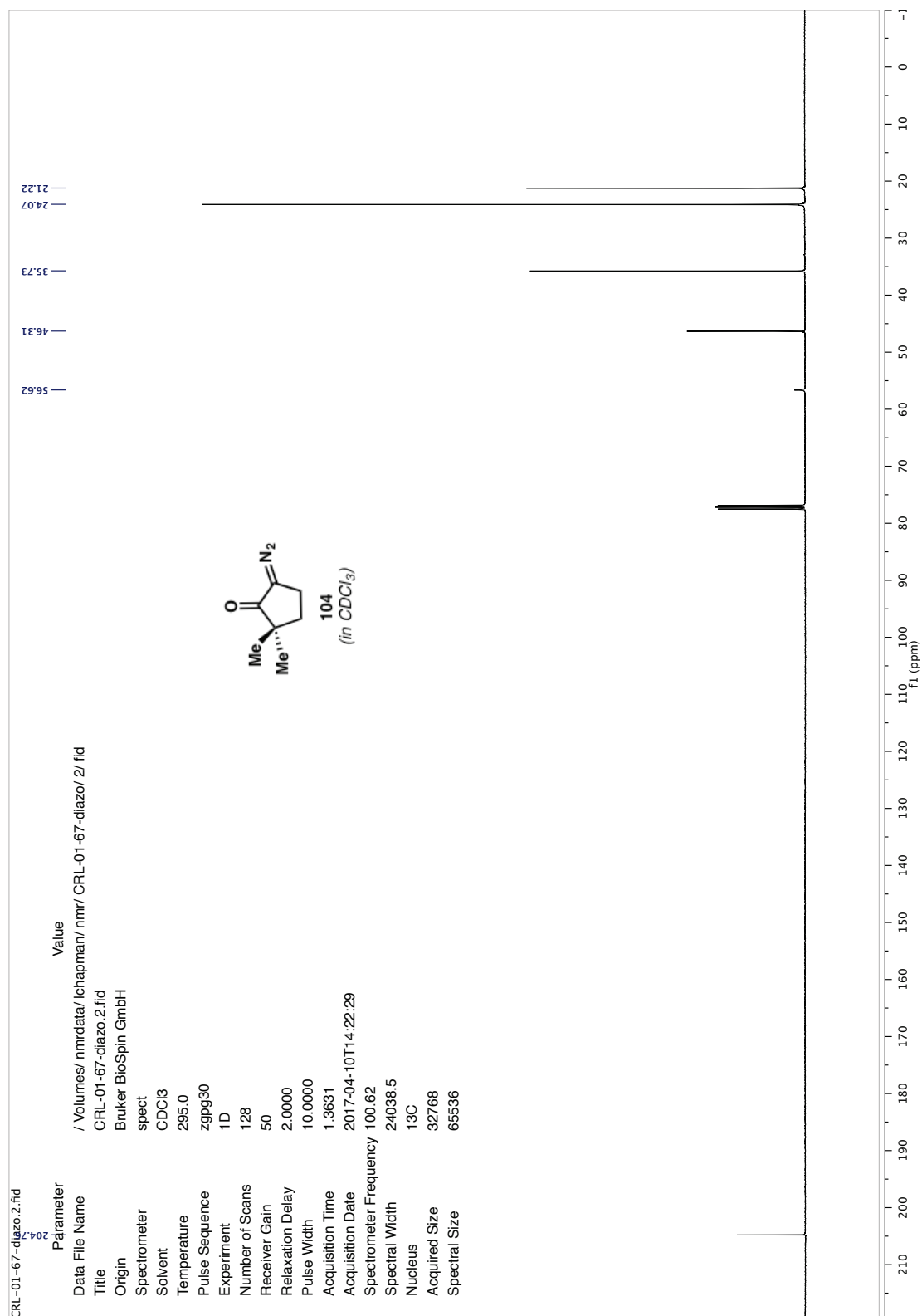
- (50) We have found that concentrated reaction mixtures (e.g. ≥ 2.2 M) react to full conversion at 0 °C, whereas more dilute reactions (i.e. 1.5 M, as reported in reference 17) often require warming to room temperature in order to initiate. This can be dangerous on large scale, as the reaction proceeds quickly and the production of H₂, combined with heat from the accompanying exotherm, can ignite a fire.
- (51) For safety reasons, *p*-4-acetamidobenzenesulfonyl azide (*p*-ABSA) was used as an alternative diazo transfer reagent in place of tosyl azide, see reference 17.
- (52) Reaction time varies with the age of the lamp. A UV-opaque film slowly develops on the inside surface of the flask facing the lamp upon prolonged irradiation. This film can be removed by soaking the flask in an alkali base bath (KOH, 4:1 *i*-PrOH/H₂O).
- (53) Minor signals in the ¹H and ¹³C spectra of **156** are consistent with 5,5-dimethyl-2-cyclopenten-1-one, see: Padwa, A.; Curtis, E. A. *J. Org. Chem.* **1996**, *61*, 73.
- (54) Prepared according to: Piers, E.; Grierson, J. R.; Lau, C. K.; Nagakura, I. *Can. J. Chem.* **1982**, *60*, 210.
- (55) Prepared according to the ligand protocol described in: Bao, H.; Qi, X.; Tambar, U. K. *J. Am. Chem. Soc.* **2011**, *133*, 1206. We found that the use of CH₂Cl₂ (vs. THF) as a reaction solvent provided higher and more reproducible yields.
- (56) Prepared from cyclohexanone according to: Banwell, M. G.; Corbett, M.; Gulbis, J.; Mackay, M. F.; Reum, M. E. *J. Chem. Soc., Perkin Trans. I* **1993**, *8*, 945.
- (57) Ohira–Bestmann reagent prepared according to: Pietruszka, J.; Witt, A. *Synthesis* **2006**, *2006*, 4266.

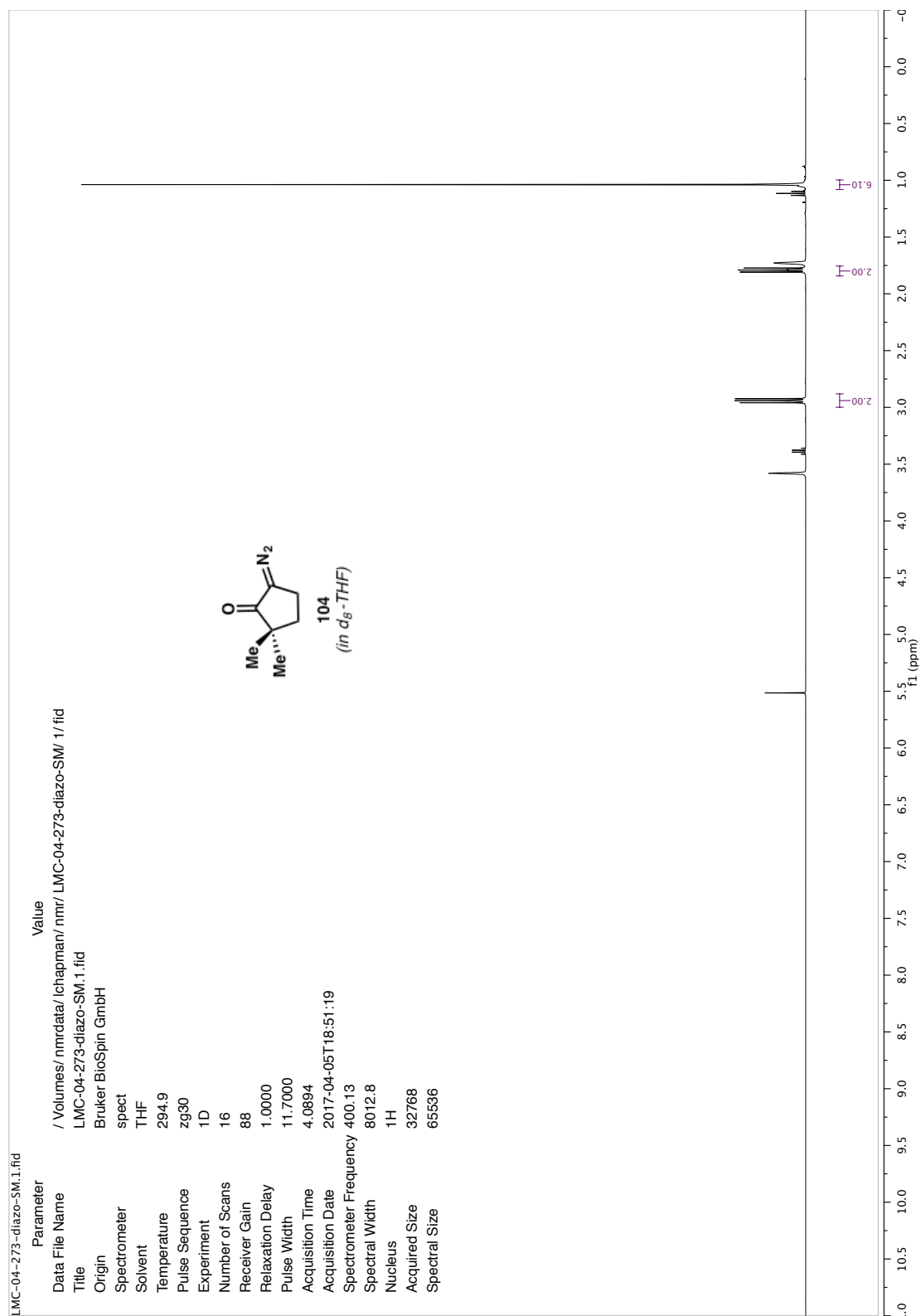
Appendix 1

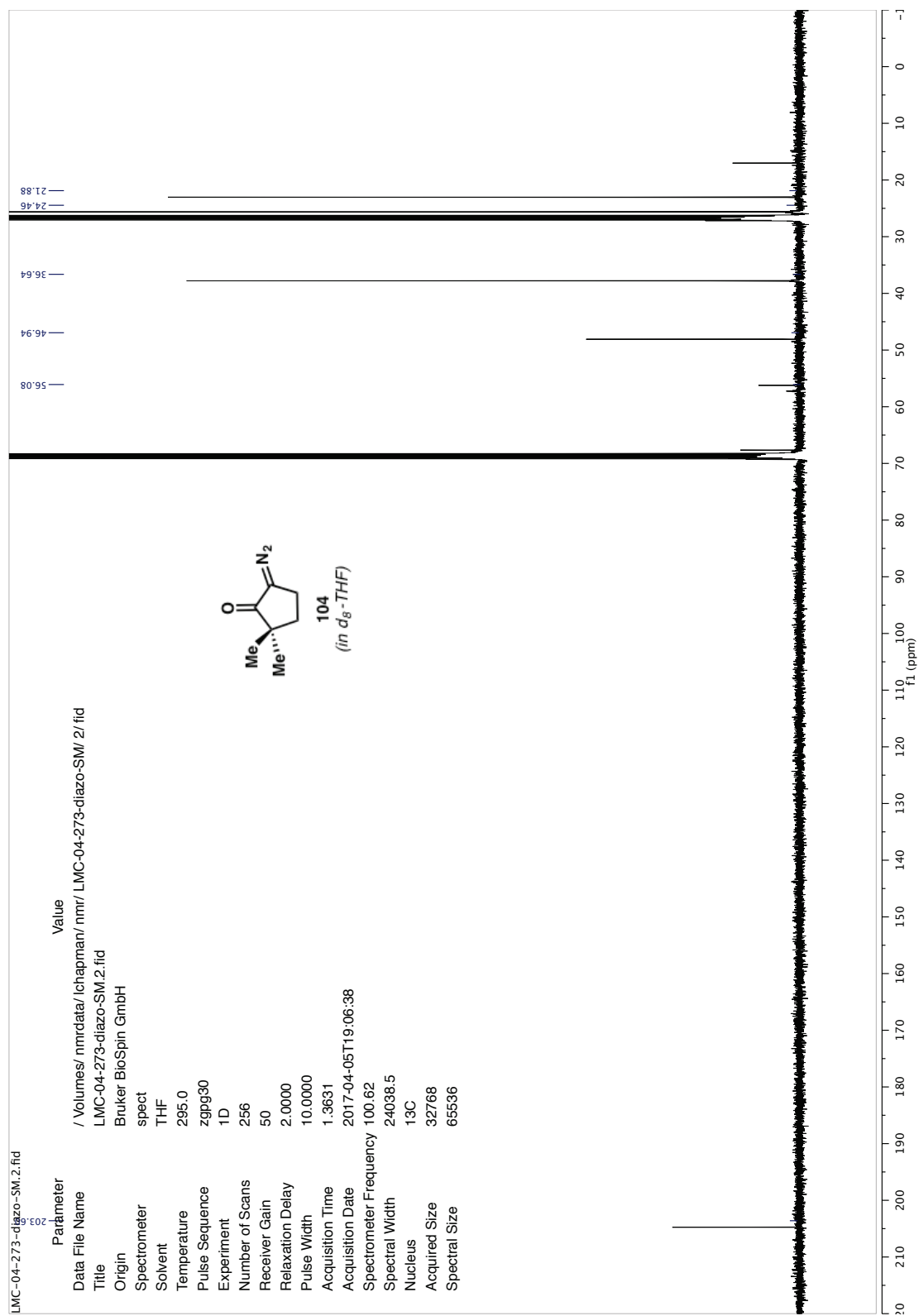
Spectra Relevant to Chapter 2:

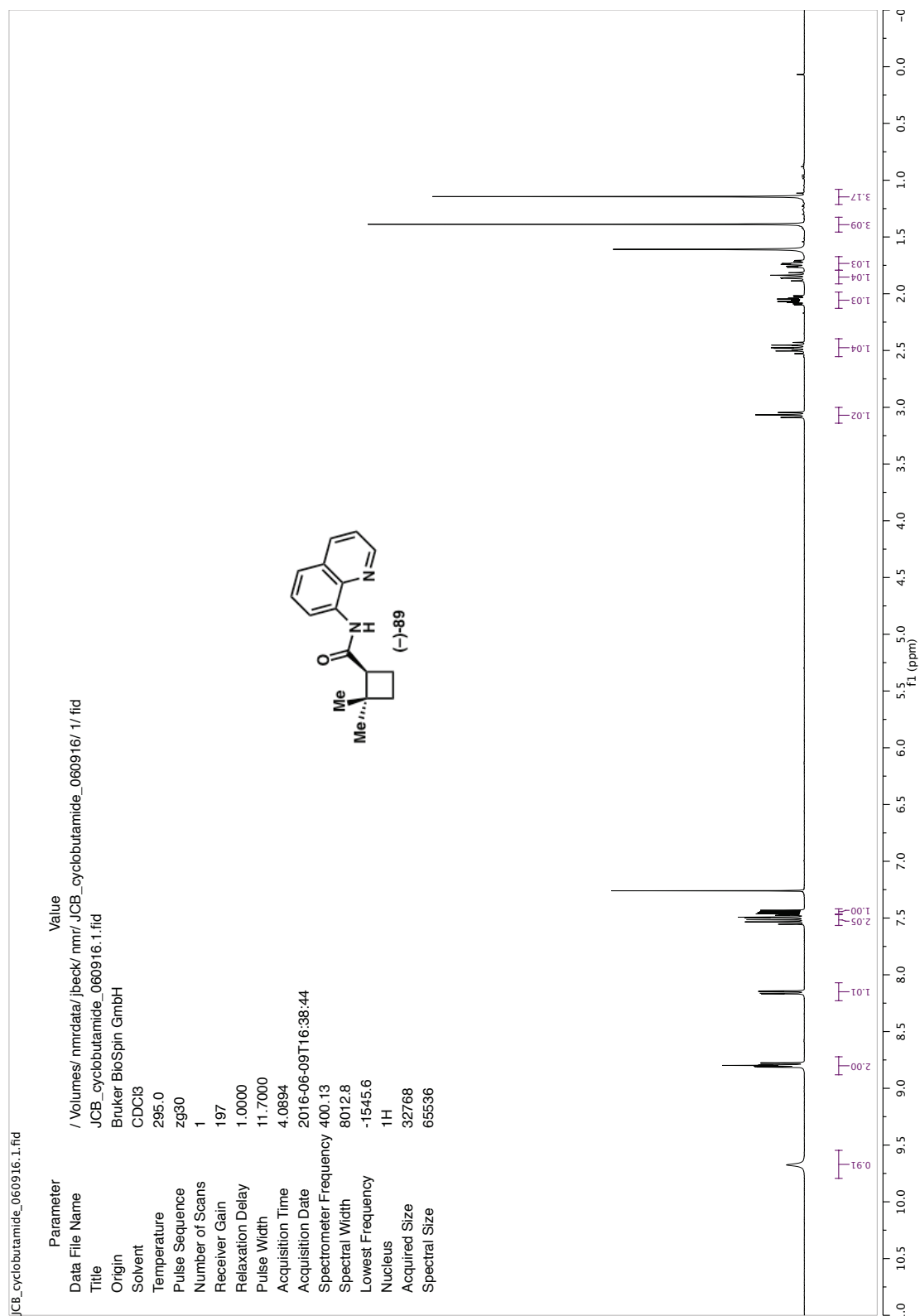
*First Generation Synthetic Strategy Toward (+)-Psiguadial B and
Development of a Catalytic, Asymmetric Wolff Rearrangement*

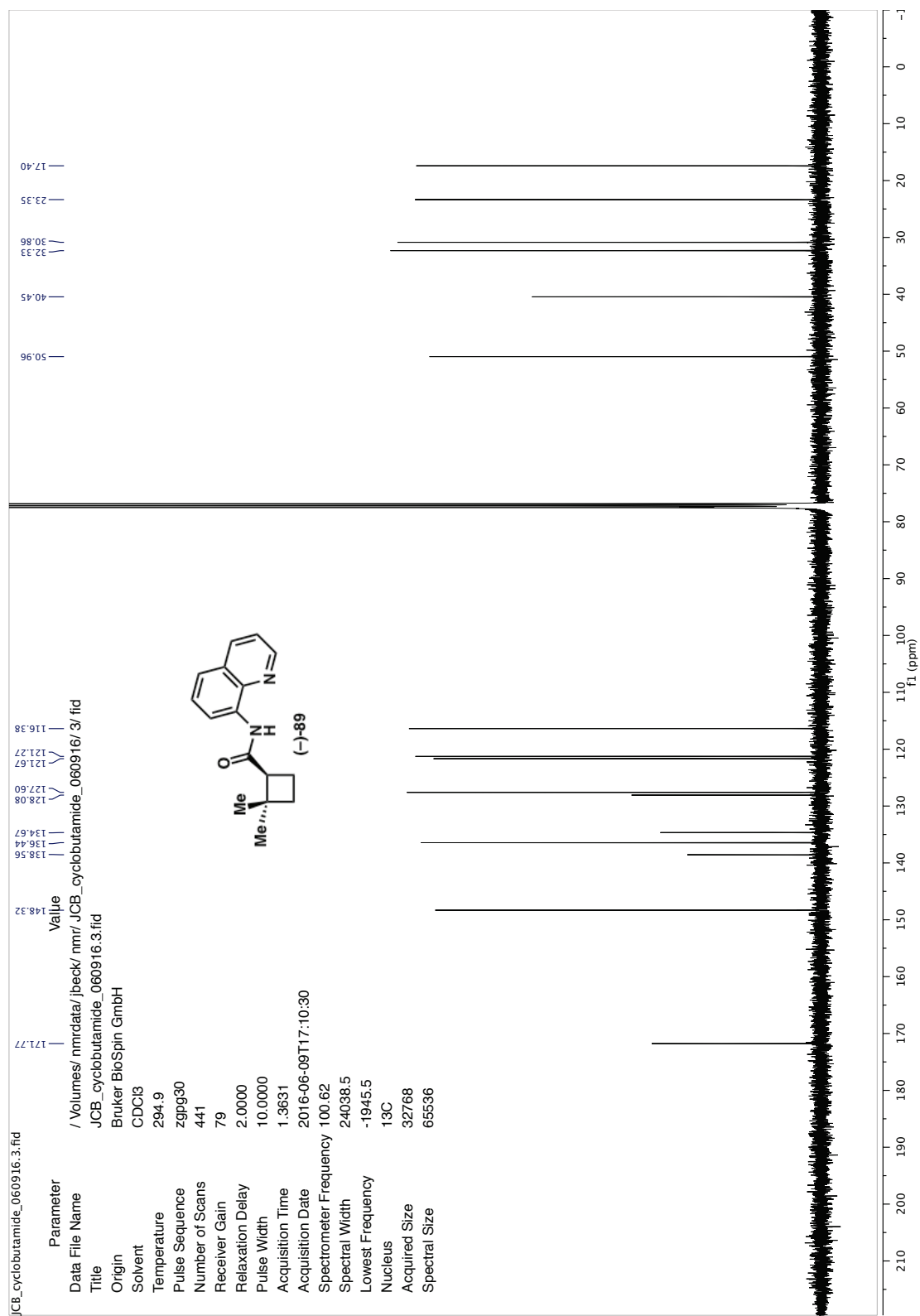


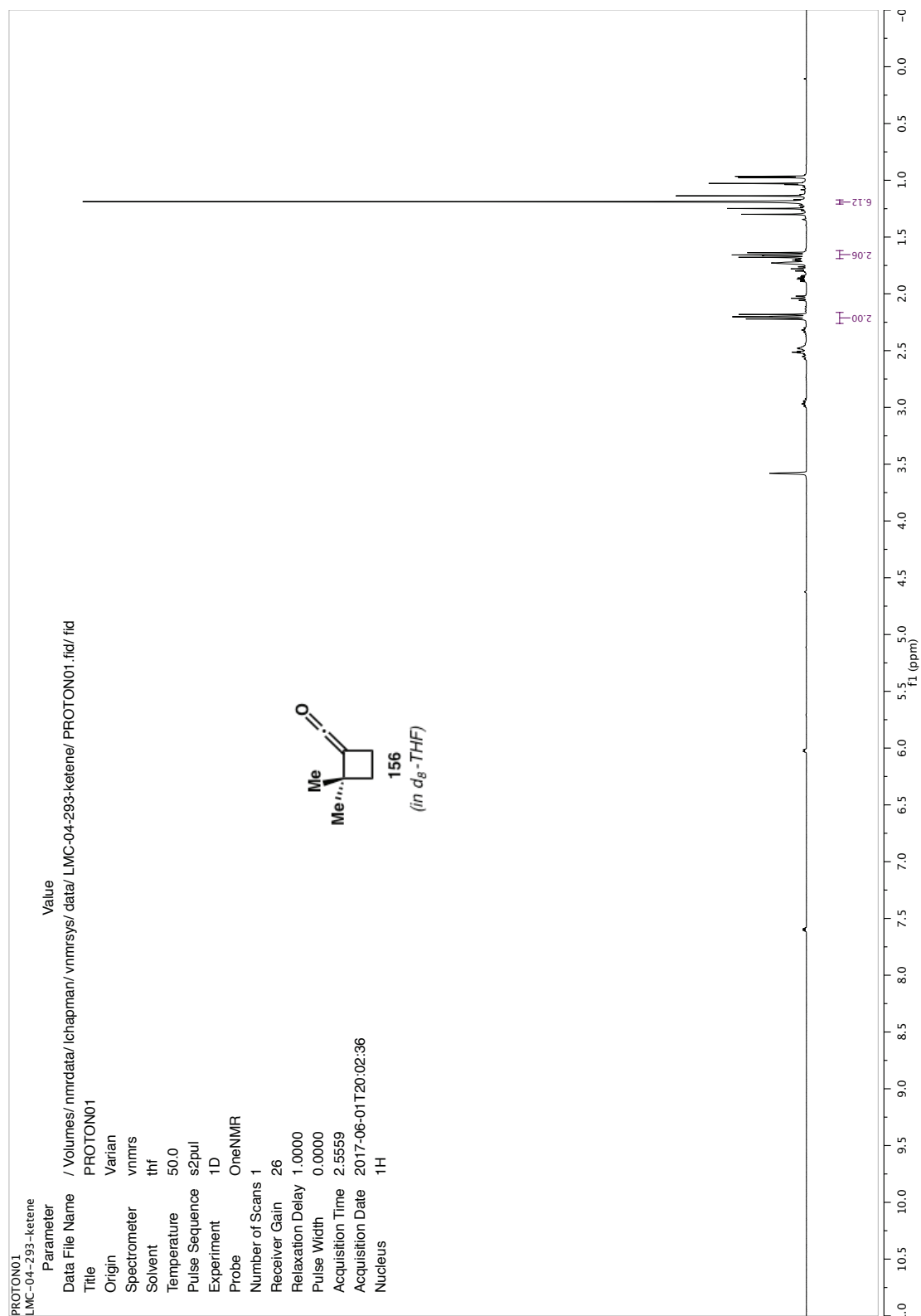


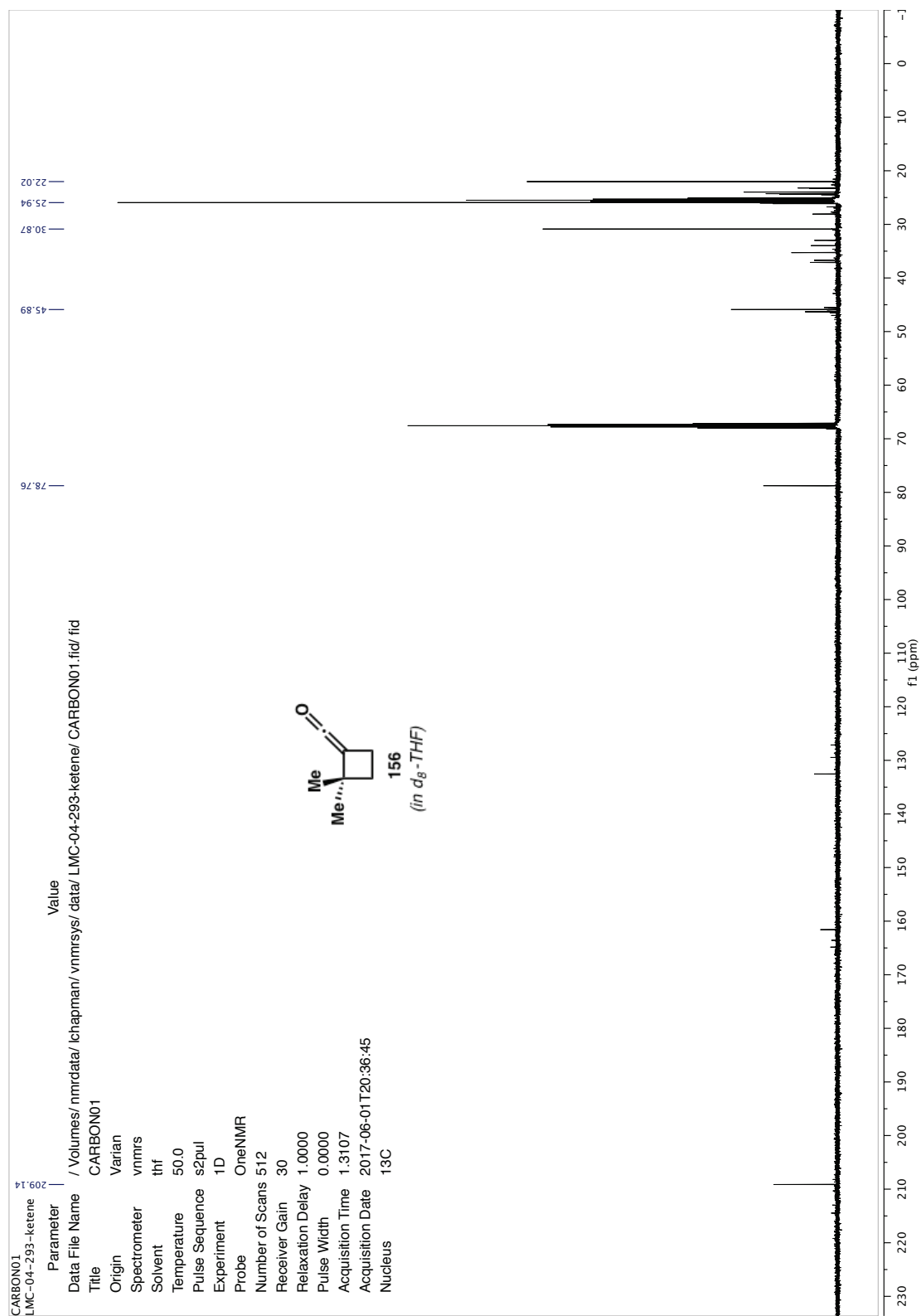


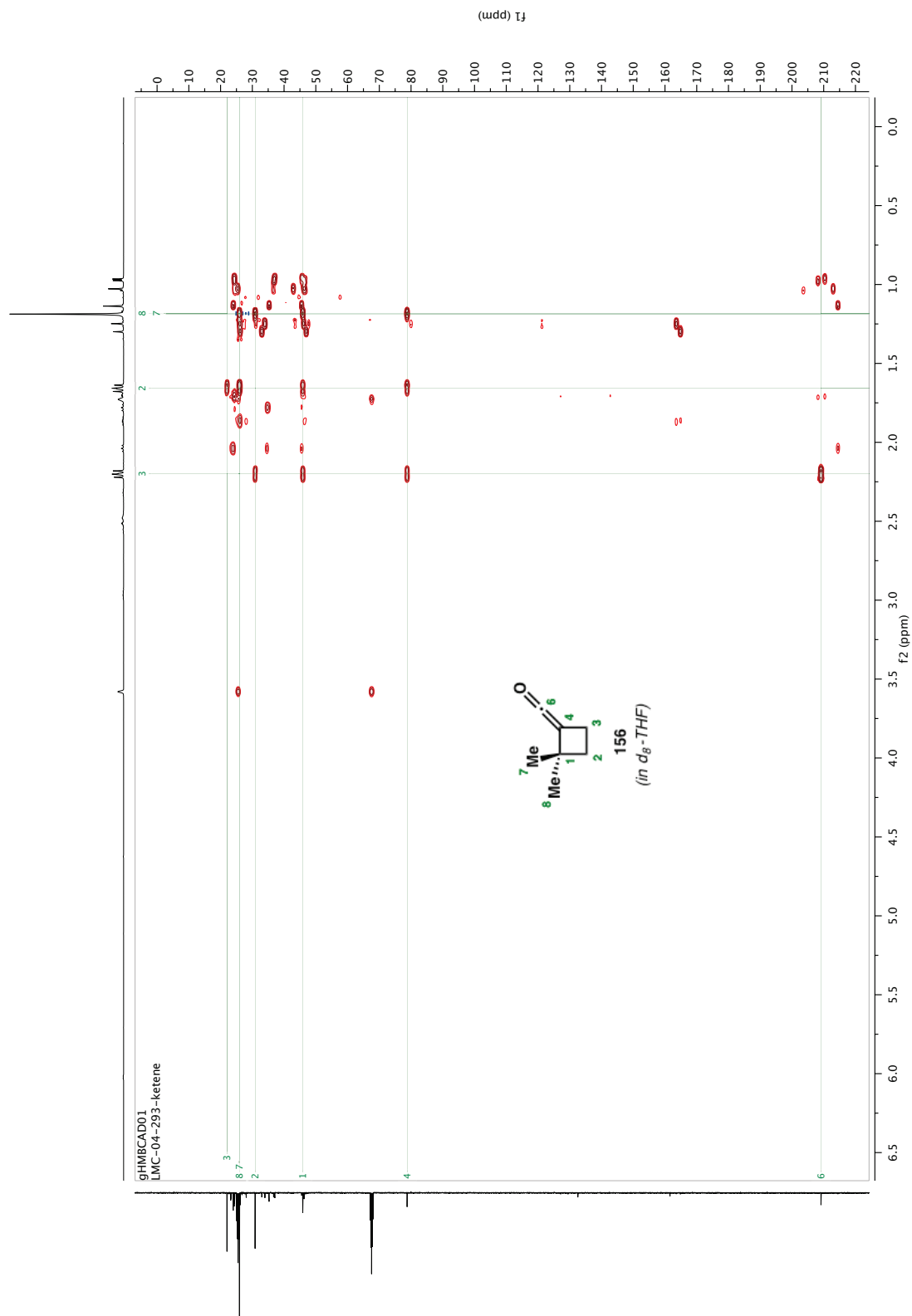


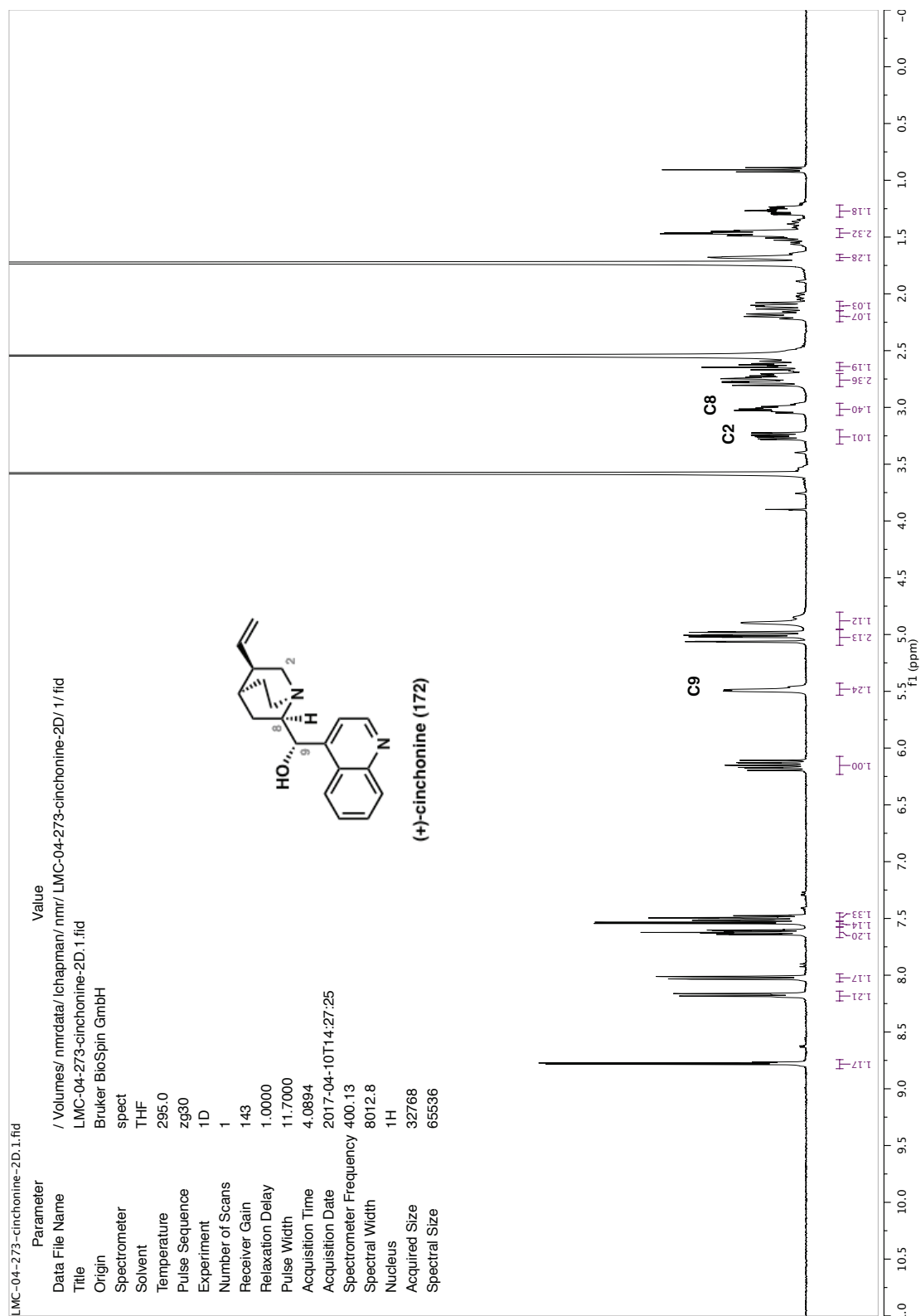


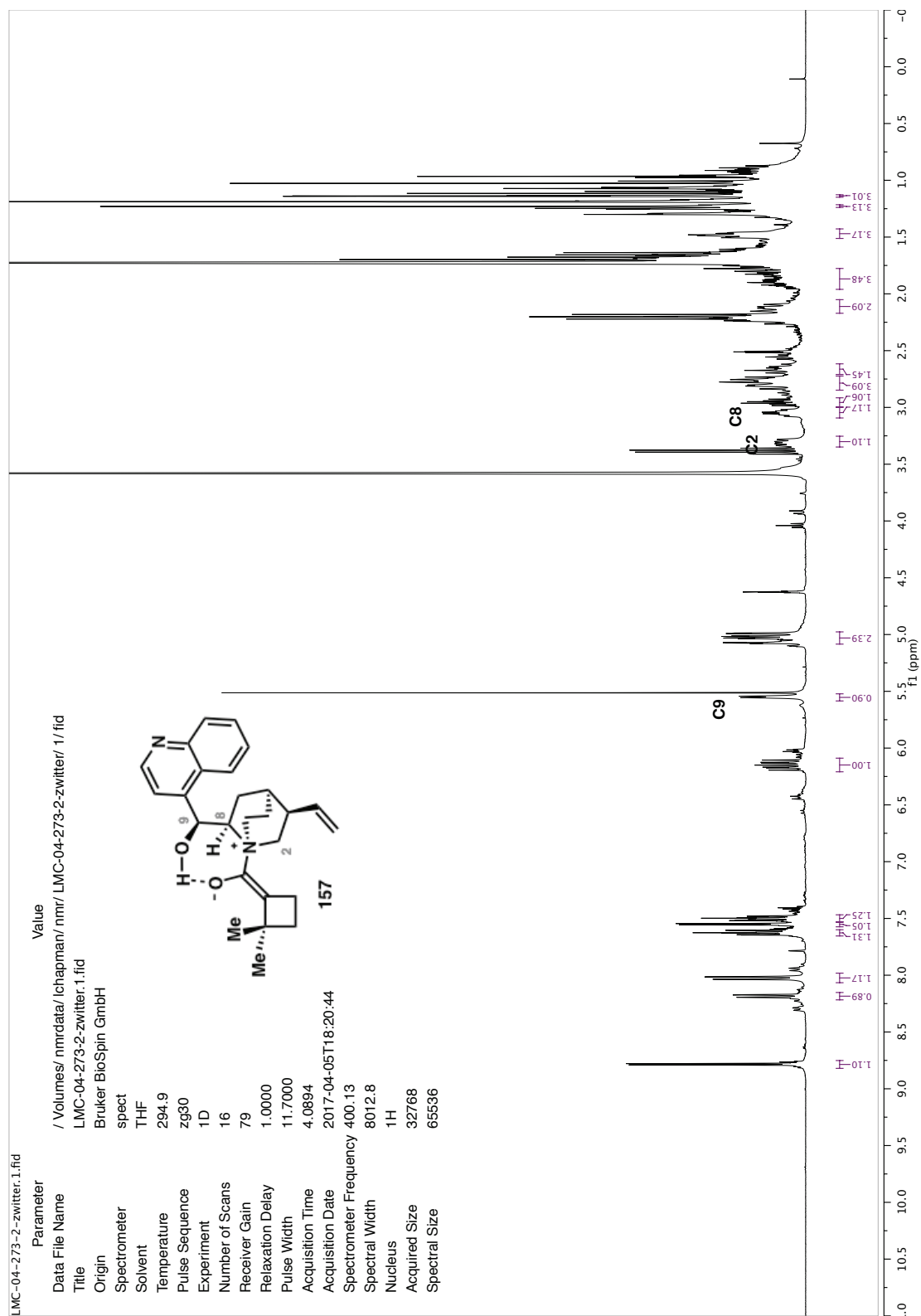


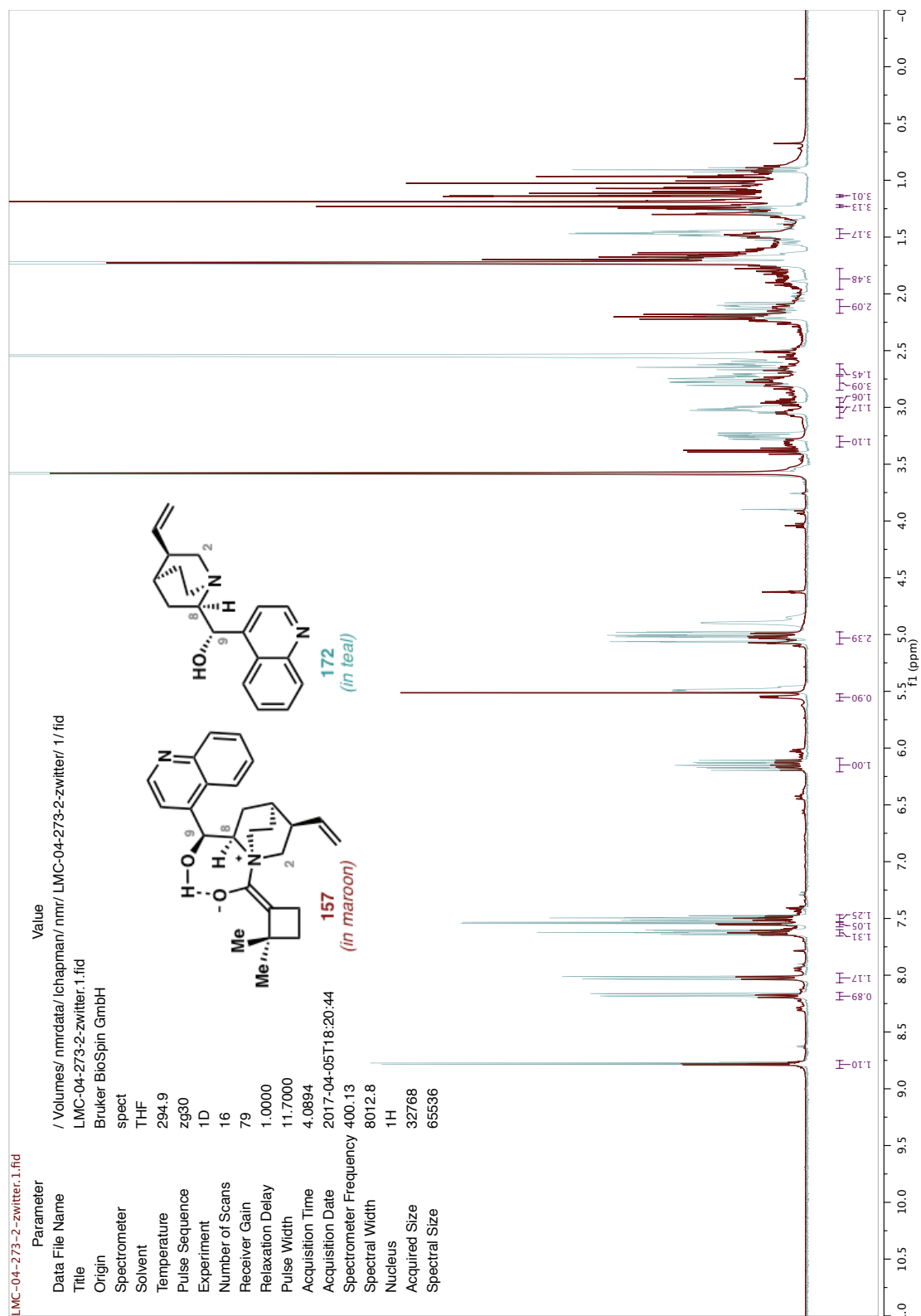


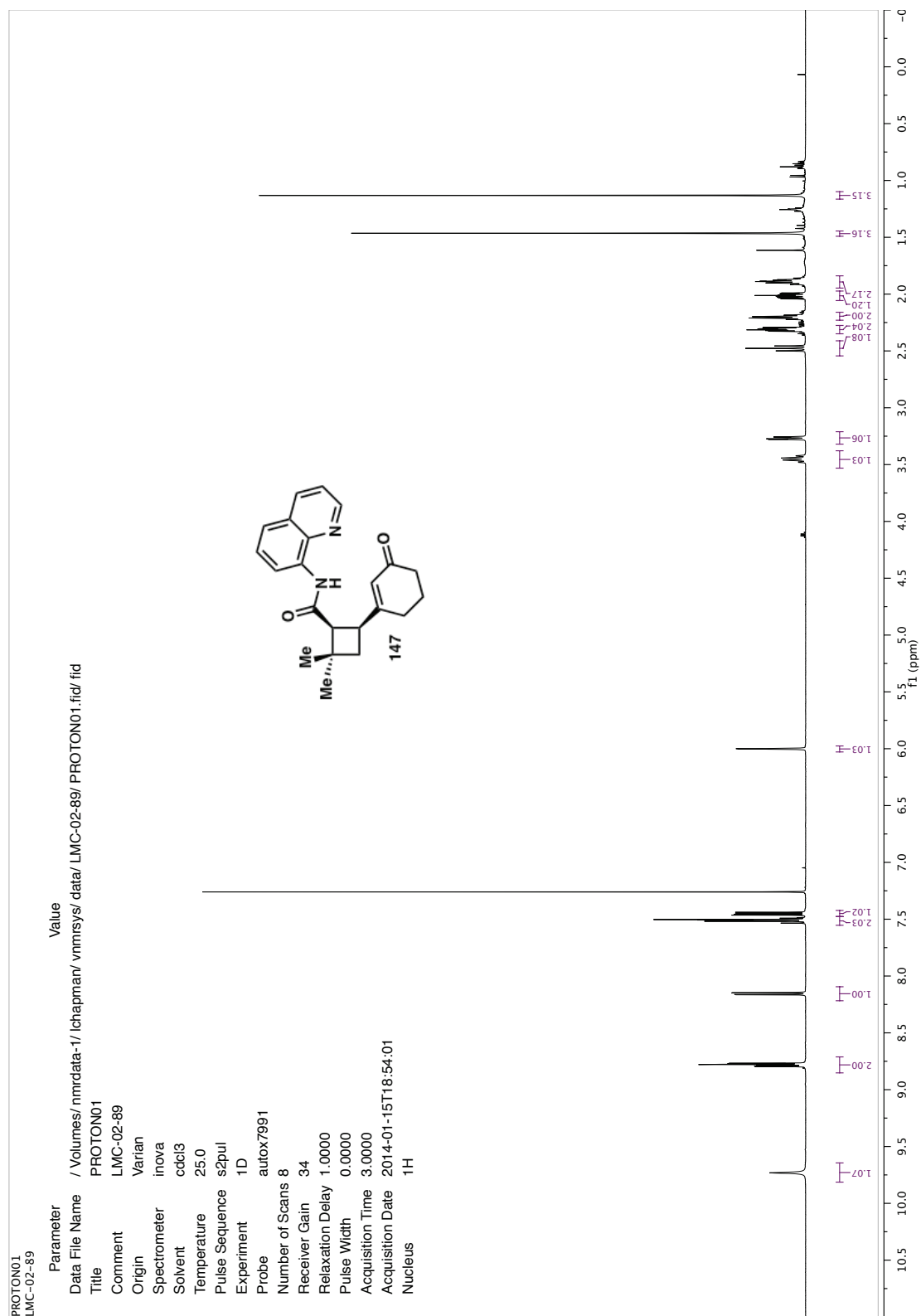


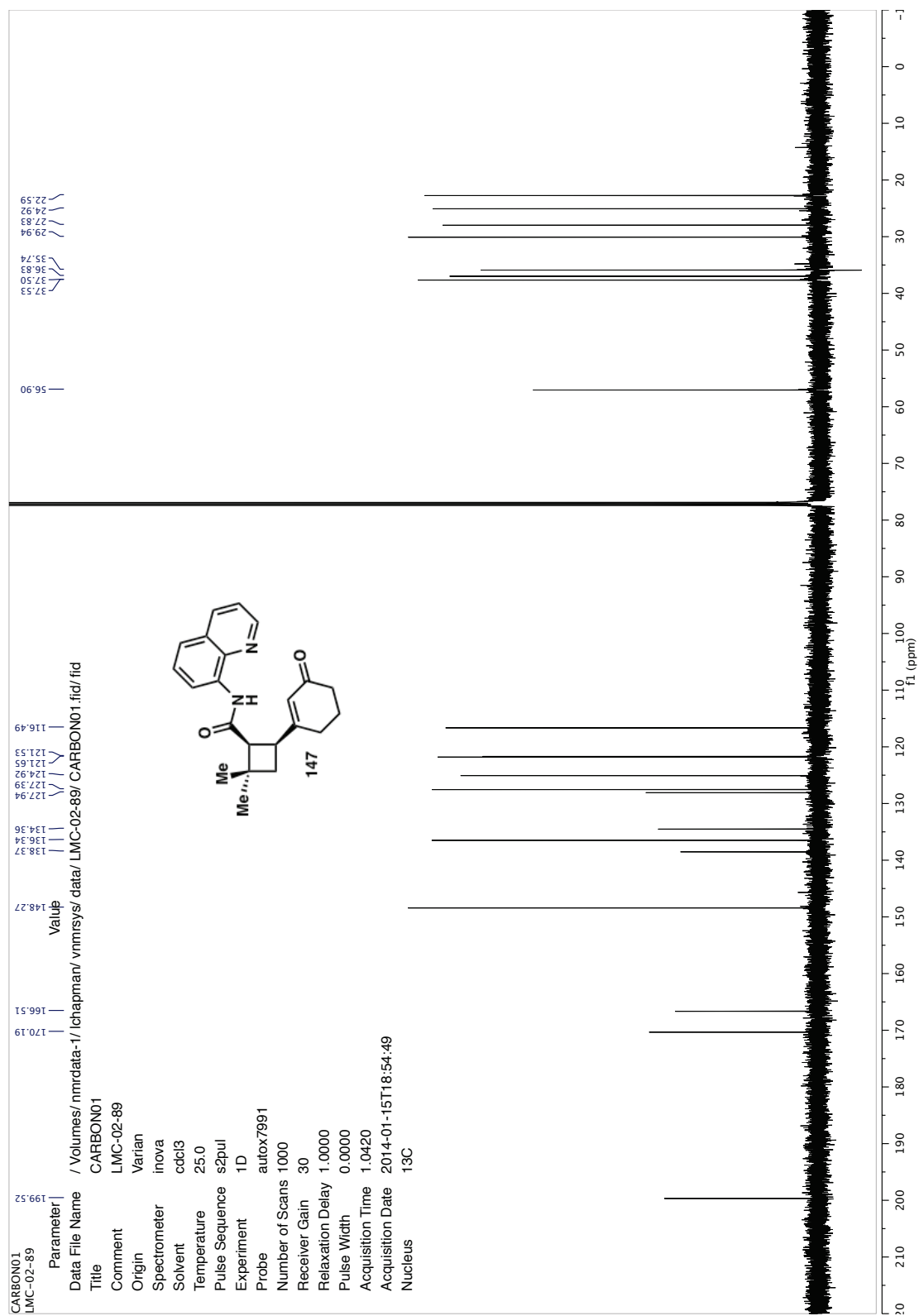


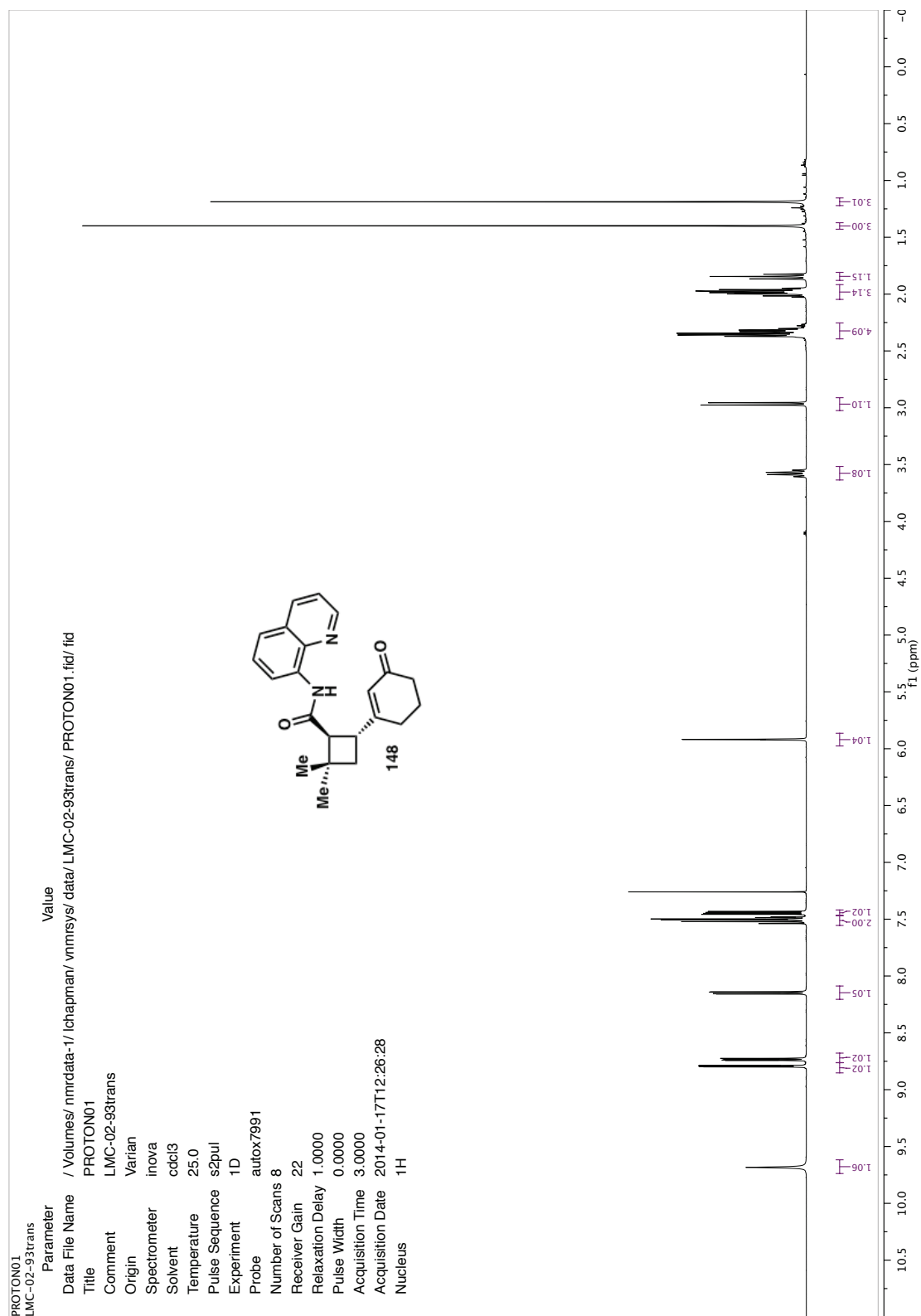


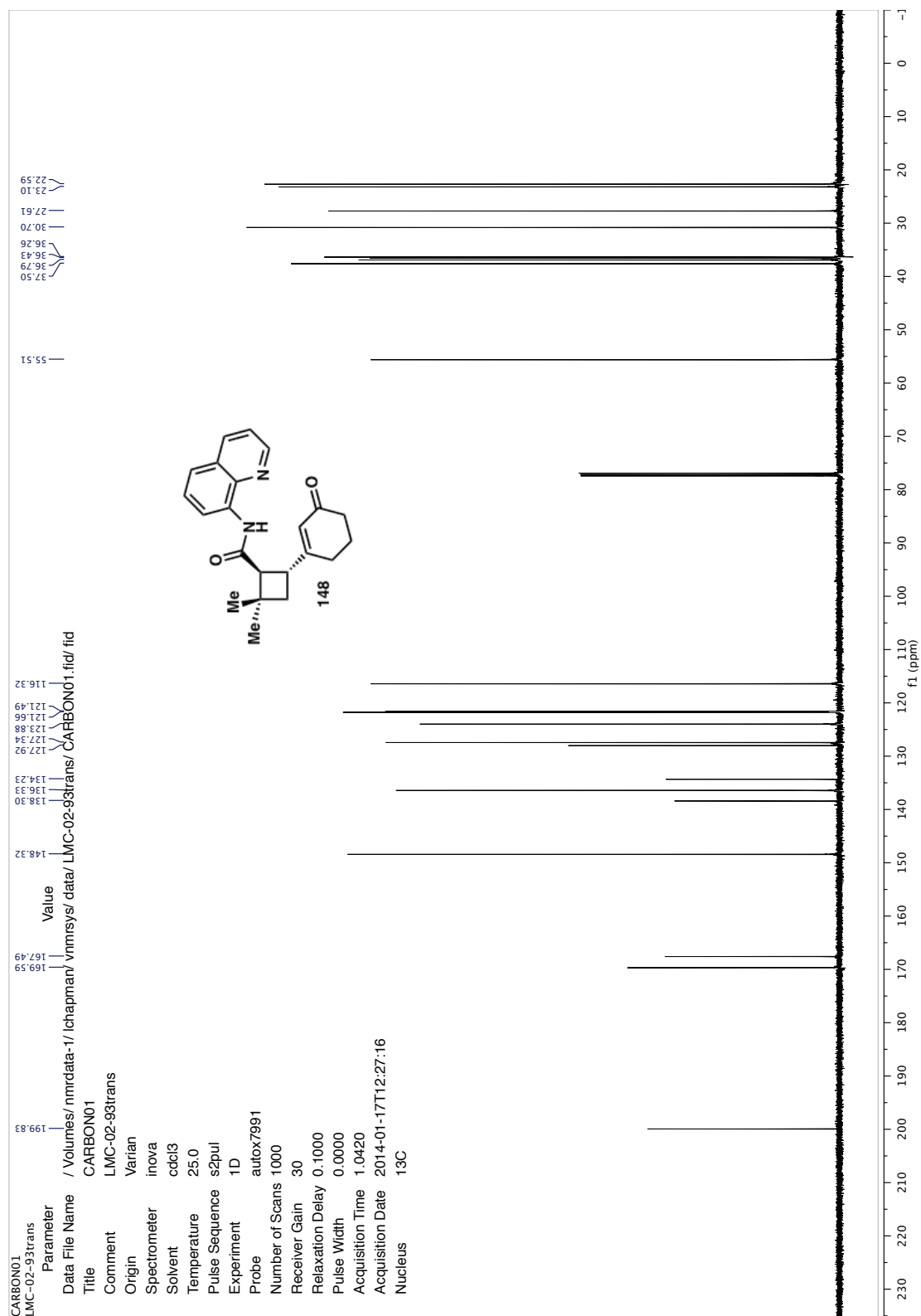


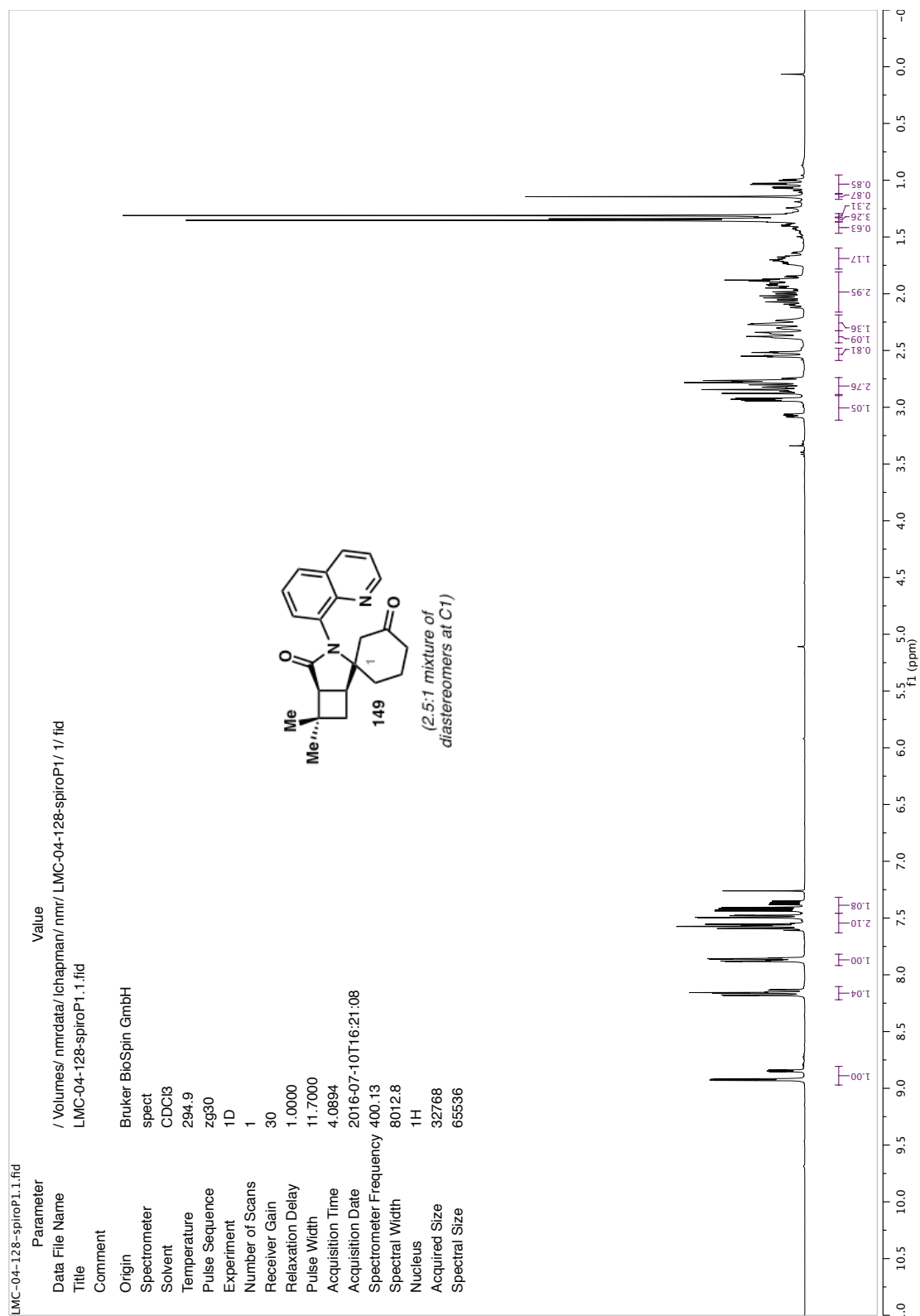


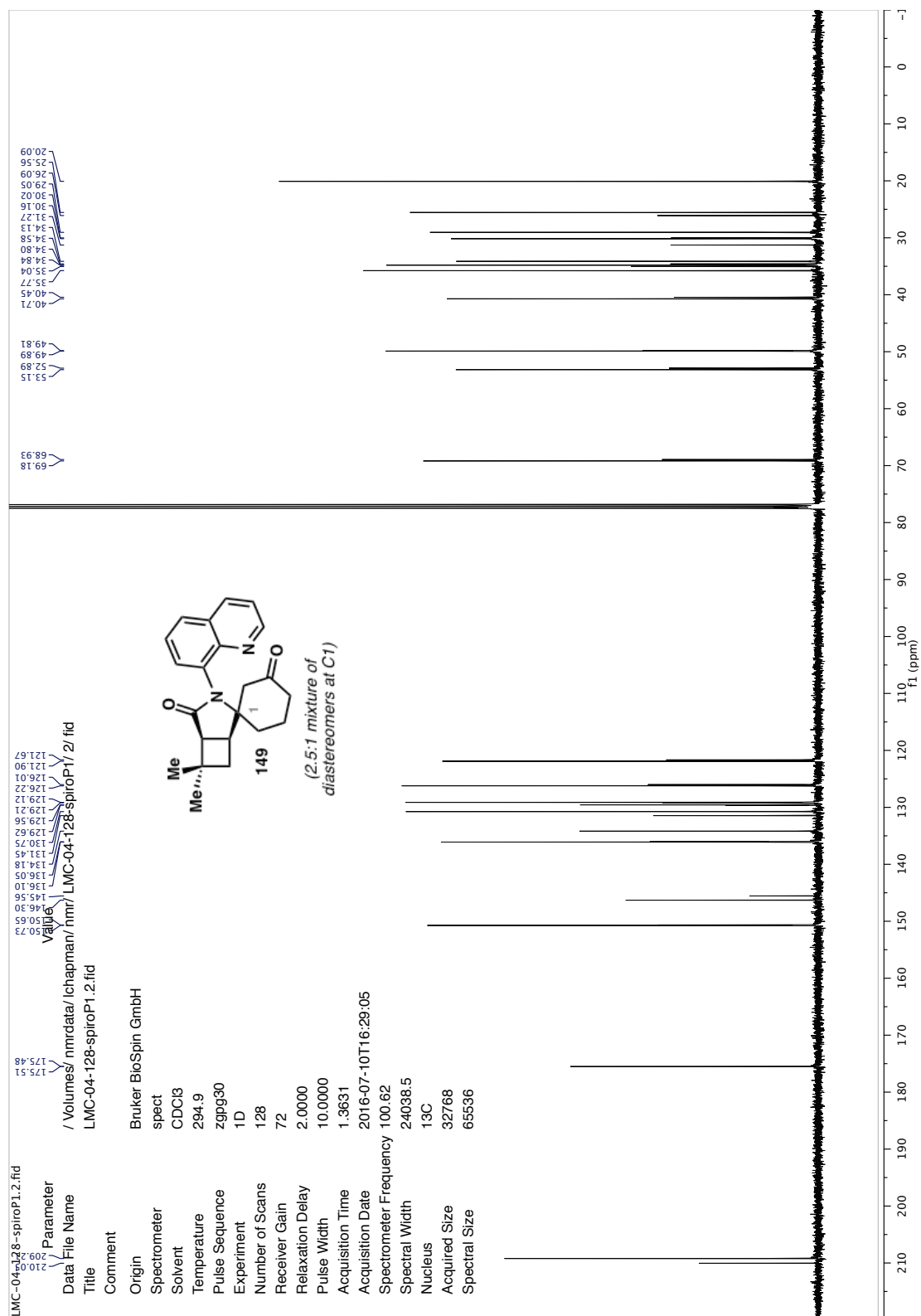


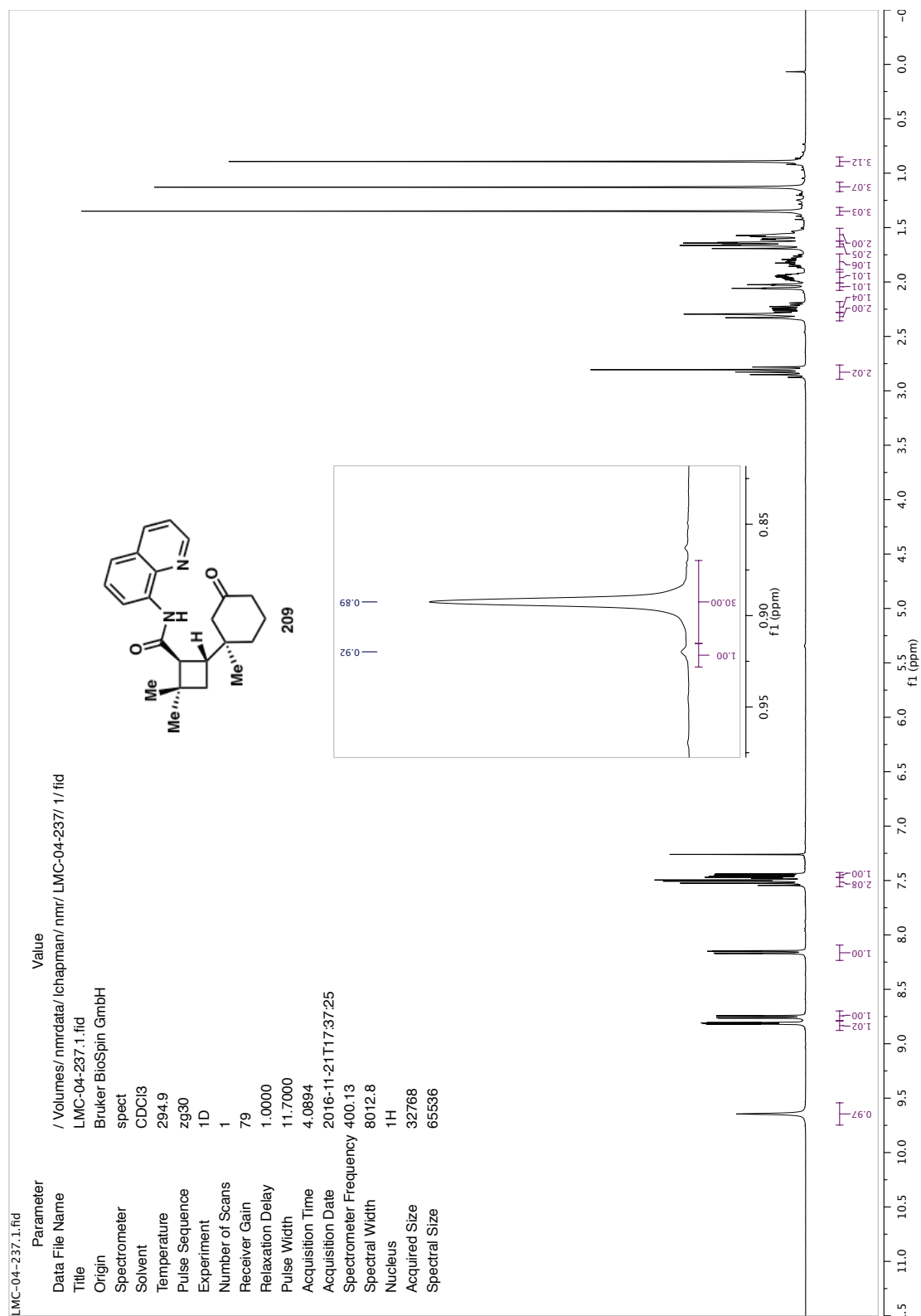


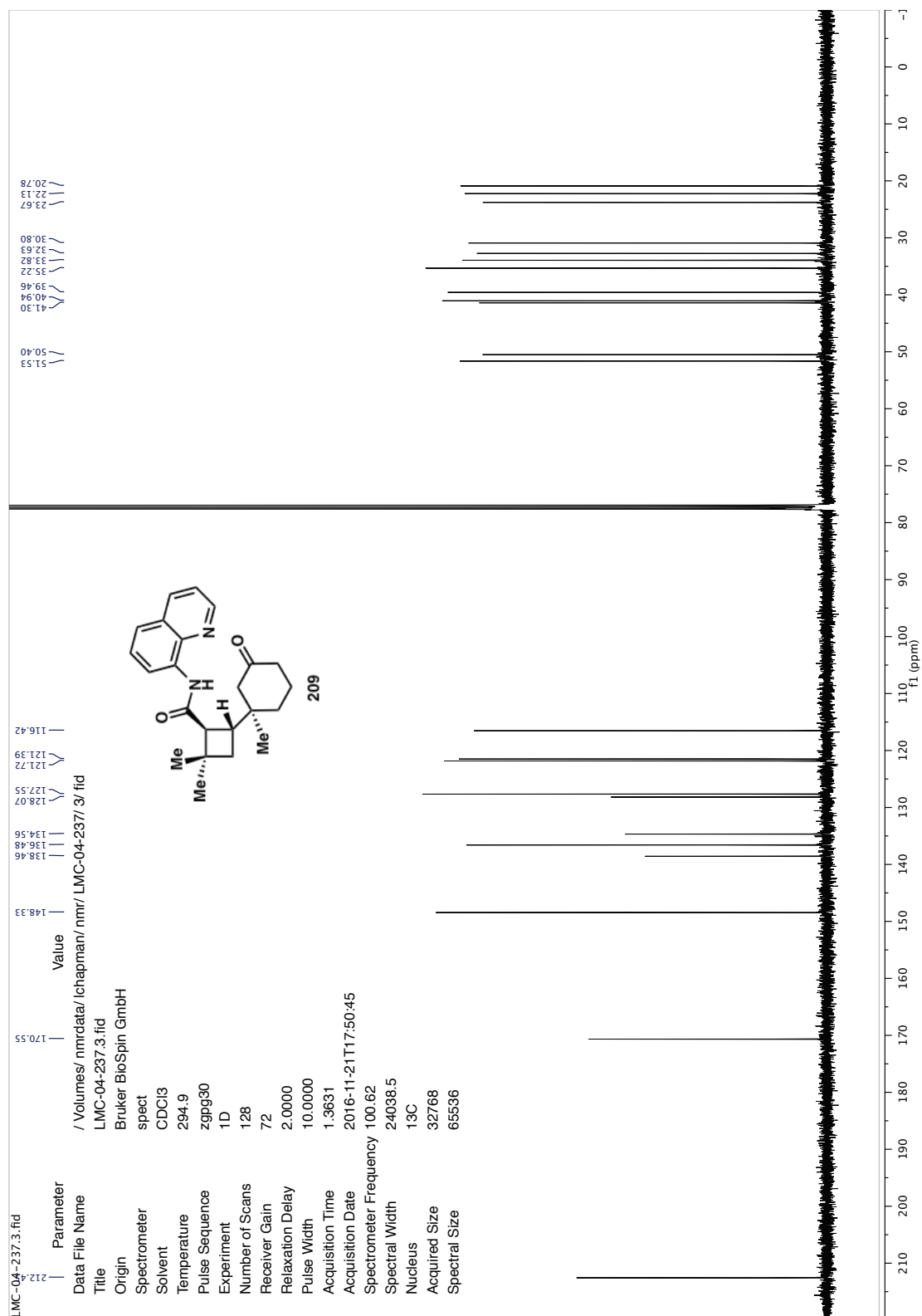


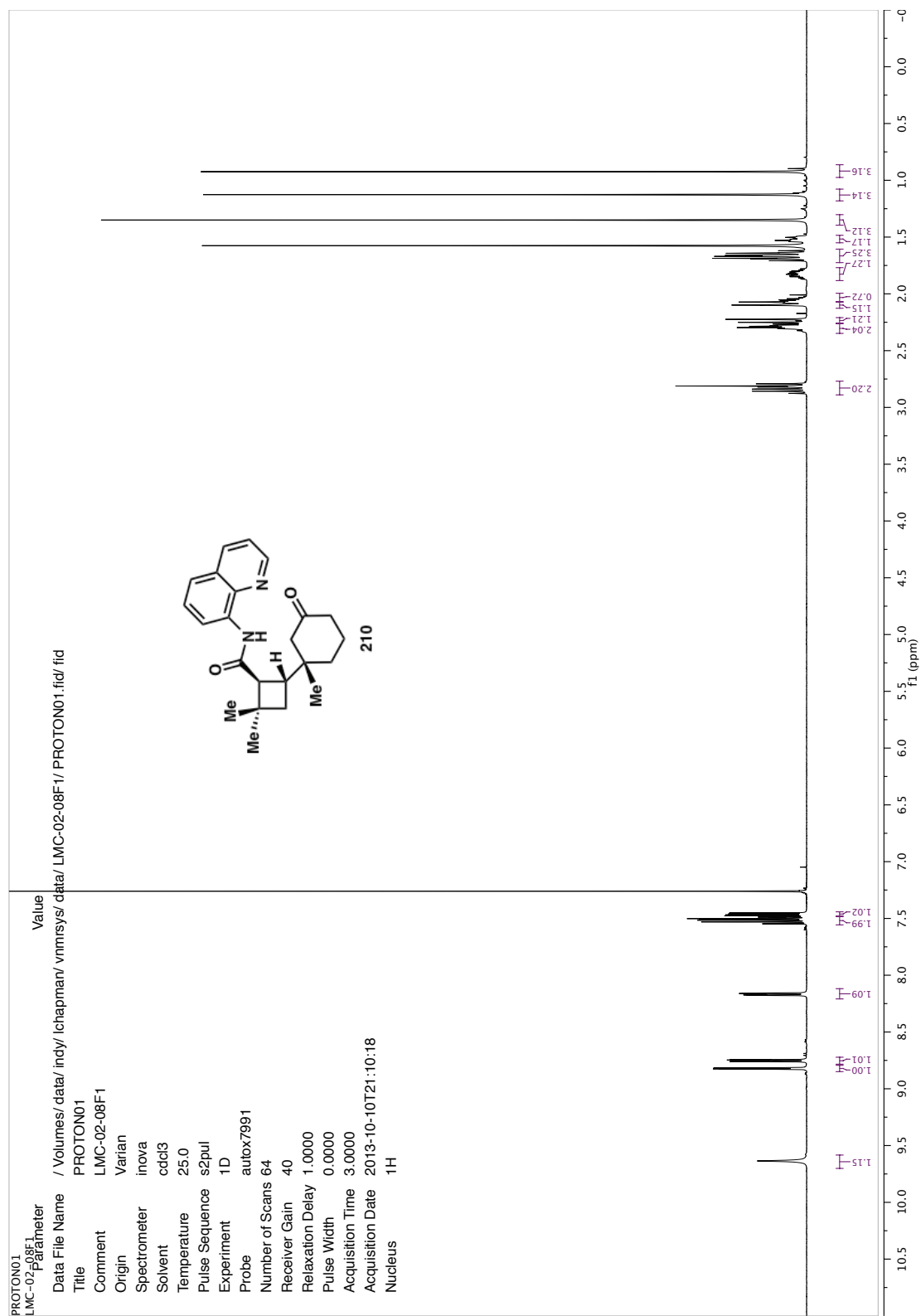


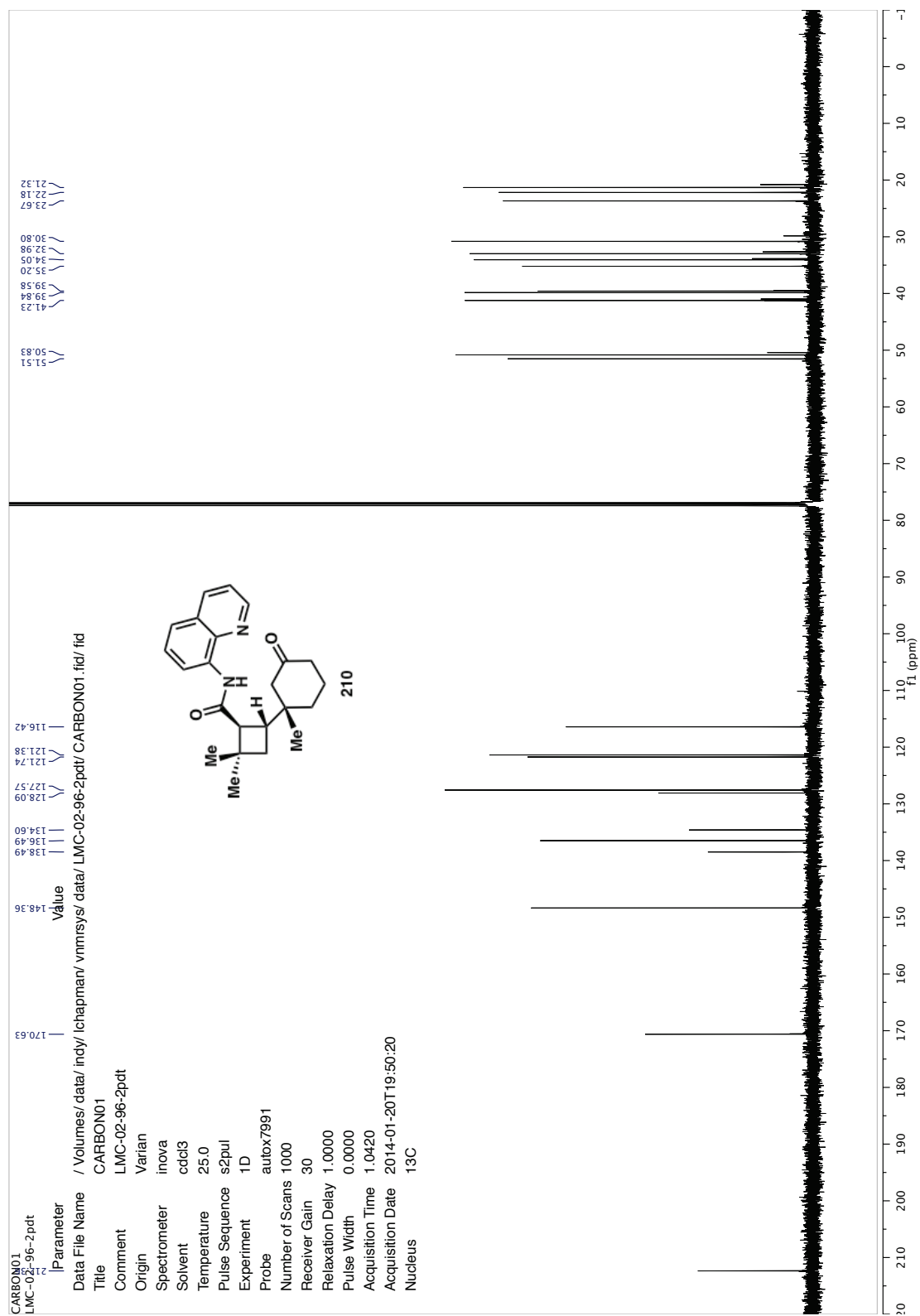


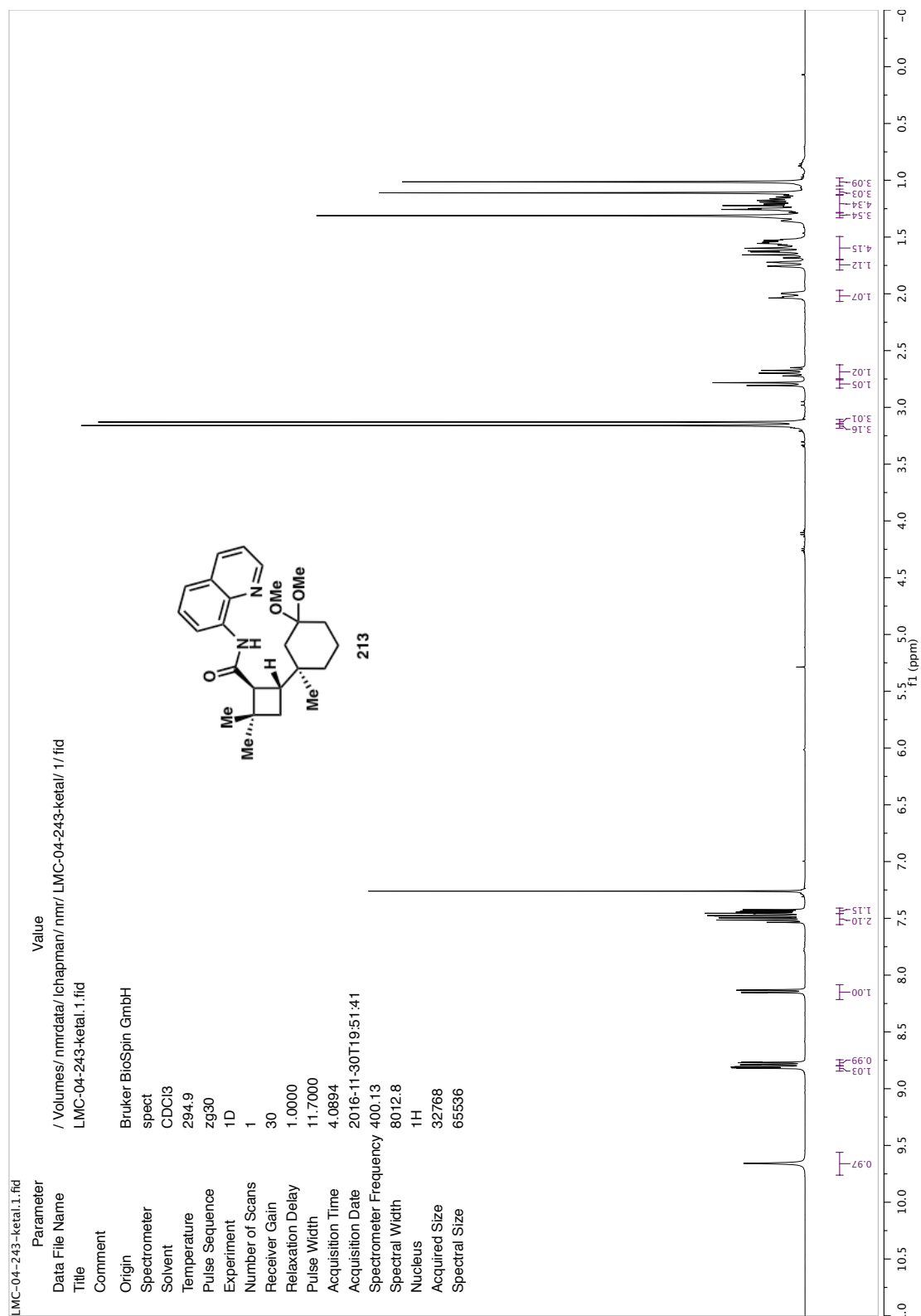


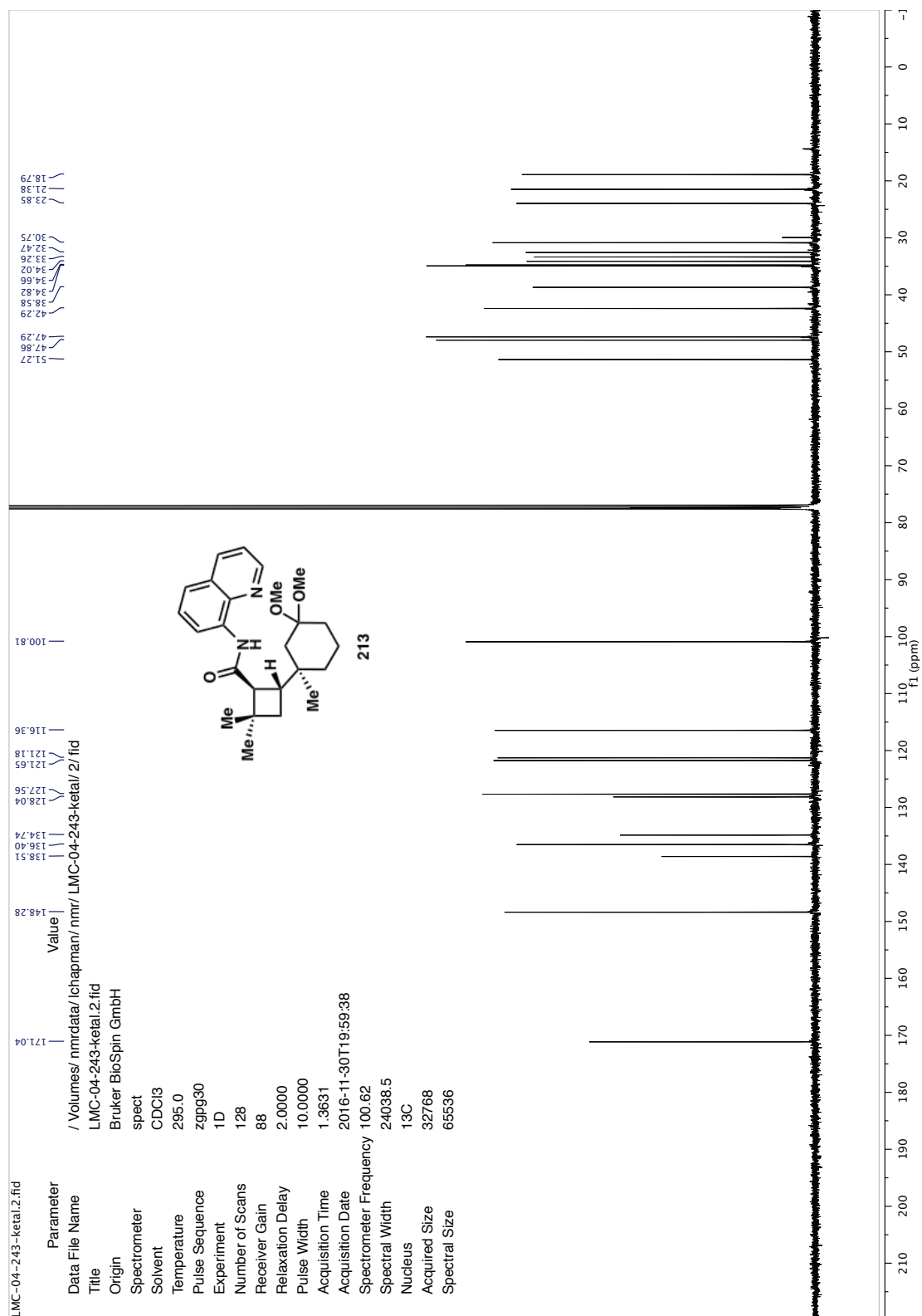


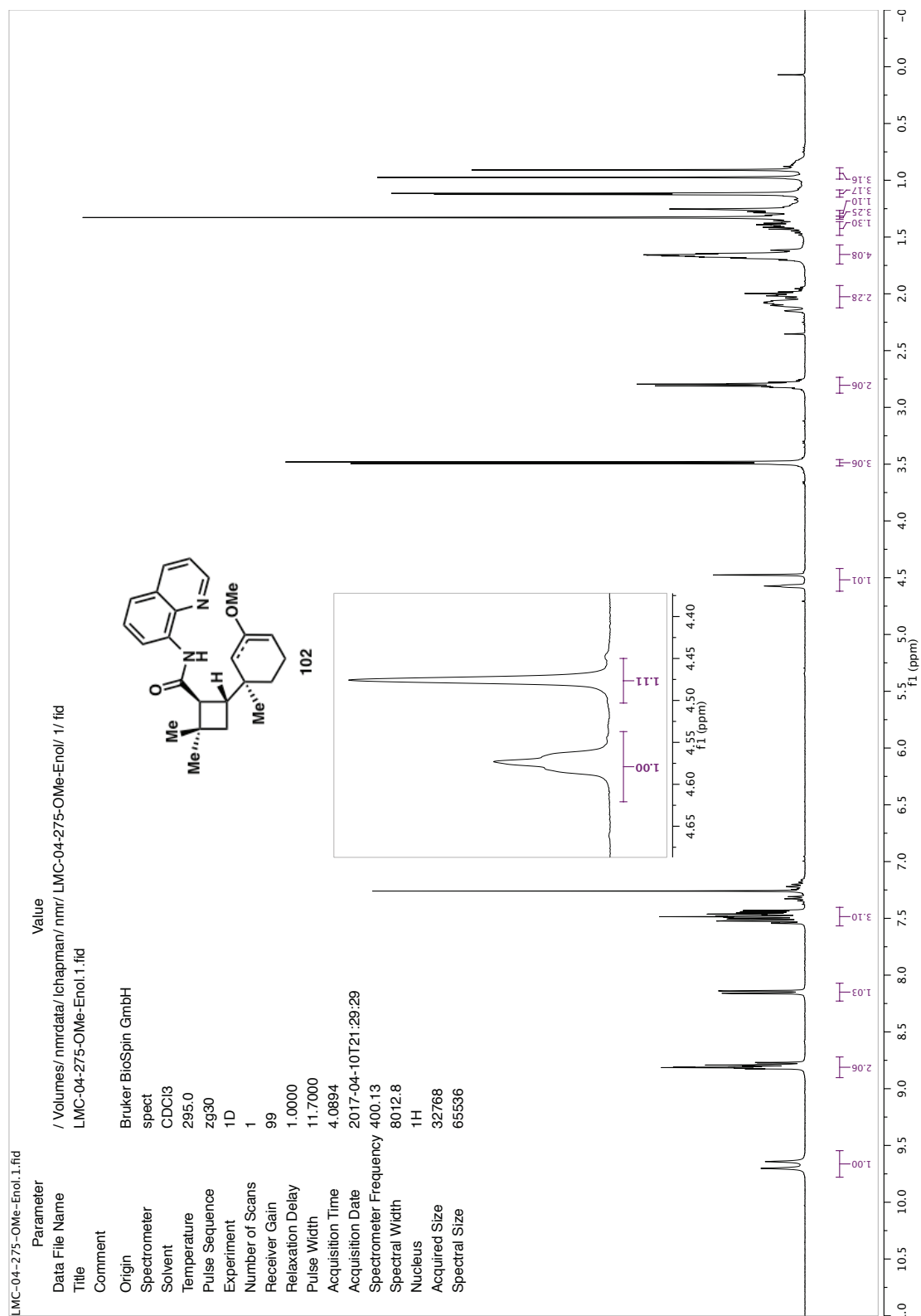


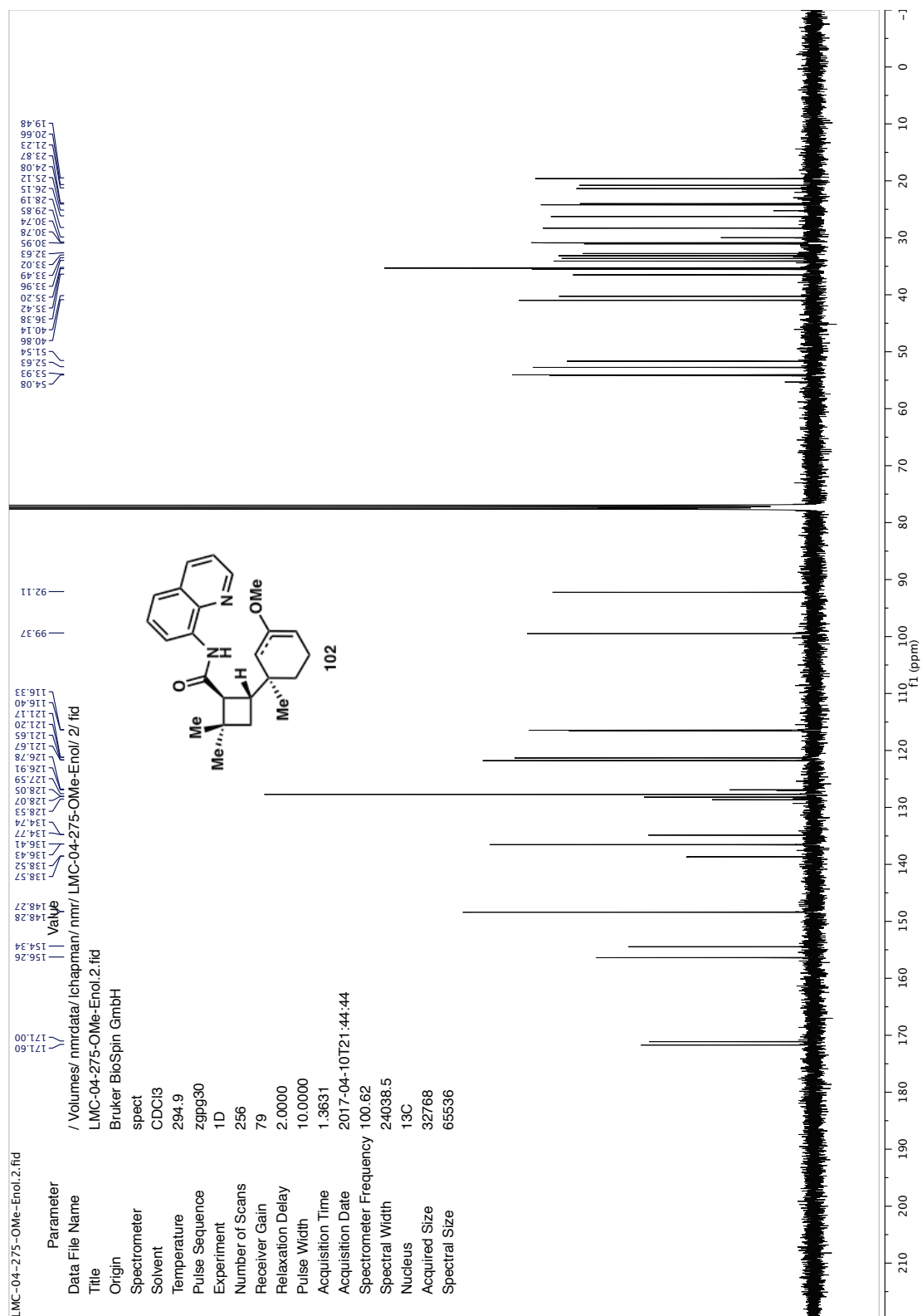


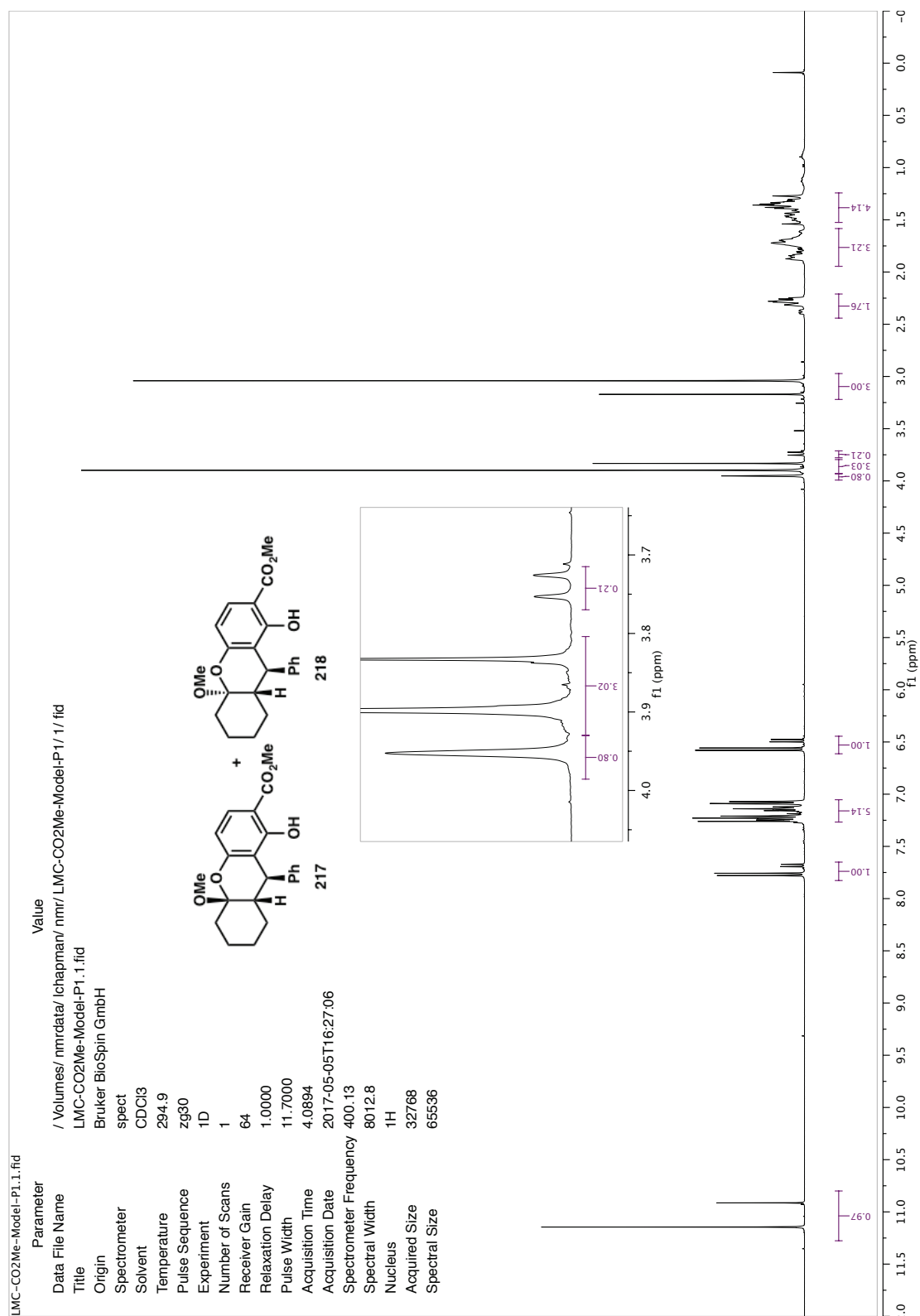


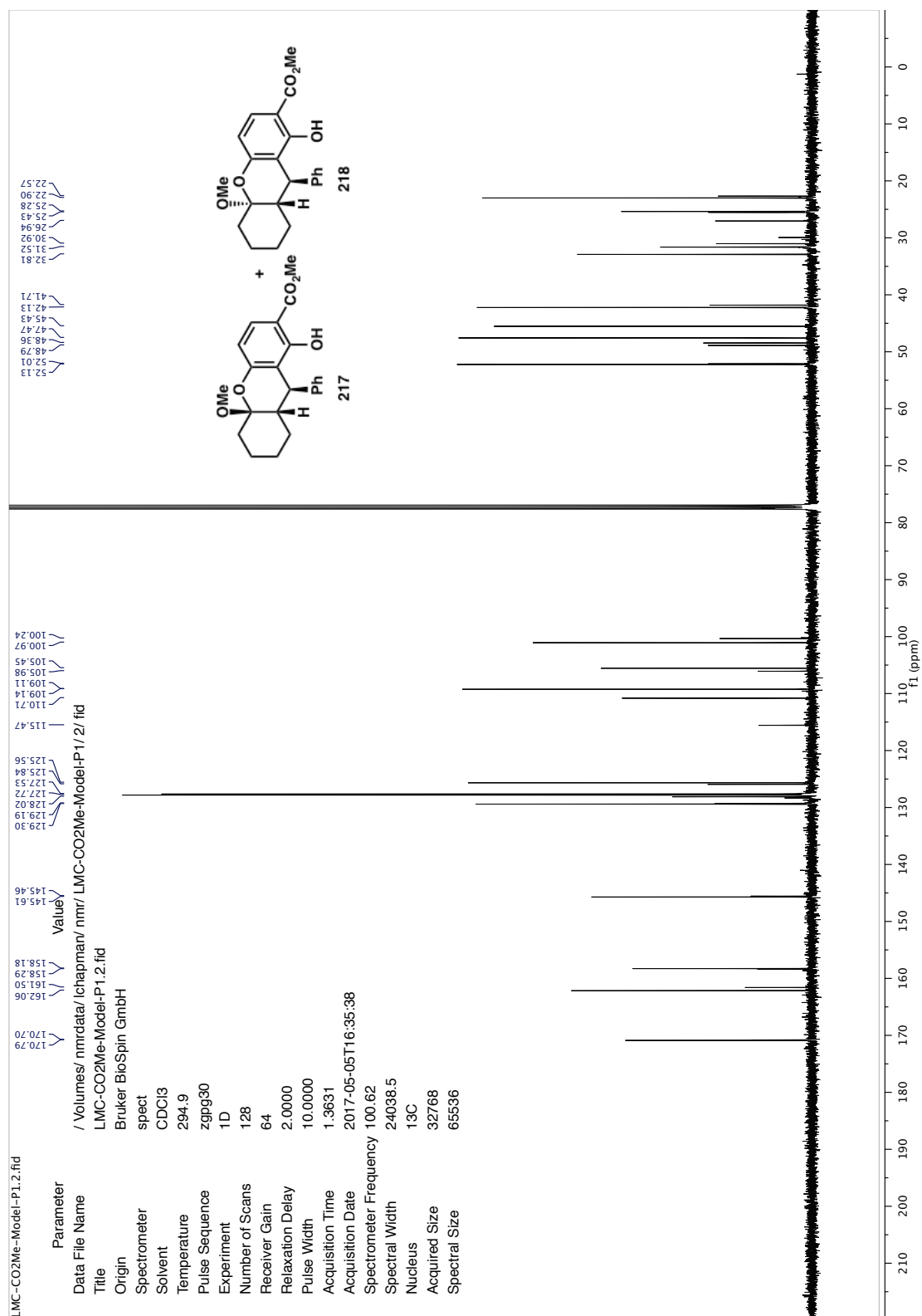


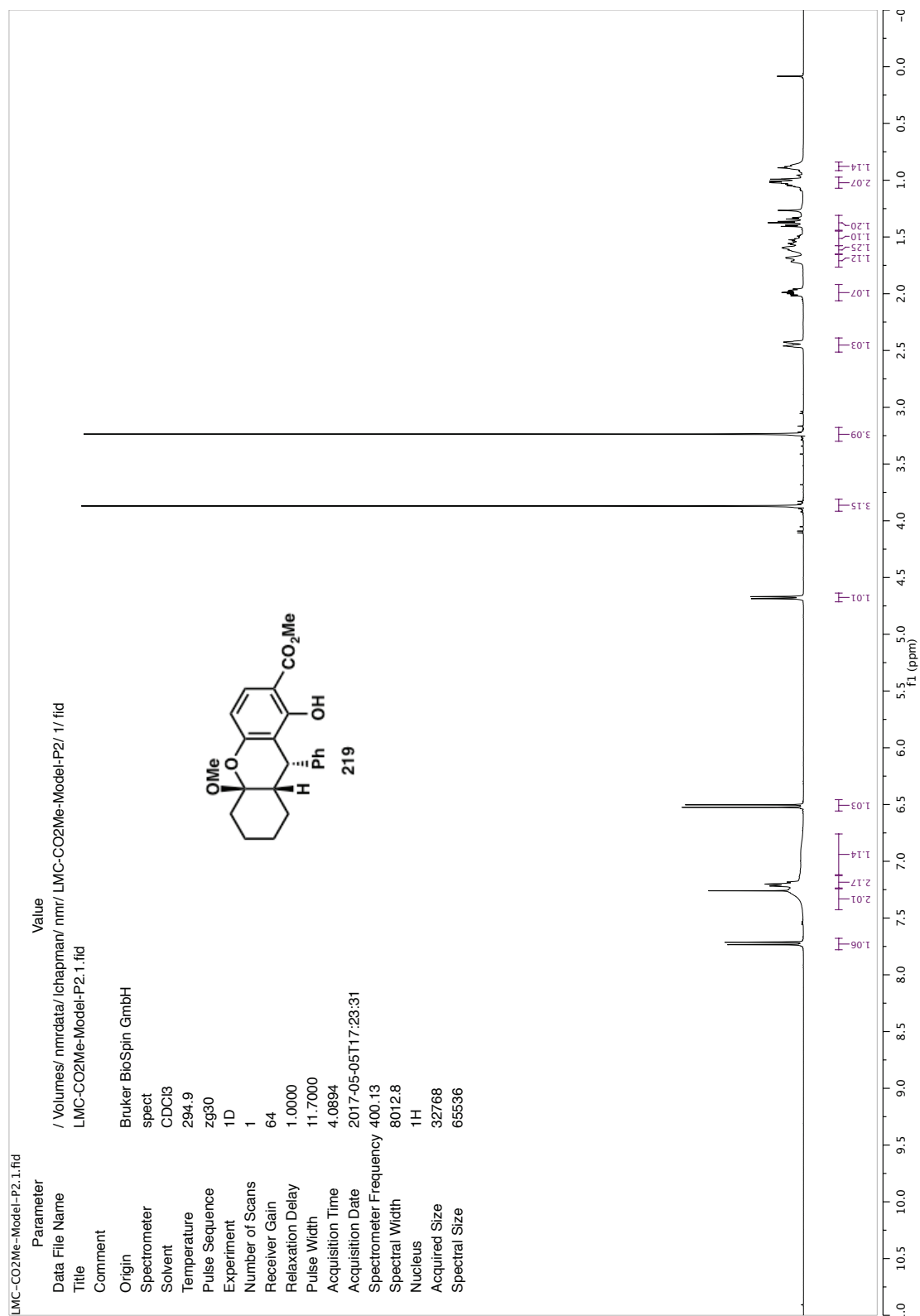


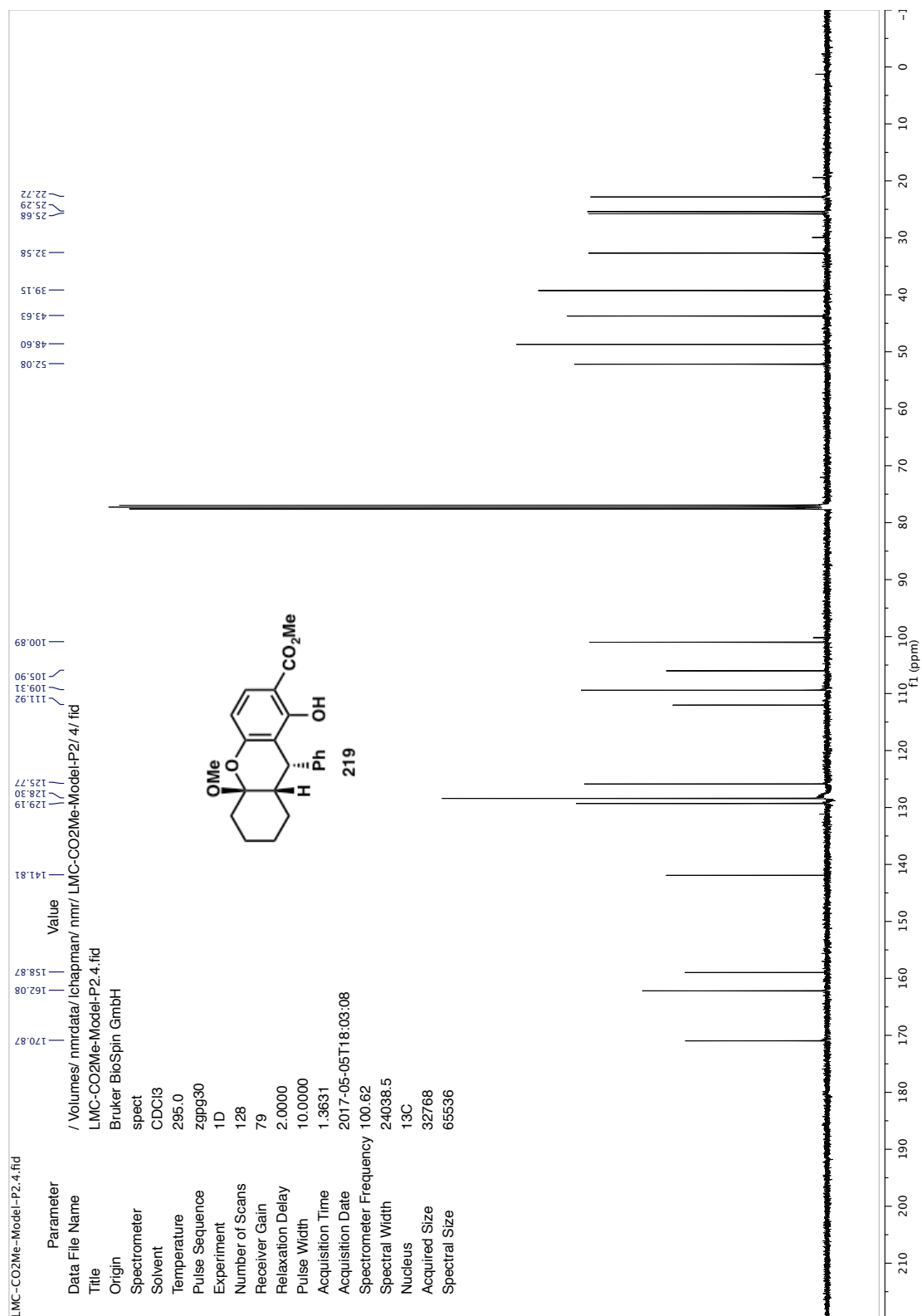


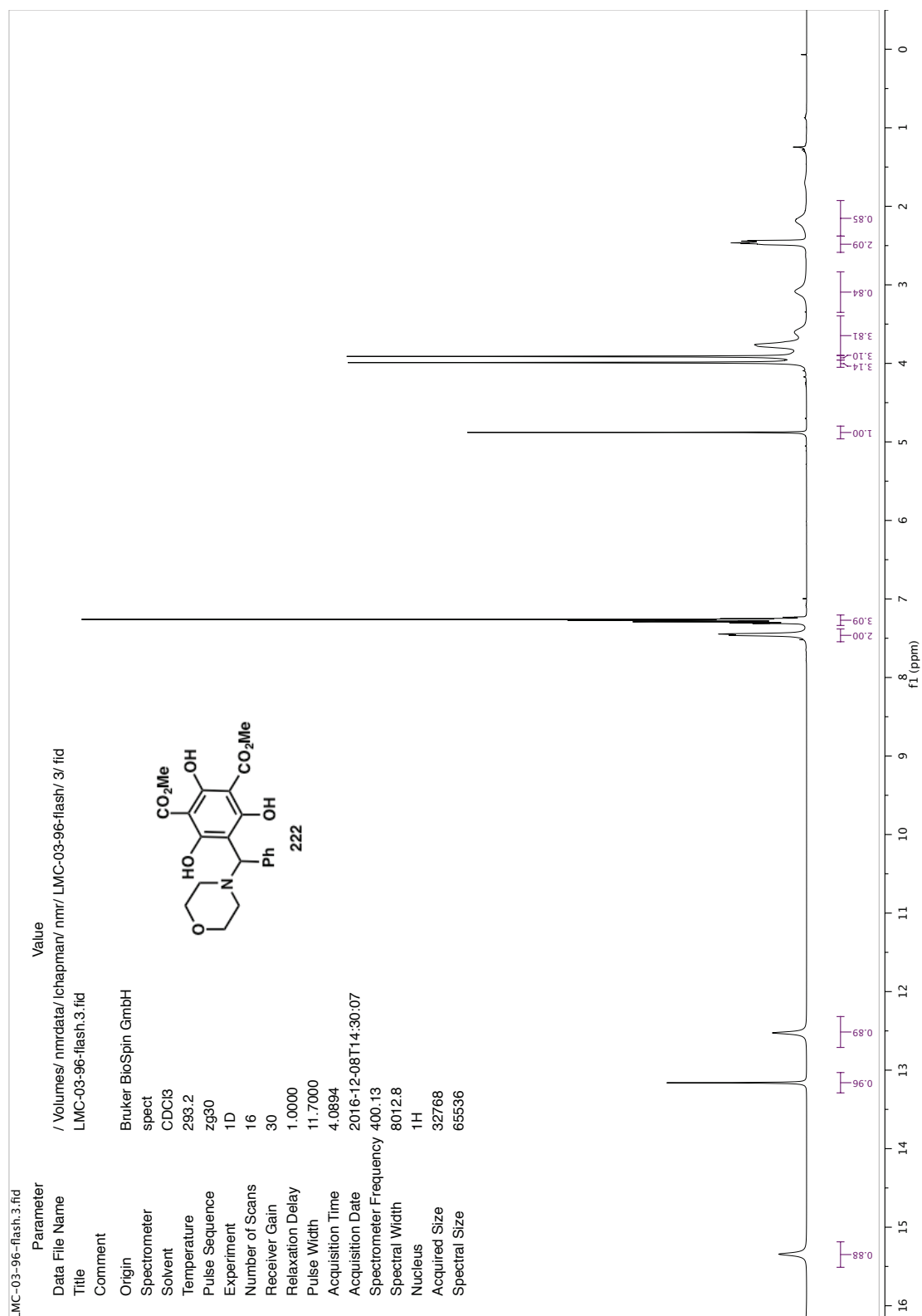


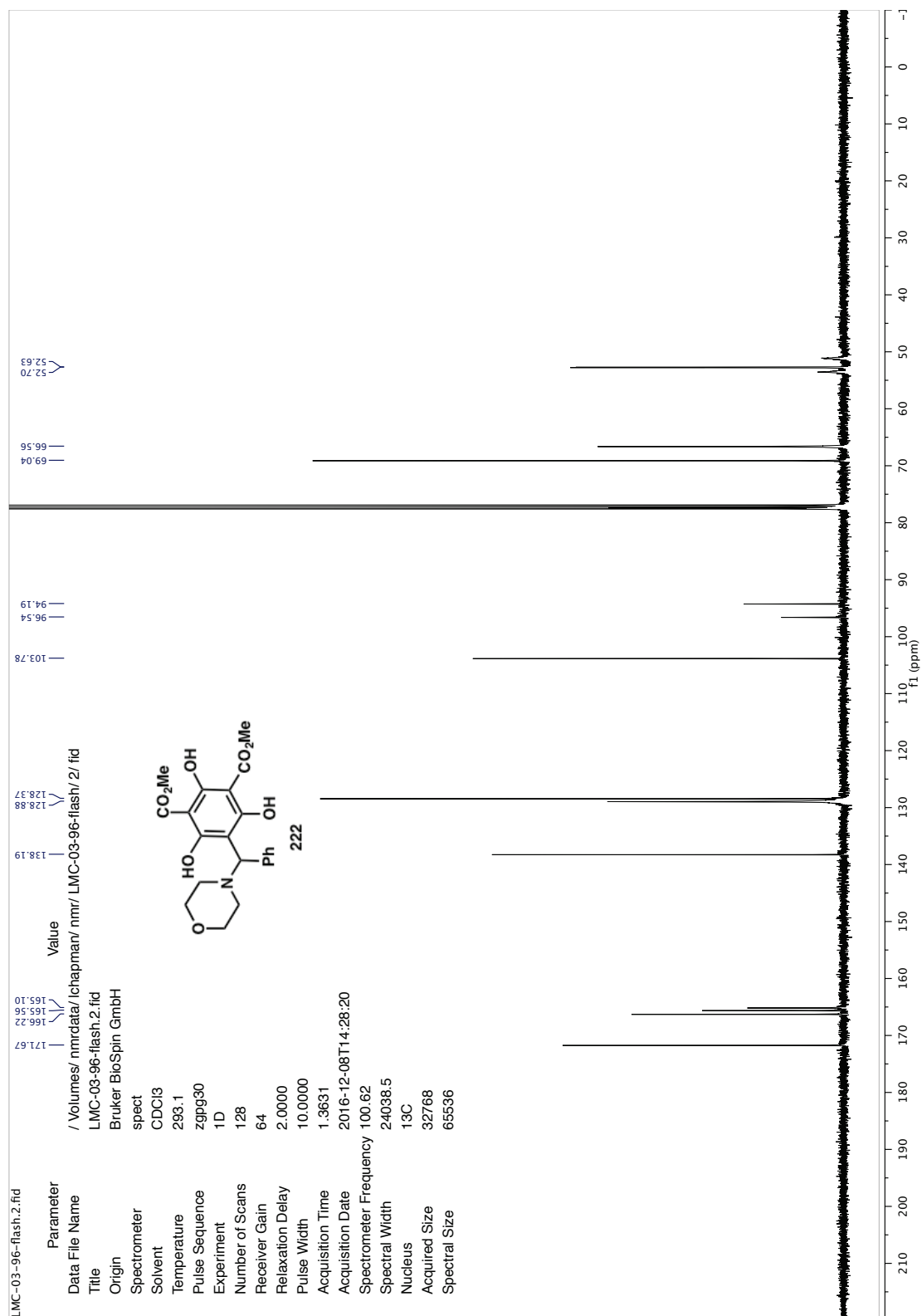


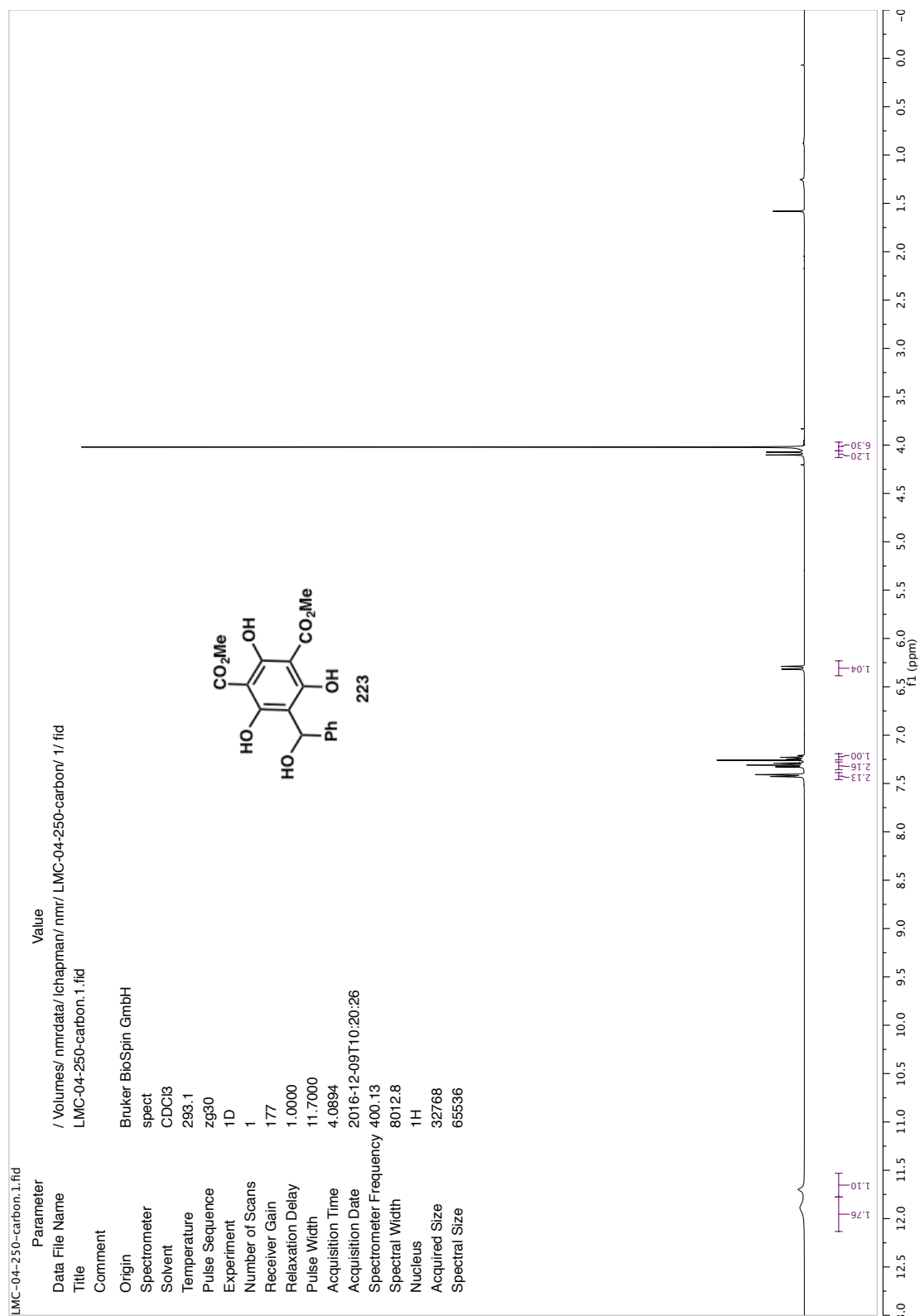


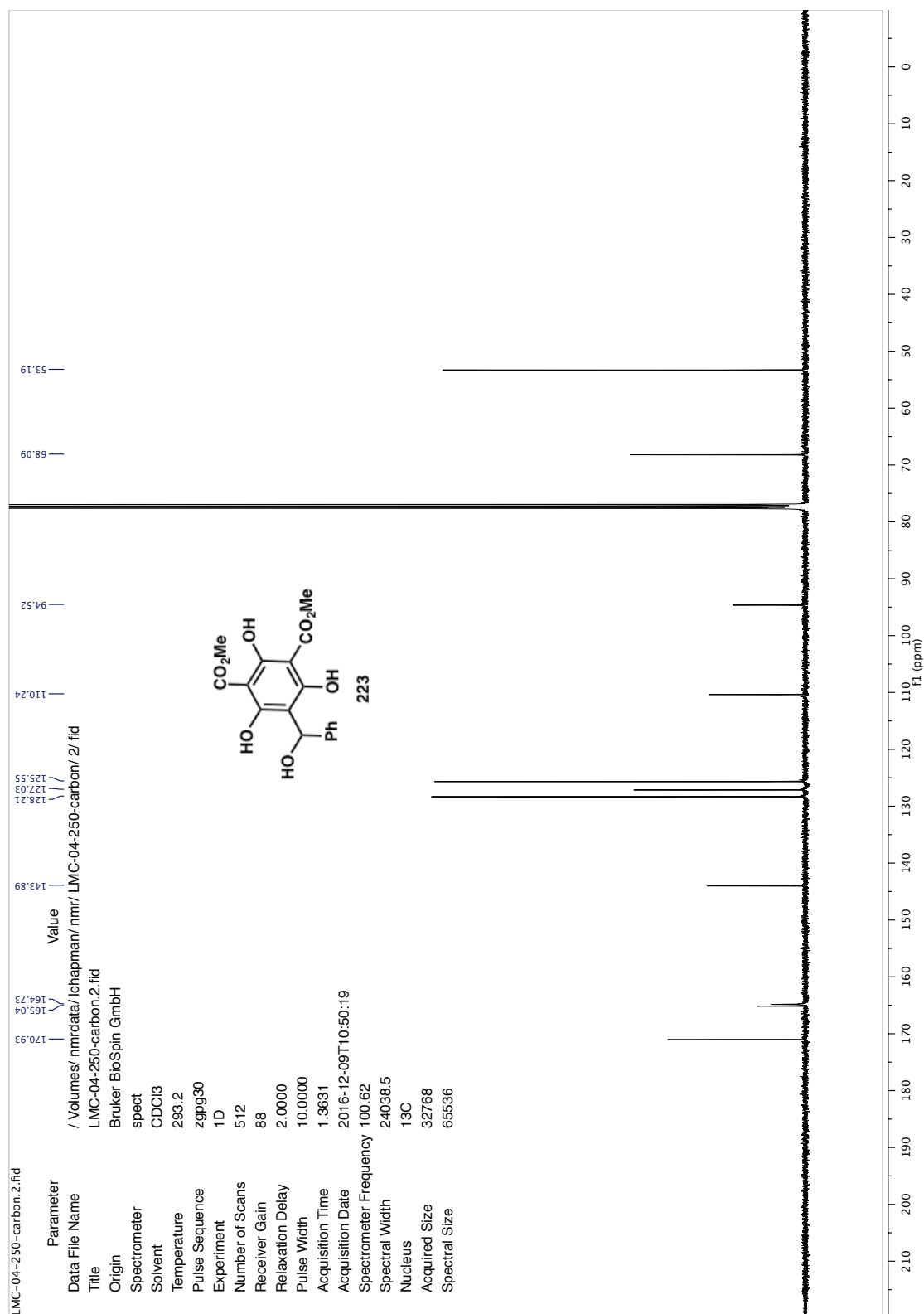


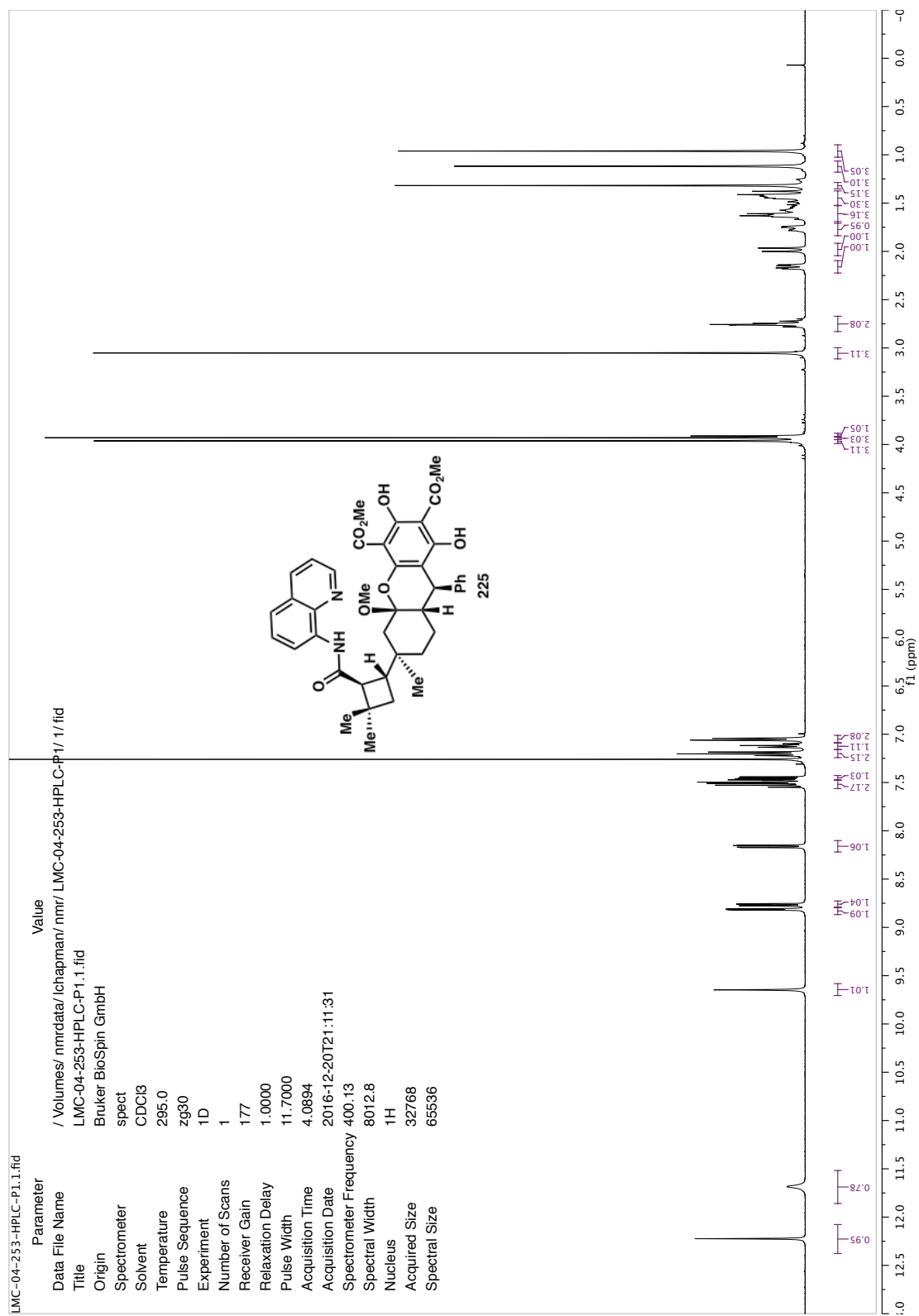


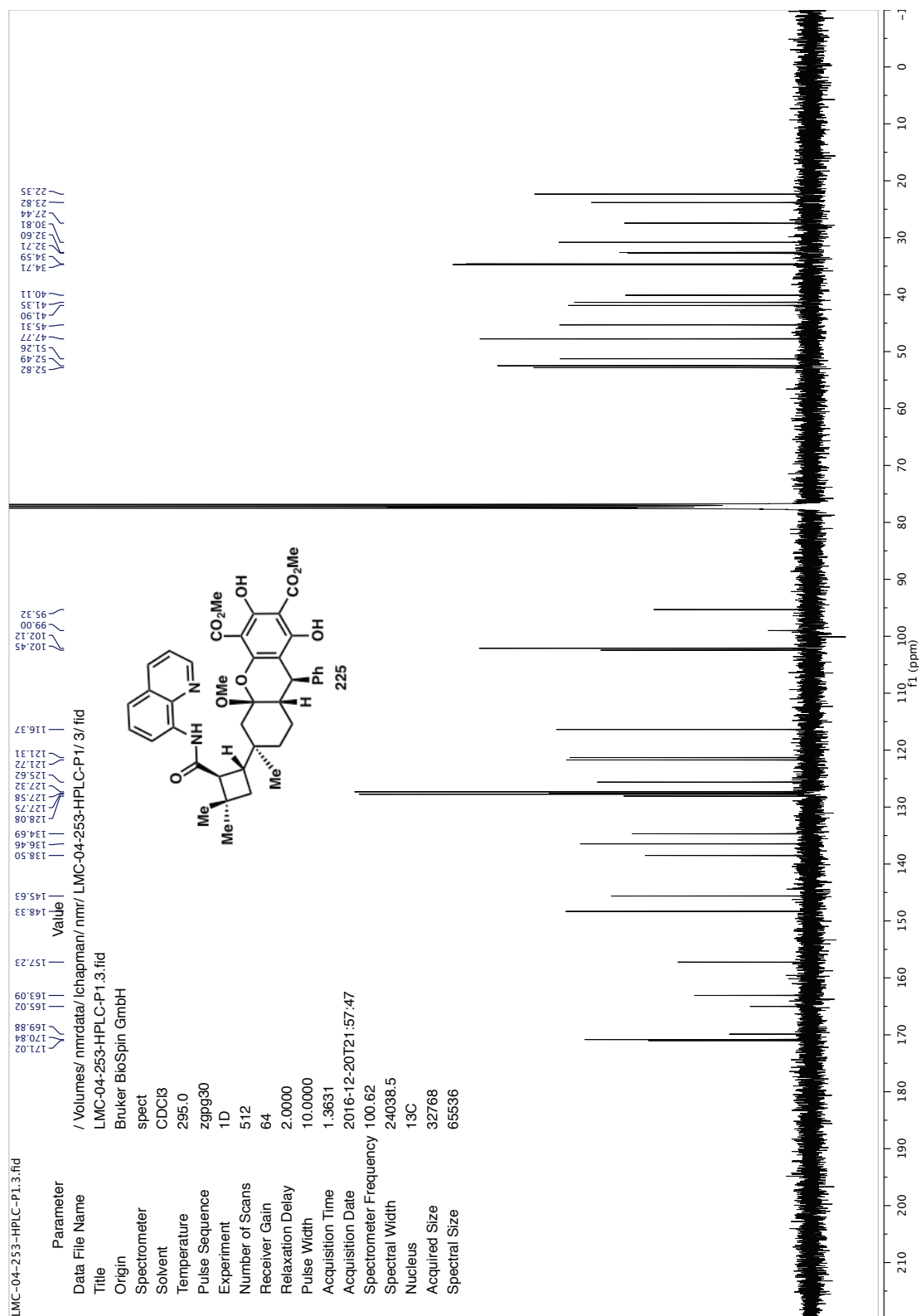


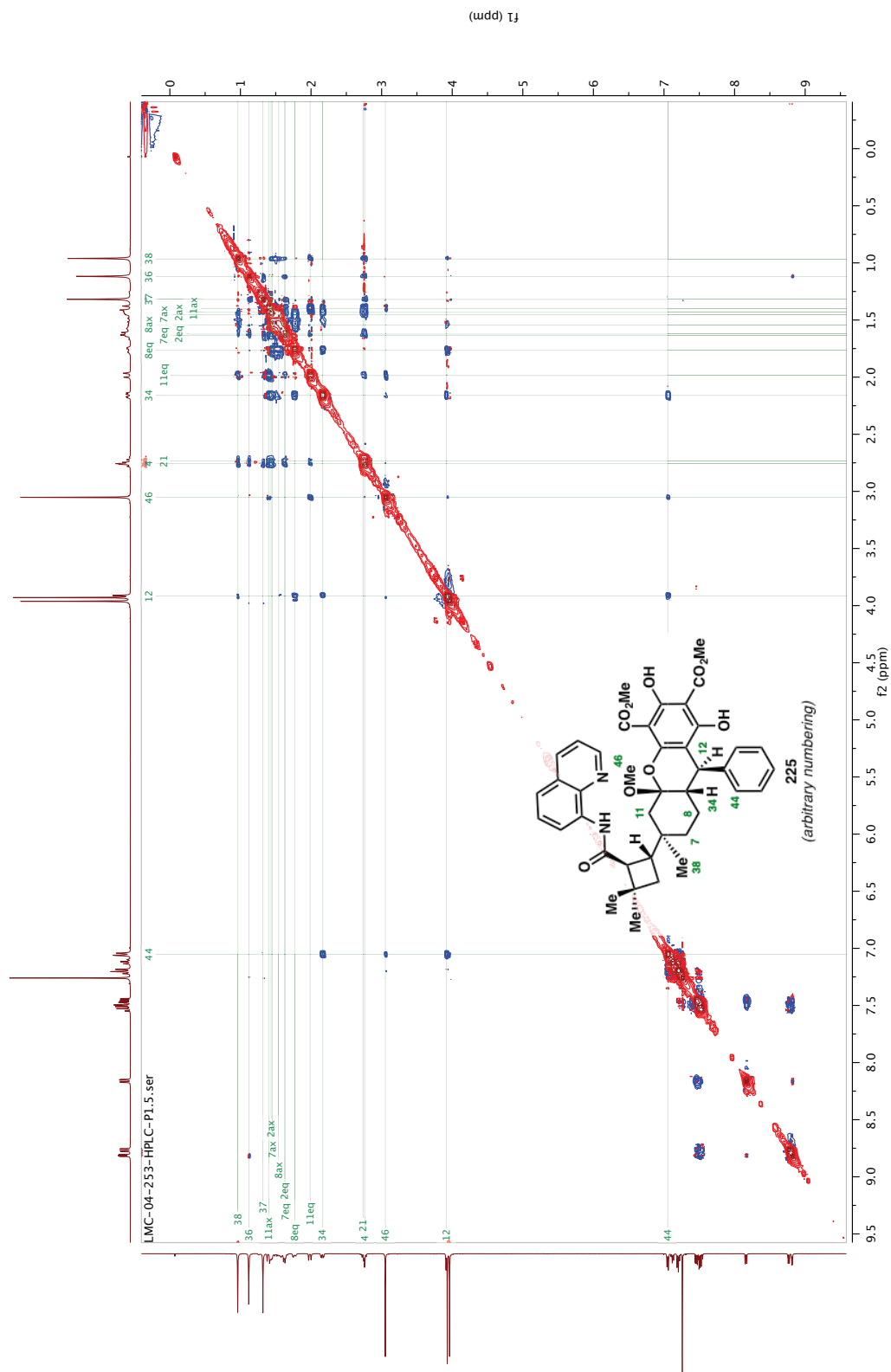


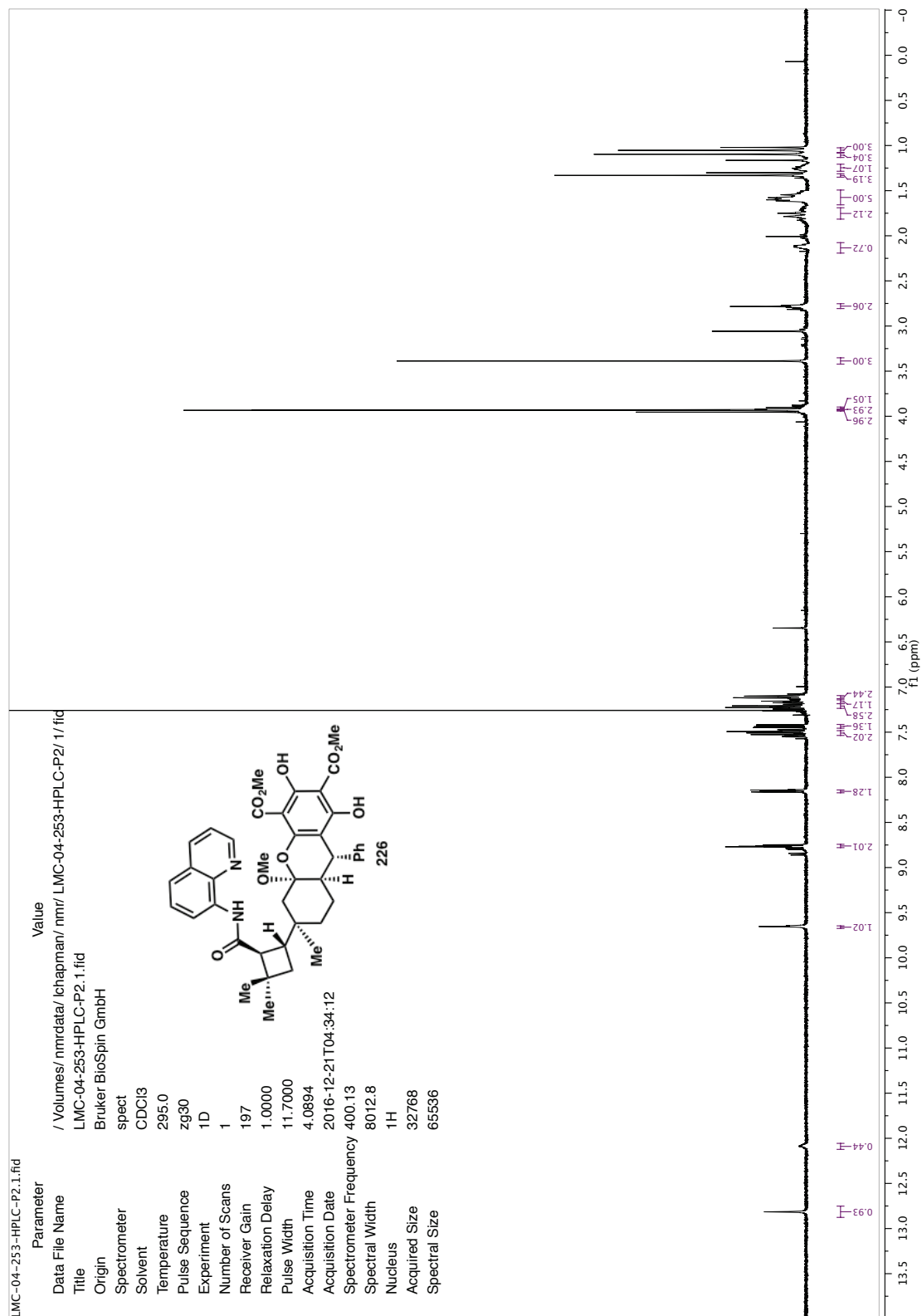


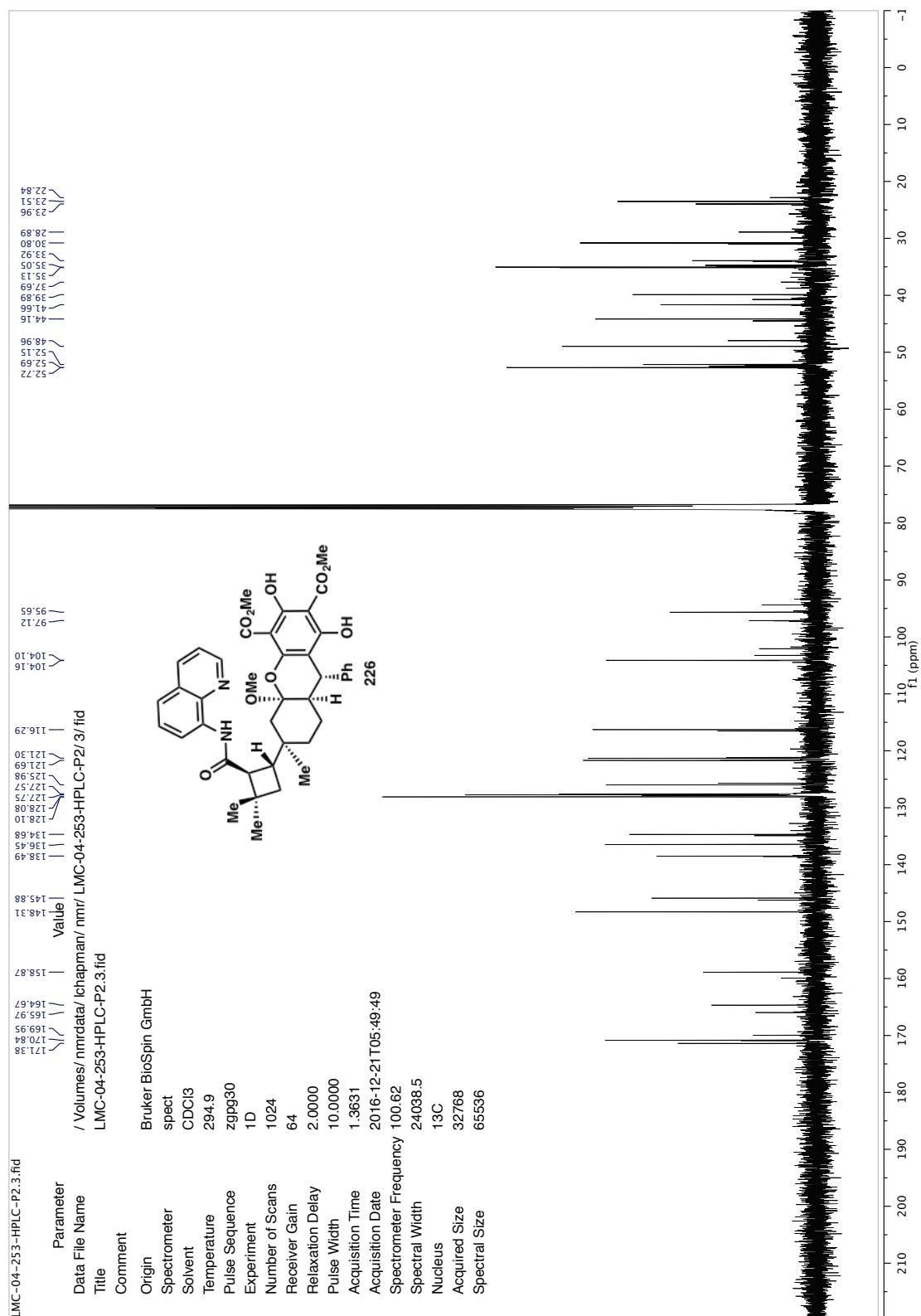


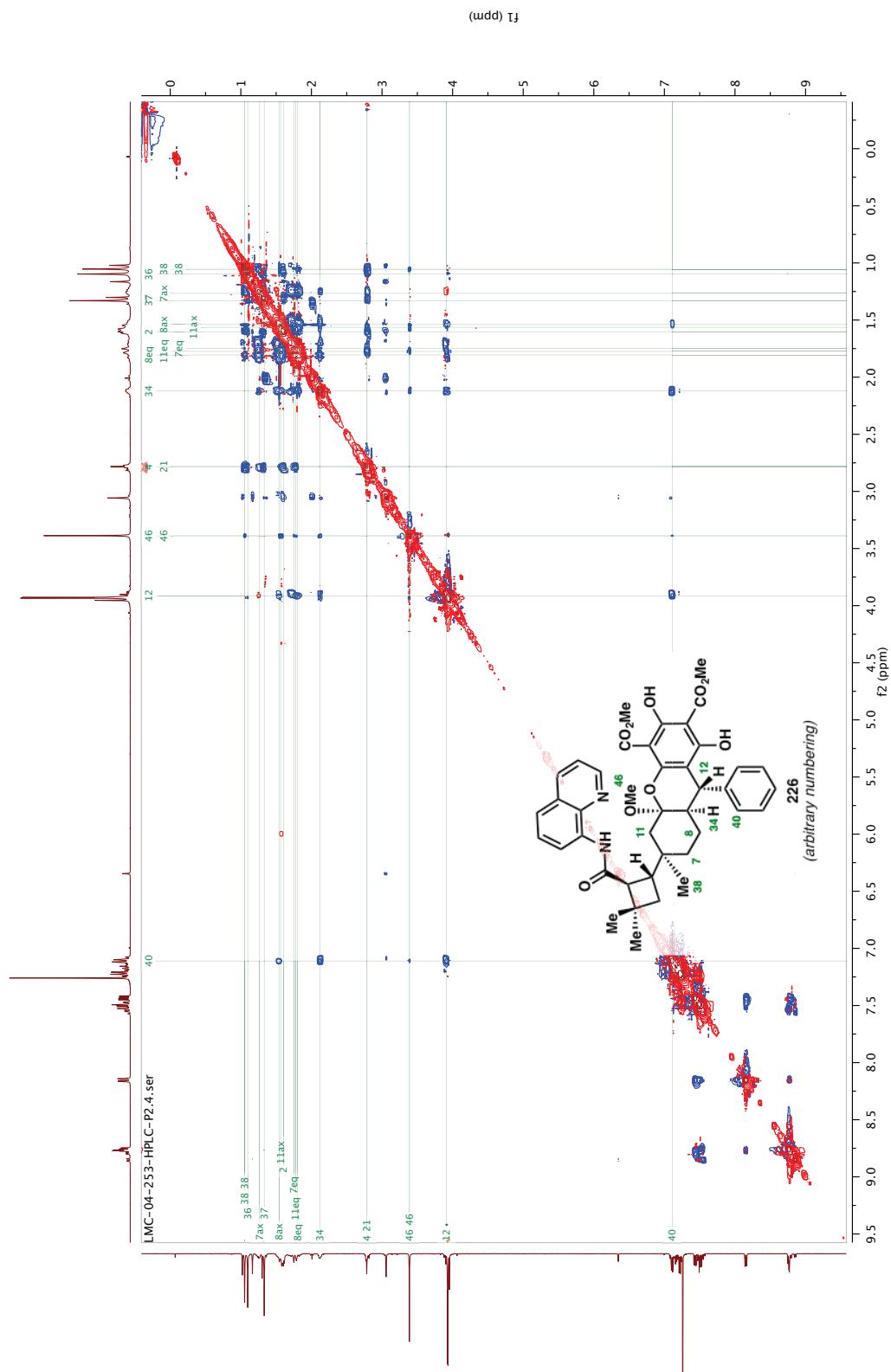


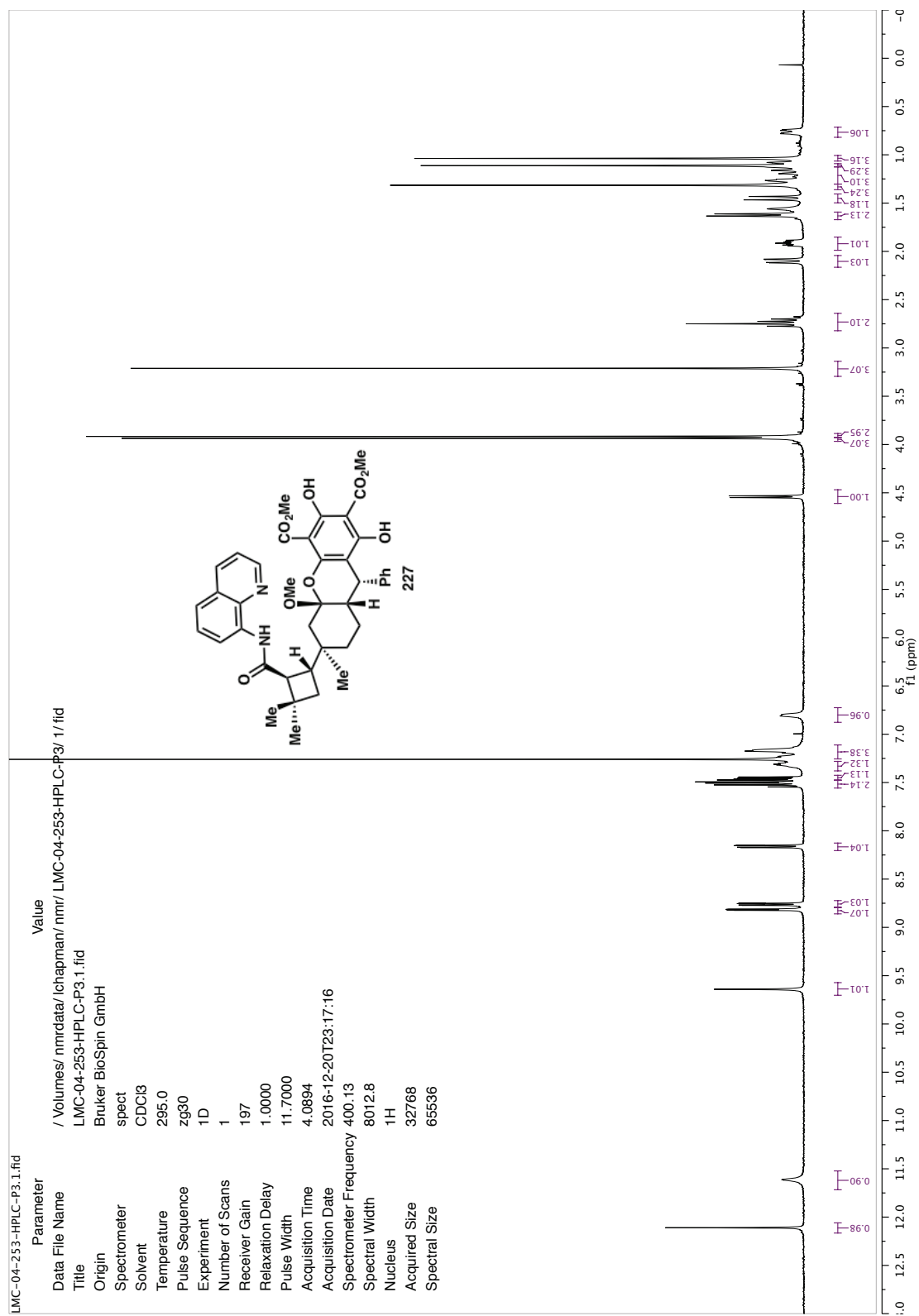


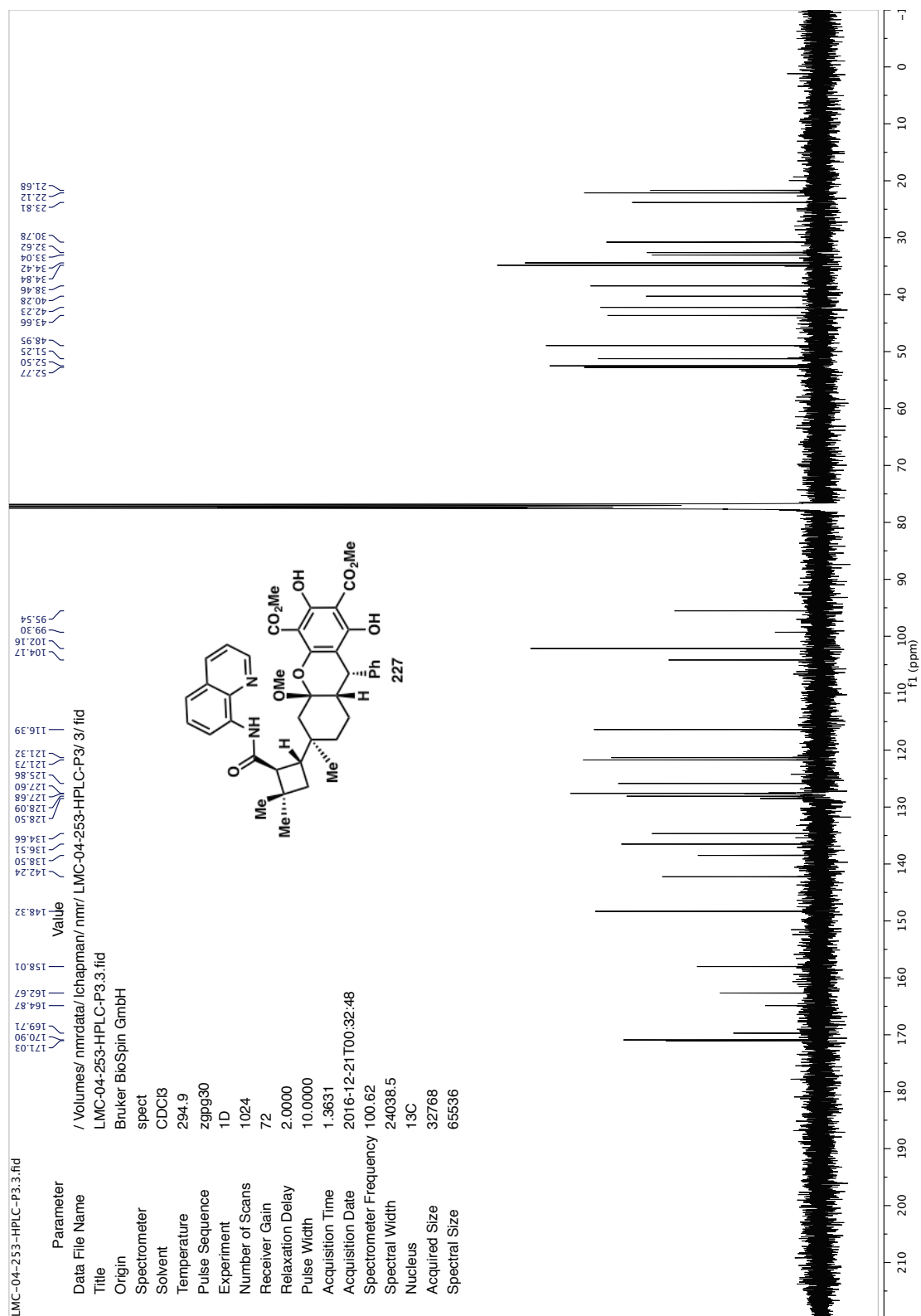


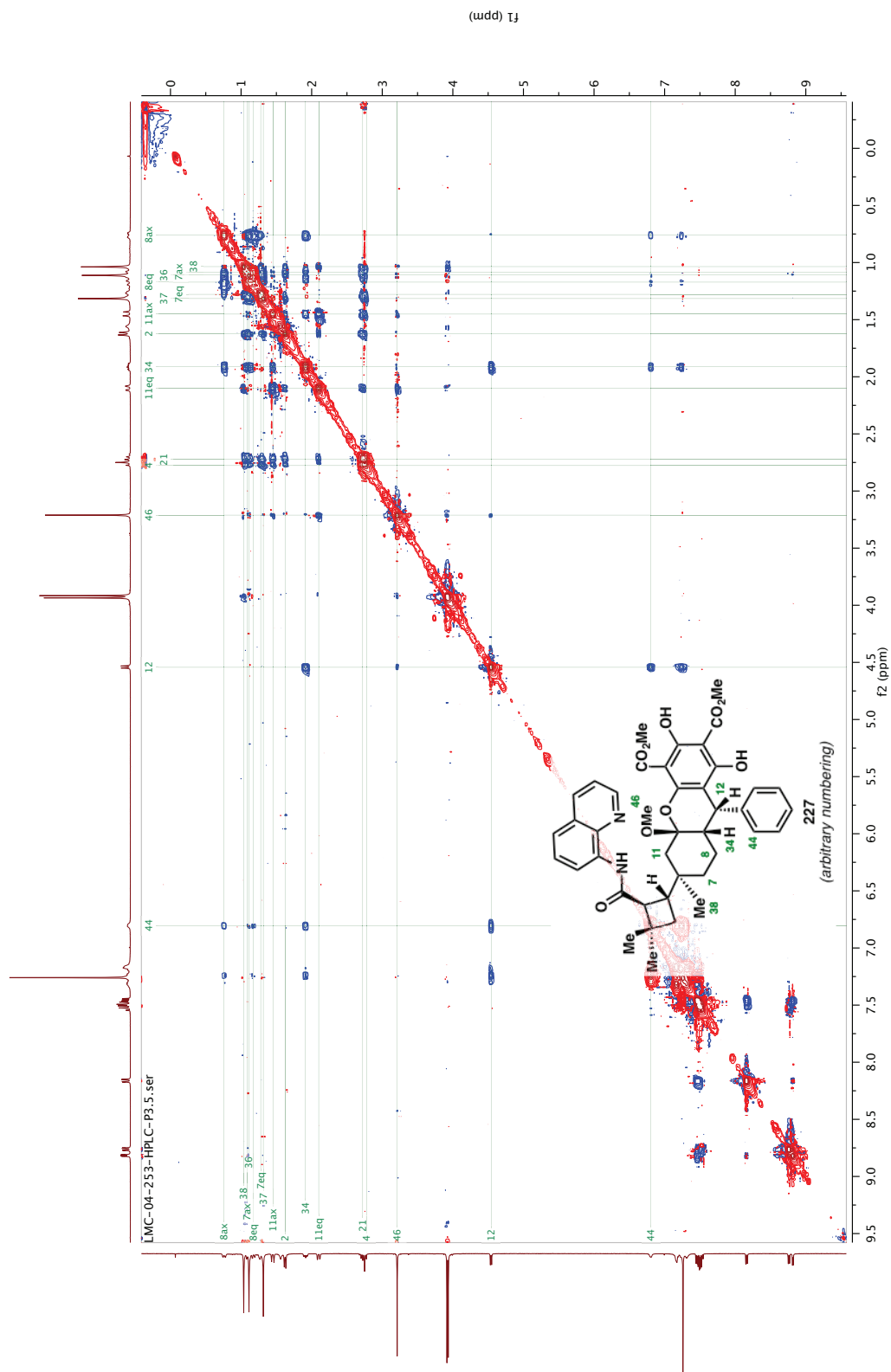


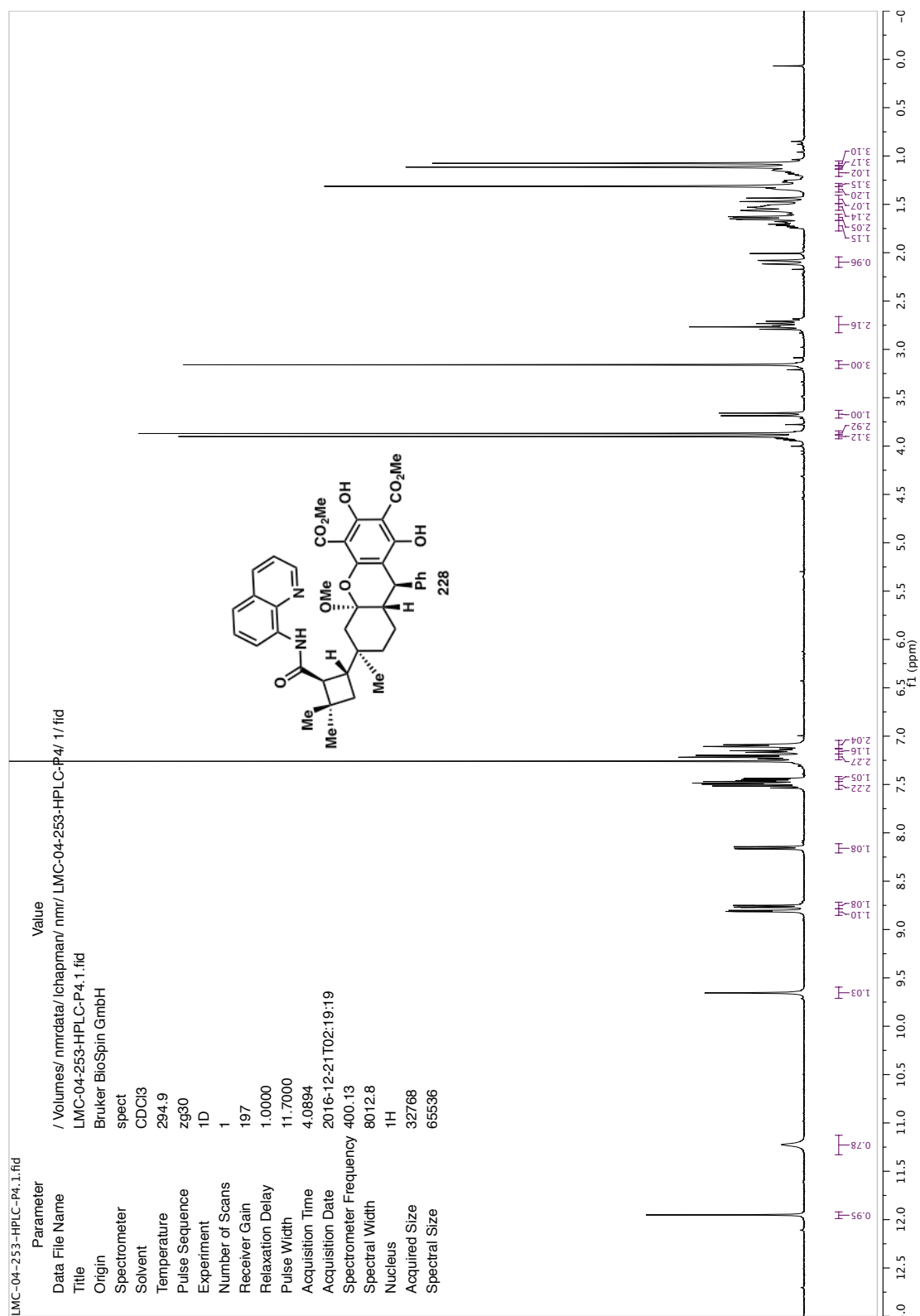


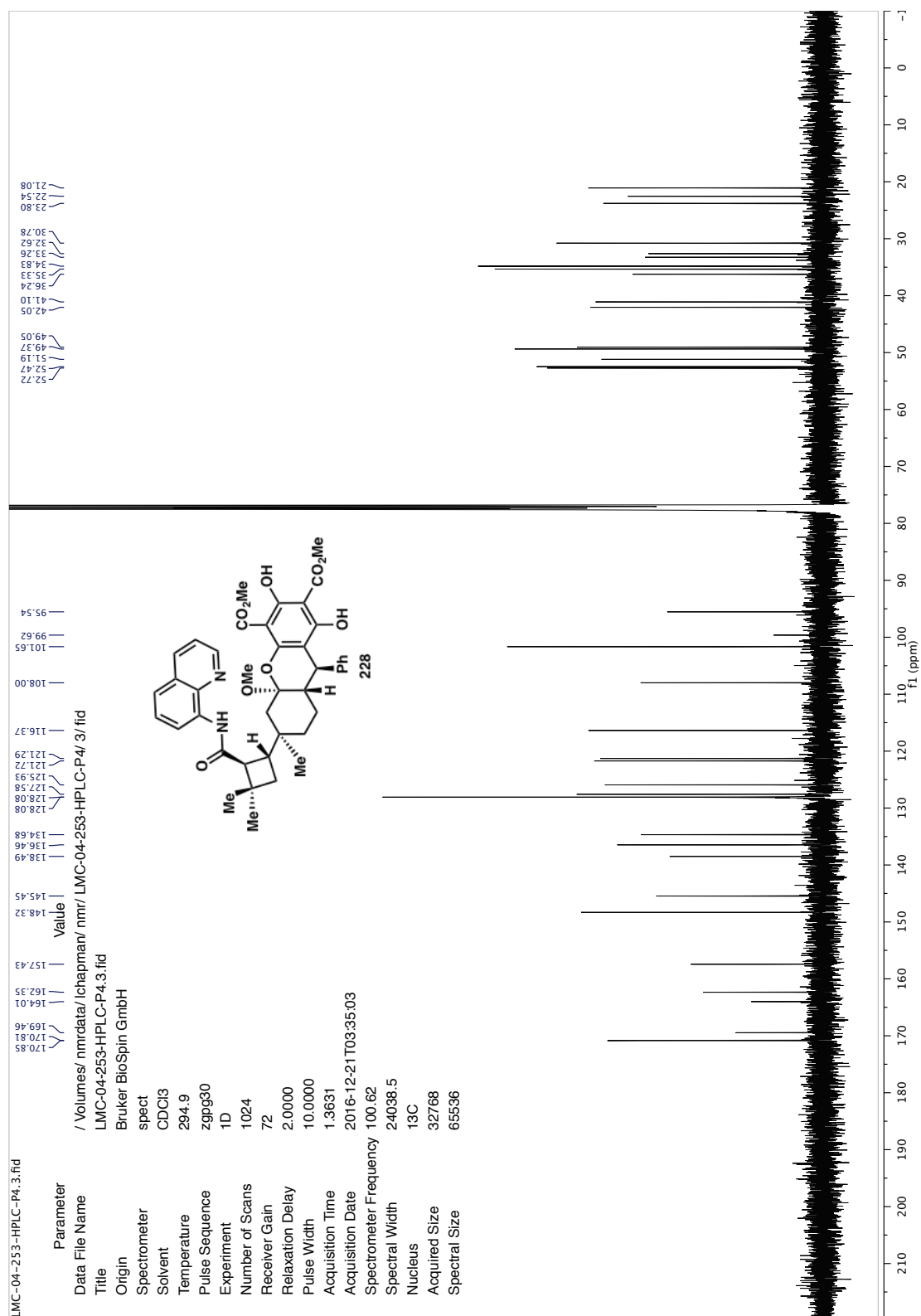


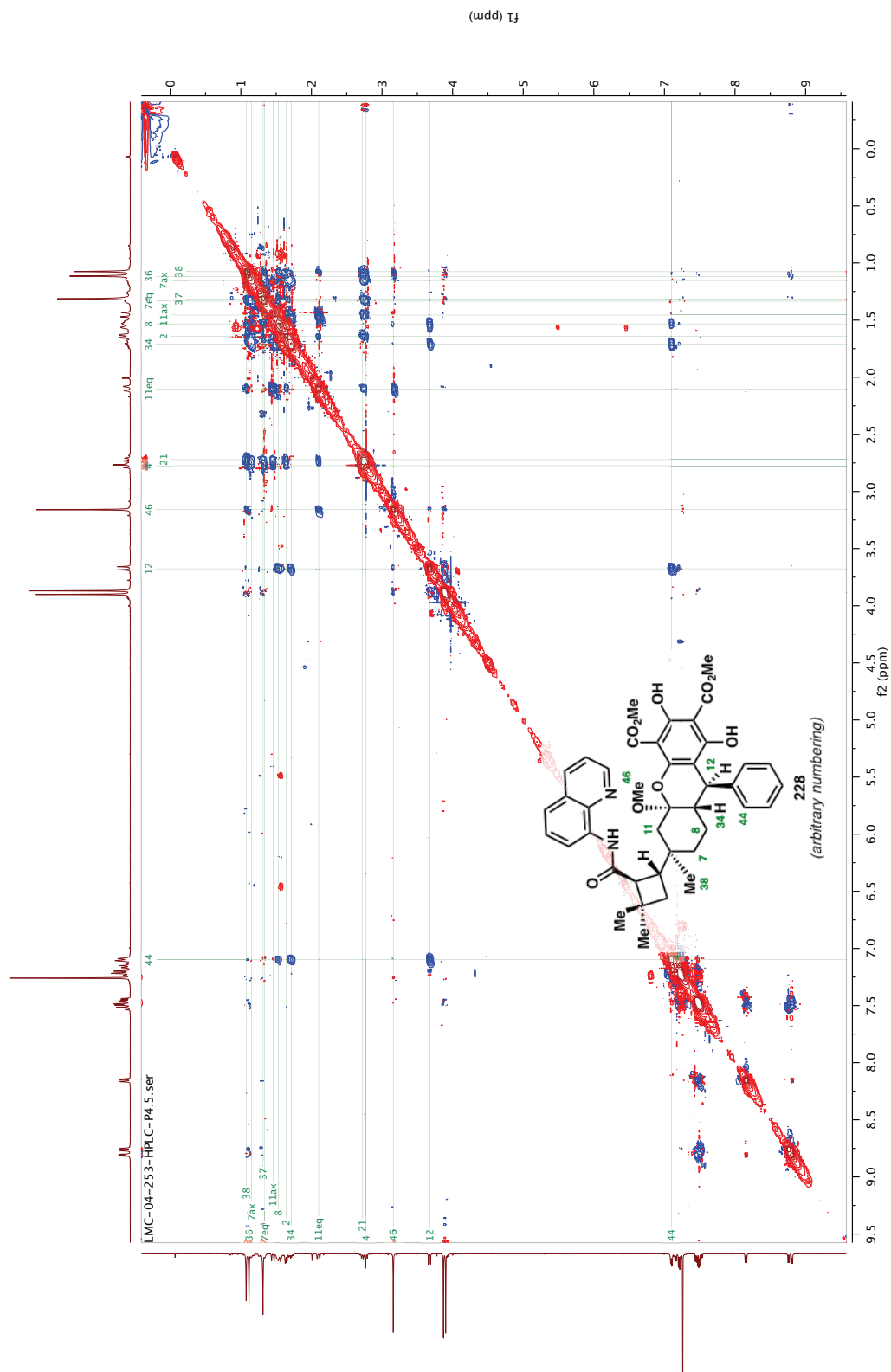


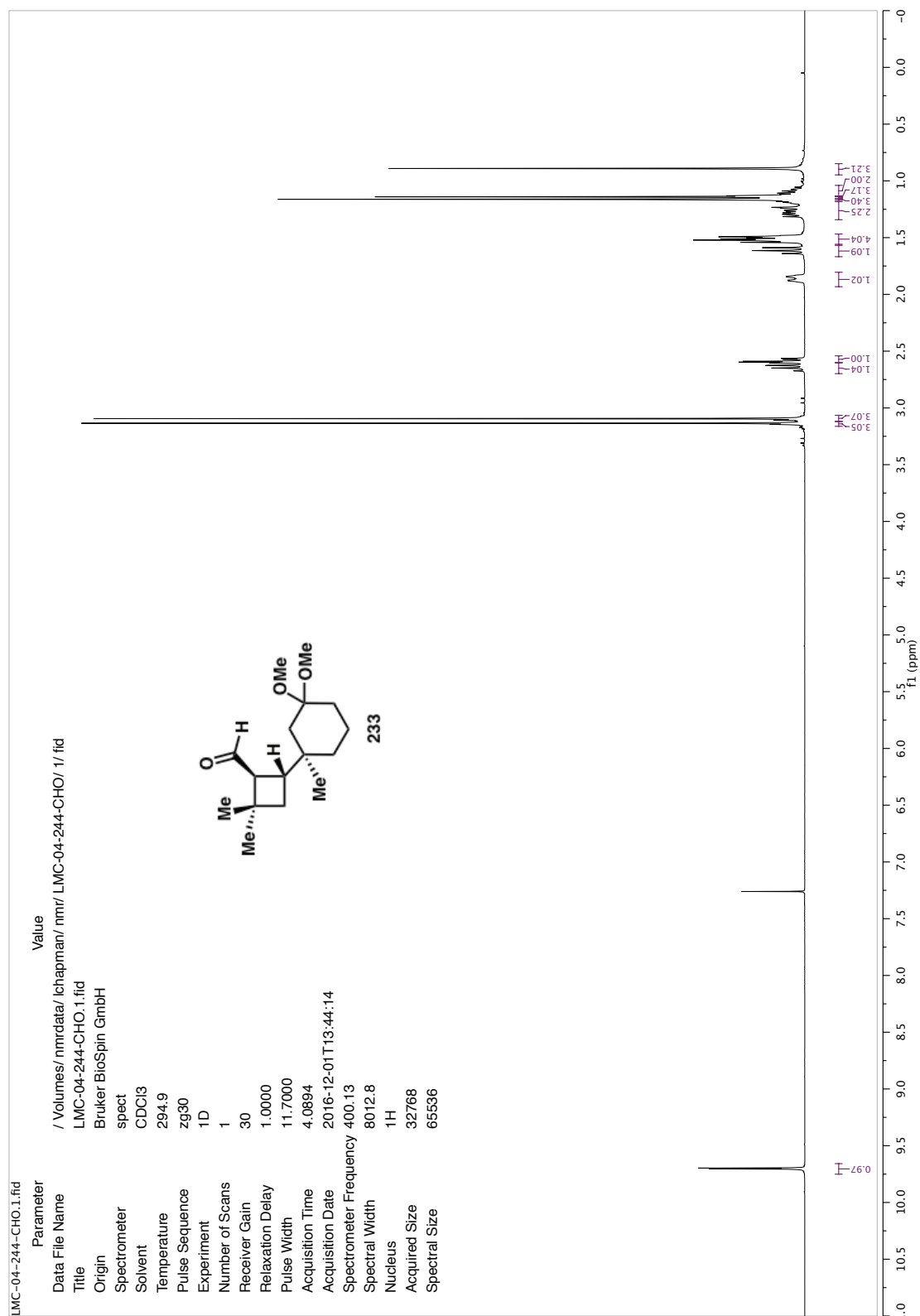


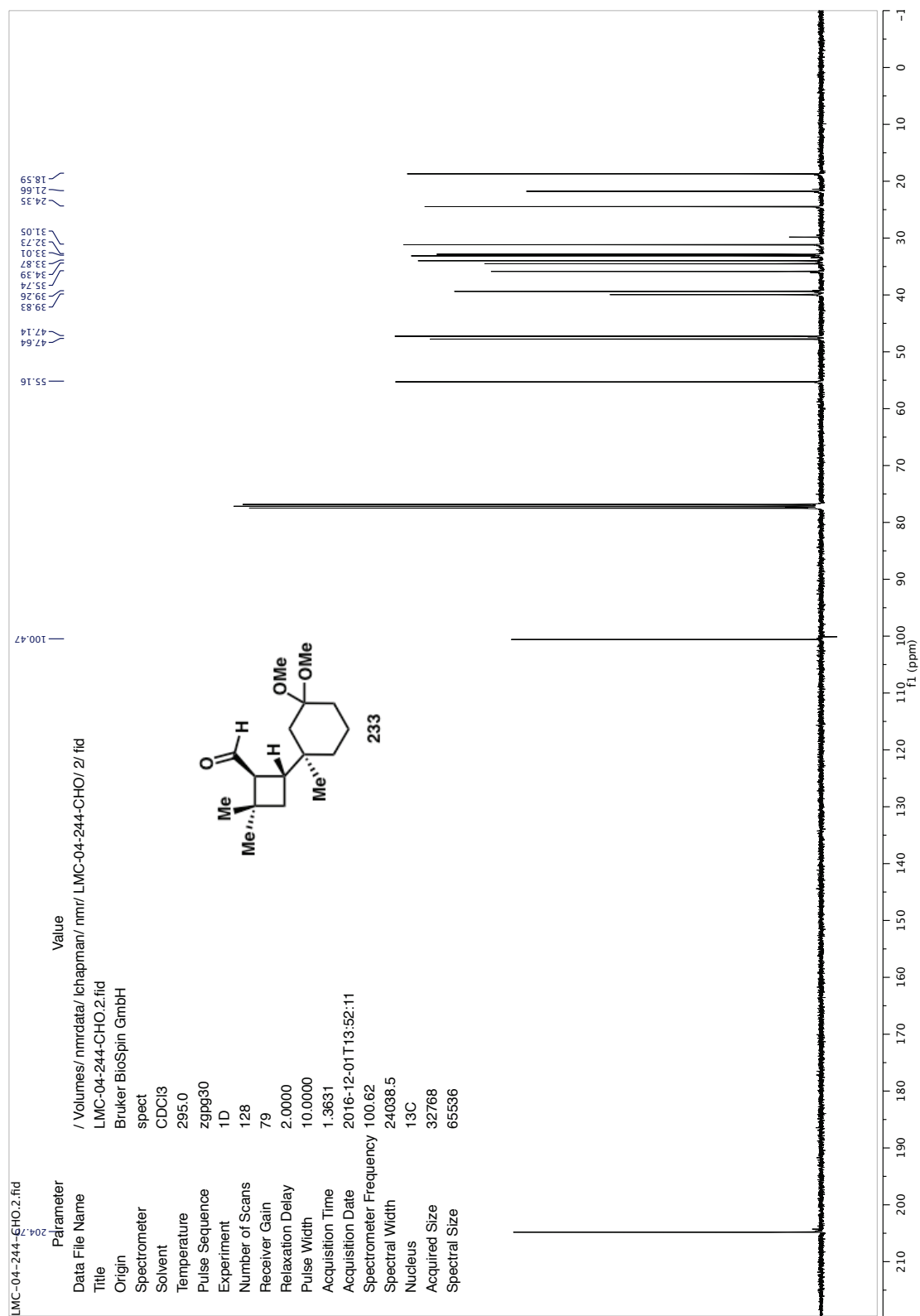


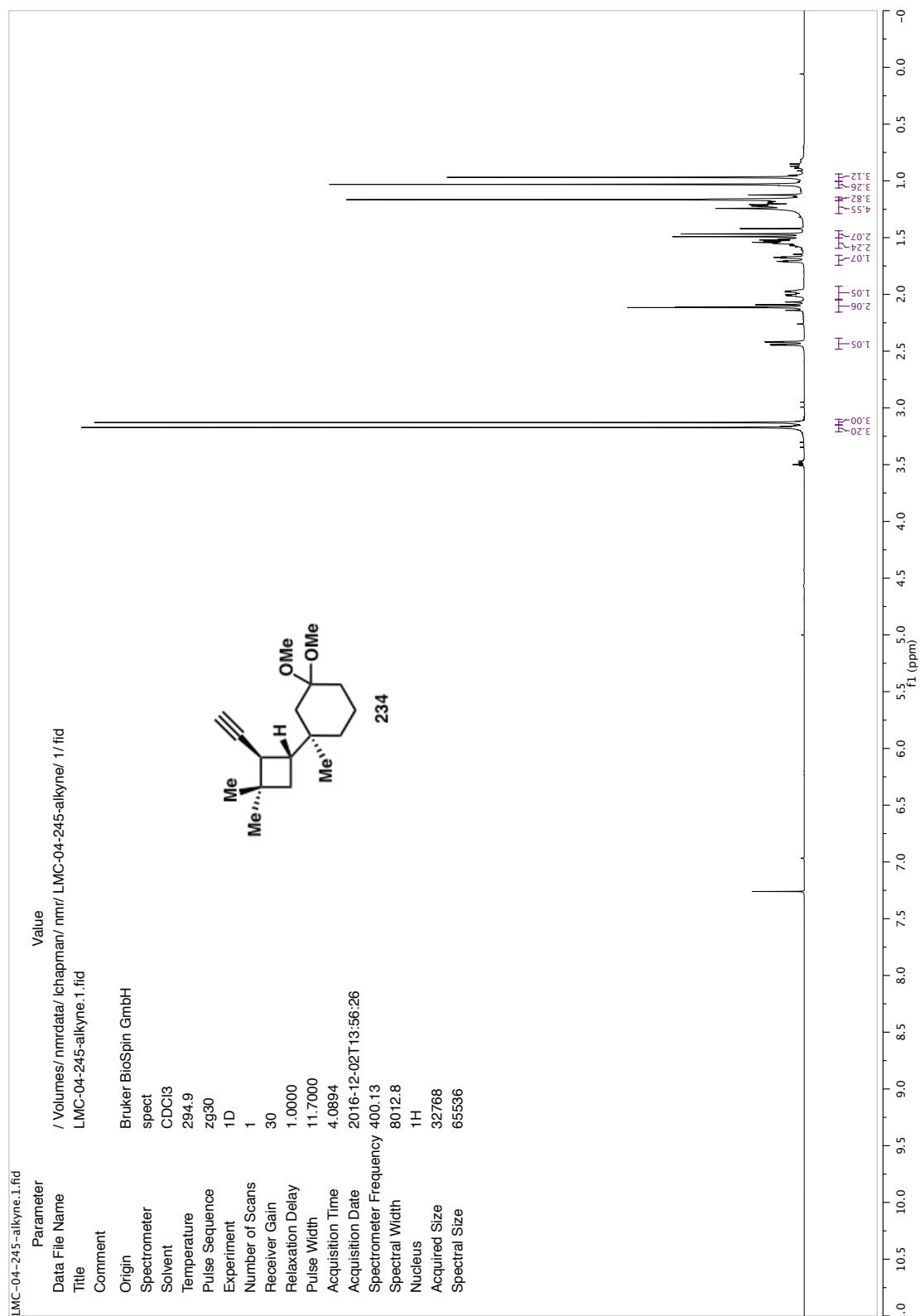


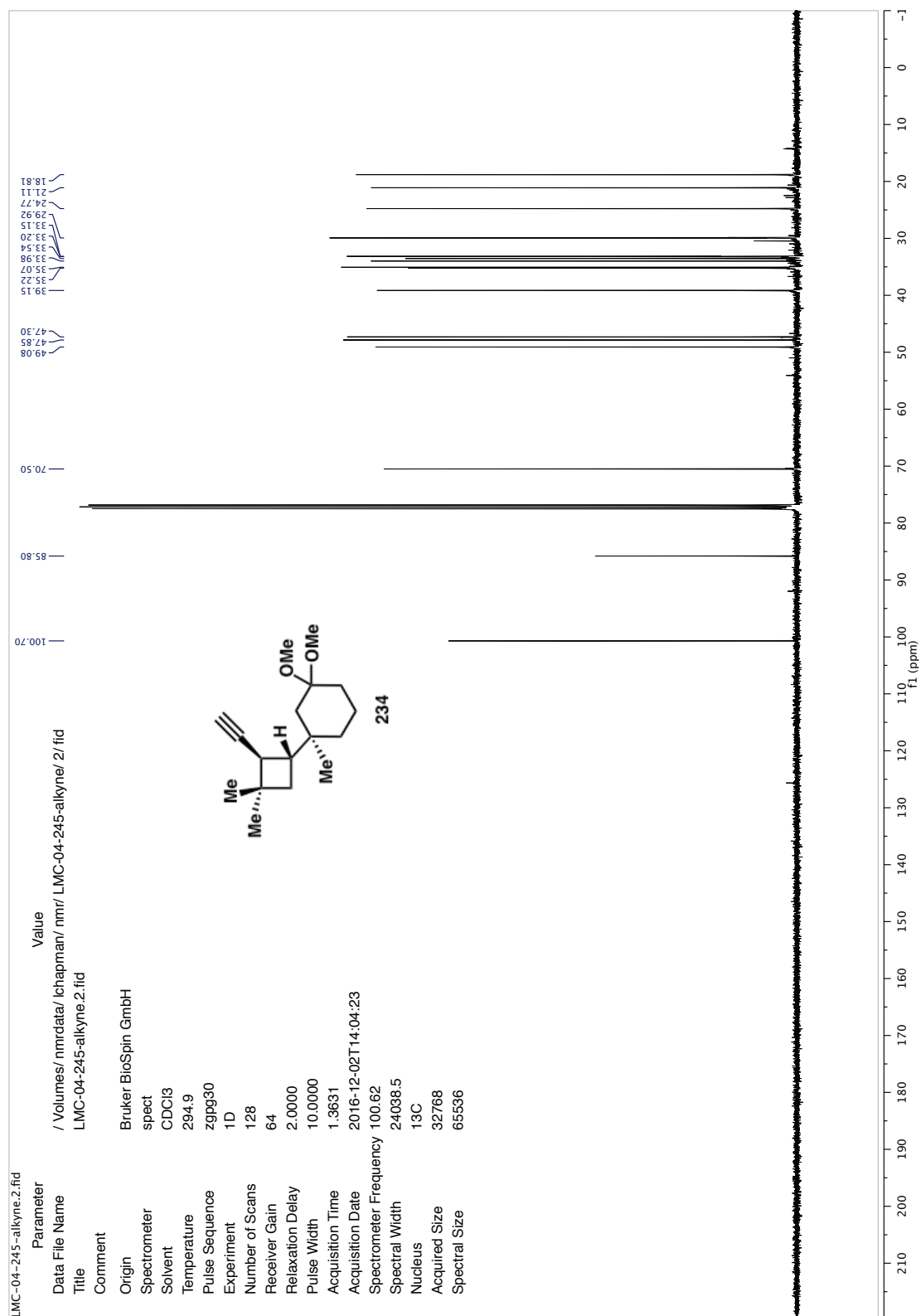


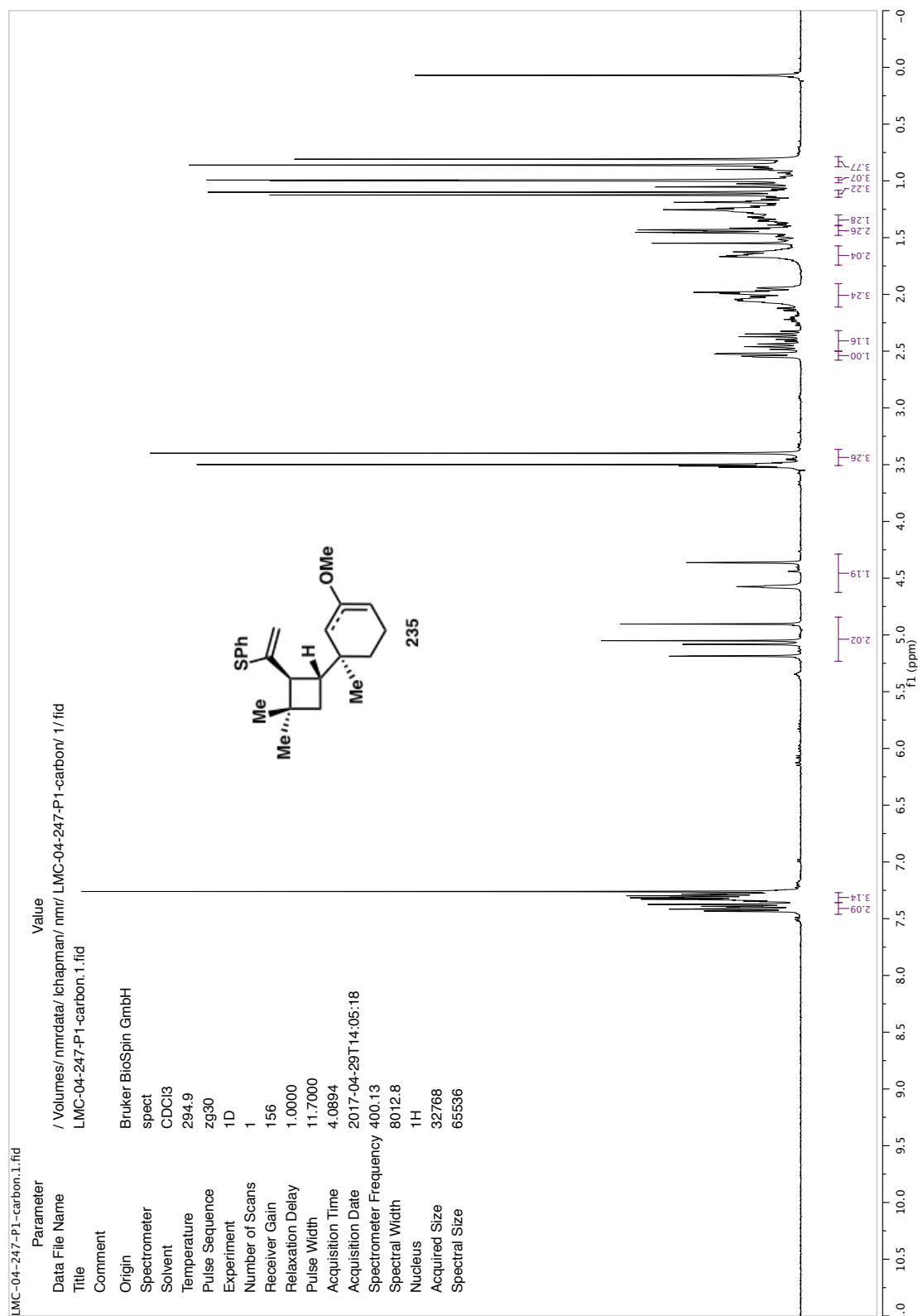


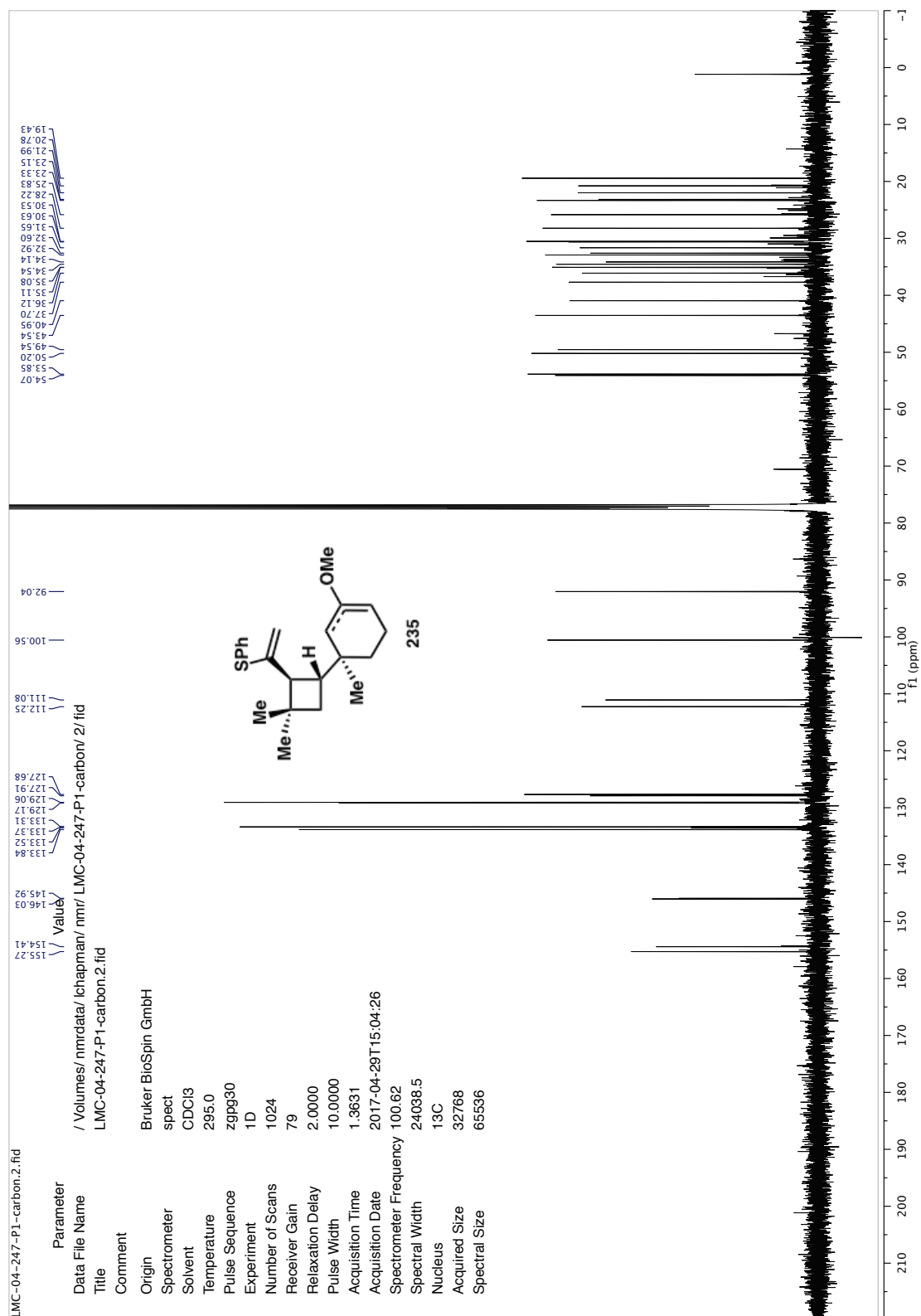


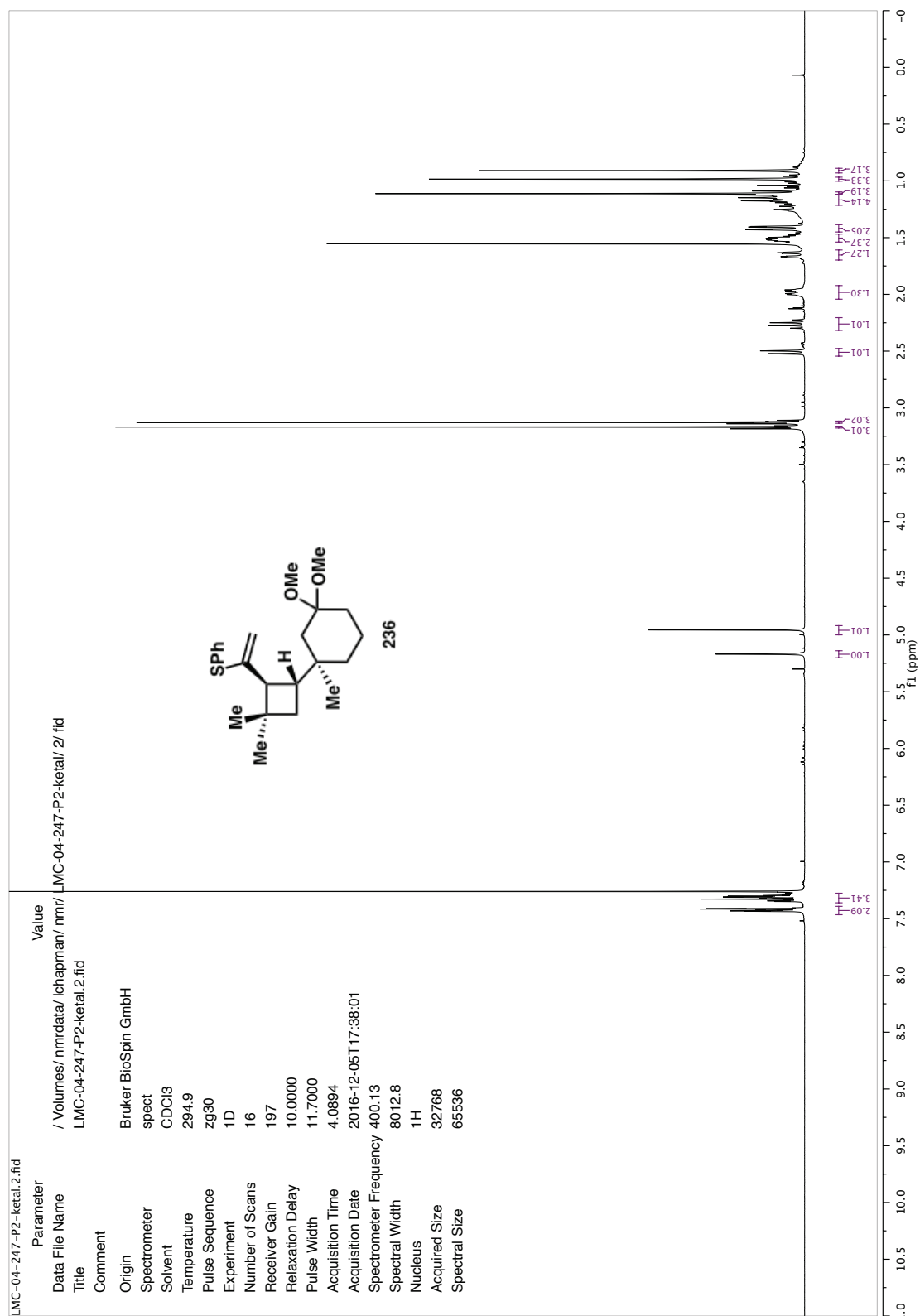


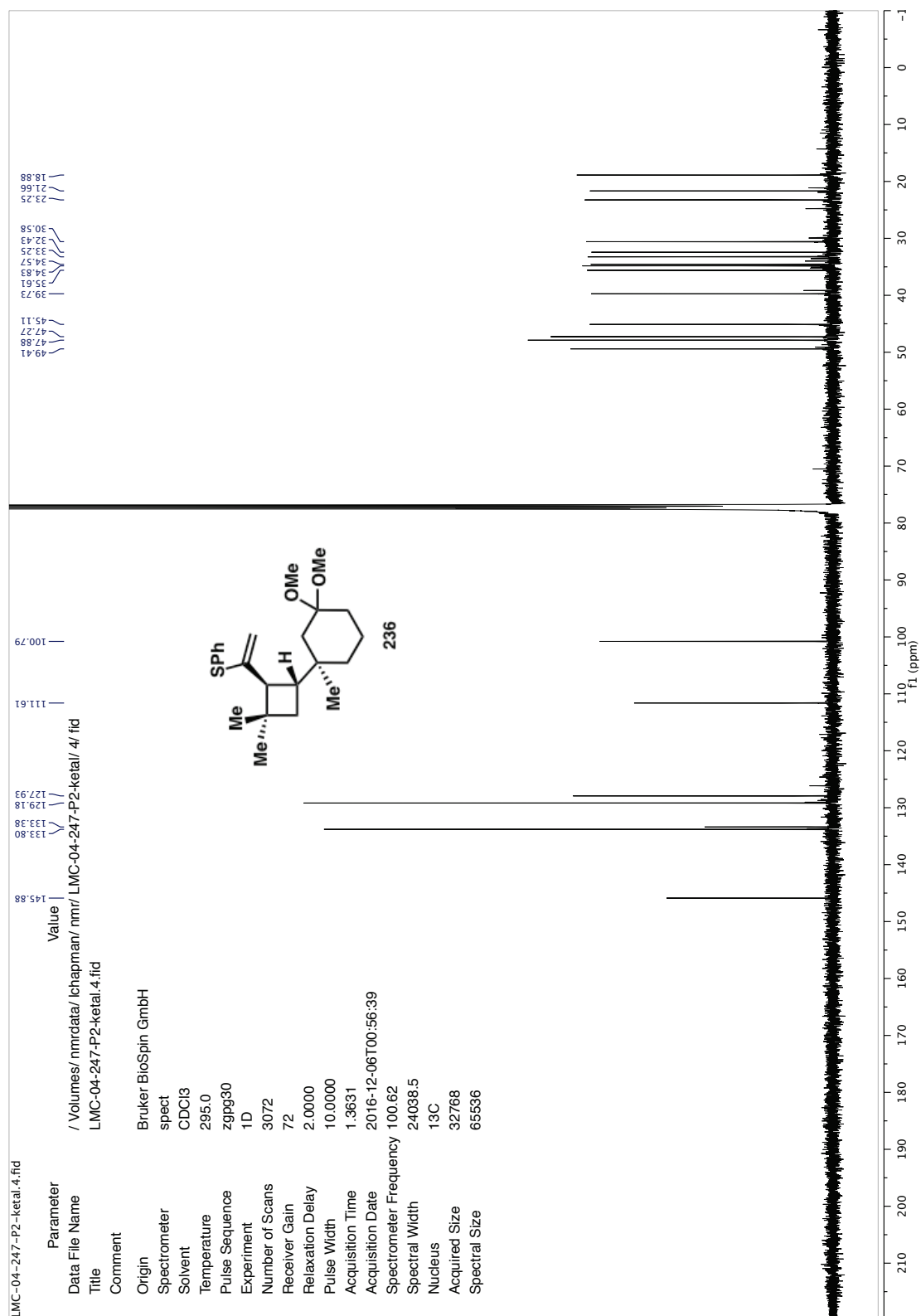


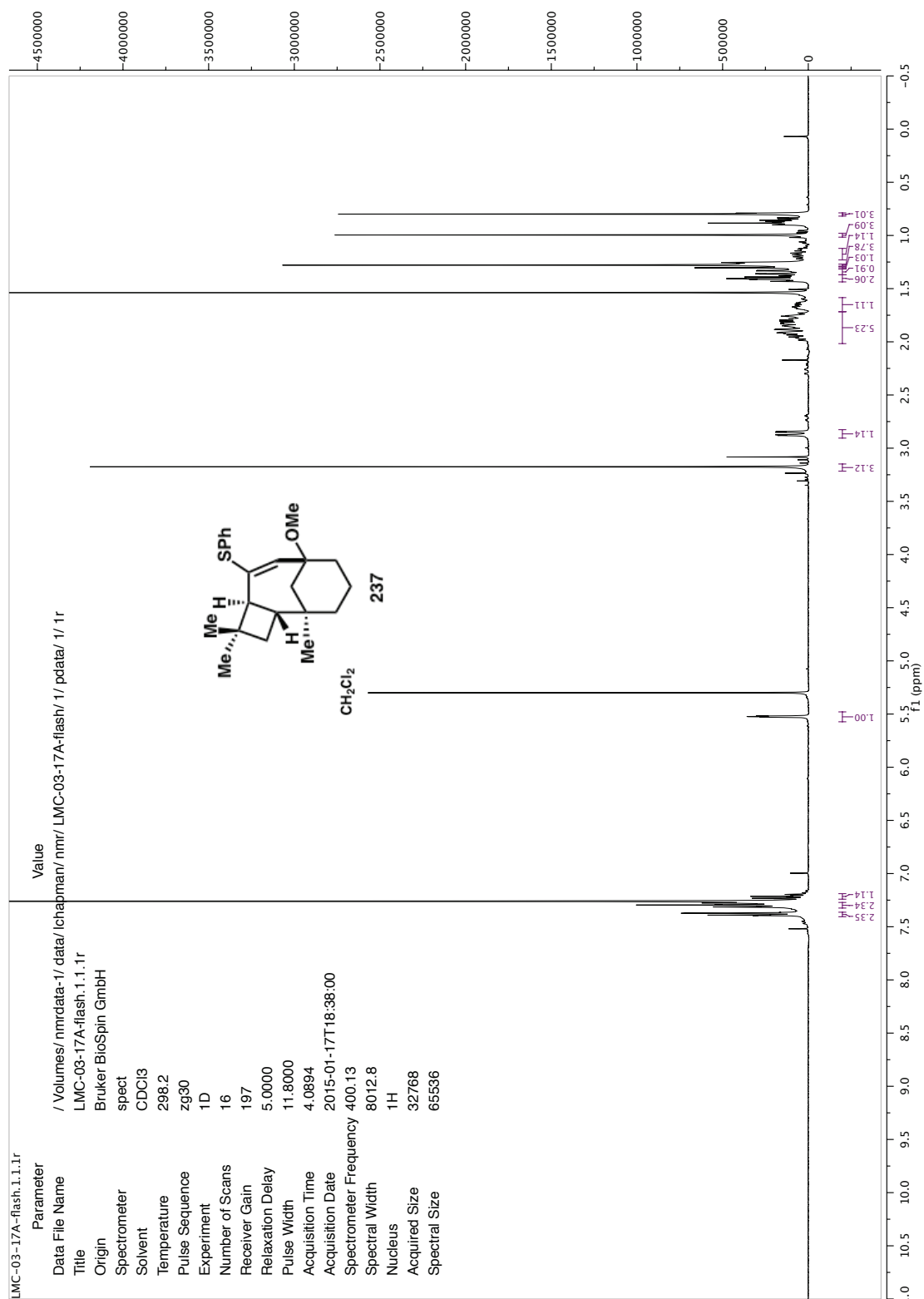


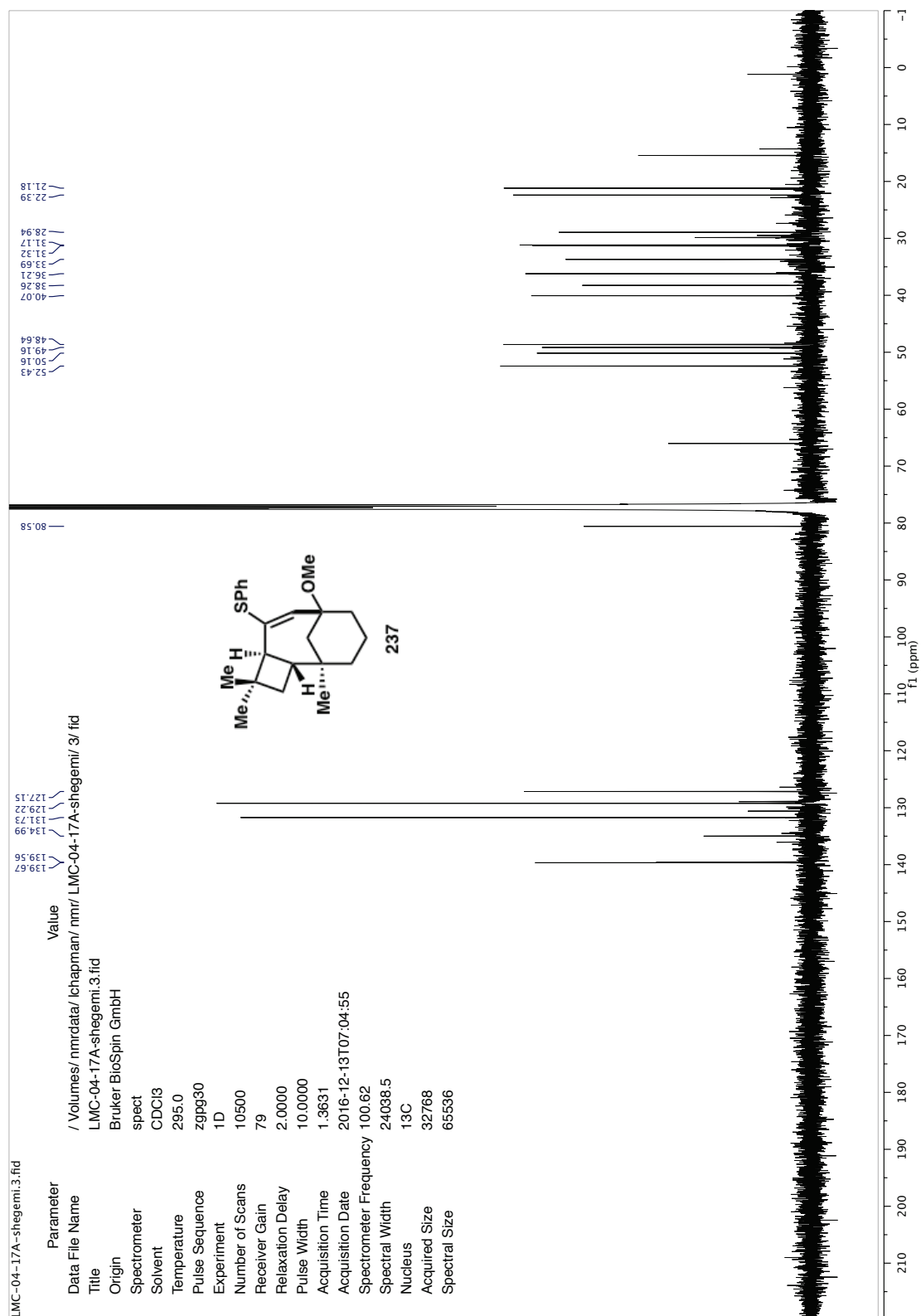


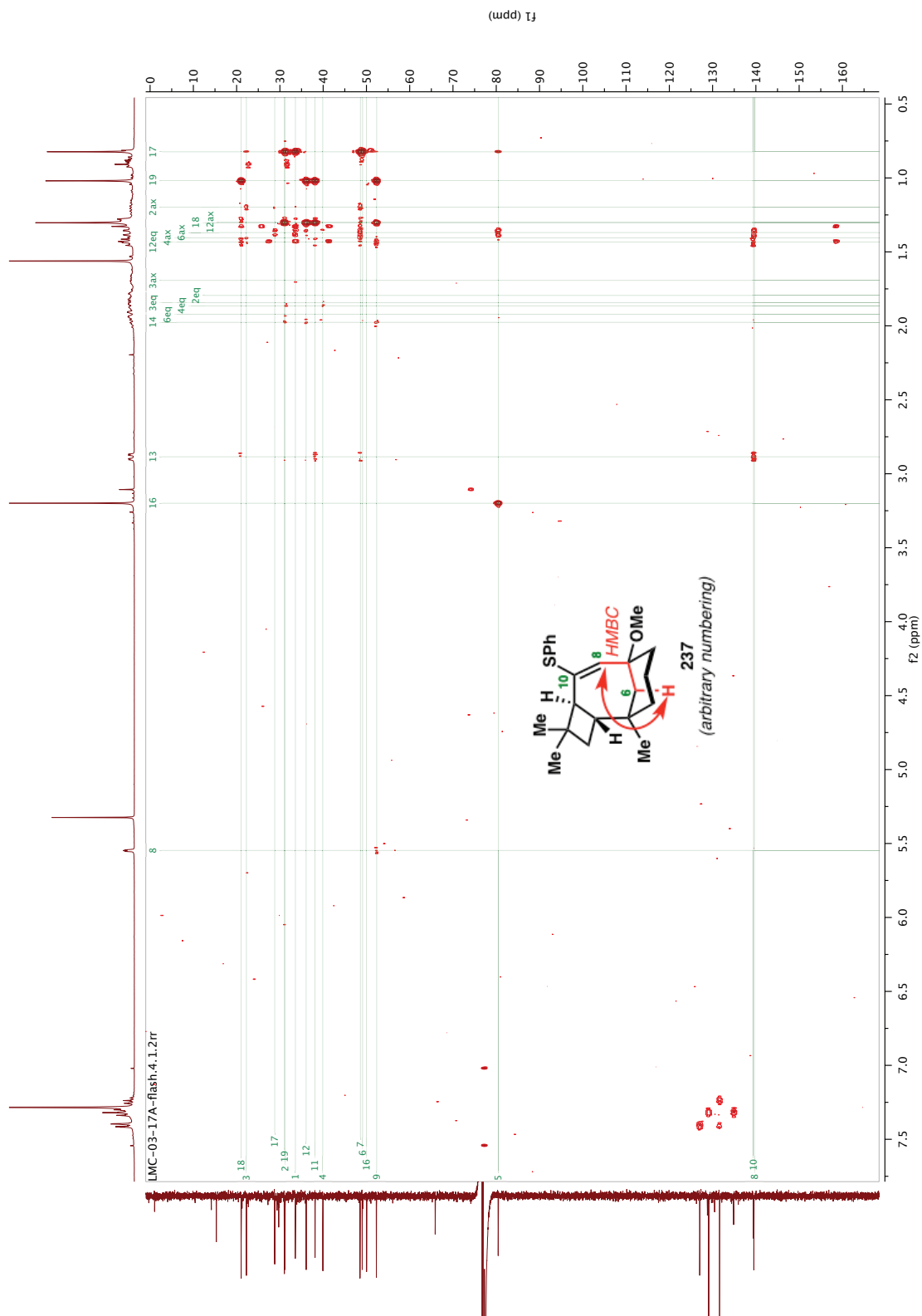


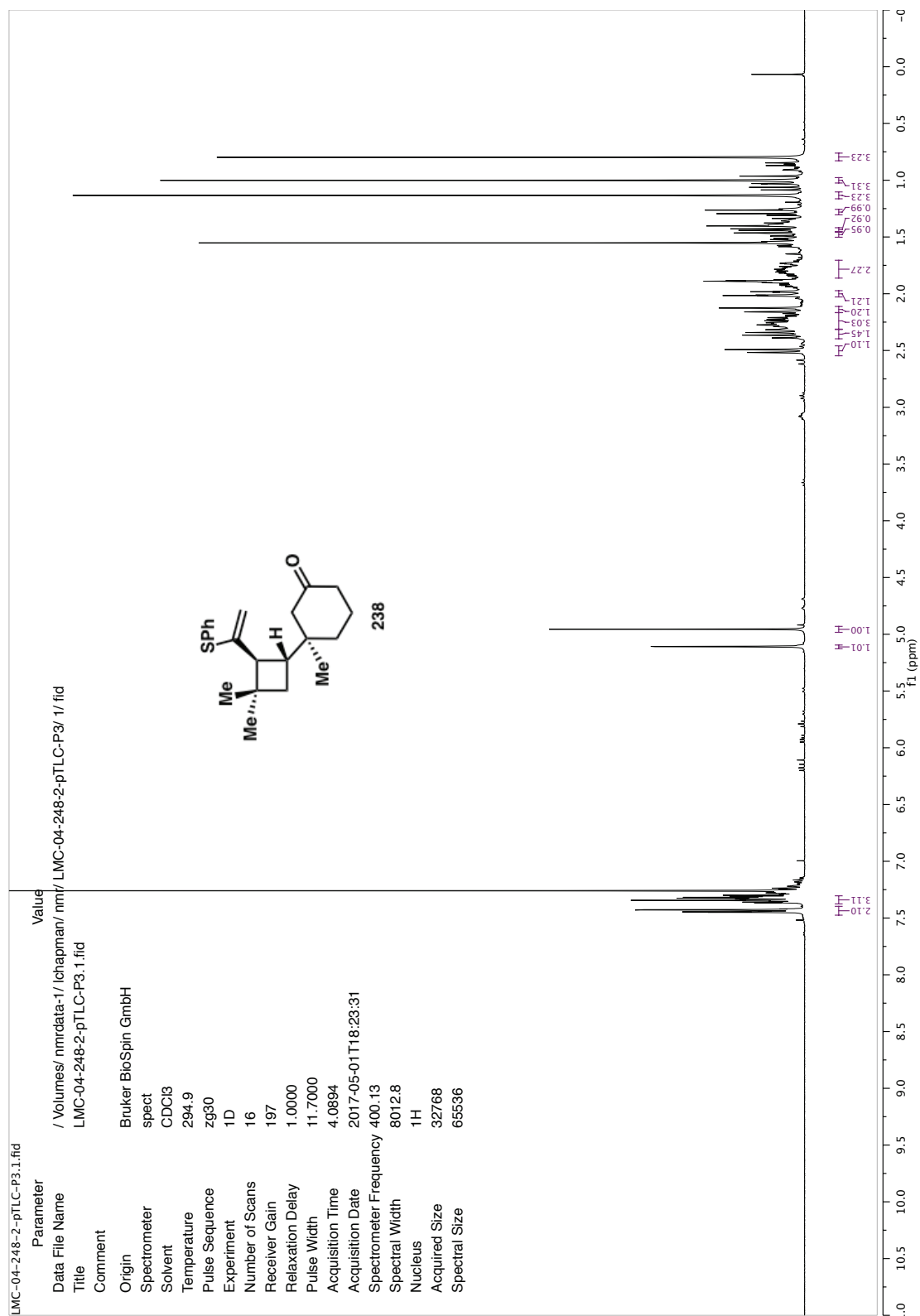


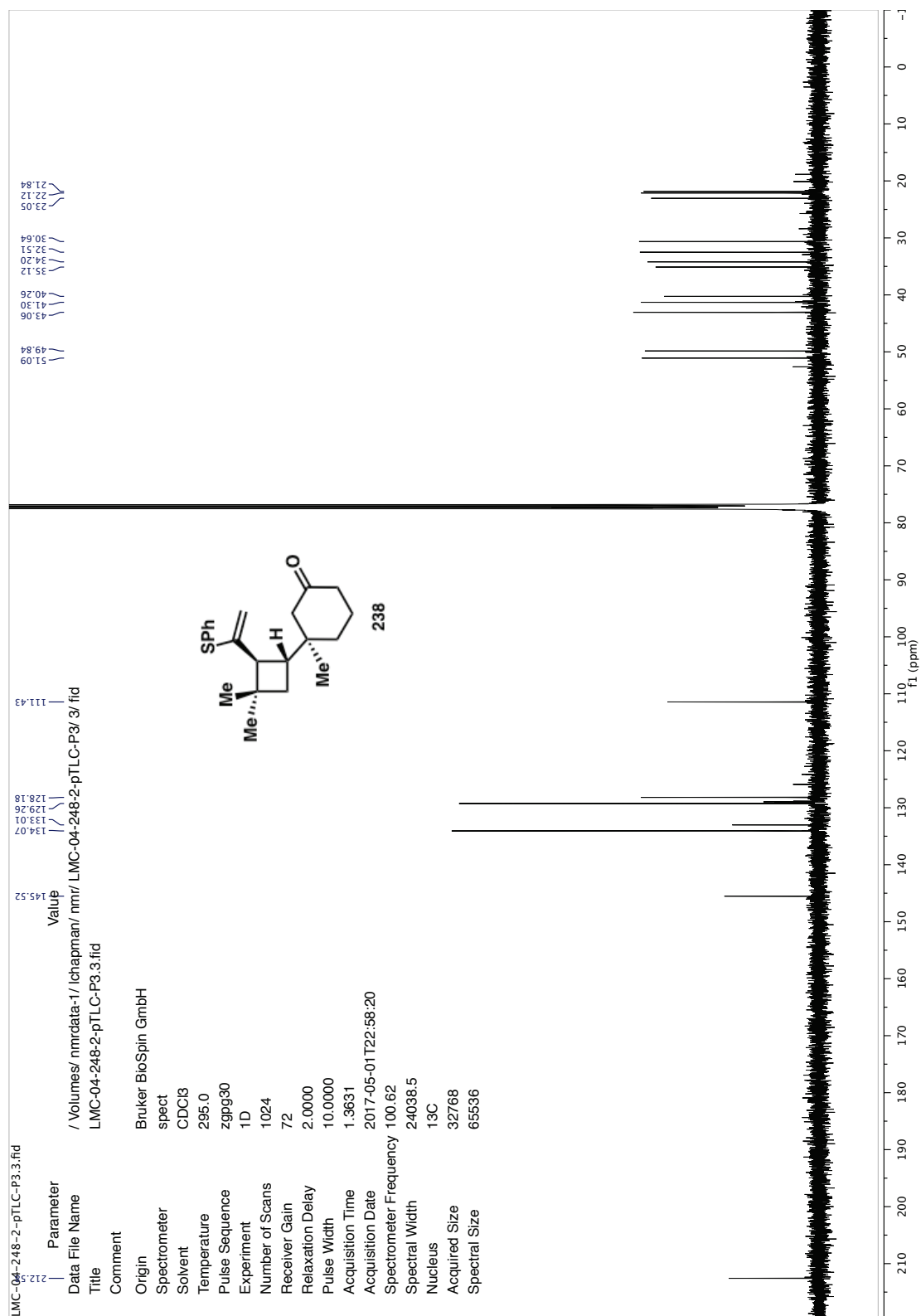












Appendix 2

*X-Ray Crystallography Reports Relevant to Chapter 2:
First Generation Synthetic Strategy Toward (+)-Psiguadial B and
Development of a Catalytic, Asymmetric Wolff Rearrangement[†]*

[†] The work disclosed in this appendix for the X-ray crystallographic analysis of **148** was completed by Dr. Allen Oliver at the University of Notre Dame in the Molecular Structure Facility and Dr. Nathan Schley, a postdoctoral researcher in the Fu lab. X-ray crystallographic analysis of **210** was completed by Dr. Michael Takase at the Caltech X-ray crystallography lab and Julie Hofstra, a graduate student in the Reisman lab.

A2.1 CRYSTAL STRUCTURE ANALYSIS: *TRANS*-CYCLOBUTANE **148**

Figure A2.1. Rendering of *trans*-cyclobutane **148**, used to establish the absolute stereochemistry across the cyclobutane ring.

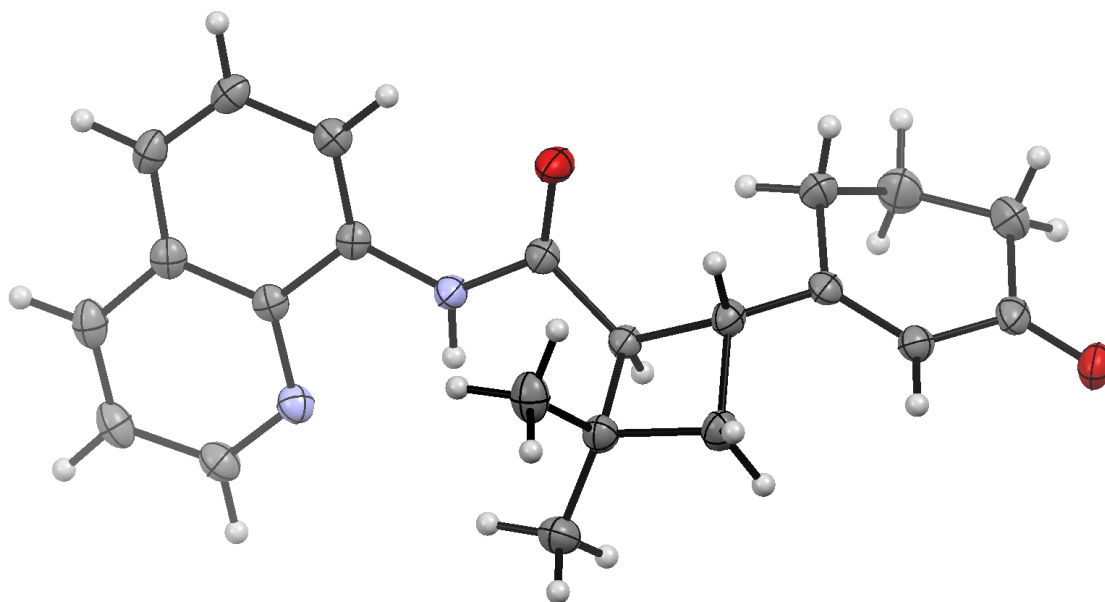


Table A2.1. Crystal data and structure refinement for *trans*-cyclobutane **148**.

Identification code	Crystal01 (or <i>trans</i> -cyclobutane 148).	
Empirical formula	C ₂₂ H ₂₄ N ₂ O ₂	
Formula weight	348.43	
Temperature	119.98 K	
Wavelength	1.54178 Å	
Crystal system	Orthorhombic	
Space group	P2 ₁ 2 ₁ 2 ₁	
Unit cell dimensions	a = 6.3942(5) Å	α = 90°.
	b = 11.6678(9) Å	β = 90°.
	c = 24.848(2) Å	γ = 90°.
Volume	1853.8(3) Å ³	
Z	4	
Density (calculated)	1.248 Mg/m ³	
Absorption coefficient	0.636 mm ⁻¹	
F(000)	744	

Crystal size	0.237 x 0.093 x 0.082 mm ³
Theta range for data collection	3.557 to 71.792°.
Index ranges	-7<=h<=7, -14<=k<=14, -28<=l<=30
Reflections collected	41642
Independent reflections	3620 [R(int) = 0.0313]
Completeness to theta = 67.679°	99.9 %
Absorption correction	Semi-empirical from equivalents
Max. and min. transmission	0.9883 and 0.8875
Refinement method	Full-matrix least-squares on F ²
Data / restraints / parameters	3620 / 0 / 237
Goodness-of-fit on F ²	1.043
Final R indices [I>2sigma(I)]	R1 = 0.0292, wR2 = 0.0782
R indices (all data)	R1 = 0.0294, wR2 = 0.0785
Absolute structure parameter	-0.04(4)
Largest diff. peak and hole	0.255 and -0.181 e/Å ⁻³

Crystallographic Analysis and Refinement Details:

A suitable crystal of C₂₂H₂₄N₂O₂ was selected for analysis. All measurements were made on a Bruker APEX-II CCD with filtered Cu-K α radiation at a temperature of 120 K. Using Olex2,¹ the structure was solved with the ShelXS² structure solution program using Direct Methods and refined with the ShelXL refinement package using Least Squares minimization. The absolute stereochemistry was determined on the basis of the absolute structure parameter. Graphical representation of the structure with 50% probability thermal ellipsoids was generated using Mercury visualization software.³

Table A2.2. Atomic coordinates ($\times 10^4$) and equivalent isotropic displacement parameters ($\text{\AA}^2 \times 10^3$) for trans-cyclobutane **148**. $U(\text{eq})$ is defined as one third of the trace of the orthogonalized U^j tensor.

	x	y	z	U(eq)
O(1)	-4024(2)	4325(1)	3741(1)	30(1)
O(2)	5981(2)	5004(1)	2361(1)	34(1)
N(1)	-3297(2)	4719(1)	4622(1)	22(1)
N(2)	-3330(2)	4949(1)	5683(1)	23(1)
C(1)	-2893(2)	4755(1)	4081(1)	21(1)
C(2)	-944(2)	5426(1)	3950(1)	19(1)
C(3)	-1002(3)	6755(1)	4055(1)	24(1)
C(4)	-3194(3)	7259(2)	3999(1)	31(1)
C(5)	36(3)	7135(2)	4574(1)	33(1)
C(6)	286(3)	6893(1)	3529(1)	26(1)
C(7)	-388(3)	5674(1)	3354(1)	22(1)
C(8)	1149(3)	4904(1)	3080(1)	22(1)
C(9)	2914(3)	5310(1)	2858(1)	23(1)
C(10)	4426(3)	4596(2)	2574(1)	26(1)
C(11)	3943(3)	3338(2)	2530(1)	38(1)
C(12)	2522(3)	2898(2)	2970(1)	40(1)
C(13)	612(3)	3648(2)	3047(1)	30(1)
C(14)	-5080(2)	4317(1)	4886(1)	20(1)
C(15)	-6783(3)	3820(1)	4640(1)	22(1)
C(16)	-8492(3)	3441(1)	4955(1)	24(1)
C(17)	-8509(3)	3560(1)	5503(1)	27(1)
C(18)	-6795(3)	4077(1)	5768(1)	24(1)
C(19)	-5062(2)	4456(1)	5460(1)	20(1)
C(20)	-3303(3)	5073(2)	6212(1)	27(1)
C(21)	-4952(3)	4734(2)	6553(1)	29(1)
C(22)	-6681(3)	4240(2)	6333(1)	29(1)

Table A2.3. Bond lengths [\AA] and angles [$^\circ$] for *trans*-cyclobutane **148**.

O(1)-C(1)	1.219(2)
O(2)-C(10)	1.224(2)
N(1)-C(1)	1.369(2)
N(1)-C(14)	1.397(2)
N(2)-C(19)	1.365(2)
N(2)-C(20)	1.320(2)
C(1)-C(2)	1.507(2)
C(2)-C(3)	1.574(2)
C(3)-C(4)	1.526(2)
C(3)-C(6)	1.554(2)
C(5)-C(3)	1.516(2)
C(7)-C(2)	1.551(2)
C(7)-C(6)	1.549(2)
C(7)-C(8)	1.495(2)
C(8)-C(13)	1.508(2)
C(8)-C(9)	1.342(2)
C(10)-C(11)	1.504(3)
C(10)-C(9)	1.459(2)
C(11)-C(12)	1.511(3)
C(13)-C(12)	1.515(3)
C(14)-C(15)	1.377(2)
C(14)-C(19)	1.436(2)
C(15)-C(16)	1.414(2)
C(17)-C(16)	1.369(2)
C(18)-C(17)	1.415(2)
C(18)-C(19)	1.417(2)
C(18)-C(22)	1.417(2)
C(20)-C(21)	1.410(3)
C(21)-C(22)	1.362(3)
O(1)-C(1)-C(2)	123.68(14)
O(1)-C(1)-N(1)	123.69(14)
O(2)-C(10)-C(11)	121.04(16)
O(2)-C(10)-C(9)	121.70(16)

N(1)-C(1)-C(2)	112.58(13)
N(1)-C(14)-C(19)	115.04(14)
N(2)-C(19)-C(14)	117.20(14)
N(2)-C(19)-C(18)	123.12(14)
N(2)-C(20)-C(21)	123.85(16)
C(1)-C(2)-C(3)	117.15(13)
C(1)-C(2)-C(7)	119.57(13)
C(1)-N(1)-C(14)	128.75(13)
C(4)-C(3)-C(2)	112.66(14)
C(4)-C(3)-C(6)	111.66(14)
C(5)-C(3)-C(2)	114.81(13)
C(5)-C(3)-C(4)	111.60(14)
C(5)-C(3)-C(6)	116.97(15)
C(6)-C(3)-C(2)	87.09(11)
C(6)-C(7)-C(2)	88.10(12)
C(7)-C(2)-C(3)	88.86(11)
C(7)-C(6)-C(3)	89.69(12)
C(7)-C(8)-C(13)	117.31(14)
C(8)-C(13)-C(12)	112.61(15)
C(8)-C(7)-C(2)	118.23(13)
C(8)-C(7)-C(6)	119.83(14)
C(8)-C(9)-C(10)	123.62(15)
C(9)-C(10)-C(11)	117.19(15)
C(9)-C(8)-C(13)	120.87(15)
C(9)-C(8)-C(7)	121.80(15)
C(10)-C(11)-C(12)	113.71(15)
C(11)-C(12)-C(13)	112.36(17)
C(14)-C(15)-C(16)	119.81(14)
C(15)-C(14)-C(19)	119.65(14)
C(15)-C(14)-N(1)	125.31(14)
C(16)-C(17)-C(18)	120.05(16)
C(17)-C(16)-C(15)	121.66(16)
C(17)-C(18)-C(19)	119.14(14)
C(17)-C(18)-C(22)	123.96(16)
C(18)-C(19)-C(14)	119.67(14)
C(20)-N(2)-C(19)	117.41(15)

C(21)-C(22)-C(18)	119.72(16)
C(22)-C(18)-C(19)	116.89(15)
C(22)-C(21)-C(20)	119.00(15)

Table A2.4. Anisotropic displacement parameters ($\text{\AA}^2 \times 10^4$) for trans-cyclobutane **148**. The anisotropic displacement factor exponent takes the form: $-2\pi^2 [h^2 a^{*2} U^{11} + \dots + 2 h k a^* b^* U^{12}]$

	U ¹¹	U ²²	U ³³	U ²³	U ¹³	U ¹²
O(1)	28(1)	43(1)	19(1)	1(1)	-2(1)	-12(1)
O(2)	28(1)	46(1)	27(1)	0(1)	8(1)	-4(1)
N(1)	20(1)	28(1)	18(1)	0(1)	0(1)	-4(1)
N(2)	24(1)	25(1)	21(1)	1(1)	-1(1)	1(1)
C(1)	20(1)	22(1)	20(1)	2(1)	-1(1)	0(1)
C(2)	19(1)	22(1)	17(1)	1(1)	-1(1)	-1(1)
C(3)	26(1)	23(1)	23(1)	0(1)	4(1)	-2(1)
C(4)	34(1)	28(1)	32(1)	4(1)	7(1)	8(1)
C(5)	38(1)	31(1)	29(1)	-6(1)	2(1)	-8(1)
C(6)	29(1)	23(1)	27(1)	2(1)	5(1)	-2(1)
C(7)	22(1)	26(1)	18(1)	4(1)	0(1)	-2(1)
C(8)	22(1)	26(1)	16(1)	-1(1)	-2(1)	-2(1)
C(9)	26(1)	25(1)	19(1)	1(1)	0(1)	-4(1)
C(10)	24(1)	37(1)	16(1)	-1(1)	0(1)	-3(1)
C(11)	36(1)	39(1)	40(1)	-16(1)	10(1)	-3(1)
C(12)	45(1)	27(1)	48(1)	-8(1)	12(1)	-4(1)
C(13)	31(1)	28(1)	32(1)	-6(1)	8(1)	-8(1)
C(14)	21(1)	18(1)	21(1)	3(1)	1(1)	3(1)
C(15)	24(1)	20(1)	21(1)	2(1)	-1(1)	2(1)
C(16)	21(1)	22(1)	31(1)	3(1)	0(1)	-1(1)
C(17)	24(1)	26(1)	31(1)	5(1)	7(1)	-1(1)
C(18)	26(1)	20(1)	24(1)	3(1)	3(1)	4(1)
C(19)	22(1)	17(1)	21(1)	2(1)	0(1)	3(1)
C(20)	32(1)	28(1)	22(1)	-1(1)	-3(1)	2(1)

C(21)	38(1)	30(1)	20(1)	1(1)	2(1)	6(1)
C(22)	34(1)	28(1)	25(1)	4(1)	8(1)	4(1)

Table A2.5. Hydrogen coordinates ($\times 10^4$) and isotropic displacement parameters ($\text{\AA}^2 \times 10^3$) for *trans*-cyclobutane **148**.

	x	y	z	U(eq)
H(1)	-2298	4985	4831	26
H(2)	286	5078	4137	23
H(4A)	-3840	6972	3667	47
H(4B)	-3104	8096	3983	47
H(4C)	-4046	7031	4309	47
H(5A)	-803	6878	4881	49
H(5B)	144	7973	4579	49
H(5C)	1438	6799	4597	49
H(6A)	-237	7508	3290	31
H(6B)	1809	6972	3590	31
H(7)	-1698	5721	3135	26
H(9)	3195	6107	2889	28
H(11A)	5272	2902	2541	46
H(11B)	3277	3190	2177	46
H(12A)	3314	2863	3312	48
H(12B)	2067	2110	2880	48
H(13A)	-363	3523	2743	36
H(13B)	-114	3417	3382	36
H(15)	-6811	3732	4260	26
H(16)	-9656	3096	4781	29
H(17)	-9674	3295	5705	32
H(20)	-2101	5411	6371	33
H(21)	-4858	4849	6930	35
H(22)	-7806	4005	6557	35

A2.2 CRYSTAL STRUCTURE ANALYSIS: MINOR KETONE 210

Figure A2.2. Rendering of minor ketone **210**, used to establish the relative stereochemistry of the methyl group at the C1 quaternary center.

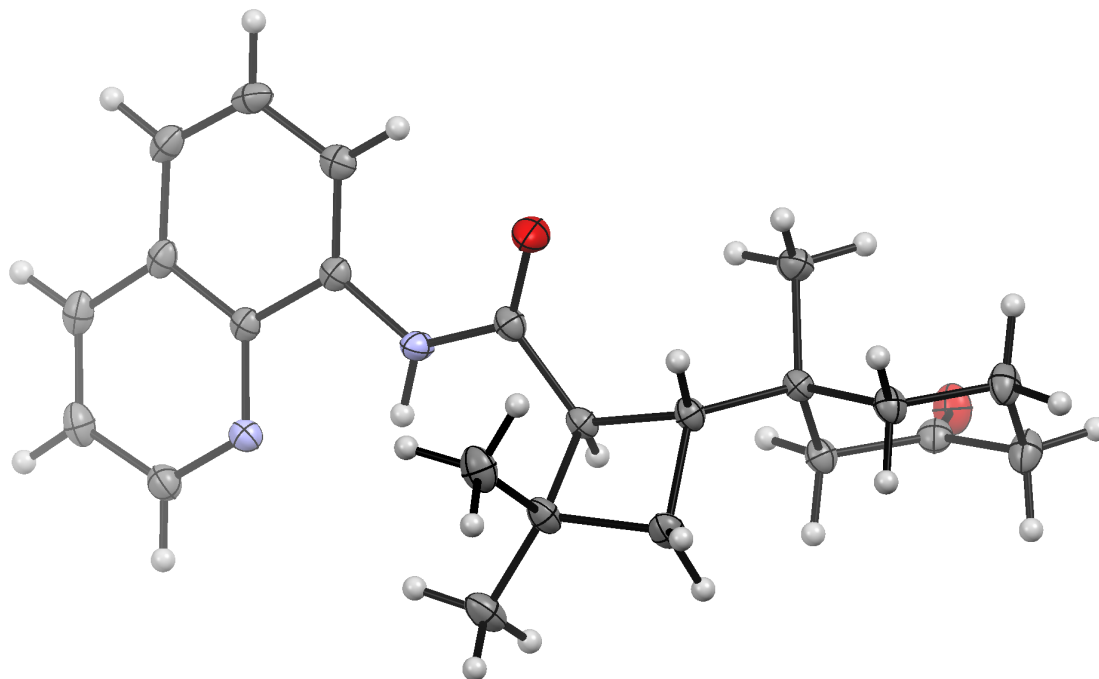


Table A2.6. Crystal data and structure refinement for minor ketone **210**.

Identification code	LMC-04-038 or minor ketone 210 .	
Empirical formula	$C_{23}H_{28}N_2O_2$	
Formula weight	364.47	
Temperature	100 K	
Wavelength	1.54178 Å	
Crystal system	Orthorhombic	
Space group	$P2_12_12_1$	
Unit cell dimensions	$a = 6.5496(4)$ Å	$a = 90^\circ$.
	$b = 10.8428(6)$ Å	$b = 90^\circ$.
	$c = 27.6666(15)$ Å	$c = 90^\circ$.
Volume	$1964.77(19)$ Å ³	
Z	4	
Density (calculated)	1.232 Mg/m ³	
Absorption coefficient	0.619 mm ⁻¹	

F(000)	784
Crystal size	0.25 x 0.15 x 0.1 mm ³
Theta range for data collection	3.195 to 79.392°.
Index ranges	-8<= <i>h</i> <=8, -13<= <i>k</i> <=13, -35<= <i>l</i> <=34
Reflections collected	24424
Independent reflections	4179 [R(int) = 0.0414]
Completeness to theta = 67.679°	100.0 %
Absorption correction	Semi-empirical from equivalents
Max. and min. transmission	0.7542 and 0.7017
Refinement method	Full-matrix least-squares on F ²
Data / restraints / parameters	4179 / 0 / 251
Goodness-of-fit on F ²	1.021
Final R indices [I>2sigma(I)]	R1 = 0.0272, wR2 = 0.0655
R indices (all data)	R1 = 0.0300, wR2 = 0.0672
Absolute structure parameter	0.08(9)
Extinction coefficient	0.0031(3)
Largest diff. peak and hole	0.187 and -0.154 e.Å ⁻³

Crystallographic Analysis and Refinement Details:

Low-temperature diffraction data (ϕ - and ω -scans) were collected on a Bruker AXS D8 VENTURE KAPPA diffractometer coupled to a PHOTON 100 CMOS detector with Cu-K α radiation (λ = 1.54178 Å) from a *I* μ S HB micro-focus sealed X-ray tube. All diffractometer manipulations, including data collection, integration, and scaling were carried out using the Bruker APEXII software.⁴ Absorption corrections were applied using SADABS.⁵ The structure was solved by intrinsic phasing using SHELXT14 and refined against F² on all data by full-matrix least squares with SHELXL-2014² using established refinement techniques.⁶ All non-hydrogen atoms were refined anisotropically. The coordinates for the hydrogen atom bound to N1 were located in the difference Fourier synthesis and refined using a riding model. All other hydrogen atoms were included into the model at geometrically calculated positions and refined using a riding model. The isotropic displacement parameters of all hydrogen atoms were fixed to 1.2 times the *U* value of the atoms they are linked to (1.5 times for methyl groups and hydroxyl groups).

Compound **210** crystallizes in the monoclinic space group $P2_12_12_1$ with one molecule in the asymmetric unit. Absolute configuration was determined by anomalous dispersion (Flack = 0.08(9)).⁷ Graphical representation of the structure with 50% probability thermal ellipsoids was generated using Mercury visualization software.³

Table A2.7. Atomic coordinates ($\times 10^4$) and equivalent isotropic displacement parameters ($\text{\AA}^2 \times 10^3$) for minor ketone **210**. $U(\text{eq})$ is defined as one third of the trace of the orthogonalized U_{ij} tensor.

	x	y	z	U(eq)
O(2)	1276(2)	7506(1)	2689(1)	28(1)
O(1)	8526(2)	4834(1)	3832(1)	28(1)
N(1)	6907(2)	5042(1)	4555(1)	17(1)
N(2)	6036(2)	5230(1)	5486(1)	17(1)
C(1)	6977(2)	4762(1)	4073(1)	17(1)
C(19)	9262(2)	6260(1)	5671(1)	18(1)
C(8)	4149(2)	4860(1)	2948(1)	15(1)
C(23)	7898(2)	5670(1)	5348(1)	15(1)
C(15)	8440(2)	5545(1)	4849(1)	16(1)
C(7)	4752(2)	3938(1)	3343(1)	16(1)
C(2)	4949(2)	4328(1)	3880(1)	16(1)
C(17)	11684(2)	6499(1)	5023(1)	21(1)
C(18)	11180(2)	6672(1)	5498(1)	21(1)
C(16)	10309(2)	5955(1)	4692(1)	19(1)
C(3)	4183(2)	3002(1)	4028(1)	19(1)
C(22)	5507(2)	5373(2)	5942(1)	21(1)
C(10)	1519(2)	6401(2)	2662(1)	19(1)
C(14)	5948(2)	5744(2)	2867(1)	22(1)
C(21)	6728(3)	5976(2)	6290(1)	24(1)
C(9)	2231(2)	5619(1)	3083(1)	18(1)
C(6)	3268(3)	2907(1)	3511(1)	20(1)
C(13)	3699(2)	4120(2)	2484(1)	19(1)
C(20)	8601(3)	6410(2)	6153(1)	22(1)

C(12)	2998(2)	4916(2)	2060(1)	22(1)
C(4)	2696(3)	2947(2)	4449(1)	25(1)
C(5)	5955(3)	2106(2)	4103(1)	26(1)
C(11)	1133(3)	5697(2)	2200(1)	24(1)

Table A2.8. Bond lengths [\AA] and angles [$^\circ$] for minor ketone **210**.

O(2)-C(10)	1.211(2)
O(1)-C(1)	1.2176(18)
N(1)-C(1)	1.3676(19)
N(1)-C(15)	1.402(2)
N(1)-H(1)	0.90(2)
N(2)-C(23)	1.364(2)
N(2)-C(22)	1.319(2)
C(1)-C(2)	1.507(2)
C(19)-C(23)	1.417(2)
C(19)-C(18)	1.416(2)
C(19)-C(20)	1.412(2)
C(8)-C(7)	1.534(2)
C(8)-C(14)	1.535(2)
C(8)-C(9)	1.548(2)
C(8)-C(13)	1.540(2)
C(23)-C(15)	1.431(2)
C(15)-C(16)	1.373(2)
C(7)-H(7)	1.0000
C(7)-C(2)	1.5486(19)
C(7)-C(6)	1.552(2)
C(2)-H(2)	1.0000
C(2)-C(3)	1.577(2)
C(17)-H(17)	0.9500
C(17)-C(18)	1.369(2)
C(17)-C(16)	1.414(2)

C(18)-H(18)	0.9500
C(16)-H(16)	0.9500
C(3)-C(6)	1.555(2)
C(3)-C(4)	1.520(2)
C(3)-C(5)	1.527(2)
C(22)-H(22)	0.9500
C(22)-C(21)	1.410(2)
C(10)-C(9)	1.514(2)
C(10)-C(11)	1.511(2)
C(14)-H(14A)	0.9800
C(14)-H(14B)	0.9800
C(14)-H(14C)	0.9800
C(21)-H(21)	0.9500
C(21)-C(20)	1.367(2)
C(9)-H(9A)	0.9900
C(9)-H(9B)	0.9900
C(6)-H(6A)	0.9900
C(6)-H(6B)	0.9900
C(13)-H(13A)	0.9900
C(13)-H(13B)	0.9900
C(13)-C(12)	1.527(2)
C(20)-H(20)	0.9500
C(12)-H(12A)	0.9900
C(12)-H(12B)	0.9900
C(12)-C(11)	1.535(2)
C(4)-H(4A)	0.9800
C(4)-H(4B)	0.9800
C(4)-H(4C)	0.9800
C(5)-H(5A)	0.9800
C(5)-H(5B)	0.9800
C(5)-H(5C)	0.9800
C(11)-H(11A)	0.9900
C(11)-H(11B)	0.9900

C(1)-N(1)-C(15)	128.85(13)
C(1)-N(1)-H(1)	119.7(13)
C(15)-N(1)-H(1)	111.4(13)
C(22)-N(2)-C(23)	117.51(13)
O(1)-C(1)-N(1)	123.29(14)
O(1)-C(1)-C(2)	124.01(13)
N(1)-C(1)-C(2)	112.68(12)
C(18)-C(19)-C(23)	119.31(14)
C(20)-C(19)-C(23)	117.04(14)
C(20)-C(19)-C(18)	123.65(15)
C(7)-C(8)-C(14)	108.23(12)
C(7)-C(8)-C(9)	112.51(12)
C(7)-C(8)-C(13)	107.68(12)
C(14)-C(8)-C(9)	109.05(13)
C(14)-C(8)-C(13)	110.57(12)
C(13)-C(8)-C(9)	108.79(12)
N(2)-C(23)-C(19)	123.01(13)
N(2)-C(23)-C(15)	117.29(13)
C(19)-C(23)-C(15)	119.68(14)
N(1)-C(15)-C(23)	114.75(13)
C(16)-C(15)-N(1)	125.50(14)
C(16)-C(15)-C(23)	119.69(14)
C(8)-C(7)-H(7)	107.9
C(8)-C(7)-C(2)	121.88(12)
C(8)-C(7)-C(6)	121.41(13)
C(2)-C(7)-H(7)	107.9
C(2)-C(7)-C(6)	87.86(11)
C(6)-C(7)-H(7)	107.9
C(1)-C(2)-C(7)	119.93(12)
C(1)-C(2)-H(2)	109.5
C(1)-C(2)-C(3)	118.23(13)
C(7)-C(2)-H(2)	109.5
C(7)-C(2)-C(3)	88.51(11)
C(3)-C(2)-H(2)	109.5

C(18)-C(17)-H(17)	119.1
C(18)-C(17)-C(16)	121.76(15)
C(16)-C(17)-H(17)	119.1
C(19)-C(18)-H(18)	120.2
C(17)-C(18)-C(19)	119.62(15)
C(17)-C(18)-H(18)	120.2
C(15)-C(16)-C(17)	119.85(14)
C(15)-C(16)-H(16)	120.1
C(17)-C(16)-H(16)	120.1
C(6)-C(3)-C(2)	86.77(11)
C(4)-C(3)-C(2)	116.02(12)
C(4)-C(3)-C(6)	117.16(14)
C(4)-C(3)-C(5)	110.98(13)
C(5)-C(3)-C(2)	111.89(13)
C(5)-C(3)-C(6)	112.06(13)
N(2)-C(22)-H(22)	118.0
N(2)-C(22)-C(21)	123.90(15)
C(21)-C(22)-H(22)	118.0
O(2)-C(10)-C(9)	123.15(15)
O(2)-C(10)-C(11)	122.04(15)
C(11)-C(10)-C(9)	114.80(14)
C(8)-C(14)-H(14A)	109.5
C(8)-C(14)-H(14B)	109.5
C(8)-C(14)-H(14C)	109.5
H(14A)-C(14)-H(14B)	109.5
H(14A)-C(14)-H(14C)	109.5
H(14B)-C(14)-H(14C)	109.5
C(22)-C(21)-H(21)	120.7
C(20)-C(21)-C(22)	118.69(15)
C(20)-C(21)-H(21)	120.7
C(8)-C(9)-H(9A)	109.4
C(8)-C(9)-H(9B)	109.4
C(10)-C(9)-C(8)	111.24(12)
C(10)-C(9)-H(9A)	109.4

C(10)-C(9)-H(9B)	109.4
H(9A)-C(9)-H(9B)	108.0
C(7)-C(6)-C(3)	89.19(11)
C(7)-C(6)-H(6A)	113.8
C(7)-C(6)-H(6B)	113.8
C(3)-C(6)-H(6A)	113.8
C(3)-C(6)-H(6B)	113.8
H(6A)-C(6)-H(6B)	111.0
C(8)-C(13)-H(13A)	108.8
C(8)-C(13)-H(13B)	108.8
H(13A)-C(13)-H(13B)	107.7
C(12)-C(13)-C(8)	113.71(13)
C(12)-C(13)-H(13A)	108.8
C(12)-C(13)-H(13B)	108.8
C(19)-C(20)-H(20)	120.1
C(21)-C(20)-C(19)	119.80(15)
C(21)-C(20)-H(20)	120.1
C(13)-C(12)-H(12A)	109.4
C(13)-C(12)-H(12B)	109.4
C(13)-C(12)-C(11)	111.00(13)
H(12A)-C(12)-H(12B)	108.0
C(11)-C(12)-H(12A)	109.4
C(11)-C(12)-H(12B)	109.4
C(3)-C(4)-H(4A)	109.5
C(3)-C(4)-H(4B)	109.5
C(3)-C(4)-H(4C)	109.5
H(4A)-C(4)-H(4B)	109.5
H(4A)-C(4)-H(4C)	109.5
H(4B)-C(4)-H(4C)	109.5
C(3)-C(5)-H(5A)	109.5
C(3)-C(5)-H(5B)	109.5
C(3)-C(5)-H(5C)	109.5
H(5A)-C(5)-H(5B)	109.5
H(5A)-C(5)-H(5C)	109.5

H(5B)-C(5)-H(5C)	109.5
C(10)-C(11)-C(12)	110.96(13)
C(10)-C(11)-H(11A)	109.4
C(10)-C(11)-H(11B)	109.4
C(12)-C(11)-H(11A)	109.4
C(12)-C(11)-H(11B)	109.4
H(11A)-C(11)-H(11B)	108.0

Table A2.9. Anisotropic displacement parameters ($\text{\AA}^2 \times 10^4$) for minor ketone **210**. The anisotropic displacement factor exponent takes the form: $-2\pi^2 [h^2 a^{*2} U^{11} + \dots + 2 h k a^* b^* U^{12}]$

	U^{11}	U^{22}	U^{33}	U^{23}	U^{13}	U^{12}
O(2)	36(1)	22(1)	27(1)	0(1)	-3(1)	8(1)
O(1)	19(1)	47(1)	18(1)	-3(1)	4(1)	-2(1)
N(1)	15(1)	21(1)	16(1)	-2(1)	3(1)	-3(1)
N(2)	18(1)	17(1)	17(1)	1(1)	1(1)	1(1)
C(1)	20(1)	16(1)	16(1)	1(1)	2(1)	2(1)
C(19)	20(1)	12(1)	21(1)	2(1)	-6(1)	2(1)
C(8)	17(1)	16(1)	14(1)	1(1)	2(1)	0(1)
C(23)	16(1)	12(1)	17(1)	1(1)	-1(1)	2(1)
C(15)	17(1)	13(1)	18(1)	0(1)	-1(1)	2(1)
C(7)	19(1)	15(1)	14(1)	0(1)	1(1)	1(1)
C(2)	18(1)	15(1)	14(1)	0(1)	3(1)	0(1)
C(17)	14(1)	16(1)	33(1)	5(1)	-1(1)	-1(1)
C(18)	20(1)	16(1)	28(1)	2(1)	-9(1)	-2(1)
C(16)	18(1)	16(1)	22(1)	2(1)	2(1)	2(1)
C(3)	26(1)	14(1)	16(1)	1(1)	3(1)	-2(1)
C(22)	23(1)	23(1)	18(1)	2(1)	1(1)	0(1)
C(10)	16(1)	22(1)	19(1)	-1(1)	2(1)	4(1)
C(14)	19(1)	23(1)	25(1)	6(1)	-1(1)	-3(1)

C(21)	32(1)	24(1)	15(1)	0(1)	-1(1)	2(1)
C(9)	20(1)	18(1)	15(1)	-1(1)	2(1)	1(1)
C(6)	25(1)	14(1)	19(1)	-1(1)	1(1)	-3(1)
C(13)	21(1)	20(1)	15(1)	-2(1)	2(1)	3(1)
C(20)	29(1)	17(1)	19(1)	-1(1)	-8(1)	2(1)
C(12)	24(1)	29(1)	15(1)	-3(1)	1(1)	7(1)
C(4)	34(1)	21(1)	21(1)	1(1)	8(1)	-6(1)
C(5)	36(1)	18(1)	22(1)	3(1)	0(1)	4(1)
C(11)	24(1)	30(1)	18(1)	-3(1)	-3(1)	7(1)

Table A2.10. Hydrogen coordinates ($\times 10^4$) and isotropic displacement parameters ($\text{\AA}^2 \times 10^3$) for minor ketone **210**.

	x	y	z	U(eq)
H(7)	6064	3539	3245	19
H(2)	3872	4950	3959	19
H(17)	12993	6751	4913	25
H(18)	12112	7066	5712	25
H(16)	10677	5874	4361	22
H(22)	4228	5051	6044	25
H(14A)	6225	6198	3166	34
H(14B)	5607	6327	2609	34
H(14C)	7162	5270	2775	34
H(21)	6258	6078	6612	28
H(9A)	1121	5052	3180	21
H(9B)	2548	6159	3361	21
H(6A)	3511	2101	3353	23
H(6B)	1810	3142	3492	23
H(13A)	4948	3668	2389	22
H(13B)	2627	3502	2556	22
H(20)	9454	6811	6382	26

H(12A)	2645	4379	1783	27
H(12B)	4127	5466	1959	27
H(4A)	3400	3189	4747	38
H(4B)	2174	2105	4483	38
H(4C)	1557	3513	4389	38
H(5A)	6918	2181	3833	38
H(5B)	5430	1261	4117	38
H(5C)	6654	2302	4406	38
H(11A)	825	6286	1936	29
H(11B)	-67	5153	2242	29
H(1)	5760(30)	4900(20)	4724(7)	29

Table A2.11. Torsion angles [°] for minor ketone **210**.

O(2)-C(10)-C(9)-C(8)	-125.20(17)
O(2)-C(10)-C(11)-C(12)	127.00(17)
O(1)-C(1)-C(2)-C(7)	0.1(2)
O(1)-C(1)-C(2)-C(3)	106.07(18)
N(1)-C(1)-C(2)-C(7)	-178.49(13)
N(1)-C(1)-C(2)-C(3)	-72.53(17)
N(1)-C(15)-C(16)-C(17)	176.96(14)
N(2)-C(23)-C(15)-N(1)	3.66(19)
N(2)-C(23)-C(15)-C(16)	-179.03(13)
N(2)-C(22)-C(21)-C(20)	-2.0(3)
C(1)-N(1)-C(15)-C(23)	-177.11(14)
C(1)-N(1)-C(15)-C(16)	5.8(3)
C(1)-C(2)-C(3)-C(6)	-144.20(13)
C(1)-C(2)-C(3)-C(4)	97.03(17)
C(1)-C(2)-C(3)-C(5)	-31.70(18)
C(19)-C(23)-C(15)-N(1)	-174.83(13)
C(19)-C(23)-C(15)-C(16)	2.5(2)
C(8)-C(7)-C(2)-C(1)	-91.02(17)

C(8)-C(7)-C(2)-C(3)	146.90(14)
C(8)-C(7)-C(6)-C(3)	-147.60(13)
C(8)-C(13)-C(12)-C(11)	-55.22(18)
C(23)-N(2)-C(22)-C(21)	1.6(2)
C(23)-C(19)-C(18)-C(17)	0.3(2)
C(23)-C(19)-C(20)-C(21)	0.9(2)
C(23)-C(15)-C(16)-C(17)	0.0(2)
C(15)-N(1)-C(1)-O(1)	6.0(3)
C(15)-N(1)-C(1)-C(2)	-175.39(14)
C(7)-C(8)-C(9)-C(10)	-172.85(13)
C(7)-C(8)-C(13)-C(12)	177.89(13)
C(7)-C(2)-C(3)-C(6)	-20.67(11)
C(7)-C(2)-C(3)-C(4)	-139.44(14)
C(7)-C(2)-C(3)-C(5)	91.84(14)
C(2)-C(7)-C(6)-C(3)	-20.99(11)
C(2)-C(3)-C(6)-C(7)	20.61(11)
C(18)-C(19)-C(23)-N(2)	179.01(14)
C(18)-C(19)-C(23)-C(15)	-2.6(2)
C(18)-C(19)-C(20)-C(21)	-179.54(15)
C(18)-C(17)-C(16)-C(15)	-2.4(2)
C(16)-C(17)-C(18)-C(19)	2.3(2)
C(22)-N(2)-C(23)-C(19)	0.2(2)
C(22)-N(2)-C(23)-C(15)	-178.22(14)
C(22)-C(21)-C(20)-C(19)	0.7(2)
C(14)-C(8)-C(7)-C(2)	71.18(17)
C(14)-C(8)-C(7)-C(6)	-179.66(13)
C(14)-C(8)-C(9)-C(10)	67.06(16)
C(14)-C(8)-C(13)-C(12)	-64.05(17)
C(9)-C(8)-C(7)-C(2)	-49.38(18)
C(9)-C(8)-C(7)-C(6)	59.77(18)
C(9)-C(8)-C(13)-C(12)	55.69(16)
C(9)-C(10)-C(11)-C(12)	-52.89(19)
C(6)-C(7)-C(2)-C(1)	142.76(14)
C(6)-C(7)-C(2)-C(3)	20.68(11)

C(13)-C(8)-C(7)-C(2)	-169.26(13)
C(13)-C(8)-C(7)-C(6)	-60.10(17)
C(13)-C(8)-C(9)-C(10)	-53.62(16)
C(13)-C(12)-C(11)-C(10)	51.44(19)
C(20)-C(19)-C(23)-N(2)	-1.4(2)
C(20)-C(19)-C(23)-C(15)	176.96(13)
C(20)-C(19)-C(18)-C(17)	-179.26(15)
C(4)-C(3)-C(6)-C(7)	138.32(14)
C(5)-C(3)-C(6)-C(7)	-91.73(14)
C(11)-C(10)-C(9)-C(8)	54.70(18)

A2.3 REFERENCES

- (1) Dolomanov, O. V.; Bourhis, L. J.; Gildea, R. J.; Howard, J. A. K.; Puschmann, H. *J. Appl. Crystallogr.* **2009**, *42*, 339.
- (2) Sheldrick, G. M. *Acta Crystallogr A* **2008**, *64*, 112.
- (3) Macrae, C. F.; Edgington, P. R.; McCabe, P.; Pidcock, E.; Shields, G. P.; Taylor, R.; Towler M.; van de Streek, J. *J. Appl. Cryst.* **2006**, *39*, 453.
- (4) APEX2, Version 2 User Manual, M86-E01078, Bruker Analytical X-ray Systems, Madison, WI, June 2006.
- (5) Sheldrick, G.M. “*SADABS (version 2008/1): Program for Absorption Correction for Data from Area Detector Frames*”, University of Göttingen, 2008.
- (6) Müller, P. *Crystallogr. Rev.* **2009**, *15*, 57.
- (7) Parsons, S.; Flack, H. D.; Wagner, T. *Acta Cryst.* **2013**, *69*, 249.

Chapter 3

Revised Strategies for the Enantioselective Synthesis of (+)-Psiguadial B[†]

3.1 INTRODUCTION

Having evaluated the key reactions proposed in our original retrosynthetic plan, we learned that the substrate employed in the *o*-QMHDA reaction (**102**, see chapter 2) was unfortunately incapable of inducing a synthetically useful level of inherent diastereoselectivity. Moreover, initial efforts to effect a *directed o*-QMHDA reaction revealed a number of additional challenges that precluded implementation of such an approach. Since the Lewis acid-promoted Prins cyclization proved capricious in a model system, a more reliable and robust method was sought to secure the 7-membered ring central to the terpene core of (+)-psiguadial B (**56**). With the successful development of an asymmetric Wolff rearrangement and application of C(sp³)-H functionalization to

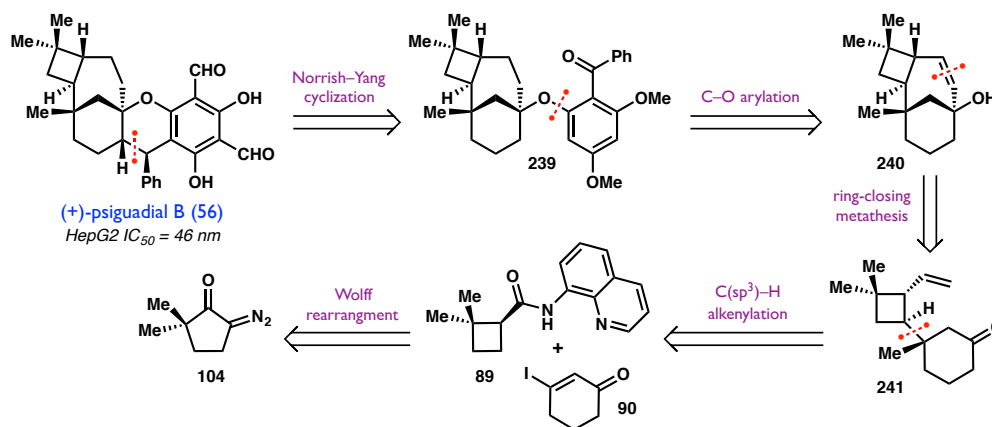
[†] Portions of this chapter were adapted from the following communication: Chapman, L. M.; Beck, J. C.; Wu, L.; Reisman, S. E. *J. Am. Chem. Soc.* **2016**, *138*, 9803, DOI: 10.1021/jacs.6b07229, copyright 2016 American Chemical Society. Studies toward the synthesis of **241** were conducted in collaboration with Jordan C. Beck, a graduate student in the Reisman Lab.

rapidly build the *trans*-cyclobutane, a new synthetic route was devised that preserved the ability to leverage these early strategic reactions.

3.1.1 Revised Retrosynthetic Analysis

In our revised retrosynthesis, we imagined that the chroman substructure could be constructed via a modified Norrish–Yang cyclization,¹ revealing benzophenone **239** as a key intermediate (Figure 3.1). Scission of the aryl C–O bond in **239** led to tertiary alcohol **240**, which would be used in the forward sense to assemble **239** via an intermolecular *O*-arylation reaction.² We reasoned that the strained 7-membered ring in **240** could be formed by a potentially challenging ring-closing metathesis, leading back to vinyl ketone **241**. In turn, it was expected that **241** should be accessible from known intermediates prepared through the previously established C(sp³)–H alkenylation/asymmetric Wolff rearrangement strategy.

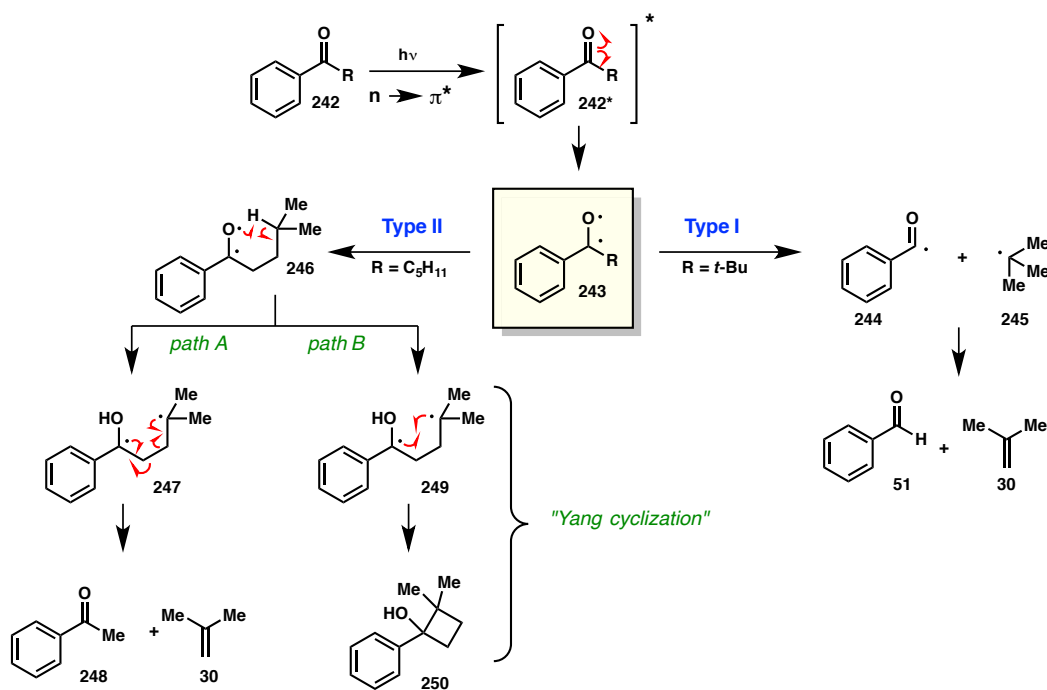
Figure 3.1. Revised retrosynthetic analysis enabled by a Norrish–Yang cyclization



With respect to the first key disconnection, benzophenones (e.g. **242**) are well known to undergo photoexcitation to the triplet state upon irradiation with UV light.³

Triplet benzophenones possess substantial diradical character and can undergo two types of subsequent fragmentation pathways (Scheme 3.1). Norrish type I fragmentation results in initial C–C bond cleavage, thus generating acyl radical species⁴ **244** and stabilized alkyl radicals such as **245**. Alternatively, Norrish type II reaction involves 1,5-hydrogen atom abstraction (e.g. **246**), and the resulting biradical may either fragment further via C–C bond cleavage (path A) or recombine to generate cyclobutanol **250**. The latter pathway is often referred to as the Norrish–Yang cyclization and has been utilized in many synthetic contexts in since its initial discovery.^{1,5}

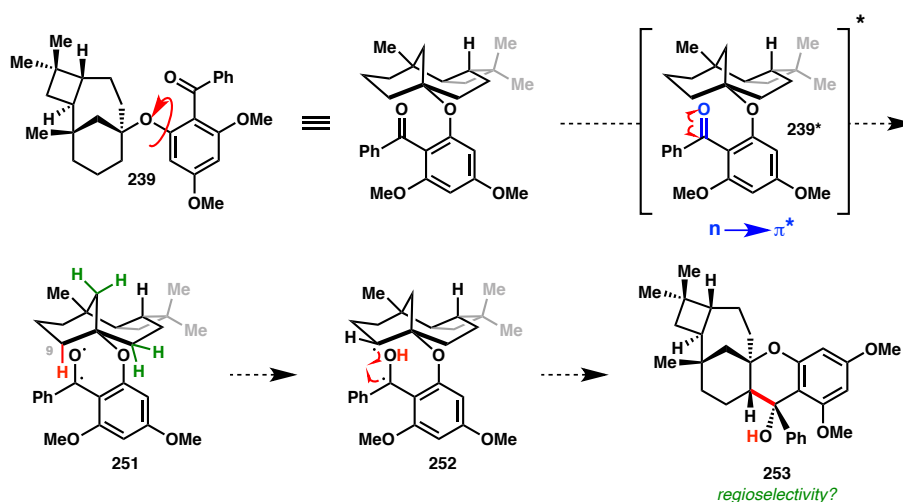
Scheme 3.1. Norrish type I and type II fragmentation pathways



In the specific case of the proposed Norrish substrate **239**, it was envisioned that the benzophenone motif could undergo photoexcitation to the triplet state upon irradiation with UV light (Scheme 3.2). It was hypothesized that, in the absence of any available γ or δ -hydrogens, triplet benzophenone **251** could abstract a hydrogen atom

from the spatially proximal site at C9 to generate diradical **252**. We anticipated that the resulting carbon-centered radicals could then recombine to form the central chroman ring in **253**, and thus complete the core of **56**.

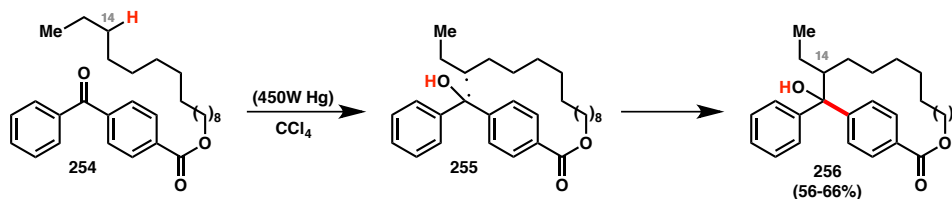
Scheme 3.2. Detailed plan for our proposed modified Norrish–Yang cyclization



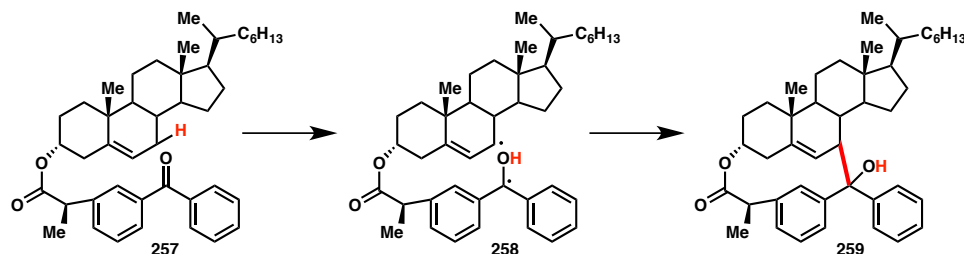
While 1,7-hydrogen atom abstraction processes are not particularly common, Breslow has established that remote C–H oxidation may be achieved by analogous Norrish–Yang type reactivity (Scheme 3.3a). For example, benzophenone **254** was shown to engage in long-range hydrogen atom abstraction predominantly at C14 of a tethered alkyl chain, thus producing macrocyclic alcohol **256** upon irradiation in CCl_4 .⁶ Likewise, Boscá and Miranda have reported the synthesis of photoadduct **259**, produced by laser flash photolysis of benzophenone **257**, which was tethered to a more rigid, steroidal framework (Scheme 3.3b).⁷ The authors of these foundational studies note that the site-selectivity of long-range hydrogen atom abstractions is typically governed by the preferred conformation that the alkyl substrates adopt in solution, which is in turn heavily influenced by solvent effects.

Scheme 3.3. Precedent for long-range hydrogen atom abstraction

a) Breslow and Winnik, 1969:



b) Boscá and Miranda, 2011:

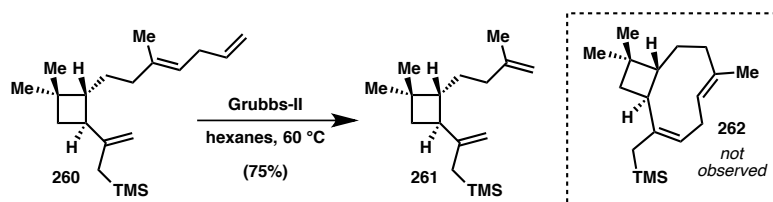


While these reports provided validation from a reactivity standpoint, we acknowledged that achieving the desired *regioselectivity* could prove challenging since **251** also possesses two other CH₂'s (highlighted in green, Scheme 3.2) within range for the same 1,7-H-atom abstraction. Although the regiochemical outcome of this transformation was uncertain, analysis of three-dimensional molecular models suggested that the product resulting from hydrogen atom abstraction at C9 would produce the least sterically encumbered chroman product. Moreover, pursuit of this strategy to access the core of (+)-psguadial B was particularly appealing since it was anticipated that **239** could be accessed in an expedient and convergent fashion.

With regard to securing the terpene framework, we hoped to harness the power of ring-closing metathesis (RCM)—a method that has proven particularly reliable for accessing medium-sized carbocycles⁸—to form the 7-membered ring in **240**. However, we were mindful that Vanderwal and Dowling were unable to effect a ring-closing metathesis with a *trans*-cyclobutane-containing substrate in their attempted synthesis of

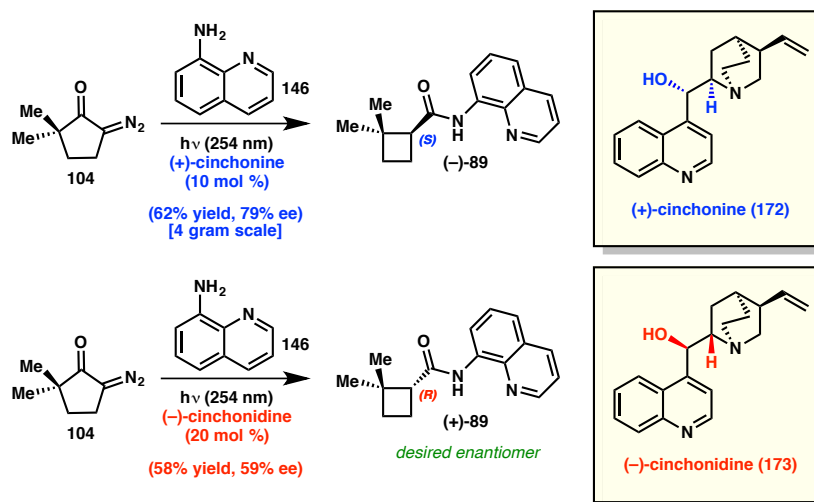
β -caryophyllene (Scheme 3.4).⁹ Unexpectedly, Vanderwal found that exposure of triene **260** to Grubbs second-generation catalyst (Grubbs-II)¹⁰ did *not* furnish the desired penultimate intermediate **262**, but rather resulted in the formation of an undesired, deallylated product **261** in high yield. Whereas RCM with the 1,1-disubstituted olefin in **260** proved challenging, formation of the 7-membered ring in retrosynthetic intermediate **240** would require reaction between two less hindered, monosubstituted vinyl groups. Therefore, it was anticipated that RCM with the planned *trans*-cyclobutane-containing substrate would be more feasible in the proposed context.

Scheme 3.4. Vanderwal's attempted RCM toward β -caryophyllene



Having established this revised retrosynthetic plan, we set out to prepare vinyl ketone **241** from intermediates already in-hand. In so doing, we wished to develop a new synthetic sequence that would address two outstanding problems encountered in the previous route. First, a substrate for conjugate addition lacking the Cu-chelating aminoquinoline was required in order to reduce the high catalyst loadings. Secondly, given that (–)-cinchonidine (**173**) provided (+)-**89** in lower yield and ee in the tandem Wolff rearrangement/asymmetric ketene addition reaction (Scheme 3.5), we sought to develop an alternative epimerization strategy that would allow preparation of natural (+)-psiguadial B (**56**) from (–)-**89**.

Scheme 3.5. Comparison of diastereomeric catalyst performance in the tandem Wolff rearrangement/asymmetric ketene addition reaction



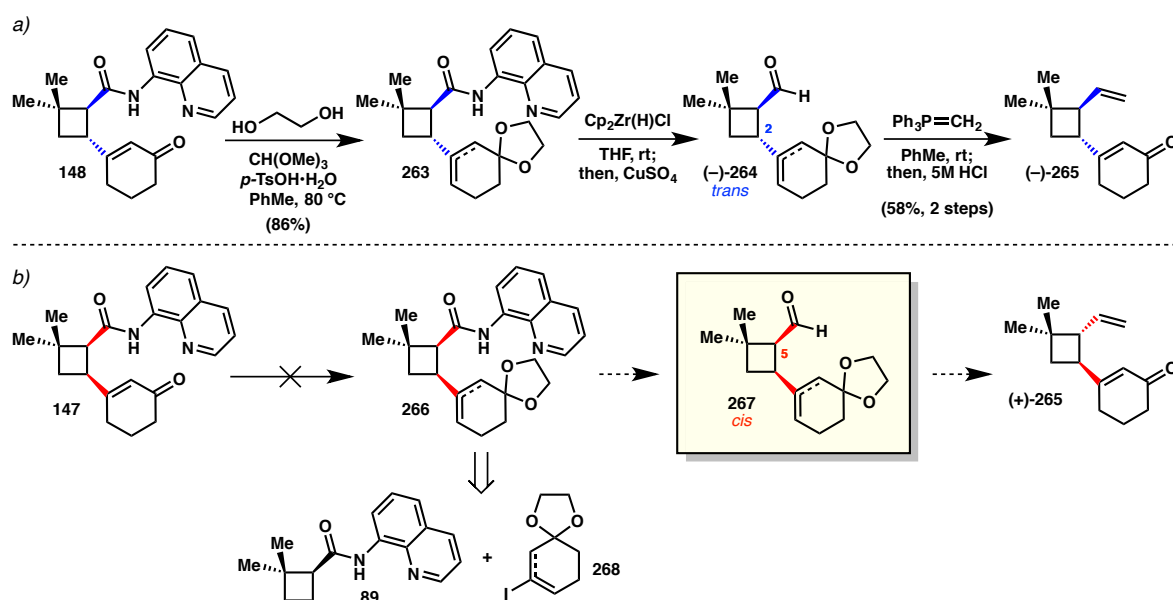
3.2 FORWARD SYNTHETIC EFFORTS

3.2.1 Development of an Alternative Epimerization Strategy

Toward the first goal, it was found that ketalization of *trans*-enone **148** enabled clean reductive cleavage of the aminoquinoline auxiliary, and the corresponding aldehyde **264** was then telescoped through Wittig olefination and hydrolysis to afford vinyl enone (–)-**265** in 58% yield over the two steps (Scheme 3.6a). With successful implementation of this chemistry, attention turned to accessing the desired enantiomer of **265** via an alternate sequence involving epimerization at C5 instead of C2 (Scheme 3.6b). To accomplish this, we reasoned that the α -proton of *cis*-aldehyde **267** would be significantly more acidic than the corresponding amide (i.e. **266**), and thus expected facile epimerization of protected aldehyde **267** at C5. Unfortunately, efforts to prepare **266** from **147** were unfruitful, resulting in facile, undesired epimerization at C2 prior to

ketalization, thus delivering **263** under a variety of canonical acidic protection conditions. Attempts to apply Noyori's aprotic ketalization protocol¹¹ caused rapid decomposition of **147**.

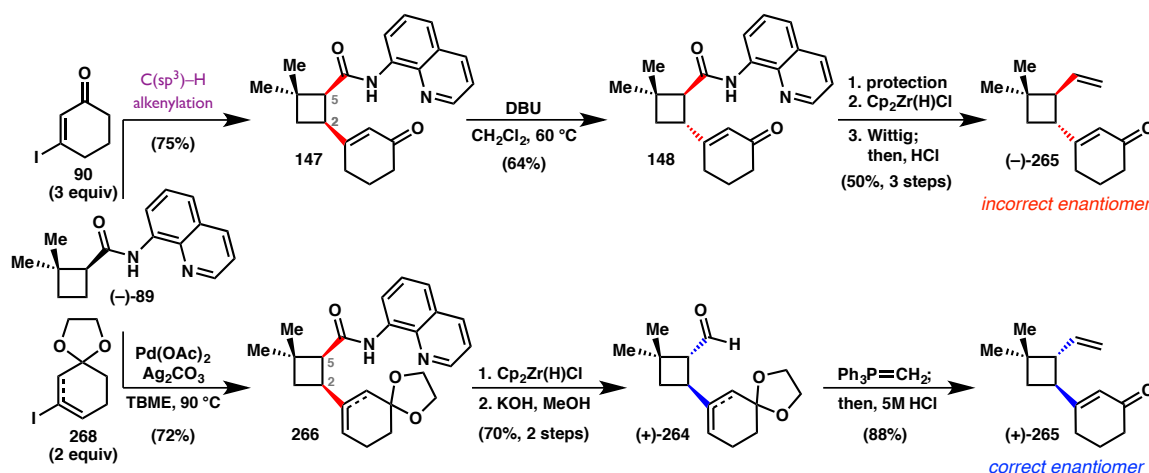
Scheme 3.6. Access to vinyl enone **265** as a better substrate for conjugate addition



At this stage, we recognized that **266** could alternatively be prepared by direct coupling of **89** and protected vinyl iodide **268**. To this end, **268** was prepared (isolated as an 8:1 mixture of olefin isomers) and subjected to the established C(sp³)–H alkenylation conditions. To our delight, protected iodide **268** performed just as well as its enone counterpart (**90**), furnishing **266** in 72% yield on a gram scale (Scheme 3.7, bottom route). Exposure of this alternative diastereomer to Schwartz's reagent effected reduction to the corresponding *cis*-aldehyde **267**, which was epimerized at C5 by treatment with KOH in methanol to give *trans*-aldehyde (+)-**264** in 70% yield over the two steps. Gratifyingly, Wittig methylenation and hydrolysis under the previously developed conditions provided (+)-**265**, the desired enantiomer. Thus, utilization of **268** as a

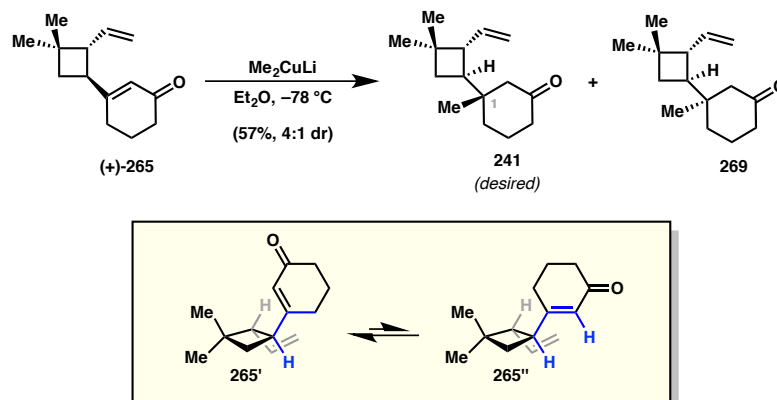
coupling partner eliminated a linear protection step and substantially improved the material throughput.¹² Moreover, it is notable that either enantiomer of **265** can be prepared using a single enantiomer of organocatalyst.

Scheme 3.7. Overview of two complementary epimerization strategies

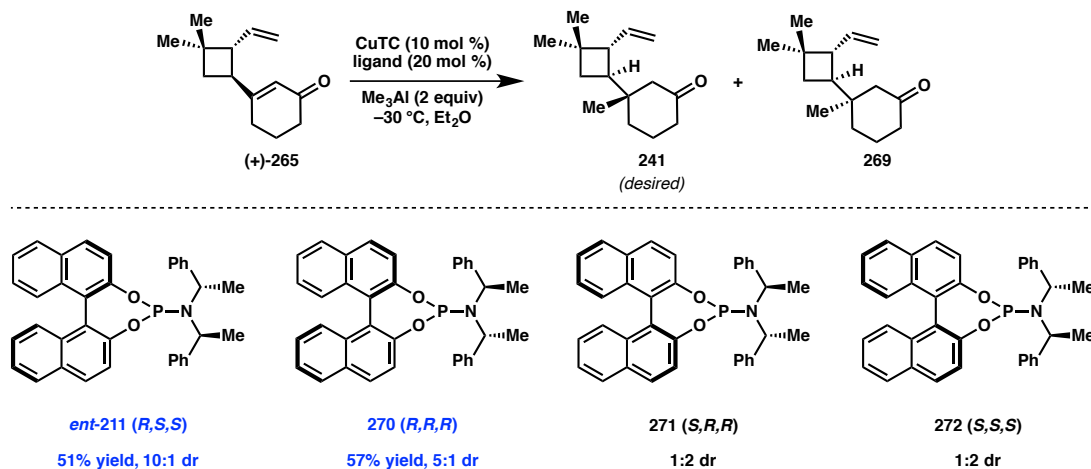


3.2.2 Optimization of a Catalytic Conjugate Addition Reaction

With the desired enantiomer of vinyl enone **265** in hand, attention turned to installation of the methyl group at the C1 quaternary center. Reaction of **265** with Gilman's reagent at -78 °C furnished a mixture of ketones **241** and **269** in moderate yield and 4:1 dr, respectively (Scheme 3.8). Once again, an inherent substrate preference for formation of the desired diastereomer **241** was observed, which is hypothesized to arise by nucleophile approach from the less hindered β-face of A^{1,3}-minimized conformer **265'**. This model also provides a possible explanation for the low levels of diastereoselectivity; either the vinyl group is too small to more effectively block the α-face, or since A^{1,3} interaction occurs between two small protons (highlighted in blue) the alternative A^{1,2} minimized conformer of **265''** may be close in energy.

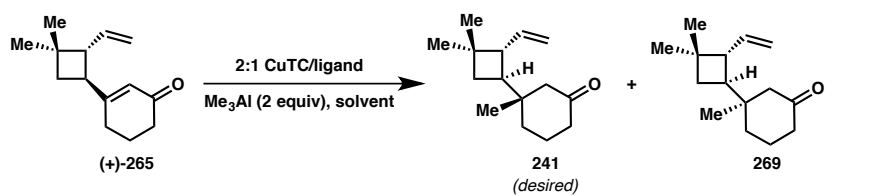
Scheme 3.8. Conjugate addition on a new substrate without aminoquinoline

Building off earlier studies, the diastereoselectivity of the conjugate addition was improved using Alexakis' copper-catalyzed asymmetric method.¹³ A survey of all four possible stereochemical permutations of BINOL-based phosphoramidite ligands *ent*-**211**, **270**–**272** confirmed that the (*R,S,S*) configuration was optimally matched for chiral substrate **265** to provide the highest selectivity, delivering **241** in 51% yield and 10:1 dr (Table 3.1). From these data, it is apparent that the configuration of the BINOL, rather than the bis-phenylethylamine, is the more dominant stereocontrolling factor of the phosphoramidite ligand.

Table 3.1. Confirming optimal ligand configuration with Alexakis' conditions

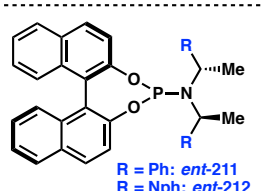
Having established **ent-211** as the optimal ligand, a series of experiments was conducted to optimize this reaction further in terms of both yield and selectivity. Unfortunately, consistent with previous studies, use of a bulkier naphthyl-substituted ligand (**ent-212**) resulted in lower selectivity, although the yield increased substantially (Table 3.2, entry 2). Interestingly, lowering the reaction temperature to $-78\text{ }^{\circ}\text{C}$ had no effect on dr (entry 3), and the selectivity began to erode in other ethereal solvents (entry 4). In the interest of increasing yield without sacrificing selectivity, the catalyst loading was increased. Gratifyingly, in the presence of 15 mol % CuTC, **241** was produced in 97% yield and 12:1 dr on a 0.10 mmol scale. On larger scales, an appreciable exotherm was observed during the addition of trimethylaluminium, which was accompanied by slightly lower levels of selectivity. To mitigate this problem, the reaction temperature was lowered to $-35\text{ }^{\circ}\text{C}$ during the addition of trimethylaluminium, and we were pleased to obtain **241** in 94% yield and 19:1 dr on a 3.7 mmol scale (entry 6).

Table 3.2. Optimization of the copper-catalyzed conjugate addition using **265**



entry ^a	Cu mol %	ligand	temp $^{\circ}\text{C}$	solvent	dr (241:269)	% yield
1	10	<i>ent</i> -211	-30	Et_2O	10:1	51
2	10	<i>ent</i> -212	-30	Et_2O	9:1	70
3	10	<i>ent</i> -211	-78	Et_2O	10:1	62
4	10	<i>ent</i> -211	-30	TBME	7:1	84
5	15	<i>ent</i> -211	-30	Et_2O	12:1	97
6 ^b	15	<i>ent</i> -211	-35	Et_2O	19:1	94

^a 0.10 mmol scale. ^b 3.7 mmol scale.

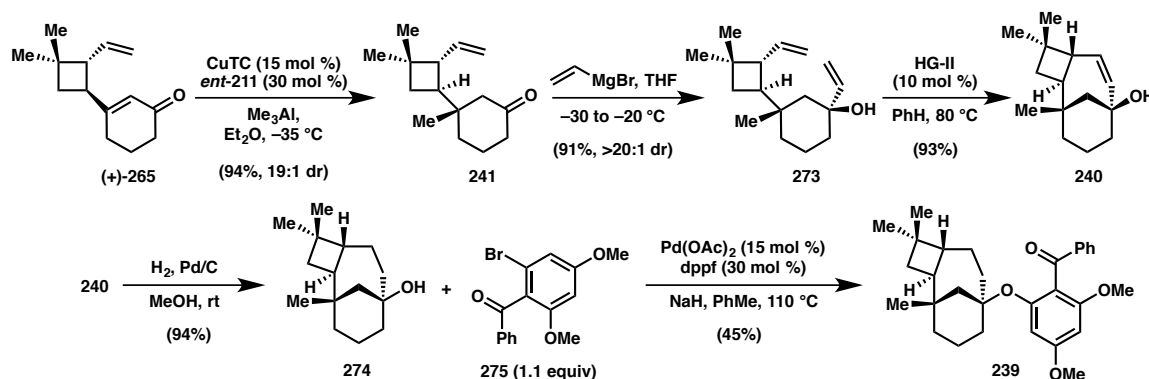


R = Ph: *ent*-211
R = Nph: *ent*-212

3.2.3 Evaluation of the Key Norrish–Yang Cyclization

With a reliable and scalable route to access vinyl ketone **241**, the key ring-closing metathesis reaction was investigated. Fortunately, vinyl Grignard addition to the ketone proceeded uneventfully, providing divinyl alcohol **273** in excellent yield and diastereoselectivity (Scheme 3.9). We were pleased to find that exposure of **273** to second-generation Hoveyda–Grubbs’ catalyst (HG-II) at elevated temperature effected smooth cyclization to bridged bicycle **240** in 93% yield. Subsequent hydrogenation under standard conditions led to tertiary alcohol **274**, which was subjected to a challenging intermolecular *O*-arylation reaction with functionalized aryl bromide **275**.¹⁴ After some experimentation, it was found that the combination of Pd(OAc)₂ and dppf² indeed produced the desired aryl ether **239**, albeit in modest yield. Unfortunately, reproducibility issues plagued this transformation and attempts to improve the yield through optimization were met without success. Nevertheless, a sufficient amount of **239** was obtained to evaluate the feasibility of the final key Norrish–Yang cyclization.

Scheme 3.9. Elaboration to the Norrish–Yang cyclization substrate

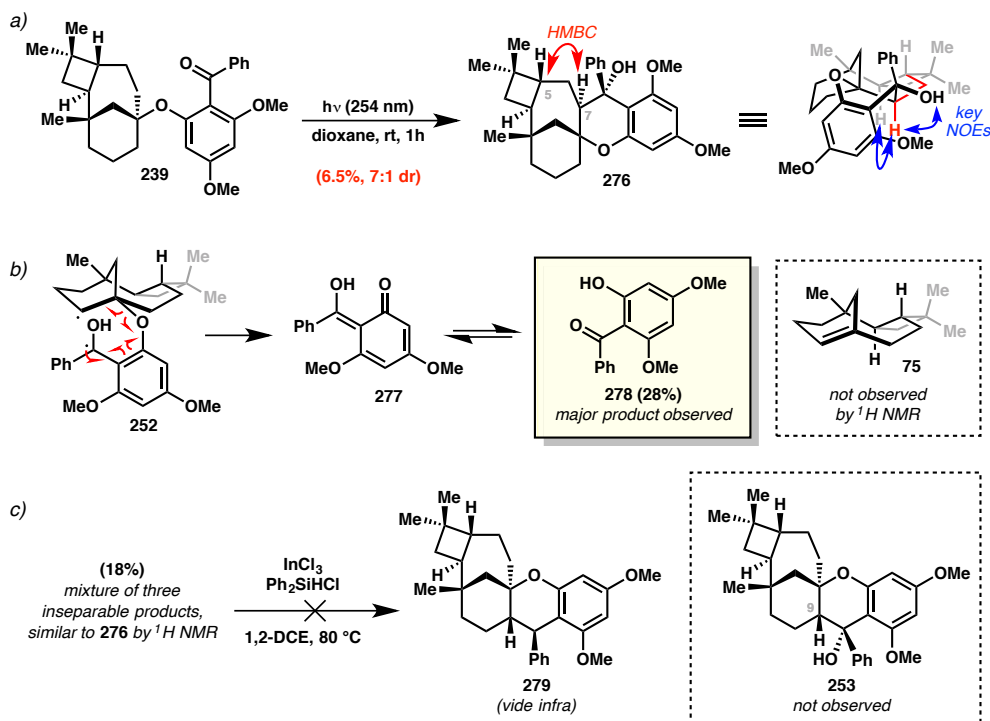


In the event, irradiation of **239** with 254 nm light in rigorously deoxygenated dioxane led to complete consumption of starting material within 1 hour and a complex

mixture of many new products. Formation of Norrish–Yang product **276** was confirmed by 2D NMR spectroscopy; a prominent HMBC correlation was apparent between the newly formed C7 methine proton and C5, in addition to key NOE signals that are consistent with the three dimensional structure as drawn (Scheme 3.10a). Thus, while the anticipated *reactivity* was achieved to some extent, it was disappointing to observe the undesired regioselectivity. Moreover, **276** was isolated in a mere 6.5% yield—a result that would be difficult to improve to synthetically useful yields.

The major product isolated from this reaction is phenol **278**,¹⁵ which was obtained in 28% yield (Scheme 3.10b). This side product presumably arises by fragmentation of diradical species **252** following Norrish type II hydrogen atom abstraction (analogous to “path A” depicted in Scheme 3.1). This apparently facile C–O bond cleavage expels enol tautomer **277**, and the resulting terpene-based radical species likely undergoes further

Scheme 3.10. Evaluation of the key Norrish–Yang cyclization reaction



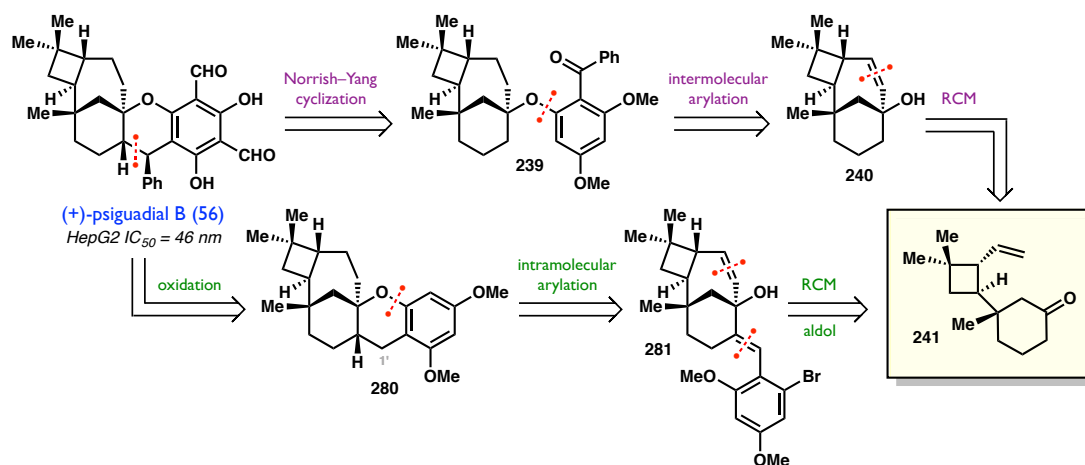
decomposition pathways, since we were unable to detect the formation of the presumably unstable bridgehead olefin **75** by ^1H NMR. In an effort to investigate whether this competing pathway could be suppressed, a number of different solvents and wavelengths were examined in a model system, but rapid formation of phenol **278** was observed in all cases.

The remaining products formed in significant quantities were obtained as a mixture of three compounds in 18% combined yield (Scheme 3.10c). Notably, the ^1H NMR spectrum of this mixture bears striking resemblance to that of **276**, but definitive characterization was hampered by the inability to purify any of these compounds under a variety of separation conditions. Thus, we turned to a chemical correlation method to determine if some of desired product **253** were present in the mixture. To this end, the mixture of three compounds was subjected to a deoxygenation protocol that had successfully been demonstrated to work well in a simpler model system. It was expected that **279**, a compound that was ultimately prepared by other means (*vide infra*), would be observed by ^1H NMR if indeed **253** had been formed in the Norrish reaction. Although a deoxygenated product was obtained that appeared quite similar to **279** (as judged by TLC and mass spectrometry), the ^1H NMR spectrum clearly did not exactly match that of **279**. Thus, while the identity of these potential Norrish–Yang products remains uncertain, we believe that a diastereomer of **253**—perhaps epimeric at C9—may have been formed in low yield. With these disappointing results in hand, an alternative strategy was sought to close the central chroman ring and complete the core (+)-psiguadial B (**56**).

3.3 REVISED SYNTHETIC ROUTE AND NEW ENGAME STRATEGY

Returning to evaluate our retrosynthetic analysis, we were pleased to have identified a robust method for the formation the strained terpene core; however, we had determined that late-stage Norrish–Yang cyclization was an untenable strategy to access **56**. We therefore revised the synthetic route again, deciding to construct the C9–C1' bond at an earlier stage, thereby simplifying **56** to **280** (Figure 3.2). Invoking the same disconnection through the C–O aryl bond as before, it was anticipated that an analogous *intramolecular* ring closure would prove more reliable than the challenging *intermolecular* arylation we had struggled with earlier. This disconnection revealed aryl bromide **281**, which would be accessed using the same ring-closing metathesis, while the arene functionality at C9 could be installed via aldol condensation with vinyl ketone **241**.

Figure 3.2. Comparison of revised retrosynthetic analyses

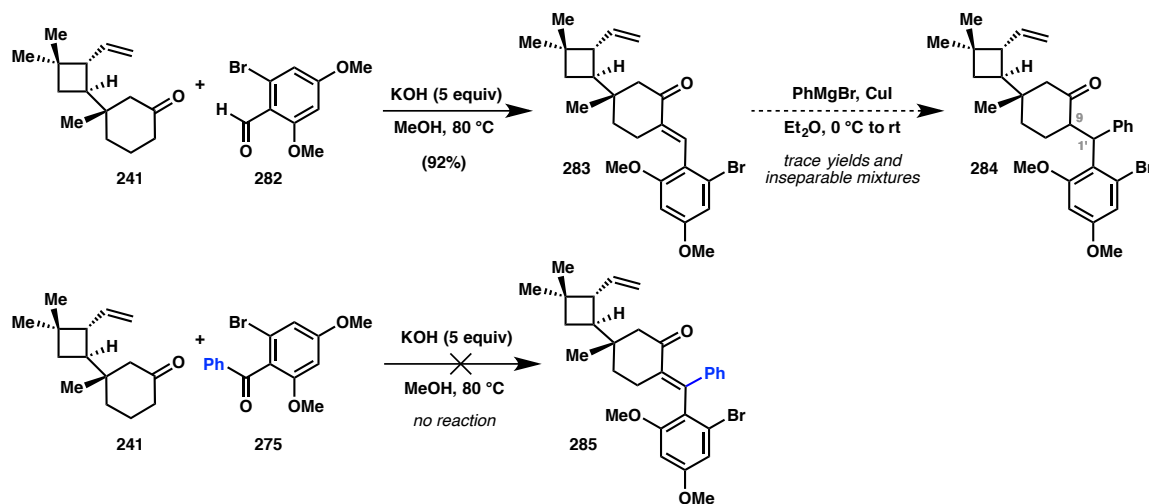


3.3.1 Completion of the Central *Psiguadial* Framework

Synthesis of the requisite aryl aldehyde **282** needed for the aldol reaction was straightforward, accomplished by a Vilsmeier–Haack formylation according to literature procedures.¹⁶ To our delight, treatment of vinyl ketone **241** and **282** with potassium

hydroxide in methanol at elevated temperature smoothly afforded *exo*-enone **283** in 92% yield (Scheme 3.11). Attempts to incorporate the C1' phenyl group via conjugate addition were met with limited success, yielding only trace amounts of **284** as an inseparable mixture of several diastereomers formed at both C9 and C1'. An alternative aldol condensation between **241** and benzophenone **275**¹⁴ did not proceed under otherwise identical conditions; likewise, Mukaiyama aldol with a silyl enol ether derived from **241** and various Lewis acids also gave no productive reaction. These results were not surprising, owing to the electron rich nature of a more hindered diaryl ketone. Despite the inability to introduce the C1' phenyl, we elected to reserve the task of installing this group at a later stage in the synthesis and moved forward with **283**, since this intermediate was readily available in excellent yield.

Scheme 3.11. Aldol reaction and attempts to incorporate the phenyl at C1'

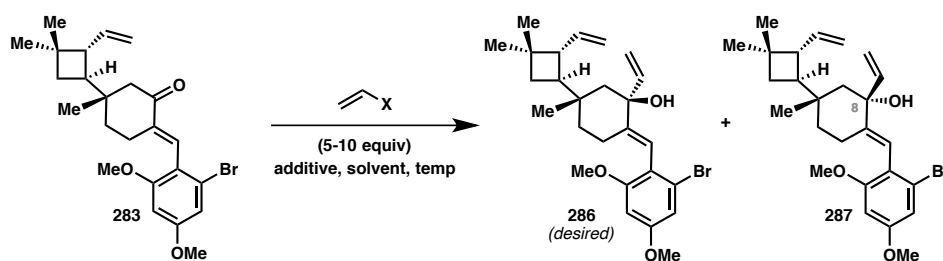


In contrast to the previous system lacking functionality at C9 (i.e. **273**), 1,2-addition into this more hindered ketone proved challenging. Treatment of **283** with vinyl magnesium bromide in THF at –35 °C led to incomplete conversion, presumably due to competitive α -deprotonation, and much lower levels of diastereoselectivity (Table 3.3,

entry 1). While lowering the temperature to $-78\text{ }^{\circ}\text{C}$ indeed improved the dr to 4.5:1, an even lower overall yield of **286** was obtained (entry 2). Alternative solvents or warmer reaction temperatures did not alleviate this problem (entries 3–5), and thus we turned to Lewis acid activators known to suppress enolization of hindered ketones.¹⁷ While additives such as CeCl_3 and $\text{LaCl}_3 \cdot 2\text{LiCl}$ indeed improved conversion, this was always accompanied by substantially lower dr, which unfortunately amounted to similar overall yields of **286** (entries 6 and 7). On the other hand, reactions with lithium salts such as LiCl and LiOCl_4 as additives still suffered from poor conversion.

Ultimately, allylic alcohol **286** was obtained in good yield with serviceable dr by employing vinyl lithium in THF at $-78\text{ }^{\circ}\text{C}$ (entry 8). Addition of $\text{La}(\text{OTf})_3$, or lowering the reaction temperature to $-100\text{ }^{\circ}\text{C}$ did not improve this reaction further (entries 9 and 10). Larger vinyl lithium nucleophiles, as well as divinylzinc were also investigated; however, use of these reagents resulted in low conversions or no reaction, respectively.

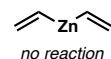
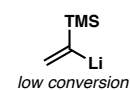
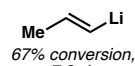
Table 3.3. Optimization of 1,2 addition using vinylmetal species



entry ^a	X	solvent	temp $^{\circ}\text{C}$	additive	% conv. ^b	dr (286:287)	% total yield (% yield 286)
1	MgBr	THF	-35	—	75	2.5:1	57 (41)
2	MgBr	THF	-78	—	56	4.5:1	41 (34)
3	MgBr	Et_2O	-35	—	ND	2.5:1	57 (41)
4	MgBr	CH_2Cl_2	0	—	85	1.9:1	69 (45)
5	MgBr	THF	0	—	60	2.0:1	50 (33)
6	MgBr	THF	-78	CeCl_3	81	1.6:1	66 (41)
7	MgBr	THF	-78	$\text{LaCl}_3 \cdot 2\text{LiCl}$	100	1.7:1	59 (37)
8	Li	THF	-78	—	86	2.1:1	77 (52)
9	Li	THF	-78	$\text{La}(\text{OTf})_3$	94	1.8:1	67 (43)
10	Li	THF	-100	—	87	1.4:1	61 (36)

^a Test reactions conducted on ~ 0.02 mmol scale. ^b Conversion determined by relative integrals using LC/MS signals detected at 254 nm.

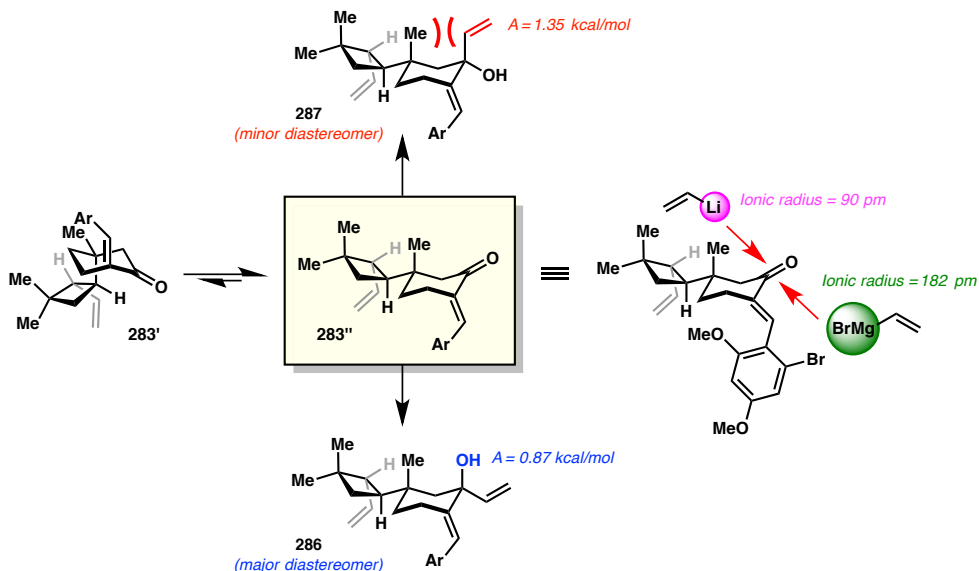
Alternative nucleophiles tested:



Lastly, Corey–Chaykovsky-type conditions,¹⁸ which are known to afford allylic alcohols in the presence of excess dimethylsulphonium methylide, led to exclusive formation of the undesired diastereomer **287**.

The conformational analysis model depicted in Figure 3.3 may explain the diastereoselectivity trends apparent in Table 3.3. Conformer **283''** orients the large cyclobutane and aryl substituents in more favorable equatorial positions and is therefore expected to be lower in energy than **283'**. Considering that a trajectory from the top face along the Bürgi–Dunitz angle places the incoming nucleophile in close proximity to the axial methyl group, it is reasonable that larger nucleophiles, such as vinylmagnesium bromide (ionic radius of $\text{Br}^- = 182$ pm), engage in equatorial attack from the bottom face with greater preference. Conversely, smaller nucleophiles such as vinyl lithium (ionic radius of $\text{Li}^+ = 90$ pm) give rise to larger amounts of **287**. This same logic applies to Lewis acid activators—large lanthanides likely coordinate to the carbonyl from the less hindered bottom face, thus eroding selectivity for **286**. With respect to the conformation

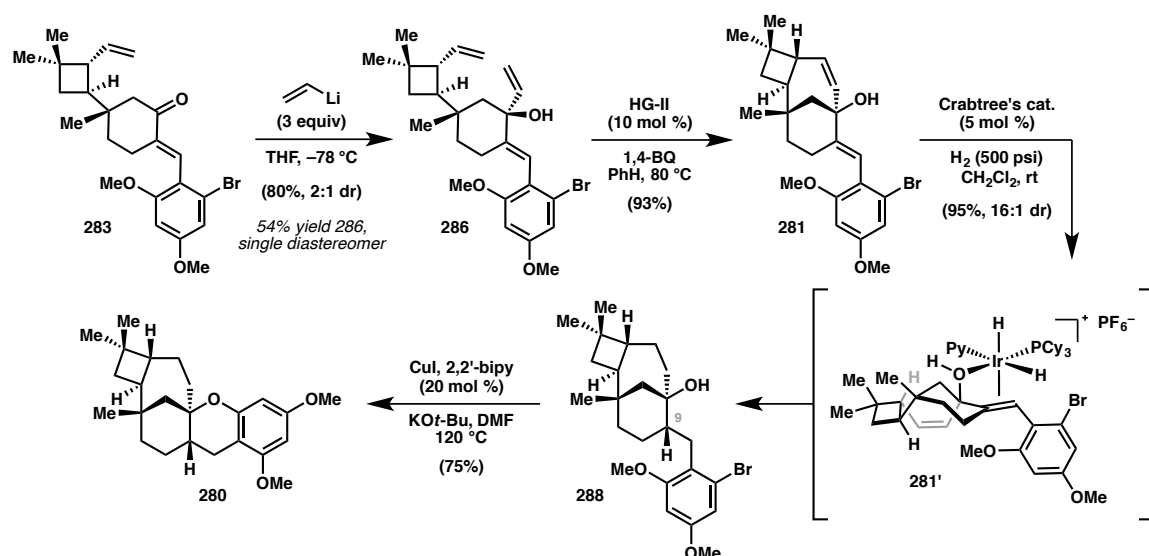
Figure 3.3. Conformational analysis and selectivity model for 1,2-addition



of the products, **287** exhibits more pronounced adverse 1,3-diaxial interactions between the methyl and vinyl group ($A = 1.35$ kcal/mol), which may contribute to the preferred formation of **286**, observed as the major diastereomer in all cases.

We were pleased to find that the results in Table 3.3, entry 8 were reproducible on large scale, delivering **286** in 54% isolated yield as a single diastereomer (Scheme 3.12). Gratifyingly, the ring-closing metathesis proceeded with equal efficiency on this new substrate to furnish **281** in 93% yield. With the strained sesquiterpene framework secured, both the di- and trisubstituted olefins in **281** were hydrogenated in the presence of Crabtree's catalyst, which engaged in a hydroxyl-directed reduction¹⁹ to establish the C9 stereogenic center with 16:1 dr, providing **288** in excellent yield. The final ring of the psiguadial framework was constructed by a significantly more facile Cu-catalyzed intramolecular *O*-arylation reaction, which furnished pentacycle **280** in 75% yield.²⁰

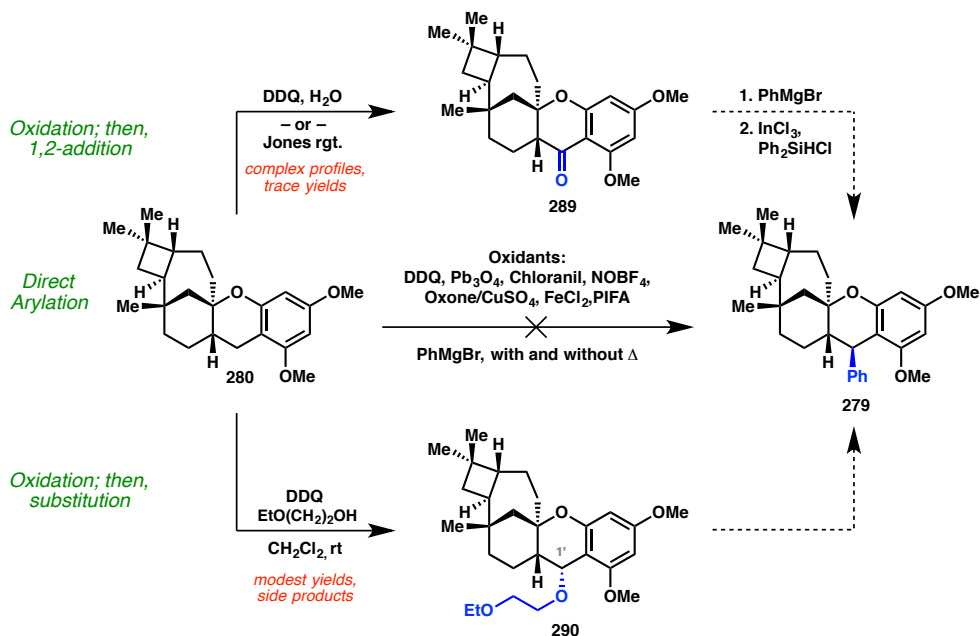
Scheme 3.12. Elaboration to complete pentacyclic core of (+)-psiguadial B



3.3.2 Appendage of the C1' Phenyl Group and Final Functionalization

Having succeeded in developing a scalable and high-yielding route to **280**, the task of appending the C1' phenyl group was now at hand. Ideally, we wished to develop a direct arylation protocol, wherein the electron rich arene in **280** might assist in benzylic oxidation at C1', followed by trapping with an appropriate phenyl nucleophile. Whereas a number of laboratories have shown that electron rich, oxidized arenes can efficiently trap benzylic cations in related systems,²¹ an electronically neutral, unsubstituted phenyl group is not sufficiently reactive to engage in this type of transformation. Nonetheless, we investigated the possibility of sequential oxidation at C1' with reagents commonly used in flavonoid chemistry, such as DDQ,^{21a,d,22} Pb₃O₄,²³ and Oxone/CuSO₄,²⁴ followed by trapping with PhMgBr, with no success (Scheme 3.13). Chloranil, a structural analog of DDQ, as well as other organic single-electron oxidants and hydride abstractors,²⁵ were also examined to no avail. Finally, efforts to apply Shi's FeCl₂-catalyzed benzylic

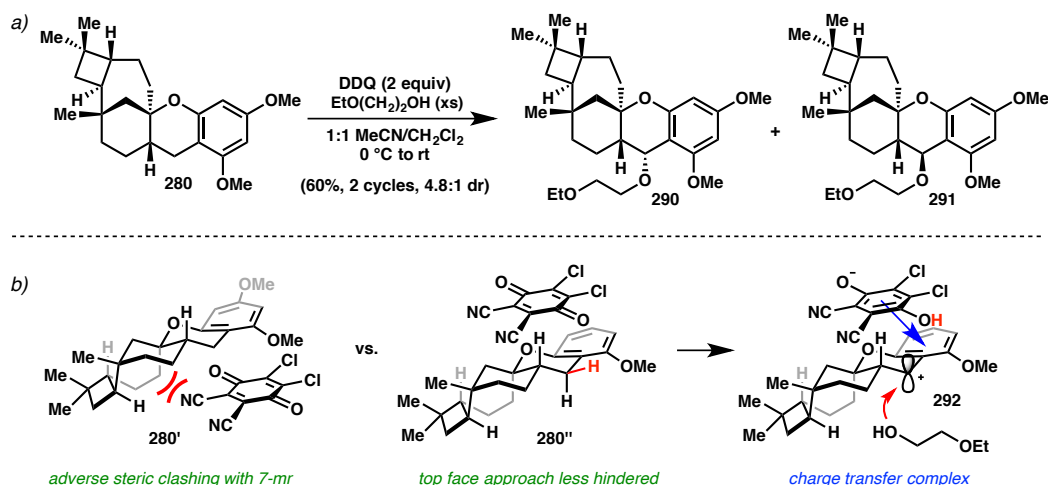
Scheme 3.13. Summary of strategies to install phenyl ring at C1'



dehydrogenative arylation,²⁶ or Muramatsu's C(sp³)–H arylation using DDQ and PIFA²⁷ were also unfruitful.

Without any success in achieving a direct arylation, a stepwise protocol was employed for the installation of the C1' phenyl substituent. Reasoning that alcohol **253** could be accessed by 1,2-addition of PhMgBr into chromanone **289**, benzylic oxidation was attempted under standard conditions but only complex reaction profiles and trace yields were observed. On the other hand, oxidation with DDQ in the presence of primary alcohols²² seemed promising; although these reactions produced several side products suspected to result from over oxidation and elimination of the newly installed benzylic ether, use of ethoxyethanol afforded **290**—a relatively stable product that could be isolated in modest yields. The possibility of accessing other benzylic ethers analogous to **290** was also explored via radical halogenation, followed by displacement with various alcohols, however these protocols led exclusively to arene bromination.

With a lead in hand, the DDQ-mediated oxidative etherification reaction was optimized. An extensive survey of reaction parameters revealed that adding acetonitrile as a co-solvent led to cleaner reaction profiles (Scheme 3.14a). Although lower conversion of starting material was observed, *productive* reactivity was much improved and synthetically useful yields of **290** were obtained after re-subjecting recovered **280** to the same reaction conditions a second time. Presumably, the presence of a high dielectric solvent helps to stabilize the intermediate benzylic cation (**291**), which can allow more efficient trapping with ethoxyethanol, rather than undergoing unproductive side reactions.

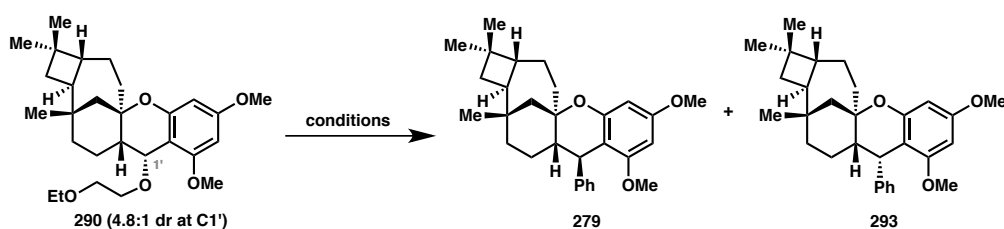
Scheme 3.14. Optimized conditions and model for observed diastereoselectivity

In regards to the stereochemistry at C1', **290** and **291** were isolated as a 4.8:1 mixture of diastereomers, respectively. Since the pseudoequatorially-disposed β -ether (i.e. **291**) is expected to be thermodynamically favored, the observed stereochemical outcome could result from an overall double inversion process that proceeds by formation of a tightly bound charge-transfer complex with DDQ (**292**, Scheme 3.14b).²⁸ Since the 7-membered ring protrudes from the bottom face of **280**, it is conceivable that DDQ preferentially approaches from the less-hindered top face, thus abstracting the β -hydrogen atom highlighted in red (**280''**). If the charge transfer complex remains closely associated, ethoxyethanol can then attack from the bottom face, thus leading to **290** as the major diastereomer.

With a functional handle now installed at C1', attention turned to its displacement with an appropriate phenyl nucleophile. Unfortunately, Smith's procedure using TMSOTf to activate ethoxyethyl benzyl ethers did not provide any of the desired phenylated product in the presence of PhB(OH)₂ or upon quench with PhMgBr (Table 3.4, entries 1 and 2).^{22b} Simple heating²⁹ or nickel-catalyzed Kumada coupling with

PhMgBr in PhMe³⁰ yielded only eliminated products and messy reaction profiles (entries 3–5). Likewise, efforts to apply Bode's conditions for addition of aryl trifluoroborates to oxonium ions generated by treatment with BF₃•OEt₂ were met without formation of **279** (entries 6 and 7).³¹ Disheartened by the apparent difficulty of this transformation, we were therefore delighted to obtain a near quantitative yield of **279** and **293** in a 1.7:1 ratio upon addition of BF₃•OEt₂ to a mixture of **290** and lithium diphenylcyanocuprate (entry 8).³² After some experimentation, it was found that the diastereoselectivity could be slightly improved to 2:1 by holding the reaction at –45 °C (entry 9), while colder temperatures led to significantly lower yields (entry 10).

Table 3.4. Attempts to displace benzylic ether using various methods

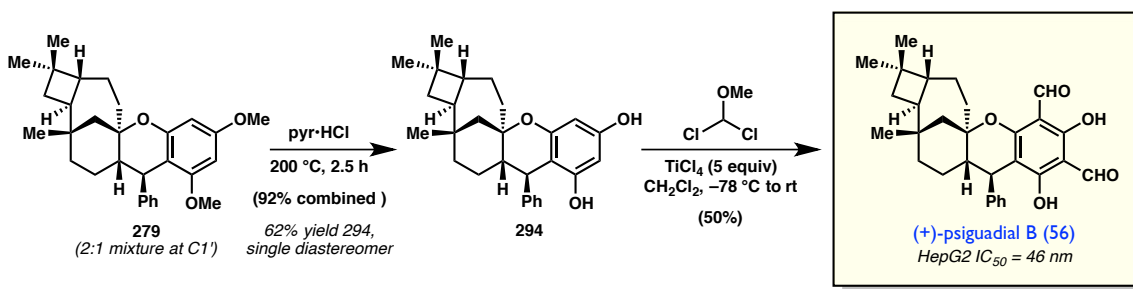


entry	Lewis acid or catalyst	nucleophile	temp °C	solvent	% yield (dr)
1	TMSOTf	PhB(OH) ₂	–78 to 0	THF	0
2	TMSOTf	PhMgBr	–78 to 0	THF	0
3	none	PhMgBr	110	PhMe	0
4	Ni(dppe)Cl ₂	PhMgBr	rt	PhMe	0
5	Ni(dppe)Cl ₂ /MgI ₂	PhMgBr	rt	PhMe	0
6	BF ₃ •OEt ₂	PhBF ₃ K	0 to rt	CH ₂ Cl ₂	0
7	BF ₃ •OEt ₂	PhBF ₃ K	0 to rt	MeCN	0
8	BF ₃ •OEt ₂	Ph ₂ Cu(CN)Li ₂	–78 to 0	Et ₂ O	99 (1.7:1)
9	BF ₃ •OEt ₂	Ph ₂ Cu(CN)Li ₂	–78 to –45	Et ₂ O	90 (2.0:1)
10	BF ₃ •OEt ₂	Ph ₂ Cu(CN)Li ₂	–78 to –60	Et ₂ O	57 (3.3:1)

As diastereomers **279** and **293** were inseparable by silica gel chromatography, the mixture was subjected to pyridine hydrochloride at 200 °C, which afforded the corresponding demethylated products in 92% combined yield (Scheme 3.15). At this stage, the diastereomeric resorcinols were readily separable by column chromatography, providing **294** in 62% yield as a single diastereomer. Finally, the remaining two aryl

aldehydes were simultaneously installed using Rieche formylation conditions,³³ delivering the (+)-psiguadial B in 50% yield. Gratifyingly, synthetic **56** was found to be spectroscopically identical in all respects to the natural sample reported by Shao et al.³⁴

Scheme 3.15. Completion of the the total synthesis of (+)-psiguadial B



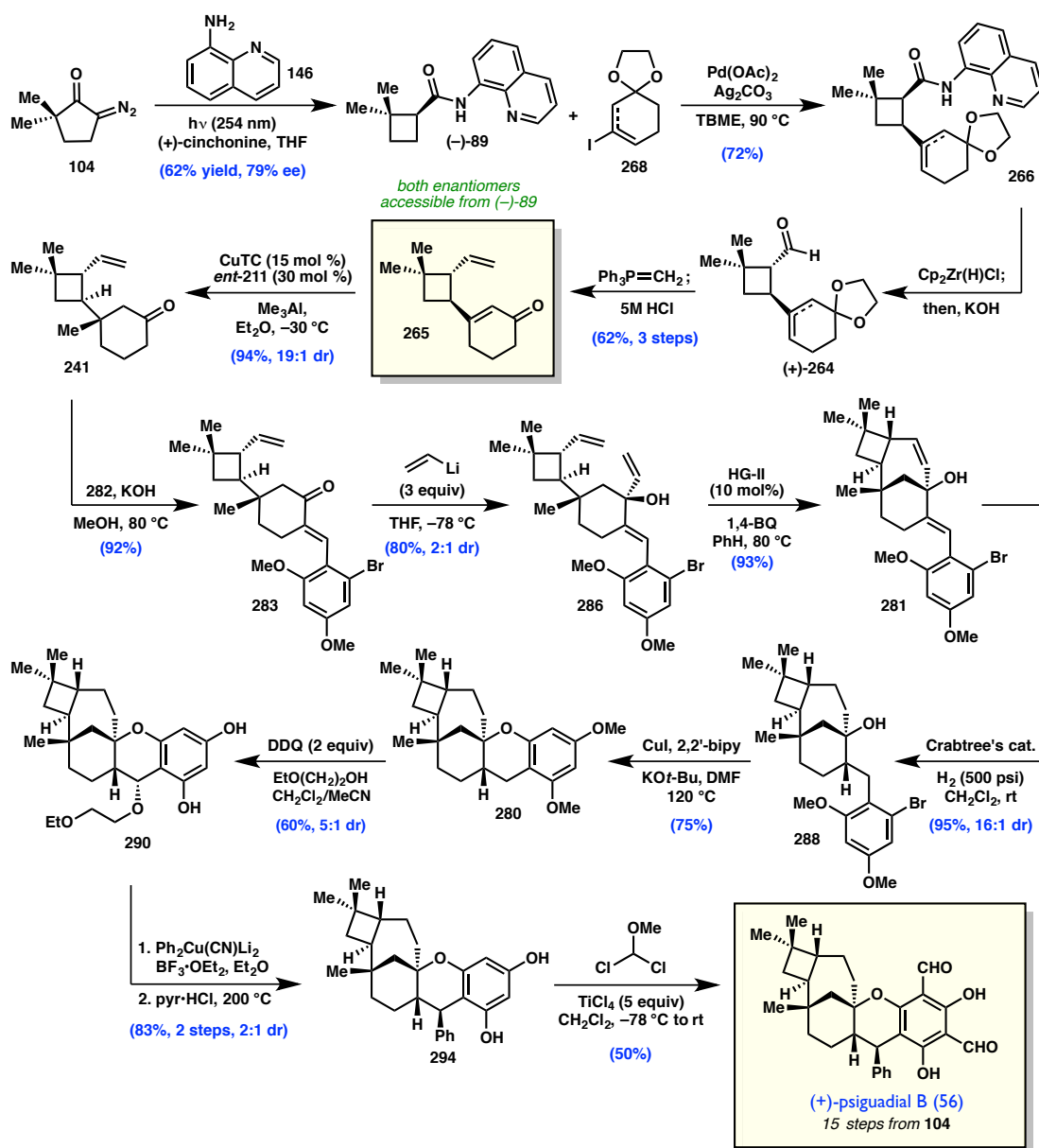
3.4 CONCLUDING REMARKS

In summary, the first enantioselective total synthesis of the cytotoxic natural product (+)-psiguadial B (**56**) has been achieved in 15 steps from diazoketone **104**.³⁵ The successful synthetic strategy was enabled by *de novo* construction of the *trans*-fused cyclobutane ring via a tandem photochemical Wolff rearrangement/asymmetric ketene addition, followed by a strategic Pd-catalyzed $\text{C}(\text{sp}^3)\text{-H}$ alkenylation reaction. Notably, both enantiomers of the natural product are accessible from a single enantiomer of organocatalyst through the development of two distinct epimerization strategies. Modification of the synthetic route facilitated the application of a *catalytic* conjugate addition reaction to secure the C1 quaternary center with excellent selectivity.

Ultimately, the strained terpene core was built via implementation of a remarkably efficient ring-closing metathesis, while the remainder of the psiguadial framework was constructed and functionalized in short order to afford the natural product in a 1.3% overall yield. We believe that the development of this expedient route to **56**

may enable the synthesis of unnatural analogs of **56** that would be difficult to access through semi-synthetic methods. To that end, several late-stage intermediates and select analogs have been prepared for the purposes of biological evaluation. Finally, efforts to expand the scope of our key reactions and apply this sequence in the synthesis of other *trans*-cyclobutane-containing natural products are currently ongoing in our laboratory.

Scheme 3.16. Overview of the final, successful route to (+)-psiguadial B



3.5 EXPERIMENTAL SECTION

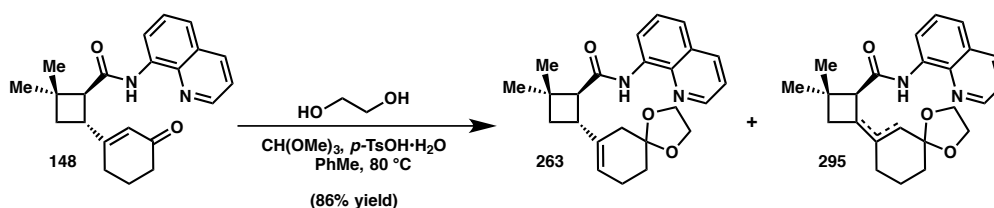
3.5.1 Materials and Methods

General Procedures. Unless otherwise stated, reactions were performed under a nitrogen atmosphere using freshly dried solvents. Tetrahydrofuran (THF), methylene chloride (CH_2Cl_2), acetonitrile (MeCN), *tert*-butyl methyl ether (TBME), benzene (PhH), and toluene (PhMe) were dried by passing through activated alumina columns. Triethylamine (Et_3N), *N,N*-diisopropylethylamine (DIPEA), and methanol (MeOH) were distilled over calcium hydride prior to use. Unless otherwise stated, chemicals and reagents were used as received. All reactions were monitored by thin-layer chromatography using EMD/Merck silica gel 60 F254 pre-coated plates (0.25 mm) and were visualized by UV, *p*-anisaldehyde, or 2,4-dinitrophenylhydrazine staining. Flash column chromatography was performed either as described by Still et al.³⁶ using silica gel (particle size 0.032-0.063) purchased from Silicycle or using pre-packaged RediSep[®] Rf columns on a CombiFlash Rf system (Teledyne ISCO Inc.). Optical rotations were measured on a Jasco P-2000 polarimeter using a 100 mm path-length cell at 589 nm. ^1H and ^{13}C NMR spectra were recorded on a Bruker Avance III HD with Prodigy cryoprobe (at 400 MHz and 101 MHz respectively), a Varian 400 MR (at 400 MHz and 101 MHz, respectively), a Varian Inova 500 (at 500 MHz and 126 MHz, respectively), or a Varian Inova 600 (at 600 MHz and 150 MHz, respectively), and are reported relative to internal CHCl_3 (^1H , δ = 7.26) and CDCl_3 (^{13}C , δ = 77.1), or C_6H_5 (^1H , δ = 7.16) and C_6D_6 (^{13}C , δ = 128). Data for ^1H NMR spectra are reported as follows: chemical shift (δ ppm) (multiplicity, coupling constant (Hz), integration). Multiplicity and qualifier abbreviations are as follows: s = singlet, d = doublet, t = triplet, q = quartet, m =

multiplet, br = broad, app = apparent. IR spectra were recorded on a Perkin Elmer Paragon 1000 spectrometer and are reported in frequency of absorption (cm^{-1}). HRMS were acquired using an Agilent 6200 Series TOF with an Agilent G1978A Multimode source in electrospray ionization (ESI), or mixed (MM) ionization mode, or obtained from the Caltech Mass Spectral Facility in fast-atom bombardment mode (FAB).

3.5.2 Preparative Procedures and Spectroscopic Data

Preparation of dioxolanes **263** and **295**.



To a flame-dried 200 mL round-bottom flask was added *trans*-cyclobutane **148** (2.59 g, 7.43 mmol) and the atmosphere was exchanged for N_2 three times. Dry PhMe (74 mL) was then added, followed by ethylene glycol (16.6 mL, 297 mmol, 40.0 equiv) and trimethyl orthoformate (2.44 mL, 22.3 mmol, 3.00 equiv) via syringe. Finally, *p*-toluenesulfonic acid monohydrate (141 mg, 0.743 mmol, 0.10 equiv) was added as a solid in one portion under a stream of N_2 . The reaction mixture was heated to 80°C for 15 hours, at which point the reaction mixture was cooled to room temperature and quenched with a saturated solution of aqueous NaHCO_3 . The layers were separated and the aqueous layer was extracted with EtOAc three times. The combined organic extracts were dried over anhydrous MgSO_4 , filtered, and concentrated *in vacuo*. The crude residue was purified by silica gel flash chromatography (isocratic: 20% EtOAc/hexane + 1%

Et₃N) to afford dioxolanes **263** and **295** (2.50 g, 86% yield) as a partially separable mixture of inconsequential olefin isomers. An analytically pure sample of the major dioxlane (**263**) was obtained and a representative spectrum of the mixture as used in the next step is also provided.

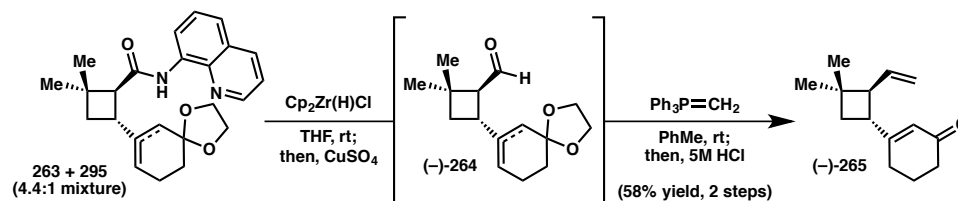
Data for **263** (major product, peak 1): $[\alpha]_D^{25.0} = -80.5^\circ$ (c = 1.40, CHCl₃)

¹H NMR (400 MHz, CDCl₃) δ 9.71 (s, 1H), 8.78 (dd, *J* = 11.0, 1.6 Hz, 1H), 8.78 (d, *J* = 1.6 Hz, 1H), 8.14 (dd, *J* = 8.3, 1.7 Hz, 1H), 7.50 (dt, *J* = 15.8, 8.2, 7.5 Hz, 2H), 7.47 (dd, *J* = 8.3, 1.6 Hz, 1H), 7.43 (dd, *J* = 8.3, 4.2 Hz, 1H), 5.54 (dt, *J* = 3.6, 1.8 Hz, 1H), 3.96 (q, *J* = 4.4, 3.9 Hz, 4H), 3.30 (q, *J* = 9.4 Hz, 1H), 2.88 (d, *J* = 9.8 Hz, 1H), 2.25 (d, *J* = 2.8 Hz, 4H), 1.87 (dd, *J* = 10.5, 8.6 Hz, 1H), 1.81 – 1.61 (m, 3H), 1.36 (s, 3H), 1.17 (s, 3H).

¹³C NMR (101 MHz, CDCl₃) δ 170.7, 148.2, 138.4, 137.3, 136.3, 134.6, 127.9, 127.4, 121.6, 121.2, 119.1, 116.3, 108.4, 64.4, 55.2, 36.7, 36.7, 36.4, 36.1, 30.9, 30.8, 24.1, 23.4.

FTIR (NaCl, thin film) 3350, 3046, 2952, 2929, 2893, 2839, 1686, 1596, 1578, 1525, 1485, 1460, 1424, 1383, 1368, 1326, 1248, 1209, 1161, 1102, 1059, 1021, 948, 826, 792, 756 cm.⁻¹

HRMS (MM) calc'd for C₂₄H₂₉N₂O₃ [M+H]⁺ 393.2173, found 393.2188.

Preparation of vinyl enone (–)-265.

Inside a N_2 -filled glovebox, two flame-dried 200 mL round-bottom flasks were each charged with Schwartz's reagent (1.60 g, 6.21 mmol, 2.04 equiv) and sealed under N_2 . The flasks were removed from the glovebox and THF (15.5 mL) was added to each via syringe. To each of the milky-white suspensions was added a mixture of dioxolanes **263** and **295** (1.19 g, 3.04 mmol) as a solution in THF (16.0 mL) in a quick drip at room temperature. The mixtures immediately began to turn yellow, darkening to orange over the course of 1 hour, at which point the reactions were quenched with saturated aqueous NaHCO_3 and combined together. The layers were separated and the aqueous layer was extracted twice with EtOAc. The combined organic layers were washed twice with 100 mL of a 0.6M aqueous solution of CuSO_4 to remove the liberated 8-aminoquinoline. The organic layer was then dried over MgSO_4 , filtered, and concentrated *in vacuo*. The crude aldehyde (**264**, 1.70 g) was dissolved in dry PhMe (20 mL) and treated with freshly prepared ylide (80 mL, 32.0 mmol, 5.26 equiv) at room temperature. The reaction was stirred for 2 hours and monitored by TLC. Upon complete conversion, the reaction was cooled to 0 °C and quenched with 5 M HCl. The layers were separated and the aqueous layer was extracted twice with Et_2O . The combined organic layers were concentrated *in vacuo* and the solvent replaced with THF (30 mL). The dioxolane was hydrolyzed by stirring vigorously with 5 M HCl for 8 hours, at which time Et_2O was added and the

layers separated. The aqueous layer was extracted twice with Et₂O and the combined organics washed with aqueous NaHCO₃, dried over MgSO₄ and concentrated *in vacuo*. The crude residue was purified by silica gel flash chromatography (isocratic: 30% Et₂O/hexanes) to afford vinyl enone (–)-**265** (715 mg, 58% yield over 2 steps) as a clear oil: $[\alpha]_D^{25.0} = -100^\circ$ (c = 1.02, CHCl₃).

¹H NMR (400 MHz, CDCl₃) δ 5.84 (q, *J* = 1.5 Hz, 1H), 5.81 (dddt, *J* = 16.8, 10.6, 7.9, 0.5, 0.5 Hz, 1H), 5.04 (qd, *J* = 1.9, 1.0 Hz, 1H), 5.01 (ddd, *J* = 10.4, 2.0, 1.1 Hz, 1H), 2.88 (q, *J* = 9.7, 9.1, 9.0 Hz, 1H), 2.48 (ddq, *J* = 9.8, 7.9, 1.0 Hz, 1H), 2.34 (t, *J* = 7.0, 6.5 Hz, 2H), 2.21 (qdd, *J* = 5.9, 1.5, 0.8 Hz, 2H), 1.95 (dt, *J* = 7.7, 6.1 Hz, 2H), 1.85 (ddd, *J* = 10.7, 8.3, 0.8 Hz, 1H), 1.67 (t, *J* = 10.4 Hz, 1H), 1.05 (s, 3H), 1.04 (s, 3H).

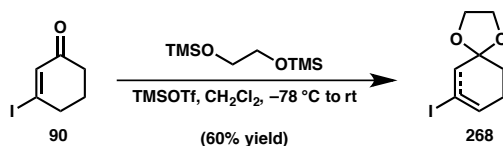
¹³C NMR (101 MHz, CDCl₃) δ 200.1, 168.7, 137.4, 123.4, 116.1, 53.8, 41.1, 37.5, 37.3, 36.0, 30.0, 27.9, 23.1, 22.6.

FTIR (NaCl, thin film) 3320, 3076, 3039, 2953, 2934, 2891, 2866, 2827, 1671, 1622, 1456, 1428, 1417, 1382, 1368, 1346, 1324, 1290, 1251, 1191, 1124, 995, 968, 942, 912, 886, 755 cm.⁻¹

HRMS (MM) calc'd for C₁₄H₂₁O [M+H]⁺ 205.1587, found 205.1587.

Preparation of Wittig ylide.

Inside a N₂-filled glovebox, methyltriphenylphosphonium bromide (22.2 g, 62.1 mmol) and KO^t-Bu (7.36 g, 65.6 mmol, 1.06 equiv) were added to a flame-dried 500 mL round-bottom flask and sealed under nitrogen. The flask was brought out of the box and dry PhMe (155 mL) was added via syringe. The flask was fitted with a reflux condenser under a stream of N₂ and heated to 110 °C for 4 hours, at which time the reaction was cooled to room temperature and the salts were allowed to settle for 3 hours before the bright yellow supernatant (~0.40 M salt-free ylide) was used for the methylenation of crude *trans*-aldehyde **264**.

Preparation of protected iodide **268.**

Inside a N₂-filled glove box, a 250 mL round bottom flask was charged with TMSOTf (0.410 mL, 0.230 mmol, 0.010 equiv) and CH₂Cl₂ (20.0 mL). The flask was sealed, removed from the glove box, and placed under a N₂ atmosphere. The reaction mixture was cooled to –78 °C, and 1,2-bis(trimethylsilyloxy)ethane (11.0 mL, 45.0 mmol, 2.00 equiv) was added via syringe. (Note: best results were obtained when 1,2-bis(trimethylsilyloxy)ethane was sparged with argon for 30 min prior to addition). Vinyl iodide **90** (5.00 g, 22.5 mmol, 1.00 equiv) was added to the flask dropwise as a solution in CH₂Cl₂ (20.0 mL), via cannula transfer. An additional portion of CH₂Cl₂ (5.00 mL) was used to complete the transfer. The colorless reaction mixture was allowed to stir at –

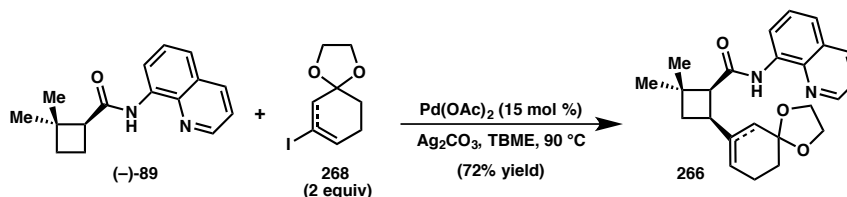
78 °C for 1 hour, at which point the reaction mixture was warmed to 0 °C. The reaction mixture became yellow immediately upon warming and was allowed to warm to room temperature over 16 hours. The reaction mixture became dark orange and was quenched with the addition of DIPEA (11.0 mL), at which point the reaction became yellow. The mixture was poured into a separatory funnel and diluted with saturated NaHCO₃ solution. The aqueous layer was extracted three times with CH₂Cl₂. The organic layers were combined, dried over a 1:1 mixture of anhydrous K₂CO₃ and Na₂SO₄, filtered, and concentrated to provide a yellow residue that was purified by flash silica gel chromatography (5% EtOAc, 1% Et₃N/hexane–20% EtOAc, 1% Et₃N/hexane) to provide **268** (3.61 g, 60% yield) as a 8:1 mixture of olefin isomers, as a pale yellow oil.

¹H NMR (400 MHz, CDCl₃) δ 6.34 (tt, *J* = 4.0, 1.9 Hz, 1H), 3.98 (p, *J* = 1.7 Hz, 4H), 2.72 (q, *J* = 2.3 Hz, 2H), 2.36 – 2.22 (m, 2H), 1.77 (t, *J* = 6.5 Hz, 2H).

¹³C NMR (101 MHz, CDCl₃) δ 136.6, 108.1, 91.1, 64.7, 49.3, 30.2, 27.5.

FTIR (NaCl, thin film) 3040, 2955, 2934, 2881, 2836, 2684, 1637, 1474, 1443, 1429, 1418, 1360, 1330, 1300, 1243, 1207, 1142, 1114, 1076, 1058, 1021, 970, 948, 889, 848, 827, 776, 738, 662 cm.⁻¹

HRMS (FAB) calc'd for C₈H₁₁IO₂ [M]⁺ 266.9876, found 266.9888.

Preparation of *cis*-dioxolane **266.**

A 100 mL, thick-walled pressure vessel was charged with Pd(OAc)₂ (132 mg, 0.590 mmol, 0.150 equiv), Ag₂CO₃ (1.08 g, 3.93 mmol, 1.00 equiv), and **89** (1.00 g, 3.93 mmol, 1.00 equiv). Vinyl iodide **268** (2.09 g, 7.86 mmol, 2.00 equiv) was then added to the flask as a solution in TBME (19.7 mL). The reaction vessel was sealed with a screw top under ambient conditions and heated to 90 °C in an oil bath. The heterogeneous reaction mixture is olive green upon addition of vinyl iodide. After heating for five minutes, the reaction mixture became black. After 16 hours, the flask was removed from the oil bath and allowed to cool to room temperature. The reaction mixture was filtered over a pad of celite and the filter cake was washed with CH₂Cl₂. The filtrate was concentrated, and the crude orange residue was purified by flash silica gel chromatography (30% EtOAc, 1% Et₃N/hexane–35% EtOAc, + 1% Et₃N/hexane) to provide **266** (1.11 g, 72% yield) as a white foam: $[\alpha]_D^{25.0} = -29.3^\circ$ (*c* = 1.95, CHCl₃).

¹H NMR (400 MHz, CDCl₃) δ 9.87 (s, 1H), 8.81 (ddd, *J* = 24.2, 7.3, 1.5 Hz, 2H), 8.13 (dd, *J* = 8.3, 1.7 Hz, 1H), 7.49 (td, *J* = 8.2, 7.5, 6.6 Hz, 1H), 7.45 (dd, *J* = 8.3, 1.6 Hz, 1H), 7.42 (dd, *J* = 8.3, 4.2 Hz, 1H), 5.65 (dd, *J* = 17.8, 9.1 Hz, 1H), 4.03 – 3.81 (m, 2H), 3.76 – 3.64 (m, 2H), 3.25 (q, *J* = 9.1, 8.2 Hz, 1H), 3.05 (dd, *J* = 8.7, 2.8 Hz, 1H), 2.46 (t, *J* = 10.9 Hz, 1H), 2.40 – 2.23 (m, 2H), 2.19 (dt, *J* = 16.5, 2.1 Hz, 1H), 2.06 – 1.97 (m,

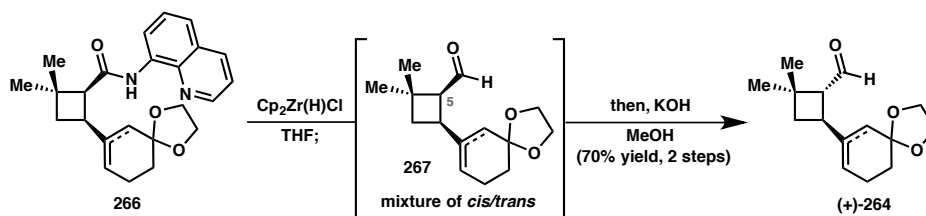
1H), 1.93 (ddd, $J = 11.1, 8.3, 2.9$ Hz, 1H), 1.71 – 1.59 (m, 1H), 1.57 – 1.48 (m, 1H), 1.40 (s, 3H), 1.11 (s, 3H).

^{13}C NMR (101 MHz, CDCl_3) δ 171.0, 147.9, 138.7, 136.3, 134.9, 134.8, 127.9, 127.5, 121.4, 121.2, 120.8, 116.6, 108.3, 64.3, 64.1, 55.9, 37.2, 37.1, 36.7, 35.4, 30.8, 30.2, 25.1, 24.4.

FTIR (NaCl, thin film) 3357, 3300, 3043, 3006, 2952, 2928, 2881, 1685, 1664, 1596, 1577, 1523, 1485, 1460, 1424, 1385, 1324, 1255, 1208, 1160, 1132, 1106, 1060, 1039, 1020, 947, 846, 826, 792, 755, 666 cm^{-1} .

HRMS (MM) calc'd for $\text{C}_{24}\text{H}_{29}\text{N}_2\text{O}_3$ $[\text{M}+\text{H}]^+$ 393.2173, found 393.2183.

Preparation of *trans*-aldehyde (+)-264.



Inside a N_2 -filled glove box, a 250 mL round bottom flask was charged with Schwartz's reagent (2.30 g, 8.92 mmol, 2.06 equiv) and THF (22.3 mL). *Cis*-dioxolane **266** (1.70 g, 4.32 mmol, 1.00 equiv) was added to the flask as a solution in THF (22.3 mL). The flask was sealed, removed from the glove box and put under a N_2 atmosphere. The flask was covered with aluminum foil and allowed to stir for one hour, at which point the reaction was quenched with the addition of saturated NaHCO_3 solution. (Note: it is important that the quench be conducted very quickly to avoid decomposition of

excess Schwartz's reagent and formation of HCl). The reaction mixture was diluted with EtOAc and the organic layer separated. The aqueous layer was filtered through a pad of celite and sand and then extracted 5x with EtOAc. The combined organics were dried over anhydrous Na₂SO₄, filtered, and concentrated to provide a yellow residue that was purified by flash silica gel chromatography (15% EtOAc, 1% Et₃N/hexanes) to provide **267** (755 mg, 3.01 mmol) as a yellow oil as a 1.8:1 (*cis/trans*) mixture of diastereomers at C5. The oil was concentrated directly into a 200 mL round bottom flask and dissolved in wet MeOH (60.0 mL). The flask was then charged with KOH (3.36 g, 59.9 mmol, 20.0 equiv) and the mixture allowed to stir for 1 hour at room temperature. The mixture was then concentrated to a volume of ~3 mL and diluted with pH 7 buffer. A pale yellow precipitate formed upon addition of buffer. The solution was slowly acidified using dilute citric acid until pH 7 was achieved. The mixture was then poured into a separatory funnel and extracted 3x with EtOAc. The combined organics were dried over anhydrous Na₂SO₄, filtered, and concentrated to provide *trans*-aldehyde (+)-**264** (755 mg, 70% over 2 steps) as a mixture of olefin isomers. The yellow oil was analytically pure and used directly in the next step: $[\alpha]_D^{25.0} = +35.2^\circ$ ($c = 0.295$, CHCl₃). Note: it is recommended that the aldehyde be used immediately in the next step to avoid decomposition.

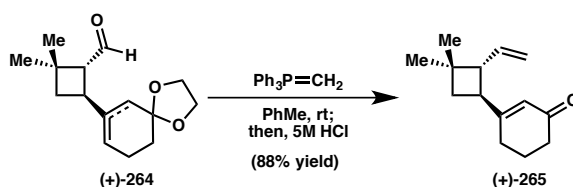
¹H NMR (400 MHz, CDCl₃) δ 9.76 (t, $J = 2.2$ Hz, 1H), 5.37 (dt, $J = 3.8, 1.9$ Hz, 1H), 3.97 (dd, $J = 2.5, 1.3$ Hz, 4H), 3.14 (q, $J = 9.2$ Hz, 1H), 2.73 (dt, $J = 10.0, 2.1$ Hz, 1H), 2.22 (dp, $J = 6.5, 2.1$ Hz, 2H), 2.16 – 1.97 (m, 2H), 1.77 (ddd, $J = 15.5, 9.4, 2.0$ Hz, 2H), 1.69 (td, $J = 6.5, 2.1$ Hz, 2H), 1.24 (s, 3H), 1.14 (s, 3H).

^{13}C NMR (101 MHz, CDCl_3) δ 203.2, 137.1, 118.8, 108.3, 64.4, 59.5, 37.3, 37.1, 36.7, 34.3, 31.2, 30.7, 24.0, 24.0.

FTIR (NaCl, thin film) 2954, 2929, 2896, 2873, 2707, 1712, 1670, 1577, 1522, 1461, 1449, 1434, 1420, 1383, 1367, 1340, 1312, 1297, 1249, 1209, 1179, 1103, 1059, 1039, 1018, 948, 846, 793 cm^{-1} .

HRMS (MM) calc'd for $\text{C}_{15}\text{H}_{23}\text{O}_3$ $[\text{M}+\text{H}]^+$ 251.1642, found 251.1645.

Preparation of vinyl enone (+)-265



A 250 mL round bottom flask was charged with aldehyde, (+)-**264** (720 mg, 2.88 mmol, 1.00 equiv). The flask was evacuated and backfilled three times with N_2 and charged with toluene (2.30 mL). The flask was then charged with freshly prepared ylide solution³⁷ (36.0 mL, 0.4 M, 5.00 equiv) and the reaction mixture was allowed to stir for 30 minutes at room temperature. The reaction was quenched with the addition of saturated NaHCO_3 solution (10.0 mL). The organic layer was separated and the aqueous layer extracted 3x with Et_2O . The combined organics were concentrated and dissolved in a 1:1 mixture of THF and 5 M HCl (28 mL.0). The reaction mixture was allowed to stir over 16 hours, at which point the mixture was diluted with Et_2O and water. The layers were separated and the aqueous layer extracted 3x with Et_2O . The combined organics were dried over anhydrous MgSO_4 , filtered, and concentrated. The crude yellow residue

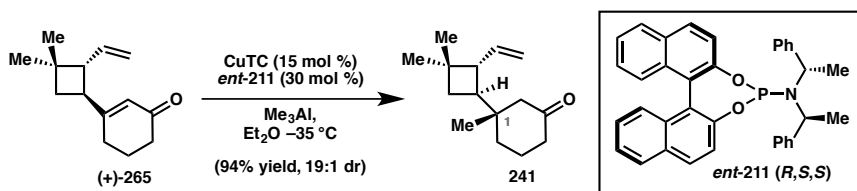
was purified by flash silica gel chromatography (20–30% Et₂O/pentane) to provide (+)-**265** (520 mg, 88%) as a pale yellow oil: $[\alpha]_D^{25.0} = +102^\circ$ (c = 0.705, CHCl₃).

¹H NMR (400 MHz, CDCl₃) δ 5.84 (q, *J* = 1.6 Hz, 1H), 5.81 (dddt, *J* = 16.8, 10.6, 7.9, 0.5, 0.5 Hz, 1H), 5.04 (qd, *J* = 1.9, 1.0 Hz, 1H), 5.01 (ddd, *J* = 10.8, 1.9, 1.1 Hz, 1H), 2.88 (q, *J* = 9.7, 9.1, 9.0 Hz, 1H), 2.48 (ddq, *J* = 9.8, 7.9, 1.0 Hz, 1H), 2.34 (t, *J* = 7.0, 6.5 Hz, 2H), 2.20 (qdd, *J* = 6.0, 1.5, 0.8 Hz, 2H), 1.95 (dt, *J* = 7.7, 6.1 Hz, 2H), 1.85 (ddd, *J* = 10.8, 8.3, 0.8 Hz, 1H), 1.67 (t, *J* = 10.3 Hz, 1H), 1.05 (s, 3H), 1.04 (s, 3H).

¹³C NMR (101 MHz, CDCl₃) δ 200.1, 168.8, 137.4, 123.4, 116.1, 53.8, 41.1, 37.5, 37.3, 36.0, 30.0, 27.9, 23.1, 22.6.

FTIR (NaCl, thin film) 3320, 3076, 3039, 2953, 2934, 2891, 2866, 2827, 1671, 1622, 1456, 1428, 1417, 1382, 1368, 1346, 1324, 1290, 1251, 1191, 1124, 995, 968, 942, 912, 886, 755 cm.⁻¹

HRMS (MM) calc'd for C₁₄H₂₁O [M+H]⁺ 205.1587, found 205.1587.

Preparation of vinyl ketone 241.

Inside a N₂-filled glovebox, CuTC (105 mg, 0.551 mmol, 0.150 equiv) and (*R,S,S*)-ligand *ent*-**211**³⁸ (594 mg, 1.10 mmol, 0.30 equiv) were added to a flame dried 100 mL round-bottom flask. The reagents were suspended in Et₂O (18.0 mL) and stirred at room temperature for 30 minutes before vinyl enone (+)-**265** (750 mg, 3.67 mmol) was added as a solution in Et₂O (18.0 mL). The reaction was sealed under N₂, removed from the glovebox and placed under a balloon atmosphere of argon. The reaction mixture was allowed to equilibrate to -35 °C for 5 minutes using a cryocool unit to maintain the temperature. Me₃Al (2.0 M in heptane; 3.67 mL, 7.34 mmol, 2.00 equiv) was then added dropwise and the reaction stirred at -35 °C for 17 hours, at which point wet MeOH (5 mL) was slowly added to quench excess Me₃Al. The mixture was warmed to room temperature, filtered over a plug of silica gel and washed thoroughly with Et₂O and CH₂Cl₂ (until no product remained in eluent). The filtrate was concentrated *in vacuo* and the crude residue purified by silica gel flash chromatography (isocratic: 20% hexane/CH₂Cl₂) to afford vinyl ketone **241** (760 mg, 94% yield) as a 19:1 mixture of inseparable diastereomers at C1, colorless oil. Note: this 19:1 mixture is carried through the next three reactions, and a single diastereomer at C1 is isolable after the ring-closing metathesis: $[\alpha]_D^{25.0} = +37.6^\circ$ ($c = 1.05$, CHCl₃).

¹H NMR (400 MHz, C₆D₆) δ 5.68 (ddd, *J* = 16.9, 10.5, 8.6 Hz, 1H), 4.96 (qd, *J* = 2.2, 0.8 Hz, 1H), 4.93 (ddd, *J* = 11.3, 2.2, 0.8 Hz, 1H), 2.20 (ddt, *J* = 9.6, 8.6, 0.9 Hz, 1H), 2.11 (dt, *J* = 13.9, 4.8, 1.4 Hz, 1H), 1.92 (dd, *J* = 3.3, 1.7 Hz, 2H), 1.90 – 1.79 (m, 2H), 1.50 – 1.40 (m, 2H), 1.31 – 1.21 (m, 2H), 1.21 – 1.13 (m, 1H), 0.99 (dt, *J* = 13.4, 4.7, 4.5, 1.5, 1.1 Hz, 1H), 0.94 (s, 3H), 0.93 (s, 3H), 0.66 (s, 3H).

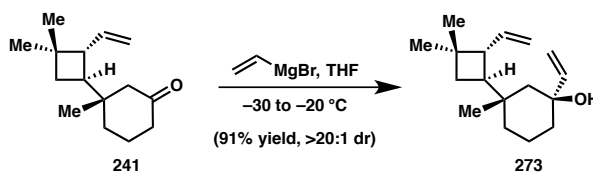
¹H NMR (400 MHz, CDCl₃) δ 5.74 (ddd, *J* = 17.1, 10.3, 8.7 Hz, 1H), 5.08 – 4.81 (m, 2H), 2.33 (ddd, *J* = 9.6, 8.7, 0.9 Hz, 1H), 2.30 – 2.19 (m, 2H), 2.16 (d, *J* = 13.5 Hz, 1H), 2.07 (td, *J* = 10.1, 8.5 Hz, 1H), 1.99 (dt, *J* = 13.4, 1.8 Hz, 1H), 1.90 (ddq, *J* = 14.0, 6.2, 4.7 Hz, 1H), 1.85 – 1.72 (m, 1H), 1.56 (ddd, *J* = 13.6, 11.1, 4.4 Hz, 1H), 1.51 – 1.34 (m, 3H), 0.98 (s, 3H), 0.97 (s, 3H), 0.83 (s, 3H).

¹³C NMR (101 MHz, CDCl₃) δ 212.8, 139.6, 115.3, 51.2, 49.5, 45.2, 41.3, 40.1, 34.8, 34.0, 33.0, 30.1, 23.7, 22.1, 21.8.

¹³C NMR (101 MHz, C₆D₆) δ 209.3, 139.9, 115.3, 51.0, 49.5, 45.2, 41.2, 39.7, 34.7, 33.9, 32.9, 30.1, 23.7, 22.1, 21.8.

FTIR (NaCl, thin film) 3075, 2953, 2873, 1713, 1633, 1460, 1422, 1382, 1368, 1312, 1285, 1253, 1228, 1172, 1049, 995, 910 cm.⁻¹

HRMS (FAB) calc'd for C₁₅H₂₄O [M]⁺ 221.1900, found 221.1897.

Preparation of divinyl alcohol 273.

To a 15 mL round-bottom flask was added vinyl ketone **241** (91.0 mg, 0.413 mmol) and the atmosphere was exchanged 3x for N₂. Dry THF (4.10 mL) was then added via syringe and the reaction cooled to –30 °C using a closely monitored acetone/CO₂ bath. Vinylmagnesium bromide (2.06 mL, 1.0 M in THF, 2.06 mmol, 5.00 equiv) was then added dropwise. The reaction was maintained at –30 °C for 30 minutes, then quenched at that temperature with saturated aqueous NaH₂PO₄. The reaction mixture was diluted with Et₂O and the layers separated. The aqueous layer was extracted with Et₂O (2 x 5 mL) and the combined organics were dried over Mg₂SO₄, filtered, and concentrated *in vacuo*. The crude residue was purified by silica gel flash chromatography (10% EtOAc/hexane) to afford **273** (92.7 mg, 91% yield) as a colorless oil: $[\alpha]_D^{25.0} = +54.4^\circ$ (c = 1.75, CHCl₃).

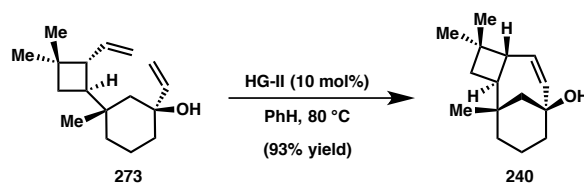
¹H NMR (400 MHz, CDCl₃) δ 5.88 (dd, *J* = 17.3, 10.6 Hz, 1H), 5.75 (ddd, *J* = 17.1, 10.2, 8.7 Hz, 1H), 5.18 (dd, *J* = 17.3, 1.3 Hz, 1H), 5.01 – 4.85 (m, 3H), 2.32 (t, *J* = 9.3 Hz, 1H), 1.92 (q, *J* = 9.6 Hz, 1H), 1.82 (qt, *J* = 13.5, 3.4 Hz, 1H), 1.55 (dddd, *J* = 14.0, 5.3, 3.5, 1.9 Hz, 1H), 1.48 (dq, *J* = 13.8, 3.5 Hz, 1H), 1.45 – 1.39 (m, 2H), 1.35 (dd, *J* = 13.5, 4.0 Hz, 1H), 1.31 – 1.22 (m, 3H), 1.16 – 1.11 (m, 1H), 1.11 (s, 1H), 1.06 (s, 3H), 0.97 (s, 3H), 0.97 (s, 3H).

^{13}C NMR (101 MHz, CDCl_3) δ 148.1, 140.6, 114.6, 110.5, 73.1, 49.0, 48.0, 45.0, 37.6, 34.6, 34.3, 33.9, 32.8, 30.1, 23.8, 22.7, 17.8.

FTIR (NaCl, thin film) 3601, 3452 (br), 3077, 2996, 2950, 2932, 2865, 1635, 1459, 1441, 1413, 1380, 1367, 1343, 1291, 1275, 1250, 1200, 1170, 1081, 1058, 994, 974, 909, 858, 846, 666 cm^{-1} .

HRMS (ESI) calc'd for $\text{C}_{17}\text{H}_{27}$ $[\text{M}-\text{OH}]^+$ 231.2107, found 231.2101.

Preparation of allylic alcohol **240**.



A 50 mL round-bottom flask containing divinyl alcohol **273** (88.0 mg, 0.355 mmol) was pumped into a N_2 -filled glovebox where Hoveyda–Grubbs second-generation catalyst (22.2 mg, 0.035 mmol, 0.100 equiv) was added. The flask was sealed under nitrogen, removed from the glovebox and dry benzene (17.7 mL) was added via syringe. The green reaction mixture was heated to 80 $^\circ\text{C}$ for 3.5 hours, then cooled to room temperature. Ethyl vinyl ether was added to inactivate the catalyst and stirred for 15 minutes before the reaction mixture was concentrated *in vacuo*. The crude residue was purified by silica gel flash chromatography (isocratic: 30% Et_2O /hexane) to afford allylic alcohol **240** (72.5 mg, 93% yield) as a pale yellow oil and a single diastereomer at C1: $[\alpha]_D^{25.0} = -62.9^\circ$ ($c = 2.67$, CHCl_3).

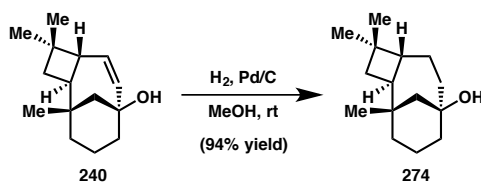
¹H NMR (400 MHz, CDCl₃) δ 5.84 (dd, *J* = 10.9, 2.5 Hz, 1H), 5.15 (ddd, *J* = 11.0, 2.9, 2.2 Hz, 1H), 2.41 (dt, *J* = 11.6, 2.7 Hz, 1H), 2.09 (td, *J* = 11.5, 10.7, 7.9 Hz, 2H), 1.69 (ddd, *J* = 13.0, 3.2, 1.1 Hz, 1H), 1.64 (s, 1H), 1.63 – 1.56 (m, 2H), 1.54 – 1.41 (m, 2H), 1.34 – 1.25 (m, 2H), 1.15 (dd, *J* = 12.8, 2.2 Hz, 1H), 1.12 – 1.06 (m, 1H), 1.05 (s, 3H), 1.03 (s, 3H), 0.87 (s, 3H).

¹³C NMR (101 MHz, CDCl₃) δ 134.1, 132.5, 75.1, 49.9, 45.3, 43.9, 39.0, 38.1, 37.8, 35.0, 32.6, 30.9, 26.9, 21.3, 20.2.

FTIR (NaCl, thin film) 3350 (br), 3004, 2948, 2930, 2866, 1460, 1443, 1369, 1380, 1366, 1329, 1270, 1256, 1238, 1175, 1106, 1044, 1030, 999, 973, 958, 925, 875, 864, 766, 723 cm.⁻¹

HRMS (MM) calc'd for C₁₅H₂₃ [M–OH]⁺ 203.1794, found 203.1790.

Preparation of tertiary alcohol **274**.



To a 100 mL round-bottom flask were added allylic alcohol **240** (107 mg, 0.486 mmol) and Pd/C (103 mg, 10% by weight, 0.097 mmol, 0.200 equiv). The flask was fitted with a septum and the atmosphere exchanged 1x for N₂. MeOH (9.7 mL) was then added via syringe and the reaction placed under a balloon atmosphere of H₂ (purged through a needle for 30 seconds). The reaction was stirred vigorously at room temperature for 2.5 hours, at which time the atmosphere was purged with argon. The

reaction mixture was filtered over celite, washed thoroughly with Et₂O, and the filtrate concentrated in vacuo. The crude residue was purified by silica gel flash chromatography (isocratic: 40% Et₂O/pentane) to afford **274** (101 mg, 94% yield) as a colorless oil: $[\alpha]_D^{25.0} = +6.37^\circ$ ($c = 0.800$, CHCl₃).

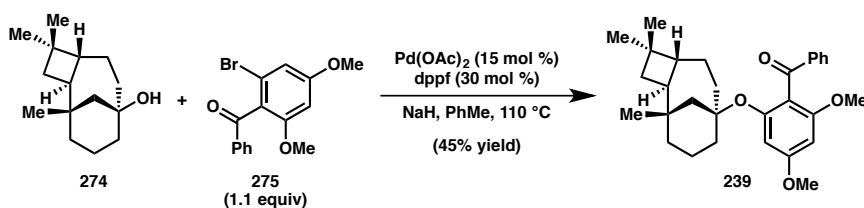
¹H NMR (400 MHz, CDCl₃) δ 1.97 (ddd, $J = 11.8, 10.7, 7.9$ Hz, 1H), 1.86 – 1.78 (m, 1H), 1.78 – 1.68 (m, 3H), 1.67 (d, $J = 0.8$ Hz, 3H), 1.51 – 1.39 (m, 2H), 1.34 (dt, $J = 3.5, 2.0$ Hz, 1H), 1.33 – 1.22 (m, 4H), 1.15 – 1.04 (m, 1H), 1.02 (d, $J = 12.8$ Hz, 1H), 0.97 (s, 3H), 0.96 (s, 3H), 0.80 (s, 3H).

¹³C NMR (101 MHz, CDCl₃) δ 74.0, 50.2, 46.3, 40.3, 40.1, 39.7, 38.2, 36.4, 34.6, 32.8, 30.7, 27.1, 22.7, 20.9, 20.7.

FTIR (NaCl, thin film) 3368 (br), 2948, 2927, 2863, 1460, 1443, 1384, 1364, 1332, 1288, 1249, 1217, 1183, 1124, 1102, 1050, 1022, 993, 976, 936, 918, 873, 862 cm.⁻¹

HRMS (ESI) calc'd for C₁₅H₂₅ [M–OH]⁺ 205.1951, found 205.1951.

Preparation of benzophenone **239**.³⁹



Inside a N₂-filled glovebox, to a 1 dram vial containing tertiary alcohol **274** (14.4 mg, 0.065 mmol) were added Pd(OAc)₂ (4.36 mg, 0.019 mmol, 0.300 equiv), dppf (21.6 mg, 0.039 mmol, 0.600 equiv), and NaH (95%, 3.11 mg, 0.130 mmol, 2.00 equiv). PhMe

(650 μ L) was then added and the orange reaction mixture stirred at room temperature for 5 minutes before aryl bromide **275**¹⁴ (22.8 mg, 0.071 mmol, 1.10 equiv) was added as a solid in one portion. The reaction was sealed with a Teflon cap and heated to 110 °C in a preheated aluminum block inside the glovebox. After 13.5 hours, the reaction was cooled to room temperature, diluted with EtOAc and saturated aqueous Na₂HPO₄ was added. The layers were separated and the aqueous layer was extracted with EtOAc until the organic layer was colorless. The combined organics were filtered over a plug of celite and Na₂SO₄. The filtrate was concentrated *in vacuo* and the crude residue purified by silica gel flash chromatography (isocratic: 30% hexane/CH₂Cl₂ + 1% EtOAc) to afford **239** (13.4 mg, 45% yield) as a milky white gum: $[\alpha]_D^{25.0} = +1.27^\circ$ (c = 0.345, CHCl₃).

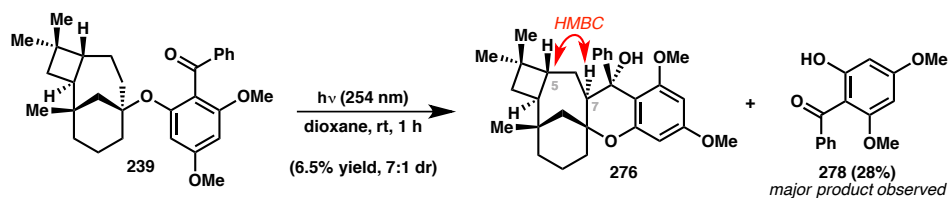
¹H NMR (400 MHz, CDCl₃) δ 7.86 – 7.76 (m, 2H), 7.51 (tt, *J* = 7.5, 2.7 Hz, 1H), 7.44 – 7.35 (m, 2H), 6.29 (d, *J* = 2.1 Hz, 1H), 6.23 (d, *J* = 2.1 Hz, 1H), 3.83 (s, 3H), 3.70 (s, 3H), 1.90 (ddd, *J* = 12.0, 10.7, 7.9 Hz, 1H), 1.78 (d, *J* = 2.3 Hz, 1H), 1.73 (t, *J* = 6.5 Hz, 2H), 1.68 (dt, *J* = 13.0, 2.3 Hz, 1H), 1.65 – 1.57 (m, 1H), 1.55 – 1.45 (m, 2H), 1.45 – 1.35 (m, 3H), 1.27 – 1.23 (m, 2H), 1.22 – 1.11 (m, 2H), 1.04 (d, *J* = 12.9 Hz, 1H), 0.92 (s, 3H), 0.91 (s, 3H), 0.69 (s, 3H).

¹³C NMR (101 MHz, CDCl₃) δ 196.0, 161.3, 158.7, 155.2, 138.8, 132.8, 129.6, 128.3, 116.8, 100.3, 92.5, 86.9, 55.9, 55.6, 47.6, 45.6, 39.7, 37.5, 36.8, 36.2, 36.1, 34.6, 32.7, 30.7, 27.1, 22.5, 20.9, 20.5.

FTIR (NaCl, thin film) 3059, 2948, 2930, 2861, 1671, 1601, 1582, 1458, 1451, 1438, 1420, 1364, 1335, 1312, 1266, 1216, 1199, 1157, 1138, 1107, 1052, 1015, 998, 948, 917, 843, 819, 802, 721, 702, 689 cm.⁻¹

HRMS (MM) calc'd for $C_{30}H_{38}NaO_4$ $[M+Na]^+$ 485.2662, found 485.2672.

Preparation of Norrish–Yang product **276**.



To a 13 x 100 quartz test tube was added benzophenone **239** (15.5 mg, 0.034 mmol). The tube was fitted with a 19/38 rubber septum and the atmosphere was exchanged 3 x for N_2 . Rigorously degassed dioxane (4.70 mL, freeze-pump-thawed 3x) was then added via syringe and the tube was sealed with electrical tape. The reaction was then placed in a bottomless test tube rack in front of a Honeywell 254 nm lamp and irradiated for 1 hour at room temperature. The reaction mixture was transferred to a cone-bottom flask and concentrated in vacuo. The crude residue was purified by preparative thin-layer chromatography (30% hexane/ CH_2Cl_2 + 1% EtOAc) to afford **278**¹⁵ (2.4 mg, 28% yield) as a white solid and **276** (1.00 mg, 6.5% yield) as a colorless oil: $[\alpha]_D^{25.0} = +13.8^\circ$ ($c = 0.050$, $CHCl_3$). Note: an additional ~18% yield of a complex mixture of products is also isolated as a single band. Although this mixture generally appears similar to **276** by 1H NMR, definitive characterization was not achieved.

1H NMR (400 MHz, $CDCl_3$) δ 7.34 – 7.26 (m, 1H), 7.24 – 7.09 (m, 4H), 6.11 (dd, $J = 2.5, 1.1$ Hz, 1H), 6.01 (dd, $J = 2.4, 1.2$ Hz, 1H), 3.95 (d, $J = 1.1$ Hz, 1H), 3.78 (d, $J = 1.2$ Hz, 3H), 3.35 (d, $J = 1.1$ Hz, 3H), 2.65 (dd, $J = 12.7, 3.5$ Hz, 1H), 2.62 – 2.52 (m, 1H), 2.40 (t, $J = 14.4$ Hz, 1H), 2.26 (q, $J = 10.4$ Hz, 1H), 2.11 – 1.90 (m, 1H), 1.86 (d, $J = 13.0$

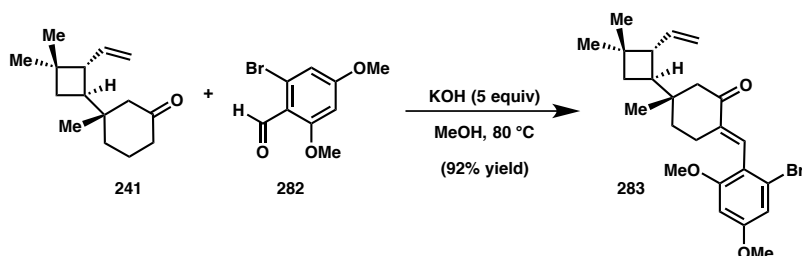
Hz, 1H), 1.83 – 1.72 (m, 1H), 1.69 – 1.57 (m, 1H), 1.43 – 1.34 (m, 2H), 1.30 – 1.09 (m, 4H), 0.80 (s, 3H), 0.78 (s, 3H), 0.75 (s, 3H), 0.50 (dt, $J = 14.5, 4.2$ Hz, 1H).

^{13}C NMR (101 MHz, CDCl_3) δ 160.5, 158.8, 154.3, 149.3, 127.4, 126.1, 125.8, 111.4, 94.2, 93.5, 80.6, 74.6, 55.6, 55.4, 48.5, 48.1, 44.0, 37.3, 36.8, 35.7, 35.5, 34.6, 33.2, 30.5, 26.4, 25.0, 20.6, 20.4.

FTIR (NaCl, thin film) 3542 (br), 3312, 3187 (br), 2960, 2924, 2854, 1738, 1726, 1710, 1666, 1614, 1592, 1492, 1462, 1453, 1445, 1423, 1376, 1366, 1351, 1332, 1261, 1215, 1203, 1150, 1112, 1045, 1020, 865, 800, 736, 702, 664 cm^{-1} .

HRMS (MM) calc'd for $\text{C}_{30}\text{H}_{37}\text{O}_3$ $[\text{M}-\text{OH}]^+$ 445.2737, found 445.2729.

Preparation of *exo*-enone **283**.



To a 200 mL round-bottom flask were added vinyl ketone **241** (884 mg, 4.01 mmol), aryl aldehyde **282**¹⁶ (1.08 g, 4.41 mmol, 1.10 equiv), and KOH (1.13 g, 20.1 mmol, 5.00 equiv). Freshly distilled MeOH (40.1 mL) was then added, the flask fitted with a reflux condenser under ambient conditions and heated to 80 °C for 12 hours. At completion, the volume of MeOH was reduced *in vacuo* and the reaction quenched with a saturated solution of aqueous NH_4Cl . Et_2O was added and the layers were separated. The aqueous layer was extracted twice with Et_2O and the combined organic layers were dried

over MgSO_4 , filtered, and concentrated *in vacuo*. The crude residue was purified by silica gel flash chromatography (isocratic: 20% Et_2O /hexane) to afford *exo*-enone **283** (1.66 g, 92% yield) as an off-white solid: $[\alpha]_D^{25.0} = +11.4^\circ$ ($c = 1.08$, CHCl_3).

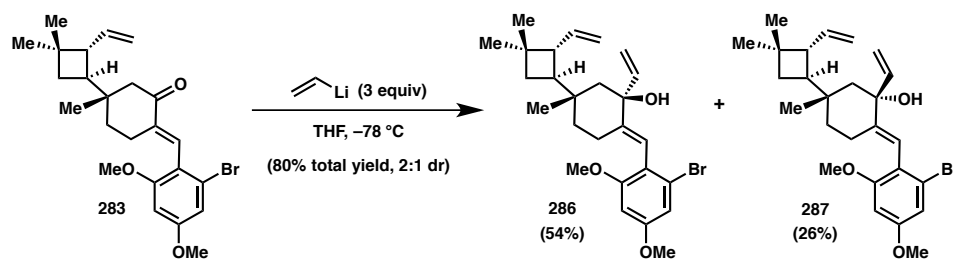
^1H NMR (400 MHz, CDCl_3) δ 7.11 (t, $J = 2.0$ Hz, 1H), 6.75 (d, $J = 2.3$ Hz, 1H), 6.40 (d, $J = 2.3$ Hz, 1H), 5.74 (ddd, $J = 17.1, 10.3, 8.6$ Hz, 1H), 4.95 (ddd, $J = 24.7, 2.1, 0.8$ Hz, 1H), 4.94 (td, $J = 2.3, 0.8$ Hz, 1H), 3.80 (s, 3H), 3.75 (s, 3H), 2.44 – 2.20 (m, 5H), 2.12 (td, $J = 10.0, 8.5$ Hz, 1H), 1.55 (ddd, $J = 13.3, 10.3, 6.0$ Hz, 1H), 1.50 (ddd, $J = 10.7, 8.4, 0.6$ Hz, 1H), 1.45 (d, $J = 10.4$ Hz, 1H), 1.38 (dtd, $J = 11.0, 5.0, 2.1$ Hz, 1H), 0.99 (s, 3H), 0.98 (s, 3H), 0.93 (s, 3H).

^{13}C NMR (101 MHz, CDCl_3) δ 202.2, 160.8, 158.6, 139.6, 139.2, 130.5, 125.1, 118.7, 115.3, 109.0, 98.1, 55.8, 55.7, 50.3, 49.4, 45.0, 36.5, 34.9, 33.2, 32.5, 30.1, 24.7, 23.7, 22.6.

FTIR (NaCl, thin film) 3073, 3000, 2952, 2863, 1686, 1599, 1558, 1482, 1461, 1435, 1407, 1381, 1367, 1303, 1259, 1214, 1153, 1051, 1035, 996, 938, 911, 960, 831, 795 cm^{-1} .

1

HRMS (MM) calc'd for $\text{C}_{24}\text{H}_{32}\text{BrO}_3$ $[\text{M}+\text{H}]^+$ 447.1529, found 447.1520.

Preparation of allylic alcohols **286 and **287**.**

A 100 mL round-bottom flask was flame dried under vacuum and backfilled with N₂. Dry THF (21.2 mL) was then added, followed by freshly prepared vinyl lithium as a solution in THF (8.42 mL, 0.756 M, 3.00 equiv). The solution was cooled to -78 °C and *exo*-enone **283** (928 mg, 2.07 mmol) was taken up in 5.0 mL THF and added dropwise over 5 minutes. After 40 minutes, the reaction was quenched with a saturated solution of NH₄Cl and warmed to room temperature. The mixture was diluted with Et₂O and the layers were separated. The aqueous layer was extracted twice with Et₂O and the combined organic layers were dried over MgSO₄, filtered, and concentrated *in vacuo*. The crude residue was purified by silica gel flash chromatography (30% hexane/CH₂Cl₂ + 1% EtOAc until unreacted **283** and **287** elute, then 5% EtOAc/CH₂Cl₂) to afford **286** (536 mg, 54%), **287** (260 mg, 26%), and recovered **283** (164 mg, 18%).

Preparation of vinyl lithium:

THF (38.0 mL) was added to a flame-dried 200 mL round-bottom flask under N₂, followed by tetravinyl tin (2.10 mL, 11.5 mmol). The solution was cooled to -78 °C and *n*-BuLi (17.3 mL, 2.5 M in hexanes, 43.3 mmol, 3.76 equiv) was added dropwise. The reaction was stirred for 20 minutes at -78 °C, then lifted out of the ice bath and allowed to warm to room temperature. The reaction was allowed to stir at room temperature for at least 2 hours before use, and provides a ~0.756 M solution of vinyl lithium (note: highest

yields for 1,2-addition are obtained after stirring for 6 hours, at which time the mixture should be slightly milky grey in appearance).

Data for **286** (major diastereomer, peak 2): $[\alpha]_D^{25.0} = -23.8^\circ$ (c = 1.07, CHCl₃).

¹H NMR (400 MHz, CDCl₃) δ 6.73 (d, *J* = 2.3 Hz, 1H), 6.40 (d, *J* = 2.3 Hz, 1H), 6.19 (dd, *J* = 17.2, 10.6 Hz, 1H), 6.04 (d, *J* = 1.5 Hz, 1H), 5.77 (ddd, *J* = 17.1, 10.2, 8.9 Hz, 1H), 5.46 (dd, *J* = 17.3, 1.6 Hz, 1H), 5.21 (dd, *J* = 10.6, 1.5 Hz, 1H), 4.92 (dddd, *J* = 17.0, 14.0, 2.2, 0.8 Hz, 2H), 3.79 (s, 3H), 3.74 (s, 3H), 2.40 – 2.22 (m, 2H), 2.07 (q, *J* = 9.6 Hz, 1H), 1.92 (dt, *J* = 14.3, 4.5 Hz, 1H), 1.51 (q, *J* = 14.0, 13.3 Hz, 2H), 1.44 (d, *J* = 12.7 Hz, 1H), 1.41 (d, *J* = 9.4 Hz, 2H), 1.35 – 1.17 (m, 2H), 1.12 (s, 3H), 0.97 (d, *J* = 1.2 Hz, 6H).

¹³C NMR (101 MHz, CDCl₃) δ 159.7, 158.3, 146.6, 145.3, 140.5, 125.3, 120.4, 119.7, 114.8, 112.9, 108.5, 98.1, 76.1, 55.8, 55.7, 49.3, 47.0, 46.1, 34.7, 34.6, 34.4, 33.1, 30.0, 23.8, 23.4, 22.9.

FTIR (NaCl, thin film) 3424 (br) 3001, 2950, 2930, 2858, 2832, 1599, 1560, 1483, 1459, 1434, 1406, 1379, 1366, 1301, 1268, 1210, 1145, 1053, 1037, 994, 910, 879, 830, 811 cm.⁻¹

HRMS (MM) calc'd for C₂₆H₃₄BrO₂ [M–OH]⁺ 457.1742, found 457.1744.

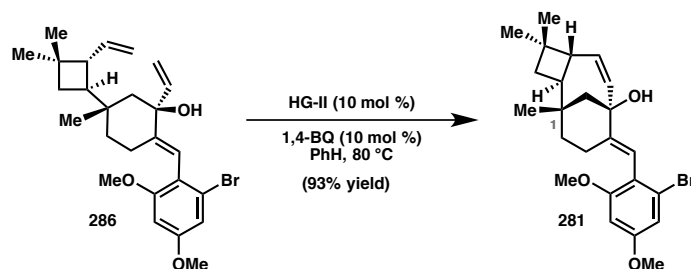
Data for **287** (minor diastereomer, peak 1): $[\alpha]_D^{25.0} = -34.2^\circ$ (c = 1.03, CHCl₃).

¹H NMR (400 MHz, CDCl₃) δ 6.75 (d, *J* = 2.4 Hz, 1H), 6.42 (d, *J* = 2.3 Hz, 1H), 6.23 (d, *J* = 1.4 Hz, 1H), 6.09 (dd, *J* = 17.4, 10.3 Hz, 1H), 5.77 (ddd, *J* = 17.2, 10.2, 8.7 Hz, 1H), 5.48 (dd, *J* = 17.4, 1.5 Hz, 1H), 5.16 (dd, *J* = 10.3, 1.5 Hz, 1H), 4.93 (dddd, *J* = 18.0, 15.2, 2.2, 0.8 Hz, 2H), 3.79 (s, 3H), 3.74 (s, 3H), 2.35 (t, *J* = 9.3 Hz, 1H), 2.15 – 2.02 (m, 2H), 1.90 (dddd, *J* = 14.3, 12.8, 4.4, 1.6 Hz, 1H), 1.77 – 1.65 (m, 2H), 1.59 (d, *J* = 13.2 Hz, 1H), 1.49 – 1.41 (m, 2H), 1.34 (td, *J* = 12.8, 4.3 Hz, 1H), 1.11 (dtd, *J* = 12.6, 4.0, 1.9 Hz, 1H), 0.97 (d, *J* = 1.1 Hz, 6H), 0.89 (s, 3H).

¹³C NMR (101 MHz, CDCl₃) δ 159.6, 158.4, 146.2, 144.9, 140.6, 125.4, 120.9, 117.9, 115.6, 114.8, 108.4, 98.1, 75.8, 55.8, 55.7, 49.6, 49.1, 46.5, 35.6, 34.9, 34.5, 33.1, 30.1, 25.0, 23.8, 22.3.

FTIR (NaCl, thin film) 3451 (br) 3073, 2998, 2951, 2934, 2858, 1630, 1560, 1560, 1482, 1461, 1434, 1406, 1380, 1366, 1301, 1266, 1211, 1150, 1038, 996, 936, 909, 884, 830, 813 cm.⁻¹

HRMS (MM) calc'd for C₂₆H₃₄BrO₂ [M–OH]⁺ 457.1742, found 457.1744.

Preparation of aryl bromide 281.

A 250 mL round-bottom flask containing allylic alcohol **286** (807 mg, 1.70 mmol) was pumped into a N₂-filled glovebox where Hoveyda–Grubbs second-generation catalyst (106 mg, 0.170 mmol, 0.100 equiv) and 1,4-benzoquinone (18.4 mg, 0.170 mmol, 0.100 equiv) were added. The flask was sealed under nitrogen, removed from the glovebox and dry benzene (85.0 mL) was added via syringe. The green reaction mixture was heated to 80 °C for 12 hours, then cooled to room temperature. Ethyl vinyl ether was added to inactivate the catalyst and stirred for 15 minutes before the reaction mixture was concentrated *in vacuo*. The crude residue was purified by silica gel flash chromatography (20–30% Et₂O/hexane) to afford aryl bromide **281** (704 mg, 93%) as a white foam and a single diastereomer at C1: $[\alpha]_D^{25.0} = +95.5^\circ$ (c = 0.815, CHCl₃).

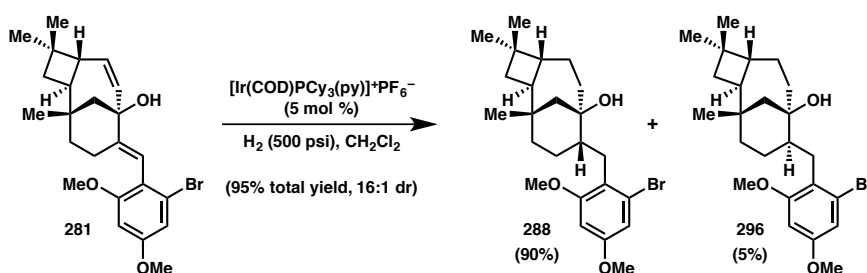
¹H NMR (400 MHz, CDCl₃) δ 6.74 (d, *J* = 2.4 Hz, 1H), 6.41 (d, *J* = 2.4 Hz, 1H), 6.32 (d, *J* = 1.7 Hz, 1H), 5.84 (dd, *J* = 10.8, 2.4 Hz, 1H), 5.34 (ddd, *J* = 10.8, 2.8, 2.1 Hz, 1H), 3.79 (s, 3H), 3.74 (s, 3H), 2.53 (dt, *J* = 11.6, 2.6 Hz, 1H), 2.37 (td, *J* = 11.2, 7.9 Hz, 1H), 2.28 (dd, *J* = 12.8, 2.3 Hz, 1H), 2.18 (dddd, *J* = 15.1, 11.0, 6.0, 1.9 Hz, 1H), 2.08 (ddd, *J* = 15.1, 5.2, 3.6 Hz, 1H), 1.75 (s, 1H), 1.60 – 1.46 (m, 2H), 1.41 (dd, *J* = 12.9, 2.2 Hz, 1H), 1.37 – 1.22 (m, 2H), 1.08 (s, 3H), 1.06 (s, 3H), 0.90 (s, 3H).

^{13}C NMR (101 MHz, CDCl_3) δ 159.6, 158.5, 147.7, 134.6, 131.6, 125.5, 120.8, 116.3, 108.5, 98.2, 76.7, 55.9, 55.7, 50.9, 45.4, 43.4, 38.3, 37.5, 35.1, 32.3, 30.9, 26.2, 24.5, 21.5.

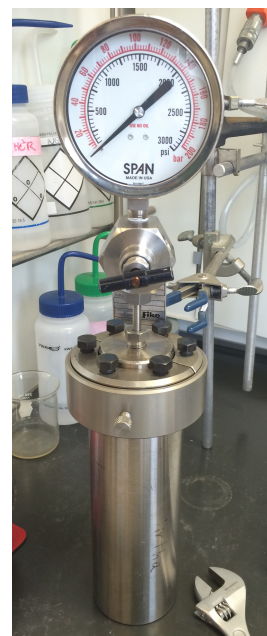
FTIR (NaCl, thin film) 3422 (br) 3002, 2949, 2930, 2862, 1599, 1562, 1481, 1462, 1455, 1434, 1405, 1366, 1302, 1267, 1211, 1149, 1037, 1015, 979, 938, 870, 858, 830, 813, 772, 755 cm^{-1} .

HRMS (MM) calc'd for $\text{C}_{24}\text{H}_{30}\text{BrO}_2$ $[\text{M}-\text{OH}]^+$ 429.1429, found 429.1429.

Preparation of tertiary alcohols **288** and **296**.



Inside a N_2 -filled glovebox, Crabtree's catalyst (59.6 mg, 0.074 mmol, 0.05 equiv) was added to a 100 mL round-bottom flask containing bromide **281** (663 mg, 1.48 mmol). CH_2Cl_2 (14.8 mL) was added and the flask was placed inside a steel bomb, which was closed under nitrogen and brought out of the glovebox. The pressure gauge was quickly attached and all bolts on the bomb tightened with a wrench. The bomb was connected to a H_2 inlet and the vessel purged with 250 psi H_2 three times before being charged



to 500 psi. The reaction was stirred at room temperature for 3 hours, at which time H₂ was vented from the reaction. The solvent was removed *in vacuo* and the crude residue purified by silica gel flash chromatography (isocratic: 40% Et₂O/hexane) to afford tertiary alcohols **288** (599 mg, 90%) and **296** (37.4 mg, 5%) as white, crystalline solids.

Data for **288** (major diastereomer, peak 2): $[\alpha]_D^{25.0} = -20.5^\circ$ (c = 0.900, CHCl₃).

¹H NMR (400 MHz, CDCl₃) δ 6.70 (d, *J* = 2.4 Hz, 1H), 6.40 (d, *J* = 2.4 Hz, 1H), 3.79 (s, 3H), 3.77 (s, 3H), 3.03 (dd, *J* = 13.2, 2.7 Hz, 1H), 2.61 (dd, *J* = 13.2, 10.0 Hz, 1H), 2.08 (ddd, *J* = 11.9, 10.6, 7.9 Hz, 1H), 1.95 (ddd, *J* = 13.8, 10.4, 3.6 Hz, 1H), 1.83 (dd, *J* = 12.8, 2.6 Hz, 1H), 1.78 – 1.57 (m, 4H), 1.57 – 1.34 (m, 5H), 1.34 – 1.23 (m, 2H), 1.01 (s, 3H), 0.99 (s, 3H), 0.96 (dd, *J* = 12.9, 5.6 Hz, 2H), 0.77 (s, 3H).

¹³C NMR (101 MHz, CDCl₃) δ 158.9, 158.9, 125.9, 122.8, 108.9, 98.4, 76.2, 55.9, 55.6, 51.7, 50.1, 45.4, 38.7, 38.0, 36.0, 35.0, 33.9, 33.3, 30.8, 28.5, 26.6, 26.3, 21.3, 21.0.

FTIR (NaCl, thin film) 3474 (br), 3000, 2946, 2930, 2862, 1603, 1568, 1482, 1461, 1435, 1410, 1294, 1272, 1212, 1198, 1151, 1130, 1054, 1038, 999, 937, 926, 876, 831, 756 cm.⁻¹

HRMS (MM) calc'd for C₂₄H₃₄BrO₂ [M–OH]⁺ 433.1737, found 433.1685.

Data for **296** (minor diastereomer, peak 1): $[\alpha]_D^{25.0} = -27.7^\circ$ (c = 0.950, CHCl₃).

¹H NMR (400 MHz, CDCl₃) δ 6.72 (d, *J* = 2.5 Hz, 1H), 6.40 (d, *J* = 2.4 Hz, 1H), 3.80 (s, 3H), 3.78 (s, 3H), 2.85 (dd, *J* = 13.6, 5.8 Hz, 1H), 2.59 (dd, *J* = 13.6, 8.1 Hz, 1H), 2.29

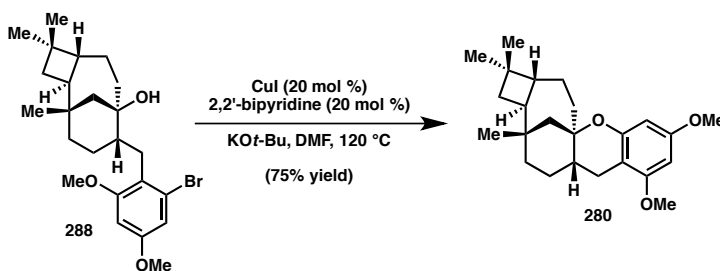
(dddd, $J = 11.4, 8.0, 5.8, 3.5$ Hz, 1H), 1.98 (ddd, $J = 11.0, 9.4, 6.7$ Hz, 2H), 1.80 – 1.52 (m, 4H), 1.52 – 1.37 (m, 4H), 1.37 – 1.26 (m, 4H), 1.25 (s, 1H), 0.94 (s, 6H), 0.78 (s, 3H).

^{13}C NMR (101 MHz, CDCl_3) δ 158.9, 158.5, 126.1, 123.0, 109.2, 98.3, 75.2, 55.8, 55.7, 49.3, 46.4, 45.4, 41.0, 38.5, 36.9, 36.6, 33.8, 30.5, 30.4, 29.2, 27.6, 24.2, 24.1, 21.5.

FTIR (NaCl, thin film) 3482 (br), 2998, 2945, 2928, 2859, 1690, 1648, 1602, 1567, 1482, 1459, 1435, 1409, 1381, 1364, 1294, 1273, 1211, 1198, 1154, 1134, 1051, 1039, 973, 937, 830, 809, 756.

HRMS (MM) calc'd for $\text{C}_{24}\text{H}_{35}\text{BrO}_3\text{Na}$ $[\text{M}+\text{Na}]^+$ 475.1818, found 475.1858.

Preparation of pentacycle 280.



Aryl bromide **288** (274 mg, 0.607 mmol) was added to each of two 20 mL scintillation vials and pumped inside a N_2 -filled glovebox, where CuI (23.1 mg, 0.121 mmol, 0.200 equiv), 2,2'-bipyridine (18.9, 0.121 mmol, 0.200 equiv), and KOt-Bu (204, 1.82 mmol, 3.00 equiv) were added as solids to each. Dry DMF (6.10 mL) was then added, the reaction sealed under N_2 with a Teflon screw-cap and heated to 120°C in a pre-heated aluminum block inside the glovebox for 3.5 hours. After cooling to room temperature, the reaction mixtures were combined and loaded directly onto a short silica

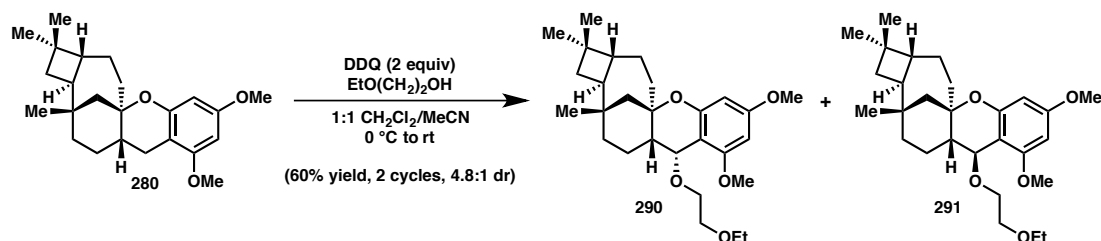
gel column, pre-equilibrated with 5% Et₂O/hexane. The column was eluted with 5% Et₂O/hexane (isocratic) to afford pentacycle **280** (339 mg, 75%) as a white solid: $[\alpha]_D^{25.0} = +42.4^\circ$ (c = 1.08, CHCl₃).

¹H NMR (400 MHz, CDCl₃) δ 6.02 (d, *J* = 2.4 Hz, 1H), 6.00 (d, *J* = 2.4 Hz, 1H), 3.77 (s, 3H), 3.74 (s, 3H), 2.55 (dd, *J* = 16.6, 4.0 Hz, 1H), 2.20 – 2.03 (m, 2H), 1.97 (dd, *J* = 12.6, 2.3 Hz, 1H), 1.77 (dddd, *J* = 18.7, 9.0, 7.4, 4.8 Hz, 2H), 1.69 – 1.55 (m, 4H), 1.52 – 1.41 (m, 3H), 1.32 (t, *J* = 10.7, 9.6 Hz, 2H), 1.32 – 1.20 (m, 1H), 1.17 (dd, *J* = 12.6, 1.1 Hz, 1H), 0.99 (s, 3H), 0.97 (s, 3H), 0.86 (s, 3H).

¹³C NMR (101 MHz, CDCl₃) δ 159.5, 158.3, 154.4, 104.5, 94.2, 90.8, 79.9, 55.5, 55.4, 48.0, 44.3, 40.9, 38.0, 36.9, 35.6, 35.1, 33.5, 30.8, 28.4, 27.1, 26.5, 22.8, 20.9, 19.9.

FTIR (NaCl, thin film) 2995, 2945, 2928, 2862, 2843, 1617, 1589, 1494, 1460, 1420, 1363, 1288, 1215, 1201, 1186, 1164, 1145, 1108, 1074, 1054, 1033, 1008, 942, 928, 810 cm.⁻¹

HRMS (MM) calc'd for C₂₄H₃₅O₃ [M+H]⁺ 371.2581, found 371.2578.

Preparation of benzylic ethers **290 and **291**.**⁴⁰

To a flame-dried 25 mL round-bottom flask was added pentacycle **280** (80.0 mg, 0.216 mmol) and the atmosphere exchanged three times for argon. A 1:1 mixture of dry MeCN/CH₂Cl₂ (6.40 mL) was then added, followed by ethoxyethanol (1.54 mL) via syringe and the solution cooled to 0 °C. A previously prepared stock solution of DDQ in dry MeCN (0.860 mL, 0.508 M, 2.00 equiv) was then added dropwise. The reaction turned grey/blue immediately upon addition of DDQ and slowly turned green-blue by the end of addition. Once the addition was complete, the reaction was lifted from the ice bath and gradually warmed to room temperature. The color became an olive green-brown after 1 hour, indicating the reaction had stalled at ~50% conversion (as judged by TLC). At this point, the reaction was quenched with a saturated solution of aqueous NaHCO₃ and stirred vigorously for 10 minutes before the layers were separated. The aqueous layer was extracted twice more with CH₂Cl₂ and the combined organic layers were washed with one portion of DI H₂O, dried over Na₂SO₄, filtered, and concentrated *in vacuo*. The crude residue was purified by silica gel flash chromatography: SiO₂ was first deactivated by applying a few drops of aqueous NH₄OH (28%) to the top of a dry column and equilibrating with 100 mL of 5% Et₂O/hexane. The crude residue was then applied and eluted with fresh 5% Et₂O/hexane until unreacted **280** elutes completely, then 20% Et₂O/hexane until complete elution of second diastereomer to afford a mixture of **290** and

291 (41.0 mg, 41% yield), and recovered starting material **280** (40.8 mg, 51%). The recovered starting material was re-subjected to the reaction conditions described above to afford additional **290** and **291** (18.8 mg, 60% total over 2 cycles) and **2** (15.2 mg, 74% overall brsm). Analytically pure samples of **290** and **291** were obtained by preparative TLC (30% Et₂O, 1% Et₃N/hexane) and a representative spectrum of the mixture as used in the next step is also provided.

Data for **290** (major diastereomer, peak 1): $[\alpha]_D^{25.0} = +43.5^\circ$ (c = 0.815, CHCl₃).

¹H NMR (400 MHz, CDCl₃) δ 6.01 (d, *J* = 2.4 Hz, 1H), 5.94 (d, *J* = 2.3 Hz, 1H), 4.27 (d, *J* = 3.3 Hz, 1H), 3.98 (dt, *J* = 9.8, 4.9 Hz, 1H), 3.81 (dd, *J* = 10.9, 5.1 Hz, 1H), 3.79 (s, 3H), 3.73 (s, 3H), 3.58 (dd, *J* = 5.9, 4.9 Hz, 2H), 3.53 (q, *J* = 7.0 Hz, 2H), 2.48 – 2.36 (m, 1H), 2.21 (qd, *J* = 14.4, 4.1 Hz, 1H), 2.10 (ddd, *J* = 12.2, 10.7, 7.9 Hz, 1H), 2.00 (dd, *J* = 12.7, 2.3 Hz, 1H), 1.79 – 1.61 (m, 3H), 1.59 – 1.41 (m, 4H), 1.42 – 1.20 (m, 4H), 1.20 (t, *J* = 7.0 Hz, 3H), 0.99 (s, 3H), 0.98 (s, 3H), 0.86 (s, 3H).

¹³C NMR (101 MHz, CDCl₃) δ 161.1, 159.7, 154.7, 106.6, 93.8, 91.2, 80.5, 72.1, 71.4, 70.5, 66.7, 55.4, 55.4, 49.3, 47.6, 46.1, 39.4, 39.3, 36.3, 34.8, 33.5, 32.4, 30.8, 26.8, 23.1, 22.3, 20.8, 15.4.

FTIR (NaCl, thin film) 2948, 2930, 2864, 1614, 1589, 1491, 1462, 1438, 1424, 1365, 1353, 1332, 1320, 1287, 1215, 1202, 1189, 1166, 1148, 1109, 1053, 1033, 1005, 951, 921, 866, 811, 731, 638 cm.⁻¹

HRMS (MM) calc'd for C₂₄H₃₃O₃ [M–O(CH₂)₂OEt]⁺ 369.2424, found 369.2430.

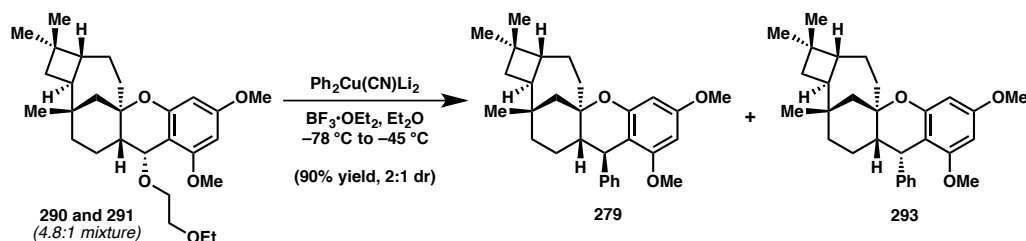
Data for **291** (minor diastereomer, peak 2): $[\alpha]_D^{25.0} = +29.6^\circ$ (c = 0.230, CHCl₃).

¹H NMR (400 MHz, CDCl₃) δ 6.02 (d, *J* = 2.4 Hz, 1H), 5.92 (d, *J* = 2.4 Hz, 1H), 4.30 (d, *J* = 10.4 Hz, 1H), 3.78 (s, 3H), 3.75 (ddd, *J* = 9.1, 3.0, 1.3 Hz, 1H), 3.73 (s, 3H), 3.58 – 3.45 (m, 5H), 2.24 – 2.04 (m, 2H), 1.92 (ddt, *J* = 14.7, 9.9, 3.2 Hz, 2H), 1.80 – 1.64 (m, 2H), 1.65 – 1.40 (m, 5H), 1.36 – 1.19 (m, 4H), 1.19 (t, *J* = 7.0 Hz, 3H), 0.97 (s, 3H), 0.96 (s, 3H), 0.86 (s, 3H).

¹³C NMR (101 MHz, CDCl₃) δ 161.0, 160.0, 155.9, 105.8, 94.2, 91.7, 81.7, 73.4, 70.5, 67.8, 66.7, 55.5, 55.4, 48.2, 47.2, 44.4, 37.8, 37.2, 35.6, 35.1, 33.2, 30.8, 28.4, 26.4, 23.7, 20.9, 20.4, 15.4.

FTIR (NaCl, thin film) 2947, 2934, 2864, 1613, 1587, 1490, 1459, 1438, 1421, 1364, 1349, 1312, 1288, 1267, 1245, 1216, 1202, 1147, 1107, 1054, 1034, 1002, 973, 943, 868, 812, 736, 636 cm.⁻¹

HRMS (MM) calc'd for C₂₄H₃₃O₃ [M–O(CH₂)₂OEt]⁺ 369.2424, found 369.2427.

Preparation of diarylmethanes **279 and **293**.**

A 10 mL round-bottom flask containing CuCN (11.9 mg, 0.133 mmol, 2.05 equiv) was flame-dried under vacuum. After cooling to room temperature, the flask was backfilled with argon and dry Et_2O (2.70 mL) was added via syringe. The suspension was cooled to -78°C under argon and PhLi (0.140 mL, 1.9 M in dibutyl ether, 0.266 mmol, 4.09 equiv) was added dropwise. After stirring at -78°C for 5 minutes, the reaction was warmed to 0°C and stirred for an additional 30 minutes. The higher-order cuprate was then cooled back to -78°C and the 4.8:1 mixture of benzylic ethers **290** and **291** (30.0 mg, 0.065 mmol) was added as a solution in Et_2O (1.00 mL). The reaction was stirred for 1-2 minutes before $\text{BF}_3 \cdot \text{OEt}_2$ (0.160 mL, 1.30 mmol, 20.0 equiv) was added dropwise via syringe. The reaction was stirred at -78°C for 10 minutes, then quickly transferred to a pre-equilibrated bath at -55°C , which was allowed to -50°C over 5 minutes, then maintained at or just below -45°C for another 30 minutes. The reaction was checked for completion by TLC, then quenched with aqueous NaHCO_3 and warmed to room temperature. The layers were separated and the aqueous layer extracted twice with Et_2O . The combined organic layers were dried over MgSO_4 , filtered, and concentrated *in vacuo*. The crude residue was purified by silica gel flash chromatography (isocratic: 5% Et_2O /hexane) to afford diarylmethanes **279** and **293** (26.3 mg, 90%) as a 2:1 inseparable mixture, white solid: $[\alpha]_D^{25.0} = +2.08^\circ$ ($c = 1.23$, CHCl_3).

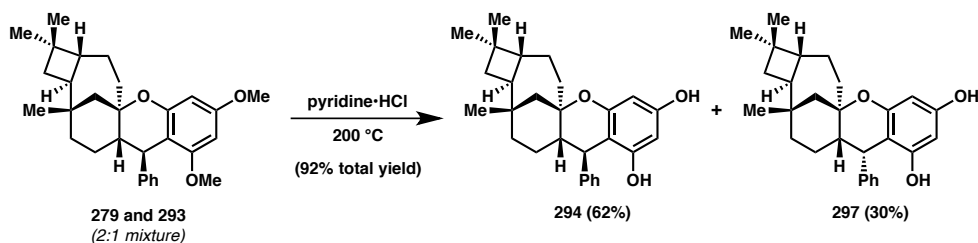
¹H NMR (2:1 dr, asterisk denotes minor diastereomer, 400 MHz, CDCl₃) δ 7.24 – 6.96 (m, 5H), 6.10* (d, *J* = 2.4 Hz, 1H), 6.07 (d, *J* = 2.5 Hz, 1H), 6.03* (d, *J* = 2.4 Hz, 1H), 5.93 (d, *J* = 2.4 Hz, 1H), 4.10* (d, *J* = 6.4 Hz, 1H), 3.79* (s, 3H), 3.76 (s, 3H), 3.46* (s, 3H), 3.47 (d, *J* = 11.3 Hz, 1H), 3.20 (s, 3H), 2.23 – 2.06 (m, 1H), 2.00 (dd, *J* = 12.7, 2.4 Hz, 1H), 1.93* (dd, *J* = 12.6, 2.5 Hz, 1H), 1.88 – 1.73 (m, 2H), 1.73 – 1.60 (m, 3H), 1.55 – 1.41 (m, 4H), 1.39 – 1.26 (m, 5H), 1.20 (q, *J* = 13.1, 12.1 Hz, 1H), 1.00 (s, 3H), 0.99 (s, 3H), 0.92* (s, 3H), 0.83 (s, 3H), 0.82* (s, 3H), 0.74* (s, 3H).

¹³C NMR (**279**, major diastereomer, 101 MHz, CDCl₃) δ 160.0, 159.2, 155.2, 146.7, 129.8, 127.7, 125.4, 109.2, 94.5, 92.7, 80.4, 55.3, 55.2, 50.7, 48.1, 44.3, 41.9, 37.9, 36.9, 35.6, 35.1, 33.3, 30.8, 28.2, 26.3, 24.3, 20.9, 20.2.

¹³C NMR (**293**, minor diastereomer 101 MHz, CDCl₃) δ 160.1, 159.2, 155.1, 141.5, 128.9, 127.0, 125.5, 106.4, 94.1, 91.5, 80.7, 55.6, 55.4, 50.0, 45.8, 44.3, 39.3, 38.5, 36.7, 35.5, 35.0, 33.2, 32.7, 30.8, 26.2, 25.8, 20.9, 20.4.

FTIR (NaCl, thin film) 3081, 3059, 3025, 2998, 2948, 2934, 2864, 2843, 1614, 1588, 1490, 1460, 1454, 1440, 1420, 1364, 1307, 1288, 1274, 1249, 1216, 1202, 1166, 1148, 1123, 1105, 1076, 1054, 1033, 1005, 943, 870, 811, 759, 740, 701 cm.⁻¹

HRMS (MM) calc'd for C₃₀H₃₉O₃ [M+H]⁺ 447.2894, found 447.2905.

Preparation of resorcinols 294 and 297.

Solid pyridine·HCl (1.44 g, 12.5 mmol, 307 equiv) was weighed into each of two 2-dram vials, containing a 2:1 mixture of diarylmethanes **279** and **293** (18.2 mg, 0.041 mmol). The vials were sealed with a Teflon screw cap under a stream of argon and heated to 200 °C in a pre-heated aluminum block for 2.5 hours. (Note: it is important to choose a vial/heating block combination that will cover the entire volume of the solid to ensure that it stays completely melted during the course of the reaction). The reactions were cooled to room temperature, during which time the mixture solidified. The crude solids were dissolved in DI H₂O, and combined by pipetting dropwise into an Erlenmeyer flask containing a saturated solution of aqueous NaHCO₃. EtOAc was then added and the layers were separated. The aqueous layer was extracted three times with EtOAc and the combined organic layers were dried over MgSO₄ and concentrated *in vacuo*. The crude residue was purified by silica gel flash chromatography (isocratic: 10% EtOAc, 1% AcOH/hexane) to separate resorcinols **294** and **297**. The concentrated fractions for each diastereomer (initially a pale orange oil) were each passed through another short plug of silica gel (eluting with 20% EtOAc/hexanes) to remove residual AcOH and remaining trace impurities to afford **294** (21.3 mg, 62%) and **297** (10.3 mg, 30%) as white solids.

Data for **294** (major diastereomer, peak 1): $[\alpha]_D^{25.0} = -28.2^\circ$ ($c = 0.475$, CHCl₃).

¹H NMR (400 MHz, CDCl₃) δ 7.44 – 7.26 (m, 5H), 6.00 (d, *J* = 2.6 Hz, 1H), 5.88 (d, *J* = 2.6 Hz, 1H), 4.73 (s, 1H), 4.46 (s, 1H), 3.49 (d, *J* = 11.4 Hz, 1H), 2.16 (ddd, *J* = 12.3, 10.4, 7.9 Hz, 1H), 2.01 (dd, *J* = 12.8, 2.3 Hz, 1H), 1.85 – 1.58 (m, 4H), 1.54 – 1.44 (m, 2H), 1.44 – 1.30 (m, 4H), 1.28 (m, 1H), 1.18 (d, *J* = 12.9 Hz, 1H), 1.10 – 1.03 (m, 1H), 1.00 (s, 3H), 0.99 (s, 3H), 0.85 (s, 3H).

¹³C NMR (101 MHz, CDCl₃) δ 156.1, 155.8, 155.4, 142.3, 128.0, 106.3, 97.7, 96.8, 80.1, 50.5, 48.1, 44.2, 41.8, 37.8, 36.9, 35.6, 35.2, 33.3, 30.8, 28.6, 26.3, 24.0, 20.9, 20.0.

FTIR (NaCl, thin film) 3511 (br), 3386 (br), 3060, 3024, 2948, 2928, 2863, 1702, 1627, 1598, 1509, 1492, 1459, 1364, 1349, 1320, 1272, 1248, 1228, 1166, 1138, 1087, 1072, 1057, 1034, 1014, 925, 869, 831, 761, 738, 703, 667, 638, 571, 516 cm.⁻¹

HRMS (MM) calc'd for C₂₈H₃₅O₃ [M+H]⁺ 419.2581, found 419.2591.

Data for **297** (minor diastereomer, peak 2): [α]_D^{25.0} = +26.7° (c = 0.180, CHCl₃).

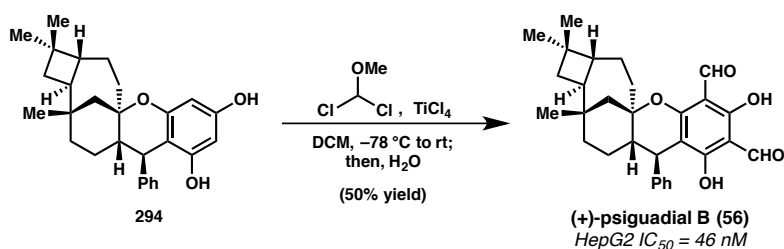
¹H NMR (400 MHz, CDCl₃) δ 7.37 – 7.21 (m, 5H), 6.02 (d, *J* = 2.5 Hz, 1H), 5.96 (d, *J* = 2.5 Hz, 1H), 4.73 (s, 1H), 4.30 (s, 1H), 4.00 (d, *J* = 7.0 Hz, 1H), 2.16 (ddd, *J* = 12.5, 7.0, 3.9 Hz, 1H), 1.93 (dd, *J* = 12.7, 2.3 Hz, 2H), 1.79 (ddd, *J* = 12.3, 10.3, 7.8 Hz, 1H), 1.66 (ddd, *J* = 12.4, 8.7, 5.4 Hz, 1H), 1.57 – 1.43 (m, 5H), 1.39 – 1.28 (m, 4H), 1.23 – 1.12 (m, 3H), 1.09 – 0.95 (m, 2H), 0.91 (s, 3H), 0.82 (s, 3H), 0.75 (s, 3H).

¹³C NMR (101 MHz, CDCl₃) δ 156.2, 155.7, 155.4, 138.6, 127.4, 104.8, 97.6, 95.9, 80.4, 49.7, 45.6, 44.2, 39.6, 38.3, 36.6, 35.4, 35.1, 33.2, 32.0, 30.8, 29.9, 26.1, 25.4, 20.8, 20.3.

FTIR (NaCl, thin film) 3385 (br), 3027, 2949, 2925, 2857, 1624, 1600, 1508, 1493, 1459, 1452, 1377, 1364, 1247, 1190, 1163, 1143, 1086, 1055, 1034, 1015, 925, 826, 761, 721, 701 cm^{-1}

HRMS (MM) calc'd for $\text{C}_{28}\text{H}_{35}\text{O}_3$ $[\text{M}+\text{H}]^+$ 419.2581, 419.2595.

Preparation of (+)-psiguadial B (**56**).



To a 2-dram vial was added resorcinol **294** (15.4 mg, 0.037 mmol) and the atmosphere exchanged three times for N_2 . CH_2Cl_2 (1.30 mL) was then added via syringe, followed by dichloromethyl methyl ether (0.083 mL, 0.920 mmol, 25.0 equiv). The solution was cooled to -78°C and a freshly prepared stock solution of TiCl_4 (0.190 mL, 0.912 M in CH_2Cl_2 , 0.173 mmol, 4.68 equiv) was added dropwise. The reaction immediately turns dark red. The reaction was stirred at -78°C for 5 minutes, then warmed to room temperature and stirred for an additional 3 hours and 40 minutes. DI H_2O (2.00 mL) was then added via syringe and the reaction stirred vigorously for 15 minutes before the layers were separated. The aqueous layer was extracted five times with CH_2Cl_2 and the combined organic layers were filtered over a plug of Na_2SO_4 and concentrated *in vacuo*. The crude residue was purified by silica gel flash chromatography (isocratic: 2% EtOAc, 1% AcOH/hexane) to afford (+)-psiguadial B (**56**) (8.7 mg, 50%) as an ivory solid. Note: **56** is streaky on SiO_2 and after an initial concentrated band elutes,

approximately 12% of the product is contained in the following very dilute fractions. The natural product is weakly UV active, but can also be visualized by TLC using 2,4-dinitrophenylhydrazine stain. $[\alpha]_D^{25.0} = +94.0^\circ$ (c = 0.265, CHCl₃).

¹H NMR (400 MHz, CDCl₃) δ 13.51 (s, 1H), 13.04 (s, 1H), 10.07 (s, 2H), 7.26 (dd, *J* = 14.6, 1.5 Hz, 2H), 7.23 – 7.17 (m, 1H), 7.10 (br s, 2H), 3.49 (d, *J* = 11.5 Hz, 1H), 2.20 – 2.12 (m, 1H), 2.09 (dd, *J* = 12.7, 2.4 Hz, 1H), 1.92 (ddd, *J* = 14.9, 12.8, 4.2 Hz, 1H), 1.82 (ddd, *J* = 12.3, 8.8, 5.6 Hz, 1H), 1.73 – 1.59 (m, 3H), 1.53 – 1.44 (m, 1H), 1.49 (ddd, *J* = 11.6, 8.1, 2.9 Hz, 2H), 1.44 – 1.29 (m, 4H), 1.05 (dd, *J* = 7.6, 5.8 Hz, 1H), 1.02 (s, 3H), 1.00 (s, 3H), 0.85 (s, 3H).

¹³C NMR (101 MHz, CDCl₃) δ 192.3, 191.5, 169.6, 168.5, 163.5, 143.4, 128.2, 126.2, 105.7, 104.6, 104.1, 84.1, 50.0, 47.4, 44.0, 40.4, 37.6, 36.9, 35.4, 35.1, 33.4, 30.6, 29.3, 26.1, 23.9, 20.7, 20.1.

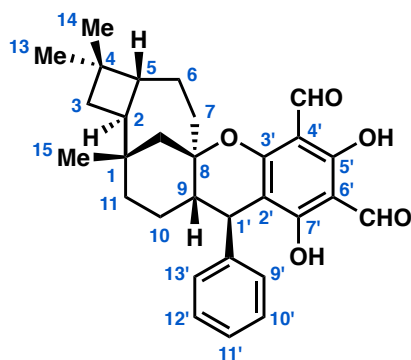
FTIR (NaCl, thin film) 3026, 2945, 2926, 2864, 2720, 1633, 1603, 1493, 1437, 1382, 1363, 1300, 1270, 1251, 1231, 1184, 1154, 1143, 1031, 1006, 976, 926, 917, 875, 851, 840, 824, 768, 701, 636, 618, 606, 564 cm.⁻¹

HRMS (MM) calc'd for C₃₀H₃₅O₅ [M+H]⁺ 475.2479, found 475.2487.

Comparison of ^1H NMR data for natural and synthetic (+)-psiguadial B (**56**).

carbon number	Natural (+)-psiguadial B ⁴¹ ^1H NMR, 500 MHz, CDCl_3	Synthetic (+)-psiguadial B ^1H NMR, 400 MHz, CDCl_3
5'-OH	δ 13.51 (s, 1H)	δ 13.51 (s, 1H)
7'-OH	13.04 (s, 1H)	13.04 (s, 1H)
14', 15'	10.08 (s, 2H)	10.07 (s, 2H)
9', 13' ⁴²	7.23 (2H)	7.26 (dd, $J = 14.6, 1.5$ Hz, 2H)
11'	7.18 (3H)	7.23 – 7.17 (m, 1H)
10', 12'	–	7.10 (br m, 2H)
1'	3.49 (d, $J = 11.5$ Hz, 1H)	3.49 (d, $J = 11.5$ Hz, 1H)
2	2.16 (1H)	2.20 – 2.12 (m, 1H)
12	2.08 (1H)	2.09 (dd, $J = 12.7, 2.4$ Hz, 1H)
7	1.93 (1H)	1.92 (ddd, $J = 14.9, 12.8, 4.2$ Hz, 1H)
5	1.82 (m, 1H)	1.82 (ddd, $J = 12.3, 8.8, 5.6$ Hz, 1H)
9	1.68 (1H)	1.73 – 1.59 (m, 3H)
6	1.65 (1H)	–
7	1.58 (m, 1H)	–
3	1.52 (1H)	1.53 – 1.44 (m, 1H)
10	1.49 (m, 2H)	1.49 (ddd, $J = 11.6, 8.1, 2.9$ Hz, 2H)
6, 11	1.41 (2H)	–
3	1.37 (1H)	1.44 – 1.29 (m, 4H)
12	1.29 (1H)	–
11	1.10 (1H)	1.05 (dd, $J = 7.6, 5.8$ Hz, 1H)
13	1.02 (s, 3H)	1.02 (s, 3H)
14	1.01 (s, 3H)	1.00 (s, 3H)
15	0.86 (s, 3H)	0.85 (s, 3H)

(+)-psiguadial B (**56**) carbon numbering as reported by Shao et al.⁴¹



Comparison of ^{13}C NMR data for natural and synthetic (+)-psiguadial B (56).

carbon number	Natural (+)-psiguadial B ⁴¹ ^{13}C NMR, 125 MHz, CDCl_3	Synthetic (+)-psiguadial B ⁴³ ^{13}C NMR, 101 MHz, CDCl_3	Δ (ppm)
15'	192.3	192.3	0.0
14'	191.4	191.5	0.1
7'	169.6	169.6	0.0
5'	168.5	168.5	0.0
3'	163.5	163.5	0.0
8'	143.4	143.4	0.0
9', 11', 13'	128.2	128.2	0.0
10', 12'	126.2	126.2	0.0
2'	105.7	105.7	0.0
4'	104.6	104.6	0.0
6'	104.2	104.1	-0.1
8	84.1	84.1	0.0
9	50.0	50.0	0.0
12	47.5	47.4	-0.1
5	44.1	44.0	-0.1
1'	40.4	40.4	0.0
11	37.6	37.6	0.0
2	37.0	36.9	-0.1
3	35.5	35.4	-0.1
4	35.1	35.1	0.0
1	33.4	33.4	0.0
13	30.6	30.6	0.0
7	29.4	29.3	-0.1
15	26.1	26.1	0.0
10	23.9	23.9	0.0
14	20.7	20.7	0.0
6	20.1	20.1	0.0

LMC-04-214-flash.2.fid

Parameter	Value
Data File Name	/Volumes/nmrdata/lchapman/nmr/LMC-04-214-flash/2/ fid
Title	LMC-04-214-flash.2.fid
Comment	
Origin	Bruker BioSpin GmbH
Spectrometer	spect
Solvent	CDCl ₃
Temperature	295.0
Pulse Sequence	zg30
Experiment	1D
Number of Scans	16
Receiver Gain	143
Relaxation Delay	10.0000
Pulse Width	11.7000
Acquisition Time	4.0894
Acquisition Date	2016-07-02T16:29:45
Spectrometer Frequency	400.13
Spectral Width	8012.8
Nucleus	¹ H
Acquired Size	32768
Spectral Size	65536

Chemical structure of (+)-psiguadial B (56):

O=C1C(O)C(O)C(=O)C1[C@H]2[C@@H](O)[C@H](C)[C@H](O)[C@H]2C

(+)-psiguadial B (56)
synthetic, this work

ppm

13.6138
13.5940
13.5081
13.4340
13.2810
13.1310
13.0861
13.0360
10.1633
10.1435
10.1366
10.1351
10.1094
10.1058
10.1002
10.0951
10.0797
10.0782
7.2790
7.2762
7.2600
7.2406
7.2281
7.2173
7.1997
7.1845
7.1815
7.1623
7.1581
7.1464
7.1420
7.1057
7.0908
5.0345
4.3773
3.5057
3.4770
2.1207
2.1140
1.5784
1.5020
1.4980
1.4661
1.4785
1.3655
1.3413
1.2856
1.2540
1.0169
1.0124
0.9654
0.8620

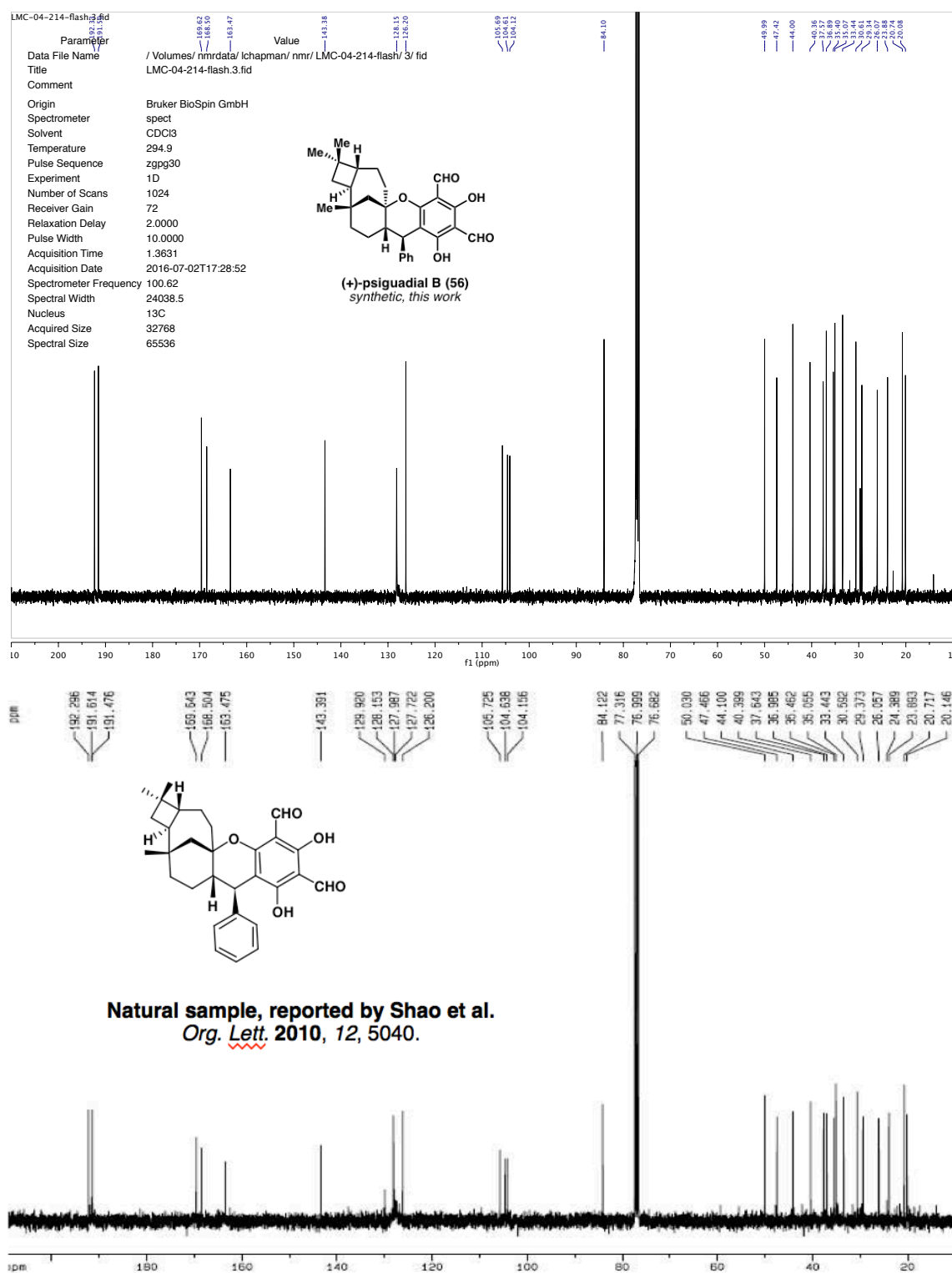
Chemical structure of (+)-psiguadial B (56):

O=C1C(O)C(O)C(=O)C1[C@H]2[C@@H](O)[C@H](C)[C@H](O)[C@H]2C

Natural sample, reported by Shao et al.
Org. Lett. 2010, 12, 5040.

ppm

14.0664
14.0428
10.1433
7.9800
7.0891
7.3349
6.8782
6.7464
4.0000
3.0629
1.4453
1.6893
3.6893
2.2601
4.2225
3.4803
2.6941
1.1217
7.9033
1.4938
4.4019

^{13}C NMR spectral comparison of natural and synthetic (+)-psiguadial B (56).

3.6 NOTES AND REFERENCES

- (1) For leading references on the Norrish–Yang cyclization, see: (a) N. C. Yang, D.-D. H. Yang, *J. Am. Chem. Soc.* **1958**, *80*, 2913. (b) Chen, C. *Org. Biomol. Chem.* **2016**, *14*, 8641. For an example in total synthesis, see Chapter 1, Scheme 1.4.
- (2) (a) Palucki, M.; Wolfe, J. P.; Buchwald, S. L. *J. Am. Chem. Soc.* **1996**, *118*, 10333. (b) Palucki, M.; Wolfe, J. P.; Buchwald, S. L. *J. Am. Chem. Soc.* **1997**, *119*, 3395. (c) Parrish, C. A.; Buchwald, S. L. *J. Org. Chem.* **2001**, *66*, 2498. (d) Vorogushin, A. V.; Huang, X.; Buchwald, S. L. *J. Am. Chem. Soc.* **2005**, *127*, 8146.
- (3) Schwinden, M. D. "The Norrish Type II reaction in organic synthesis." (1990). Retrospective Theses and Dissertations. Paper 9890.
- (4) Chatgililoglu, C.; Crich, D.; Komatsu, M.; Ryu, I. *Chem. Rev.* **1999**, *99*, 1991.
- (5) For select examples, see: (a) Bach, T.; Aechtner, T.; Neumüller, B. *Chem. Eur. J.* **2002**, *8*, 2464. (b) Renata, H.; Zhou, Q.; Baran, P. S. *Science* **2013**, *339*, 59. (c) Singhal, N.; Koner, A. L.; Mal, P.; Venugopalan, P.; Nau, W. M.; Moorthy, J. N. *J. Am. Chem. Soc.* **2005**, *127*, 14375.
- (6) (a) Winnik, M. A.; Breslow, R. *J. Am. Chem. Soc.* **1969**, *91*, 3038. (b) Breslow, R.; Rothbard, J.; Herman, F.; Rodriguez, M. L. *J. Am. Chem. Soc.* **1978**, *100*, 1213.
- (7) Andreu, I.; Palumbo, F.; Tilocca, F.; Morera, I. M.; Boscá, F.; Miranda, M. A. *Org. Lett.* **2011**, *13*, 4096.
- (8) (a) Maier, M. E. *Angew. Chem. Int. Ed.* **2000**, *39*, 2073. (b) Michalak, M.; Wicha,

- J. *Synlett* **2005**, 2005, 2277.
- (9) Dowling, M. S.; Vanderwal, C. D. *J. Org. Chem.* **2010**, 75, 6908.
- (10) Scholl, M.; Ding, S.; Lee, C. W.; Grubbs, R. H. *Org. Lett.* **1999**, 1, 953.
- (11) Tsunoda, T.; Suzuki, M.; Noyori, R. *Tetrahedron Lett.* **1980**, 21, 1357.
- (12) Formation of spirocyclic lactam **149** (see Chapter 2) is precluded using this alternative sequence, since the *in situ* aza-Michael addition observed with **148** cannot occur when the enone is protected as the corresponding dioxolane.
- (13) (a) d'Augustin, M.; Palais, L. T.; Alexakis, A. *Angew. Chem., Int. Ed.* **2005**, 44, 1376. (b) Vuagnoux-d'Augustin, M.; Alexakis, A. *Chem. Eur. J.* **2007**, 13, 9647.
- (14) Prepared according to: Gambacorti-Passerini, C.; Mologni, L.; Scapozza, L.; Bisson, W.; Ahmed, S.; Goekjian, P.; Tardy, S.; Orsato, A.; Gueyrard, D.; Benoit, J. *Alpha-carbolines for the treatment of cancer*. WO2013167730, 2013.
- (15) Spectroscopic data for **278** matches that reported in the literature: Lee, H.; Yi, C. *S. Eur. J. Org. Chem.* **2015**, 2015, 1899.
- (16) Prepared according to: Wong, N. C. W.; Tucker, J. E. L.; Hansen, H. C.; Chiacchia, F. S.; McCaffrey, D. *Compounds for the prevention and treatment of cardiovascular diseases*. WO2008092231, 2008.
- (17) (a) Imamoto, T.; Takiyama, N.; Nakamura, K.; Hatajima, T.; Kamiya, Y. *J. Am. Chem. Soc.* **1989**, 111, 4392. (b) Collins, S.; Hong, Y.; Hoover, G. J.; Veit, J. R. *J. Org. Chem.* **1990**, 55, 3565.
- (18) Harnett, J. J.; Alcaraz, L.; Mioskowski, C.; Martel, J. P.; Le Gall, T.; Shin, D. -S.; Falck, J. R. *Tetrahedron Lett.* **1994**, 35, 2009.
- (19) For an example of a tertiary alcohol-directed hydrogenation using Crabtree's

- catalyst, see: (a) Hong, A. Y.; Stoltz, B. M. *Angew. Chem. Int. Ed.* **2014**, *53*, 5248.
- For a review, see: (b) Hoveyda, A. H.; Evans, D. A.; Fu, G. C. *Chem. Rev.* **1993**, *93*, 1307.
- (20) Suchand, B.; Krishna, J.; Mritunjoy, K.; Satyanarayana, G. *RSC Adv.* **2014**, *4*, 13941.
- (21) For select examples, see: (a) Selenski, C.; Pettus, T. R. R. *Tetrahedron* **2006**, *62*, 5298. (b) Achilonu, M. C.; Bonnet, S. L.; van der Westhuizen, J. H. *Org. Lett.* **2008**, *10*, 3865. (c) Bezuidenhoudt, B. C. B.; Brandt, E. V.; Roux, D. G. *J. Chem. Soc., Perkin Trans. 1* **1984**, 2767. (d) Hayes, C. J.; Whittaker, B. P.; Watson, S. A.; Grabowska, A. M. *J. Org. Chem.* **2006**, *71*, 9701, and references cited therein.
- (22) (a) Saito, A.; Nakajima, N.; Tanaka, A.; Ubukata, M. *Tetrahedron* **2002**, *58*, 7829. (b) Dennis, E. G.; Jeffery, D. W.; Johnston, M. R.; Perkins, M. V.; Smith, P. A. *Tetrahedron* **2012**, *68*, 340.
- (23) Feng, Z. G.; Bai, W. J.; Pettus, T. R. R. *Angew. Chem. Int. Ed.* **2015**, *54*, 1864.
- (24) Hendrik, C.; Mouton, L.; Steenkamp, J. A.; Young, D. A.; Bezuidenhoudt, B. C. B.; Ferreira, D. *Tetrahedron* **1990**, *46*, 6885.
- (25) (a) Day, J. J.; McFadden, R. M.; Virgil, S. C.; Kolding, H.; Alleva, J. L.; Stoltz, B. M. *Angew. Chem. Int. Ed.* **2011**, *50*, 6814. (b) Olah, G. A.; Salem, G.; Staral, J. S.; Ho, T.-L. *J. Org. Chem.* **1978**, *43*, 173.
- (26) Li, Y. Z.; Li, B. J.; Lu, X. Y.; Lin, S.; Shi, Z. J. *Angew. Chem. Int. Ed.* **2009**, *48*, 3817.
- (27) Muramatsu, W.; Nakano, K. *Org. Lett.* **2014**, *16*, 2042.
- (28) Steenkamp, J. A.; Mouton, C.; Ferreira, D. *Tetrahedron* **1991**, *47*, 6705.

- (29) Willson, T. M.; Amburgey, J.; Denmark, S. E. *J. Chem. Soc., Perkin Trans. 1* **1991**, 12, 2899.
- (30) (a) Greene, M. A.; Yonova, I. M.; Williams, F. J.; Jarvo, E. R. *Org. Lett.* **2012**, 14, 4293. (b) Yonova, I. M.; Johnson, A. G.; Osborne, C. A.; Moore, C. E.; Morrisette, N. S.; Jarvo, E. R. *Angew. Chem. Int. Ed.* **2014**, 53, 2422. (c) Dawson, D. D.; Jarvo, E. R. *Org. Process Res. Dev.* **2015**, 19, 1356.
- (31) (a) Mitchell, T. A.; Bode, J. W. *J. Am. Chem. Soc.* **2009**, 131, 18057. (b) Vo, C.-V. T.; Mitchell, T. A.; Bode, J. W. *J. Am. Chem. Soc.* **2011**, 133, 14082.
- (32) (a) Lipshutz, B. H.; Wilhelm, R. S.; Kozlowski, J. A. *J. Org. Chem.* **1984**, 49, 3938. (b) Lipshutz, B. H.; Parker, D. A.; Kozlowski, J. A.; Nguyen, S. M. *Tetrahedron Lett.* **1984**, 25, 5959.
- (33) (a) Rieche, A.; Gross, H.; Höft, E. *Chem. Ber.* **1960**, 93, 88. (b) Aukrust, I. R.; Skattebol, L. *Acta Chem. Scand.* **1996**, 50, 132. (c) Kraus, G. A.; Mengwasser, J.; Maury, W.; Oh, C. *Bioorg. Med. Chem. Lett.* **2011**, 21, 1399.
- (34) Shao, M.; Wang, Y.; Liu, Z.; Zhang, D.-M.; Cao, H.-H.; Jiang, R.-W.; Fan, C.-L.; Zhang, X.-Q.; Chen, H.-R.; Yao, X.-S.; Ye, W.-C. *Org. Lett.* **2010**, 12, 5040.
- (35) Chapman, L. M.; Beck, J. C.; Wu, L.; Reisman, S. E. *J. Am. Chem. Soc.* **2016**, 138, 9803.
- (36) Still, W. C.; Kahn, M. & Mitra, A. *J. Org. Chem.* **1978**, 43, 2923.
- (37) See procedure for ylide preparation on page 222.
- (38) Prepared according to the ligand protocol described in: Bao, H.; Qi, X.; Tambar,

U. K. *J. Am. Chem. Soc.* **2011**, *133*, 1206. We found that the use of CH₂Cl₂ as a reaction solvent provided higher and more reproducible yields, compared with THF.

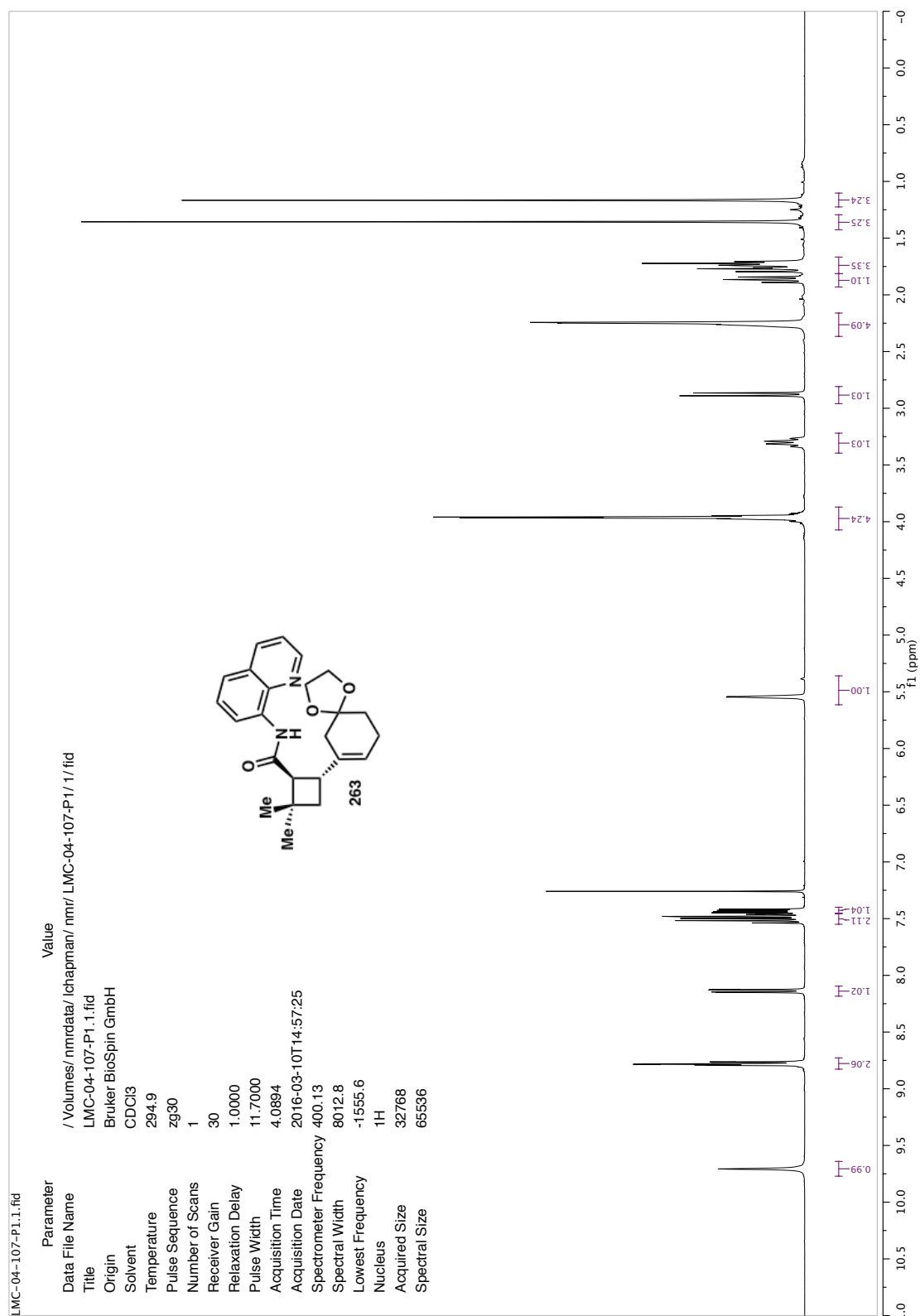
- (39) This reaction is particularly capricious—on multiple occasions, two identical reactions have been set up in parallel using the protocol described above. Often, one reaction works, whereas the other results in no reaction. In the latter case, **274** is recovered in >80% yield. The origin of this irreproducibility is unclear at this time.
- (40) Extensive optimization aimed at increasing conversion of this reaction resulted in either significant decomposition, a variety of over-oxidation products, or trapping by 2,3-dichloro-5,6-dicyanohydroquinone. As a result, we found that the most efficient material throughput was achieved by running the reaction to ~50% conversion using the above protocol, and resubjecting the recovered starting material to the reaction conditions.
- (41) Isolation of psiguadials A and B: Shao, M.; Wang, Y.; Liu, Z.; Zhang, D.-M.; Cao, H.-H.; Jiang, R.-W.; Fan, C.-L.; Zhang, X.-Q.; Chen, H.-R.; Yao, X.-S.; Ye, W.-C. *Org. Lett.* **2010**, *12*, 5040. Except where designated, multiplicities are not specified.
- (42) Shao et al. report the two protons at 7.23 ppm as corresponding to the carbon signal at 126.2 ppm (carbons 10' and 12'). This is assumed to be a typographical error based on the reported plot of their HSQC spectrum and our own data showing a correlation between the proton signal at 7.26 ppm and the more downfield carbon shift at 128.2 ppm, which corresponds to carbons 9' and 13'.

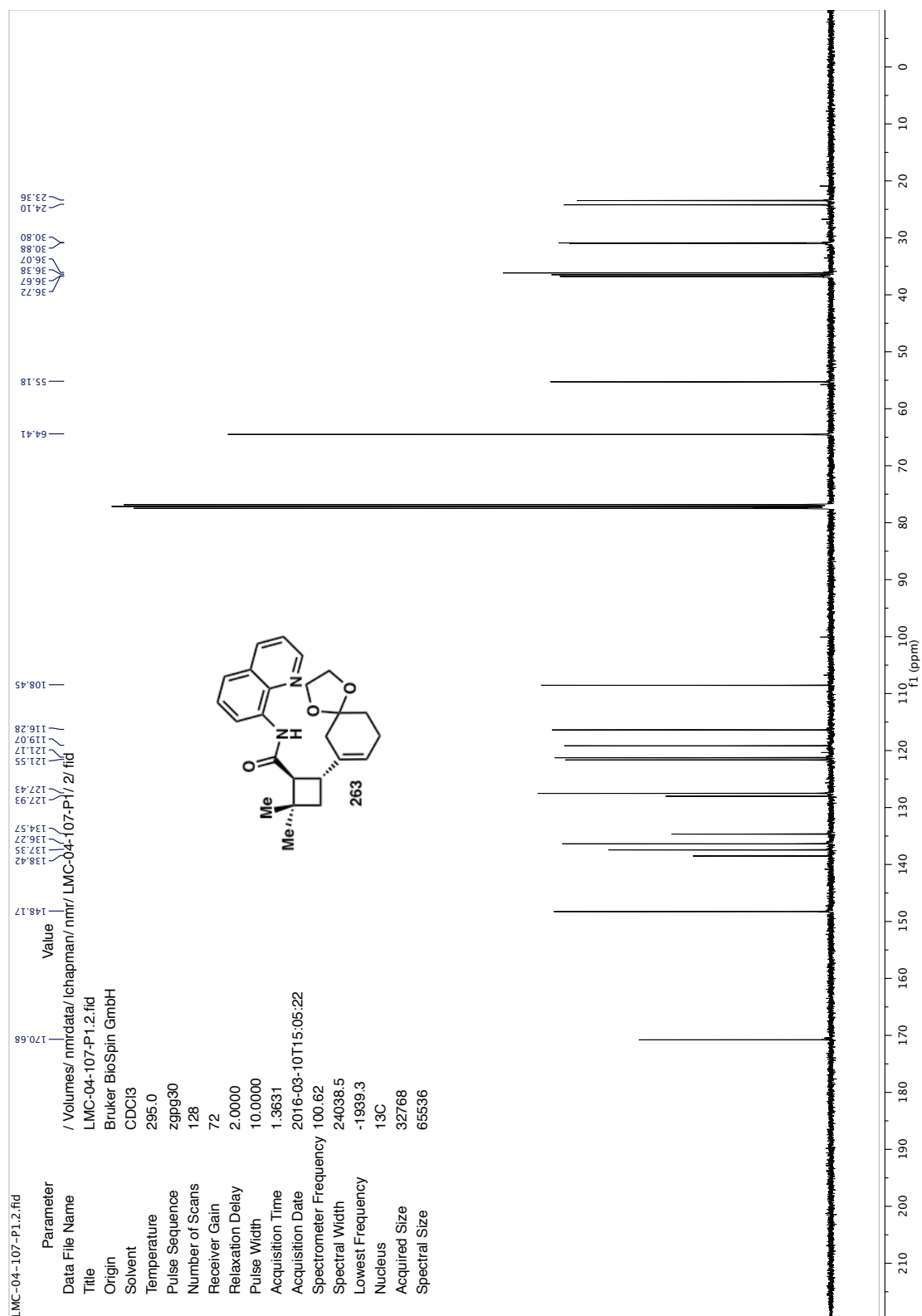
The remaining three aromatic proton signals are adjusted accordingly in the comparison list.

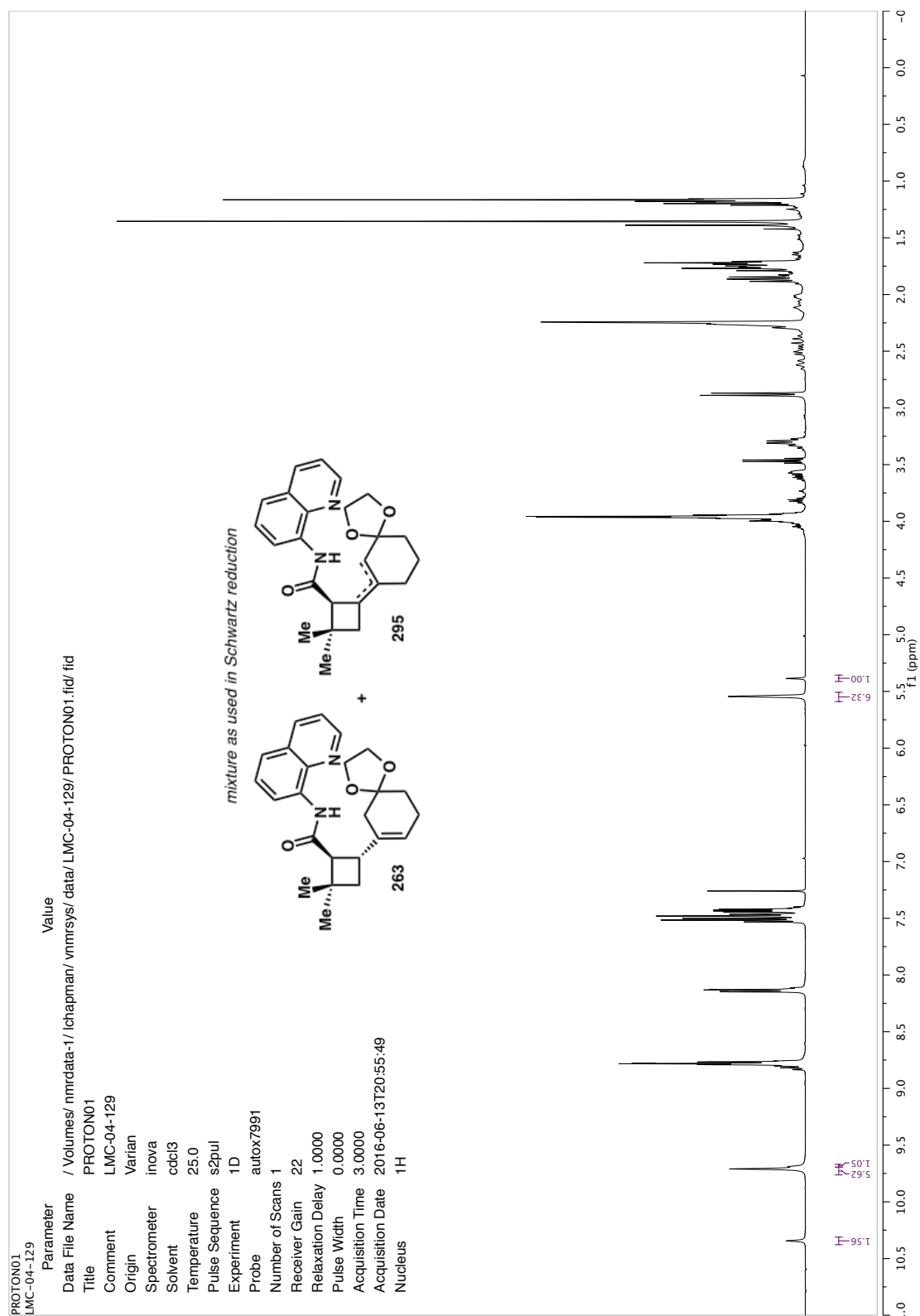
- (43) Center peak of CDCl_3 is referenced to 76.999 ppm, as shown in the Shao et al. report, see ^{13}C spectral comparison.

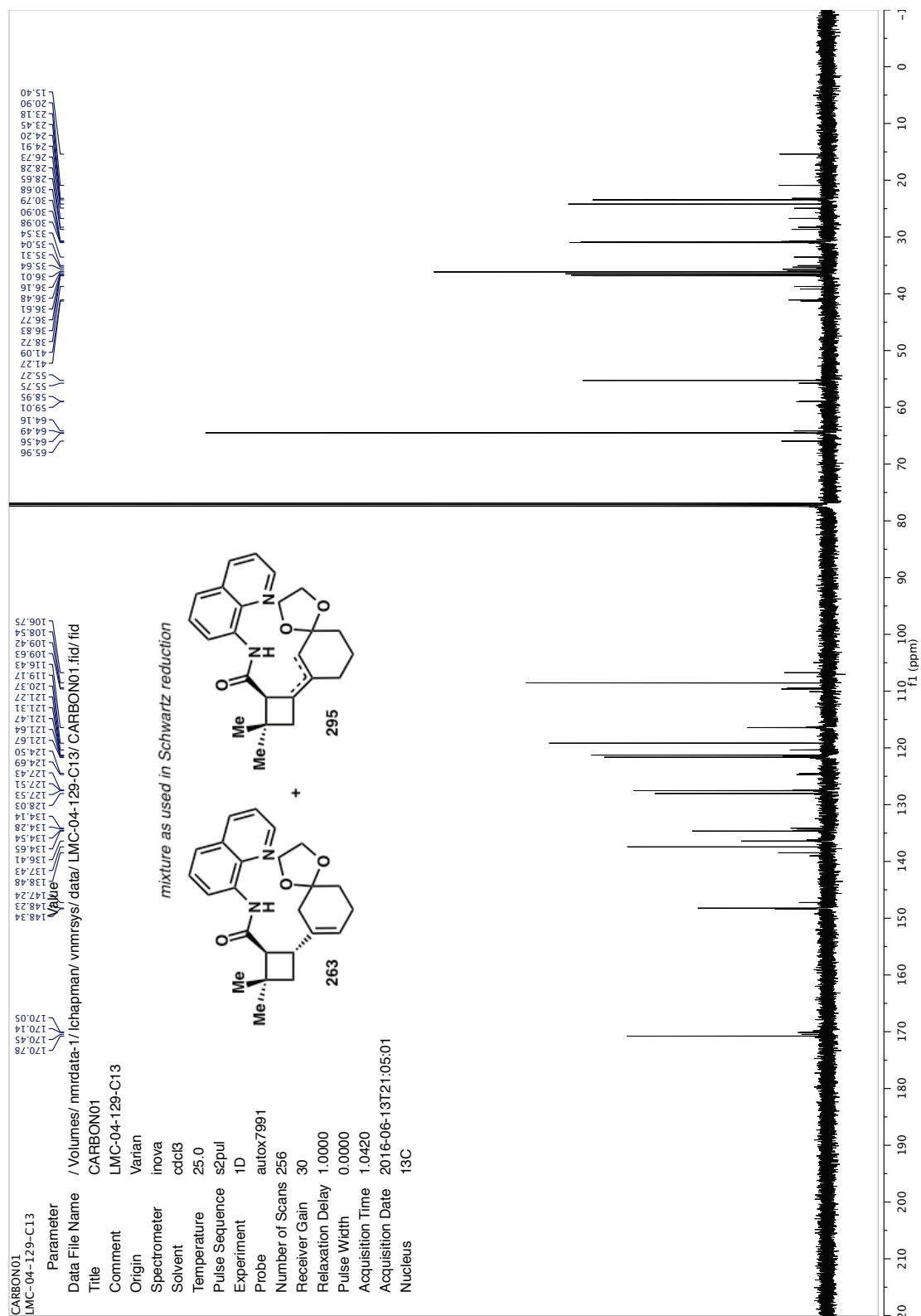
Appendix 3

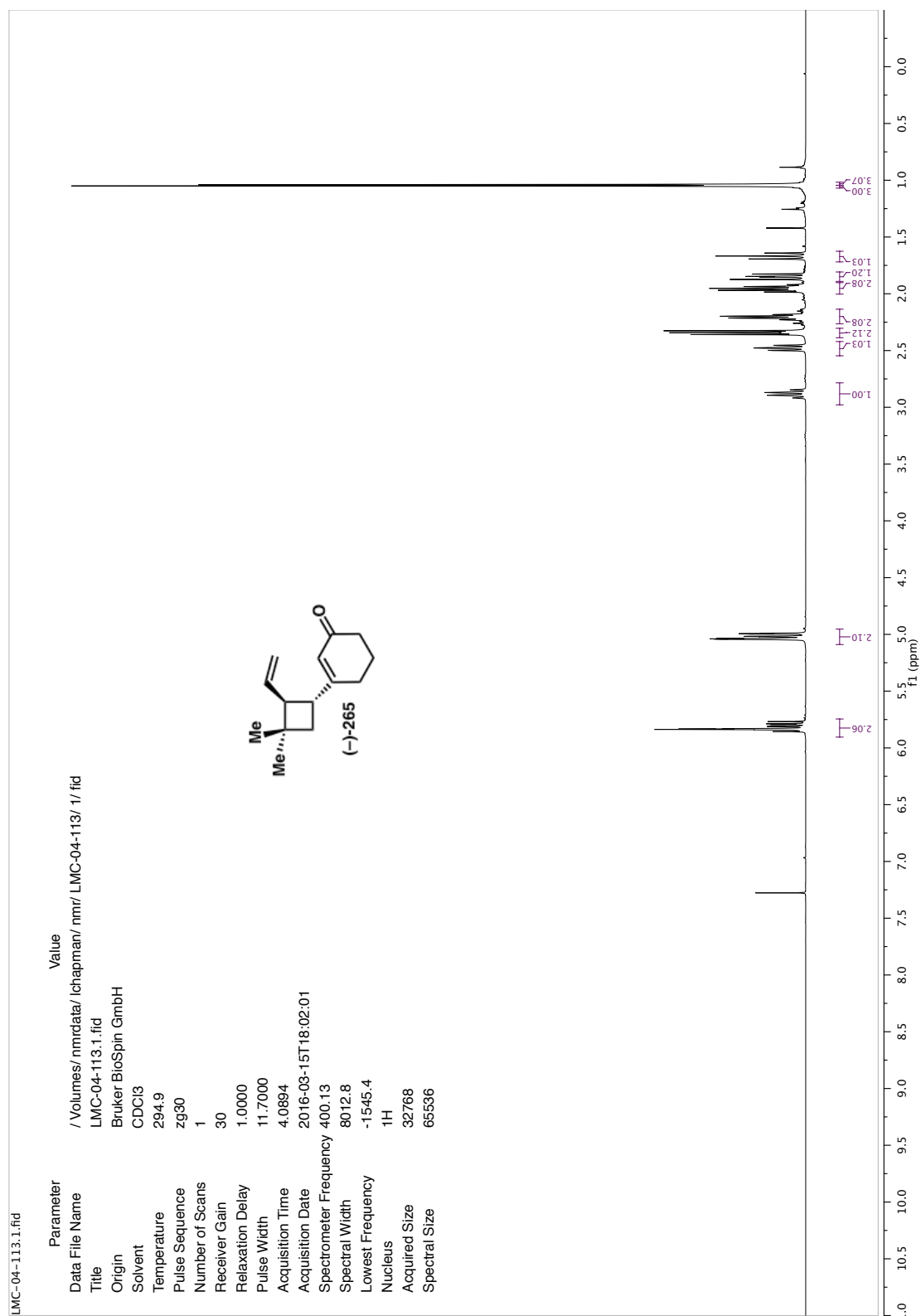
*Spectra Relevant to Chapter 3:
Revised Strategies for the Enantioselective
Total Synthesis of (+)-Psiguadial B*

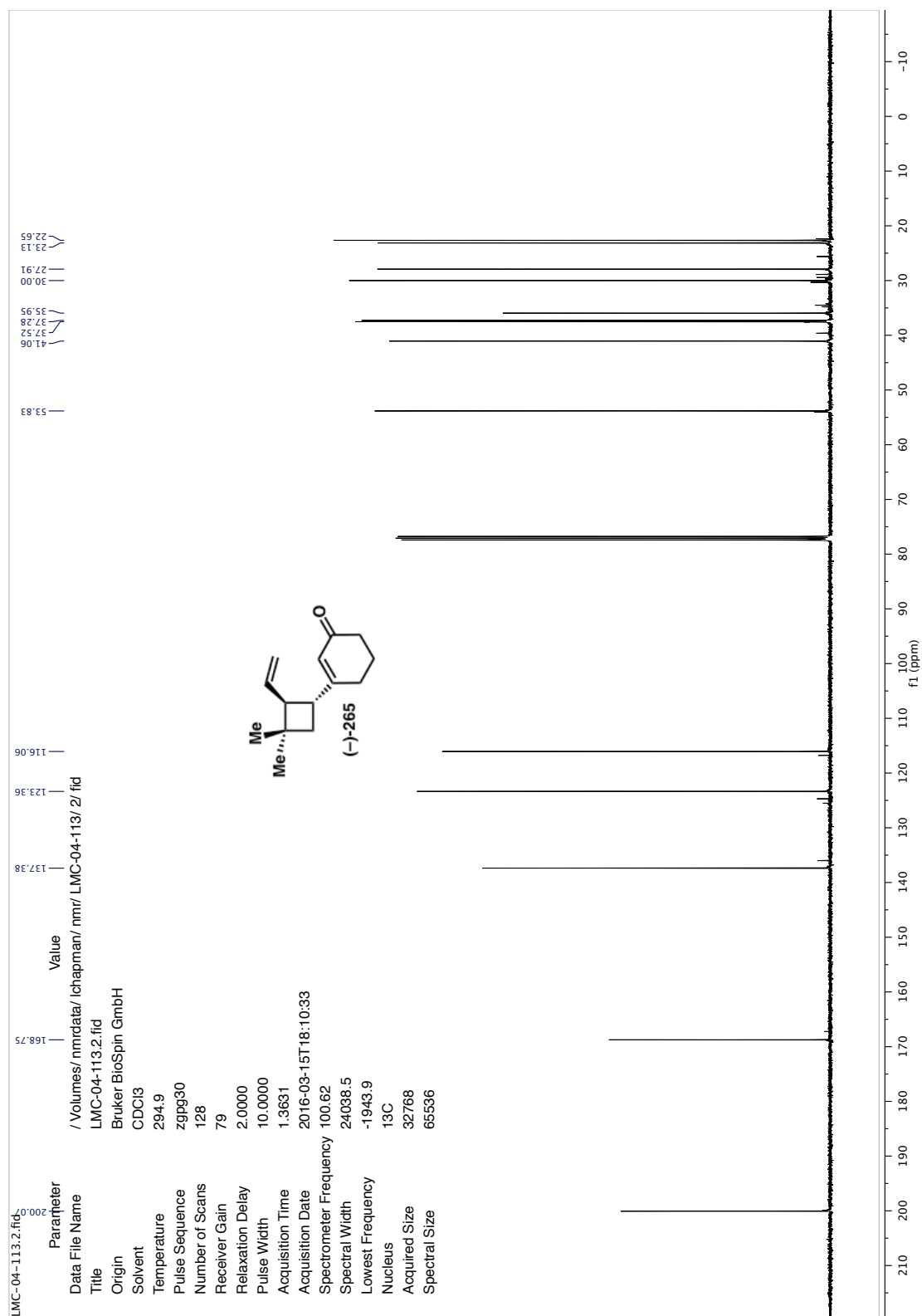


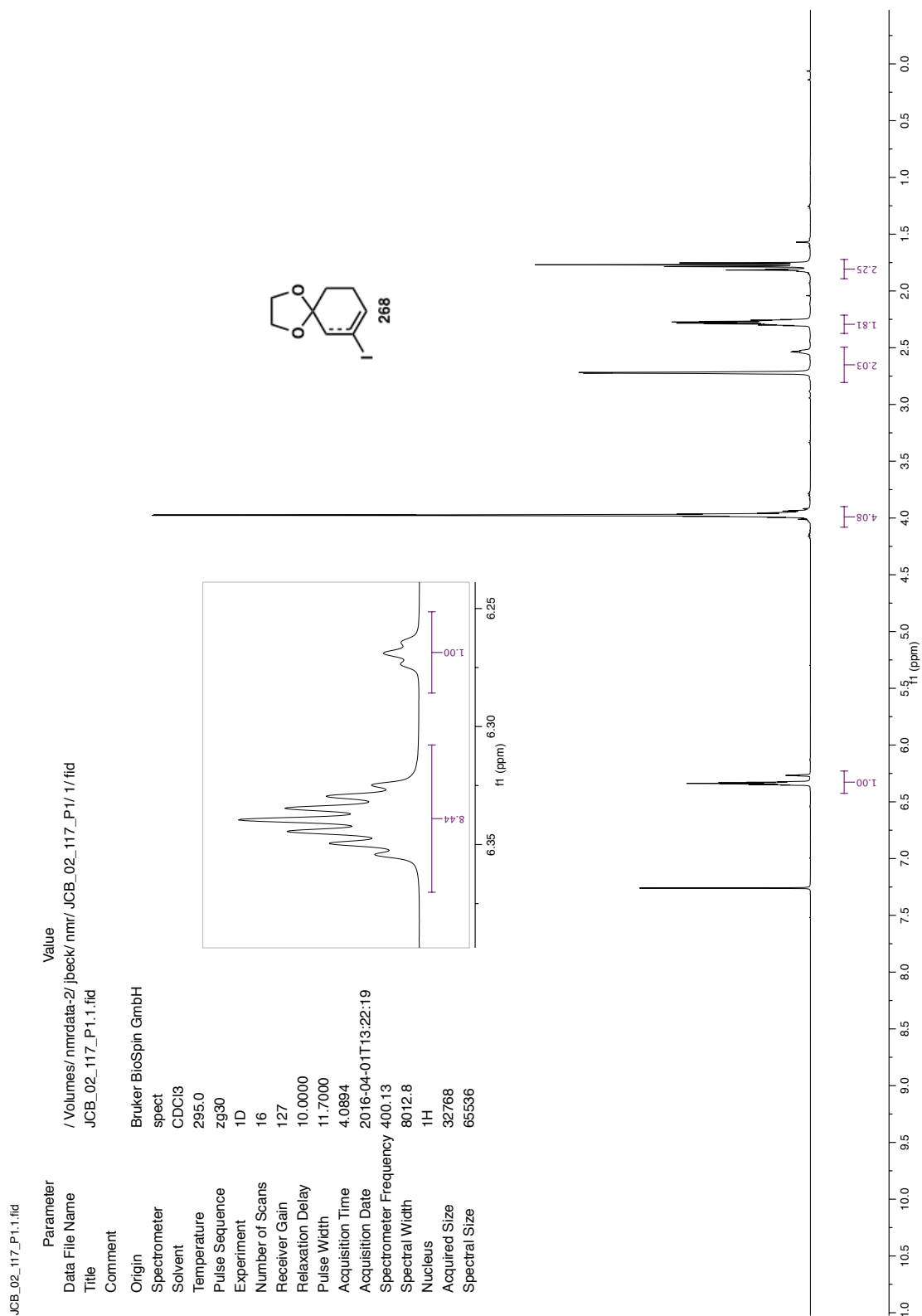


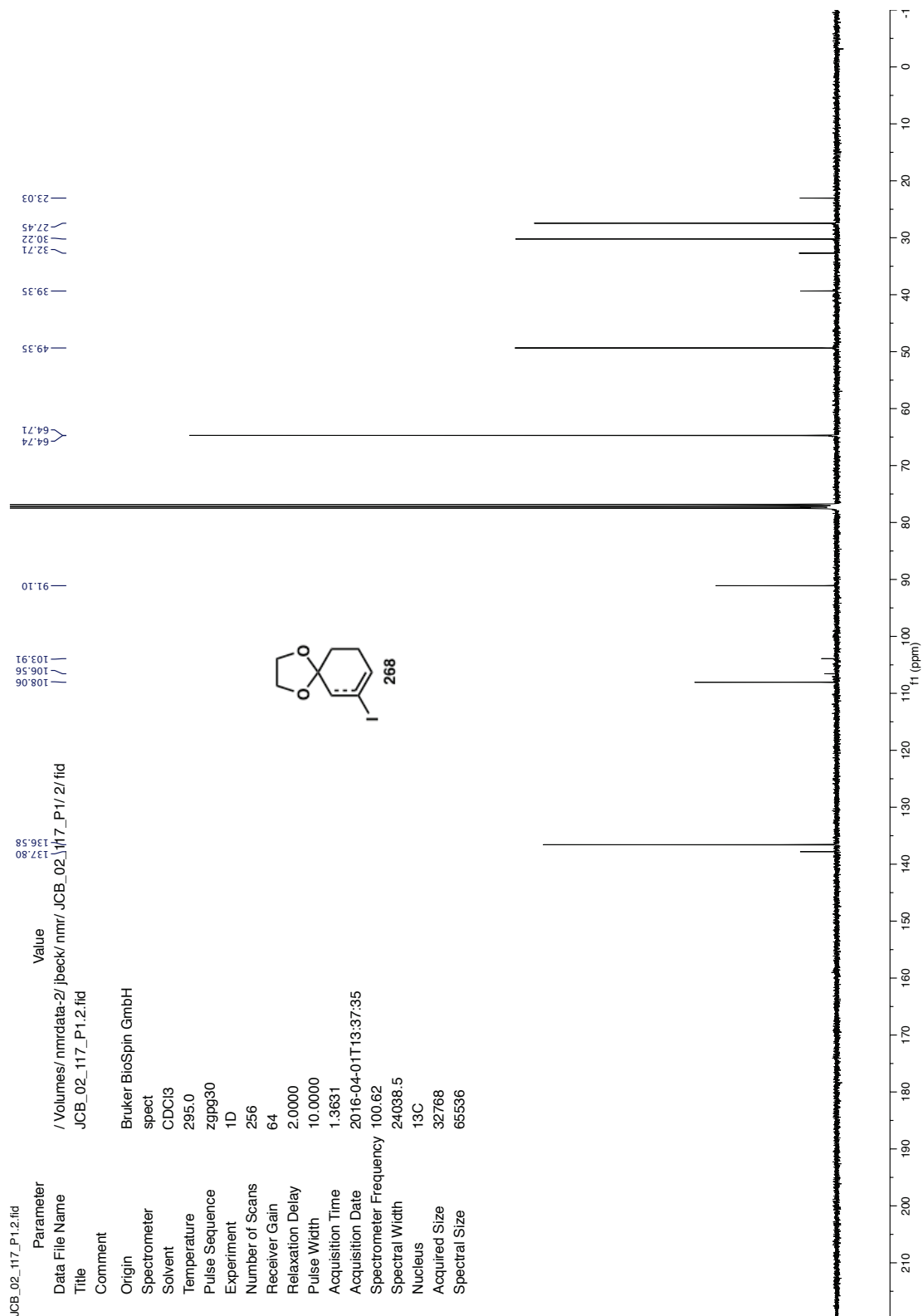


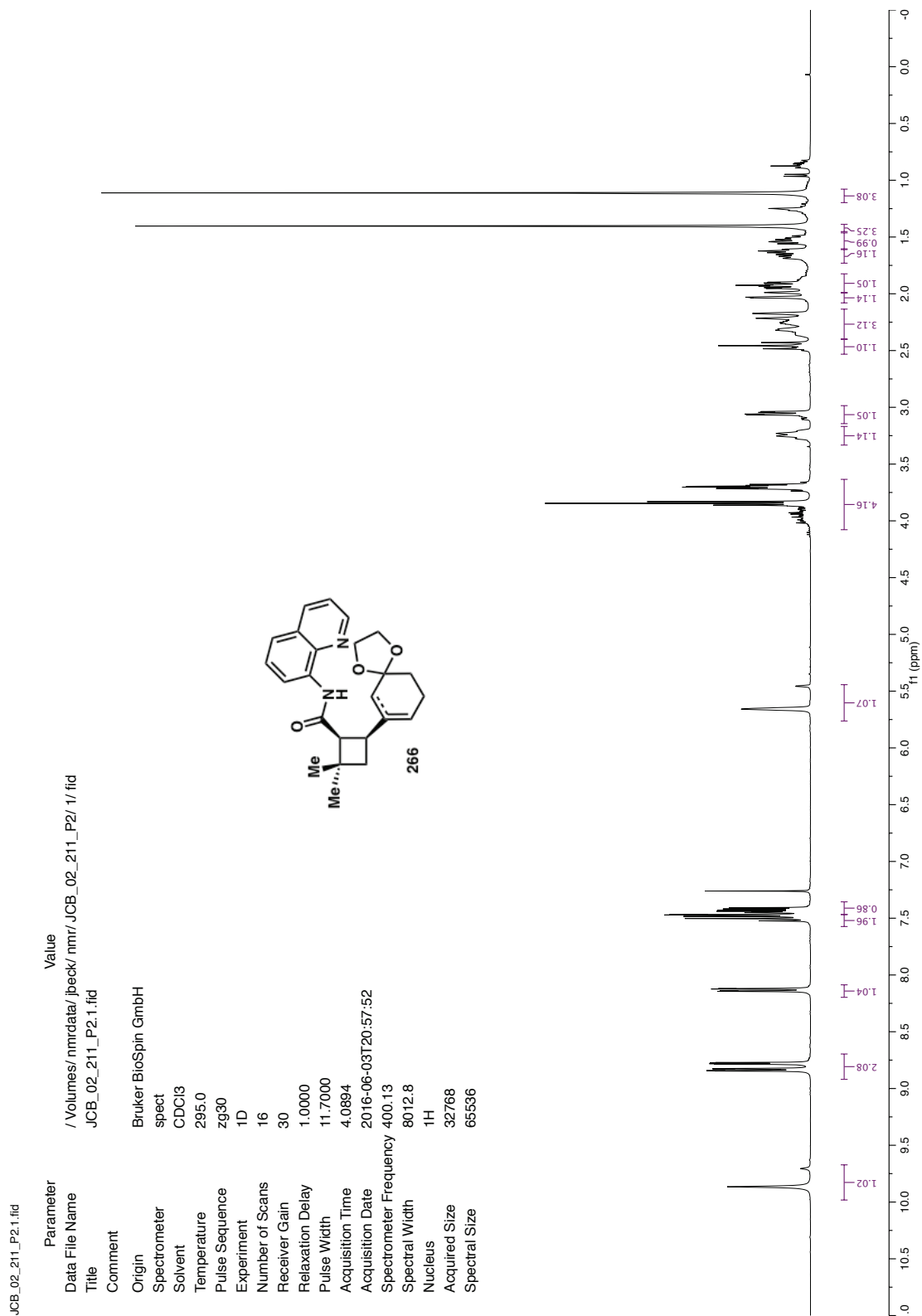


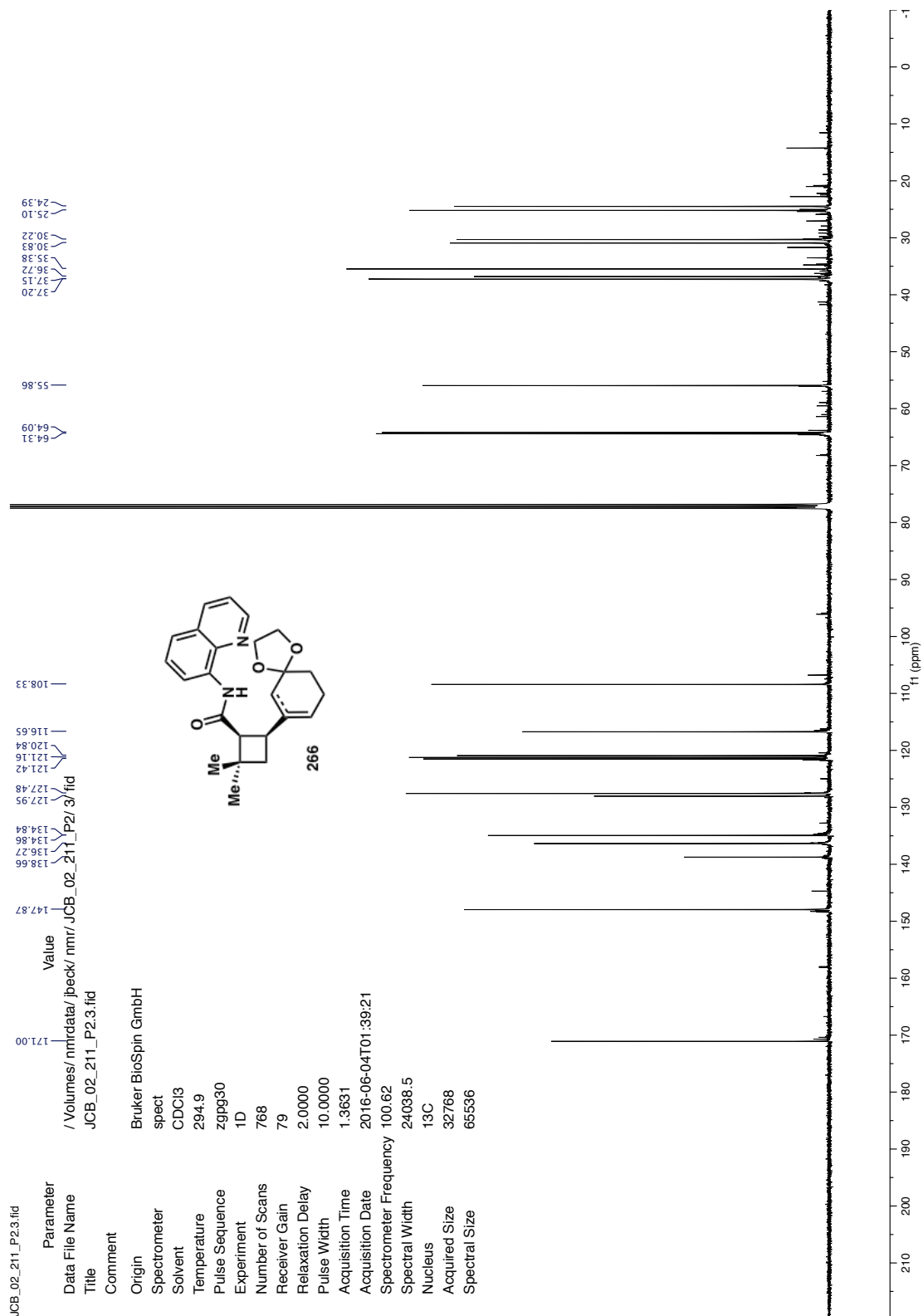


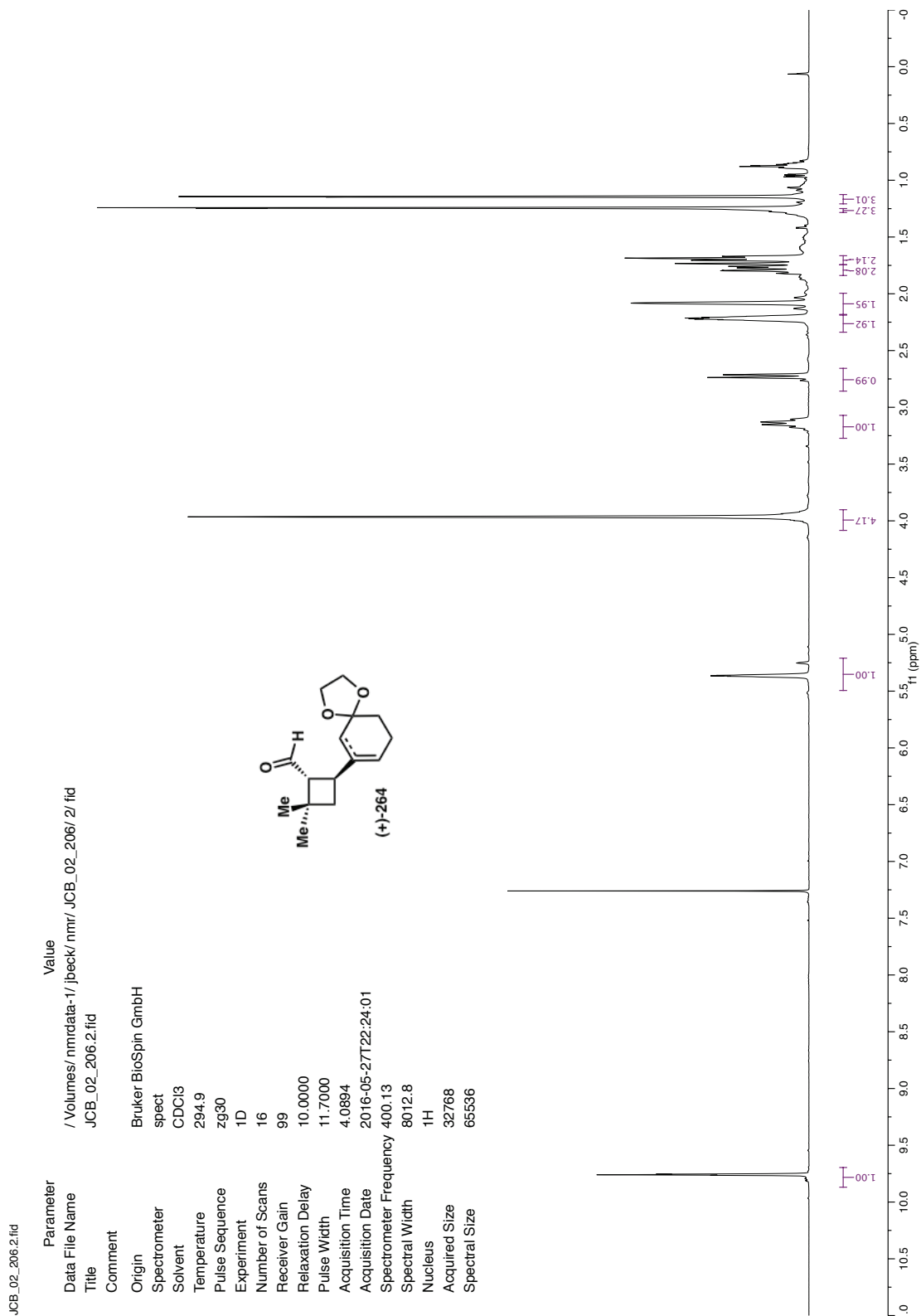


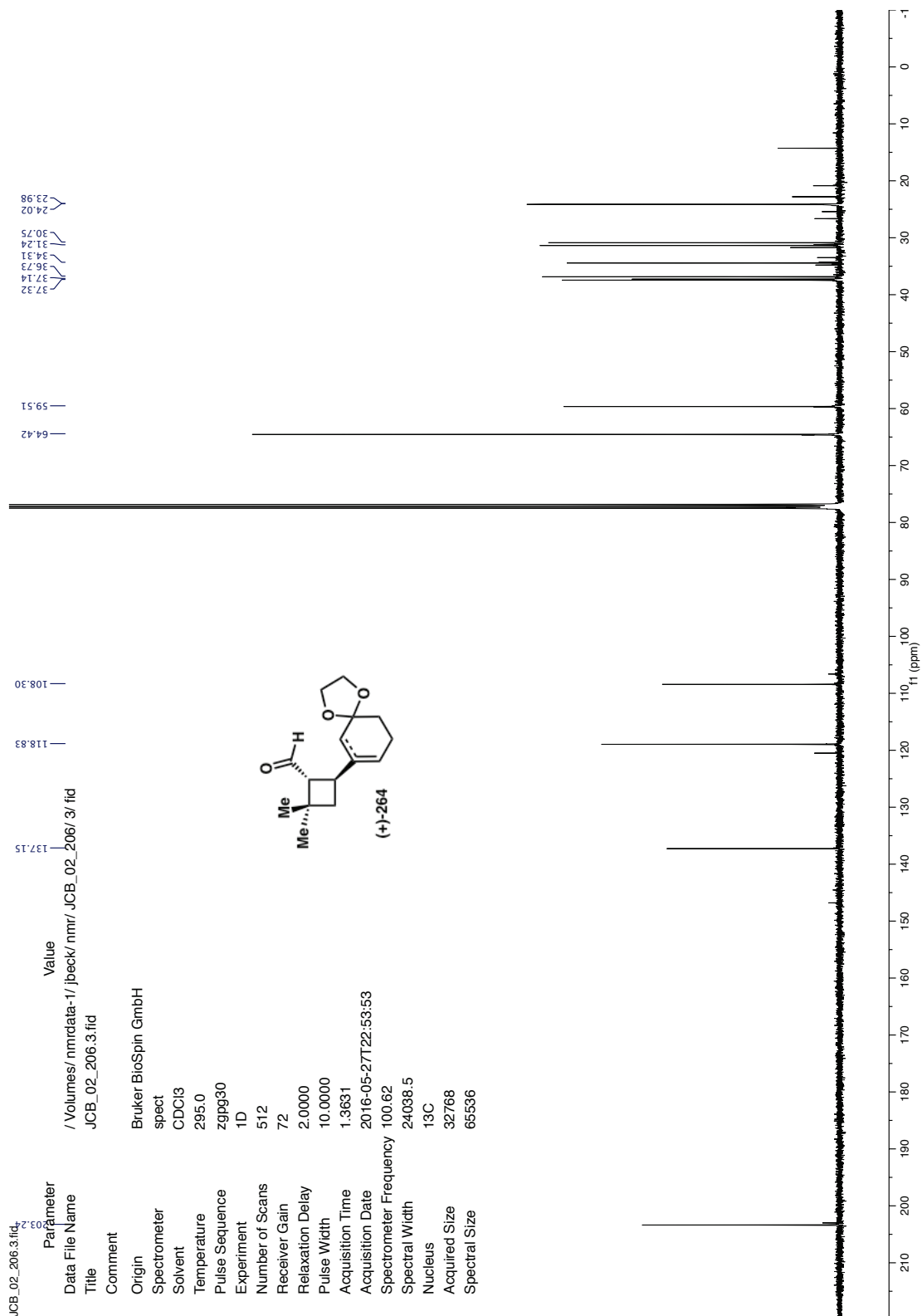


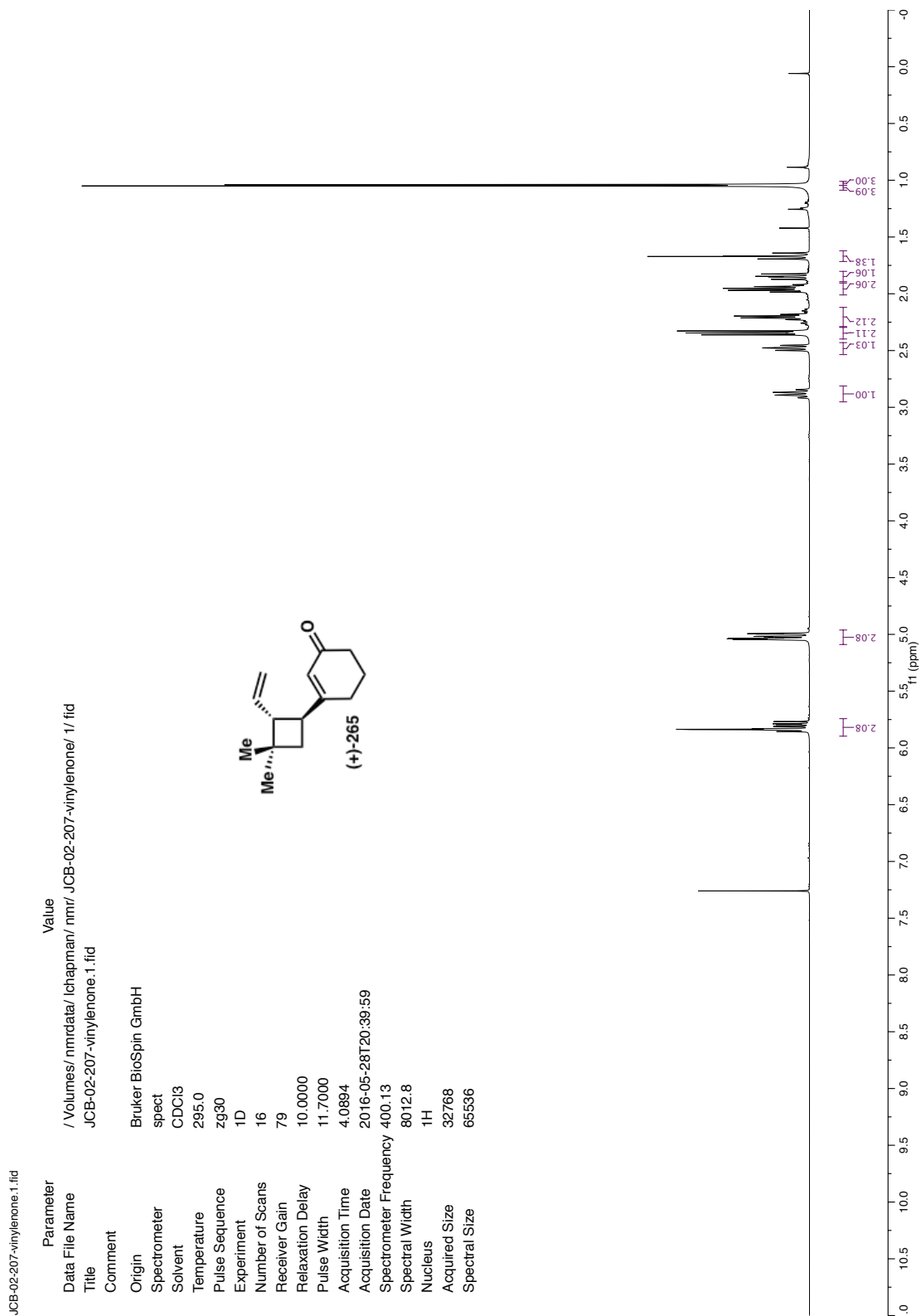


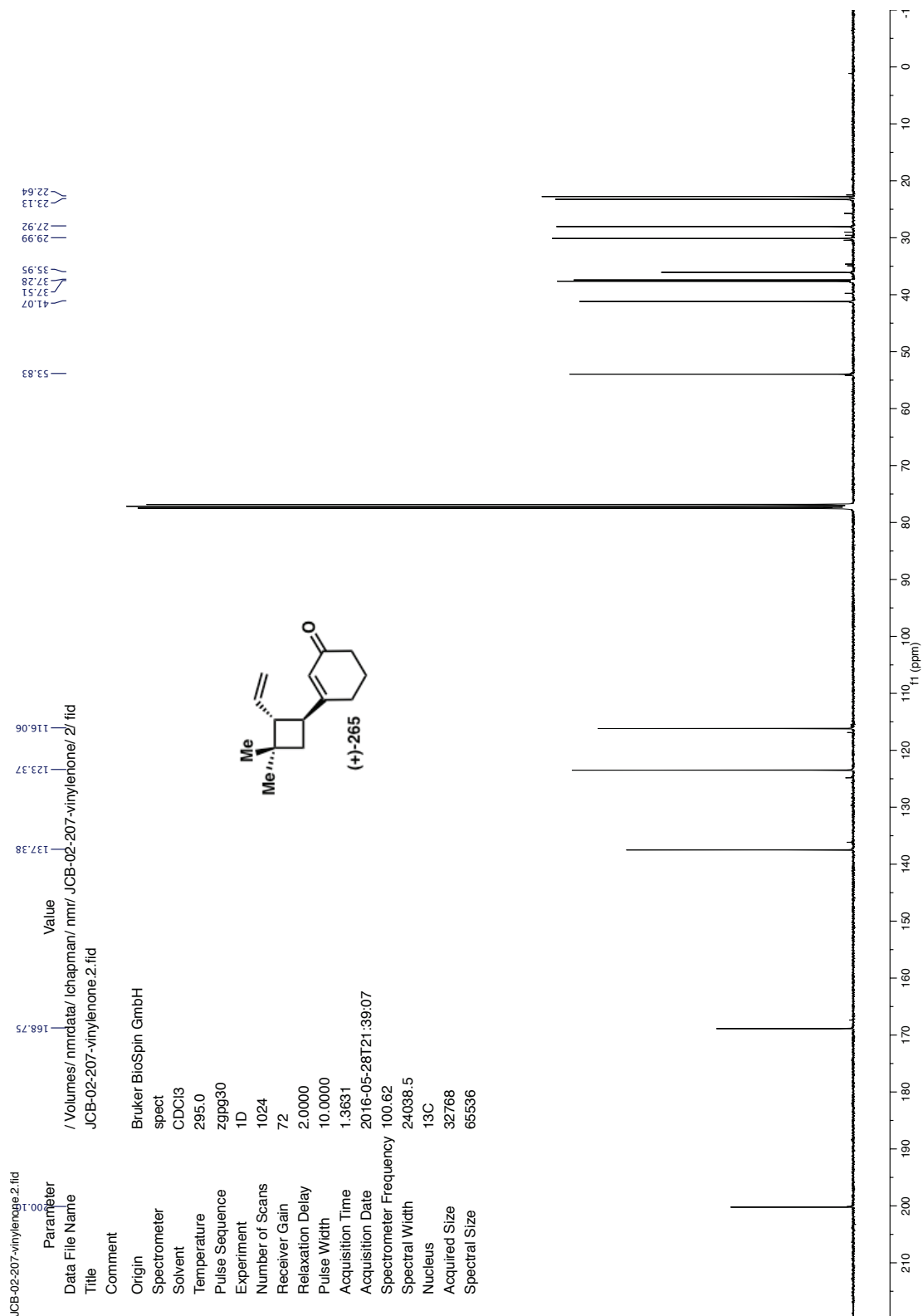


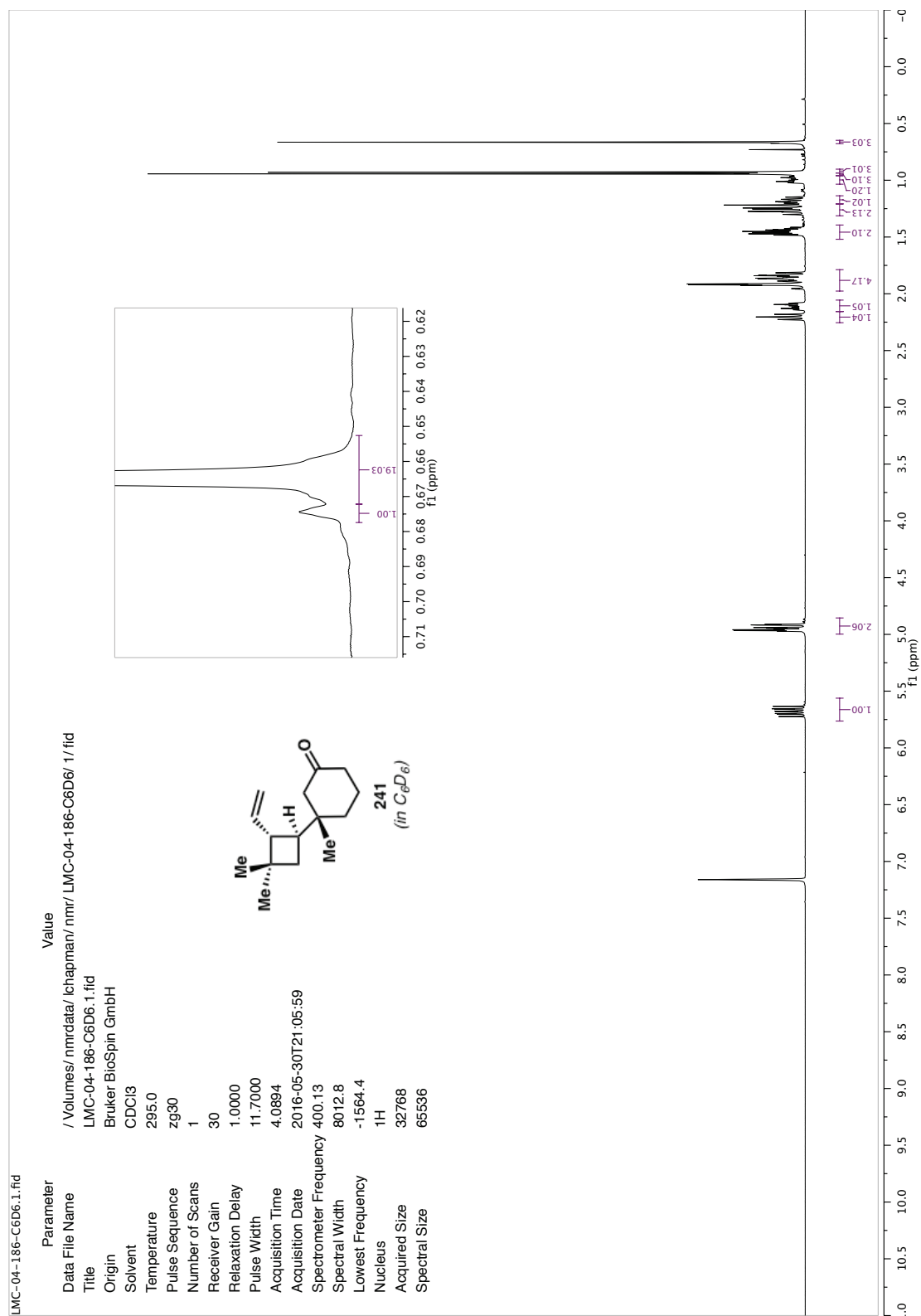


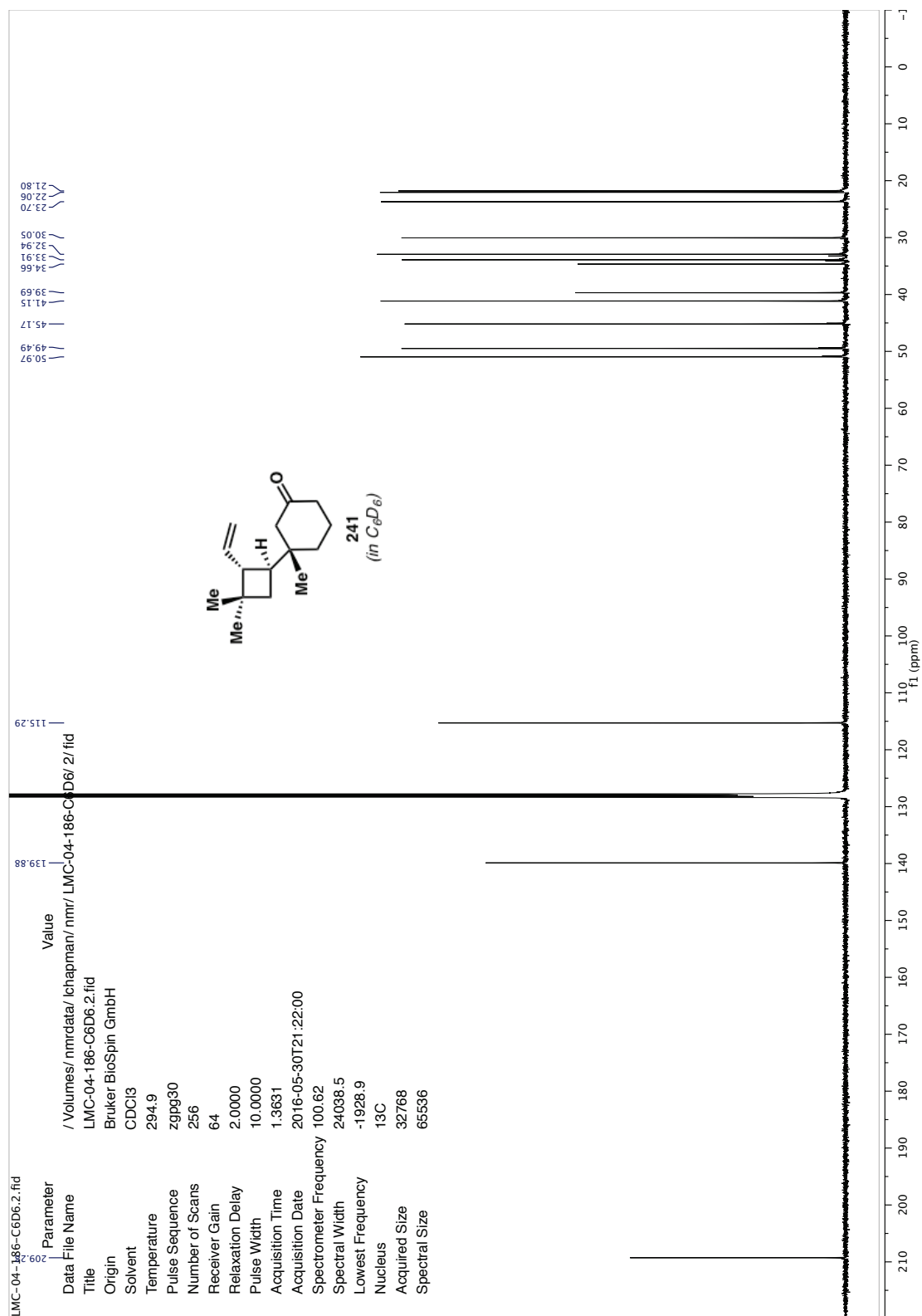


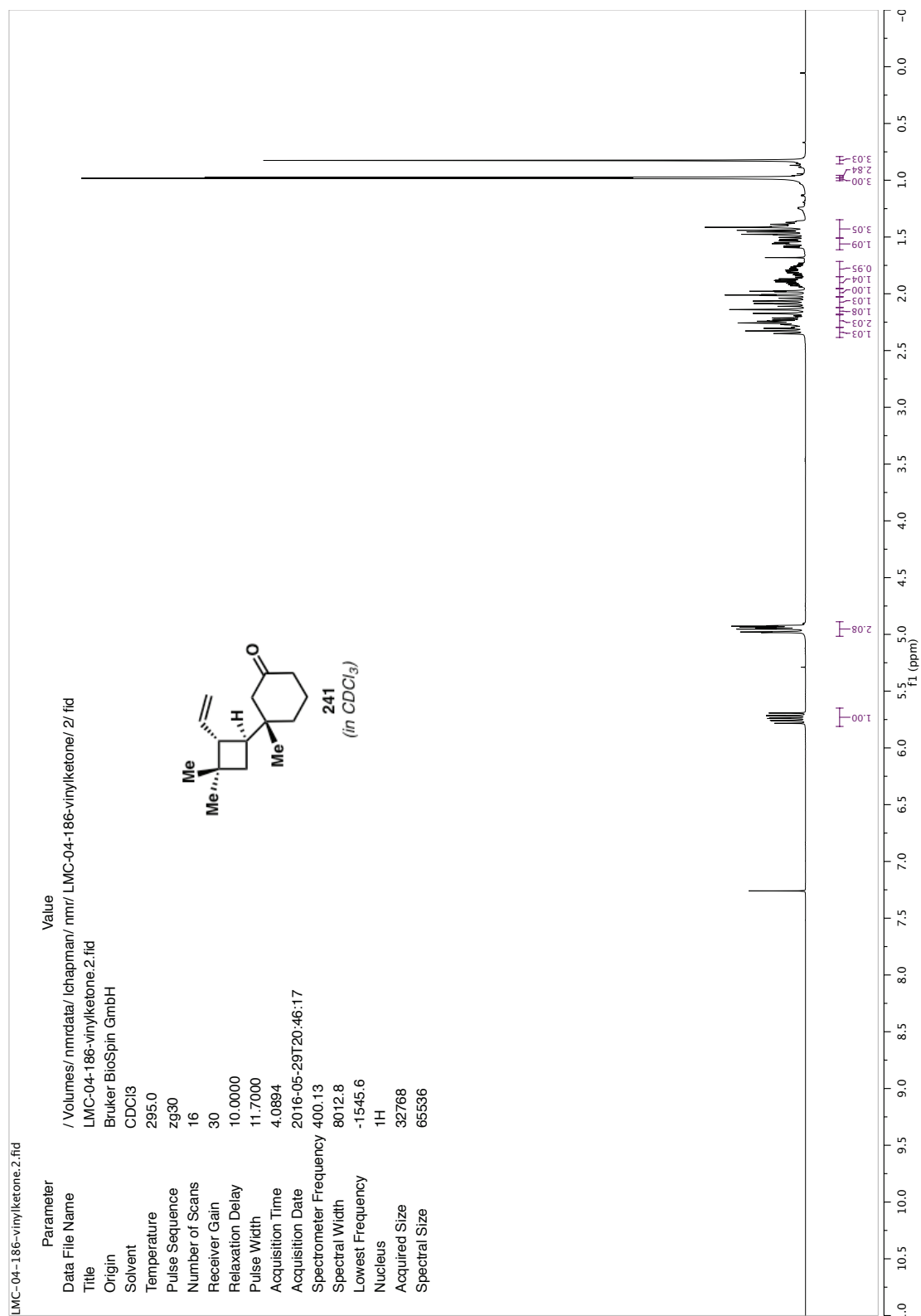


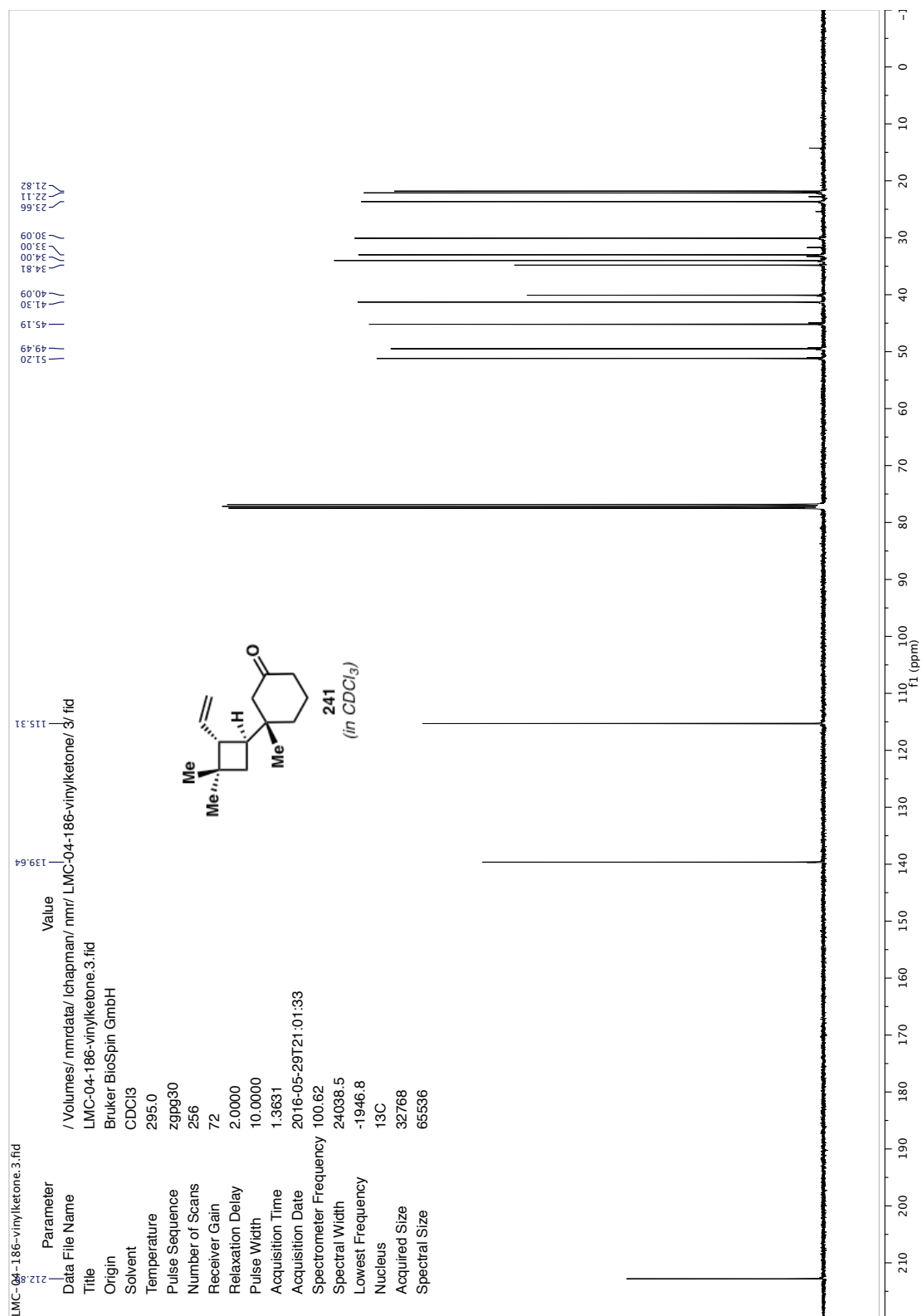


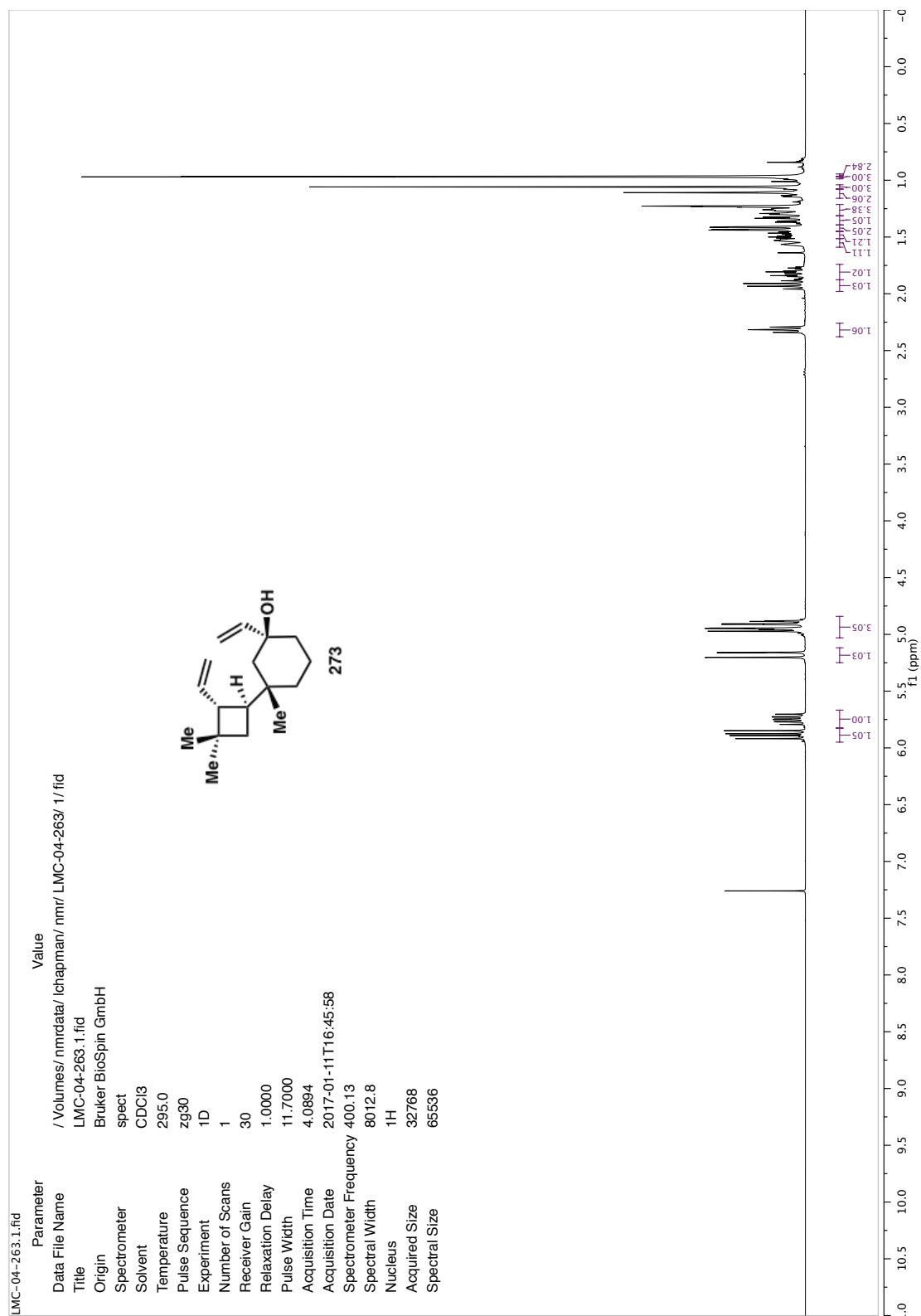


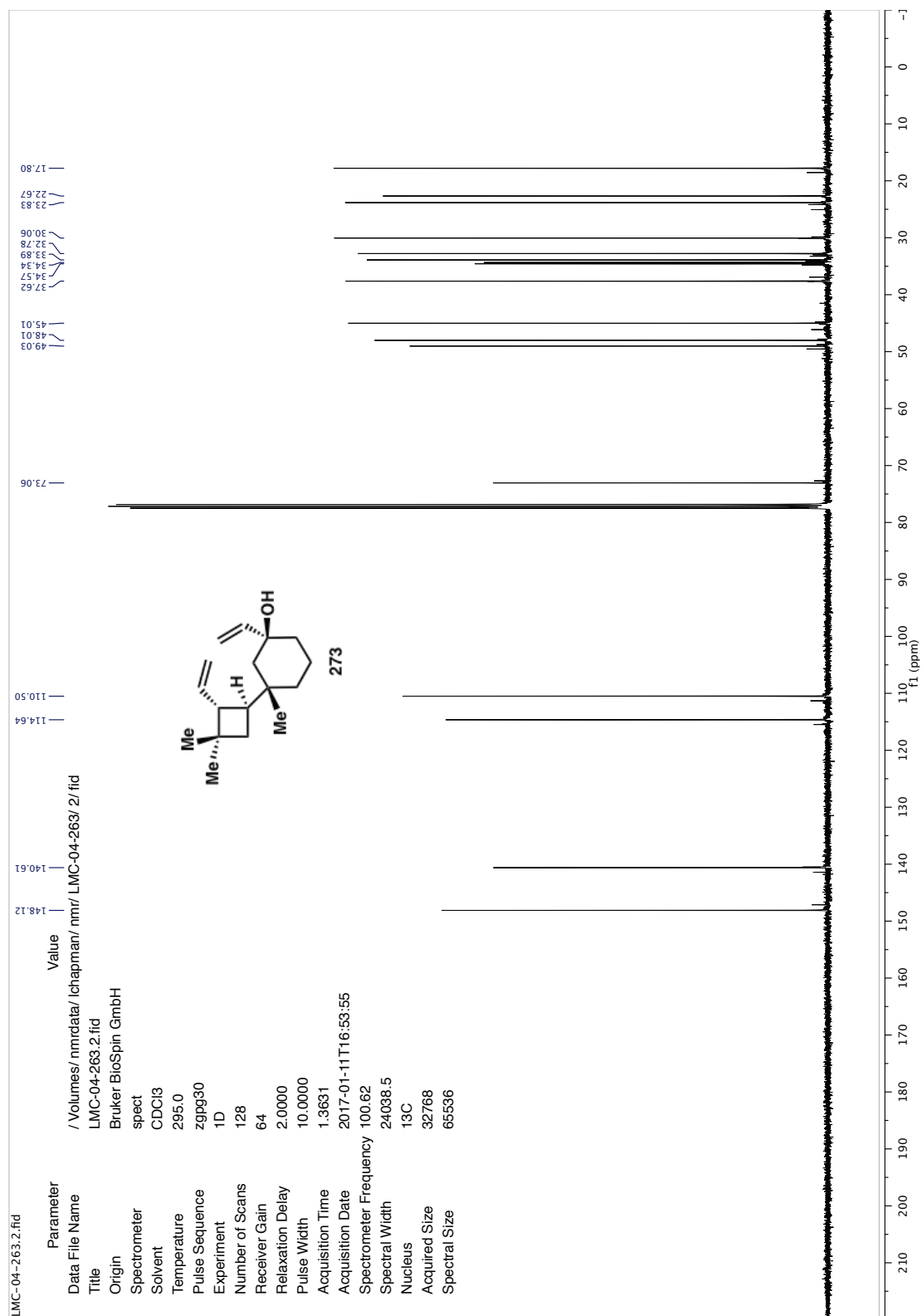


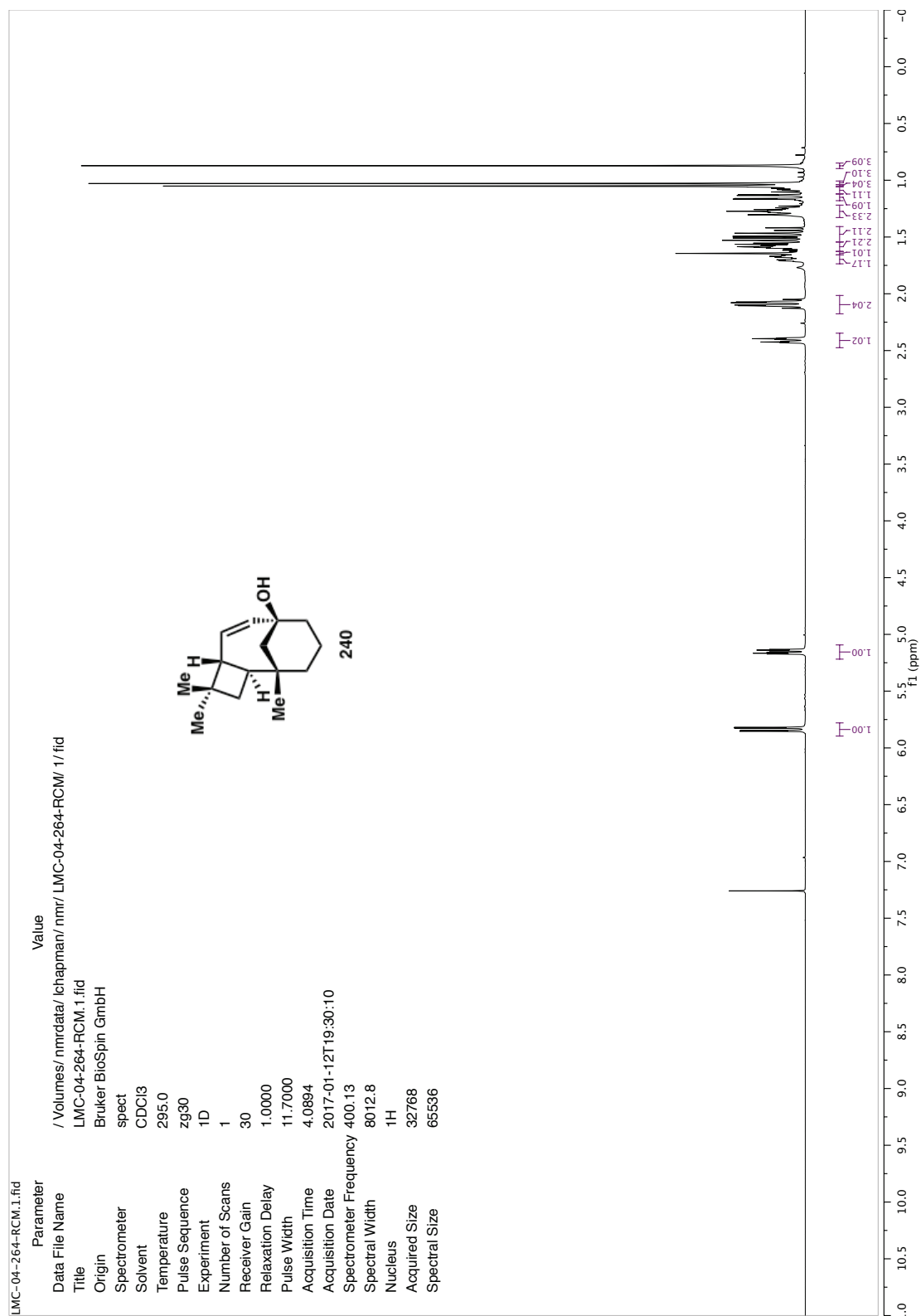


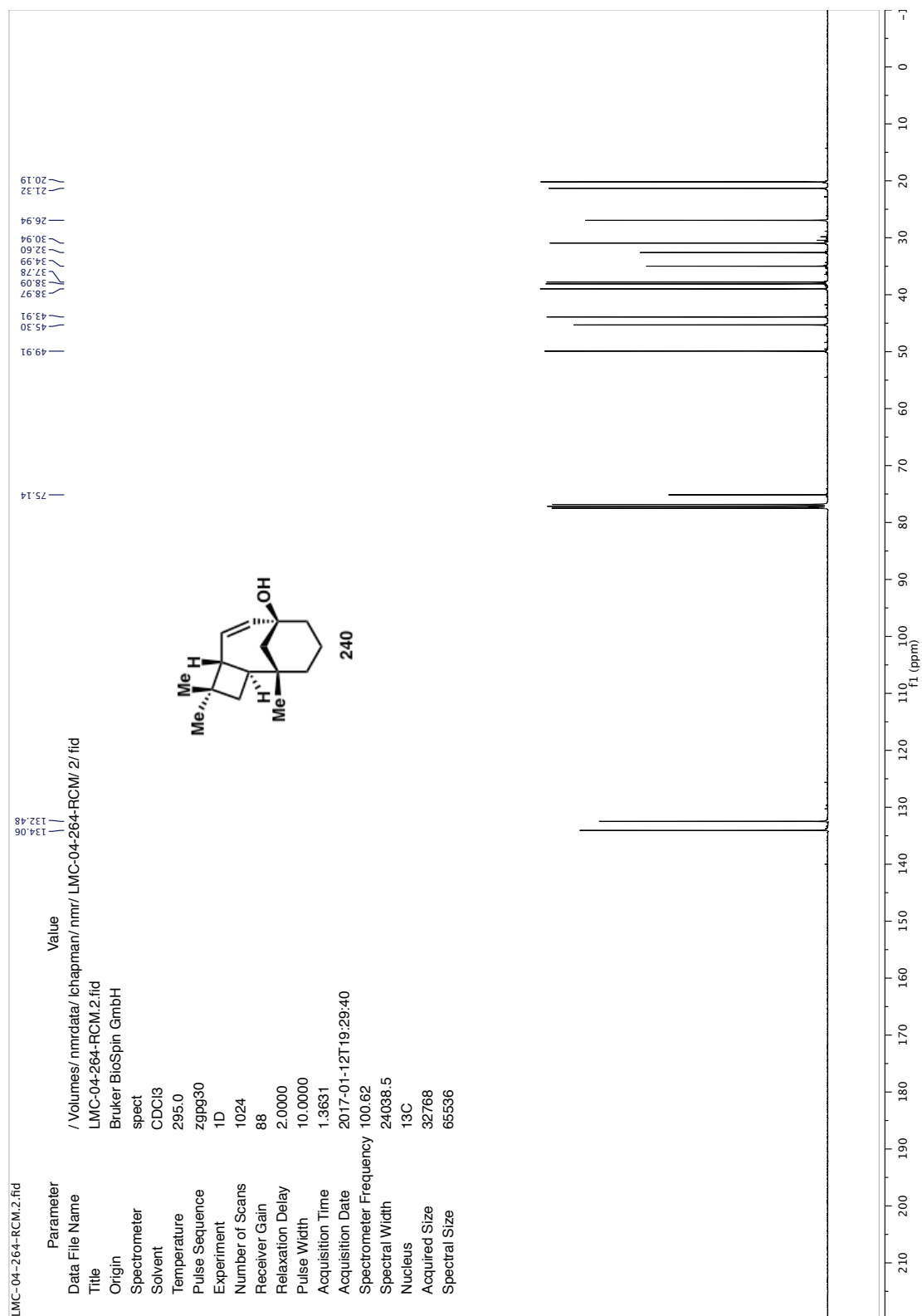


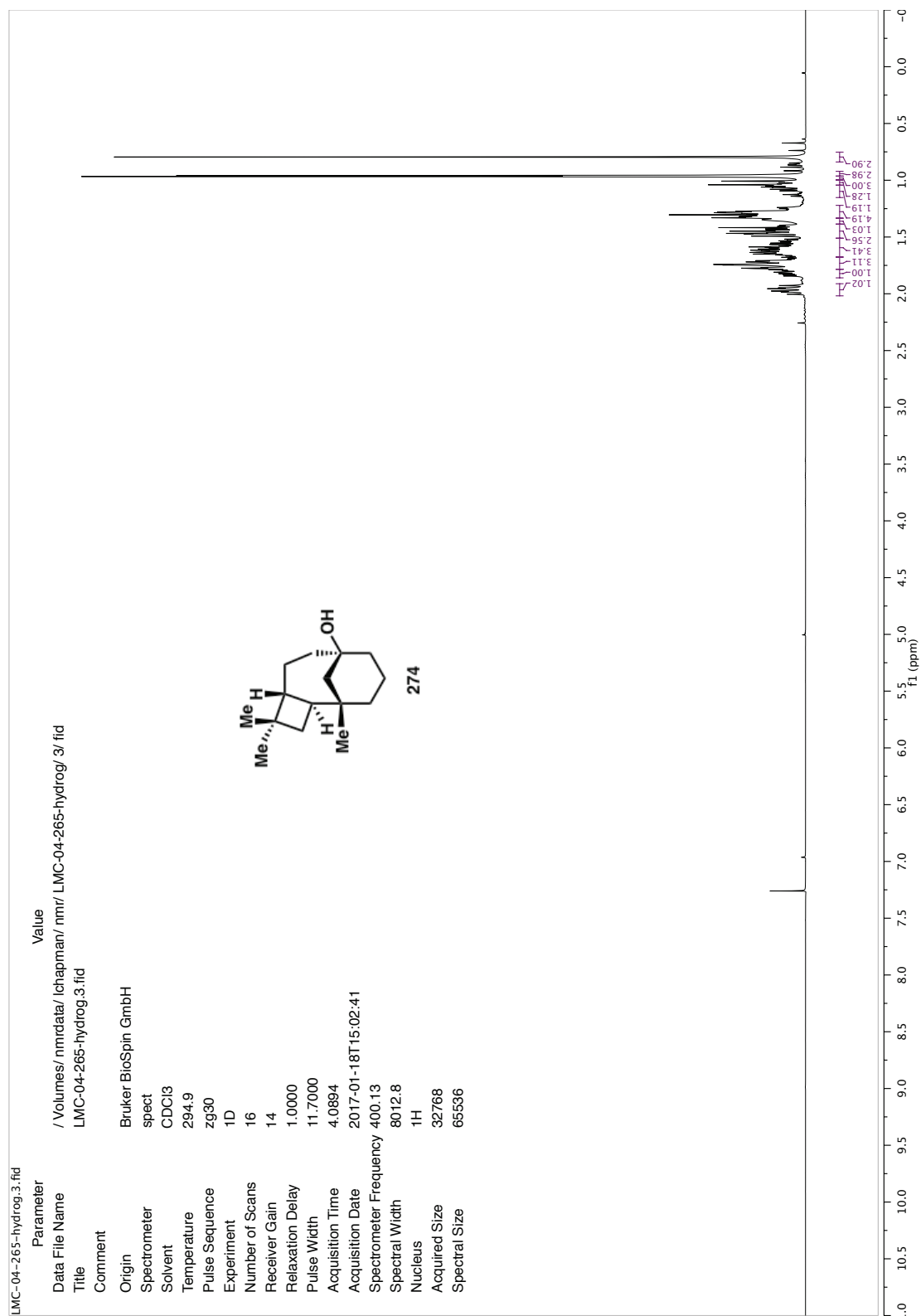


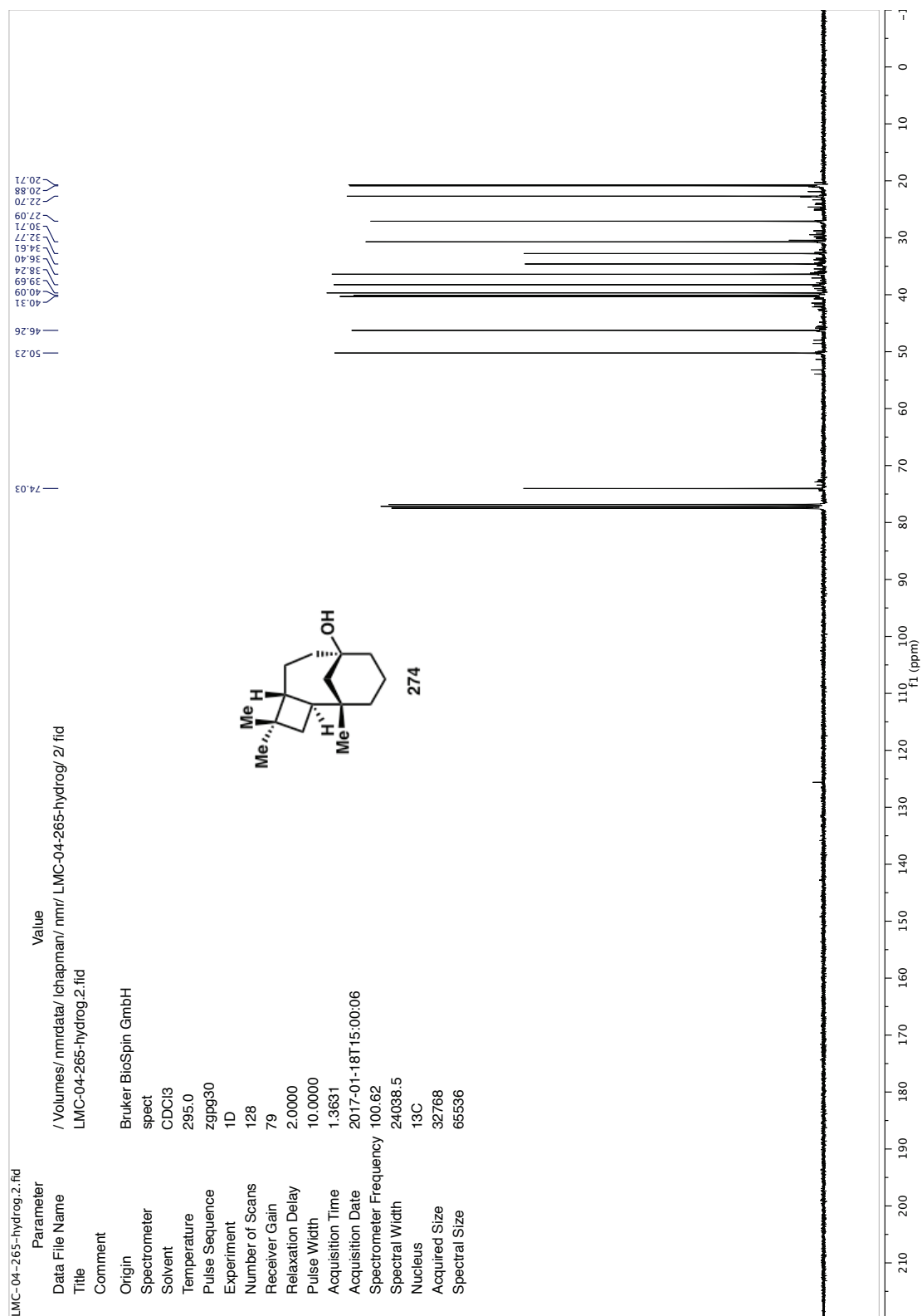


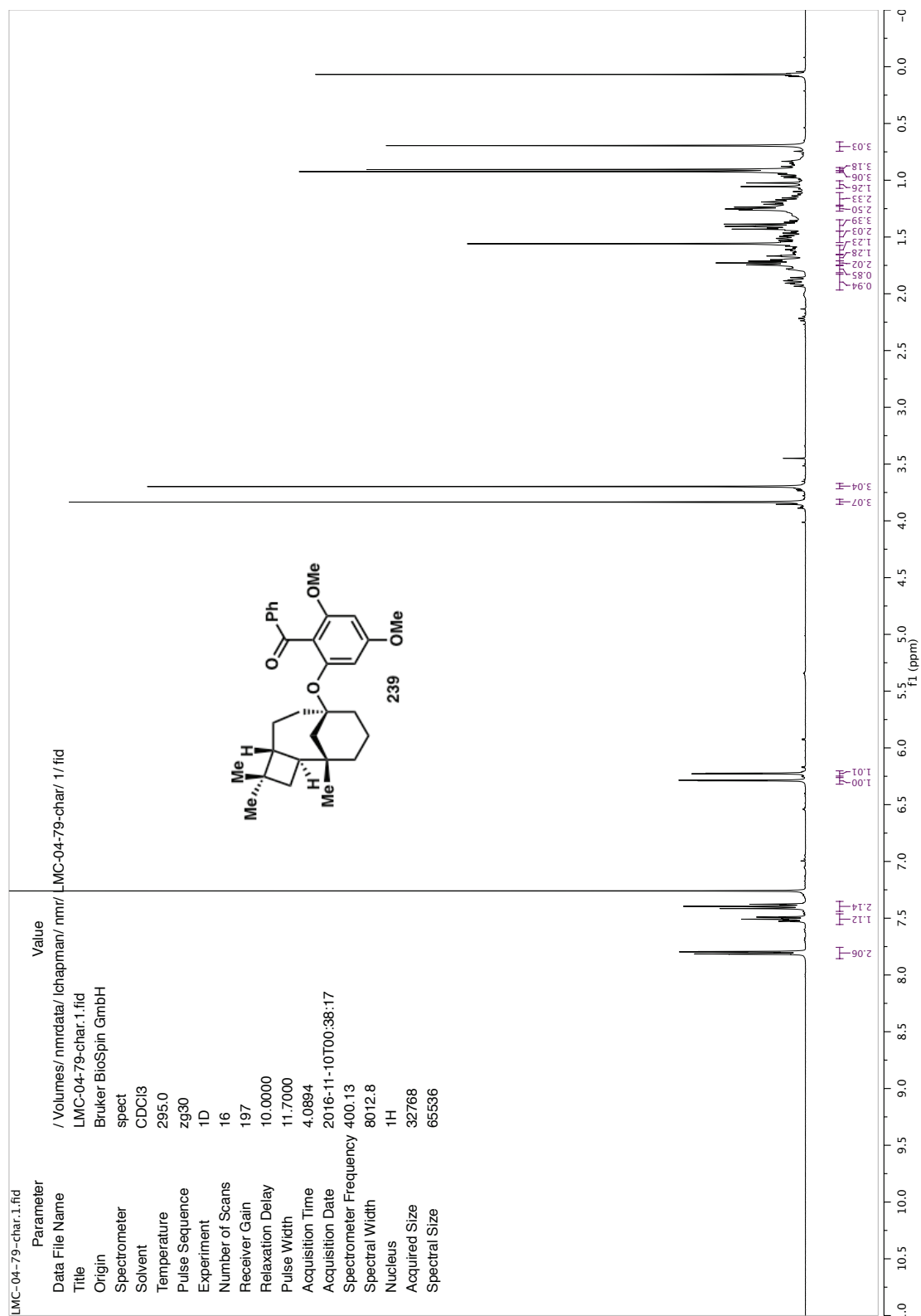


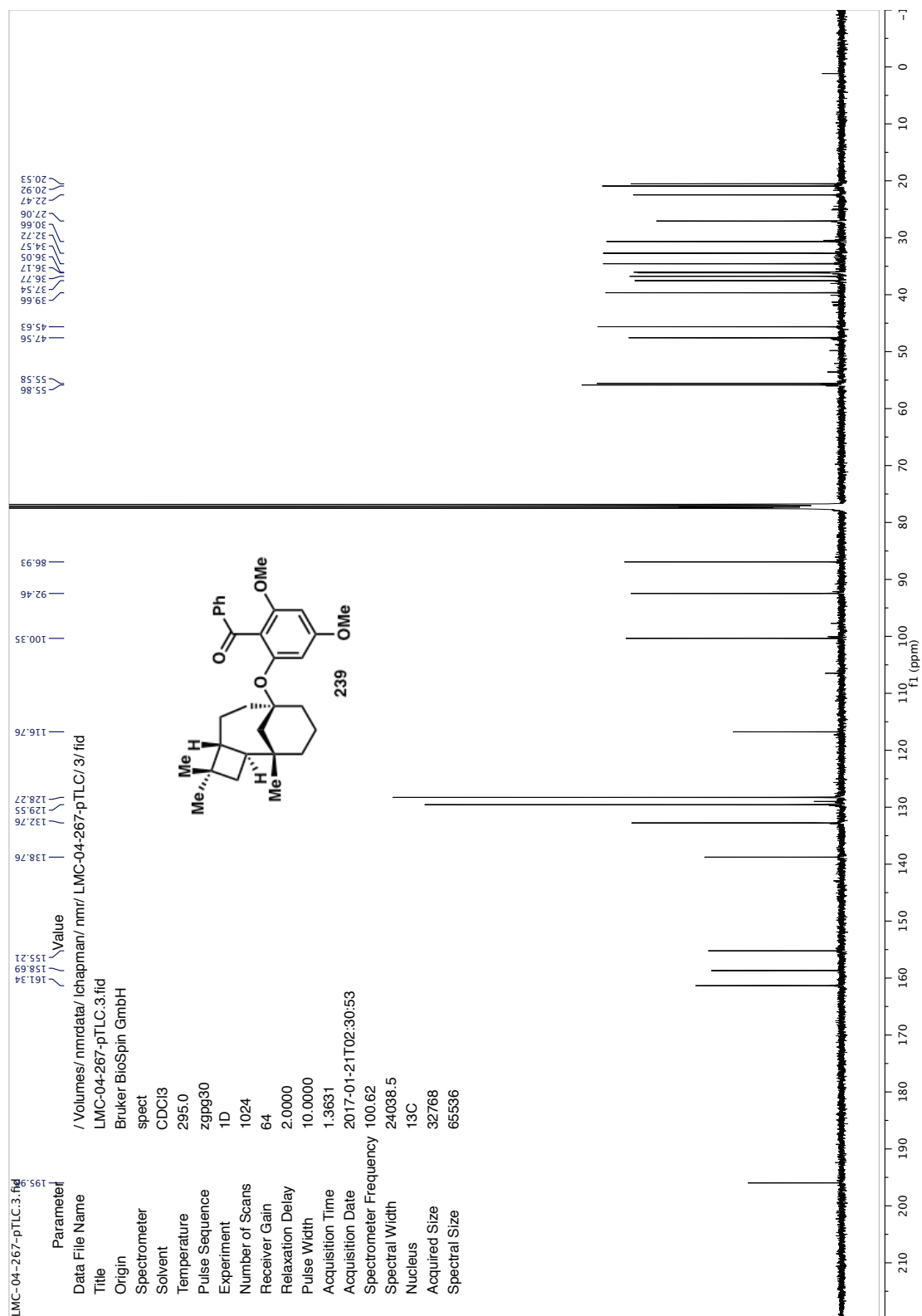


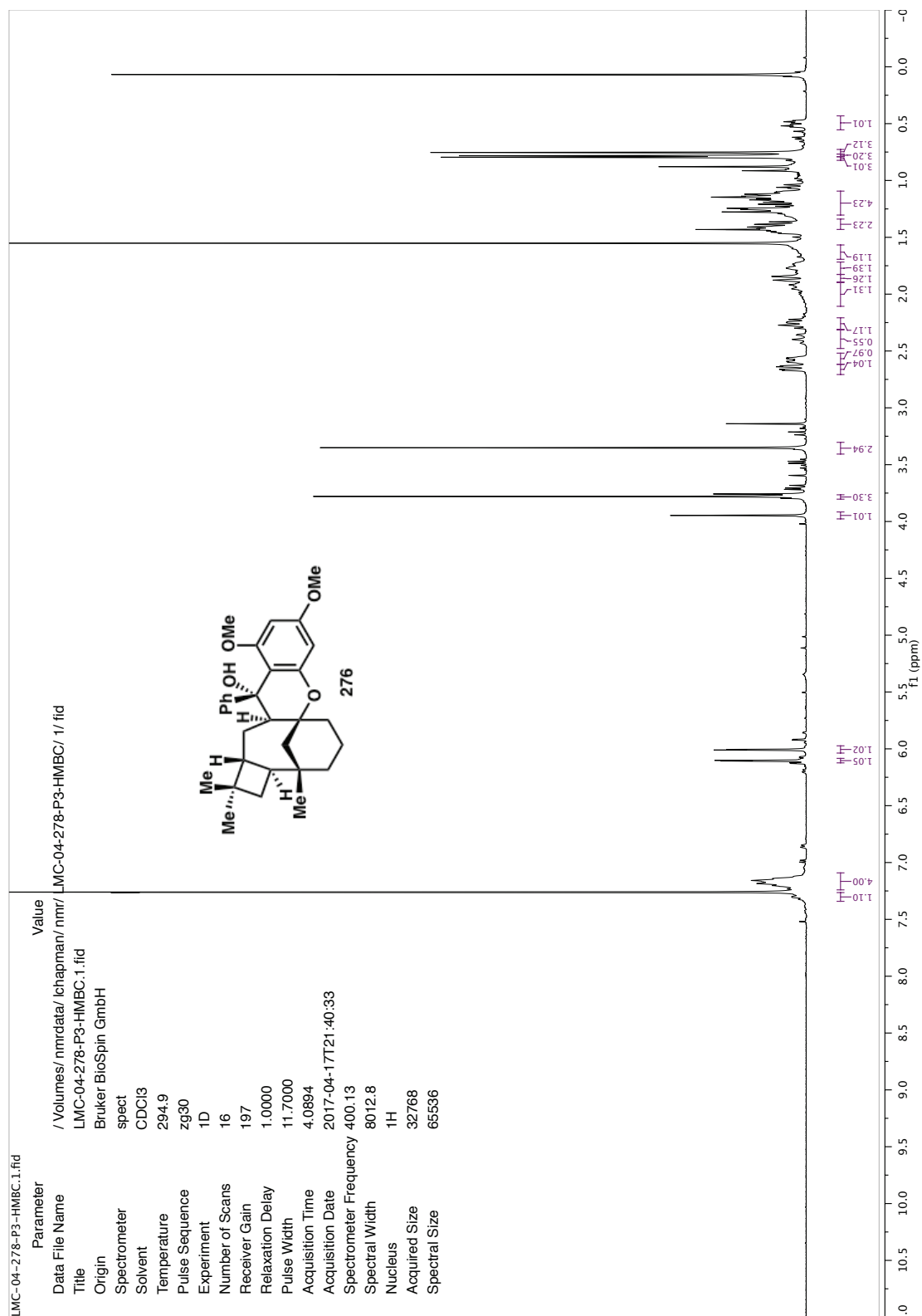


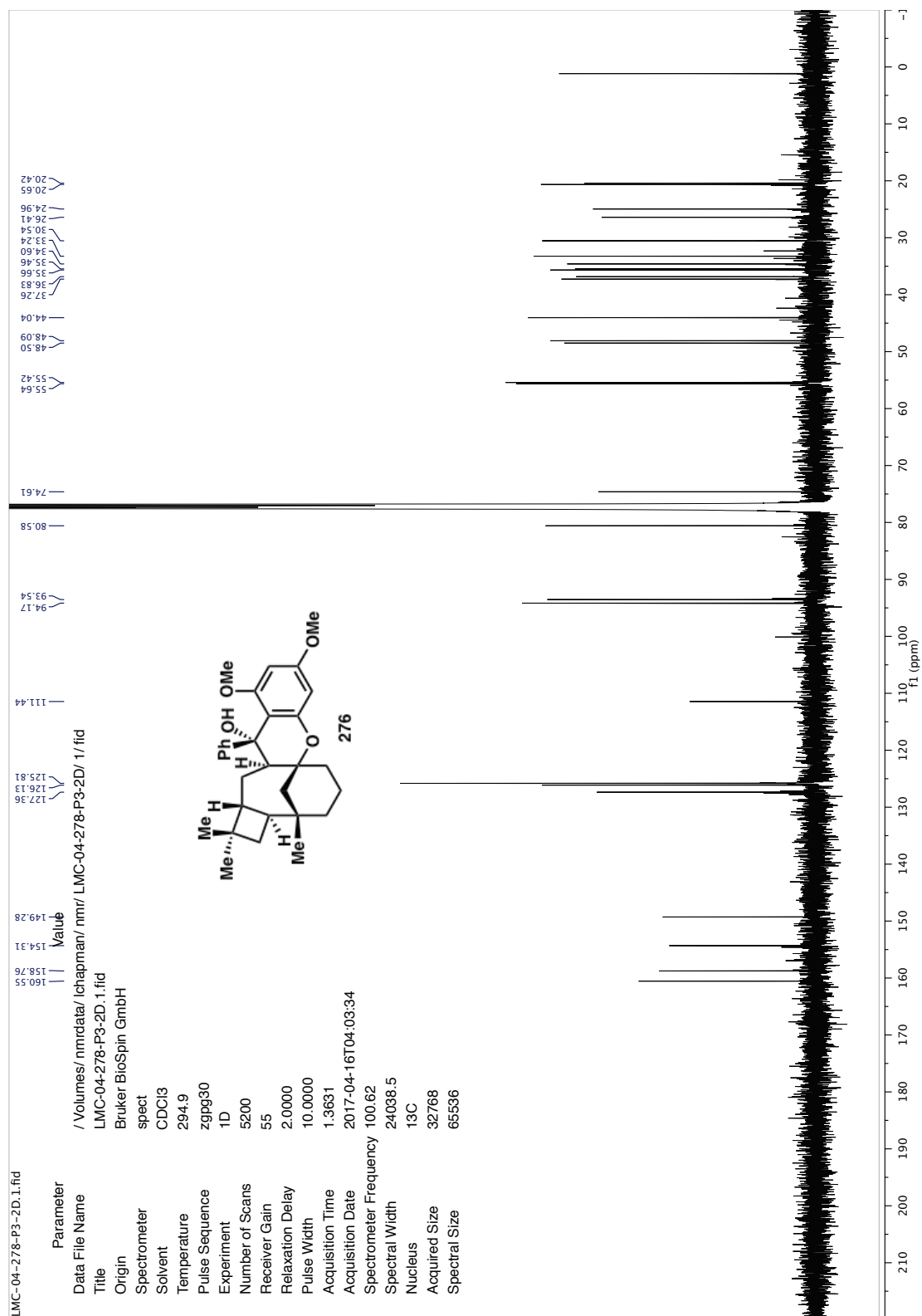


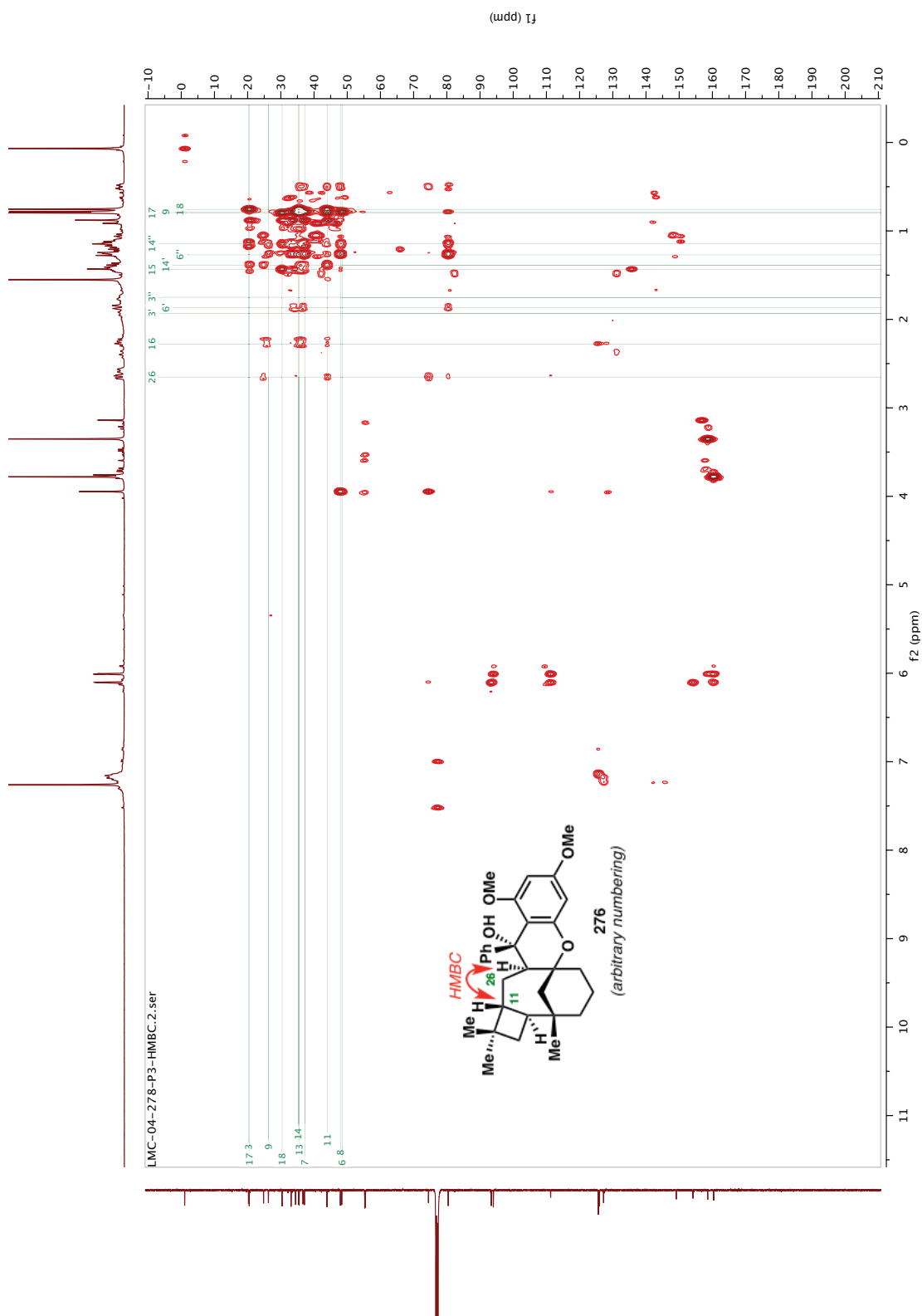


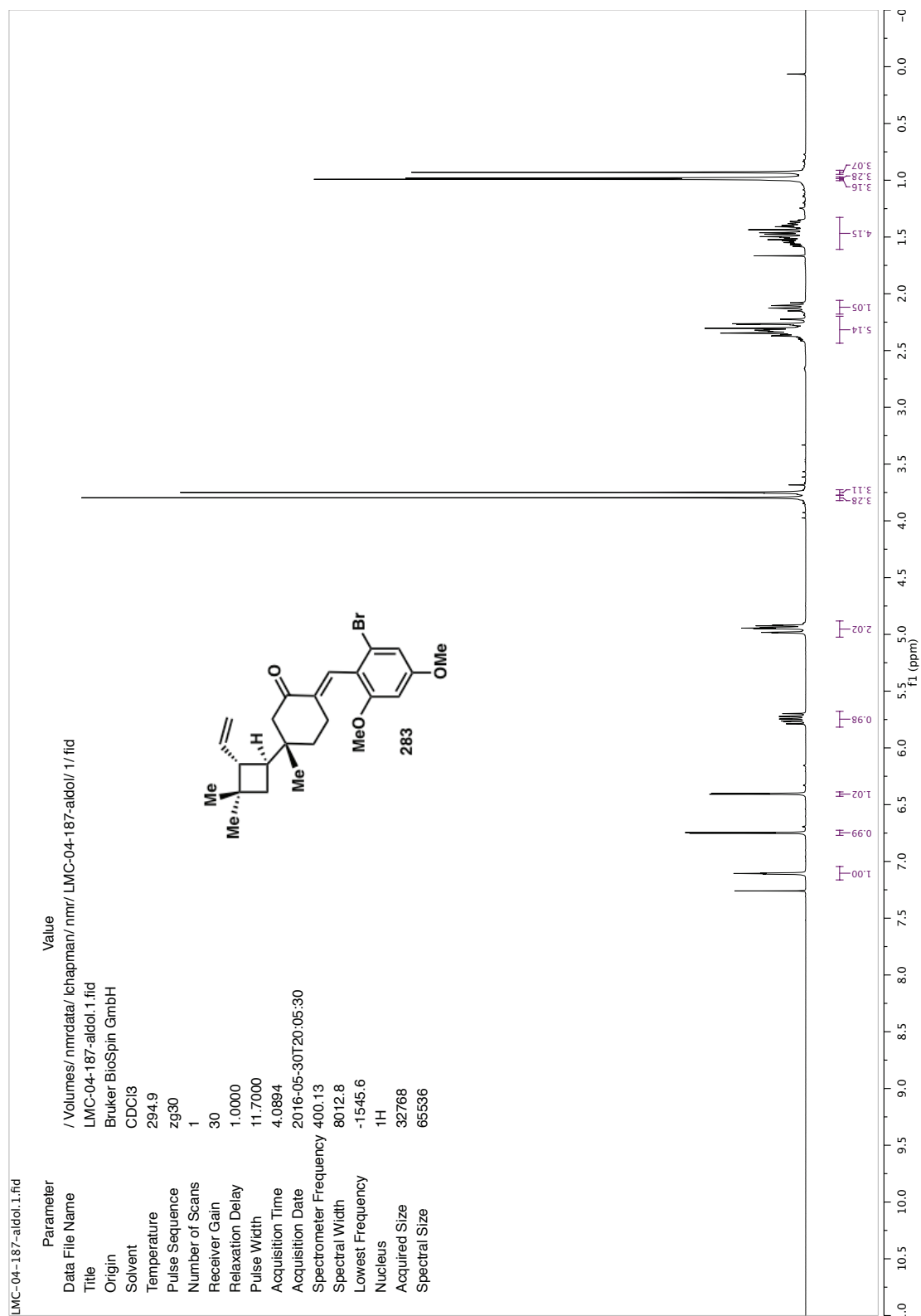


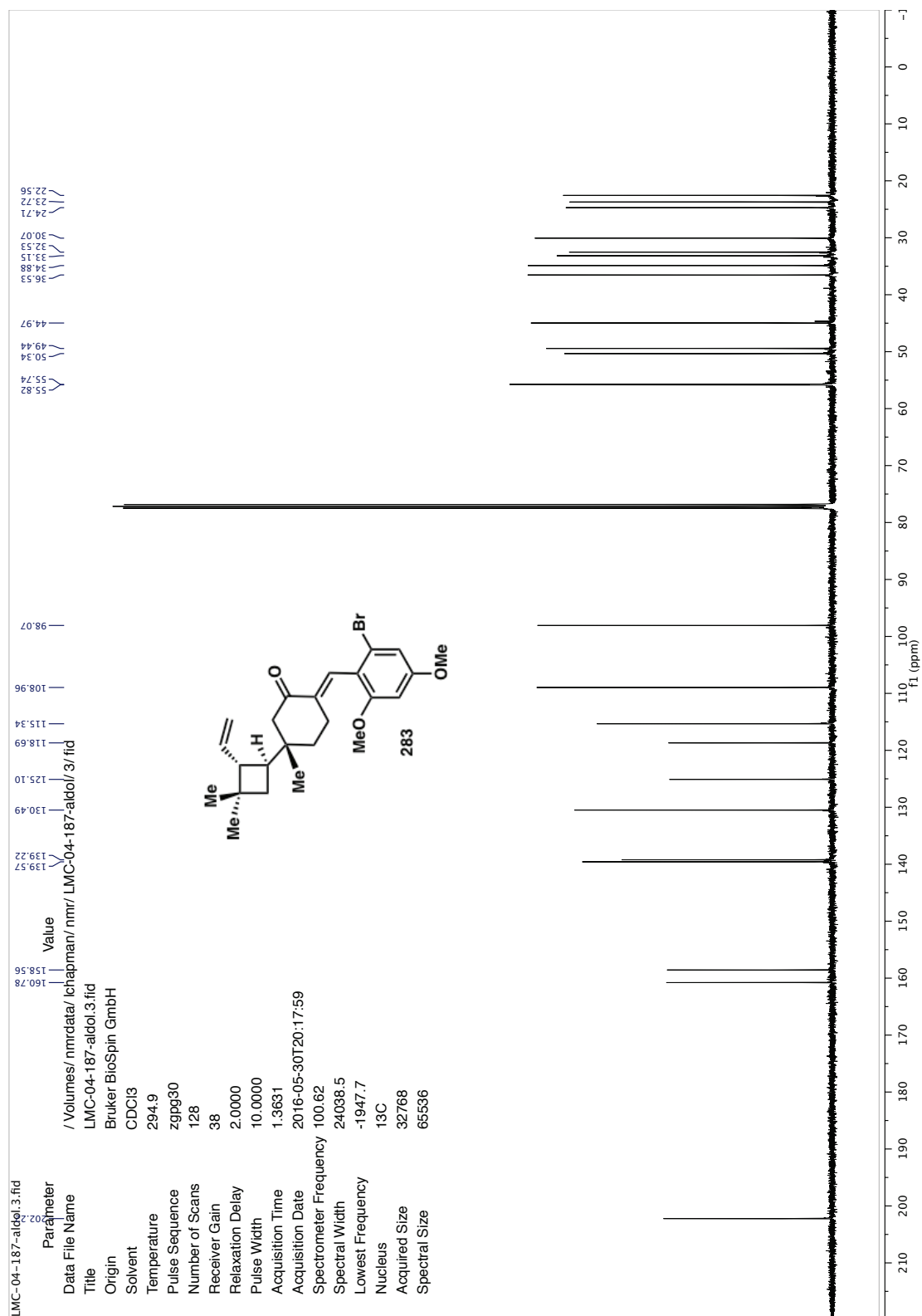


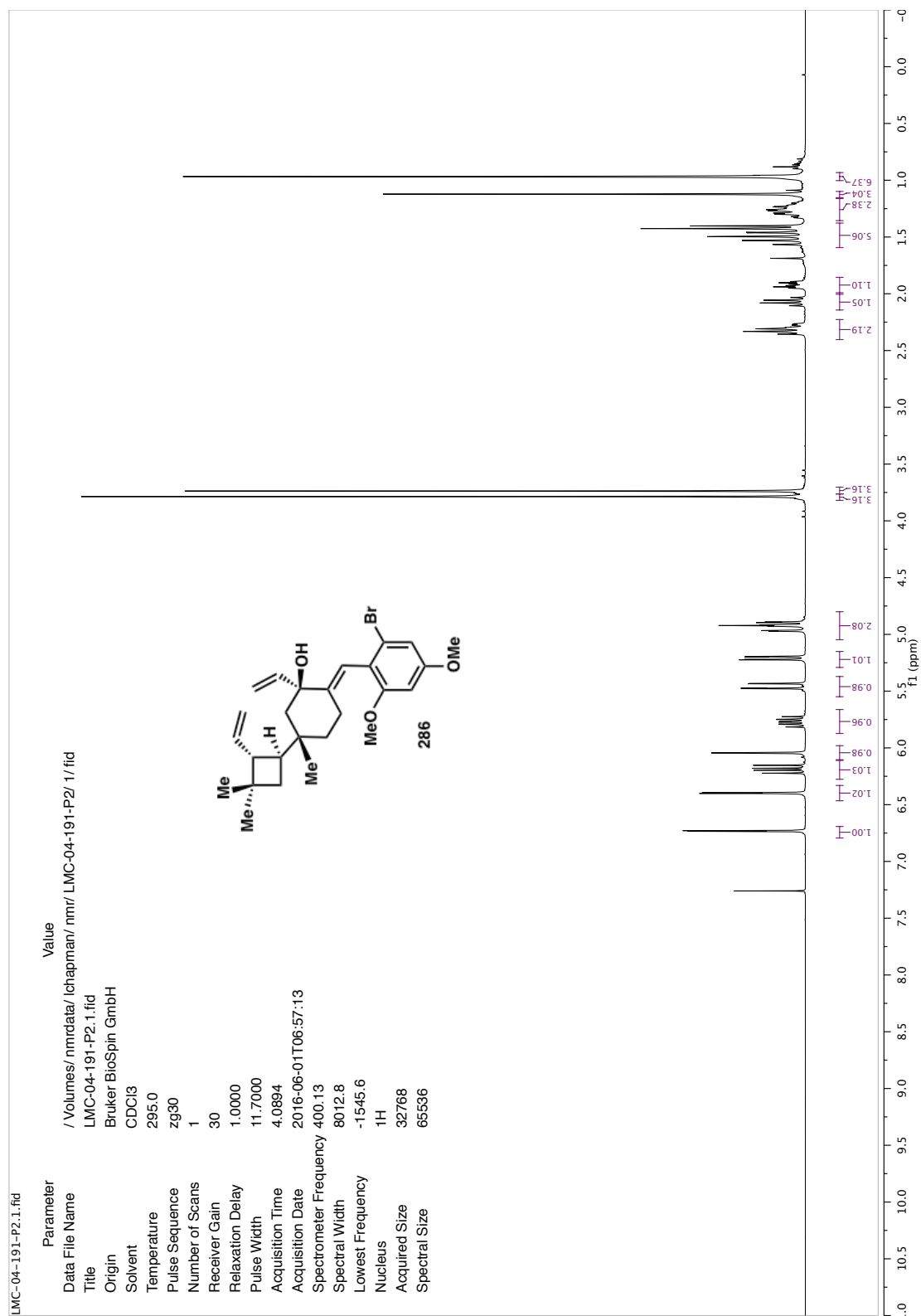


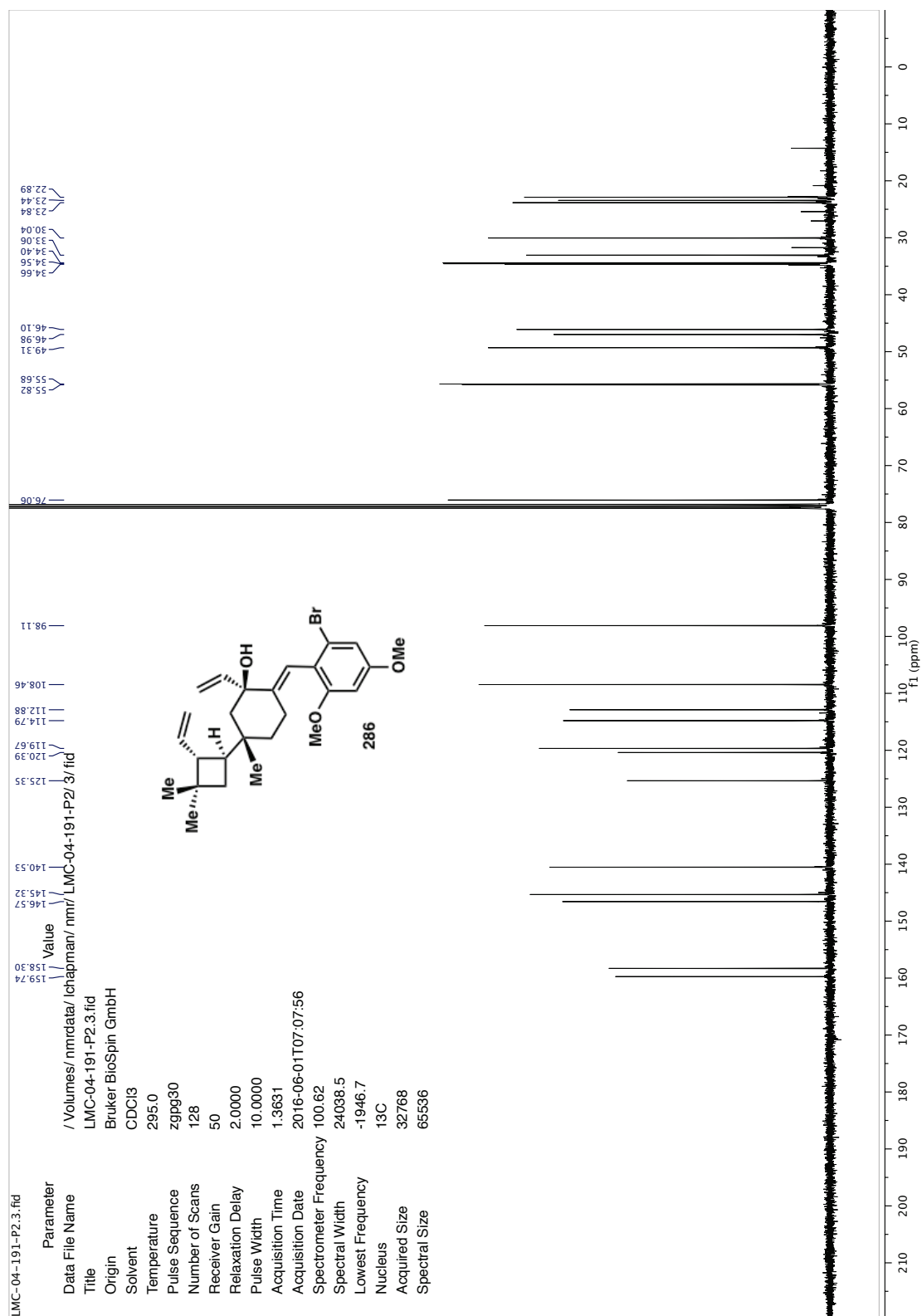


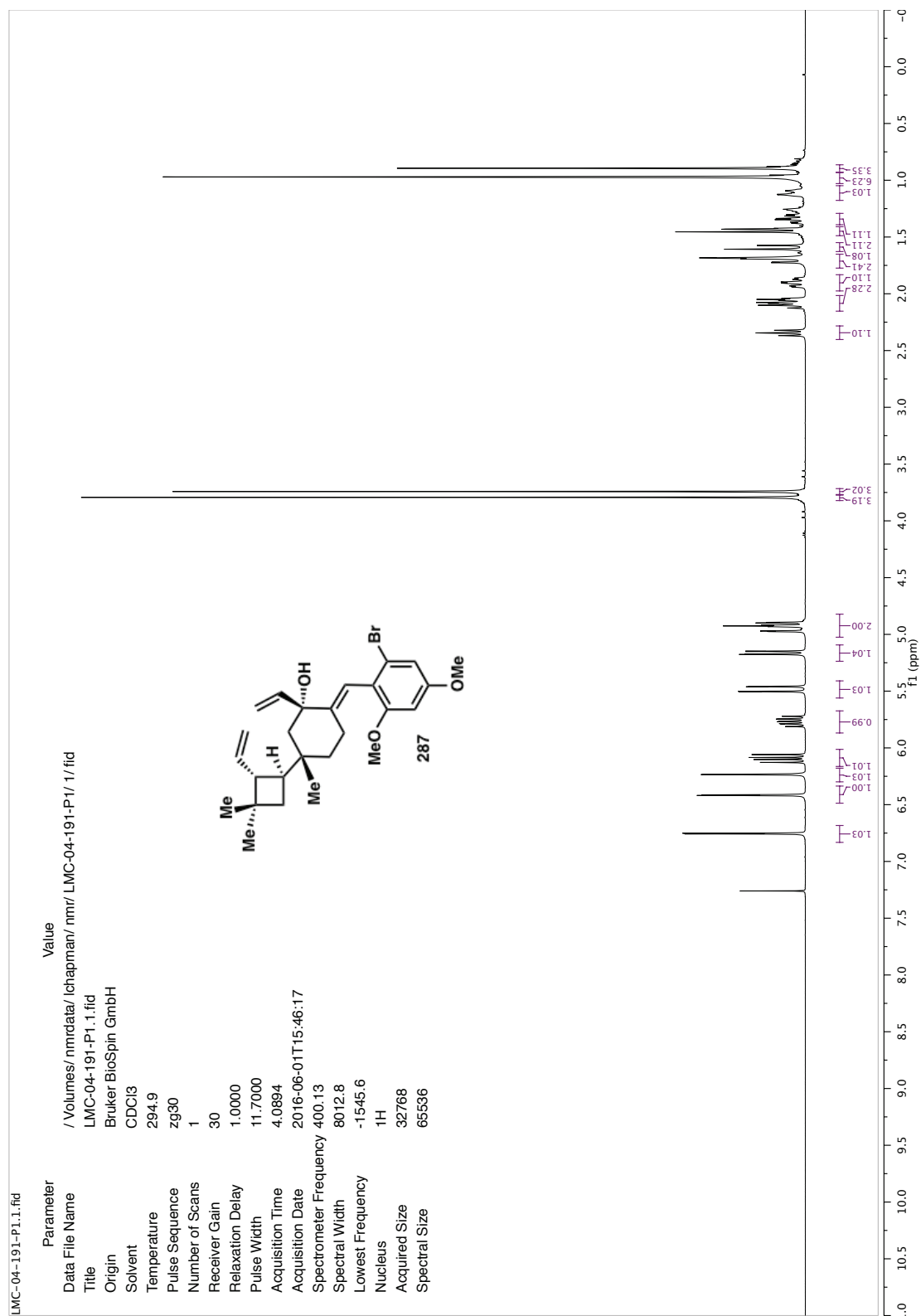


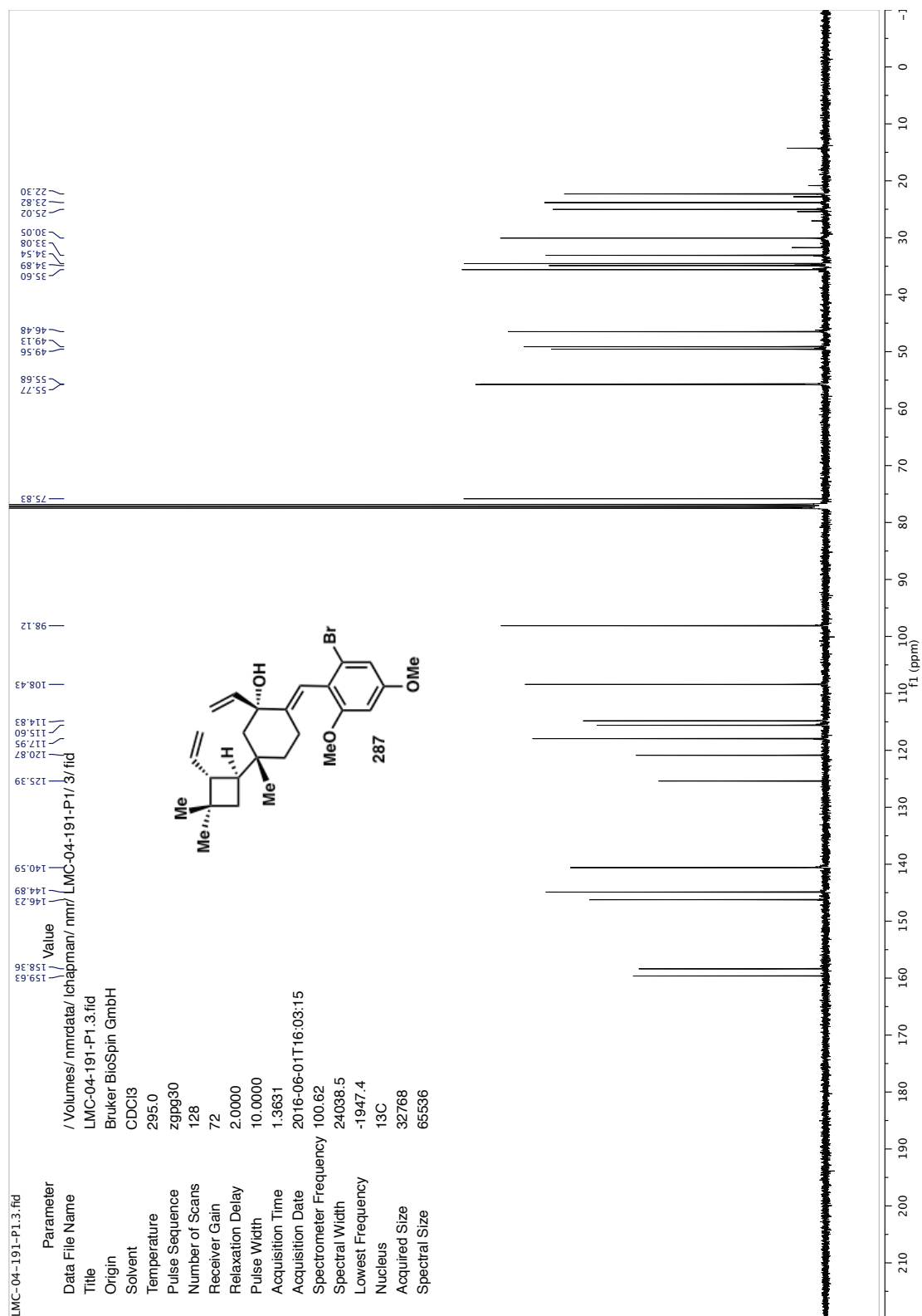


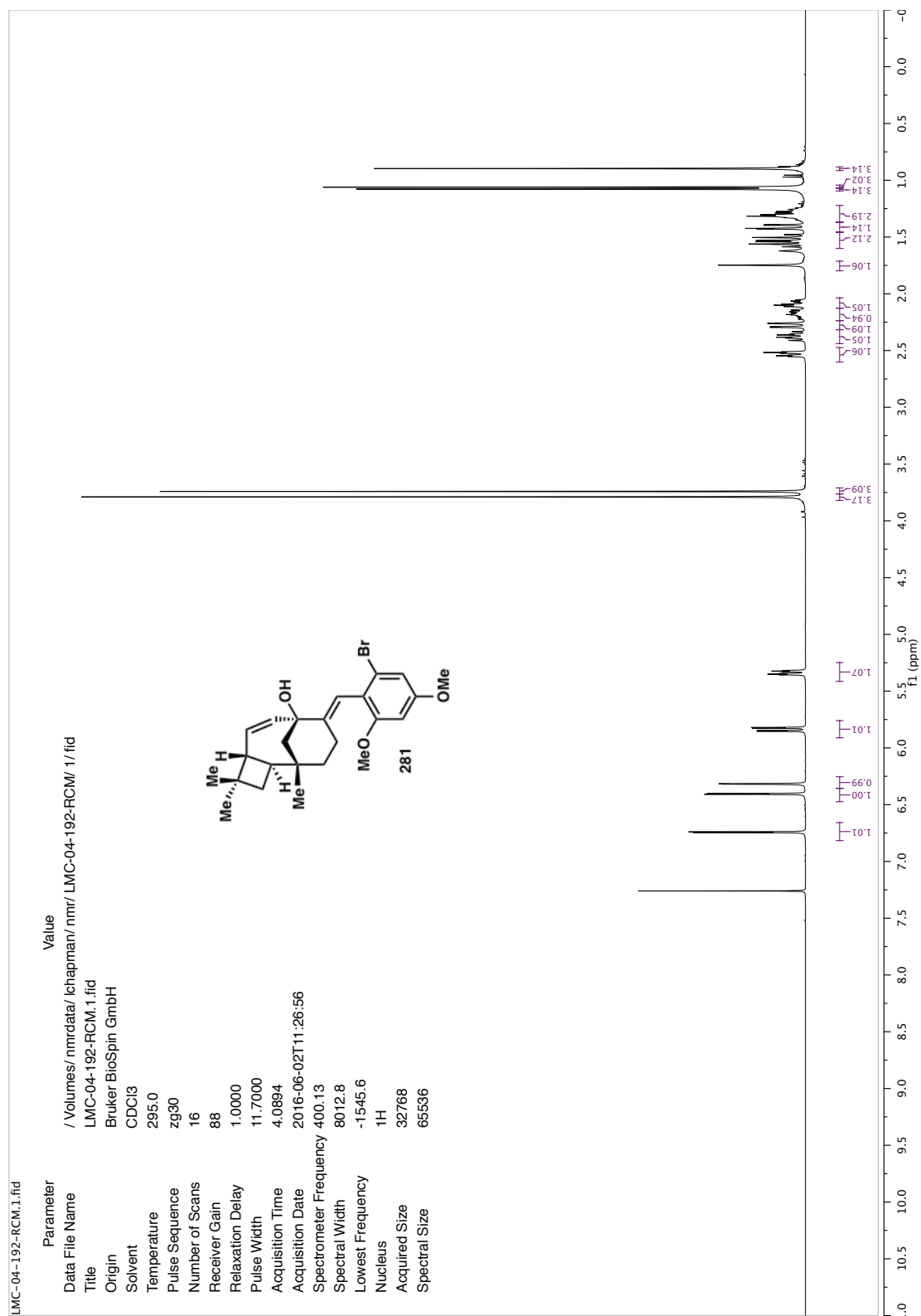


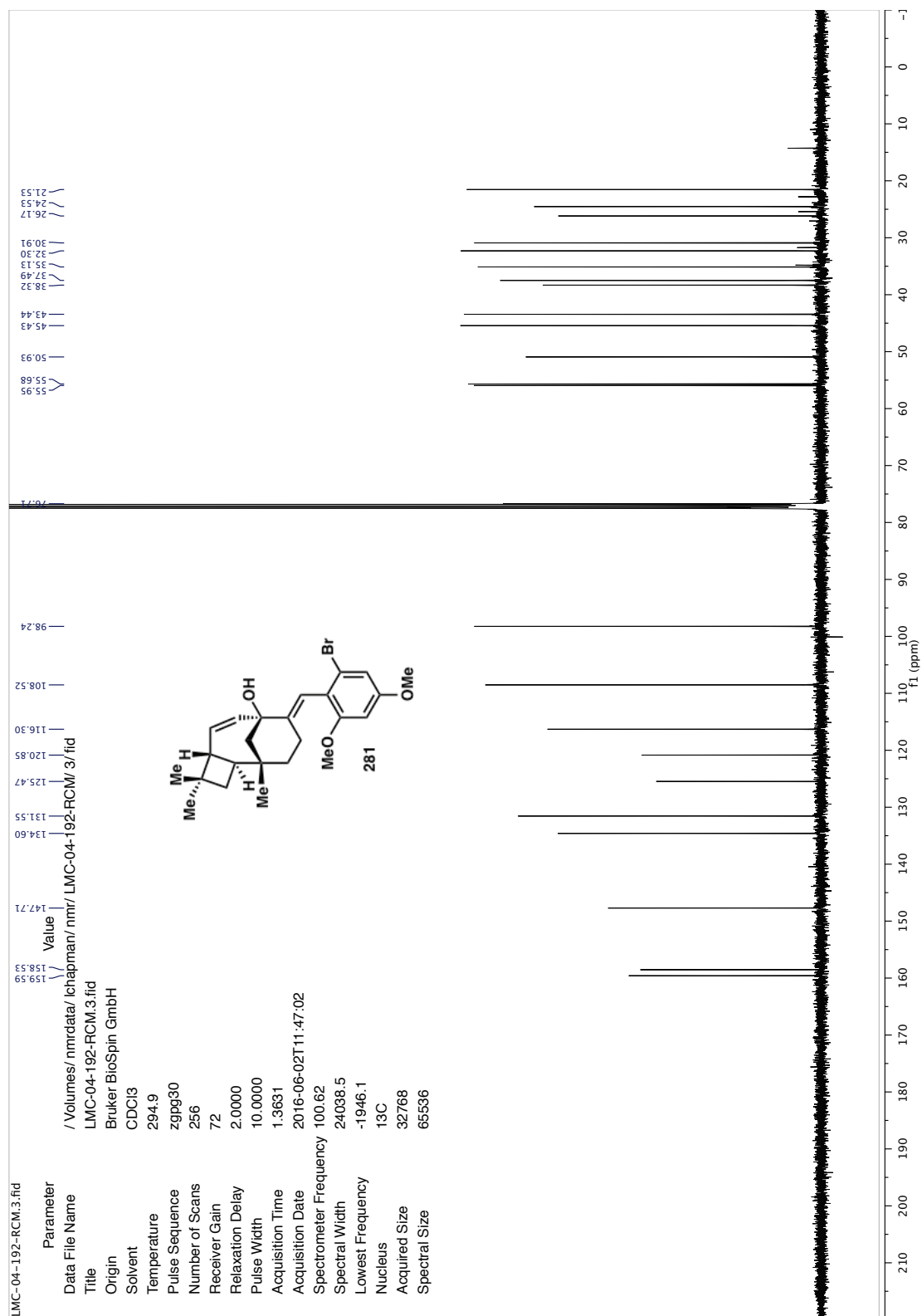


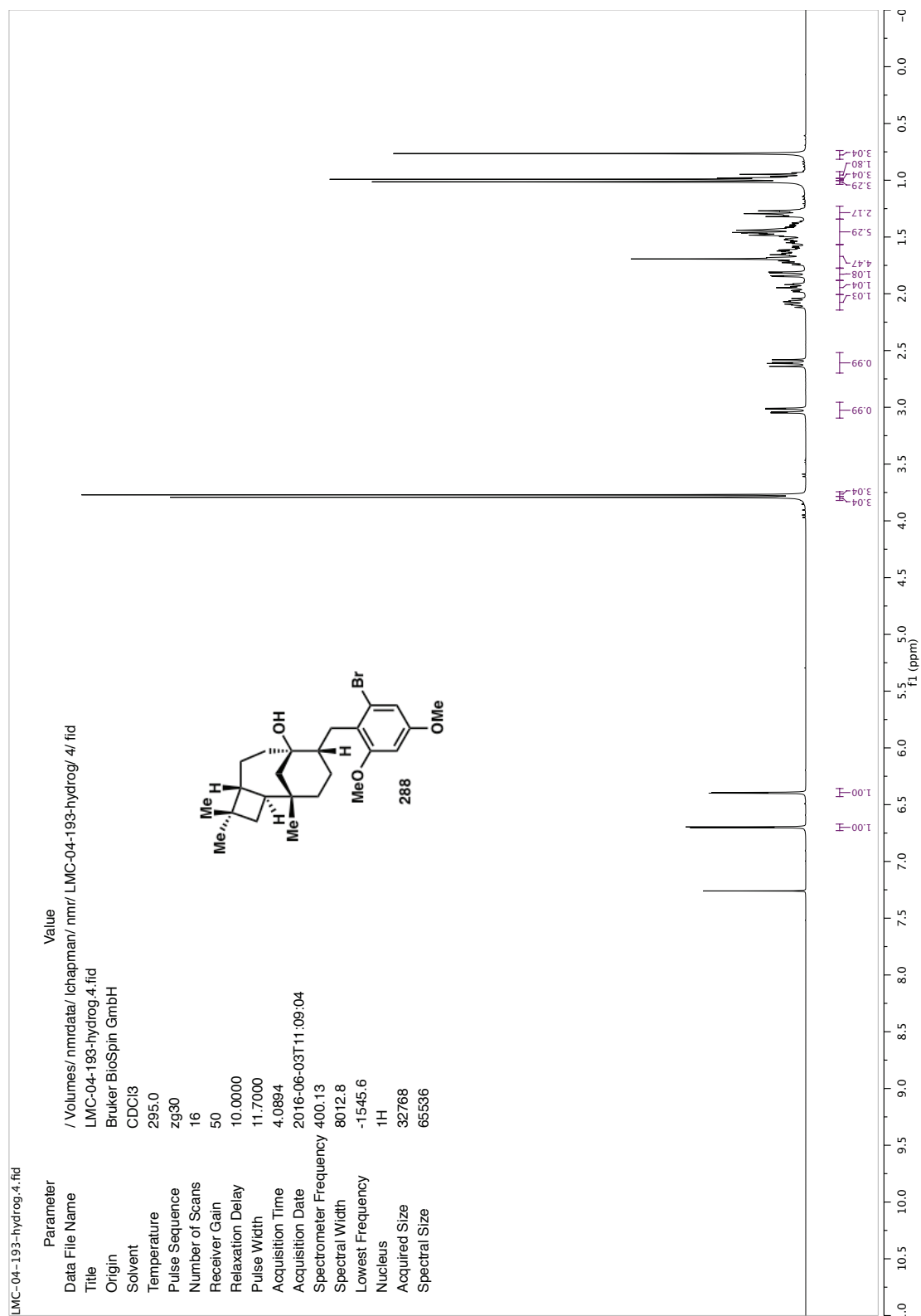


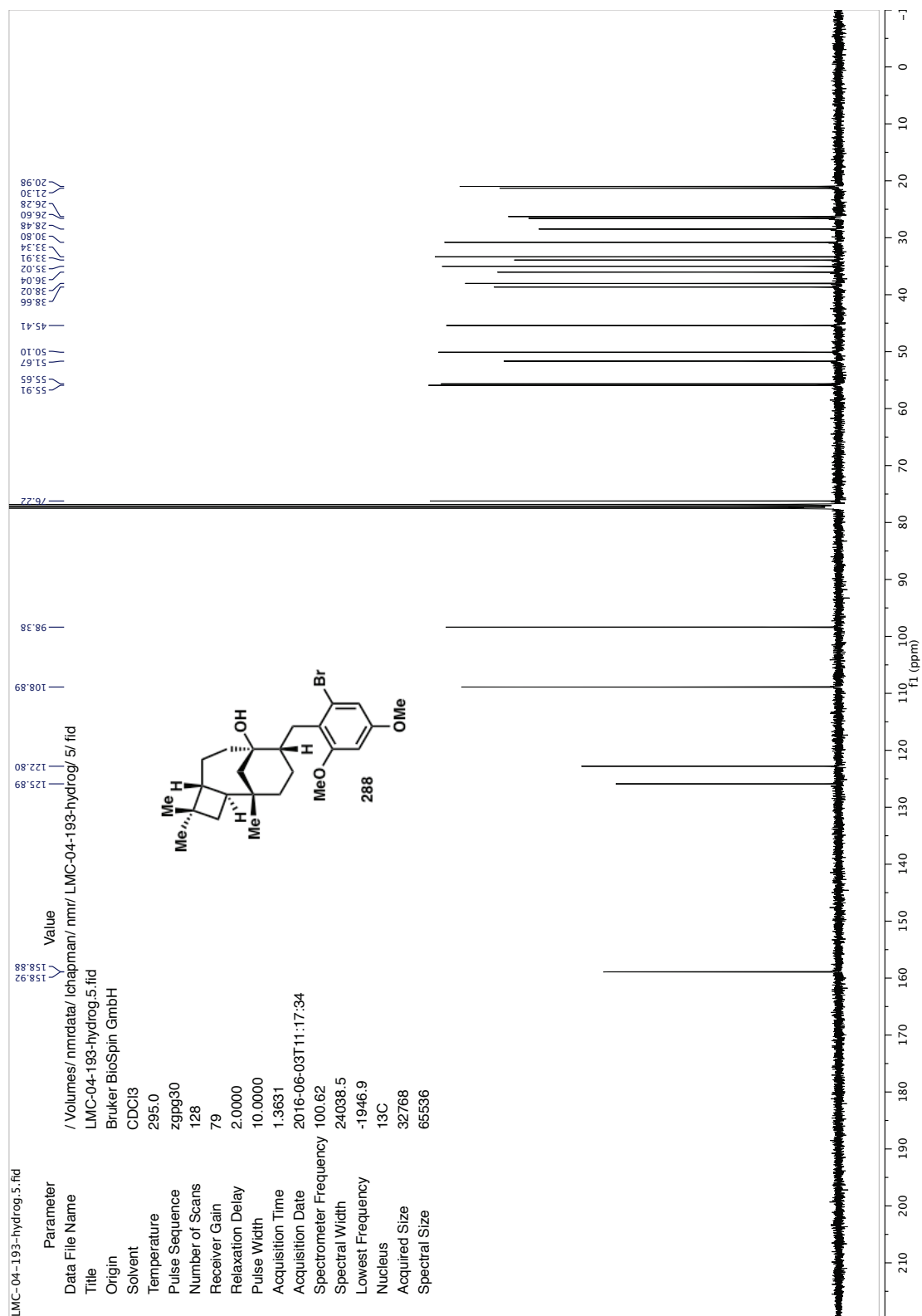


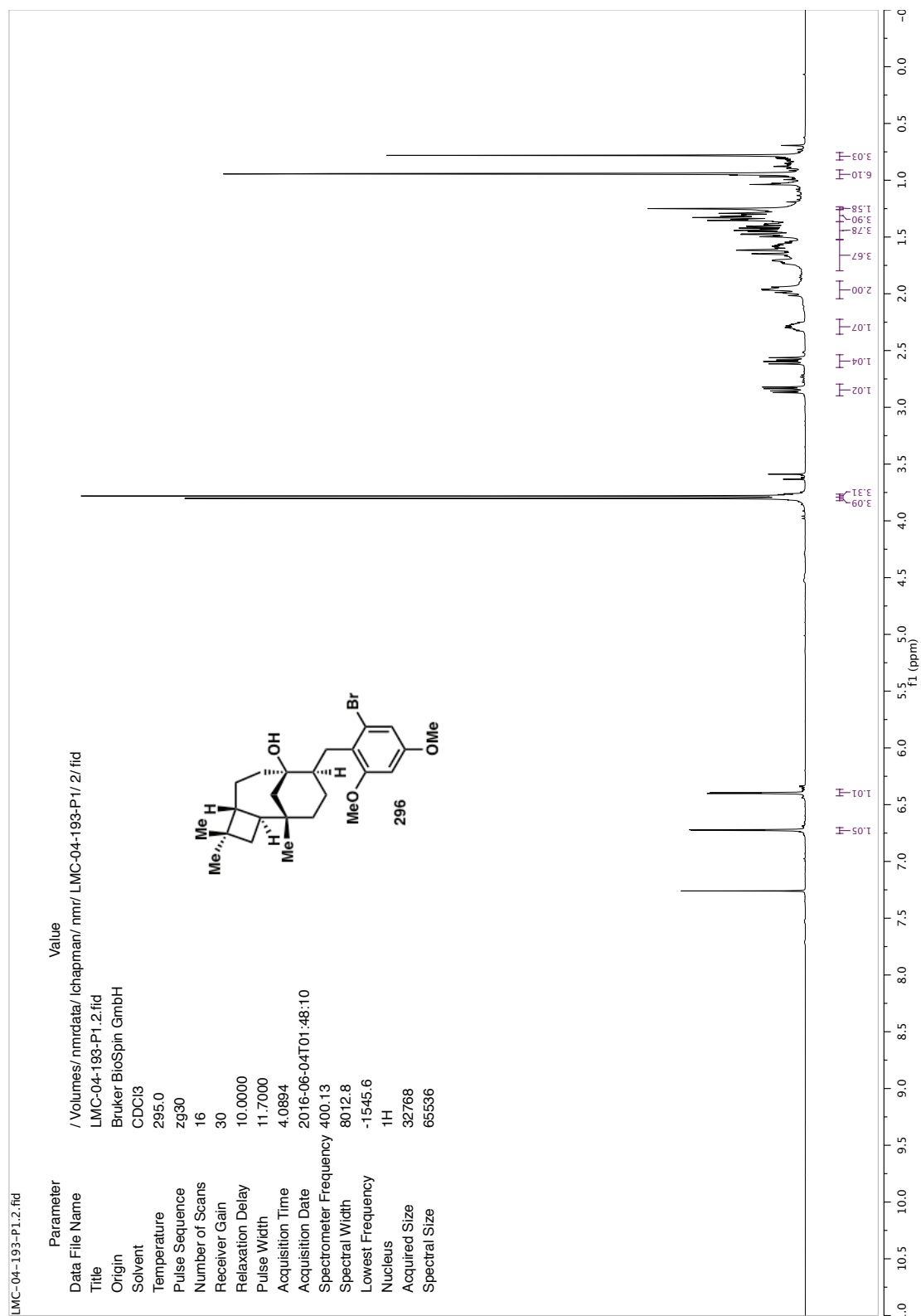


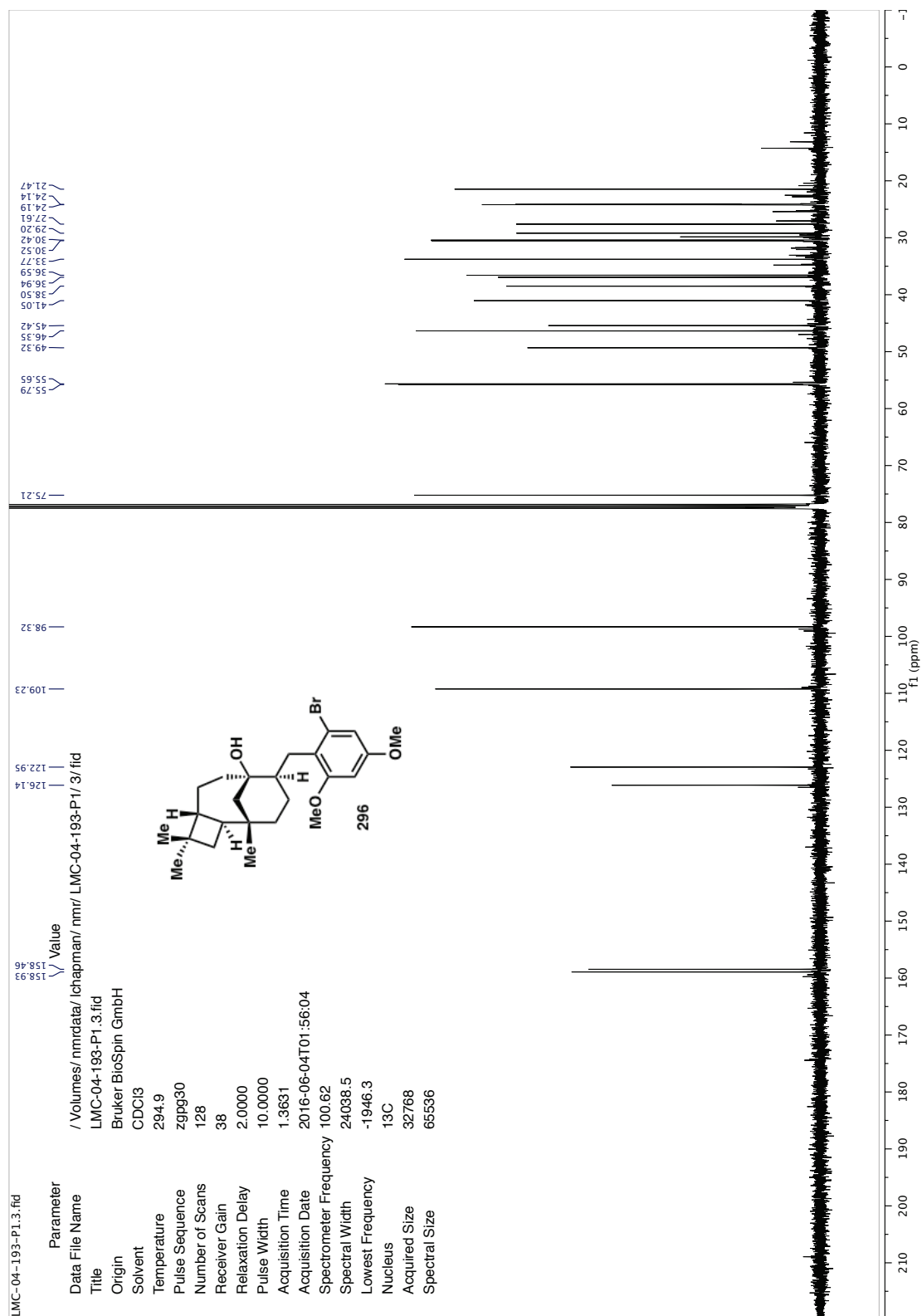


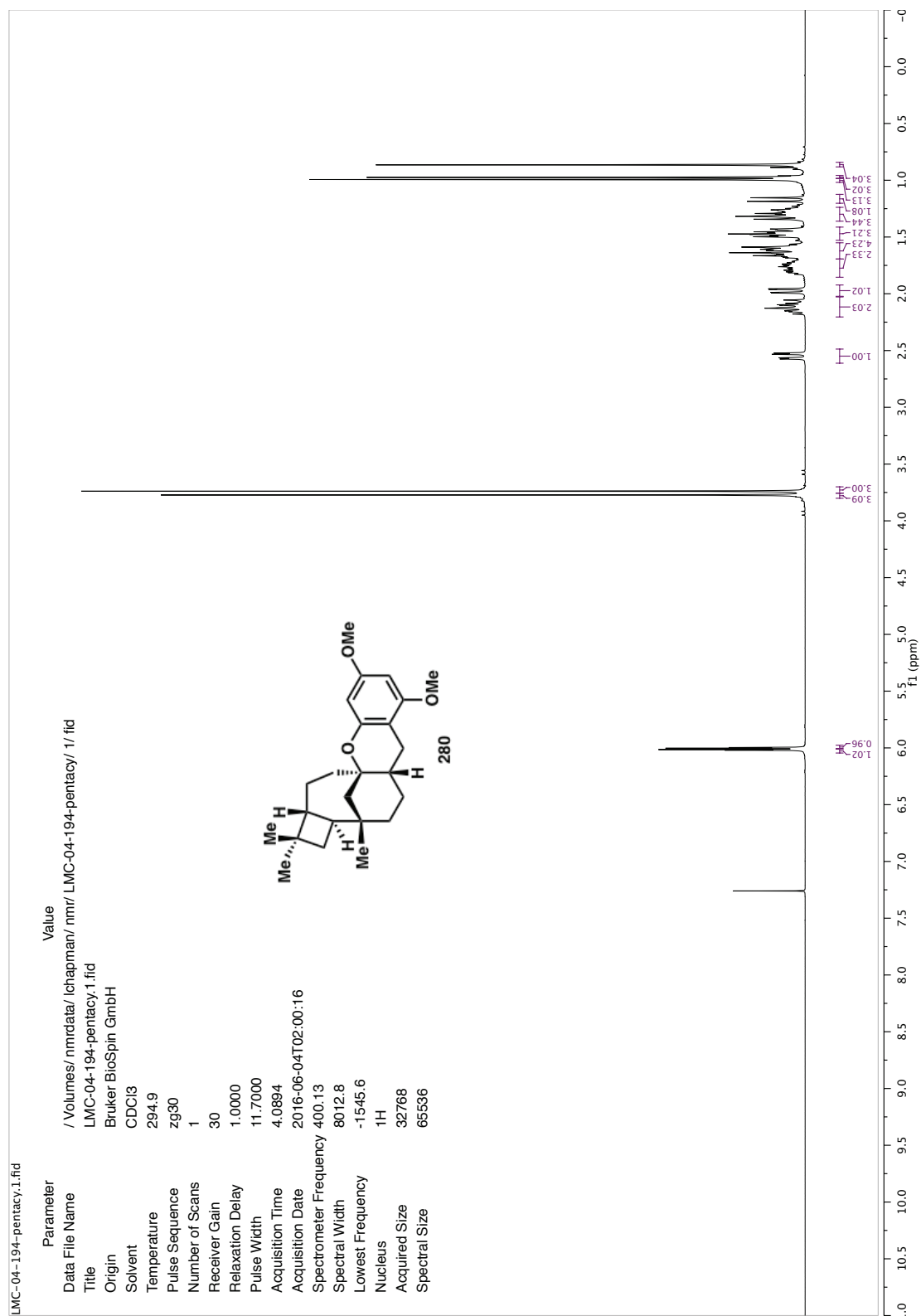


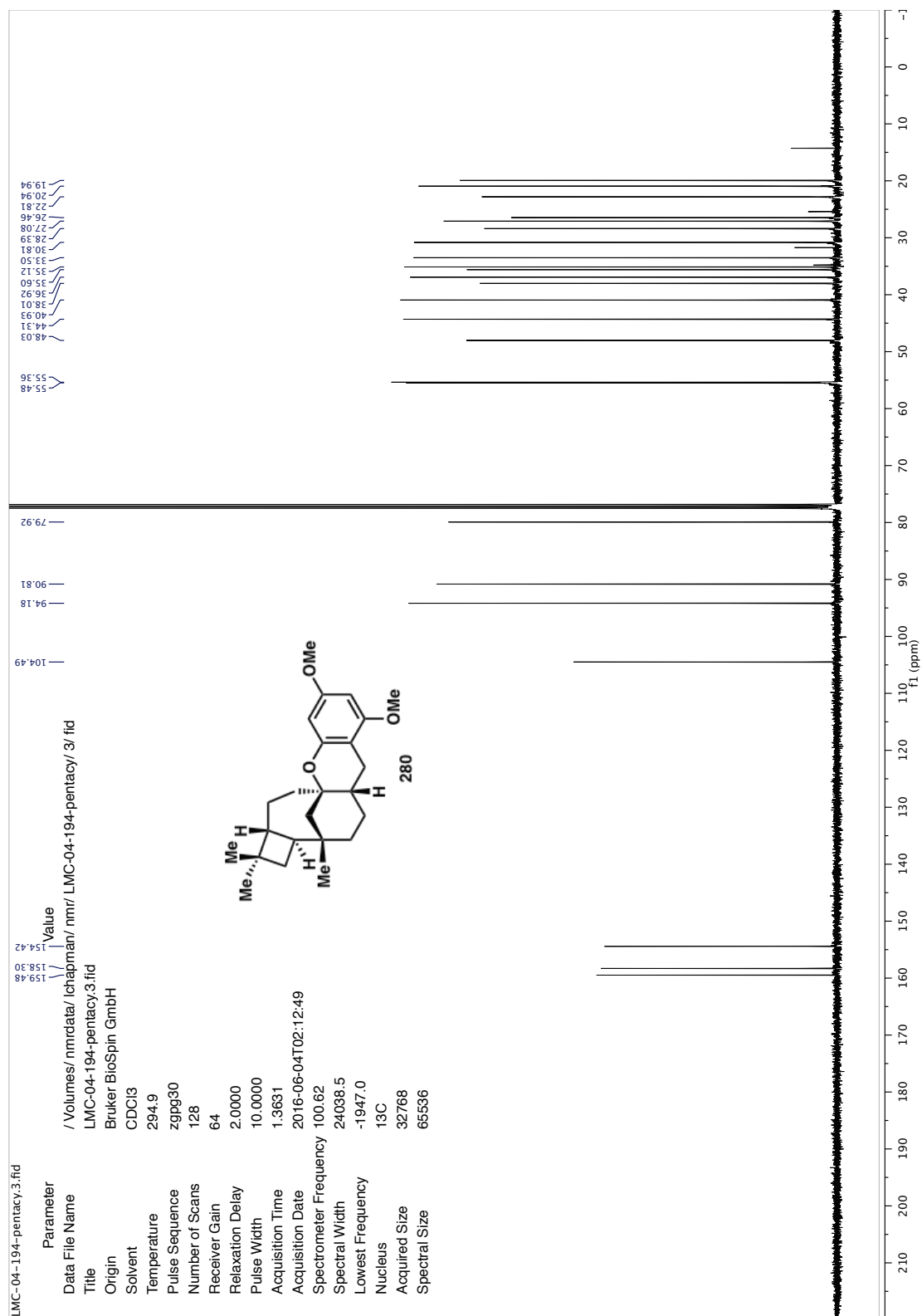


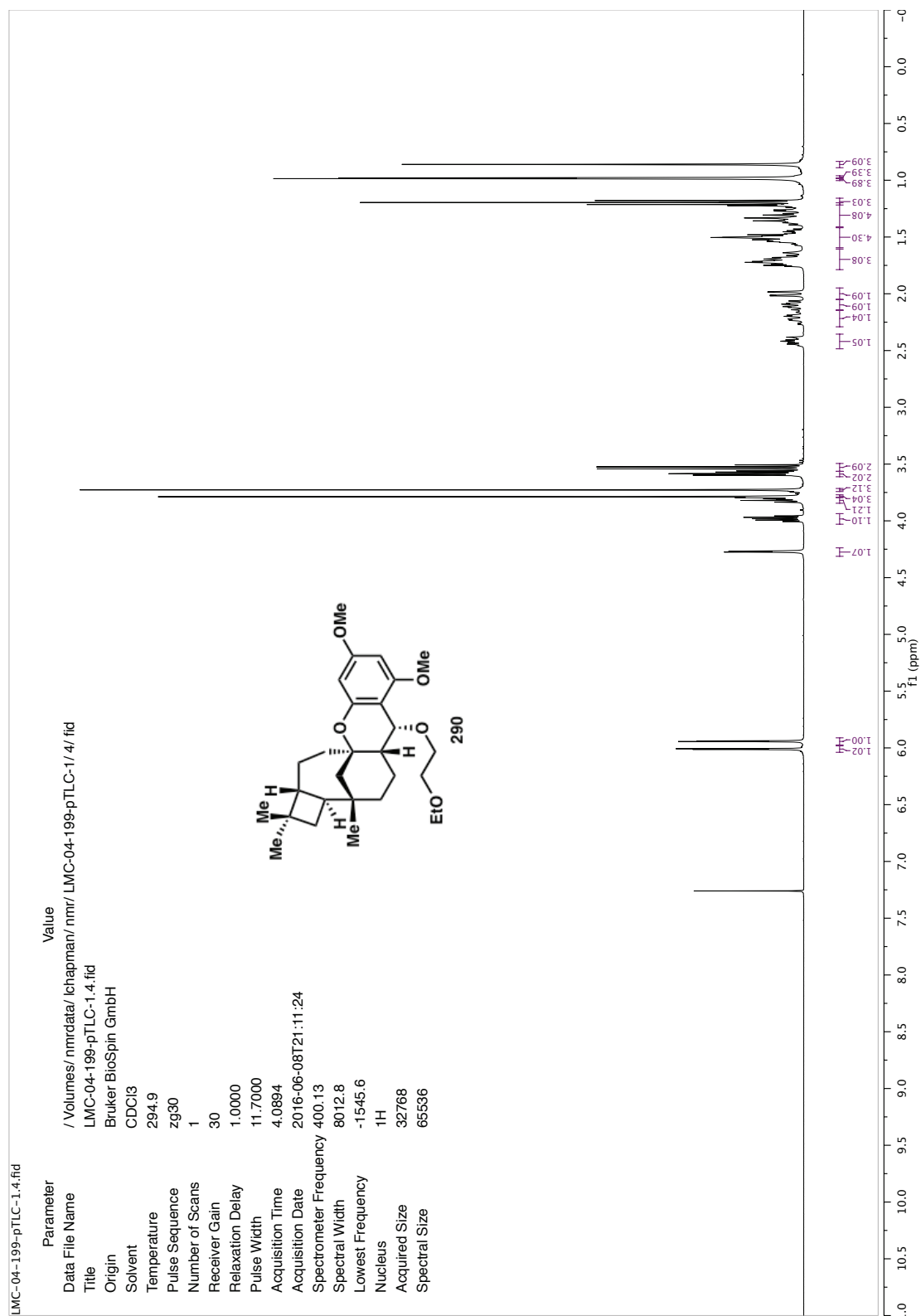


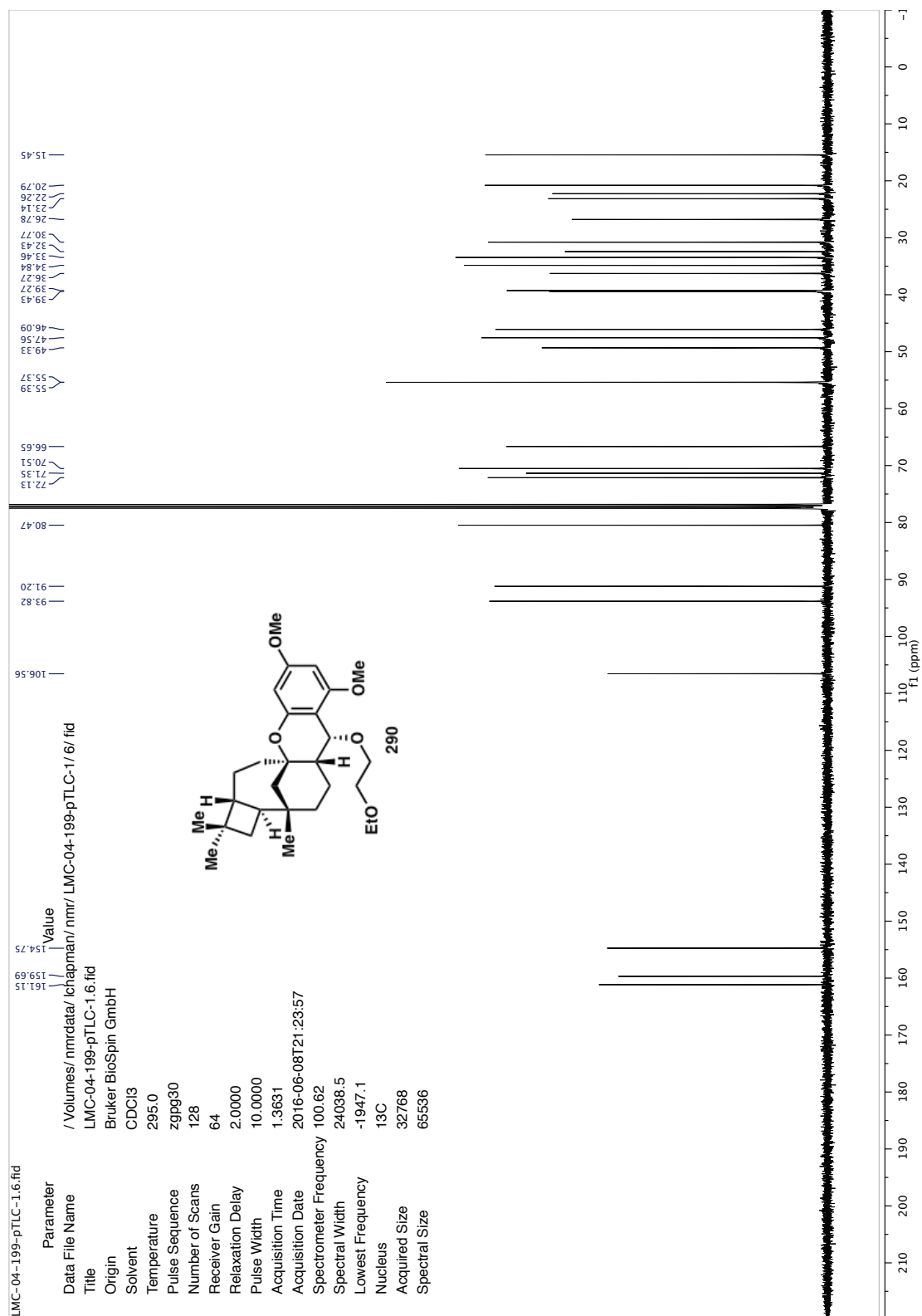


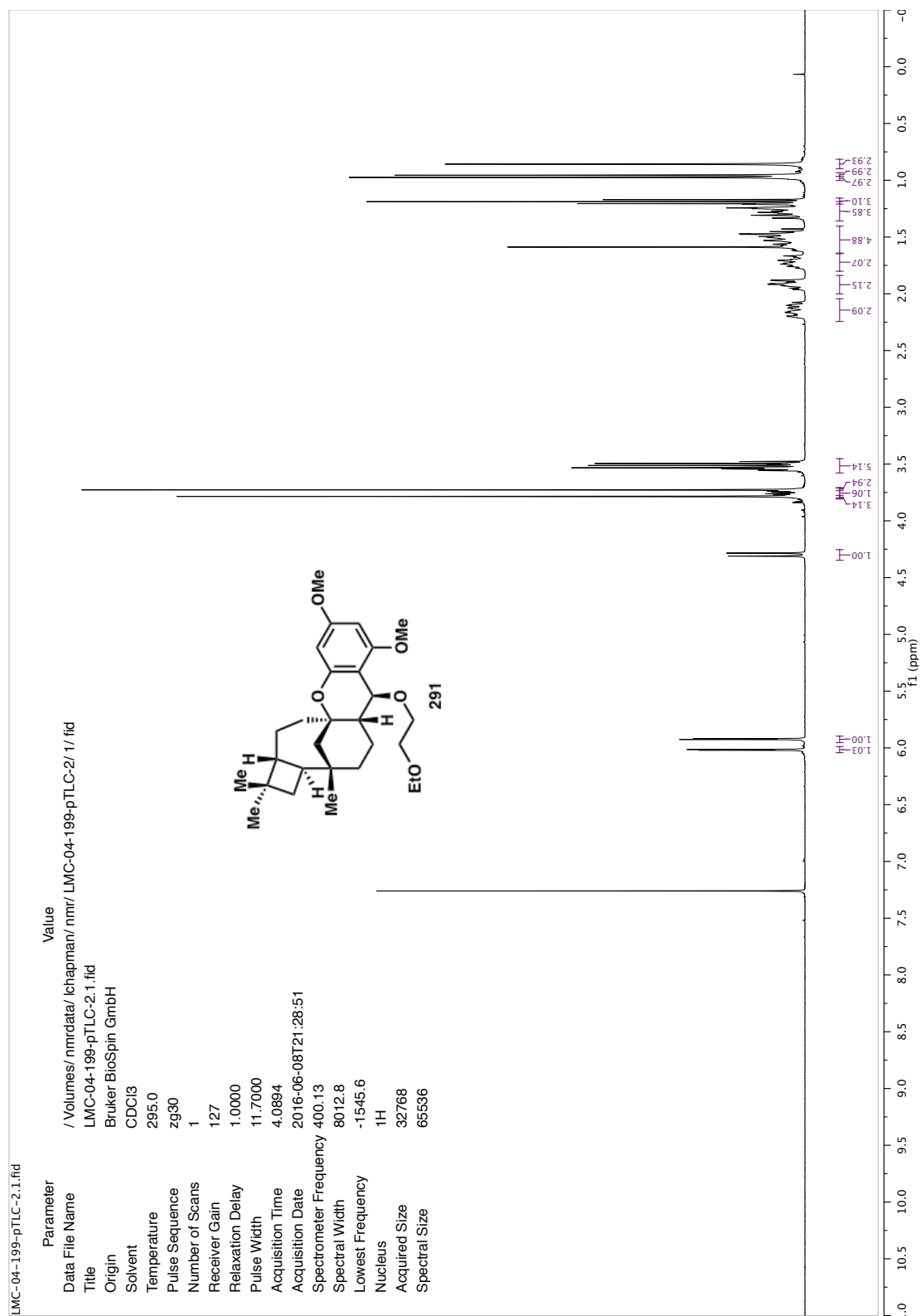


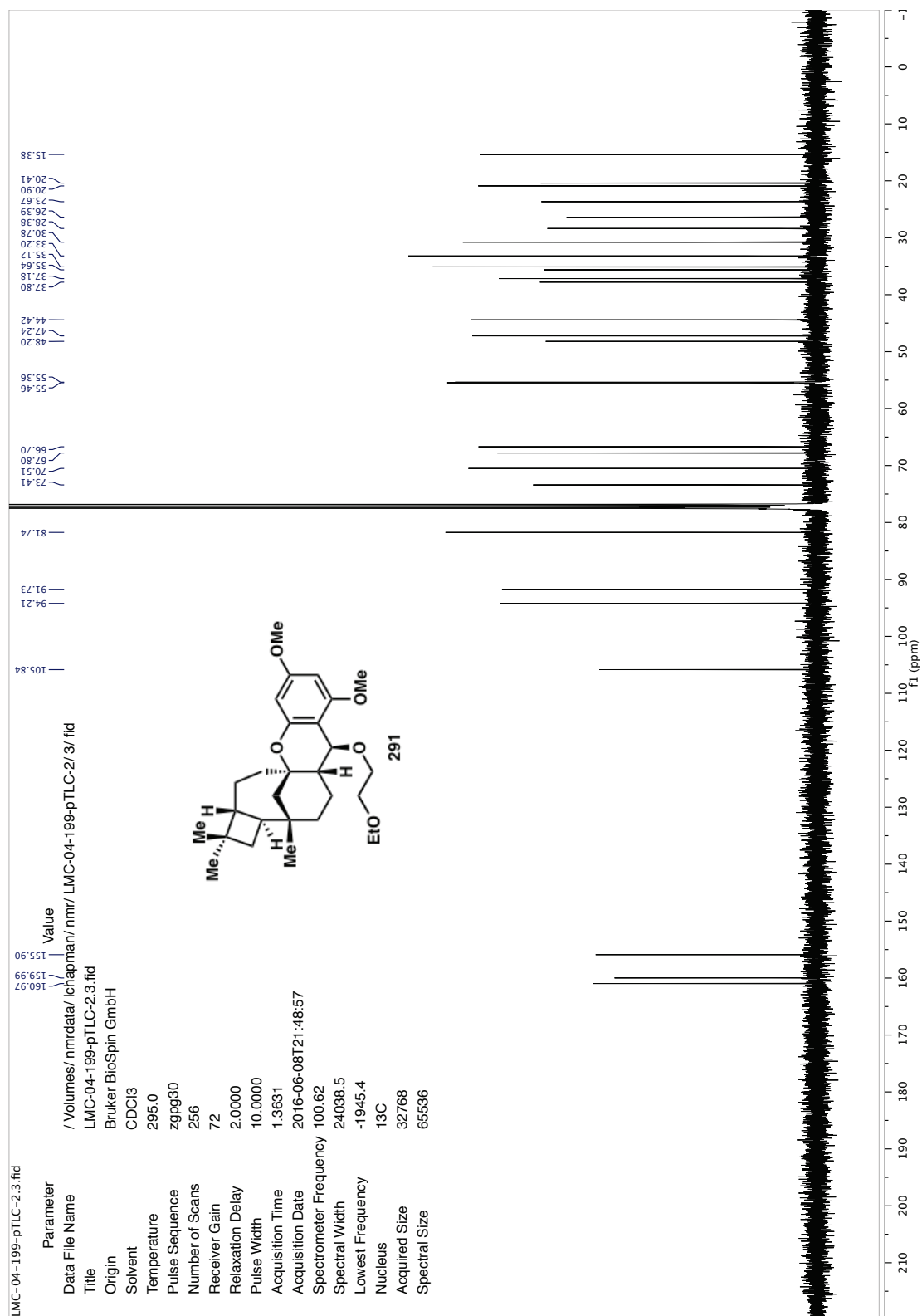


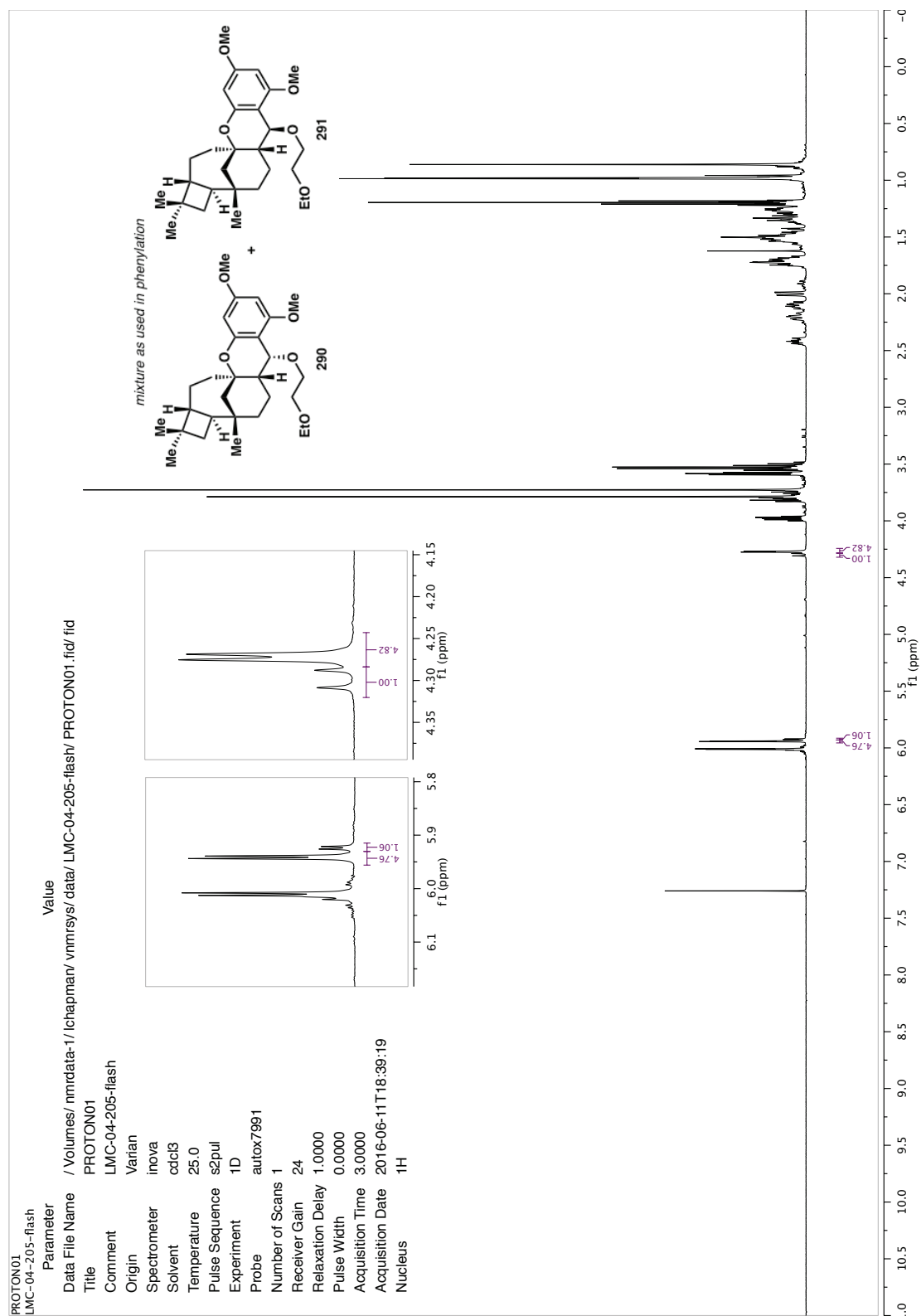


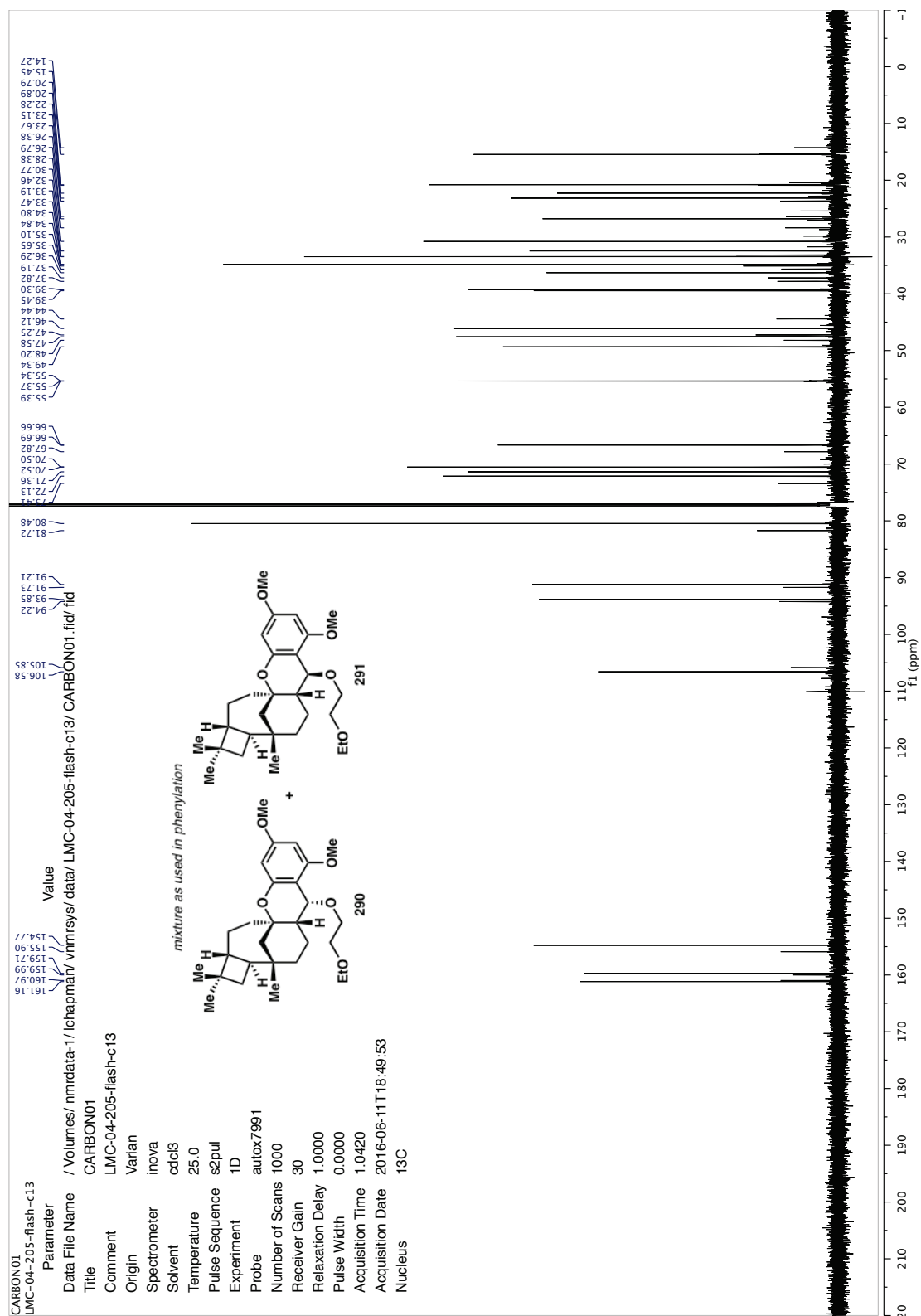


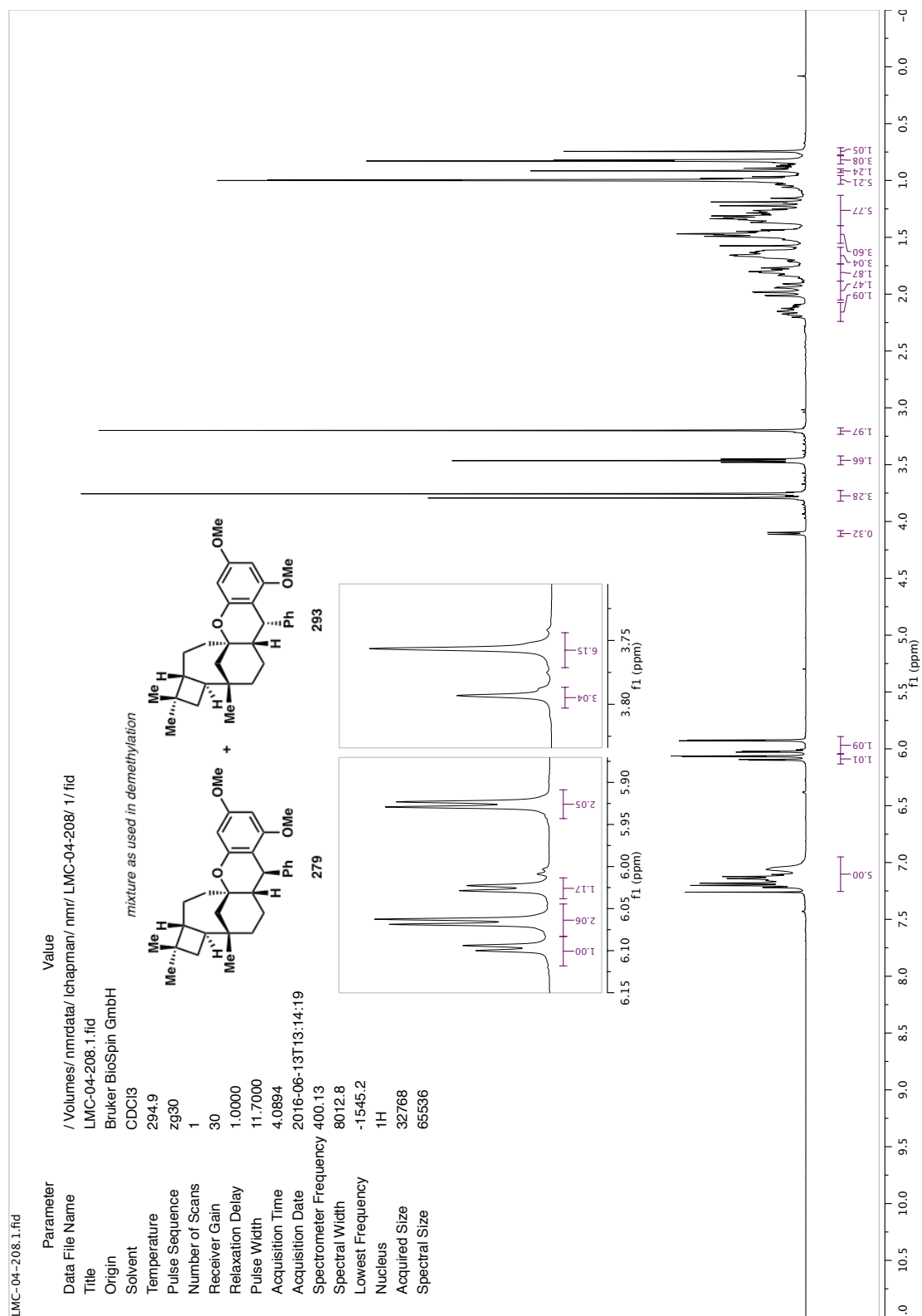


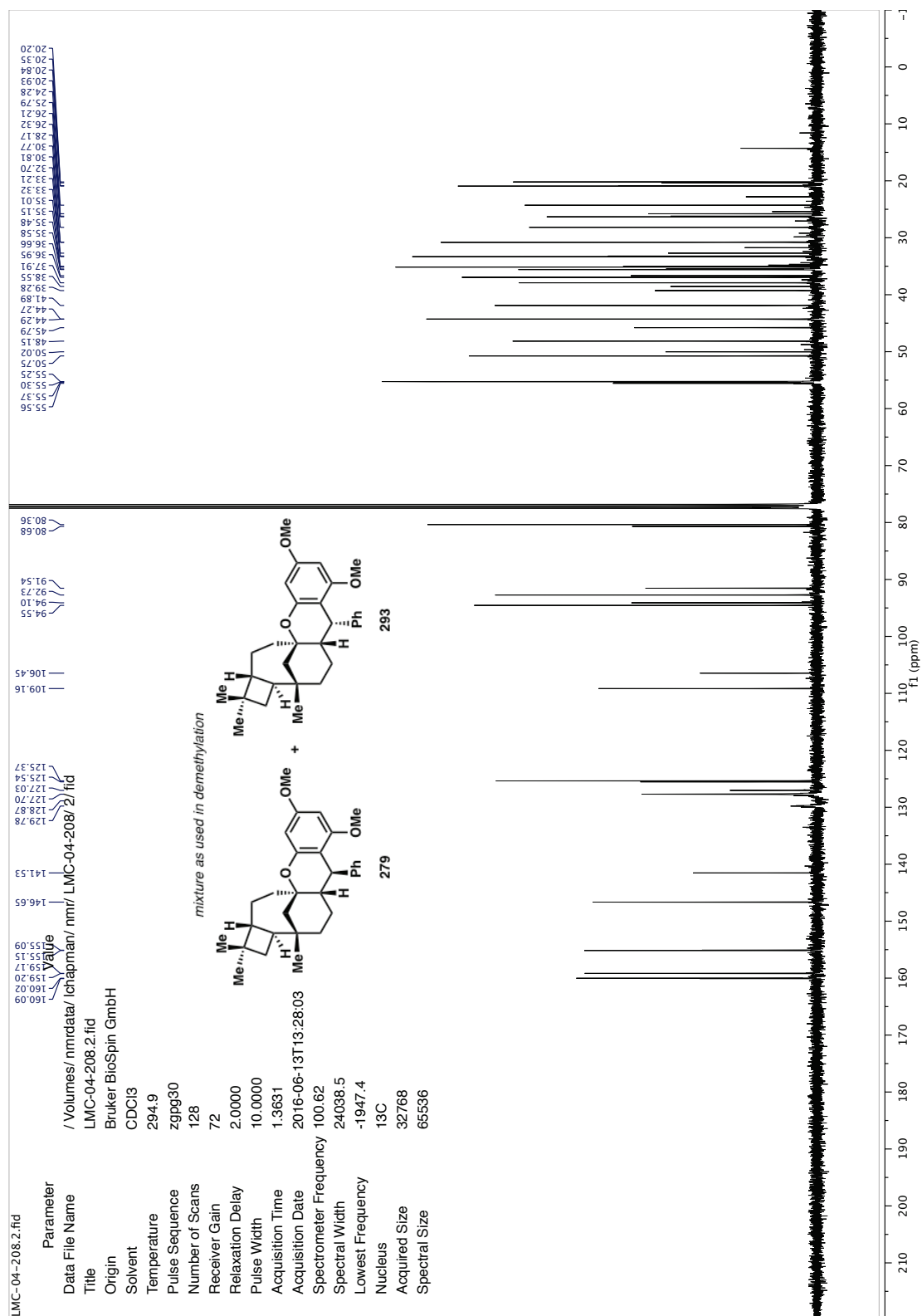


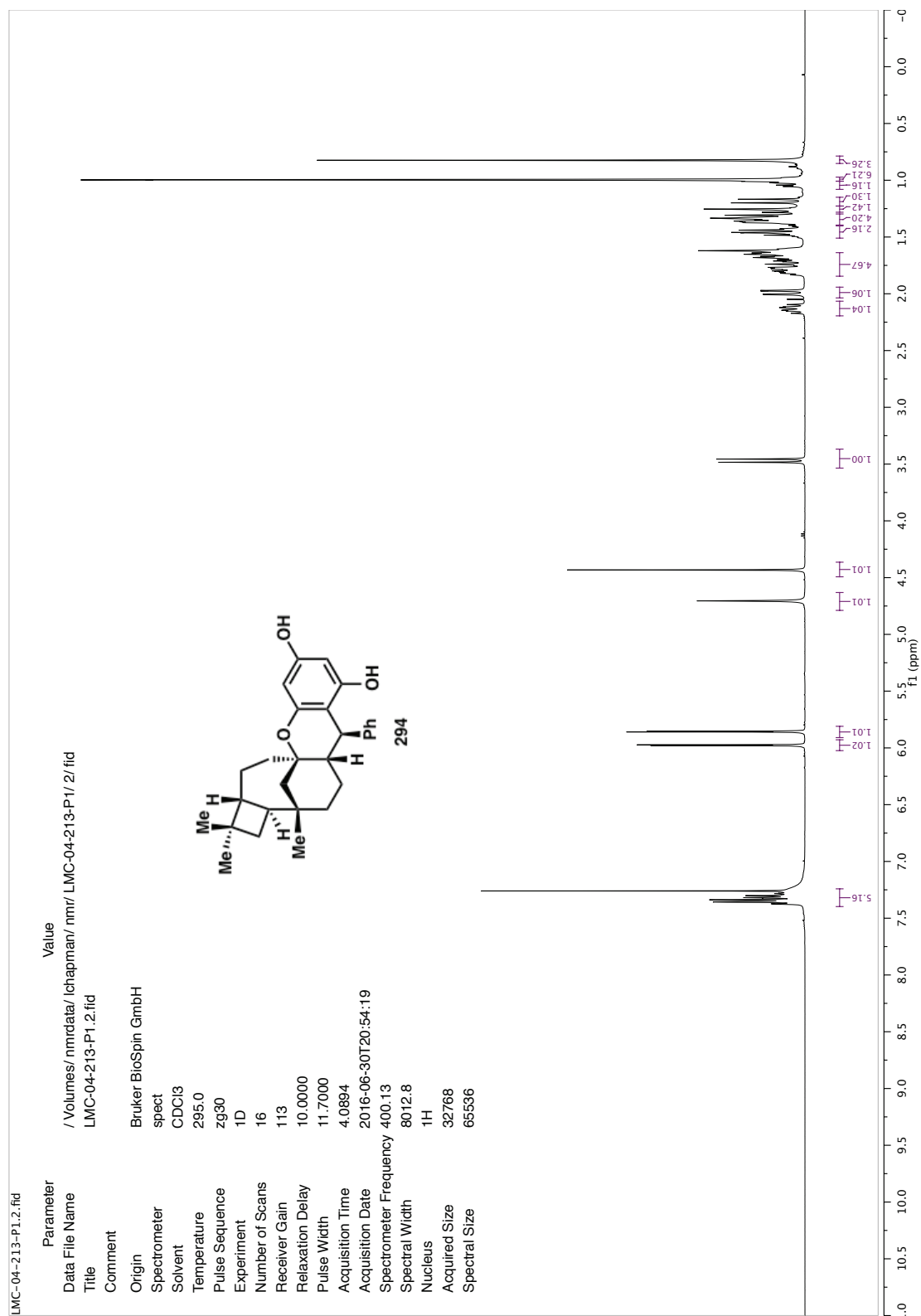


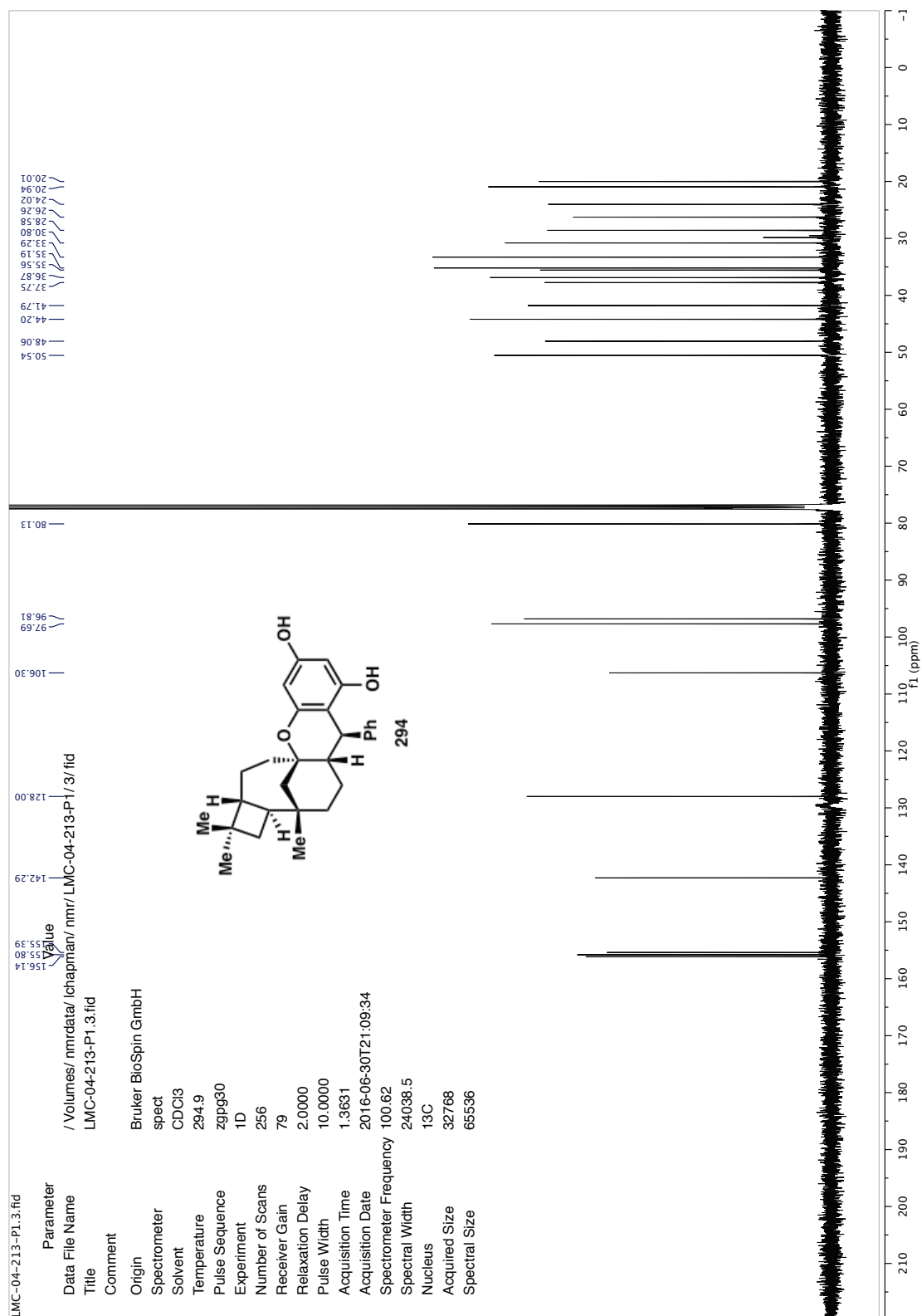


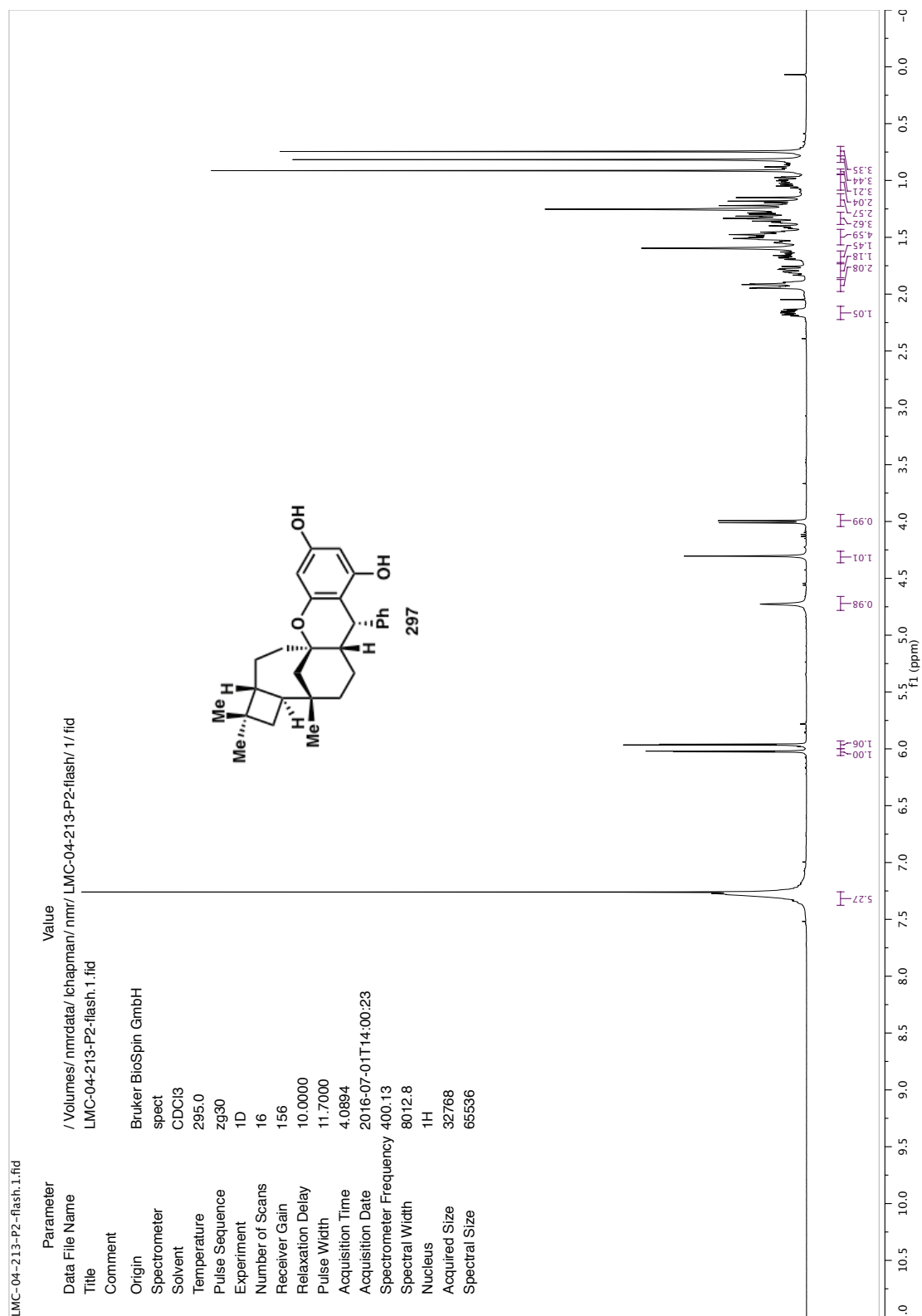


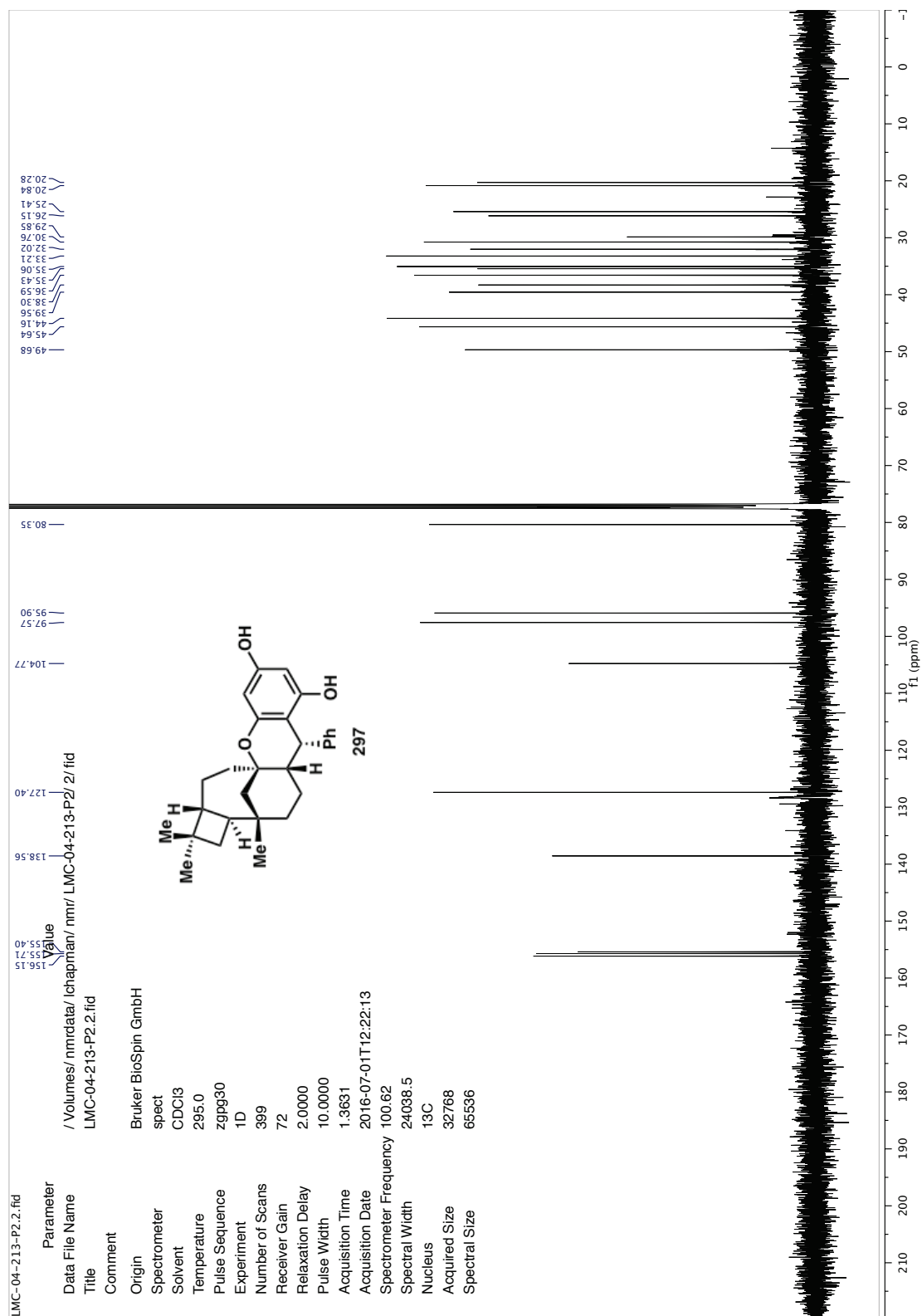


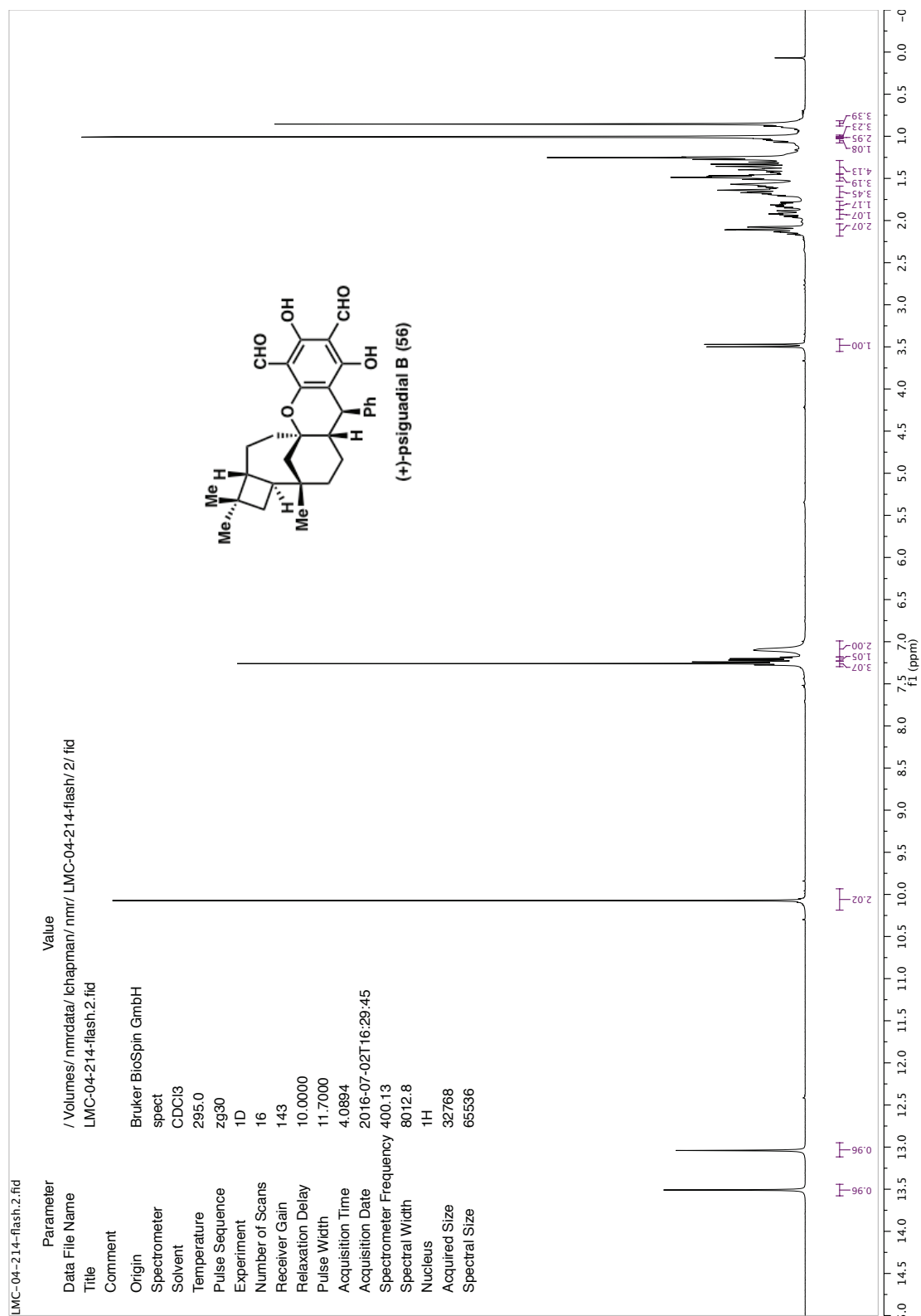


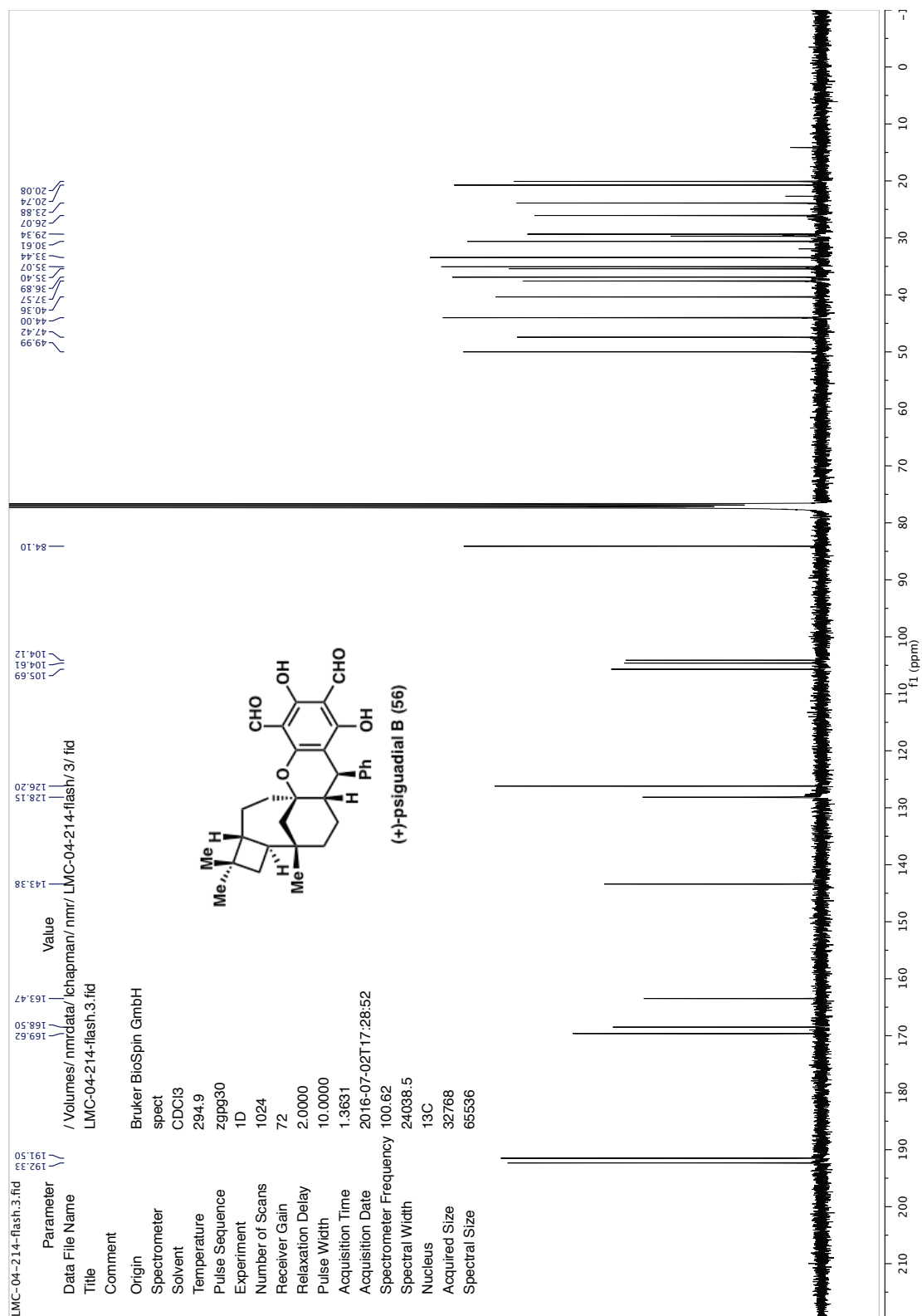












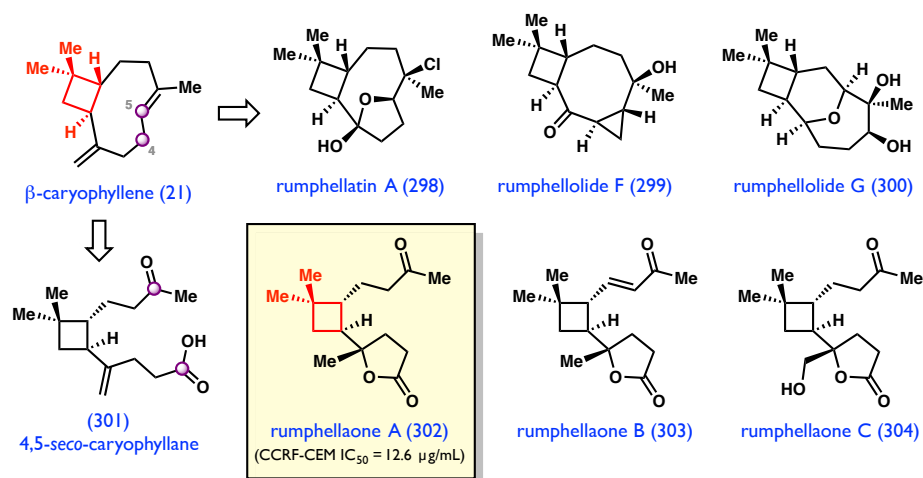
Appendix 4

Progress Toward a Concise Total Synthesis of (+)-Rumphellaone A

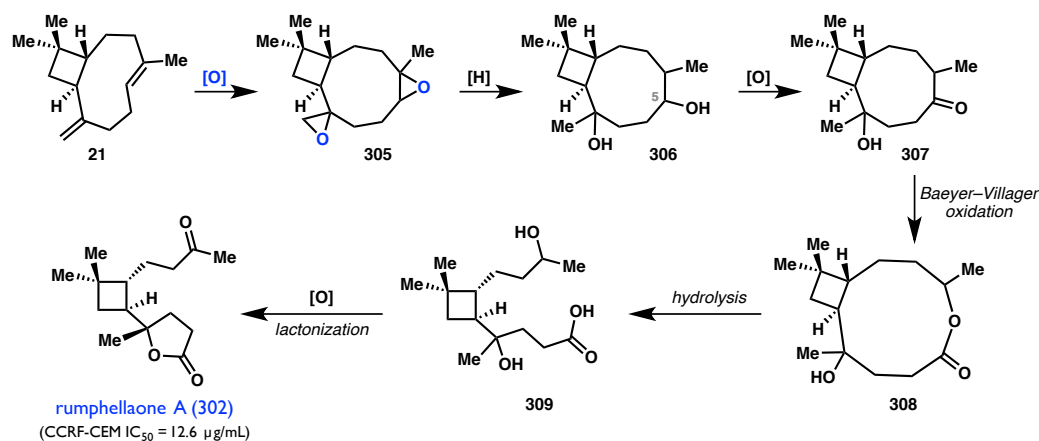
4.1 INTRODUCTION

4.1.1 Isolation and Biosynthetic Origins

A variety of β -caryophyllene-derived natural products, such as **298–300**, have been isolated from the gorgonian coral, *Rumphella antipathies* (Figure 4.1).¹ In 2010, Chung and coworkers reported the discovery of (+)-rumphellaone A (**302**), which was found to exhibit cytotoxicity against a human T-cell acute lymphoblastic leukemia tumor cell line (CCRF-CEM $IC_{50} = 12.6 \mu\text{g/mL}$). From a structural standpoint, **302** is a novel 4,5-*seco*-caryophyllane sesquiterpenoid; although several C4-C5 oxidative cleavage products of β -caryophyllene (**21**) have been reported previously (e.g. **301**),² **302** possesses an unprecedented γ -butyrolactone.³ Two additional members of this family, rumphellaones B and C (**303** and **304**), were isolated from the same marine invertebrate several years later and were shown to possess anti-inflammatory activity.⁴

Figure 4.1. Rumphellaone A and related β -caryophyllene-derived natural products

Biosynthetically, **302** is proposed to originate from β -caryophyllene (**21**) by double epoxidation, followed by reduction to give diol **306** (Scheme 4.1).² Oxidation of the secondary alcohol at C5 affords ketone **307**, which may undergo Baeyer–Villiger oxidative ring expansion to produce **308**. Hydrolysis of this 10-membered lactone gives rise to 4,5-*seco*-caryophyllane **309**, a possible precursor for other members of this family (e.g. **301**, Figure 4.1). Lactonization of **309** and a final oxidation then provides the natural product, (+)-rumphellaone A (**302**).

Scheme 4.1. Proposed biosynthesis of (+)-rumphellaone A

4.2 PREVIOUS TOTAL SYNTHESSES OF (+)-RUMPHELLAONE A

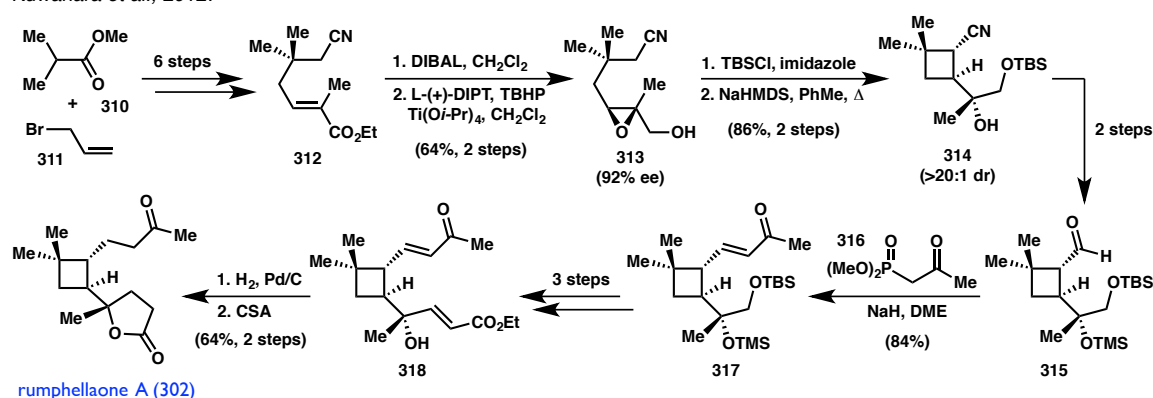
4.2.1 Kuwahara's Enantioselective Synthesis

The first enantioselective total synthesis of (+)-rumphellaone A (**302**) was achieved by Kuwahara and coworkers in 2012 (Scheme 4.2).⁵ Nitrile **312** was obtained in 6 steps from methyl isobutylate (**310**) and allyl bromide (**311**). Chemoselective reduction of the ester in **312** using DIBAL gave an allylic alcohol that was used to effect a Sharpless asymmetric epoxidation, furnishing **313** in 92% ee and 64% yield, over the two steps. Following protection of the primary alcohol, the cyclobutane ring was formed via a key epoxy nitrile cyclization,⁶ providing *trans*-cyclobutane **314** in excellent yield and diastereoselectivity. Initial efforts to develop this transformation provided mixtures of *cis* and *trans* cyclobutanes; however, the use of excess base at elevated temperatures was found to be crucial for complete conversion to the thermodynamic *trans* product.

Reduction of nitrile **314** to aldehyde **315** then facilitated installation of rumphellaone's "northern" methyl ketone via homologation with Wittig reagent **316**. The remaining carbons were introduced using a Horner–Wadsworth–Emmons reaction to

Scheme 4.2. Kuwahara's enantioselective total synthesis of (+)-rumphellaone A

Kuwahara et al., 2012:

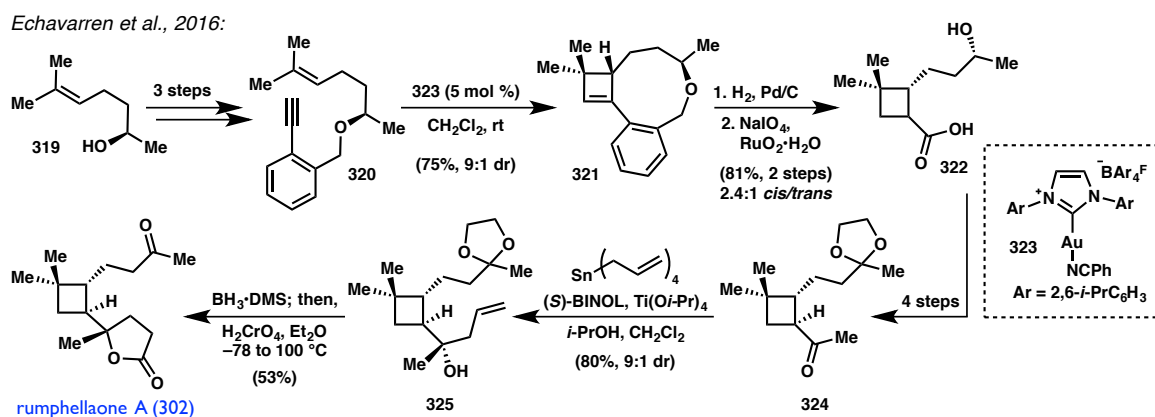


afford **318** after 3 steps. Global hydrogenation and a final lactonization then furnished (+)-**302** in 18 steps from commercially available starting materials.

4.2.2 Echavarren's Asymmetric Synthesis

Four years after Kuwahara's initial disclosure, Echavarren and coworkers reported a markedly different strategy toward **302**⁷ that highlights the utility of their previously developed gold(I)-catalyzed [2+2] cycloaddition of 1,10-enynes⁸ (Scheme 4.3). The key cycloaddition substrate **320** was accessed in short order from enantioenriched alcohol **319** via *O*-benzylation and a Sonogoshira reaction. Treatment of **320** with 5 mol % of gold catalyst **323** provided macrocyclic cyclobutene **321** in 75% yield and 9:1 dr. Hydrogenolysis of the benzyl ether in **321**, followed by oxidative cleavage of the aryl group gave carboxylic acid **322**. A 4-step sequence involving base-mediated epimerization of an ester generated *in situ* provided *trans*-ketone **324**, which was subjected to an asymmetric allylation reaction, delivering tertiary alcohol **325** in 80% yield and 9:1 dr. Finally, a one-pot procedure⁹ converted the homoallylic alcohol in **325** into the γ -butyrolactone with concomitant deprotection to afford **302** in 12 total steps.

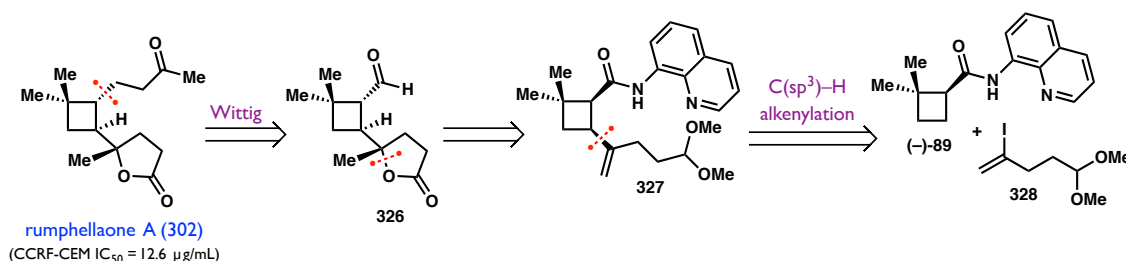
Scheme 4.3. Echavarren's asymmetric total synthesis of (+)-rumphellaone A



4.3 RETROSYNTHETIC ANALYSIS

Having developed an enantioselective total synthesis of (+)-psiguadial B (**56**), we sought to apply the key strategy concepts in the context of other bioactive, *trans*-cyclobutane-containing natural products, such as (+)-rumphellaone A (**302**). We reasoned that **302** could be obtained through a late-stage Wittig reaction with *trans*-aldehyde **326**, using the reaction conditions developed by Kuwahara.⁵ In turn, *trans*-aldehyde **326** would be accessed using the Schwartz reduction/epimerization sequence previously developed for the synthesis of **56**. Construction of the γ -butyrolactone was envisioned to be enabled by hydration of the vinyl group in **327**, which would be the direct product of a C(sp³)-H alkenylation reaction between cyclobutane (–)-**89** and vinyl iodide **328**. Thus, our studies commenced by determining the feasibility of joining these two fragments.

Figure 4.2. Retrosynthetic analysis for (+)-rumphellaone A

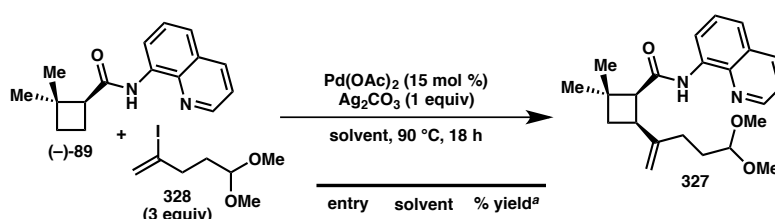


4.4 FORWARD SYNTHETIC EFFORTS

Vinyl iodide **328** was easily prepared via ketalization of the corresponding known aldehyde.¹⁰ Subjection of (–)-**89** and 3 equiv **328** to the standard Pd-catalyzed C(sp³)-H alkenylation reaction conditions resulted in formation of the expected product, **327** as a single diastereomer, albeit in only 11% yield (Table 4.1, entry 1). The reaction profile

was quite clean and analysis of the crude mixture by TLC and ^1H NMR revealed that the low yield resulted from poor conversion of the starting materials, both of which remained intact. Given that solvent choice proved critical in the optimization of this transformation for the synthesis of **147** (see Chapter 2, Table 2.1), both toluene and dioxane were investigated (entries 2 and 3), but each gave similarly disappointing results. A more thorough survey of reaction parameters is currently ongoing with parallel efforts to identify alternative iodides that might react more efficiently than **328**.

Table 4.1. Preliminary solvent screen for $\text{C}(\text{sp}^3)\text{--H}$ alkenylation with iodide **328**



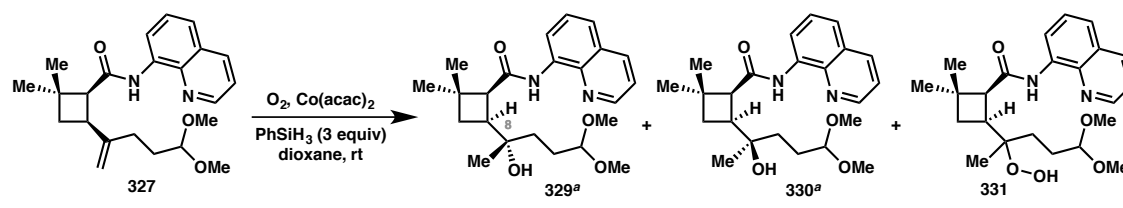
entry	solvent	% yield ^a
1	TBME	11
2	PhMe	12
3	dioxane	13

^a Determined by ^1H NMR against an added internal standard.

With modest quantities of **327** in hand, Markovnikov hydration of the 1,1-disubstituted olefin was accomplished using Mukaiyama's protocol.¹¹ Exposure of **327** to 20 mol % $\text{Co}(\text{acac})_2$ and phenyl silane under a balloon atmosphere of O_2 effected slow conversion to **329** and **330**, as well as peroxide **331**, each as a ~1:1 mixture of diastereomers at C8 (Table 4.2, entry 1). Increasing the catalyst loading to 40 mol % significantly reduced reaction time, and the addition of 2 equiv triphenylphosphine after workup led to the disappearance of **331**, allowing isolation of **329** and **330** as the sole products in a combined 44% yield (entry 2). Formation of peroxide **331** was not observed when triphenylphosphine was present *during* the reaction,¹² though a more complex reaction profile and lower overall yield was observed with the use of 1 equiv $\text{Co}(\text{acac})_2$

(entry 3). Although **329** and **330** could be separated using preparative TLC, determination of the configuration at C8 could not be established by 2D NMR spectroscopy.¹³

Table 4.2. Mukaiyama hydration of terminal olefin **327**



entry	scale (mg)	Co(acac) ₃	PPh ₃ (2 equiv)	time for full conversion	% yield (329:330)	% 331
1	3.4	20 mol %	none	5 h	37 (ND)	49
2	7.4	40 mol %	after wrkp	2 h	44 (1.3:1)	0
3	8.3	100 mol %	during rxn	1.5 h	24 (1.3:1)	0

^a Configuration at C8 is assigned arbitrarily.

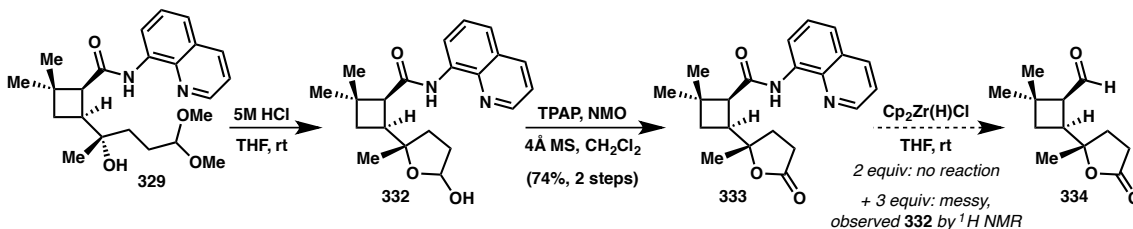
Deprotection of the dimethylacetal in **329** was accomplished using aqueous HCl in THF and the crude mixture of diastereomeric lactols (**332**) was subjected to standard Ley oxidation conditions, which smoothly afforded γ -butyrolactone **333** in 74% yield, over the two steps (Scheme 4.4a). However, no reaction was observed when **333** was exposed to 2 equiv Schwartz's reagent—a result that was quite surprising.¹⁴ Upon the addition of excess reagent, the reaction profile became complex. Although Georg has reported several examples of chemoselective reduction of amides over esters using Schwartz's reagent,¹⁵ analysis of the crude reaction mixture by ¹H NMR showed only the formation of lactol **332**, with no evidence of aminoquinoline cleavage.

Discouraged by the inability to achieve a chemoselective amide reduction in the presence of the lactone, attention turned to reduction at an earlier stage. Unfortunately, attempted Schwartz reduction of **330** also resulted in no reaction; in this case, adding another portion of Schwartz reagent resulted in only recovered starting material (Scheme 4.4b). Likewise, an attempt to employ a stronger reducing agent was unsuccessful;

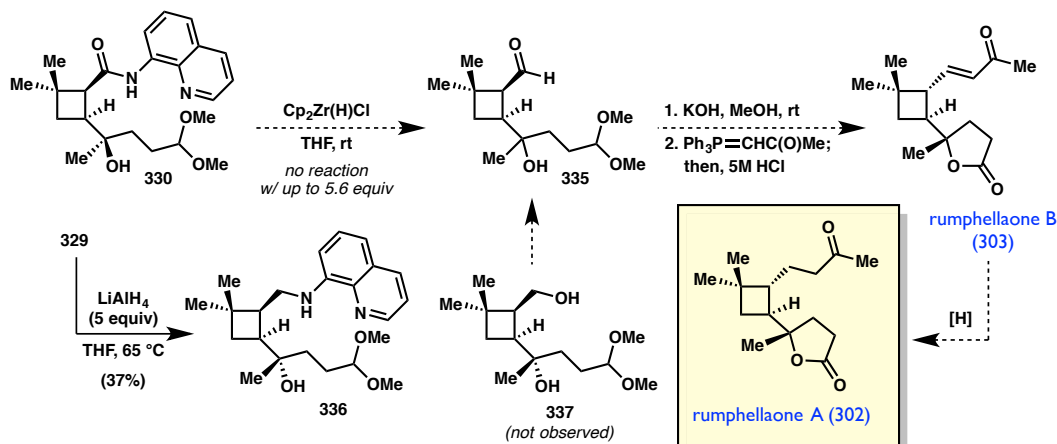
treatment of **329** with excess LiAlH_4 in refluxing THF led to isolation of secondary aryl amine **336** in 37% yield without any evidence that the desired alcohol **337** had formed.

Scheme 4.4. Construction of γ -butyrolactone and attempted Schwartz reduction

a) Completion of the γ -butyrolactone and efforts to cleave the auxiliary



b) Attempts toward amide reduction at an earlier stage

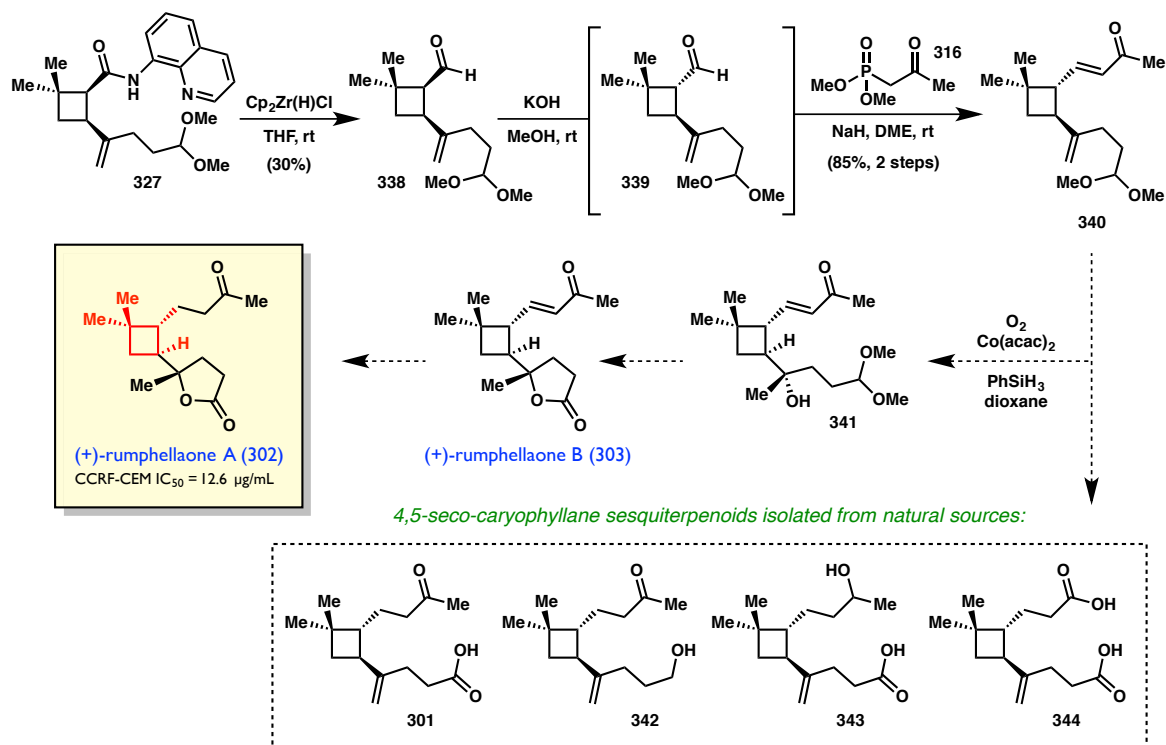


Since these initial attempts to remove the aminoquinoline auxiliary were met without success, we considered that a survey of other reducing agents, or conversion to a more activated tertiary amide, might allow access to **335** from **329/330**.¹⁶ Alternatively, it was hypothesized that cleavage of the auxiliary in **327** prior to olefin functionalization might be possible; although competitive hydrosilylation could prove problematic with Schwartz reagent, it was anticipated that the hindered nature of the 1,1-disubstituted olefin in **327** might permit chemoselective reduction of the amide. Moreover, we recognized that synthesis of *trans*-aldehyde **339** would enable rapid access to several

members of the broader 4,5-*seco*-caryophyllane sesquiterpenoid family (i.e. **301** and **342–344**, see Scheme 4.5). Thus, investigation of this route was pursued.

Gratifyingly, smooth reductive cleavage of the aminoquinoline auxiliary was observed upon exposure of amide **327** to Schwartz reagent, delivering *cis*-aldehyde **338** in 30% yield (Scheme 4.5). Notably, side products resulting from hydrozirconation were not observed, and the low yield obtained from this experiment is attributed to incomplete conversion of starting material, as well as the dilute reaction concentration used on small scale.¹⁴ Subjection of **338** to the standard epimerization protocol gave *trans*-aldehyde **339**, which was telescoped through a Wittig olefination with phosphonate **316**⁵ to furnish enone **340** in 85% yield over the 2 steps. An initial attempt to apply the previously established conditions for Mukaiyama hydration of the 1,1-disubstituted olefin in **340**

Scheme 4.5. Preliminary synthetic studies toward (+)-rumphellaones A and B



led to the detection of new products by mass spectrometry with the desired molecular weight of **341**; however, the structure of these (presumably) diastereomeric products could not be definitively confirmed by ^1H NMR, due to the small scale (0.7 mg) on which this preliminary experiment was conducted. Efforts to reproduce this synthetic sequence and confirm that Mukaiyama hydration of **340** indeed affords the desired tertiary alcohol **341** are currently underway.

4.5 CONCLUDING REMARKS AND FUTURE DIRECTIONS

In summary, initial studies are disclosed toward a concise synthesis of the bioactive *trans*-cyclobutane-containing natural product, (+)-rumphellaone A (**302**). Although the preliminary results reveal that considerable optimization will be required to obtain synthetically useful yields of **327**, a $\text{C}(\text{sp}^3)\text{--H}$ alkenylation reaction between (–)-**89** and vinyl iodide **328** has been realized. Moreover, a Mukaiyama hydration reaction was successfully employed to transform **327** into tertiary alcohol **329**, which was used to complete the γ -butyrolactone ring of the natural product.

Ultimately, a chemoselective reduction of the aminoquinoline auxiliary in **327** was achieved and the corresponding aldehyde was elaborated to enone **340**, which may serve as a precursor to a variety of naturally occurring 4,5-*seco*-caryophyllane sesquiterpenoids. Current efforts are directed toward utilizing this intermediate to confirm the structure of tertiary alcohol **341**, which would require only a remaining 2 or 3 steps to access (+)-rumphellaone B, and (+)-rumphellaone A, respectively. If successful, the implementation of this synthetic strategy would constitute the shortest route to (+)-rumphellaone A reported to date.

4.6 EXPERIMENTAL SECTION

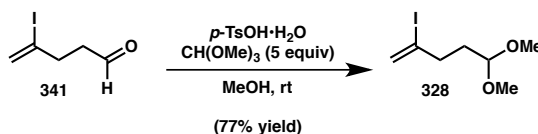
4.6.1 Materials and Methods

General Procedures. Unless otherwise stated, reactions were performed under a nitrogen atmosphere using freshly dried solvents. Tetrahydrofuran (THF), methylene chloride (CH_2Cl_2), *tert*-butyl methyl ether (TBME), toluene (PhMe), and dioxane were dried by passing through activated alumina columns. Methanol (MeOH) was distilled over calcium hydride prior to use. Unless otherwise stated, chemicals and reagents were used as received. All reactions were monitored by thin-layer chromatography using EMD/Merck silica gel 60 F254 pre-coated plates (0.25 mm) and were visualized by UV, *p*-anisaldehyde staining. Flash column chromatography was performed either as described by Still et al.¹⁷ using silica gel (particle size 0.032-0.063) purchased from Silicycle or using pre-packaged RediSep[®]Rf columns on a CombiFlash Rf system (Teledyne ISCO Inc.). ^1H and ^{13}C NMR spectra were recorded on a Bruker Avance III HD with Prodigy cryoprobe (at 400 MHz and 101 MHz respectively), a Varian 400 MR (at 400 MHz and 101 MHz, respectively), a Varian Inova 500 (at 500 MHz and 126 MHz, respectively), or a Varian Inova 600 (at 600 MHz and 150 MHz, respectively), and are reported relative to internal CHCl_3 (^1H , $\delta = 7.26$) and CDCl_3 (^{13}C , $\delta = 77.1$). Data for ^1H NMR spectra are reported as follows: chemical shift (δ ppm) (multiplicity, coupling constant (Hz), integration). Multiplicity and qualifier abbreviations are as follows: s = singlet, d = doublet, t = triplet, q = quartet, m = multiplet, br = broad, app = apparent. IR spectra were recorded on a Perkin Elmer Paragon 1000 spectrometer and are reported in frequency of absorption (cm^{-1}). HRMS were acquired using an Agilent 6200 Series TOF

with an Agilent G1978A Multimode source in electrospray ionization (ESI), or mixed (MM) ionization mode.

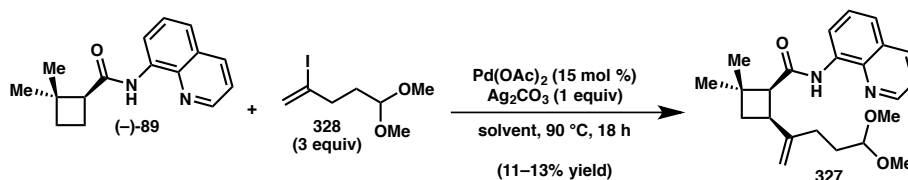
4.6.2 Preparative Procedures and Spectroscopic Data

Preparation of vinyl iodide **328**.



To a flame-dried 15 mL flask were added aldehyde **341**¹⁰ (371 mg, 1.77 mmol) and freshly distilled MeOH (5.00 mL). Trimethylorthoformate (966 μL , 8.83 mmol, 5.00 equiv) was then added, followed by *p*-toluenesulfonic acid monohydrate (16.8 mg, 0.088 mmol, 0.05 equiv). The reaction was allowed to stir at room temperature for 20 minutes, at which time the reaction was determined complete by TLC analysis. The reaction was quenched with saturated aqueous NaHCO_3 , diluted with Et_2O and the layers were separated. The aqueous layer was extracted with Et_2O (3 x 5 mL), and the combined organics were dried over MgSO_4 , filtered, and concentrated *in vacuo*. The crude residue was purified by silica gel flash chromatography (isocratic: 6% Et_2O /pentane) to afford **328** (348 mg, 77% yield) as a colorless oil.

¹H NMR (400 MHz, CDCl_3) δ 6.05 (q, J = 1.4 Hz, 1H), 5.70 (dd, J = 1.5, 0.7 Hz, 1H), 4.37 (t, J = 5.7 Hz, 1H), 3.33 (s, 6H), 2.52 – 2.40 (m, 2H), 1.87 – 1.76 (m, 2H).

Preparation of vinyl acetal 327.

To each of 3x flame-dried 1 dram vials were added (–)-**89** (30.0 mg, 0.118 mmol), **328** (90.6 mg, 0.354 mmol, 3.00 equiv), Pd(OAc)_2 (3.97 mg, 0.018 mmol, 0.150 equiv), and Ag_2CO_3 (32.5 mg, 0.118 mmol, 1.00 equiv). TBME, PhMe, or dioxane (590 μL) was then added and the vials were sealed with a Teflon screw cap under ambient conditions and heated to 90 °C in a preheated aluminum block for 18 hours. The reactions were then cooled to room temperature and each was filtered through a small plug of celite and washed with EtOAc until the filtrate runs colorless. The filtrates were concentrated *in vacuo* and 1,2,4,5-tetrachloro-3-nitrobenzene (5.90 mg, 0.023 mmol) was added as an internal standard to determine the respective yields of **327** as indicated in Table 4.1 by ^1H NMR analysis. The reaction mixtures were then combined and purified by silica gel flash chromatography (10–20% EtOAc/hexane) to afford **327** (17.3 mg, 13% yield) as an amorphous white residue.

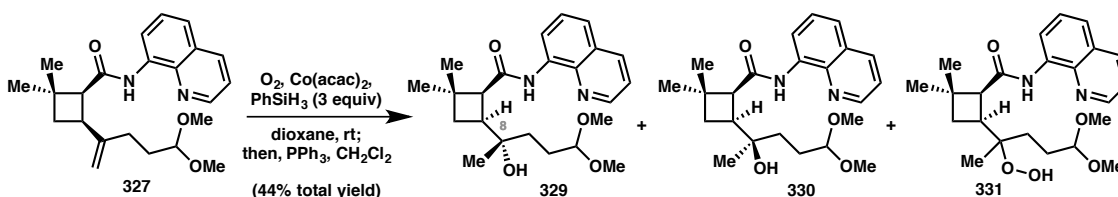
^1H NMR (400 MHz, CDCl_3) δ 9.79 (s, 1H), 8.83 (dd, $J = 7.1, 2.0$ Hz, 1H), 8.79 (dd, $J = 4.2, 1.7$ Hz, 1H), 8.14 (dd, $J = 8.3, 1.7$ Hz, 1H), 7.54 – 7.46 (m, 2H), 7.44 (dd, $J = 8.3, 4.2$ Hz, 1H), 5.01 (dd, $J = 2.1, 1.3$ Hz, 1H), 4.94 (dd, $J = 2.2, 1.2$ Hz, 1H), 4.26 (t, $J = 5.7$ Hz, 1H), 3.38 – 3.28 (m, 1H), 3.18 (s, 3H), 3.15 (s, 3H), 3.11 (ddd, $J = 8.6, 2.9, 0.7$ Hz, 1H), 2.49 (t, $J = 10.8$ Hz, 1H), 2.10 – 1.95 (m, 2H), 1.96 – 1.89 (m, 1H), 1.82 – 1.62 (m, 2H), 1.43 (s, 3H), 1.13 (s, 3H).

^{13}C NMR (101 MHz, CDCl_3) δ 171.1, 148.3, 148.1, 138.7, 136.4, 134.9, 128.0, 127.6, 121.6, 121.3, 116.7, 109.6, 104.1, 56.3, 52.9, 52.4, 37.3, 37.0, 35.3, 30.6, 30.2, 29.3, 25.2.

FTIR (NaCl, thin film) 3359, 3047, 2952, 2928, 2866, 2829, 1688, 1670, 1523, 1485, 1460, 1424, 1386, 1324, 1258, 1193, 1160, 1127, 1077, 1059, 903, 826, 792 cm^{-1} .

HRMS (MM) calc'd for $\text{C}_{23}\text{H}_{31}\text{N}_2\text{O}_3$ $[\text{M}+\text{H}]^+$ 383.2329, found 383.2340.

Preparation of hydration products **329** and **330**.



To a 1 dram vial containing **327** (7.40 mg, 0.019 mmol) was added dioxane (500 μL) and O_2 was bubbled through the resulting solution for 15 minutes before stock solutions of $\text{Co}(\text{acac})_2$ (80.0 μL , 0.100M, 0.008 mmol, 0.414 equiv) and PhSiH_3 (100 μL , 0.582M, 0.058 mmol, 3.00 equiv) were added successively via syringe. The reaction was stirred vigorously at room temperature for 2 hours, then quenched with saturated aqueous $\text{Na}_2\text{S}_2\text{O}_4$ and diluted with Et_2O . The aqueous layer was extracted 5x with Et_2O and the organics filtered through a small plug of Na_2SO_4 and concentrated *in vacuo*. The crude residue was taken up in CH_2Cl_2 (500 μL) and solid PPh_3 (10.1 mg, 0.039 mmol, 2.00 equiv) was added. The reaction was stirred for 1 hour, at which point analysis by LC/MS had indicated the disappearance of peroxide **331**. The reaction mixture was concentrated and purified by silica gel preparative thin-layer chromatography (50% EtOAc /hexane) to

afford **329** (1.90 mg, 25% yield) and **330** (1.50 mg, 19% yield) each as colorless residues.

Note: the stereochemical configuration at C8 is arbitrarily assigned.

Data for **329** (major diastereomer):

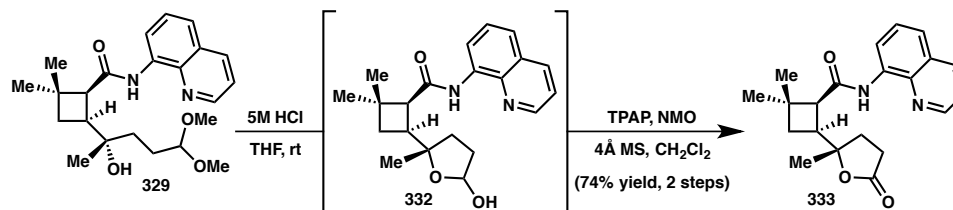
¹H NMR (400 MHz, CDCl₃) δ 9.81 (s, 1H), 8.81 (dd, *J* = 4.3, 1.7 Hz, 2H), 8.17 (dd, *J* = 8.2, 1.7 Hz, 1H), 7.55 (d, *J* = 3.4 Hz, 2H), 7.54 (s, 1H), 7.47 (dd, *J* = 8.3, 4.2 Hz, 1H), 6.18 (s, 1H), 4.35 (t, *J* = 5.7 Hz, 1H), 3.33 (s, 3H), 3.33 (s, 3H), 3.13 (ddd, *J* = 8.9, 2.3, 0.9 Hz, 1H), 2.67 (dt, *J* = 11.1, 9.0 Hz, 1H), 2.46 (t, *J* = 11.1 Hz, 1H), 1.79 (ddd, *J* = 11.2, 9.1, 2.3 Hz, 1H), 1.75 – 1.62 (m, 2H), 1.49 (ddd, *J* = 13.4, 11.6, 5.4 Hz, 1H), 1.42 (s, 3H), 1.37 – 1.28 (m, 1H), 1.15 (s, 3H), 1.10 (s, 3H).

¹³C NMR (101 MHz, CDCl₃) δ 174.2, 148.3, 138.4, 136.5, 134.0, 127.9, 127.4, 122.0, 121.7, 116.9, 105.3, 70.4, 56.1, 52.9, 52.8, 41.4, 35.8, 35.5, 34.5, 30.6, 27.2, 25.1, 24.8.

Data for **330** (minor diastereomer):

¹H NMR (600 MHz, CDCl₃) δ 9.79 (s, 1H), 8.81 (dd, *J* = 4.2, 1.7 Hz, 1H), 8.77 (dd, *J* = 6.6, 2.2 Hz, 1H), 8.17 (dd, *J* = 8.3, 1.7 Hz, 1H), 7.58 – 7.51 (m, 2H), 7.47 (dd, *J* = 8.2, 4.2 Hz, 1H), 5.99 (s, 1H), 4.28 (t, *J* = 5.7 Hz, 1H), 3.38 – 3.28 (m, 2H), 3.22 (d, *J* = 1.1 Hz, 3H), 3.19 (s, 3H), 3.11 (dd, *J* = 8.9, 2.1 Hz, 1H), 2.67 (q, *J* = 9.5 Hz, 1H), 2.49 (t, *J* = 11.2 Hz, 1H), 1.91 – 1.77 (m, 2H), 1.66 – 1.60 (m, 1H), 1.43 (s, 3H), 1.11 (s, 3H), 1.03 (s, 3H).

¹³C NMR (101 MHz, CDCl₃) δ 174.3, 148.4, 138.5, 136.6, 134.1, 128.1, 127.5, 122.1, 121.8, 117.0, 105.0, 70.9, 56.0, 53.0, 52.4, 41.4, 35.8, 35.2, 34.0, 30.7, 27.5, 25.0, 24.4.

Preparation of γ -butyrolactone **333.**

To a 2 dram vial containing **329** (1.70 mg, 0.004 mmol) was added a 1:1 mixture of THF/5M HCl (500 μ L). The reaction was stirred at room temperature for 2.5 hours, then quenched with saturated aqueous NaHCO₃ and diluted with Et₂O. The aqueous layer was extracted 5x with Et₂O and the organics filtered through a small plug of Na₂SO₄ and concentrated *in vacuo*. The crude lactol **332** was analyzed by ¹H NMR, then concentrated into another 2 dram vial and dried under high vacuum. *N*-methylmorpholine *N*-oxide (1.13 mg, 0.010 mmol, 2.27 equiv) and previously flame-dried, activated 4Å mol sieves were quickly added to the vial as a solid and the atmosphere exchanged for N₂ 1x. CH₂Cl₂ (500 μ L) was then added via syringe, followed by TPAP (1.7 mg, 0.005 mmol, 1.14 equiv) as a solid in one portion. The reaction immediately turns yellow, then brown, and was stirred at room temperature. Analysis of an aliquot of the reaction mixture by LC/MS indicated full conversion of starting material after 1 hour, at which time the reaction was diluted with CH₂Cl₂, filtered through a plug of silica gel, and concentrated to afford **333** (1.10 mg, 74% yield) as a colorless residue that was used directly in the next step.

Data for intermediate lactol **332** (mixture of diastereomers):

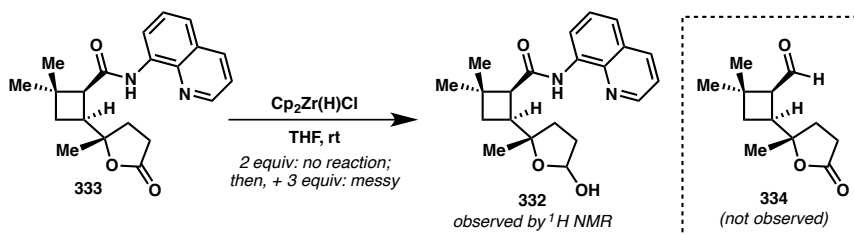
¹H NMR (500 MHz, CDCl₃) δ 11.43 (s, 1H), 9.80 (s, 1H), 9.11 – 8.64 (m, 2H), 8.19 (ddt, *J* = 14.3, 6.2, 3.0 Hz, 1H), 7.59 – 7.49 (m, 2H), 7.47 (dd, *J* = 8.4, 4.3 Hz, 1H), 3.25 – 3.05

(m, 1H), 2.95 – 2.43 (m, 2H), 2.14 (td, $J = 11.6, 8.1$ Hz, 3H), 1.67 (ddd, $J = 11.8, 7.9, 2.3$ Hz, 1H), 1.42 (s, 3H), 1.26 (s, 3H), 1.23 – 1.19 (m, 1H), 1.12 (s, 3H).

Data for γ -butyrolactone **333**:

^1H NMR (600 MHz, CDCl_3) δ 9.79 (s, 1H), 8.81 (dd, $J = 4.2, 1.7$ Hz, 1H), 8.77 (dd, $J = 7.3, 1.7$ Hz, 1H), 8.15 (dd, $J = 8.2, 1.7$ Hz, 1H), 7.56 – 7.48 (m, 2H), 7.45 (dd, $J = 8.2, 4.2$ Hz, 1H), 3.14 (dd, $J = 9.4, 2.6$ Hz, 1H), 3.06 (dt, $J = 11.1, 9.1$ Hz, 1H), 2.62 – 2.55 (m, 1H), 2.53 (dd, $J = 9.4, 3.7$ Hz, 1H), 2.51 – 2.45 (m, 1H), 2.37 (t, $J = 11.0$ Hz, 1H), 1.94 (ddd, $J = 13.1, 9.6, 3.0$ Hz, 1H), 1.88 (ddd, $J = 11.1, 8.8, 2.6$ Hz, 1H), 1.54 (s, 3H), 1.42 (s, 3H), 1.23 (s, 4H).

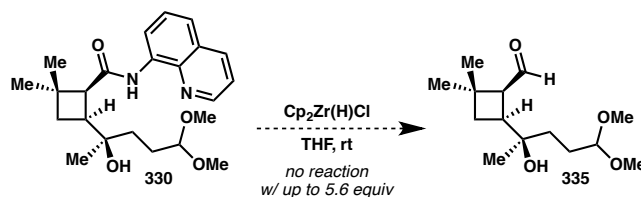
Attempted preparation of aldehyde **334**.



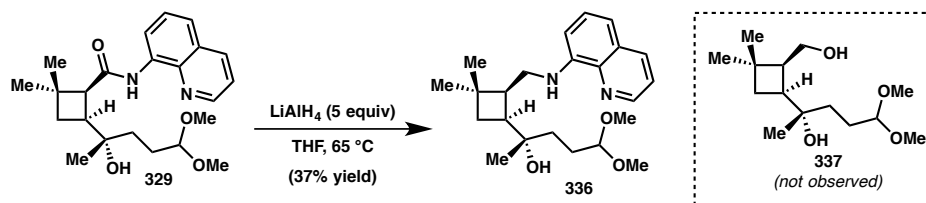
Inside a N_2 -filled glovebox, Schwartz reagent (1.60 mg, 0.006 mmol, 2.00 equiv) was added to an oven-dried vial. The vial was sealed under N_2 and brought out of the box, where THF (250 μL) was added via syringe. To the resulting suspension was added **333** (1.10 mg, 0.003 mmol) as a solution in 300 μL THF in a quick drip. The reaction was stirred at room temperature for 1 hour, at which time TLC analysis indicated that no reaction had occurred. The vial was sealed under a stream of N_2 with a Teflon screw cap and pumped into the glovebox where additional Schwartz reagent (2.40 mg, 0.010 mmol,

3.00 equiv) was added as a solid in one portion. The reaction was allowed to stir for an additional 2.5 hours, then quenched with aqueous NaHCO_3 and diluted with Et_2O . The aqueous layer was extracted 5x with Et_2O and the organics filtered through a small plug of Na_2SO_4 and concentrated *in vacuo*. Analysis of the crude reaction mixture by TLC and ^1H NMR showed a complex mixture including **332** as the major, discernable product.

Attempted preparation of aldehyde **335**.



Inside a N_2 -filled glovebox, Schwartz reagent (1.93 mg, 0.008 mmol, 2.00 equiv) was added to an oven-dried vial. The vial was sealed under N_2 and brought out of the box, where THF (250 μL) was added via syringe. To the resulting suspension was added **330** (1.50 mg, 0.004 mmol) as a solution in 300 μL THF in a quick drip. The reaction was stirred at room temperature for 2 hours, at which time TLC analysis indicated that no reaction had occurred. The vial was sealed under a stream of N_2 with a Teflon screw cap and pumped into the glovebox where additional Schwartz reagent (3.48 mg, 0.013 mmol, 3.60 equiv) was added as a solid in one portion. The reaction was allowed to stir for >24 hours, then quenched with aqueous NaHCO_3 and diluted with Et_2O . The aqueous layer was extracted 5x with Et_2O and the organics filtered through a small plug of Na_2SO_4 and concentrated *in vacuo*. Analysis of the crude reaction mixture by TLC and ^1H NMR showed no evidence of **335**, with only **330** remaining.

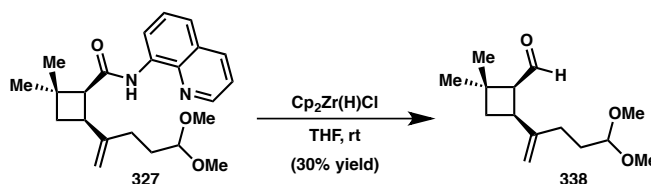
Preparation of aryl amine 336.

The atmosphere inside a ½ dram vial containing alcohol **329** (1.40 mg, 0.003 mmol) was exchanged for N_2 3x, and THF (200 μL) was added via syringe, followed by a commercial solution of LiAlH_4 (1M in THF, 17 μL , 0.017 mmol, 5.00 equiv) at room temperature. The reaction turned yellow upon addition of LiAlH_4 . The vial was sealed under a stream of N_2 with a Teflon screw cap and electrical tape, then heated to 65 °C in a preheated aluminum block for 2 hours. The reaction turns orange in the first 15 minutes of heating, then back to a bright yellow by the end of the reaction. Note: reaction turns orange/red upon exposure to ambient conditions for TLC. The reaction was then cooled to 0 °C, carefully quenched with a saturated aqueous solution of Rochelle's salt, and diluted with Et_2O . The aqueous layer was extracted 5x with Et_2O and the organics filtered through a small plug of Na_2SO_4 and concentrated *in vacuo*. The crude yellow residue was purified by silica gel preparative thin-layer chromatography (50% EtOAc /hexane) to afford **336** (0.500 mg, 37% yield) as a yellow residue. Note: several other bands on the TLC plate were collected, but none contained any spectroscopic evidence of **337**.

^1H NMR (600 MHz, CDCl_3) δ 8.70 (dd, $J = 4.1, 1.7$ Hz, 1H), 8.04 (dd, $J = 8.2, 1.7$ Hz, 1H), 7.38 (t, $J = 7.9$ Hz, 1H), 7.35 (dd, $J = 8.2, 4.2$ Hz, 1H), 7.06 (dd, $J = 8.1, 1.2$ Hz, 1H), 6.76 (d, $J = 7.7$ Hz, 1H), 6.04 (s, 1H), 4.31 (t, $J = 5.6$ Hz, 1H), 3.80 (dt, $J = 13.1, 7.0$ Hz, 1H), 3.47 – 3.40 (m, 1H), 3.31 (s, 3H), 3.30 (s, 3H), 2.53 (ddt, $J = 18.7, 7.4, 3.5$ Hz,

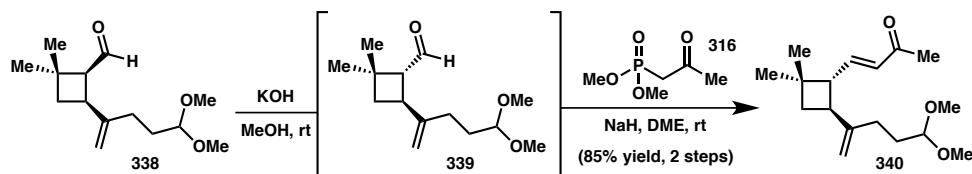
3H), 1.98 (t, $J = 10.8$ Hz, 1H), 1.65 (dddd, $J = 30.5, 19.2, 13.7, 11.1, 5.4$ Hz, 3H), 1.48 – 1.40 (m, 1H), 1.35 (ddd, $J = 13.7, 11.4, 5.4$ Hz, 1H), 1.28 (s, 3H), 1.28 (s, 3H), 1.09 (s, 3H).

Preparation of *cis*-aldehyde **338**.



Inside a N_2 -filled glovebox, Schwartz reagent (5.50 mg, 0.021 mmol, 2.18 equiv) was added to an oven-dried vial. The vial was sealed under N_2 and brought out of the box, where THF (200 μL) was added via syringe. To the resulting suspension was added a previously prepared stock solution of **327** (100 μL , 0.049 M in THF, 3.74 mg, 0.010 mmol) in a quick drip. The reaction was stirred at room temperature for 1 hour, then quenched with aqueous NaHCO_3 and diluted with Et_2O . The aqueous layer was extracted 5x with Et_2O and the organics filtered through a small plug of Na_2SO_4 and concentrated *in vacuo*. The crude residue was purified by silica gel preparative thin-layer chromatography (30% EtOAc /hexane) to afford **338** (0.70 mg, 30% yield) as a pale yellow residue.

^1H NMR (600 MHz, CDCl_3) δ 9.80 (d, $J = 6.4$ Hz, 1H), 4.95 (s, 1H), 4.86 (s, 1H), 4.33 (t, $J = 5.7$ Hz, 1H), 3.31 (dd, $J = 3.2, 0.8$ Hz, 7H), 3.25 (q, $J = 9.2$ Hz, 1H), 2.69 – 2.59 (m, 1H), 2.38 (t, $J = 11.0$ Hz, 1H), 2.06 (ddd, $J = 11.3, 8.4, 3.3$ Hz, 1H), 1.95 (dd, $J = 10.2, 6.0$ Hz, 1H), 1.88 (dd, $J = 10.4, 5.2$ Hz, 1H), 1.79 – 1.71 (m, 1H), 1.67 (ddd, $J = 16.0, 11.8, 5.7$ Hz, 1H), 1.31 (s, 4H), 1.08 (s, 3H).

Preparation of *trans*-enone 340.

To a 2 dram vial containing *cis*-aldehyde **338** (0.700 mg, 0.003 mmol) were added KOH (3.30 mg, 0.059 mmol, 20.2 equiv), and wet methanol (300 μ L). The vial was sealed under ambient conditions with a Teflon screw cap and allowed to stir vigorously at room temperature for 14 hours. The reaction was then quenched with pH 7 buffer, followed by a saturated aqueous solution of NH_4Cl . The mixture was stirred vigorously for 30 seconds before being diluted with Et_2O . The aqueous layer was extracted 6x with Et_2O , and the organics filtered through a small plug of Na_2SO_4 and concentrated *in vacuo*. The crude *trans*-aldehyde **339** (0.800 mg, quantitative yield) was analyzed by ^1H NMR, then concentrated into a 1 dram vial. The atmosphere inside the vial was exchanged 3x for N_2 , and a previously prepared stock slurry of Wittig ylide (see below: 300 μ L, 0.054 mmol, 18.6 equiv) was added using an wide-bore, 18G needle. The reaction was stirred at room temperature for 6.5 hours, then quenched with a saturated aqueous solution of NH_4Cl . The reaction mixture was diluted with Et_2O . The aqueous layer was extracted 6x with Et_2O , and the organics filtered through a small plug of Na_2SO_4 and concentrated *in vacuo* to afford *trans*-enone **340** (0.700 mg, 85% yield, 2 steps) as a colorless residue. Analysis by ^1H NMR indicated that the material was of sufficient purity to use in the next step without further manipulation.

Data for crude *trans*-aldehyde **339**:

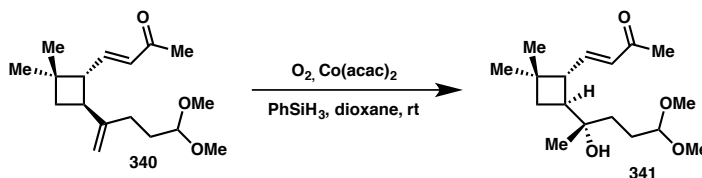
¹H NMR (600 MHz, CDCl₃) δ 9.78 (d, *J* = 2.0 Hz, 1H), 4.83 – 4.76 (m, 1H), 4.69 (d, *J* = 1.5 Hz, 1H), 4.35 (t, *J* = 5.7 Hz, 1H), 3.32 (s, 3H), 3.32 (s, 3H), 3.24 (q, *J* = 9.6 Hz, 1H), 2.77 (dt, *J* = 9.4, 1.2 Hz, 1H), 2.38 – 2.30 (m, 1H), 1.98 (t, *J* = 8.4 Hz, 2H), 1.92 – 1.84 (m, 1H), 1.75 – 1.72 (m, 2H), 1.27 (s, 3H), 1.16 (s, 3H).

Data for crude *trans*-enone **340**:

¹H NMR (600 MHz, CDCl₃) δ 6.80 (dd, *J* = 15.9, 7.7 Hz, 1H), 6.05 (dd, *J* = 16.0, 1.2 Hz, 1H), 4.75 (t, *J* = 1.4 Hz, 1H), 4.70 (s, 1H), 4.34 (t, *J* = 5.6 Hz, 1H), 3.31 (s, 6H), 2.82 (q, *J* = 9.4 Hz, 1H), 2.63 (t, *J* = 8.7 Hz, 1H), 1.99 (t, *J* = 8.2, 7.4 Hz, 2H), 1.90 (td, *J* = 8.8, 8.5, 1.7 Hz, 1H), 1.75 – 1.67 (m, 2H), 1.64 (t, *J* = 10.4 Hz, 1H), 1.10 (s, 3H), 1.07 (s, 3H).

Preparation of Wittig ylide:⁵

Inside a N₂-filled glovebox, sodium hydride (95%, 10.0 mg, 0.417 mmol) and dry DME (1.00 mL) were added to a 1 dram vial and sealed with a septum under nitrogen. The vial was brought out of the box and dimethyl (2-oxopropyl)phosphonate **316** (50.0 μL, 0.362 mmol) was added via syringe (note: gas bubbles form immediately upon addition). The reaction was allowed to stir at room temperature for 1 hour before another 1.0 mL DME was added to dilute the resulting thick, white slurry (~0.181 M ylide), which was used directly for the methylenation of crude *trans*-aldehyde **339**.

Attempted preparation of tertiary alcohol 341.

To a 1 dram vial containing **340** (0.700 mg, 0.003 mmol) were successively added stock solutions of $Co(acac)_2$ (300.0 μ L, 0.003 M, 0.001 mmol, 0.400 equiv) and $PhSiH_3$ (100 μ L, 0.075 M, 0.008 mmol, 2.67 equiv), which were each prepared in dioxane and sparged with O_2 for 15 minutes prior to use. The reaction was stirred vigorously at room temperature under an atmosphere of O_2 for 3 hours, then quenched with saturated aqueous $Na_2S_2O_4$ and stirred for 20 minutes before Et_2O was added. The aqueous layer was extracted 5x with Et_2O and the organics filtered through a small plug of Na_2SO_4 and concentrated *in vacuo*. Analysis of the crude residue by LC/MS-TOF revealed several peaks in the chromatogram corresponding to the expected mass of **341**; however, the amount of material obtained was insufficient to give discernable 1H NMR signals needed to confirm the structure.

4.7 NOTES AND REFERENCES

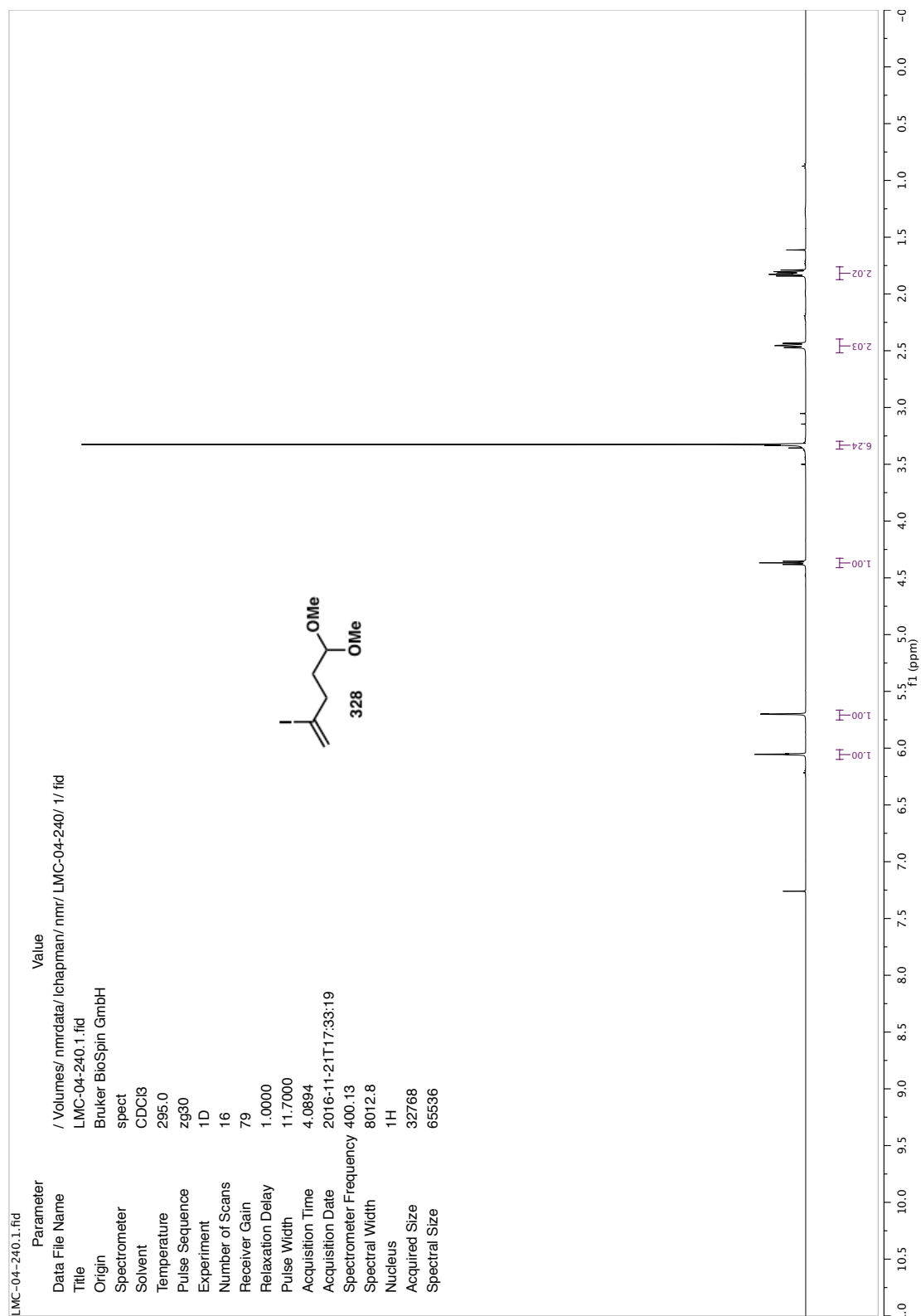
- (1) For rumphellatins A–D, see: (a) Sung, P. J.; Chuang, L. F.; Kuo, J.; Fan, T. Y.; Hu, W. P. *Tetrahedron Lett.* **2007**, 48, 3987. (b) Sung, P.-J.; Chuang, L.-F.; Hu, W.-P. *Bull. Chem. Soc. Jpn.* **2007**, 80, 2395. (c) Sung, P.-J.; Su, Y.-D.; Hwang, T.-L.; Chuang, L.-F.; Chen, J.-J.; Li, J.-J.; Fang, L.-S.; Wang, W.-H. *Chem. Lett.* **2008**, 37, 12320. For rumphellolides A–I, see: (d) Sung, P.-J.; Chuang, L.-F.; Kuo,

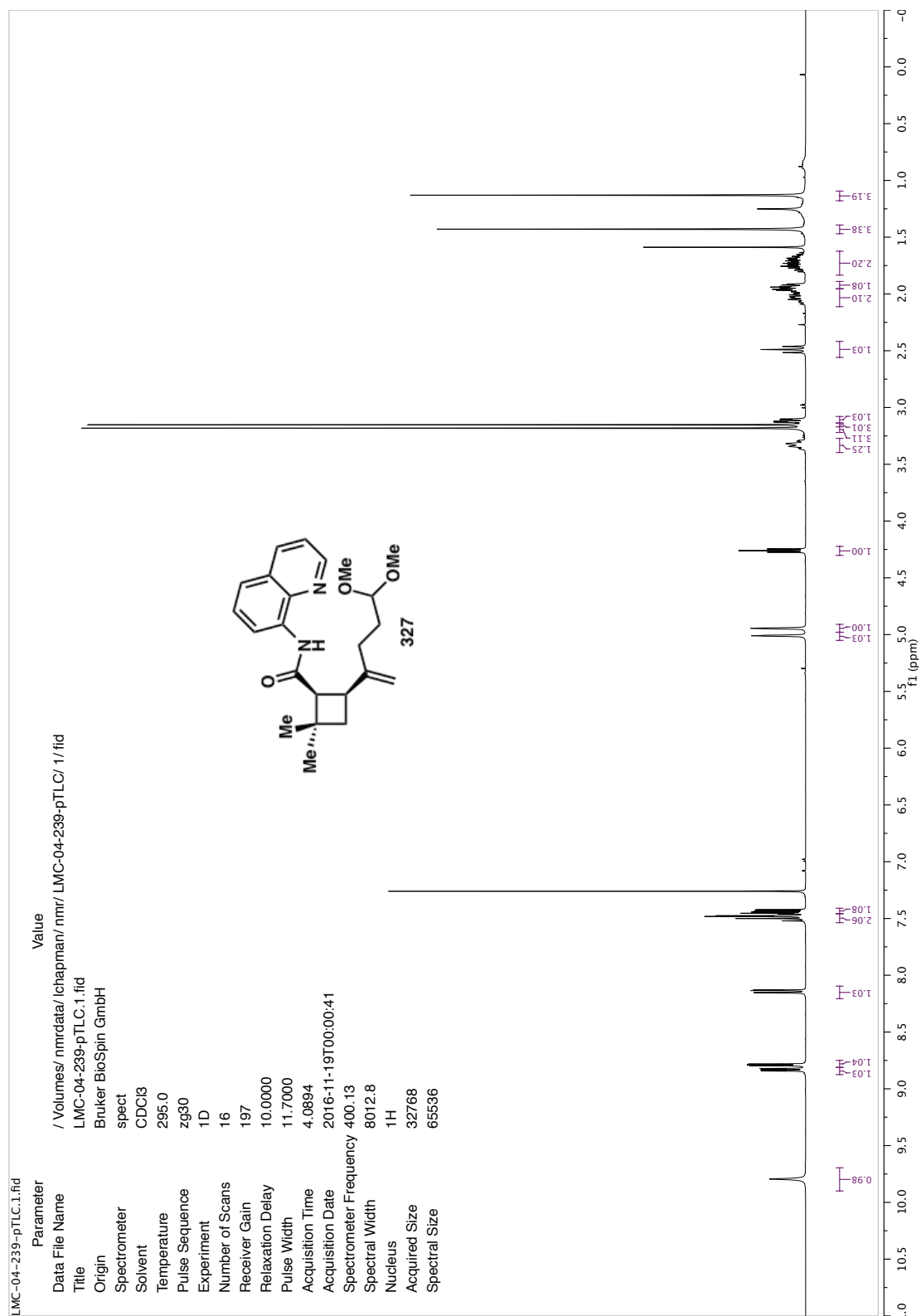
- J.; Chen, J.-J.; Fan, T.-Y.; Li, J.-J.; Fang, L.-S.; Wang, W.-H. *Chem. Pharm. Bull.* **2007**, *55*, 1296. (e) Sung, P.-J.; Chuang, L.-F.; Fan, T.-Y.; Chou, H.-N.; Kuo, J.; Fang, L.-S.; Wang, W.-H. *Chem. Lett.* **2007**, *36*, 1322. (f) Sung, P. J.; Su, Y. D.; Hwang, T. L.; Chuang, L. F.; Chung, H. M. *Chem. Lett.* **2009**, *38*, 282.
- (2) Chung, H. M.; Chen, Y. H.; Lin, M. R.; Su, J. H.; Wang, W. H. *Tetrahedron Lett.* **2010**, *51*, 6025.
- (3) (a) Bohlmann, F.; Zdero, C.; King, R. M.; Robinson, H. *Liebigs Ann. Chem.* **1984**, 503. (b) Jakupovic, J.; Pathak, V. P.; Bohlmann, F.; King, R. M.; Robinson, H. *Phytochemistry* **1987**, *26*, 803. (c) Zdero, C.; Bohlmann, F.; Anderberg, A.; King, R. M. *Phytochemistry* **1991**, *30*, 2643. (d) Quijano, L.; Vasquez-C, A.; Ríos, T. *Phytochemistry* **1995**, *38*, 1251. (e) Jaoui, M.; Lewandowski, M.; Kleindienst, T. E.; Offenber, J. H.; Edney, E. O. *Geophys. Res. Lett.* **2007**, *34*, 1.
- (4) Chung, H.-M.; Wang, W.-H.; Hwang, T.-L.; Li, J.-J.; Fang, L.-S.; Wu, Y.-C.; Sung, P.-J. *Molecules* **2014**, *19*, 12320.
- (5) (a) Hirokawa, T.; Nagasawa, T.; Kuwahara, S. *Tetrahedron Lett.* **2012**, *53*, 705. (b) Hirokawa, T.; Kuwahara, S. *Tetrahedron Lett.* **2012**, *68*, 4581.
- (6) For a seminal study, see: Stork, G.; Cohen, J. F. *J. Am. Chem. Soc.* **1974**, *96*, 5270.
- (7) Ranieri, B.; Obradors, C.; Mato, M.; Echavarren, A. M. *Org. Lett.* **2016**, *18*, 1614.
- (8) Obradors, C.; Leboeuf, D.; Aydin, J.; Echavarren, A. M. *Org. Lett.* **2013**, *15*, 1576.
- (9) Mandal, A. K.; Mahajan, S. W. *Synthesis* **1991**, *4*, 311.
- (10) Prepared according to: Holmes, M.; Kwon, D.; Taron, M.; Britton, R. *Org. Lett.* **2015**, *17*, 3868. For an alternative procedure to access this same aldehyde, see: Gao, F.; Hoveyda, A. H. *J. Am. Chem. Soc.* **2010**, *132*, 10961.

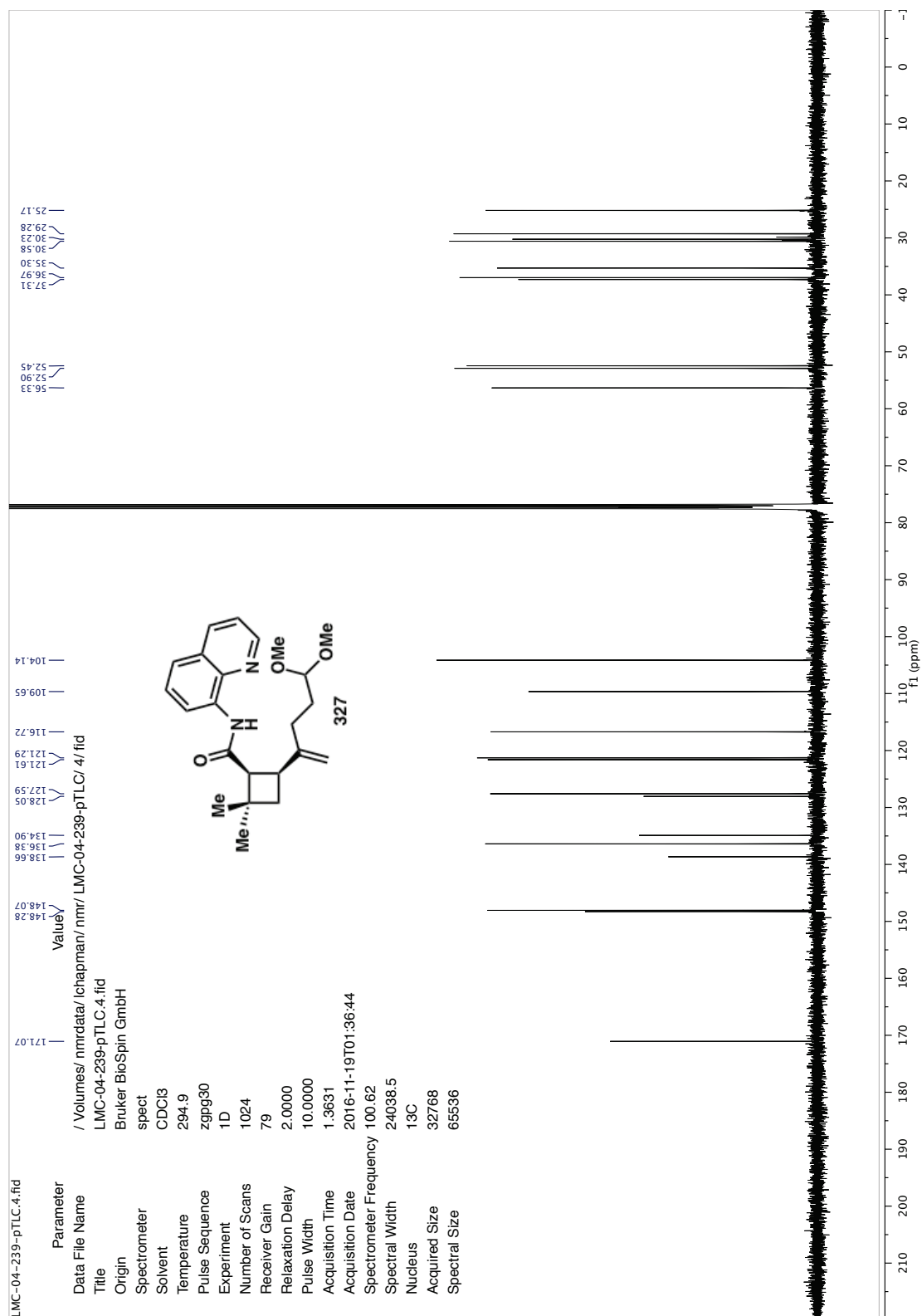
- (11) Isayama, S.; Mukaiyama, T. *Chem. Lett.* **1989**, 18, 1071.
- (12) Kawamura, S.; Chu, H.; Felding, J.; Baran, P. S. *Nature* **2016**, 532, 90.
- (13) At present, the diastereomers as drawn in this appendix are assigned arbitrarily.
- (14) In our previous studies toward (+)-psiguadial B (**56**), we have often noted that the Schwartz reduction can be sensitive to reaction concentration. Due to the small amount of material employed in these preliminary results (~1 mg), the necessarily dilute concentrations may contribute to hindrance of the desired reactivity.
- (15) (a) White, J. M.; Tunoori, A. R.; Georg, G. I. *J. Am. Chem. Soc.* **2000**, 122, 11995.
(b) Spletstoser, J. T.; White, J. M.; Tunoori, A. R.; Georg, G. I. *J. Am. Chem. Soc.* **2007**, 129, 3408.
- (16) We have also considered converting the amide to the corresponding ester using the nickel-catalyzed protocol reported recently, though this method may prove limited to aryl substrates, see: Hie, L.; Fine Nathel, N. F.; Shah, T. K.; Baker, E. L.; Hong, X.; Yang, Y.-F.; Liu, P.; Houk, K. N.; Garg, N. K. *Nature* **2015**, 524, 79.
- (17) Still, W. C., Kahn, M. & Mitra, A. *J. Org. Chem.* **1978**, 43, 2923.

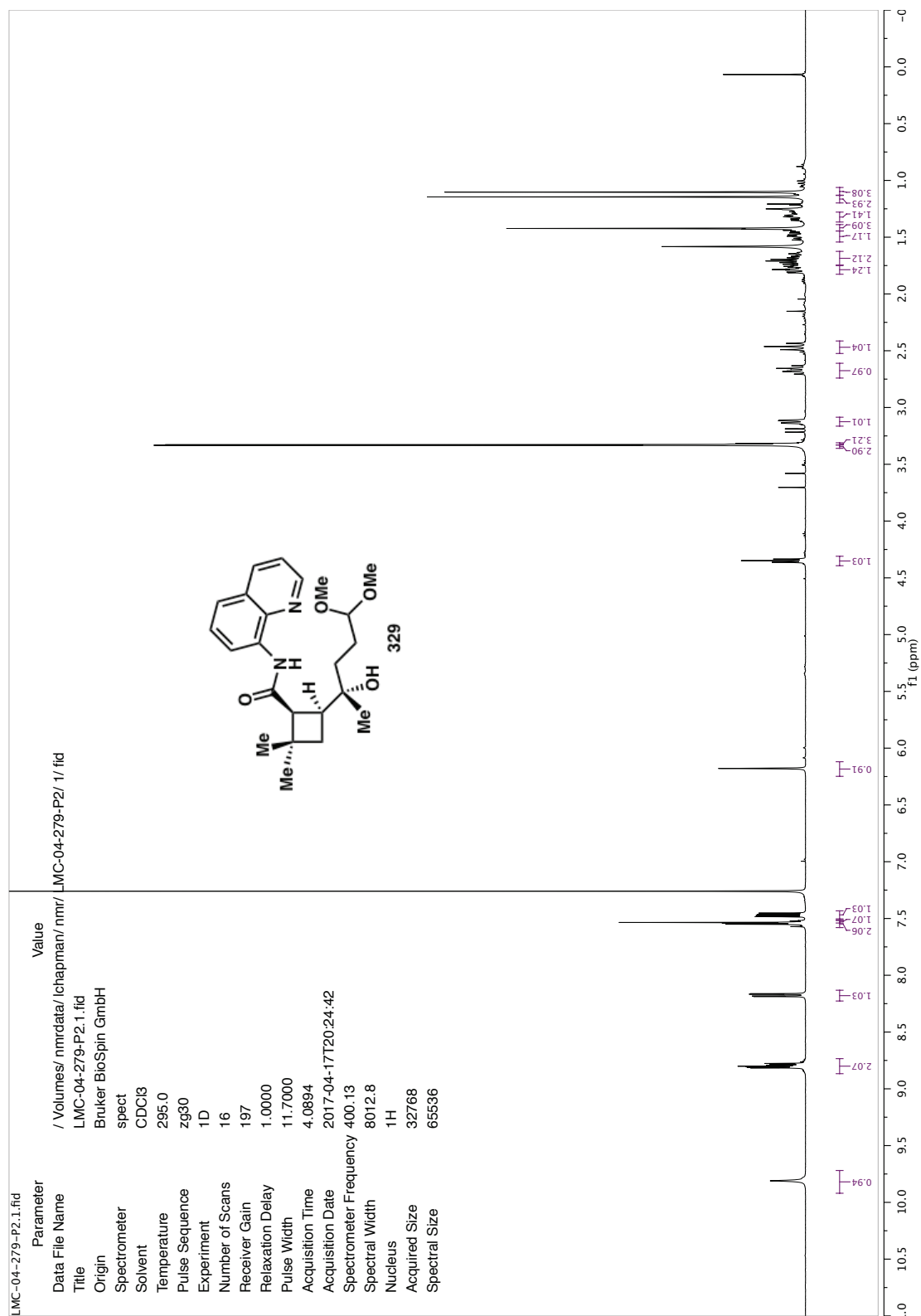
Appendix 5

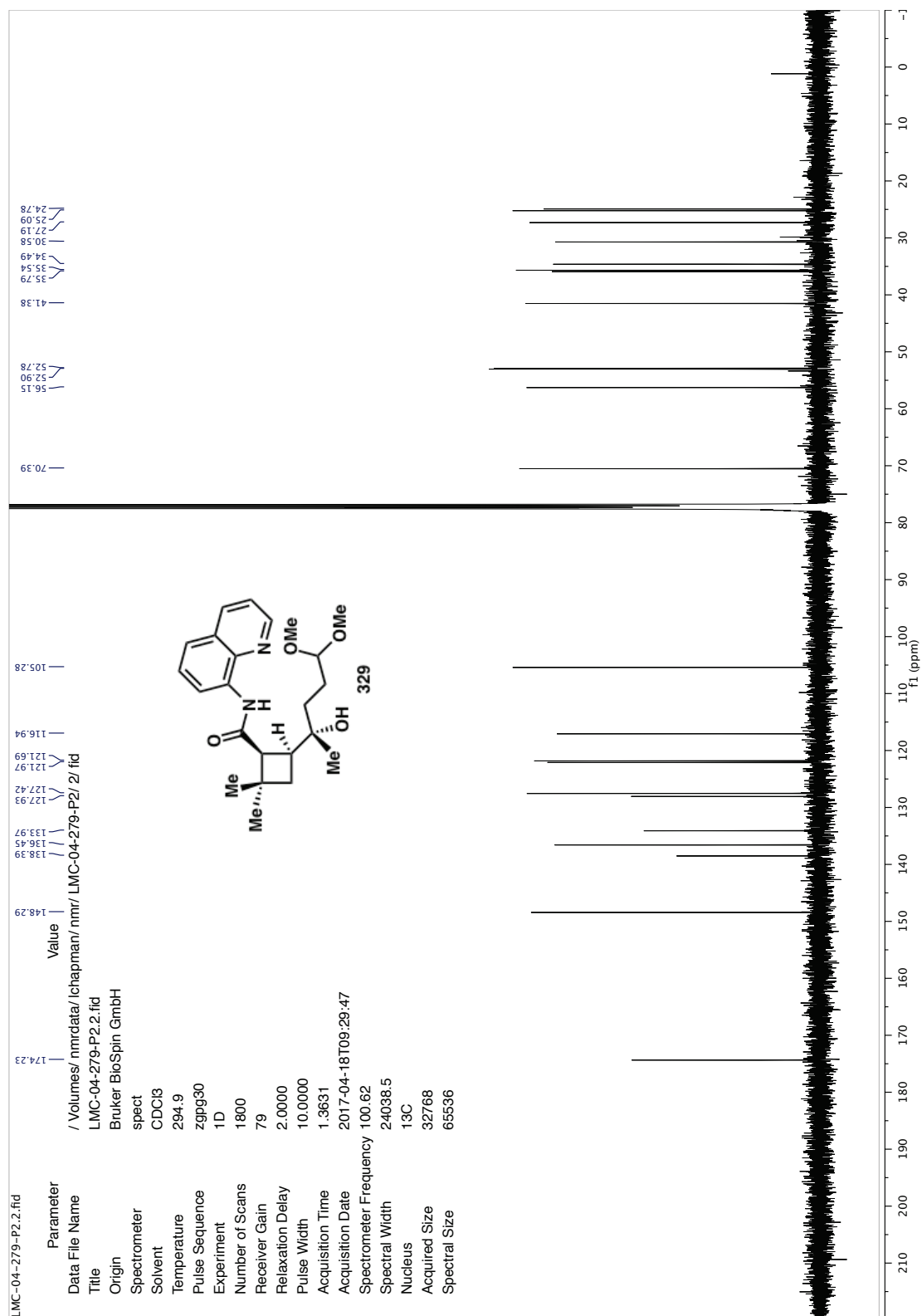
*Spectra Relevant to Appendix 4:
Progress Toward a Concise Total Synthesis of (+)-Rumphellaone A*

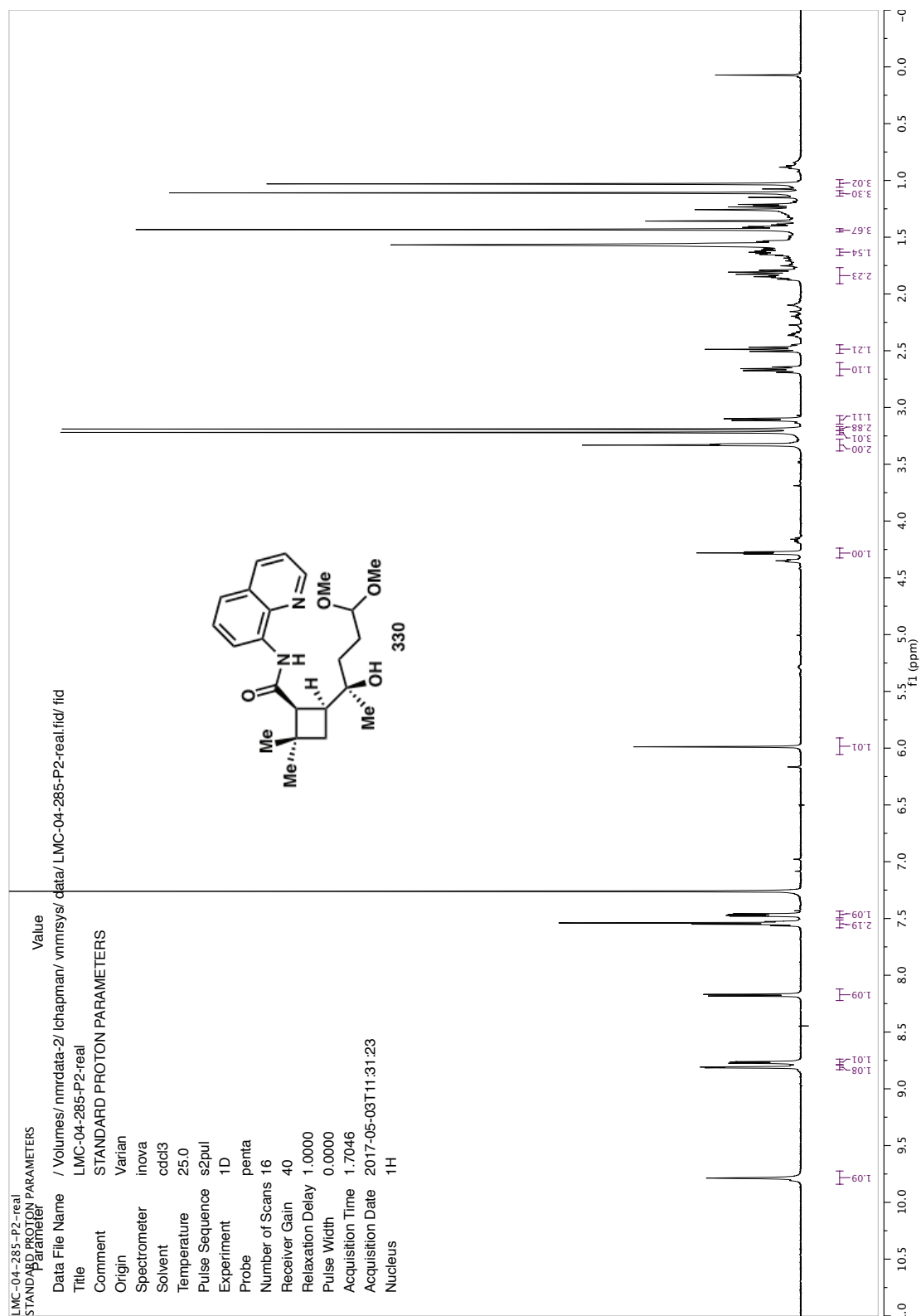


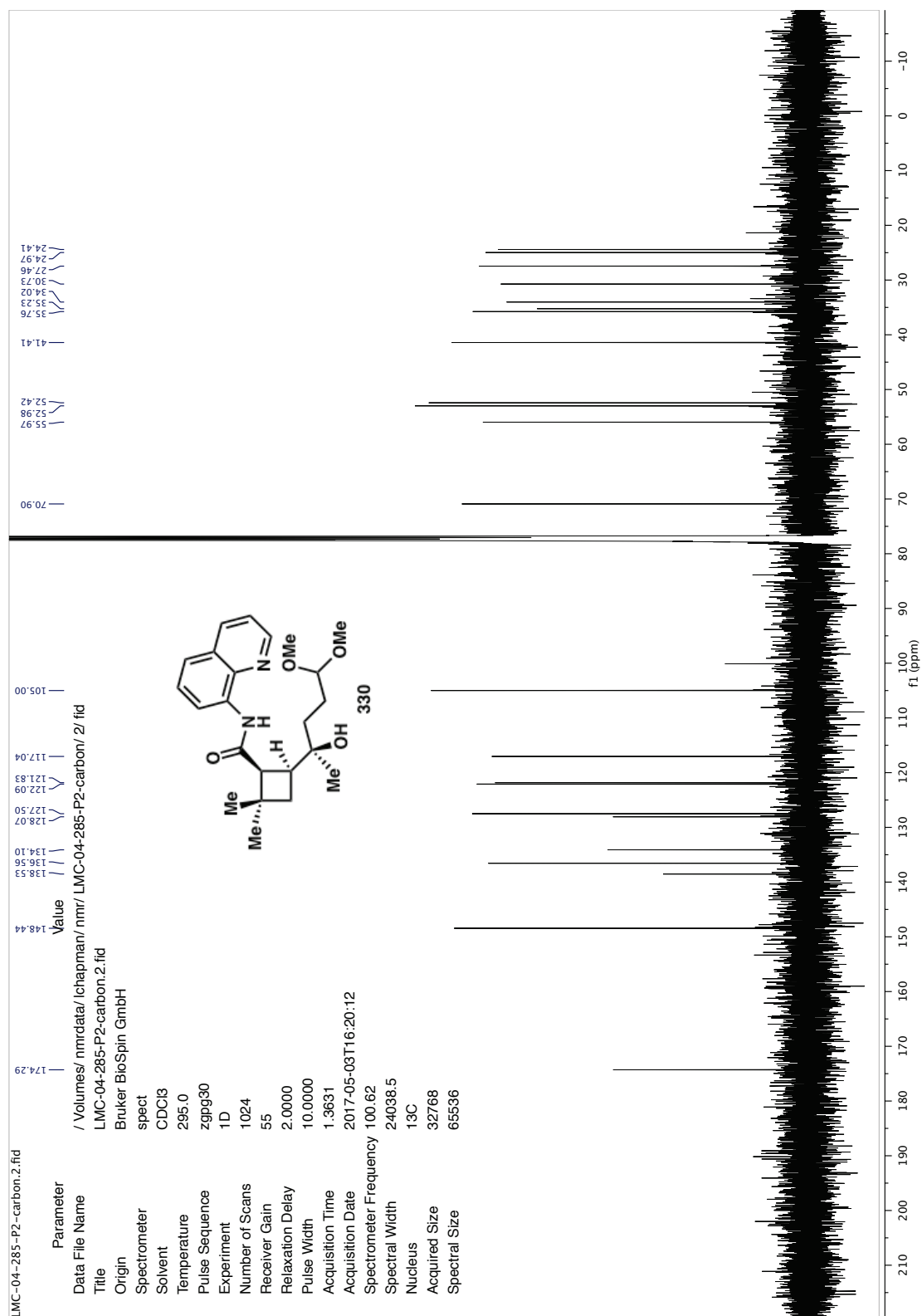


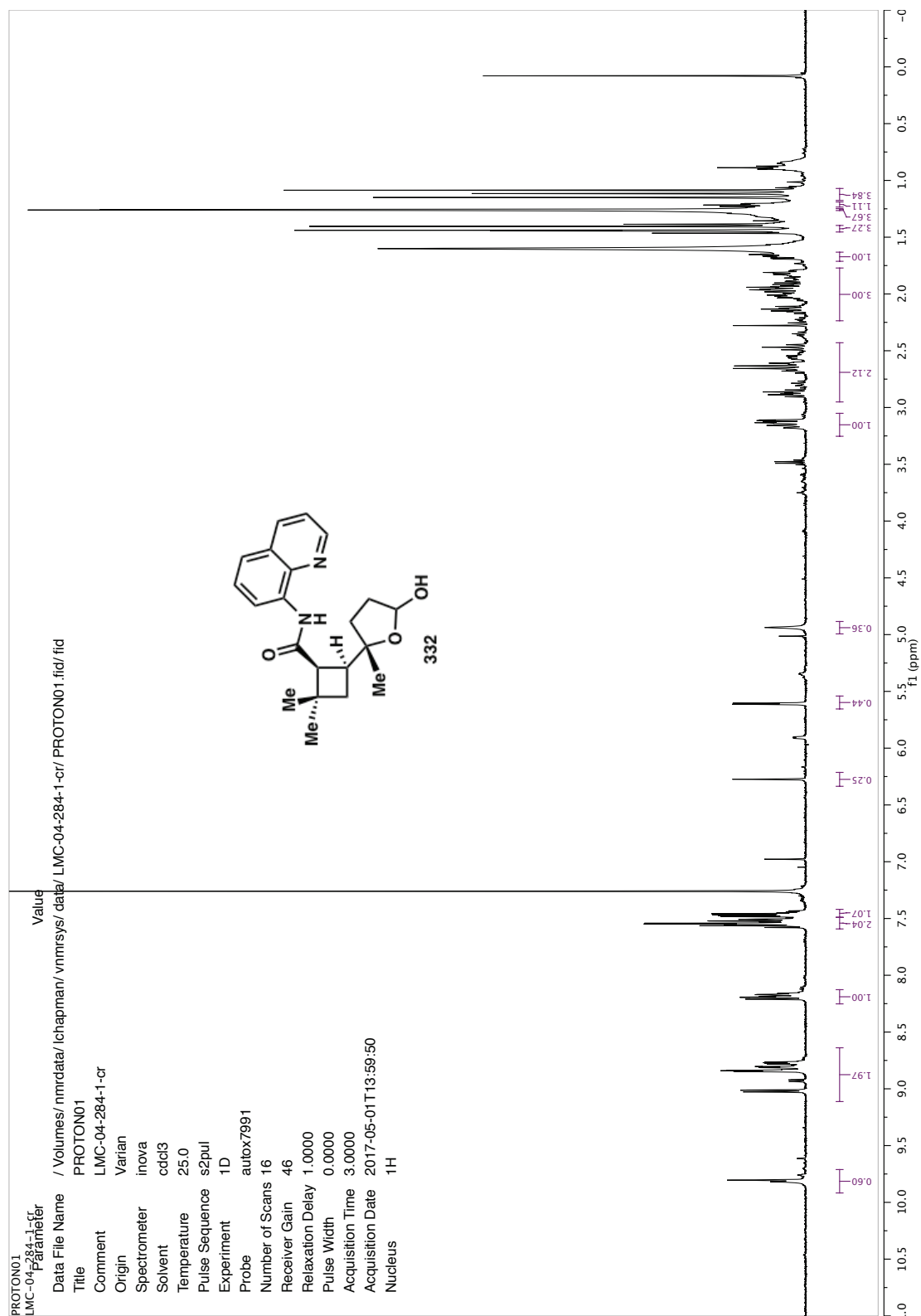


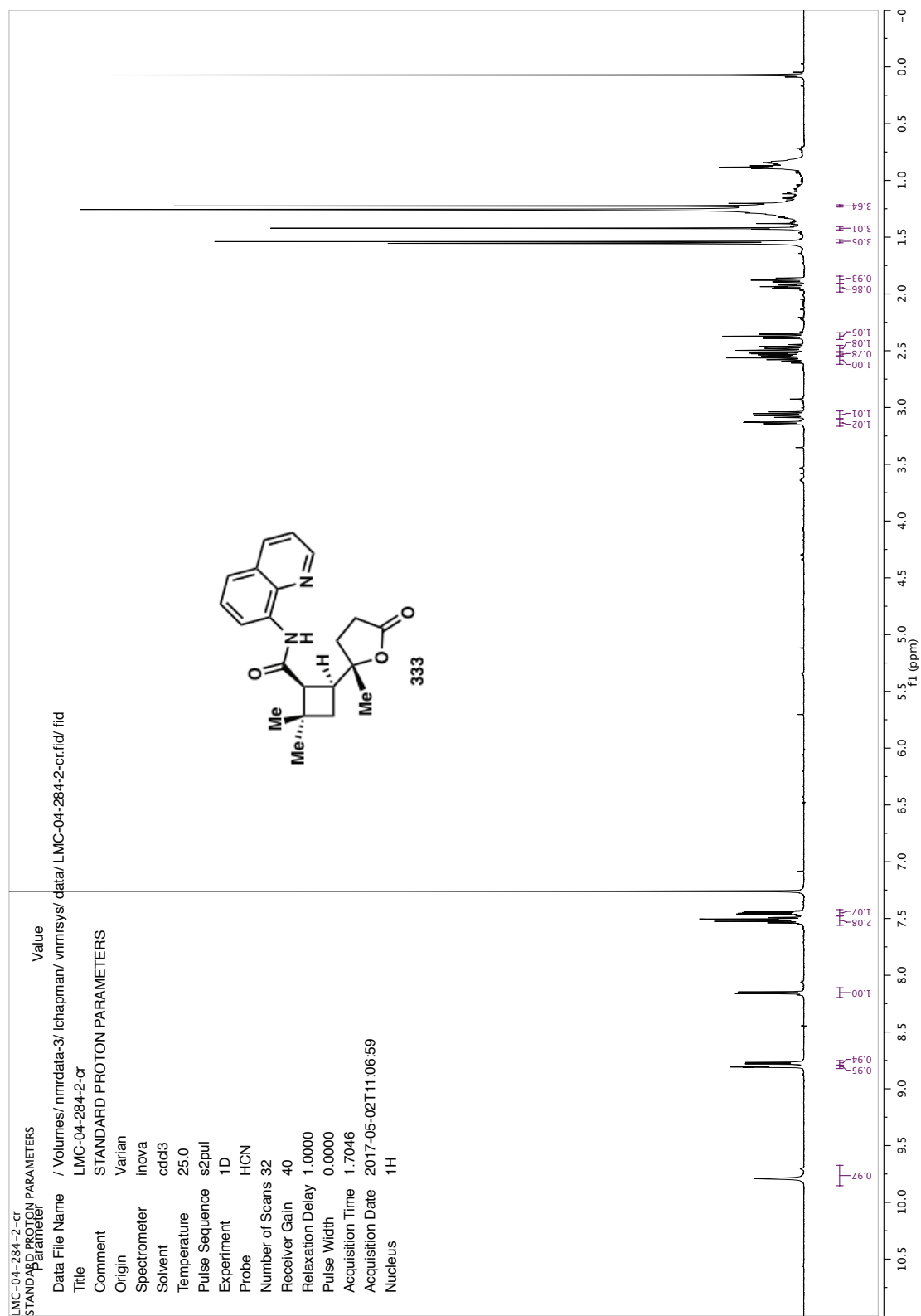


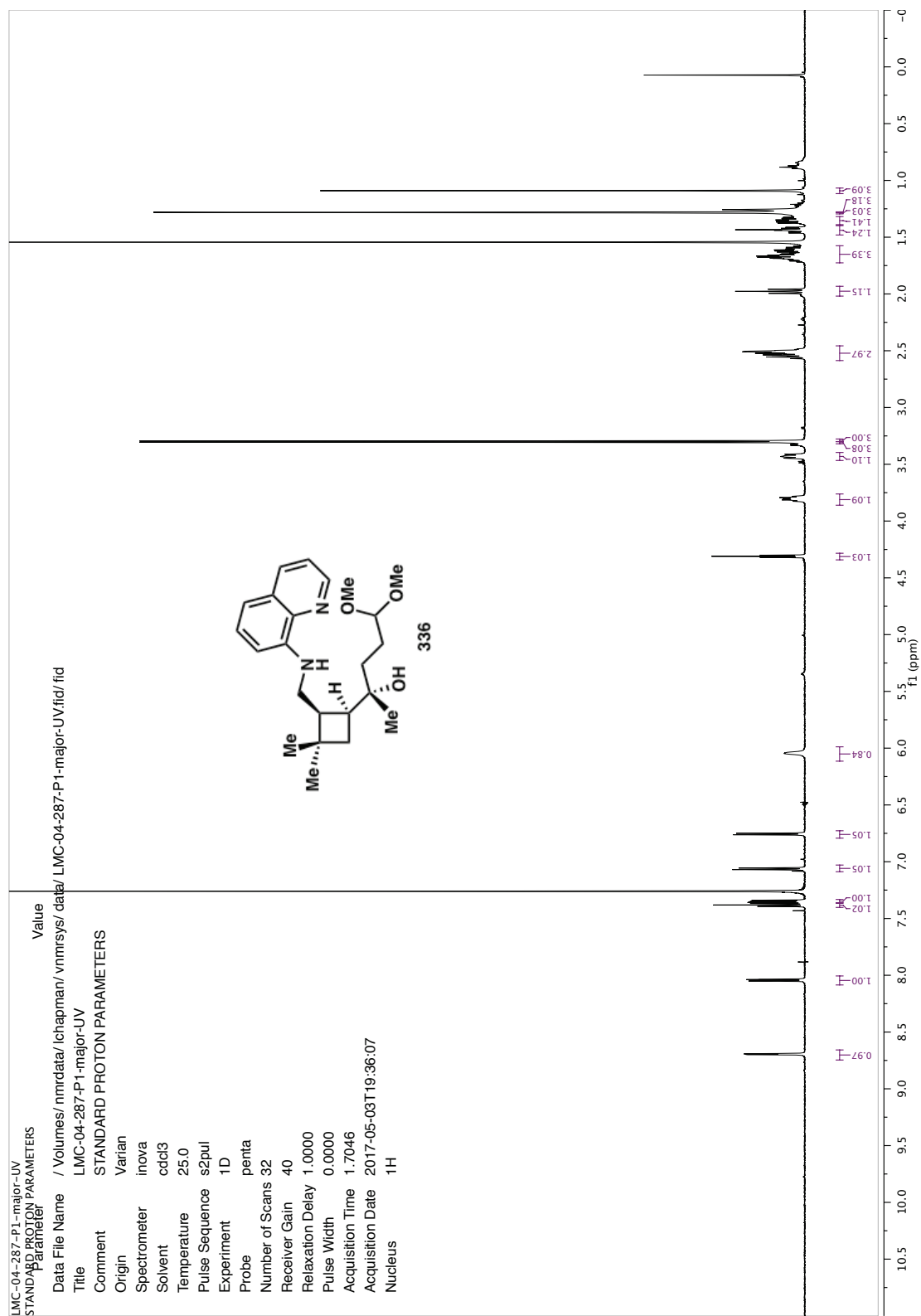


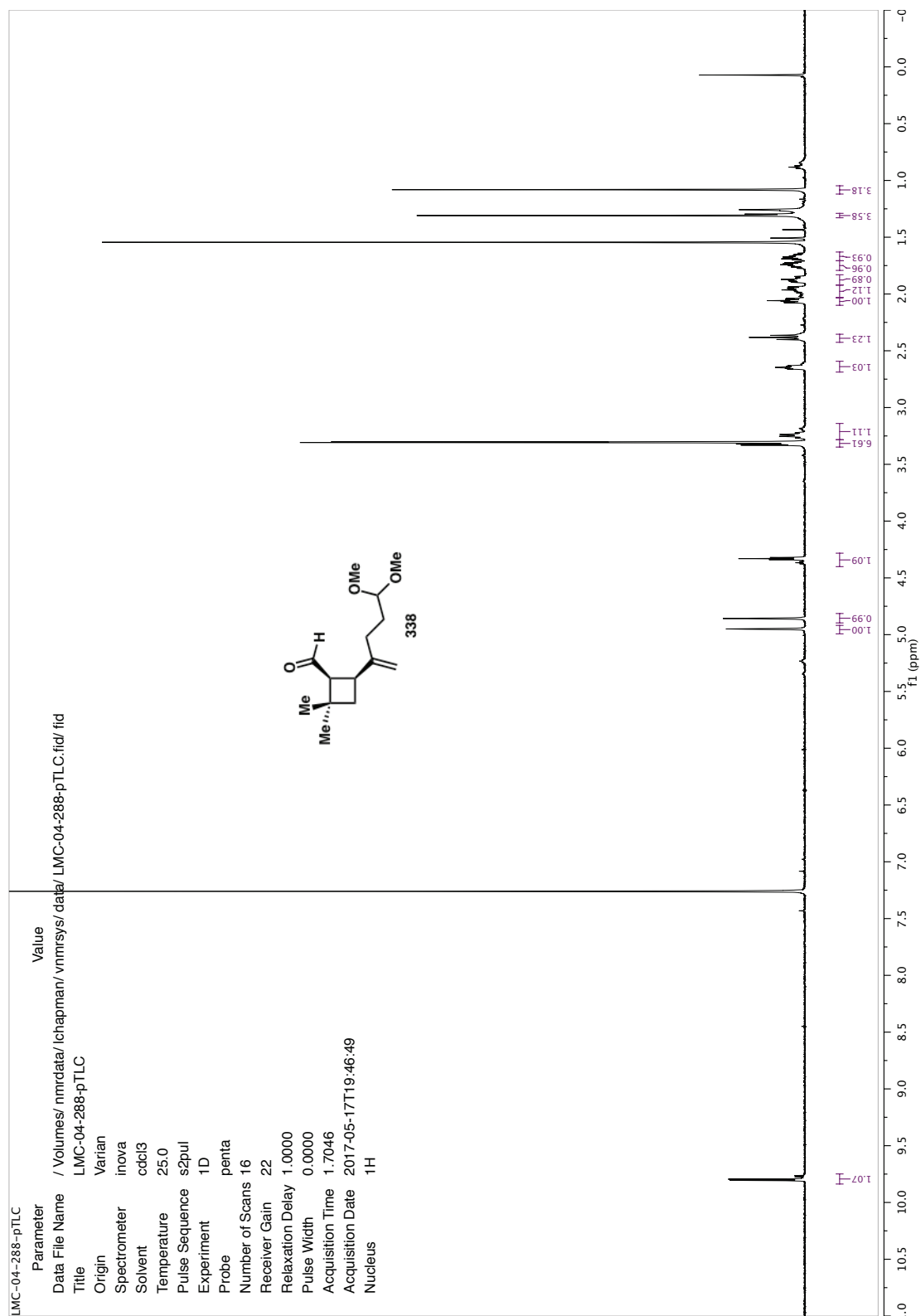


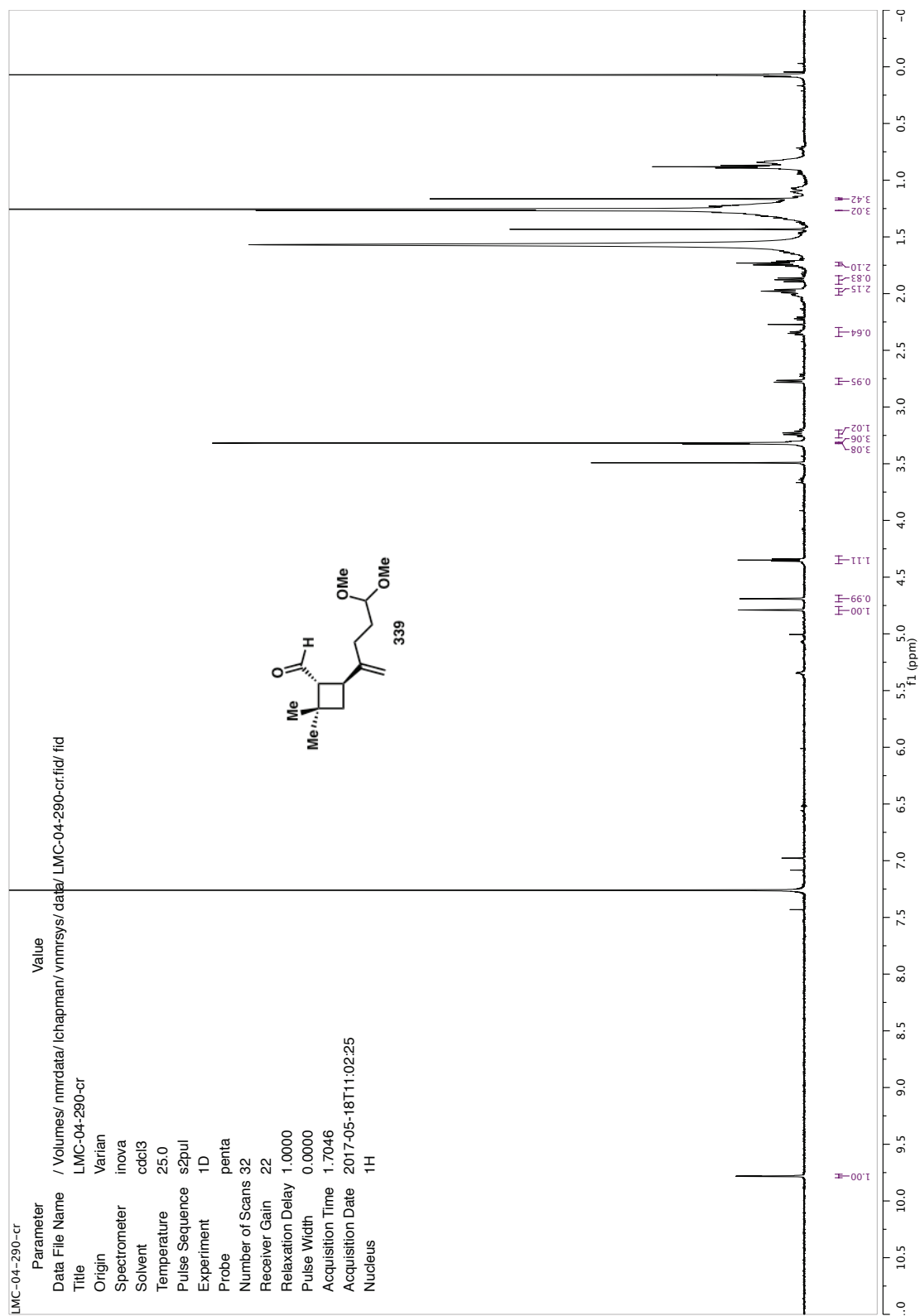


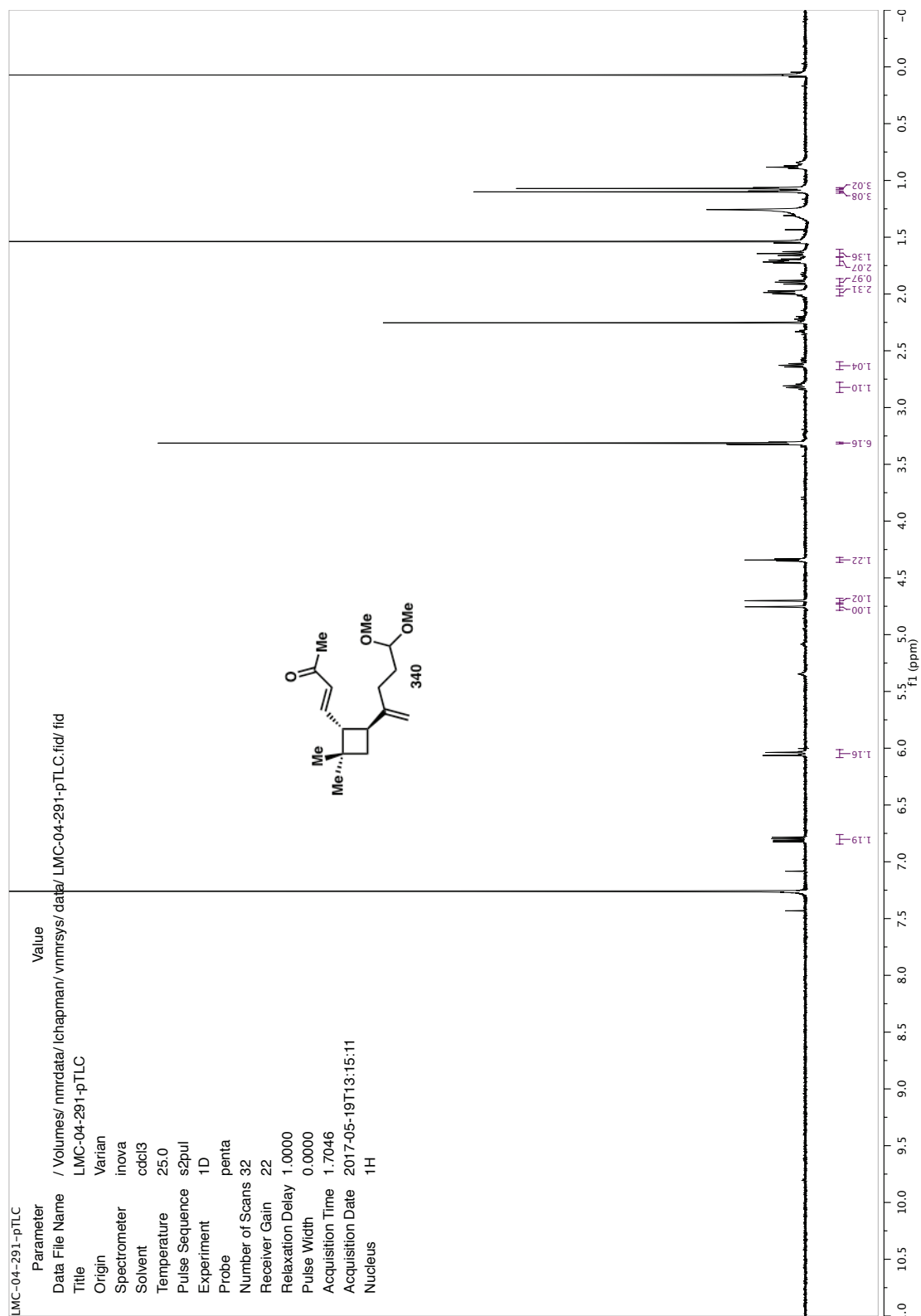












ABOUT THE AUTHOR

Lauren Marie Chapman was born on June 9th, 1986 to Garland (Gary) J. Chapman and Debra J. Chapman in White Plains, New York. She grew up in a small lake town and enjoyed swimming, fishing, boating, and ice-skating as a child. Lauren attended Mahopac High School, where her interest in science was first sparked by her chemistry teacher, who held many memorable after-school laboratory demos involving colorful fires, controlled explosions, and the synthesis of acetylsalicylic acid.

In 2004, Lauren moved to Boston, Massachusetts where she earned a joint B.S./M.S. degree at Northeastern University as a double major in chemistry and biochemistry. She also completed a minor in graphic design and served as the layout and design editor for the Spectrum Literary Arts Magazine for several years. As a participant in Northeastern's co-op program, Lauren worked at Millennium Pharmaceuticals, Merck Research Laboratories, and Northeastern's Center for Drug Discovery—three pivotal experiences that cemented her decision pursue a career in medicinal chemistry.

Lauren joined Cubist Pharmaceuticals as an associate chemist in 2009, where she worked for three years before moving to the California Institute of Technology to earn her doctoral degree under the direction of Professor Sarah Reisman. Her research has focused on developing a strategy to access *trans*-cyclobutane-containing natural products and has culminated in the first enantioselective total synthesis of (+)-psiguadial B. As an avid scuba diver, Lauren looks forward to cruising the world-class coral reefs of French Polynesia following the completion of her PhD in June of 2017. She will then move to Emeryville, California, where she is excited to join the medicinal chemistry team at the Novartis Institutes for BioMedical Research.